

Pre- and post-pyrolysis treatments in biochar-based fertilization

Dissertation

der Mathematisch-Naturwissenschaftlichen Fakultät
der Eberhard Karls Universität Tübingen
zur Erlangung des Grades eines
Doktors der Naturwissenschaften
(Dr. rer. nat.)

vorgelegt von
M.Sc. Jannis Grafmüller
aus Emmendingen

Tübingen
2025

Gedruckt mit Genehmigung der Mathematisch-Naturwissenschaftlichen Fakultät der
Eberhard Karls Universität Tübingen.

Tag der mündlichen Qualifikation:	04.11.2025
Dekan:	Prof. Dr. Thilo Stehle
1. Berichterstatter/-in:	Prof. Dr. E. Marie Muehe
2. Berichterstatter/-in:	Prof. Dr. Daniel Kray
3. Berichterstatter/-in:	Prof. Dr. Yvonne Oelmann

Acknowledgements

I would like to express my deepest gratitude to the many people who have supported me during my PhD project in the last four years. My work was funded within the EU Horizon 2020 project HyPErFarm, for which I would like to express my appreciation.

I am very grateful to Daniel Kray for enabling and supervising my PhD thesis. He offered me a lot of freedom in my work and placed a large amount of trust in me. I want to thank all my colleagues of the PVT research group in Offenburg for the very pleasant working atmosphere.

I would also like to express a special thank you to Marie Muehe for co-supervising my PhD thesis in a very appreciative and constructive manner. Her feedback and comments on my manuscripts helped a lot to improve their scientific quality and I am grateful that the doors to her lab were always open to me. Further, I want to thank her research group at UFZ Leipzig for warmly welcoming me in their lab and I am grateful to Paul-Georg Richter and Mara Breit for their kind assistance and teaching on microbiological analysis.

I would also like to thank Yvonne Oelmann and Peter Grathwohl for their willingness to act as reviewers in my doctoral examination procedure.

I am especially grateful to Nikolas Hagemann, who enabled the start of my journey in biochar research with supervising my MSc thesis in 2020. His ongoing support and supervision during my PhD time was irreplaceable. He encouraged me to be less hard on myself, to let go of some setbacks and refocus on the present. Thank you for your reliable support!

Hans-Peter Schmidt shaped many ideas underlying to my thesis and has always been reliable in providing valuable feedback on experimental data and manuscripts, for which I am very grateful to him.

I want to thank Thomas Bucheli for providing many helpful and critical comments on manuscripts and experimental methodology, through which I learnt a lot. I am also grateful to him for offering access to lab equipment and infrastructure at Agroscope Zurich during my PhD time. In this context, I want to thank his research group for welcoming me and especially Isabel Hilber, Martin Zuber and Ayah Aziz for helping me with experimental work. I also want to thank Dilani Rathnayake and Vinayak Kamra for their support with pyrolysis experiments in Zurich.

I want to thank Jens Möllmer for conduction of porosity analysis on many of my biochar samples at INC Leipzig, which helped to better understand and interpret my experimental data.

In this context, I want to thank Haike Mäurer and Markus Lange for further help with experimental work at INC and Reiner Staudt who established contact with the INC for me.

Claudia Kammann helped me with the experimental design of the greenhouse experiment on N₂O emissions and provided critical and valuable feedback on manuscript drafts. I also want to thank her research group members Christina Funk and Alexandra Schuld for their assistance.

Many of my working days in the greenhouse or lab would have been more demanding and less joyful without the valuable help of Viola Bartsch, Lea-Elena Anders, Sara Cebulla and Mohammed Kusaybati, who supported me as student assistants during the last years.

Without it being in their area of responsibility, Regina Brämer, Andrea Seigel, Barbara Anders, Almuth Henninger, Barbara Kast, Melanie Broszat, Olivia Warnsmann, Andreas Wilke, Thomas Eisele, Christiane Zell, Susanne Gleißle, Tobias Duri, Sascha Reißmann, Sascha Himmelbach, Corinna Henninger, Uzair Ahmed, Olga Zilienska and Hector Duran assisted me a lot at Offenburg University either with help on analysis of my samples, providing lab space and equipment or providing advice on experimental realization of my ideas. Thank you all for your support!

I am thankful to Heiko Peisert for providing access to XPS equipment at Tuebingen University and to Syed Mustafa Hussein for supporting me during the measurements.

I further want to thank Pellegrino Conte and Calogero Librici for giving me the opportunity to visit their lab at University of Palermo and introducing me to the Sicilian culture, which I enjoyed a lot.

Further, I want to thank Jochen Schweiger as well as Peter Bissert for offering greenhouse space for my experiments. I am also grateful to all farmers providing soils for greenhouse experiments, especially Thomas Margenfeld, Johannes Witt, Alois Huber and Andreas Harlander.

The support from my family and friends throughout my studies and PhD has been invaluable. I want to thank my parents for their support throughout my whole life, never judging me by what I am doing and always offering a place to sleep and eat, when I was tired of commuting during the last years. Philipp, thank you for the longstanding friendship and hosting me in Zurich. I am very grateful to my family in-law for their support and lots of valuable advice during the last years that helped me to get things done. Finally, I am deeply grateful for the unconditional support of my wife Greta, who always stands by my side and motivates me to keep going.

Table of Contents

Abstract	6
Zusammenfassung	8
1. Introduction to biochar-based fertilization and objectives of this thesis	11
2. Wood ash additives for improved yield and nutrient content of biochar and related formation of polychlorinated pollutants during biochar production	26
a. Increasing biochar yield in pyrolysis by adding ash	26
b. Biochars from chlorine-rich feedstock are low in polychlorinated dioxins, furans and biphenyls	78
3. Physical modification of biochar for use in biochar-based fertilizers	94
a. Root-zone amendments of biochar-based fertilizers: yield increases of white cabbage in temperate climate	94
b. Preparation of biochar microparticles by milling: effect on biochar and soil water holding capacity, biochar porosity and growth of white cabbage	114
c. Granulation compared to co-application of biochar plus mineral fertilizer and its impacts on crop growth and nutrient leaching	146
d. Contrasting effects of granulated biochar-based fertilizer on nitrogen leaching in sandy loam and silt loam	163
e. Soil-borne N ₂ O emissions were not reduced with granulated biochar-based fertilizer at agricultural relevant biochar and nitrogen dosage	184
4. Acidification of biochar for use in biochar-based fertilizers	237
a. Citric acid treatment reduced nitrate leaching but impaired macronutrient uptake in spinach, depending on biochar type	237
b. Biochar acidification increased sorption and reduced leaching of nitrate	275
5. Discussion and conclusion	289

Abstract

Biochar is produced by pyrolysis of biomass and applied to soil for carbon sequestration. Its application further aims to improve crop yield in agriculture and to reduce nutrient leaching and soil-borne nitrous oxide (N₂O) emissions. Still, little is known if these co-benefits attributed to high, but uneconomic biochar application rates can be observed when using biochar as biochar-based fertilizer (BBF), a combination of biochar and fertilizer in one product, resulting in low biochar application rates to soil of ~1-5 t ha⁻¹ season⁻¹. In this thesis, BBF production methods applied before (pre-) or after (post-) pyrolysis were elucidated on their effects on the pyrolysis process, biochar properties and agricultural performance. An underlying aim of this work was to investigate the extent to which wood ash as pyrolysis additive can increase biochar yields and how BBF production methods, mainly granulation and liquid fertilizer-enrichment, affect agronomic performance of low biochar application rates to soil.

Biomass was amended with wood ash before pyrolysis, aiming to recycle ash-derived nutrients and to increase dry and ash-free biochar yield. Ash amendment was most effective to elevate biochar yield when applied to woody biomass while negative effects were observed for gramineous biomass. Results from pilot-plant scale were confirmed by pyrolysis on industrial scale, which has the potential to reduce biochar production costs.

Wood ash and pyrolysis feedstocks like marine biomass can be enriched with chlorine, potentially leading to biochar contamination with polychlorinated aromatic hydrocarbons (PCB+PCDD/F), a largely unexplored topic in biochar production. In pyrolysis experiments performed in this thesis, the use of chlorine-rich feedstock did not increase PCB+PCDD/F contamination of biochar above limit values set in the European Biochar Certificate, enabling biochar producers to use chlorine enriched additives and biomass in the future.

Impacts of different post-pyrolysis treatments on crop growth, nutrient leaching and soil-borne N₂O emissions were studied in greenhouse experiments. Biochar, liquid enriched with fertilizer and applied concentrated in the root-zone at low dosage (~1 t ha⁻¹), increased yields of white cabbage by up to 21% compared to fertilized soil without a biochar amendment. The underlying mechanisms remained unclear; a better nutrient supply might have occurred due to BBF application directly below seedlings.

A further focus was on the preparation of granulated BBF. It was hypothesized that the close contact of fertilizer and biochar after granulation reduces the nutrient release rate from BBF leading to decreased nutrient leaching and soil-borne N₂O emissions. Granulated BBF reduced nutrient leaching by up to 35% in sandy loam, similar to non-granulated biochar. Still, higher crop yields compared to non-amended soil were only observed with non-granulated biochar co-

applied with fertilizer, which was associated with immobilization of macronutrients in granulated BBF. In silt loam, granulated BBF increased nitrogen leaching by 32% compared to non-amended soil, highlighting that BBF application strategies need to be adapted to soil types. Soil borne N₂O emissions were not reduced with a low biochar application rate resulting from granulated BBF amendment (~1 t ha⁻¹). However, reductions could occur after repeated use over several years.

Lastly, acidification of biochar was studied as a tool to reduce nitrate (NO₃⁻) leaching from soil. Citric acid treated and NO₃⁻-enriched biochar reduced NO₃⁻ leaching more effectively than non-acidified biochar in a greenhouse experiment with sandy loam. Still, unintended side-effects of citric-acid treatment, like decreased macronutrient uptake in spinach and an increase in soil pH, potentially due to decarboxylation of citrate, make this method unsuitable for BBF application. Further, nitric acid was used for acidification to systematically study sorption mechanisms of NO₃⁻ to biochar at soil relevant pH (pH 5 and pH 7) by avoiding interference with competing anions, such as citrate. Previous research reported increased NO₃⁻ sorption at higher biochar production temperature and at decreased in equilibration pH, which was confirmed by the experiments in this thesis, but so far, sorption mechanisms remained unclear. The experiments in this thesis indicated that NO₃⁻ sorption at soil relevant pH is dominated by sorption to protonated, condensed aromatic structures of biochar. Nitric-acid enriched BBF amended to LUFA standard soils reduced NO₃⁻ leaching by up to 20% in soil with pH below 6 while leaching from soil with neutral pH was only marginally affected compared to non-amended soil.

The most consistent effect of using low biochar application rates applied as BBF in this thesis was an averaged 42 ± 16% reduction in nitrogen leaching from sandy soil, which likely enabled BBF-induced increases in crop yields by 14 ± 12% following leaching events across different experiments. In absence of leaching, crop yields were changed by +5 ± 9% across all greenhouse experiments, here, significant differences to non-treated soil could only be rarely observed.

This thesis highlighted the potential of wood ash as an additive in biomass pyrolysis and established a basic understanding on contamination of biochar with PCB+PCDD/F. Further, BBF application at low biochar application rate to soil has the potential to reduce nutrient leaching from soil while reductions in N₂O emissions and increases in crop yields are uncertain, which needs to be further studied under field conditions.

Zusammenfassung

Pflanzenkohle wird über die Pyrolyse von Biomasse hergestellt und zur Kohlenstoff-Sequestrierung in Böden eingebracht. Ein weiterer Beweggrund ihrer Anwendung ist die Erhöhung landwirtschaftlicher Ernten und die Reduktion der Nährstoffauswaschung sowie der Emission von Lachgas (N_2O) aus Böden. Jedoch ist bisher wenig bekannt, ob diese positiven Nebeneffekte, die mit hohen, jedoch unwirtschaftlichen Pflanzenkohleapplikationen in Verbindung gebracht werden, beobachtet werden können, wenn Pflanzenkohle in Form Pflanzenkohle-basierter Düngemittel (engl. „biochar-based fertilizer“, abgekürzt mit „BBF“) angewendet wird, was in geringen Pflanzenkohle-Anwendungsraten von circa $1-5 \text{ t ha}^{-1}\text{Saison}^{-1}$ resultiert. In der vorliegenden Arbeit wurden Herstellungsverfahren von BBF, angewandt vor oder nach der Pyrolyse, hinsichtlich ihrer Auswirkungen auf den Pyrolyseprozess, die Pflanzenkohleeigenschaften und agronomische Parameter untersucht. Ziel dieser Arbeit war es, Holzasche als Additiv im Kontext der Steigerung des Pflanzenkohleertrags in der Pyrolyse zu untersuchen und herauszufinden, wie sich verschiedene BBF-Herstellungsverfahren, hauptsächlich Granulierung und Anreicherung mit Flüssigdünger, auf die agronomische Leistung von niedrigen Pflanzenkohle-Applikationsraten auswirken.

Die Anwendung von Holzasche als Additiv in der Pyrolyse kann Nährstoffkreisläufe schließen und den asche-freien Pflanzenkohleertrag steigern. Die Asche steigerte die Pflanzenkohleerträge am stärksten, wenn sie holziger Biomasse zugegeben wurde, negative Effekte wurden für grasartige Biomassen beobachtet. Die auf Pilotmaßstab erzielten Ergebnisse wurden durch Pyrolyseexperimente auf industriellem Maßstab bestätigt und könnten dazu beitragen, zukünftig die Herstellungskosten von Pflanzenkohle zu senken.

Holzasche und Pyrolyse-Eingangsstoffe wie marine Biomasse können mit Chlor angereichert sein, was zu einer Kontamination von Pflanzenkohle mit polychlorierten aromatischen Kohlenwasserstoffen (PCB+PCDD/F) führen kann - ein bisher weitestgehend unerforschtes Thema in der Pflanzenkohleherstellung. In den hier durchgeführten Pyrolyseversuchen führte die Verwendung von chlorreichen Eingangsstoffen zu keiner Überschreitung der Grenzwerte des europäischen Pflanzenkohlezertifikats, was den Weg für den Einsatz von Chlor-enthaltenden Additiven oder Biomassen in der industriellen Pflanzenkohleherstellung ebnet.

In Gewächshausversuchen wurde die Auswirkung verschiedener BBF auf das Pflanzenwachstum, die Nährstoffauswaschung sowie N_2O Emissionen aus Böden untersucht. Ein BBF, der über die Flüssiganreicherung von Pflanzenkohle mit Dünger in niedriger Pflanzenkohle-Dosierung von circa 1 t ha^{-1} konzentriert in der Wurzelzone appliziert wurde, steigerte die Erträge von Weißkohl um bis zu 21% im Vergleich zu gedüngtem Boden ohne

Pflanzkohlezusatz. Der Wirkmechanismus blieb unklar, die Nährstoffversorgung könnte durch die BBF-Applikation direkt unterhalb der Pflanzen verbessert worden sein.

Ein weiterer Schwerpunkt dieser Arbeit lag in der Herstellung eines granulierten BBF. Es wurde die These aufgestellt, dass der durch die Granulierung entstehende unmittelbare Kontakt zwischen Pflanzkohle und Düngemittel die Freisetzungsrates von Nährstoffen aus dem BBF verlangsamt und dies zu einer geringeren Auswaschung von Nährstoffen und geringeren N_2O Emissionen führt. Das granuliert BBF reduzierte die Stickstoffauswaschung in sandigem Lehm um bis zu 35%, vergleichbar mit der Anwendung von nicht granulierter Pflanzkohle. Höhere Ernteerträge, verglichen zu nicht behandeltem Boden, wurden jedoch nur unter Verwendung von nicht granulierter Pflanzkohle, die separat zu einem Düngemittel ausgebracht wurde, beobachtet, was mit der Immobilisierung von Makronährstoffen im granulierten BBF zusammenhing. In schluffigem Lehm wiederum erhöhte das granuliert BBF die Stickstoffauswaschung um 32% verglichen zu nicht behandeltem Boden, wodurch verdeutlicht wurde, dass BBF-Anwendungen an die Bodenart angepasst werden sollten.

Emissionen von N_2O wurden durch die niedrige Pflanzkohle-Anwendungsrate, die sich aus der Düngung mit granuliertem BBF ergab (circa 1 t ha^{-1}), nicht reduziert, was jedoch nach wiederholter Anwendung über mehrere Jahre hinweg auftreten könnte.

Schließlich wurde die Ansäuerung von Pflanzkohle zur Verringerung der Nitratauswaschung aus einem sandigen Lehm untersucht. Zitronensäure- und mit Nitrat (NO_3^-)-angereicherte Pflanzkohle reduzierte die Auswaschung deutlicher als nicht angesäuerte Pflanzkohle. Unbeabsichtigte Nebenwirkungen der Zitronensäurebehandlung, wie eine verringerte Aufnahme von Makronährstoffen durch die Spinatkultur und ein Anstieg des pH-Wertes des Bodens, der auf die Decarboxylierung von Citrat zurückzuführen ist, machen diese Methode jedoch für die BBF-Herstellung ungeeignet. Stattdessen wurde Salpetersäure (HNO_3) zur Ansäuerung von Pflanzkohle verwendet, um die Sorptionsmechanismen von NO_3^- bei bodenrelevanten pH-Werten (pH 5 und pH 7) systematisch zu untersuchen, wodurch weiterhin eine Störung durch konkurrierende Anionen wie Citrat vermieden wurde. Frühere Untersuchungen ergaben, dass die Sorptionskapazität mit der Pyrolysetemperatur der Pflanzkohle und mit einer Abnahme des pH-Wertes während der Sorption zunehmen, was durch die Experimente in dieser Arbeit bestätigt wurde, jedoch blieben die Sorptionsmechanismen zuvor unklar. Die Ergebnisse dieser Arbeit deuten an, dass die Sorption von NO_3^- bei bodenrelevanten pH-Werten von protonierten, aromatischen Strukturen der Pflanzkohle bestimmt wird. Die Einbringung von mit HNO_3 behandeltem BBF in zwei LUFA-Standardböden verringerte die NO_3^- -Auswaschung im Boden mit einem pH-Wert von

5.7 um bis zu 20%, während sich in einem Boden mit neutralem pH-Wert nur geringfügige Effekte ergaben.

Die konsistenteste Auswirkung niedrig dosierter, über BBF angewandter Pflanzenkohle-Applikationen war eine durchschnittliche Verringerung der Stickstoffauswaschung aus sandigem Boden um $42 \pm 16\%$, was mutmaßlich zur durchschnittlichen Steigerung der Ernteerträge um $14 \pm 12\%$ führte. Ohne die Durchführung von Auswaschungsereignissen veränderten sich die Erträge über alle Versuche hinweg um nur $+5 \pm 9\%$, hier konnte nur in wenigen Versuchen ein signifikanter Unterschied zu nicht-behandeltem Boden festgestellt werden.

Diese Arbeit hat das Potential von Holzasche als Additiv in der Biomassepyrolyse aufgezeigt und ein grundlegendes Verständnis zur Kontamination von Pflanzenkohle mit PCB+PCDD/F aufgebaut. Darüber hinaus konnte gezeigt werden, dass niedrig dosierte Pflanzenkohle-Anwendungen über BBF das Potential haben, die Nährstoffauswaschung zu verringern, während die Reduktion von N₂O-Emissionen und Auswirkungen auf Ernteerträge ungewiss sind, was unter Feldbedingungen weiter untersucht werden sollte.

Chapter 1

Introduction to biochar-based fertilization and objectives of this thesis

The need for maintaining high productivity due to the permanently increasing human population and providing high product quality at less negative environmental implications, such as groundwater pollution or greenhouse gas emissions, imposes a challenging burden on global agriculture^{1,2}. The widespread use of synthetic fertilizer on agricultural soil ensures productivity over multiple growing seasons, yet simultaneously causes negative environmental impacts of modern agriculture, such as soil acidification, nitrate (NO_3^-) leaching to groundwater and the release of the potent greenhouse gas nitrous oxide (N_2O) from soil^{3,4}.

Motivated to address these challenges, research on biochar application in agriculture has been ongoing for nearly two decades, which is extensively summarized in a recent review of meta-analyses⁵. Biochar is defined as the solid product of biomass pyrolysis⁶. It predominantly consists of condensed aromatic carbon structures⁷, with up to 80% of its total carbon content estimated to be persistent against mineralization on a centennial timescale⁸. Biochar production from sustainably sourced biomass and application to soil is thus considered a carbon sequestration tool to mitigate climate change and referred to as Pyrogenic Carbon Capture and Storage (PyCCS)⁹. Beside climate-change mitigation, biochar application in agriculture can provide co-benefits. According to recent meta-analyses, biochar application can increase crop yields by 10%¹⁰, reduce NO_3^- leaching by 12%¹¹, and decrease N_2O emissions from soil by 38%^{11,12}. These improvements, however, were predominantly achieved with biochar application rates of 10-50 t ha⁻¹, which are not considered economic for farmers, as current biochar prices amount to 800-1500 € t⁻¹ in e.g., Germany, Austria, and Switzerland¹³. High costs and the lack of crop-specific application protocols are considered to be the main reasons why biochar use in agriculture remains limited so far¹⁴. Thus, its potential as a tool for carbon sequestration and reducing negative impacts of agriculture remains unexploited.

Early studies focused on using biochar as a soil conditioner, applying pristine biochar separately from fertilizer. More recently, attention has alternated towards the use of biochar-based fertilizers (BBF), which combine biochar and fertilizer in a single product¹⁵. It is hypothesized that this combination improves interactions between biochar and nutrients, such as sorption of nutrients to the biochar surface leading to improved nutrient retention in soil, which could be favorable for crop nutrition, enabling biochar to be effective at lower application rates (1-5 t ha⁻¹)^{16,17}. BBF could be applied repetitively over multiple cropping seasons allowing

biochar to accumulate in the soil. A recent meta-analysis suggests that one-time BBF application at biochar application rates equal to $\sim 1 \text{ t ha}^{-1}$ can increase crop productivity by 10%¹⁵. However, little is known if BBF can also mitigate nutrient leaching and soil-borne N_2O emissions and if this is dependent on different BBF production methods. To improve our understanding in this area, this thesis investigated BBF production through various pre- and post-pyrolysis treatments. The focus is on **(1)** applying post-pyrolysis treatments to study their effect on the agricultural performance of BBF while reducing negative environmental impacts of fertilization and **(2)** to identify synergies between pre-pyrolysis nutrient enrichment of biomass using wood ash and biochar production to improve nutrient recycling and reduce biochar production costs.

There are multiple ways to modify biochar for BBF production, as summarized in Figure 1, which serves to contextualize the experiments included in this thesis without claiming for completeness. Both pre- and post-pyrolysis treatments, either applied individually or in combination, can be used for BBF production, as described in further detail below.

Pre-pyrolysis treatments

Pre-pyrolysis options include the choice of feedstock material and the use of additives. Depending on the feedstock material and their inherent contents of nutrients and potentially toxic elements (PTE), the resulting biochars, due to neglectable volatilization of nutrients like phosphorus (P), potassium (K) and magnesium (Mg) and PTE during pyrolysis¹⁸, differ in their fertility but also applicability to soil in accordance with the European Biochar Certificate (EBC¹⁹). For example, feedstocks like manure or sewage sludge are comparable rich in nutrients but might also be contaminated to a higher extent with PTE as compared to woody feedstocks, which are usually poor in nutrients^{18,20}. The macromolecular structure of a biomass, i.e., the content of lignin, cellulose, hemicellulose and ash can influence the resulting biochar porosity²¹, determining e.g., the sorption capacity of nutrients on the biochar surface.

The use of additives applied to biochar feedstocks include the application of pure salts, such as AlCl_3 or KCl to improve NO_3^- and phosphate (PO_4^{3-}) sorption capacity²², K-containing salts to improve P-availability in sewage sludge biochars²⁰ and the treatment of biomass with acids and bases (e.g., H_3PO_4 or NaOH) to increase biochar's specific surface area (SSA)^{23–25}. Further, mineral additives such as wood ash or rock powder were used as additives to increase biochar yields, enrich biochar with nutrients and to study potential co-benefits of enhanced rock weathering and biochar application^{26–28}.

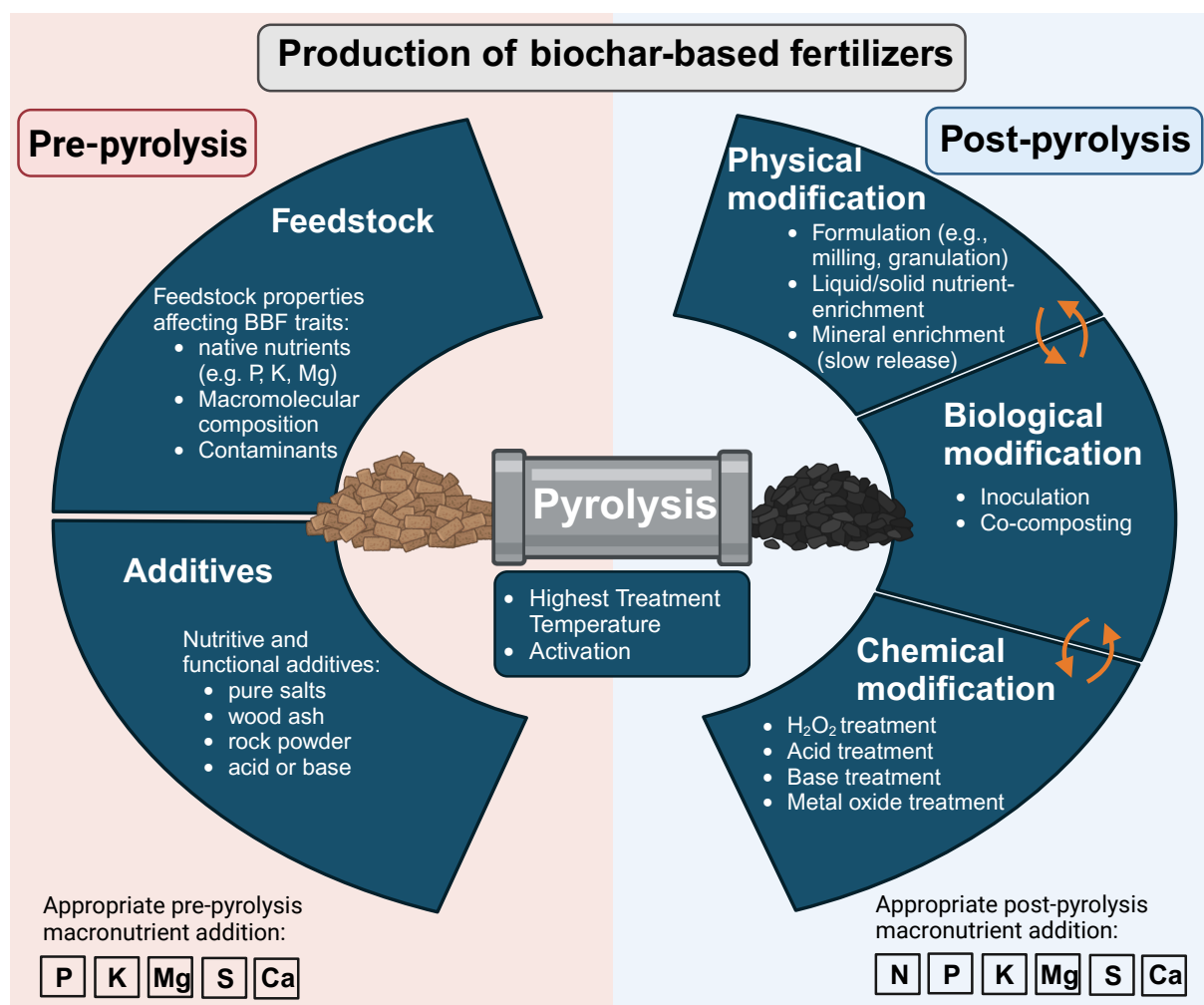


Figure 1: Overview of different strategies to produce and modify biochar-based fertilizers (BBF) separated into pre- and post-pyrolysis treatments.

Post-pyrolysis treatments

Post-pyrolysis treatments for BBF production use pristine biochars as educt for further modification. The treatments can be differentiated in those changing the physical, biological or chemical properties of the biochar (Figure 1).

a. Physical modification

One of the simplest physical modifications is milling to reduce the variation of the inherent particle size distribution of biochar making it available for combined soil application with fertilizer via e.g., box or auger spreaders. A more advanced modification is the combined granulation of finer milled biochar with fertilizer, to obtain a granulated BBF that can be applied in the same way as conventional granulated fertilizers most commonly used in agriculture²⁹⁻³¹. Further, BBF can be prepared by simple mixing of biochar and solid fertilizer or preparing a suspension of biochar and solubilized fertilizer to allow biochar to absorb a nutritive solution in its porous structure³². Enrichment of biochar with clay minerals can be used to improve the

slow-release of nutrients from biochar spiked with liquid fertilizer through partial pore clogging³³.

b. Biological modification

Biological modifications of biochar include inoculation with P solubilizing bacteria to improve the plant-availability of barely soluble calcium phosphates in sewage sludge biochars³⁴. Similarly, biochar inoculation with arbuscular mycorrhizal fungi was proposed to mediate phosphorus solubilization from biochar and stimulate plant nutrient uptake³⁵. Further, biochar can be co-composted allowing the development of a thin coating on the biochar surface rich in humic substances that captures plant-available mineral N^{36,37}. Biological modifications of biochar, however, have not been applied in the present thesis.

c. Chemical modification

Chemical modification techniques all aim to modify the surface of biochar to improve either the sorption capacity for cations or anions, to facilitate slow release of nutrients from BBF, which is key to reduce nutrient leaching from soil. Treatment of pristine biochars with H₂O₂, bases like KOH or acids such as H₂SO₄ increased the content of oxygenated functional groups and SSA resulting in improved sorption of cations to biochar³⁸. Impregnation of biochar surface, which is usually negatively charged³⁹, with positively charged metals³⁸ resulted in an improved sorption capacity of modified biochars for anions such as NO₃⁻ or PO₄³⁻.

In addition to the abovementioned methods, the highest treatment temperature or the application of a water-based activation treatment during pyrolysis can influence biochar characteristics relevant for BBF applications, such as biochar SSA^{21,40}. More general, given that nitrogen (N) is largely volatilized during pyrolysis¹⁸, it is the only macronutrient recommended to add during post-pyrolysis treatment (Figure 1).

Objectives of this thesis

The present thesis includes both pre- and post-pyrolysis treatments for BBF production, with the main aim to increase biomass use-efficiency of PyCCS to potentially lower biochar production costs, to improve the applicability of biochar in agriculture by physical post-pyrolysis treatments and to improve NO₃⁻ sorption capacity of pristine biochars with a simple post-pyrolysis treatment to provide a short-cut to the earlier observed improved NO₃⁻ retention in soil-aged or co-composted^{36,37} biochar. The focus was on (1) applying wood ash as an additive in pre-pyrolysis treatments, (2) producing BBF via granulation during post-pyrolysis modification to elucidate its effect on crop growth, nutrient leaching and soil-borne N₂O emissions and (3) using biochar acidification during post-pyrolysis modification as a tool to improve NO₃⁻ sorption to biochar. In the following, a brief introduction is given to the specific chapters included in this thesis and to the research questions that were addressed.

Chapter 2 focuses on using wood ash as additive in biomass pyrolysis, which has the potential to increase dry and ash-free (daf) biochar yield and enrich biochar with ash-derived nutrients^{27,28}. This way, a BBF with essential macronutrients such as K, Mg and Ca is produced while biochar production costs could be lowered due to biochar yield increases during pyrolysis. Motivated by our previous observation of a dose-response relation of daf biochar yield with ash-amendment of softwood with low native ash content²⁸, **chapter 2.a** aimed to (1) quantify the increase in daf biochar yield upon ash amendment of different biomasses with varying native ash contents, to (2) link changes in yield to the properties of different ash additives and (3) to transfer the ash treatment to biomass pyrolysis on industrial scale. Based on the observation that amending softwood with chlorine-containing wood ash increased the content of polychlorinated aromatic hydrocarbons in biochar (PCB and PCDD/F)²⁸, a contaminant group regulated by the EBC¹⁹, **chapter 2.b** focused on the formation of these contaminants in pyrolysis of chlorine-enriched biomass to find out, if there is a risk for PCB+PCDD/F contamination when using ash-additives with potential chlorine enrichment. While extensive research was already done on the formation of polyaromatic hydrocarbons during pyrolysis⁴¹⁻⁴³, the formation of polychlorinated pollutants during biochar production was largely unexplored so far.

The experiments in **Chapter 3** focused on physical post-pyrolysis treatments in BBF production. In the experiment presented in **chapter 3a**, the focus was on liquid nutrient-enrichment of biochar to produce BBF. Liquid nutrient-enrichment is a simple method to

increase the nutrient content of any biochar by utilizing its water holding capacity of usually 100-200% (w/w) for absorption of liquid fertilizers. There are several studies that observed increased crop yields by application of liquid-enriched BBF, also at low absolute biochar application rates (Table 1). Here, most positive results were obtained with cow urine-enriched biochars applied to the root-zone of several crop types in field trials in Nepal conducted by Schmidt et al.^{17,32}. Crop yields were increased in the following order: urine-enriched biochars > mineral NPK enriched biochars > sole mineral NPK fertilization. In contrast, Kizito et al.⁴⁴ reported negative effects for organically enriched BBF compared to sole mineral NPK fertilizer amendment to soil. As this study used digestate for biochar enrichment, which was assumed to have a significantly lower content of mineralized nitrogen compared to urine, the negative effects found by Kizito and colleagues were attributed to reduced mineral N content and low mineralization rates of the digestate. Beside improved crop growth observed by Schmidt and Pandit et al. when applying liquid enriched BBF, Luyama and colleagues⁴⁵ observed increased root:shoot ratios for liquid enriched BBF, indicating reduced nutrient availability under BBF amendment (Table 1).

An identified knowledge gap is a comparison of different mineral nitrogen species for liquid-enrichment of biochar, which has only been partly conducted by Schmidt and colleagues^{17,32} without allowing direct comparisons between individual mineral N fertilizers. In this thesis, liquid enrichments of biochar were performed using urea (in analogy to cow urine), ammonium-nitrate or ammonium sulphate. Due to ammonia volatilization observed during liquid enrichment of biochar with ammonium sulphate, this fertilizer was however not further included in the experimental setup. Secondly, differences between liquid enriched biochars and co-application of non-enriched biochar in combination with top-dress fertilization have not been studied so far. Lastly, the positioning of liquid-enriched BBF in proximity to the plant might affect crop growth due to alternation of nutrient availability in soil. Therefore, as a third factor, the BBF were either positioned as a “Hotspot” below seedlings or homogeneously applied in the plant’s root zone.

This was studied in greenhouse trial presented in **chapter 3a** which was conducted with white cabbage using a fertile, silt loam soil, in accordance to previously performed field trials on silt loams in Nepal^{17,32}. The promising results from Pandit et al.⁴⁶ when applying biochars with hot infused liquid fertilizers were unfortunately not incorporated in the present thesis but should be further investigated in the future (Table 1). To build up on the results of Luyama et al.⁴⁵, the effects of the liquid-enriched BBF on root architecture were analyzed using a Shovelomics protocol according to Colombi et al.⁴⁷ in the present thesis.

Chapter 1: Introduction to biochar-based fertilization and objectives of this thesis

Table 1: Literature overview on plant growth studies performed with liquid-enriched biochars to produce biochar-based fertilizers.

Author, year and title	Biochar	Liquid enrichment source	Biochar application rates [t ha ⁻¹]	Trial and soil type	Results
Schmidt et al. 2017¹⁷ : Biochar-Based Fertilization with Liquid Nutrient Enrichment: 21 Field Trials Covering 13 Crop Species in Nepal	Ageratina adenophora (700°C)	(1) Cow urine (2) Urea (3) Diammonium-phosphate	0.5-2	Field Trials in Nepal Soils: Silt loam SOC: 1.5-6% pH: 5-7	Yield Increases for various crops: - 123±76 % for urine-BC compared to organic fertilization only - 103±12% for organically compared to mineral enriched BC - 15-30% for NPK-enriched BC compared to NPK only
Kizito et al. 2019⁴⁴ : Role of Nutrient-Enriched Biochar as a Soil Amendment During Maize Growth: Exploring Practical Alternatives to Recycle Agricultural Residuals and to Reduce Chemical Fertilizer Demand	Fig tree (600°C) Corn cub (600°C)	Digestate	(1) 10 (2) 20	Clay loam soil (2% SOC) and overall low fertility	Yield decreases in maize compared to NPK: - 20-30% lower yield at 20 t ha ⁻¹ - 45-50% lower yield at 10 t ha ⁻¹ When co-applied with NPK (no liquid enrichment), yield differences were lower for 10 t ha ⁻¹ (-25-30%)
Schmidt et al. 2015³² : Fourfold Increase in Pumpkin Yield in Response to Low-Dosage Root Zone Application of Urine-Enhanced Biochar to a Fertile Tropical Soil	Ageratina adenophora (700°C)	Cow urine	0.75	Field trial in Nepal, fertile silt loam	Pumpkin yield increases: 300% increase with urine enriched BC compared to urine only and 85% compared to biochar only
Pandit et al. 2017⁴⁶ : Biochar from "Kon Tiki" flame curtain and other kilns: Effects of nutrient enrichment and kiln type on crop yield and soil chemistry	Eupatorium adenophorum (700°C)	Mineral NPK fertilizer via hot or cold nutrient enrichment (hot or cold)	(1) 20 (2) 80	Pot trial with Inceptisol from Nepal with pH 4.5	Increases in maize biomass: 150-200% with hot NPK enrichment and 10-50% with cold NPK enrichment, while lower application rate was always more advantageous than higher application rate.
Luyima et al. 2021⁴⁵ : Nutrient Dynamics in Sandy Soil and Leaf Lettuce Following the Application of Urea and Urea-Hydrogen Peroxide Impregnated Co-Pyrolyzed Animal Manure and Bone Meal	Cow dung + 25% or 50% bone meal (no HTT provided)	(1) Urea (2) Urea hydrogen peroxide	5	Pot trial with sandy soil	Higher root:shoot ratio of lettuce for all enriched biochars but no crop yields provided.

Chapter 3b focused on the production of biochar microparticles, which are essential for processes such as BBF granulation. The study investigated how microparticles produced using two different milling technologies differed in particle size distribution, biochar porosity, and their effects on soil water-holding capacity and growth of white cabbage. The aim was to provide recommendations on how biochar microparticles should be prepared for granulated BBF (gBBF) production.

Chapters **3 c-d** focused on gBBF application to soil. Granulated BBF might be the simplest way for farmers to apply biochar to soil with common agricultural machinery, however, research on the effect of gBBF on crop growth, nutrient leaching and soil-borne N₂O emissions is limited (Table 2). Shi et al.³¹ observed reduced nitrogen release rates and increased maize growth with the amendment of an urea-based gBBF compared to sole urea fertilization. However, the authors also added clay minerals like bentonite and sepiolite to the gBBF, that were not added with sole urea fertilization. Therefore, it is challenging to separate biochar-effects and effects related to the added mineral contained in the gBBF in this experiment. Li and colleagues⁴⁸ prepared three gBBF based on a mineral compound fertilizer that was amended with different biochar concentrations before granulation. The effects on reduction of N leaching compared to the sole application of compound fertilizer to the soil were marginal (<10% reduction of N leaching), which might be attributed to the low contents of biochar in the gBBFs (up to 15%, w/w). Jia et al. coated granulated urea with a biochar layer to prepare a gBBF (23% biochar content, w/w)³⁰. Amended to an acidic soil, this gBBF reduced nitrogen leaching significantly compared to pure urea but also compared to the co-application of non-granulated biochar and urea. However, their gBBF treatment contained a tenfold lower biochar application rate to soil compared to the co-application treatment. On the one hand, this highlights the effectivity of the biochar coating in the gBBF, however, it does not allow a direct comparison of the gBBF with the co-application treatment. In contrast, Liao et al. found increased nutrient leaching with granulated biochar compared to milled biochar application to soil⁴⁹ without focusing on BBF application. However, this study generally highlighted that granulated and non-granulated biochar application to soil at similar application rate differ in their effects on nutrient leaching. To identify effects of biochar granulation itself, a more systematic comparison of gBBF application with the co-application of non-granulated biochar and fertilizer is needed. Further, while there are some studies focusing on gBBF effects on crop growth and N leaching (Table 2), no study so far focused on the effect on soil-borne N₂O emissions. The experiments performed in chapters 3 c-e therefore study effects of gBBF amendment on crop growth, nutrient leaching and N₂O emissions:

- **Chapter 3c** examined whether well-established benefits of biochar application to soil, namely increased crop yields and reduced nutrient leaching, can be enhanced at low biochar application rate when biochar is applied in the form of gBBF rather than in its non-granulated form, the latter being the most common application method in both research and practice. White cabbage was used as the test crop, with a conventional NPK compound fertilizer serving as reference fertilization.
- **Chapter 3d** explored the effects of gBBF amendment on two contrasting soil types to determine whether the promising N leaching reductions observed in Chapter 3c in sandy soil could also be achieved in silt- and clay-rich soil. Annual ryegrass was used as the test plant, with a conventional NPK fertilizer serving as the control.
- **Chapter 3e** presents a greenhouse trial with spinach to investigate whether a low biochar application rate, applied to soil with a gBBF, is sufficient to reduce soil-borne N₂O emissions compared to a conventional NPK-fertilized control. Additionally, biochar was co-applied with NPK fertilizer in non-granulated form at the same rate to determine whether the granulation process influences the effect of biochar on N₂O emissions. Furthermore, a tenfold higher biochar amount (relative to the gBBF treatment) was co-applied with NPK in non-granulated form to match the biochar dosage used in previous studies^{50,51} that reported significant reductions in soil-borne N₂O emissions.

Chapter 1: Introduction to biochar-based fertilization and objectives of this thesis

Table 2: Literature overview on plant growth and leaching studies performed with granulated biochar-based fertilizers.

Author, year, and title	Biochar	Study type	Granule components	Reference treatment	Results
Shi et al. 2020 ³¹ : Biochar bound urea boosts plant growth and reduces nitrogen leaching	Green waste biochar (450-550 °C)	Soil column leaching experiment and greenhouse trial (soil type not specified)	Biochar (22%) Urea (44%) Bentonite (27%) Sepiolite (7%)	Granulated urea	(1) Significant lower nitrogen release rates from biochar-blended granules in soil column leaching experiment (2) +13.8% aboveground biomass, +25.1% root biomass, and +24% nitrogen use efficiency with BBF amendment compared to sole urea fertilization.
Yunlong Li et al. 2019 ⁴⁸ : Effects of biochar-based fertilizers on nutrient leaching in a tobacco-planting soil	Tobacco stalks (Temperature unknown)	Soil column leaching experiment (limestone soil, pH 7.8)	Biochar added at 3%, 9%, and 15% mass ratio to a compound fertilizer (composition of fertilizer unknown) before granulation process	Granulated compound fertilizer (composition unknown)	Decrease in total nitrogen leaching by 8%, 7% and 6% with 3%, 9%, and 15% biochar content in BBF compared to pure compound fertilizer
Jia et al. 2021 ³⁰ : Application of biochar-coated urea controlled loss of fertilizer nitrogen and nitrogen use efficiency.	Vinasse (600°C)	Pot experiment with oilseed rape including leaching events (red soil pH 5.9)	Urea granules coated with biochar (23%, w/w biochar). Traces of resin and paraffin wax added to the outer surface of the granules.	(1) Urea (2) Biochar + Urea (co-application)	36% lower nitrogen leaching loss with biochar-coated urea compared to pure urea and 33% lower compared to co-application of biochar co-applied with urea. No significant difference in crop yields observed among the treatments.
Liao et al. 2022 ⁴⁹ : Biochar granulation, particle size, and vegetation effects on leachate water quality from a green roof substrate	Sawmill waste (625 °C)	Pot trial on vegetated roof substrate	Biochar only to obtain granules in five different sieving fractions: (1-2mm; 2-2.8mm; 2.8-4mm; 4-6.3 mm)	Non-granulated biochar at five sieving fractions: 0.25-0.5 mm; 0.5-1mm; 1-2mm; 2-2.8mm; 2.8-4mm)	Higher reduction in nutrient leaching with non-granulated biochar for the different sieving fractions. Enhanced plant performance with granulated biochar.

Chapter 4 was inspired by recent findings that the interaction of organic acids, e.g. citric acid, and biochar can enhance the sorption of NO_3^- to biochar⁵². This chapter investigated whether an acidification treatment could be used to produce NO_3^- -enriched BBF that slowly release NO_3^- and thereby reduce NO_3^- leaching from soil. In **Chapter 4a**, two citric acid-treated BBF were tested in a greenhouse trial with spinach to examine NO_3^- release to soil porewater and NO_3^- leaching losses, compared to non-acidified BBF and compared to an untreated soil control. In **chapter 4b**, pH-dependent sorption of NO_3^- to different wood-based biochars was studied. Unlike the experiment in chapter 4a, where citric acid was used for biochar acidification, or previous research that used HCl for pH adjustment⁵³, HNO_3 was chosen aiming to maximize NO_3^- sorption by avoiding interference from additional anions such as citrate or chloride. Building up on previous research⁵³, sorption capacities were linked to different biochar properties to gain a more mechanistic understanding of pH-dependent⁵³ NO_3^- sorption to biochar. Finally, the release dynamics of HNO_3 -treated BBF were assessed in a column experiment using two LUFA standard soils.

References

- (1) FAO. Greenhouse Gas Emissions from Agrifood Systems - Global, Regional and Country Trends, 2000-2022, 2024. <https://openknowledge.fao.org/handle/20.500.14283/cd3167en> (accessed 2025-03-17).
- (2) Robertson, G. P.; Swinton, S. M. Reconciling Agricultural Productivity and Environmental Integrity: A Grand Challenge for Agriculture. *Front. Ecol. Environ.* **2005**, *3* (1), 38–46. [https://doi.org/10.1890/1540-9295\(2005\)003\[0038:RAPAEI\]2.0.CO;2](https://doi.org/10.1890/1540-9295(2005)003[0038:RAPAEI]2.0.CO;2).
- (3) Ayoub, A. T. Fertilizers and the Environment. *Nutr. Cycl. Agroecosystems* **1999**, *55* (2), 117–121. <https://doi.org/10.1023/A:1009808118692>.
- (4) Goucher, L.; Bruce, R.; Cameron, D. D.; Lenny Koh, S. C.; Horton, P. The Environmental Impact of Fertilizer Embodied in a Wheat-to-Bread Supply Chain. *Nat. Plants* **2017**, *3* (3), 17012. <https://doi.org/10.1038/nplants.2017.12>.
- (5) Schmidt, H.-P.; Kammann, C.; Hagemann, N.; Leifeld, J.; Bucheli, T. D.; Sánchez Monedero, M. A.; Cayuela, M. L. Biochar in Agriculture – A Systematic Review of 26 Global Meta-analyses. *GCB Bioenergy* **2021**, *13*, 1708–1730. <https://doi.org/10.1111/gcbb.12889>.
- (6) *Biochar for Environmental Management: Science, Technology and Implementation*, Second edition.; Lehmann, J., Joseph, S., Eds.; Routledge, Taylor & Francis Group: London ; New York, 2015.
- (7) Chia et al. Characteristics of Biochar: Physical and Structural Properties. In *Biochar for environmental management: science, technology and implementation*; Lehmann, J., Joseph, S., Eds.; Routledge, Taylor & Francis Group: London;New York, 2015. <https://doi.org/10.4324/9780203762264-12>.
- (8) McBeath, A. V.; Wurster, C. M.; Bird, M. I. Influence of Feedstock Properties and Pyrolysis Conditions on Biochar Carbon Stability as Determined by Hydrogen Pyrolysis. *Biomass Bioenergy* **2015**, *73*, 155–173. <https://doi.org/10.1016/j.biombioe.2014.12.022>.
- (9) Schmidt, H.-P.; Anca-Couce, A.; Hagemann, N.; Werner, C.; Gerten, D.; Lucht, W.; Kammann, C. Pyrogenic Carbon Capture and Storage. *GCB Bioenergy* **2019**, *11* (4), 573–591. <https://doi.org/10.1111/gcbb.12553>.

- (10) Ye, L.; Camps-Arbestain, M.; Shen, Q.; Lehmann, J.; Singh, B.; Sabir, M. Biochar Effects on Crop Yields with and without Fertilizer: A Meta-analysis of Field Studies Using Separate Controls. *Soil Use Manag.* **2020**, *36* (1), 2–18. <https://doi.org/10.1111/sum.12546>.
- (11) Borchard, N. Biochar, Soil and Land-Use Interactions That Reduce Nitrate Leaching and N₂O Emissions: A Meta-Analysis. *Sci. Total Environ.* **2019**, 11.
- (12) Kaur, N.; Kieffer, C.; Ren, W.; Hui, D. How Much Is Soil Nitrous Oxide Emission Reduced with Biochar Application? An Evaluation of Meta-analyses. *GCB Bioenergy* **2023**, *15* (1), 24–37. <https://doi.org/10.1111/gcbb.13003>.
- (13) Grafmüller, J.; Hagemann, N.; Kray, D. *Deliverable 4.2: Report on the comparison of pyrolysis with other CDR technologies available*. HyPERFarm EU Project. <https://hyperfarm.eu/wp-content/uploads/2025/03/D4.2.pdf> (accessed 2025-03-21).
- (14) Bach, M.; Wilske, B.; Breuer, L. Current Economic Obstacles to Biochar Use in Agriculture and Climate Change Mitigation. *Carbon Manag.* **2016**, *7* (3–4), 183–190. <https://doi.org/10.1080/17583004.2016.1213608>.
- (15) Melo, L. C. A.; Lehmann, J.; Carneiro, J. S. da S.; Camps-Arbestain, M. Biochar-Based Fertilizer Effects on Crop Productivity: A Meta-Analysis. *Plant Soil* **2022**. <https://doi.org/10.1007/s11104-021-05276-2>.
- (16) Joseph, S.; Graber, E.; Chia, C.; Munroe, P.; Donne, S.; Thomas, T.; Nielsen, S.; Marjo, C.; Rutledge, H.; Pan, G.; Li, L.; Taylor, P.; Rawal, A.; Hook, J. Shifting Paradigms: Development of High-Efficiency Biochar Fertilizers Based on Nano-Structures and Soluble Components. *Carbon Manag.* **2013**, *4* (3), 323–343. <https://doi.org/10.4155/cmt.13.23>.
- (17) Schmidt, H.-P.; Pandit, B. H.; Cornelissen, G.; Kammann, C. I. Biochar-Based Fertilization with Liquid Nutrient Enrichment: 21 Field Trials Covering 13 Crop Species in Nepal: Biochar-Based Fertilization. *Land Degrad. Dev.* **2017**, *28* (8), 2324–2342. <https://doi.org/10.1002/ldr.2761>.
- (18) Rathnayake, D.; Schmidt, H.; Leifeld, J.; Mayer, J.; Epper, C. A.; Bucheli, T. D.; Hagemann, N. Biochar from Animal Manure: A Critical Assessment on Technical Feasibility, Economic Viability, and Ecological Impact. *GCB Bioenergy* **2023**, *15* (9), 1078–1104. <https://doi.org/10.1111/gcbb.13082>.
- (19) EBC 2012-2024. “European Biochar Certificate - Guidelines for a Sustainable Production of Biochar.” Carbon Standards International (CSI), Frick, Switzerland. ([Http://European-Biochar.Org](http://European-Biochar.Org)). Version 10.4 from 20th Dec 2024, 2024.
- (20) Buss, W.; Bogush, A.; Ignatyev, K.; Mašek, O. Unlocking the Fertilizer Potential of Waste-Derived Biochar. *ACS Sustain. Chem. Eng.* **2020**, *8* (32), 12295–12303. <https://doi.org/10.1021/acssuschemeng.0c04336>.
- (21) Ippolito, J. A.; Cui, L.; Kammann, C.; Wrage-Mönnig, N.; Estavillo, J. M.; Fuertes-Mendizabal, T.; Cayuela, M. L.; Sigua, G.; Novak, J.; Spokas, K.; Borchard, N. Feedstock Choice, Pyrolysis Temperature and Type Influence Biochar Characteristics: A Comprehensive Meta-Data Analysis Review. *Biochar* **2020**. <https://doi.org/10.1007/s42773-020-00067-x>.
- (22) Dieguez-Alonso, A.; Anca-Couce, A.; Frišták, V.; Moreno-Jiménez, E.; Bacher, M.; Bucheli, T. D.; Cimò, G.; Conte, P.; Hagemann, N.; Haller, A.; Hilber, I.; Husson, O.; Kammann, C. I.; Kienzl, N.; Leifeld, J.; Rosenau, T.; Soja, G.; Schmidt, H.-P. Designing Biochar Properties through the Blending of Biomass Feedstock with Metals: Impact on Oxyanions Adsorption Behavior. *Chemosphere* **2019**, *214*, 743–753. <https://doi.org/10.1016/j.chemosphere.2018.09.091>.
- (23) Chu, G.; Zhao, J.; Huang, Y.; Zhou, D.; Liu, Y.; Wu, M.; Peng, H.; Zhao, Q.; Pan, B.; Steinberg, C. E. W. Phosphoric Acid Pretreatment Enhances the Specific Surface Areas of Biochars by Generation of Micropores. *Environ. Pollut.* **2018**, *240*, 1–9. <https://doi.org/10.1016/j.envpol.2018.04.003>.
- (24) Bentley, M. J.; Kearns, J. P.; Murphy, B. M.; Summers, R. S. Pre-Pyrolysis Metal and

Base Addition Catalyzes Pore Development and Improves Organic Micropollutant Adsorption to Pine Biochar. *Chemosphere* **2022**, 286, 131949.

<https://doi.org/10.1016/j.chemosphere.2021.131949>.

(25) Hina, K.; Bishop, P.; Arbestain, M. C.; Calvelo-Pereira, R.; Maciá-Agulló, J. A.; Hindmarsh, J.; Hanly, J. A.; Macías, F.; Hedley, M. J. Producing Biochars with Enhanced Surface Activity through Alkaline Pretreatment of Feedstocks. *Soil Res.* **2010**, 48 (7), 606. <https://doi.org/10.1071/SR10015>.

(26) Maria-Elena Vorrath; Drewer, J. M. Z.; Reinaldy Poetra; Hagemann, N.; Amann, T.; Hartmann, J. ROCKCHAR - Co-Pyrolysis of Biomass and Industrial Side Products for Cost-Efficient Carbon Dioxide Removal. **2024**. <https://doi.org/10.13140/RG.2.2.13092.08328>.

(27) Buss, W.; Jansson, S.; Mašek, O. Unexplored Potential of Novel Biochar-Ash Composites for Use as Organo-Mineral Fertilizers. *J. Clean. Prod.* **2019**, 208, 960–967. <https://doi.org/10.1016/j.jclepro.2018.10.189>.

(28) Grafmüller, J.; Böhm, A.; Zhuang, Y.; Spahr, S.; Müller, P.; Otto, T. N.; Bucheli, T. D.; Leifeld, J.; Giger, R.; Tobler, M.; Schmidt, H.-P.; Dahmen, N.; Hagemann, N. Wood Ash as an Additive in Biomass Pyrolysis: Effects on Biochar Yield, Properties, and Agricultural Performance. *ACS Sustain. Chem. Eng.* **2022**, 10 (8), 2720–2729. <https://doi.org/10.1021/acssuschemeng.1c07694>.

(29) Tahery, S.; Munroe, P.; Marjo, C. E.; Rawal, A.; Horvat, J.; Mohammed, M.; Webber, J. B. W.; Arns, J.-Y.; Arns, C. H.; Pan, G.; Bian, R.; Joseph, S. A Comparison between the Characteristics of a Biochar-NPK Granule and a Commercial NPK Granule for Application in the Soil. *Sci. Total Environ.* **2022**, 832, 155021. <https://doi.org/10.1016/j.scitotenv.2022.155021>.

(30) Jia, Y.; Hu, Z.; Ba, Y.; Qi, W. Application of Biochar-Coated Urea Controlled Loss of Fertilizer Nitrogen and Increased Nitrogen Use Efficiency. *Chem. Biol. Technol. Agric.* **2021**, 8 (1), 3. <https://doi.org/10.1186/s40538-020-00205-4>.

(31) Shi, W.; Ju, Y.; Bian, R.; Li, L.; Joseph, S.; Mitchell, D. R. G.; Munroe, P.; Taherymoosavi, S.; Pan, G. Biochar Bound Urea Boosts Plant Growth and Reduces Nitrogen Leaching. *Sci. Total Environ.* **2020**, 701, 134424. <https://doi.org/10.1016/j.scitotenv.2019.134424>.

(32) Schmidt, H.; Pandit, B.; Martinsen, V.; Cornelissen, G.; Conte, P.; Kammann, C. Fourfold Increase in Pumpkin Yield in Response to Low-Dosage Root Zone Application of Urine-Enhanced Biochar to a Fertile Tropical Soil. *Agriculture* **2015**, 5 (3), 723–741. <https://doi.org/10.3390/agriculture5030723>.

(33) Liu, X.; Liao, J.; Song, H.; Yang, Y.; Guan, C.; Zhang, Z. A Biochar-Based Route for Environmentally Friendly Controlled Release of Nitrogen: Urea-Loaded Biochar and Bentonite Composite. *Sci. Rep.* **2019**, 9 (1), 9548. <https://doi.org/10.1038/s41598-019-46065-3>.

(34) Efthymiou, A.; Grønlund, M.; Müller-Stöver, D. S.; Jakobsen, I. Augmentation of the Phosphorus Fertilizer Value of Biochar by Inoculation of Wheat with Selected Penicillium Strains. *Soil Biol. Biochem.* **2018**, 116, 139–147. <https://doi.org/10.1016/j.soilbio.2017.10.006>.

(35) Hammer, E. C.; Balogh-Brunstad, Z.; Jakobsen, I.; Olsson, P. A.; Stipp, S. L. S.; Rillig, M. C. A Mycorrhizal Fungus Grows on Biochar and Captures Phosphorus from Its Surfaces. *Soil Biol. Biochem.* **2014**, 77, 252–260. <https://doi.org/10.1016/j.soilbio.2014.06.012>.

(36) Hagemann, N.; Joseph, S.; Schmidt, H.-P.; Kammann, C. I.; Harter, J.; Borch, T.; Young, R. B.; Varga, K.; Taherymoosavi, S.; Elliott, K. W.; McKenna, A.; Albu, M.; Mayrhofer, C.; Obst, M.; Conte, P.; Dieguez-Alonso, A.; Orsetti, S.; Subdiaga, E.; Behrens, S.; Kappler, A. Organic Coating on Biochar Explains Its Nutrient Retention and Stimulation of Soil Fertility. *Nat. Commun.* **2017**, 8 (1), 1089. <https://doi.org/10.1038/s41467-017-01123->

0.

- (37) Haider, G.; Joseph, S.; Steffens, D.; Müller, C.; Taherymoosavi, S.; Mitchell, D.; Kammann, C. I. Mineral Nitrogen Captured in Field-Aged Biochar Is Plant-Available. *Sci. Rep.* **2020**, *10* (1), 13816. <https://doi.org/10.1038/s41598-020-70586-x>.
- (38) Sizmur, T.; Fresno, T.; Akgül, G.; Frost, H.; Moreno-Jiménez, E. Biochar Modification to Enhance Sorption of Inorganics from Water. *Bioresour. Technol.* **2017**, *246*, 34–47. <https://doi.org/10.1016/j.biortech.2017.07.082>.
- (39) Banik, C.; Lawrinenko, M.; Bakshi, S.; Laird, D. A. Impact of Pyrolysis Temperature and Feedstock on Surface Charge and Functional Group Chemistry of Biochars. *J. Environ. Qual.* **2018**, *47* (3), 452–461. <https://doi.org/10.2134/jeq2017.11.0432>.
- (40) Borchard, N.; Wolf, A.; Laabs, V.; Aeckersberg, R.; Scherer, H. W.; Moeller, A.; Amelung, W. Physical Activation of Biochar and Its Meaning for Soil Fertility and Nutrient Leaching - a Greenhouse Experiment: Physical Activation of Biochar. *Soil Use Manag.* **2012**, *28* (2), 177–184. <https://doi.org/10.1111/j.1475-2743.2012.00407.x>.
- (41) Bucheli et al. Polycyclic Aromatic Hydrocarbons and Polychlorinated Aromatic Compounds in Biochar. In *Biochar for Environmental Management*; Lehmann, J., Joseph, S., Eds.; Routledge, 2015; pp 627–656.
- (42) Hilber, I.; Blum, F.; Leifeld, J.; Schmidt, H.-P.; Bucheli, T. D. Quantitative Determination of PAHs in Biochar: A Prerequisite To Ensure Its Quality and Safe Application. *J. Agric. Food Chem.* **2012**, *60* (12), 3042–3050. <https://doi.org/10.1021/jf205278v>.
- (43) Buss, W.; Hilber, I.; Graham, M. C.; Mašek, O. Composition of PAHs in Biochar and Implications for Biochar Production. *ACS Sustain. Chem. Eng.* **2022**, *10* (20), 6755–6765. <https://doi.org/10.1021/acssuschemeng.2c00952>.
- (44) Kizito, S.; Luo, H.; Lu, J.; Bah, H.; Dong, R.; Wu, S. Role of Nutrient-Enriched Biochar as a Soil Amendment during Maize Growth: Exploring Practical Alternatives to Recycle Agricultural Residuals and to Reduce Chemical Fertilizer Demand. *Sustainability* **2019**, *11* (11), 3211. <https://doi.org/10.3390/su11113211>.
- (45) Luyima, D.; Egyir, M.; Yun, Y.-U.; Park, S.-J.; Oh, T.-K. Nutrient Dynamics in Sandy Soil and Leaf Lettuce Following the Application of Urea and Urea-Hydrogen Peroxide Impregnated Co-Pyrolyzed Animal Manure and Bone Meal. *Agronomy* **2021**, *11* (8), 1664. <https://doi.org/10.3390/agronomy11081664>.
- (46) Pandit, N. R.; Mulder, J.; Hale, S. E.; Schmidt, H. P.; Cornelissen, G. Biochar from “Kon Tiki” Flame Curtain and Other Kilns: Effects of Nutrient Enrichment and Kiln Type on Crop Yield and Soil Chemistry. *PLOS ONE* **2017**, *12* (4), e0176378. <https://doi.org/10.1371/journal.pone.0176378>.
- (47) Colombi, T.; Kirchgessner, N.; Le Marié, C. A.; York, L. M.; Lynch, J. P.; Hund, A. Next Generation Shovelomics: Set up a Tent and REST. *Plant Soil* **2015**, *388* (1–2), 1–20. <https://doi.org/10.1007/s11104-015-2379-7>.
- (48) Li, Y.; Cheng, J.; Lee, X.; Chen, Y.; Gao, W.; Pan, W.; Tang, Y. Effects of Biochar-Based Fertilizers on Nutrient Leaching in a Tobacco-Planting Soil. *Acta Geochim.* **2019**, *38* (1), 1–7. <https://doi.org/10.1007/s11631-018-0307-2>.
- (49) Liao, W.; Drake, J.; Thomas, S. C. Biochar Granulation, Particle Size, and Vegetation Effects on Leachate Water Quality from a Green Roof Substrate. *J. Environ. Manage.* **2022**, *318*, 115506. <https://doi.org/10.1016/j.jenvman.2022.115506>.
- (50) Cayuela, M. L.; Sánchez-Monedero, M. A.; Roig, A.; Hanley, K.; Enders, A.; Lehmann, J. Biochar and Denitrification in Soils: When, How Much and Why Does Biochar Reduce N₂O Emissions? *Sci. Rep.* **2013**, *3* (1), 1732. <https://doi.org/10.1038/srep01732>.
- (51) Kammann, C.; Ratering, S.; Eckhard, C.; Müller, C. Biochar and Hydrochar Effects on Greenhouse Gas (Carbon Dioxide, Nitrous Oxide, and Methane) Fluxes from Soils. *J. Environ. Qual.* **2012**, *41* (4), 1052–1066. <https://doi.org/10.2134/jeq2011.0132>.

- (52) Heaney, N.; Ukpong, E.; Lin, C. Low-Molecular-Weight Organic Acids Enable Biochar to Immobilize Nitrate. *Chemosphere* **2020**, *240*, 124872.
<https://doi.org/10.1016/j.chemosphere.2019.124872>.
- (53) Fidel, R. B.; Laird, D. A.; Spokas, K. A. Sorption of Ammonium and Nitrate to Biochars Is Electrostatic and pH-Dependent. *Sci. Rep.* **2018**, *8* (1), 17627.
<https://doi.org/10.1038/s41598-018-35534-w>.

Chapter 2a

Increasing biochar yield in pyrolysis by adding ash

Jannis Grafmüller^{1,2,3,4}, Michael Tobler⁵, Philipp Vögelin⁶, Thomas D. Bucheli³, Hans-Peter Schmidt¹, Nikolas Hagemann^{1,3}

¹: Ithaka Institut, Arbaz, Switzerland and Goldbach, Germany

²: Institute of Sustainable Energy Systems (INES), Offenburg University, Offenburg, Germany

³: Environmental Analytics, Agroscope, Zurich, Switzerland

⁴: Plant Biogeochemistry, Department of Geosciences, University of Tübingen, Tübingen, Germany

⁵: Holz & Forst Consulting GmbH, 4102 Binningen, Switzerland

⁶: Industrielle Werke Basel (IWB); Margarethenstrasse 40; 4002 Basel, Switzerland

Working paper

Chapter 2: Wood ash additives in biochar production and related formation of polychlorinated contaminants

Statement of personal and co-author contributions, plus non-listed contributors

Authors	Position of candidate in list of authors	Scientific ideas by the author [%]	Data generation by the author [%]	Analysis and interpretation by the author [%]	Paper writing done by the author [%]
Jannis Grafmüller	1	20	35	50	65
Michael Tobler	2	10	10	0	0 ^a
Philipp Vögelin	3	10	10	0	0 ^a
Thomas D. Bucheli	4	10	0	0	5
Hans-Peter Schmidt	5	10	0	0	5
Nikolas Hagemann	6	40	35	50	25
Contribution by other parties not listed as authors (e.g., commercial analysis laboratories, student assistants)					
Eurofins Umwelt Ost GmbH, Bobritzsch Hilbersdorf, Germany		0	9	0	0
QMinerals BVBA, Heverlee, Belgium		0	1	0	0
Publication status	unpublished				
Explanations	<p>The experiments in this chapter were conceptualized by Nikolas Hagemann with equal contributions from all other authors. Biochar production on experimental scale was carried out in equal proportions by Nikolas Hagemann and me. Severin Neukom supported with maintenance of the pyrolysis plant. The ash samples were sampled and provided by Michael Tobler. Philipp Vögelin, Michael Tobler, Nikolas Hagemann and me planned and conducted the pyrolysis experiments on industrial scale. Sara Cebulla and two technical employees of Industrielle Werke Basel, who are not known by name, supported the experiments on industrial scale. Biomass, ash and biochar characterization was performed by Eurofins Umwelt Ost GmbH (Bobritzsch-Hilbersdorf, Germany) and QMinerals BVBA (Heverlee, Belgium). Data analysis and interpretation was conducted by Nikolas Hagemann and me. I wrote the draft of the chapter and Nikolas Hagemann, Thomas D. Bucheli, and Hans-Peter Schmidt improved the quality of the manuscript. Main funding of the project was acquired by Michael Tobler, Nikolas Hagemann and Thomas D. Bucheli.</p>				

^a: Contribution set to 0, as the co-author did not yet review the manuscript.

Abstract

Wood ash additives increase biochar yield in pyrolysis via catalysis by alkali and alkaline earth metals. However, the extent to which this depends on ash and biomass properties is unknown. Here, we pyrolyzed pelleted and ash-amended woody and gramineous biomasses at 500-550 °C. At pilot-scale, 5% (w/w) amendment of different ashes increased dry and ash-free biochar yield (y_{daf}) by 13-37% and carbon yield (y_C) by 2-33% for woody feedstocks and decreased yields by 5-6% for grass or straw. Accordingly, mixing grass with softwood at increasing ratios reduced the effects of added ash. The yield increase depended on biomass type rather than on the intrinsic ash content of the biomass, as positive effects were observed even for woody feedstocks with relatively high ash content, unlike gramineous biomass. Yield increases observed for different added ashes did not correlate with ash properties, pending further investigation. Toxic hexavalent chromium from ash additives was not detected in biochar, suggesting its reduction to non-toxic Cr(III) during biochar production. At industrial scale, y_{daf} increased by 11% and y_C by 6% through adding 4% ash to landscaping-wood, demonstrating the scalability of wood ash use. Adding ash to woody feedstock increased biochar production, pyrolysis economy, and carbon sink potential.

1. Introduction

Biomass pyrolysis and non-oxidative use of biochar are the key elements of the carbon dioxide removal strategy called Pyrogenic Carbon Capture and Storage (PyCCS).¹ The removal of CO₂ from the atmosphere occurs during photosynthesis, so that the climate impact of this approach is determined in the long-term by both the availability of biomass and the yield of biochar from pyrolysis. Biomass is a limited resource due to the availability of land for cultivation, suitable climate, and the competition with food production and other sustainability goals.^{2,3} Therefore, optimizing biochar yields is essential to efficiently use the available biomass.

In pyrolysis of lignocellulosic biomass, alkali and alkaline earth metals (AAEM), most importantly calcium (Ca), magnesium (Mg), potassium (K), and sodium (Na) are known to catalyze the pyrolysis process, leading to higher yields of char and pyrolysis gas while reducing the yield of liquid products, both by affecting primary and secondary pyrolysis reaction pathways.⁴⁻⁶ Alkali and alkaline earth metals can be deliberately added to biomass prior to pyrolysis via different types of materials, including wood ash.^{4,7-10} Adding wood ash in biomass pyrolysis also adds the macronutrient K, as well as other nutrients, in a plant-available form to biochars, helping to close AAEM nutrient cycles.^{8,9,11} Using biomass ash in biochar production could synergistically link PyCCS with Bioenergy Carbon Capture and Storage (BECCS), which includes biomass combustion, resulting in nutrient-rich ashes to be disposed of.¹¹ However, knowledge is limited on how different ashes alter biochar yields and properties when blended with biomass feedstocks.

To evaluate the effect of ash additives on biomass pyrolysis, the mass yield (y_M) of biochar production is not expedient (see equation 2 in the Supporting Information- SI). Therefore, the dry and ash-free biochar yield (y_{daf}) and biochar carbon yield (y_C) of pyrolysis have been investigated.^{8,9} For y_{daf} , the biochar mass, minus its ash and water content, is related to the feedstock mass minus its ash and water content (see equation 3 in the SI). For the calculation of y_C , the mass of total carbon in the biochar is related to the total carbon present in the feedstock before pyrolysis (equation 4 in the SI).

For woody biomass, adding ash prior to the pyrolysis increased y_{daf} by up to 40-90% with ash amendments of up to 40-50%.^{8,9} However, ash was most effective when added at a concentration of 5-10% (w/w) to softwood. Yield increases per amount of added ash were lower for amendments higher than 20%.⁹ Further, adding ash to ash-rich biomass had no effect on y_{daf} for biogas residue and even decreased it for maize silage at a pyrolysis temperature of 500 °C.¹² These previous studies have each tested only one combination of biomass and ash. There has

been no systematic comparison of blending different biomasses or ashes. Yet, combining this limited existing data allows to conclude that the effect of an ash amendment on y_{daf} and y_C might vary with biomass and ash type, and can even have no or negative effects, when a biomass with, e.g., high absolute intrinsic ash content, such as straw, is pyrolyzed. The ash composition could further be of importance, since different AAEM may impact differently the catalyzing char formation in biomass pyrolysis.⁵

Besides AAEM, biomass ash contains potentially toxic elements (PTE),¹³ which may limit compliance with fertilizer regulations and thus its direct soil application. One of these PTE is chromium, in particular its hexavalent speciation (Cr(VI)),¹⁴ which is highly toxic and carcinogenic.¹⁵ Bottom ashes can be enriched in Cr(VI),¹³ due to the low volatility of Cr and the oxidative atmosphere in combustion systems. The reductive atmosphere in pyrolysis reactors is supposed to reduce Cr(VI) to less-toxic Cr(III), which has not been explored systematically yet.

On pilot-plant scale, we first varied the biomass composition by mixing low-ash softwood with ash-rich grass to study the effect of an ash amendment on y_{daf} and y_C in dependence on biomass properties. In addition, four further biomasses were used to test a broader range of properties. Secondly, we tested four different wood ashes and one gasifier coke with a high ash content to link their individual AAEM contents, solubility, and speciation with their effects on softwood-biochar production. Detailed analyses of the ashes can be found in section 2.1 in the SI. Thirdly, we tested whether Cr(VI) originating from an ash additive remains inert or is reduced during pyrolysis. Fourthly, we applied wood ash in biomass pyrolysis at an industrial scale (300 kg biomass input per hour) to quantify effects on y_{daf} and y_C . With this study, we aim to gain more knowledge on the mechanisms and overall potential of ash-induced increases in y_{daf} and y_C of pyrolysis products and intend to provide practical recommendations for the biochar industry.

2. Materials and Methods

2.1. Sampling of ash additives

Five different ashes from wood-fired power plants in Switzerland were sampled by the plant operators and labeled according to their origin: Sissach, Brislach, Möhlin, Gruyère, and Zeglingen. The Zeglingen sample was an ash-rich gasifier coke from a combined heat and power unit, while all other samples were bottom ashes from burning chambers. All systems processed untreated Swiss forest wood. The ash from Gruyère was used both for pyrolysis at the pilot-plant and at industrial scale, obtained from two different sampling dates, which were

Chapter 2: Wood ash additives in biochar production and related formation of polychlorinated contaminants

approximately two months apart. The Gruyère sample used for pyrolysis at industrial scale is referred to as “Gruyère_large”. The ashes were sieved to a particle size of < 2 mm to separate stones, residual char pieces in the gasifier coke, and other artefacts (Table S1 in Supporting Information - SI).

2.2. Biomass selection and pelletization for pyrolysis on pilot-plant scale

The following six biomasses were used as feedstock for biochar production (elemental composition displayed in Table S6): commercial softwood bedding (GermanHorse, AllSpan, Karlsruhe Germany), mixed Swiss forest wood, grass (long grass from an urban area managed with single-cut mowing), wheat straw, conifer bark mulch (both from Landi Schweiz AG, Dotzingen, Switzerland), and waste timber category A2/A3 (Lindum AS, Norway, cf. Sørmo *et al.*¹⁶).

In pilot-plant pre-experiments, pelleting biomass with ash consistently resulted in increases of y_{daf} and y_C compared to loose mixing (Figure S7). Therefore, forest wood, grass, wheat straw, and waste timber were first milled with a hammer mill to < 12 mm (HM420B, EverTec, Groß-Zimmern, Germany). Softwood bedding and bark were obtained ready for pelletization. Pellets with a diameter of 6 mm were produced using a pellet press (WK230, EverTec, Groß-Zimmern, Germany) after homogenization of the respective biomass with the ash additive and water to achieve a water content of 25% (w/w). Obtained pellets were dried to 5-15% (w/w) residual water content at 40 °C for 12 hours, sieved to > 6 mm, and stored at room temperature prior to pyrolysis (~7 days storage time). In total, 22 sets of pellets from different feedstock blends were prepared (Table S2).

2.3. Pyrolysis at pilot-plant scale

Pyrolysis experiments on pilot-plant scale were sequentially performed on a PYREKA research pyrolysis unit (Pyreg GmbH, Dörth, Germany), a continuously operated, electrically heated auger reactor.¹⁷ The reactor was purged with 2 l min⁻¹ N₂ that passed the reactor (8 cm diameter) concurrently with solids. The biomass was fed continuously via a rotary valve, and the biochar was collected in a water-cooled container that was emptied intermittently. Pyrolysis was performed at the highest treatment temperature (HTT) of 500 °C with a feedstock residence time (RT) of 10 minutes in the reactor. After a stabilization time of five RT, during which the product was discarded, biochar was sampled without replicates for a total of three RT.

2.4. Pyrolysis at industrial scale

Industrial-scaled experiments were carried out on a PX1500 (Pyreg GmbH, Dörth, Germany) operated by Industrielle Werke Basel (IWB, Basel-Kleinhüningen, Switzerland).¹⁸ The reactor had a biomass throughput of 300 kg h⁻¹ or 2,200 t year⁻¹ (dry matter). This pyrolysis plant consists of two horizontally mounted double screw reactors that are supplied with biomass from a storage tank via rotary feeders. The reactors are double-walled and heated indirectly by hot exhaust gases from pyrolysis gas combustion (Figure S1). The pyrolysis was conducted with a RT of 20 minutes and a HTT of 550 °C. The pyrolysis reactors were continuously fed with pre-dried landscaping wood (elemental composition: Table S6). The storage container was filled with biomass from the bunker at 15-minute intervals via a conveyor belt, which took a minute each time. The biomass input over time to the reactors was determined by recording the load cell of the storage tank over time and was obtained as an averaged value over the whole experimental runtime (Figure S2). The wood ash (sample Gruyère_large) was scattered into the biomass stream each time the storage tank was automatically filled (5 kg of ash per fill with 90-100 kg dry biomass, Figure S3), which resulted in 4% (w/w) ash amendment. After an initial process stabilization time of four RTs (4 x 20 minutes), biochar samples were taken. For each sample, biochar was sequentially filled for 6 minutes in a separate 15 kg bag, which was weighed to 0.1 kg accuracy to determine biochar mass flow. This process was performed nine times for both the control biochar (no ash amendment) and the ash-amended biochar. From these nine subsamples, three times three samples were combined to form a total of three subsamples. These three combined samples were then representatively sampled,¹⁹ so that three representative biochar samples per treatment were analyzed.

2.5. Biomass, ash and biochar analysis

Ash, biomass, and biochar analysis was conducted by Eurofins Umwelt Ost GmbH (Bobritzsch-Hilbersdorf, Germany). Basic ash, biomass, and biochar analyses were conducted following international guidelines as detailed in Table S3 in the SI. Soluble AAEM contents in the ashes were quantified following DIN EN ISO 17294-2²⁰ in aqueous eluates prepared by shaking horizontally at 150 rpm for 1 hour at a solid:liquid ratio of 1:10. Quantitative X-ray diffraction analysis (XRD) of the ashes was performed by QMineral (Heverlee, Belgium).

2.6. Data analysis

Biochar yields (y_M , y_{daf} , and y_C) and increase in nitrogen yield (Δy_N) of pyrolysis were calculated according to literature⁹ as detailed in equations 2-4 in the SI. Deviations of biochar yields at pilot-plant scale were calculated based on the variation of biomass mass flow through the non-heated reactor according to the error propagation law (equations 6-14 in the SI). For industrial experiments, nine individual values for y_M , y_{daf} and y_C per treatment were calculated and statistically evaluated with GraphPad Prism v9.4.1 (one-way ANOVA and the Šídák multiple comparison test, $\alpha < 0.05$). Significance tests were not applied to yield data from experiments on pilot-plant scale, since biochar sampling was performed with single replicates and, therefore, the biomass mass flow was the only variable contributing to deviations, which was deemed insufficient to perform further statistical analysis. The H/C_{org} molar ratios from biochars produced at pilot-plant scale, with or without an ash amendment, were compared by an unpaired t-test ($\alpha < 0.05$). The observed increases of y_{daf} and y_C due to ash amendment to varying biomasses were modeled in JMP 18 (SAS Institute, Cary, North Carolina, USA), applying a multivariate regression analysis using the intrinsic lignin, cellulose, hemicellulose, and ash contents of the biomasses as variables. Variables identified as non-significant with JMP ($p > 0.05$) were excluded from the model. Linear regression analysis of y_{daf} , y_C , or Δy_N with ash properties was performed by calculating Pearson correlation coefficients (r) with GraphPad Prism.

3. Results and Discussion

3.1. Impact of ash addition on biochar production at pilot-plant scale

3.1.1. Effect of ash amendment on biochar yield of different biomasses

Amending softwood with 5% Sissach ash increased y_{daf} and y_C by 13% and 9%, respectively (Figure 1a and Table 1). This was also achieved when the ash was added to a mixture containing 25% grass and 75% softwood (Figure 1a). The more grass was added to the softwood, the lower the increase in yields due to the ash amendment. At a grass content of 75%, no substantial yield changes occurred anymore (Figure 1a). For pure grass, the ash amendment reduced y_{daf} and y_C by 5% and 6%, respectively, compared to the non-amended grass feedstock (Figure 1a). A similar yield-reducing effect was observed when ash was added to straw feedstock (Figure 1b). Effects on forest wood and bark were comparable to those of softwood, while the ash blending of waste timber at 5% of Sissach ash decreased y_{daf} and y_C by 6% and 8%, respectively (Figure 1b). Waste timber was, thus, the only woody feedstock for which a decline in y_{daf} and y_C occurred upon the ash-amendment. The observed decrease with waste timber feedstock is inconclusive based on our other experiments and literature using woody feedstock^{8,9}, and requires further verification. Waste timber contains plastics and other polymers, which might not fully degrade by pyrolysis at 500 °C.²¹ Alkali earth metals are well-known catalysts in pyrolytic plastic recycling as these metals catalyze fragmentation reactions.²² Thus, AAEM might have supported the complete volatilization of synthetic polymers already at 500 °C and thus reduced char yields from waste timber in our experimental setup.²²

The bark had an intrinsic ash content of 6.7% (Table S6), which was similar to grass and straw but considerably higher compared to softwood and forest wood (<1%). Therefore, the comparable high increases in y_{daf} and y_C observed for ash-amended bark (Figure 1b) were not expected. It indicates that the extent of yield increases upon addition of ash is not solely affected by the intrinsic ash content of a biomass but most likely also by the general biomass composition. The observed increases in y_{daf} and y_C can be well modeled by applying a multivariate regression using the intrinsic contents of lignin, cellulose, hemicellulose, and ash in the biomasses as input variables (Figure S6). Only the cellulose and hemicellulose contents had a significant impact ($p < 0.05$) in this model, the other variables were therefore withdrawn. However, due to the small number of data pairs (eight pairs, waste timber was excluded due to the abovementioned reasons), it is not yet possible to reliably determine which biomass components can best be used to approximate the potential effects of added ash on y_{daf} and y_C . According to this model, biomasses with high cellulose combined with low hemicellulose

Chapter 2: Wood ash additives in biochar production and related formation of polychlorinated contaminants

contents will respond most positively to an ash amendment, at least for Sissach ash. The results must be further validated with more biomass feedstocks, but also with pure lignin, cellulose, and e.g. xylan (representative for hemicellulose) amended with ash, to gain a more mechanistic understanding.

A key knowledge gap is understanding why increases in y_{daf} and y_C became negative when ash-rich straw and grass samples were amended with additional ash, rather than remaining constant. It could be due to higher biochar reactivity in the pyrolysis reactor and gasification reactions catalyzed by AAEM, particularly by K, when interacting with gasification agents like CO₂ during pyrolysis.²³⁻²⁵

Chapter 2: Wood ash additives in biochar production and related formation of polychlorinated contaminants

Table 1(continued on next page): Biochar properties: elemental analysis (organic and total carbon (C_{org} and C , respectively), hydrogen (H), nitrogen (N), sulfur (S)), ash content, and molar H/C_{org} ratio. Mass yield of biochar (y_M), dry and ash-free biochar yield (y_{daf}) and carbon yield of pyrolysis (y_C). The different biomasses were amended with the specified amounts (in %, w/w) of the following ashes, when indicated: Sissach, Zeglingen, Möhlin, Gruyère, Gruyere_large, and Brislach. Biochars were pyrolyzed at 500 °C with 10 minutes residence time at pilot-plant scale. Biochars produced from landscaping wood were pyrolyzed on an industrial plant at an estimated 550 °C with 20 minutes residence time. Errors were calculated according to the error propagation law, unless otherwise specified.

Biochar	C [%]	C_{org} [%]	H [%]	N [%]	Ash [%]	H/C_{org}	y_M [%]	y_{daf} [%]	y_C [%]
Softwood	87	87	2.8	0.2	2.0	0.38	22 ± 1	21 ± 1	38 ± 1
Softwood/Grass (75:25)	79	79	2.8	0.6	8.2	0.42	26 ± 1	24 ± 1	42 ± 2
Softwood/Grass (50:50)	75	75	2.6	0.8	14	0.41	27 ± 1	24 ± 0	42 ± 1
Softwood/Grass (25:75)	72	72	2.0	1.0	19	0.33	29 ± 0	25 ± 0	43 ± 1
Grass	66	66	2.2	1.3	23	0.40	30 ± 1	26 ± 1	43 ± 1
Softwood + 5% Sissach	72	72	2.6	0.1	16	0.43	27 ± 1	24 ± 1	41 ± 1
Softwood/Grass (75:25) + 5% Sissach	68	68	2.4	0.4	21	0.42	32 ± 0	27 ± 0	48 ± 1
Softwood/Grass (50:50) + 5% Sissach	57	56	2.0	0.6	25	0.42	33 ± 1	27 ± 0	41 ± 1
Softwood/Grass (25:75) + 5% Sissach	59	59	2.1	0.9	29	0.43	33 ± 0	26 ± 0	43 ± 0
Grass + 5% Sissach	56	55	2.0	1.0	33	0.43	32 ± 1	24 ± 1	40 ± 1
Straw	71	69	2.3	0.8	18	0.40	29 ± 0	26 ± 0	46 ± 1
Forest Wood	83	83	2.8	0.3	5.0	0.40	21 ± 0	20 ± 0	35 ± 1
Bark	76	75	2.8	0.9	11	0.44	32 ± 1	31 ± 1	50 ± 1
Waste timber	84	83	3.1	1.7	4.0	0.45	24 ± 1	23 ± 1	41 ± 1
Straw + 5% Sissach	62	61	2.0	0.7	27	0.39	30 ± 1	24 ± 1	43 ± 1
Forest Wood + 5% Sissach	73	72	2.6	0.2	16	0.43	27 ± 0	24 ± 0	41 ± 1
Bark + 5% Sissach	69	68	2.5	0.7	19	0.44	40 ± 0	37 ± 0	59 ± 0
Waste timber + 5% Sissach	70	70	2.7	1.2	18	0.46	25 ± 0	19 ± 0	37 ± 1
Softwood + 5% Zeglingen	79	78	2.8	0.2	10	0.43	31 ± 0	29 ± 0	50 ± 1
Softwood + 5% Möhlin	73	72	2.7	0.3	15	0.45	30 ± 1	27 ± 1	45 ± 1

Chapter 2: Wood ash additives in biochar production and related formation of polychlorinated contaminants

Biochar	C [%]	C_{org} [%]	H [%]	N [%]	Ash [%]	H/C_{org}	y_M [%]	y_{daf} [%]	y_C [%]
Softwood + 5% Gruyère	71	70	2.9	0.2	16	0.49	31 ± 1	28 ± 1	46 ± 2
Softwood + 5% Brislach	70	69	2.7	0.2	15.1	0.47	27 ± 1	24 ± 0	38 ± 1
Softwood + 10% Brislach	62	60	2.1	0.3	23.5	0.42	32 ± 1	27 ± 1	42 ± 1
Softwood + 20% Brislach	49	45	1.6	0.2	34.6	0.42	47 ± 1	38 ± 1	53 ± 1
Landscaping Wood ^a	72 ± 1	71 ± 1	2.5 ± 0.1	0.8 ± 0.1	14.2 ± 0.1	0.43 ± 0.03	37 ± 1	33 ± 2	53 ± 2
Landscaping Wood + 4% Gruyère large ^a	59 ± 1	58 ± 1	2.2 ± 0.1	1.0 ± 0.1	26.9 ± 0.4	0.46 ± 0.02	48 ± 2	36 ± 2	57 ± 2

^aFor biochars produced from Landscaping Wood, errors indicate the standard deviation of three replicates for elemental analysis and of nine replicates for y_M, y_{daf} and y_C.

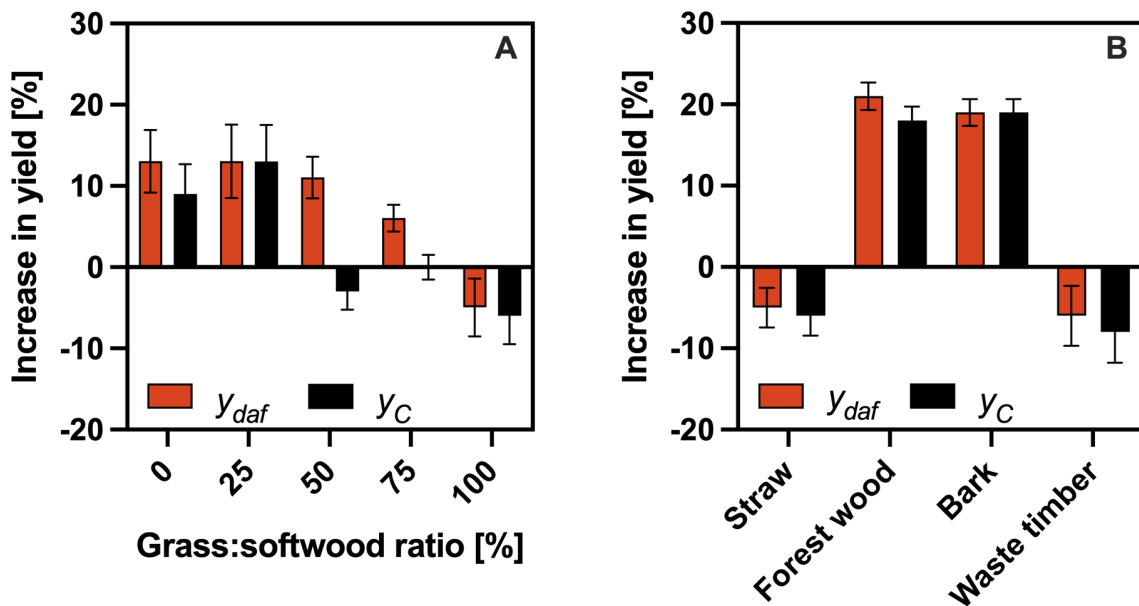


Figure 1: (A) Increases in yield of dry and ash-free biochar (y_{daf}) and in carbon yield (y_C) of biochar production due to addition of 5% (w/w) Sissach ash to different mixtures of grass and softwood at the indicated mass ratios. (B) Increases in y_{daf} and y_C due to addition of 5% (w/w) Sissach ash to different biomasses. All biochars were produced at 500°C with 10 minutes residence time in the pilot-scale pyrolysis reactor. Error bars were calculated according to the error propagation law based on the variation of the biomass transport in the pyrolysis unit.

3.1.2. Effect of different ashes amended to softwood on biochar yield

For all the five ashes amended to softwood at 5% (w/w), y_{daf} and y_C increased in the range of 11-37% and 2-33%, respectively, compared to non-amended softwood (Figure 2). Using the Brislach ash at a rate of 5% led to the lowest yield increases, while the highest increases were obtained with the Zeglingen gasifier coke. With the Gruyère and Möhlin ash, yield increases were in a similar range as with the Zeglingen ash. In particular, the high yield increases obtained with the Zeglingen gasifier coke ash are promising, as gasifier coke can contain relevant amounts of polycyclic aromatic hydrocarbons and is mostly not allowed for direct soil application unless properly treated beforehand, e.g. by co-pyrolysis.²⁶ Interestingly, yield increases observed with the different ashes were not significantly correlated with individual AAEM contents or their sum in the ash additives (Table S7).

Wet impregnation of biomass with AAEM additives is generally more effective in enhancing biochar yield than dry mixing.⁵ In our study, moistening the dry mixture of biomass and ash to a water content of 25% before pelleting may have partially solubilized AAEM, improving their

Chapter 2: Wood ash additives in biochar production and related formation of polychlorinated contaminants

catalytic activity. However, y_{daf} and y_C were not significantly correlated to the absolute soluble amount of AAEM from the ashes (Table S7), despite the highest absolute soluble content of AAEM in the Zeglingen and the lowest content for the Sissach samples (Table S5), in line with their contrasting effects on y_{daf} and y_C .

Melting of AAEM-containing minerals was shown to increase biochar yields by trapping pyrolysis gases inside the solid particles, which leads to higher transformation rates of biomass to biochar.²⁷ However, this was probably irrelevant in our study, as wood ashes have melting points well above the pyrolysis temperature of 500 °C used in the present study (1000 °C).^{28,29} Lastly, the speciation of AAEM in the ash might be decisive for its catalytic activity, which was investigated with XRD analyses (Figure S4 and chapter 2.1 in the SI). The Sissach sample had the highest absolute content and relative share of AAEM in the form of Dicalcium-silicate (Figure S4), where Ca is allocated within the crystalline structure, leading to an assumed low interaction with the surrounding solid and gas phase during pyrolysis, which could explain the low effect observed for this ash. The Zeglingen sample, in contrast, had not any AAEM bound in silicates but the highest absolute and relative contribution of AAEM bound in carbonates, especially CaCO_3 , where Ca is assumed to be better accessible for interaction. Still, correlations of y_{daf} and y_C with AAEM speciation, either as carbonates, phosphates, sulphates, oxides, hydroxides, or silicates in the ashes did not lead to any significant correlation (Table S7). To establish a more mechanistic understanding of this and to identify causalities instead of correlations only, we recommend performing pyrolysis experiments using pure minerals as additives to predict the catalytic activity of complex mineral mixtures, such as wood ash, in biomass pyrolysis. So far, the effect of a specific ash on biochar yields can be estimated at best, if at all, by means of a solubility analysis, as seen for the Zeglingen sample.

The increase in y_{daf} and y_C was also dependent on the amount of ash added. Amending the Brislach ash at a rate of 10% to the softwood increased y_{daf} and y_C by 26% and 15%, respectively, while at an amendment rate of 20%, increases of 78% and 50%, respectively, were achieved (Figure 2). This dosage dependent increase in y_{daf} and y_C is in line with literature.^{8,9}

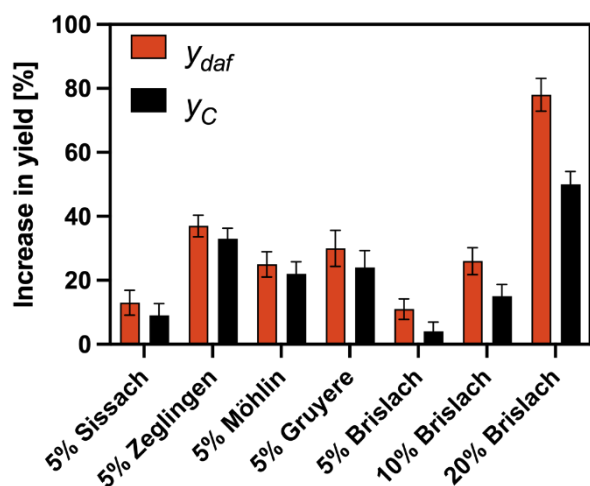


Figure 2: Increases in yield of dry and ash-free biochar (y_{daf}) and in carbon yield (y_C) of biochar production due to the addition of different wood ashes to softwood at the indicated ratios (w/w). All biochars were produced at 500°C with a 10-minute residence time in the pilot-scale pyrolysis reactor. Error bars were calculated according to the error propagation law based on the variation of the biomass transport in the pyrolysis unit.

3.1.3. H/C_{org} ratio and increase in N yield of biochars

The H/C_{org} molar ratio of biochars produced at pilot-plant scale was not significantly changed by an ash amendment where a decline in y_{daf} was observed. When y_{daf} increased upon ash amendment, H/C_{org} molar ratios were significantly higher for ash-amended biochars compared to non-amended biochars (Figure 3A). This indicates a lower share of C_{org} was speciated as aromatic carbon in these biochars produced with ash amendments and/or that the degree of condensation and with that the average size of aromatic clusters was reduced.³⁰ Still, this needs to be interpreted with caution since H/C_{org} molar ratios are only a proxy and not a direct measure for biochar aromaticity.³⁰ The increase in H/C_{org} molar ratios of ash-amended biochars is not in line with a previous study.⁹ Still, irrespective of the ash amendment, all biochars had H/C_{org} molar ratios well below the EBC limit of 0.7.³¹

Nitrogen yield of biochar production tended to decrease under the amendment of Sissach ash at a rate of 5% (w/w) to all tested biomasses (Figure 3B). All other ashes, when added to softwood, increased y_N by 22-120% compared to pyrolysis of non-amended softwood. An increase in y_N is linked to a lower amount of N being released to the gas phase, which could reduce the risk of NO_x formation during pyrogas combustion, a gas that is strictly regulated under national emission control.³² An AAEM-induced fixation of N in the biochar, inhibiting the formation of NO_x precursors such as NH₃ and HCN during pyrolysis, was observed in

previous studies.^{33,34} Despite this, the differences in effects on y_N through the Sissach ash compared to all other ashes were not correlated to the ash properties, such as AAEM content, investigated in the present study (Table S7).

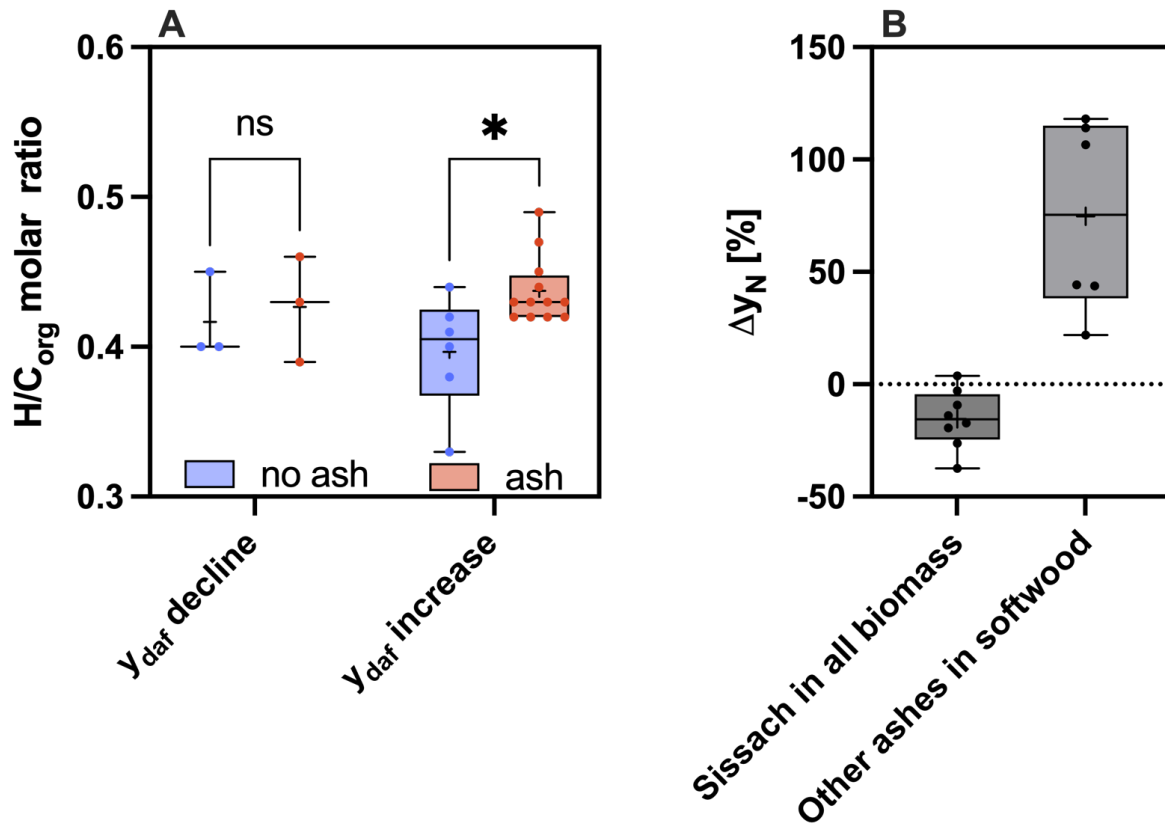


Figure 3: (A) Hydrogen to organic carbon molar ratio (H/C_{org}) of all biochars produced on pilot-plant scale without or with an ash amendment to feedstocks separated into two groups: biomasses for which a decline or an increase in dry and ash-free biochar yield (y_{daf}) due to ash amendment was observed. (B) Increase in nitrogen yield (Δy_N) due to amendment of 5% (w/w) Sissach ash to all tested biomasses and due to amendment of other ash samples at 5-20% (w/w) to softwood. All biochars were produced at 500°C with 10 minutes residence time in the pilot-scale pyrolysis reactor. Error bars indicate the range of minimum to maximum observation, the "+" in boxplots indicate the mean values, and asterisks above error bars indicate a significant difference between treatments in panel A ($p < 0.05$, unpaired t -test, ns: not significant).

3.1.4. Reduction of Cr(VI) during pyrolysis

Due to elevated Cr(VI) contents, four out of the six ash/coke samples would not have been allowed for soil application in Europe³⁵⁻³⁷ (Table S4 and chapter 2.1 in the SI). However, none of the biochars produced from softwood amended with 0%, 10% or 20% of the highly Cr(VI)-contaminated Brislach ash contained Cr(VI) above the quantification limit of 0.1 mg kg⁻¹. If Cr(VI) were inert during feedstock preparation and biochar production, biochar would contain 6 to 8 mg Cr(VI) kg⁻¹, with a 10% and 20% ash amendment, respectively, which is well above the quantification limit. Recovery rates of total Cr in ash-amended biochars were 93% and 152%, for 10% and 20% ash amendment, respectively; i.e., Cr volatilization during pyrolysis at 500 °C can be excluded. Recovery rates >100% can be explained by abrasion from the steel reactor, which does not interfere with Cr(VI) quantification. If elevated Cr(VI) contents prevented the use of ash as fertilizer, the AAEM-nutrients it contains, in particular K, would be lost when disposed as waste. Pyrolysis that eliminates Cr(VI) could enable AAEM-nutrient recycling, as such treated ashes could be applied to soil embedded in biochar.

The mechanism of Cr(VI) reduction during biochar production could not be clearly elucidated, but several hypotheses can be formulated. Firstly, Cr(VI) might be reduced to Cr(III) due to the reductive conditions in the pyrolysis reactor, i.e., the oxygen contained in chromate or dichromate (CrO_4^{2-} and $\text{Cr}_2\text{O}_7^{2-}$) is released during pyrolysis and used up as an oxidizing agent. Secondly, the contact of Cr(VI) with the lignocellulose matrix during pelleting might reduce it to Cr(III), as described for the “fixation process” when wood is impregnated with the Cr(VI)-containing preservative chromium-copper-arsenate (CCA).³⁸ Thirdly, the moistening of the wood and ash mixture prior to pelleting to a water content of 25% might lead to Cr(VI) reduction, as is observed after moistening and storage of wood ash for several weeks, where water limits oxygen transport within the solid particles, leading to reduction to Cr(III).^{13,14,39} The relevance of these potential mechanisms would need further investigation.

3.2. Impact of ash amendment on biochar production at industrial scale

3.2.1. Biochar yield

During pyrolysis at industrial scale, amending landscaping wood with 4% Gruyère_large ash increased y_M by 30% ($p < 0.001$), y_{daf} by 11% ($p < 0.0021$), and y_C by 7% ($p < 0.0021$) compared to the non-amended feedstock (Table 1). This demonstrates the potential of using ash as an additive for woody feedstocks in industrial biochar production, even when only adding loose ash intermittently to the wood in the biomass feed container, without moistening, pelleting, or

extensive homogenization. The increase in y_{daf} observed at industrial scale was at the lower end of the range seen in experimental-scale trials (13%–38%, Figure 2), likely due to the lower ash dosage (4% vs. 5%), a relatively high intrinsic ash content in the landscaping wood (11%), and the absence of feedstock pelleting. Simply adding ash to wood in the biomass feed container without pelleting is a more practical and cost-effective approach for operators.

Converted to the annual production of this specific pyrolysis plant (2200 t a⁻¹ biomass throughput with a carbon content of 50%, dry matter), the yearly produced amount of biochar could increase from 810 t to 1050 t (based on observed y_M , Table 1) and the C-sink potential increases from 2154 t CO₂ equivalents (CO_{2e}) to 2293 t CO_{2e} (based on observed y_C and a conversion factor of 3.67 CO_{2e} per amount of C). With a market value of € 800 t⁻¹ of biochar and €100-250 t⁻¹ of sequestered CO_{2e}⁴⁰, this corresponds to an increase in revenue of € 194'000 due to a higher amount of physical biochar and € 13'900-34'750 for additional C-sink certificates. Thus, with little effort for plant operators, cycles of AAEM-nutrients can be closed, additional C is sequestered, and pyrolysis plants become more economic. However, the effect of ash addition on biochar degradation when applied to soil has not been investigated yet. The increased H/C_{org} ratio may indicate increased degradation.⁴¹

3.2.2. Biochar properties

The ash-amended biochar produced had a similar H/C_{org} molar ratio as the non-amended biochar (Table 1), in contrast to the increase observed at pilot-plant scale. The ash amendment increased y_N in biochar by 65%, similar to the observation on pilot-plant scale with the Gruyère ash sample (44% increase in y_N at pilot scale), thus, lower amounts of N were released to the gas phase under ash amendment.

The PTE content of biochars increased compared to the non-amended biochar (Table S8), as was expected due to their non-volatile character during pyrolysis.⁴² Still, the ash-amended biochar met the limit values for the EBC AgroOrganic³¹ certification for contents of PTE (Table S8). The sum of the 16 polycyclic aromatic hydrocarbons prioritized by the Environmental Protection Agency (16 EPA PAH) remained largely unchanged by the ash amendment and remained within the EBC guideline (Table S10), in line with the literature.⁹ Also, it is well established that contamination of biochars obtained from slow-pyrolysis with organic compounds is a matter of process control, i.e., separation of pyrolysis gases and biochar at sufficiently high temperature to avoid contaminant condensation onto biochar.^{43–45}

3.3. Legislative status quo for use of wood ash as an additive in European biochar production

The application of wood ash as additive in biomass pyrolysis is permitted according to the EBC to date³¹, as long as the limit values of the resulting biochar are met, which are related to soil protection and fertilizer guidelines e.g., in Germany, Switzerland and the EU.⁴⁶⁻⁴⁸ According to Regulation 2019/1009³⁶ of the European Union (EU, Fertiliser Product Regulation) under component material category (CMC) 14, the use of additives of up to 25% (w/w) to feedstock materials are permitted in pyrolysis, provided that they “improve the process performance or the environmental performance of the pyrolysis or gasification process”. Such additives, however, are not allowed, if they are considered wastes according to Directive 2008/98EC (Article 3, point 1).⁴⁹ In this context, ashes are often considered waste, as they are a byproduct of wood combustion, where the primary product is heat, and the ash is usually discarded. Therefore, the legal basis for the use of ash in biochar production for soil application still requires careful examination on a case-by-case basis, whereas the application of AAEM salts⁷ is straightforward. Also, we are not aware of any comparable restrictions on the use of ash-amended biochar in (construction) materials, although it does not contribute to nutrient recycling.

4. Conclusion

Ash amendment in biochar production is a useful tool for increasing the conversion rate of biomass-C into biochar-C, as demonstrated in the present study for various ash and biomass types, both at a pilot-plant and industrial scale. While we could not provide mechanistic insights beyond the literature, ash amendment consistently increased y_{daf} and y_C for natural woody feedstocks, with the positive effect being independent of their intrinsic ash content (tested with up to 11% intrinsic ash content in landscaping wood). In contrast, we found no evidence that ash addition can enhance yields in gramineous biomass. More research is needed to understand the mechanisms by which different ashes influence pyrolysis. For the time being, AAEM solubility may serve as a proxy for the effectiveness of ash as an additive in biochar production. Ash amendment on industrial pyrolysis plants can be implemented directly without pelletizing biomass and ash, which would enhance the carbon sequestration potential of industrial biochar production and enable ash-derived nutrient recycling. Furthermore, pyrolysis should be discussed and researched as a viable tool for treating Cr(VI)-contaminated biomass streams. Yet, when dealing with Cr(VI)-contaminated ashes as pyrolysis additives, workplace safety has

Chapter 2: Wood ash additives in biochar production and related formation of polychlorinated contaminants

to be assured by using skin and respiratory protection and ash dosage must be carried out in such a way that no ash dust is released to the environment.

Beyond PyCCS, BECCS also stands out as a crucial negative emissions technology, often relying on wood combustion. Our industrial-scale demonstrations now clearly show that these two technologies can be effectively integrated through the strategic use of ash in pyrolysis. This approach proves beneficial even with biomasses already high in ash, like bark or landscaping wood, which are only partially suitable for combustion. To facilitate the broader adoption of this combined strategy, the EU must integrate regulations to simplify the use of ash additives in biochar production.

References:

- (1) Schmidt, H.-P.; Anca-Couce, A.; Hagemann, N.; Werner, C.; Gerten, D.; Lucht, W.; Kammann, C. Pyrogenic Carbon Capture and Storage. *GCB Bioenergy* **2019**, *11* (4), 573–591. <https://doi.org/10.1111/gcbb.12553>.
- (2) Braun, J.; Werner, C.; Gerten, D.; Stenzel, F.; Schaphoff, S.; Lucht, W. Multiple Planetary Boundaries Preclude Biomass Crops for Carbon Capture and Storage Outside of Agricultural Areas. *Commun. Earth Environ.* **2025**, *6* (1), 102. <https://doi.org/10.1038/s43247-025-02033-6>.
- (3) Werner, C.; Lucht, W.; Gerten, D.; Kammann, C. Potential of Land-Neutral Negative Emissions Through Biochar Sequestration. *Earths Future* **2022**, *10* (7), e2021EF002583. <https://doi.org/10.1029/2021EF002583>.
- (4) Anca-Couce, A. Reaction Mechanisms and Multi-Scale Modelling of Lignocellulosic Biomass Pyrolysis. *Prog. Energy Combust. Sci.* **2016**, *53*, 41–79. <https://doi.org/10.1016/j.peccs.2015.10.002>.
- (5) Giudicianni, P.; Gargiulo, V.; Grottola, C. M.; Alfè, M.; Ferreira, A. I.; Mendes, M. A. A.; Fagnano, M.; Ragucci, R. Inherent Metal Elements in Biomass Pyrolysis: A Review. *Energy Fuels* **2021**, *35* (7), 5407–5478. <https://doi.org/10.1021/acs.energyfuels.0c04046>.
- (6) Di Blasi, C.; Galgano, A.; Branca, C. Influences of the Chemical State of Alkaline Compounds and the Nature of Alkali Metal on Wood Pyrolysis. *Ind. Eng. Chem. Res.* **2009**, *48* (7), 3359–3369. <https://doi.org/10.1021/ie801468y>.
- (7) Mašek, O.; Buss, W.; Brownsort, P.; Rovere, M.; Tagliaferro, A.; Zhao, L.; Cao, X.; Xu, G. Potassium Doping Increases Biochar Carbon Sequestration Potential by 45%, Facilitating Decoupling of Carbon Sequestration from Soil Improvement. *Sci. Rep.* **2019**, *9* (1), 5514. <https://doi.org/10.1038/s41598-019-41953-0>.
- (8) Buss, W.; Jansson, S.; Mašek, O. Unexplored Potential of Novel Biochar-Ash Composites for Use as Organo-Mineral Fertilizers. *J. Clean. Prod.* **2019**, *208*, 960–967. <https://doi.org/10.1016/j.jclepro.2018.10.189>.
- (9) Grafmüller, J.; Böhm, A.; Zhuang, Y.; Spahr, S.; Müller, P.; Otto, T. N.; Bucheli, T. D.; Leifeld, J.; Giger, R.; Tobler, M.; Schmidt, H.-P.; Dahmen, N.; Hagemann, N. Wood Ash as an Additive in Biomass Pyrolysis: Effects on Biochar Yield, Properties, and Agricultural Performance. *ACS Sustain. Chem. Eng.* **2022**, *10* (8), 2720–2729. <https://doi.org/10.1021/acssuschemeng.1c07694>.
- (10) Buss, W.; Wurzer, C.; Manning, D. A. C.; Rohling, E. J.; Borevitz, J.; Mašek, O. Mineral-Enriched Biochar Delivers Enhanced Nutrient Recovery and Carbon Dioxide Removal. *Commun. Earth Environ.* **2022**, *3* (1), 67. <https://doi.org/10.1038/s43247-022-00394-w>.
- (11) Buss, W.; Jansson, S.; Wurzer, C.; Mašek, O. Synergies between BECCS and Biochar—Maximizing Carbon Sequestration Potential by Recycling Wood Ash. *ACS Sustain. Chem. Eng.* **2019**, *7* (4), 4204–4209. <https://doi.org/10.1021/acssuschemeng.8b05871>.
- (12) Wu, W.; Yan, B.; Zhong, L.; Zhang, R.; Guo, X.; Cui, X.; Lu, W.; Chen, G. Combustion Ash Addition Promotes the Production of K-Enriched Biochar and K Release Characteristics. *J. Clean. Prod.* **2021**, *311*, 127557. <https://doi.org/10.1016/j.jclepro.2021.127557>.
- (13) Bachmaier, H.; Kuptz, D.; Hartmann, H. Wood Ashes from Grate-Fired Heat and Power Plants: Evaluation of Nutrient and Heavy Metal Contents. *Sustainability* **2021**, *13* (10), 5482. <https://doi.org/10.3390/su13105482>.
- (14) Pohlandt-Schwandt, K. Treatment of Wood Ash Containing Soluble Chromate. *Biomass Bioenergy* **1999**, *16* (6), 447–462. [https://doi.org/10.1016/S0961-9534\(99\)00013-6](https://doi.org/10.1016/S0961-9534(99)00013-6).
- (15) Costa, M. Toxicity and Carcinogenicity of Cr(VI) in Animal Models and Humans.

- Crit. Rev. Toxicol.* **1997**, 27 (5), 431–442. <https://doi.org/10.3109/10408449709078442>.
- (16) Sørmo, E.; Silvani, L.; Bjerkli, N.; Hagemann, N.; Zimmerman, A. R.; Hale, S. E.; Hansen, C. B.; Hartnik, T.; Cornelissen, G. Stabilization of PFAS-Contaminated Soil with Activated Biochar. *Sci. Total Environ.* **2021**, 763, 144034. <https://doi.org/10.1016/j.scitotenv.2020.144034>.
- (17) Hagemann, N.; Schmidt, H.-P.; Kägi, R.; Böhrer, M.; Sigmund, G.; Maccagnan, A.; McArdell, C. S.; Bucheli, T. D. Wood-Based Activated Biochar to Eliminate Organic Micropollutants from Biologically Treated Wastewater. *Sci. Total Environ.* **2020**, 730. <https://doi.org/10.1016/j.scitotenv.2020.138417>.
- (18) *PYREG PX Pyrolyse-Anlagen: premium Karbonisierungstechnologie für ein tragfähiges Business.* <https://pyreg.com/de/unsere-technologie/>.
- (19) Bucheli, T. D.; Bachmann, H. J.; Blum, F.; Bürge, D.; Giger, R.; Hilber, I.; Keita, J.; Leifeld, J.; Schmidt, H.-P. On the Heterogeneity of Biochar and Consequences for Its Representative Sampling. *J. Anal. Appl. Pyrolysis* **2014**, 107, 25–30. <https://doi.org/10.1016/j.jaap.2014.01.020>.
- (20) DIN EN ISO 17294-2:2024-03, Wasserbeschaffenheit - Anwendung Der Induktiv Gekoppelten Plasma-Massenspektrometrie (ICP-MS) - Teil 2: Bestimmung von Ausgewählten Elementen Einschließlich Uran-Isotope (ISO 17294-2:2023); Deutsche Fassung EN ISO 17294-2:2023, 2024. <https://doi.org/10.31030/3503779>.
- (21) Hilber, I.; Hagemann, N.; De La Rosa, J. M.; Knicker, H.; Bucheli, T. D.; Schmidt, H. Biochar Production From Plastic-Contaminated Biomass. *GCB Bioenergy* **2024**, 16 (11), e70005. <https://doi.org/10.1111/gcbb.70005>.
- (22) Chen, S.; Hu, Y. H. Chemical Recycling of Plastic Wastes with Alkaline Earth Metal Oxides: A Review. *Sci. Total Environ.* **2023**, 905, 167251. <https://doi.org/10.1016/j.scitotenv.2023.167251>.
- (23) Hawley, M. C.; Boyd, M.; Anderson, C.; DeVera, A. Gasification of Wood Char and Effects of Intraparticle Transport. *Fuel* **1983**, 62 (2), 213–216. [https://doi.org/10.1016/0016-2361\(83\)90201-6](https://doi.org/10.1016/0016-2361(83)90201-6).
- (24) Nzihou, A.; Stanmore, B.; Sharrock, P. A Review of Catalysts for the Gasification of Biomass Char, with Some Reference to Coal. *Energy* **2013**, 58, 305–317. <https://doi.org/10.1016/j.energy.2013.05.057>.
- (25) Mitsuoka, K.; Hayashi, S.; Amano, H.; Kayahara, K.; Sasaoaka, E.; Uddin, Md. A. Gasification of Woody Biomass Char with CO₂: The Catalytic Effects of K and Ca Species on Char Gasification Reactivity. *Fuel Process. Technol.* **2011**, 92 (1), 26–31. <https://doi.org/10.1016/j.fuproc.2010.08.015>.
- (26) Hagemann, N.; Pollex, A.; Zeng, T.; Schmidt, H.-P. Holzvergaserkoks: Abfall oder Rohstoff? *MÜLL ABFALL* **2024**, No. 3, 8. <https://doi.org/10.37307/j.1863-9763.2024.03.08>.
- (27) Jalalabadi, T.; Glenn, M.; Tremain, P.; Moghtaderi, B.; Donne, S.; Allen, J. Modification of Biochar Formation during Slow Pyrolysis in the Presence of Alkali Metal Carbonate Additives. *Energy Fuels* **2019**, 33 (11), 11235–11245. <https://doi.org/10.1021/acs.energyfuels.9b02865>.
- (28) Radačovská, L.; Holubčík, M.; Nosek, R.; Jandačka, J. Influence of Bark Content on Ash Melting Temperature. *Procedia Eng.* **2017**, 192, 759–764. <https://doi.org/10.1016/j.proeng.2017.06.131>.
- (29) Link, S.; Yrjas, P.; Lindberg, D.; Trikkel, A.; Mikli, V. Ash Melting Behaviour of Reed and Woody Fuels Blends. *Fuel* **2022**, 314, 123051. <https://doi.org/10.1016/j.fuel.2021.123051>.
- (30) Wiedemeier, D. B.; Abiven, S.; Hockaday, W. C.; Keiluweit, M.; Kleber, M.; Masiello, C. A.; McBeath, A. V.; Nico, P. S.; Pyle, L. A.; Schneider, M. P. W.; Smernik, R. J.; Wiesenberger, G. L. B.; Schmidt, M. W. I. Aromaticity and Degree of Aromatic

Chapter 2: Wood ash additives in biochar production and related formation of polychlorinated contaminants

Condensation of Char. *Org. Geochem.* **2015**, 78, 135–143.

<https://doi.org/10.1016/j.orggeochem.2014.10.002>.

(31) EBC 2012-2024. “European Biochar Certificate - Guidelines for a Sustainable Production of Biochar.” Carbon Standards International (CSI), Frick, Switzerland.

(<Http://European-Biochar.Org>). Version 10.4 from 20th Dec 2024, 2024.

(32) German Federal Office of Justice. *Neununddreißigste Verordnung zur Durchführung des Bundes-Immissionsschutzgesetzes*) (Verordnung über Luftqualitätsstandards und Emissionshöchstmengen - 39. BImSchV)*. https://www.gesetze-im-internet.de/bimschv_39/index.html#BJNR106510010BJNE000100000 (accessed 2025-08-03).

(33) Liu, X.; Shen, J.; Deng, S.; Wang, S.; Chen, B.; Wang, Z.; Zhang, H.; Guo, Y. Unveiling the Role of Sodium Ion in the Conversion of Amino Acid Intermediates and the Formation Mechanism of NOx Precursors during Kitchen Waste Pyrolysis. *J. Anal. Appl. Pyrolysis* **2023**, 173, 106085. <https://doi.org/10.1016/j.jaap.2023.106085>.

(34) Guo, S.; Liu, T.; Hui, J.; Che, D.; Li, X.; Sun, B.; Li, S. Effects of Calcium Oxide on Nitrogen Oxide Precursor Formation during Sludge Protein Pyrolysis. *Energy* **2019**, 189, 116217. <https://doi.org/10.1016/j.energy.2019.116217>.

(35) BGH. *Bundesgütegemeinschaft Holz asche: Verwertung von Holz aschen*. URL Accessed on 18.07.2021.

https://www.kompost.de/fileadmin/docs/Archiv/Thema_Position/5.3.2_Thema_Verwertung_von_Holz aschen_2013-final.pdf (accessed 2021-02-08).

(36) European Union. *REGULATION (EU) 2019/1009 OF THE EUROPEAN PARLIAMENT AND OF THE COUNCIL of 5 June 2019*; 2019. <https://eur-lex.europa.eu/legal-content/EN/TXT/?uri=CELEX%3A02019R1009-20241120> (accessed 2025-03-06).

(37) Walter, B.; Mostbauer, P.; Karigl, B. *Biomasse-Ascheströme in Österreich*. URL accessed on 30.10.2022.

<https://www.umweltbundesamt.at/fileadmin/site/publikationen/REP0561.pdf>.

(38) Hingston, J. A.; Collins, C. D.; Murphy, R. J.; Lester, J. N. Leaching of Chromated Copper Arsenate Wood Preservatives: A Review. *Environ. Pollut.* **2001**, 111 (1), 53–66. [https://doi.org/10.1016/S0269-7491\(00\)00030-0](https://doi.org/10.1016/S0269-7491(00)00030-0).

(39) Schilling, S. Steuerungsmöglichkeiten Der Qualität Und Eignung von Holz aschen Für Deren Einsatz Bei Der Waldkalkung. *Master Thesis Albert-Ludwigs-Univ. Freibg.* **2020**.

(40) CDR.FYI. *CDR.FYI*. <https://www.cdr.fyi>. accessed 25th March 2024. (accessed 2024-03-15).

(41) Woolf, D.; Lehmann, J.; Ogle, S.; Kishimoto-Mo, A. W.; McConkey, B.; Baldock, J. Greenhouse Gas Inventory Model for Biochar Additions to Soil. *Environ. Sci. Technol.* **2021**, 55 (21), 14795–14805. <https://doi.org/10.1021/acs.est.1c02425>.

(42) Rathnayake, D.; Schmidt, H.; Leifeld, J.; Mayer, J.; Epper, C. A.; Bucheli, T. D.; Hagemann, N. Biochar from Animal Manure: A Critical Assessment on Technical Feasibility, Economic Viability, and Ecological Impact. *GCB Bioenergy* **2023**, 15 (9), 1078–1104. <https://doi.org/10.1111/gcbb.13082>.

(43) Buss, W.; Hilber, I.; Graham, M. C.; Mašek, O. Composition of PAHs in Biochar and Implications for Biochar Production. *ACS Sustain. Chem. Eng.* **2022**, 10 (20), 6755–6765. <https://doi.org/10.1021/acssuschemeng.2c00952>.

(44) Bucheli et al. Polycyclic Aromatic Hydrocarbons and Polychlorinated Aromatic Compounds in Biochar. In *Biochar for Environmental Management*; Lehmann, J., Joseph, S., Eds.; Routledge, 2015; pp 627–656.

(45) Grafmüller, J.; Rathnayake, D.; Hagemann, N.; Bucheli, T. D.; Schmidt, H.-P. Biochars from Chlorine-Rich Feedstock Are Low in Polychlorinated Dioxins, Furans and

Chapter 2: Wood ash additives in biochar production and related formation of polychlorinated contaminants

Biphenyls. *J. Anal. Appl. Pyrolysis* **2024**, *183*, 106764.

<https://doi.org/10.1016/j.jaap.2024.106764>.

(46) German Federal Office of Justice. Bundes-Bodenschutz- Und Altlastenverordnung (BBodSchV), 1999. <https://www.gesetze-im-internet.de/bbodschv/BBodSchV.pdf> (accessed 2021-01-03).

(47) Schweizerischer Bundesrat. *Verordnung Über Belastungen Des Bodens (VBBo)*; 2016.

(48) German Federal Ministry of Justice and Consumer Protection. Verordnung Über Das Inverkehrbringen von Düngemitteln, Bodenhilfsstoffen, Kultursubstraten Und Pflanzenhilfsmitteln (Düngemittelverordnung - DüMV), 2012.

(49) European Union. *DIRECTIVE 2008/98/EC OF THE EUROPEAN PARLIAMENT AND OF THE COUNCIL*; 2008. <https://eur-lex.europa.eu/eli/dir/2008/98/oj/eng>.

Supporting Information to:

Increasing biochar yield in pyrolysis by adding ash

Jannis Grafmüller^{1,2,3,4}, Michael Tobler⁵, Philipp Vögelin⁶, Thomas D. Bucheli³, Hans-Peter Schmidt¹, Nikolas Hagemann^{1,3}

¹: Ithaka Institut, Arbaz, Switzerland and Goldbach, Germany

²: Institute of Sustainable Energy Systems (INES), Offenburg University, Offenburg, Germany

³: Environmental Analytics, Agroscope, Zurich, Switzerland

⁴: Plant Biogeochemistry, Department of Geosciences, University of Tübingen, Tübingen, Germany

⁵: Holz & Forst Consulting GmbH, 4102 Binningen, Switzerland

⁶: Industrielle Werke Basel (IWB); Margarethenstrasse 40; 4002 Basel, Switzerland

1. Supplemental description of Materials and Methods

1.1. Additional information on wood ashes

Table S1: Origins of the wood ashes used for the pyrolysis experiments and their particle size fractions.

Ash description	Ash Type	Biomass feedstock	Mass Fraction >2mm [%]	Mass fraction <2mm [%]
Sissach	Bottom ash	Natural forest wood (hard and softwood)	17%	83%
Brislach	Bottom ash	Natural forest wood (hard and softwood)	7%	93%
Möhlin	Bottom ash	Natural forest wood (hard and softwood)	6%	94%
Gruyère	Bottom ash	Sawmill residual wood without bark (softwood)	41%	59%
Gruyère_large ^a	Bottom ash	Sawmill residual wood without bark (softwood)	n.d.	n.d.
Zeglingen	Wood gasifier coke	Sawmill residual wood with bark (softwood)	27%	73%

^a: Gruyère_large was used for industrial pyrolysis

1.2. Pelletized feedstocks for pyrolysis at pilot-plant scale

Table S2: All biomass and ash mixtures used for pelleting for the pyrolysis experiments at pilot-plant scale. The analyses of the ashes and biomasses can be found in Tables S4 and S5, respectively.

Biomass ID	Biomass (mixture)	Ash amendment to feedstock [%] (w/w, dry)	Ash type
<i>Effect of ash amendment under variation of intrinsic biomass ash content</i>			
1	100% Softwood	0	n.a.
2	75% Softwood	0	n.a.
	25% Grass		n.a.
3	50% Softwood	0	n.a.
	50% Grass		
4	25% Softwood	0	n.a.
	75% Grass		
5	100% Grass	0	n.a.
6	100% Softwood	5	Sissach
7	75% Softwood	5	Sissach
	25% Grass		
8	50% Softwood	5	Sissach
	50% Grass		
9	25% Softwood	5	Sissach
	75% Grass		
10	100% Grass	5	Sissach
<i>Effect of ash amendment on pyrolysis of different feedstocks</i>			
1	Softwood	0	n.a.
11	Forest Wood	0	n.a.
12	Waste Timber	0	n.a.
13	Straw	0	n.a.
14	Bark	0	n.a.
6	Softwood	5	Sissach
15	Forest Wood	5	Sissach
16	Waste Timber	5	Sissach
17	Straw	5	Sissach
18	Bark	5	Sissach
<i>Effect of ash amendment dependent on ash type</i>			
1	Softwood	0	n.a.
6	Softwood	5	Sissach
19	Softwood	5	Gruyère
20	Softwood	5	Brislach
21	Softwood	5	Möhlin
22	Softwood	5	Zeglingen
<i>Effect of Pyrolysis on Cr(VI)</i>			
1	Softwood	0	n.a.
23	Softwood	10	Brislach
24	Softwood	20	Brislach

1.3. Reactor scheme of industrial pyrolysis plant

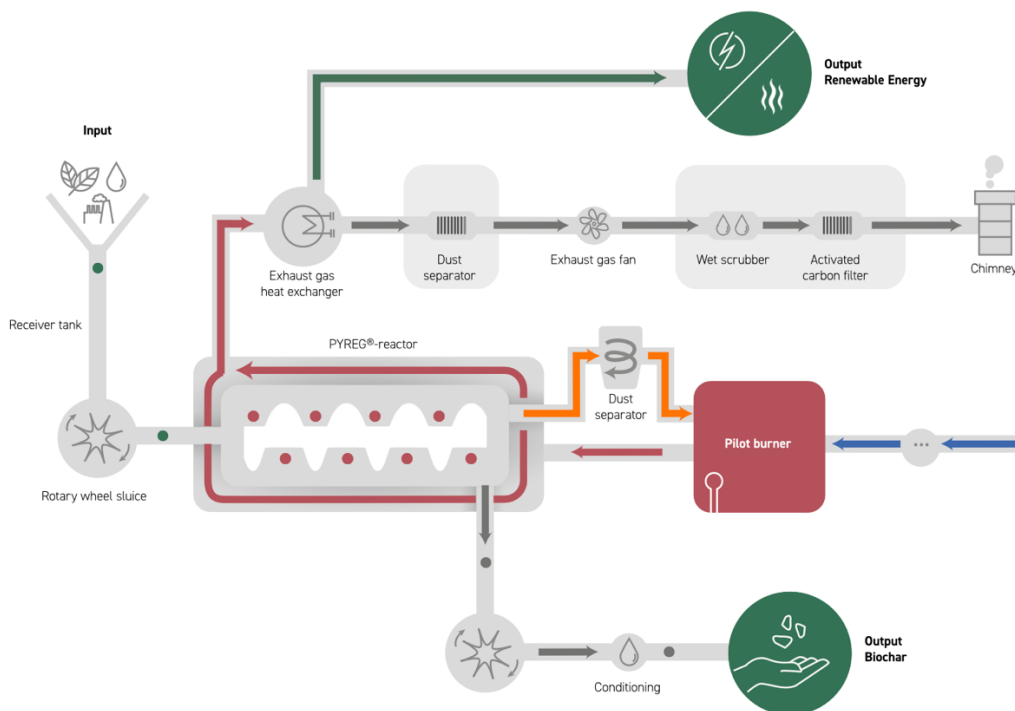


Figure S1: Process scheme of industrial pyrolysis plant PX1500 (Pyreg GmbH, Dörth, Germany). Scheme was retrieved from the manufacturer's website, where further information can be found: <https://pyreg.com/our-technology/>.

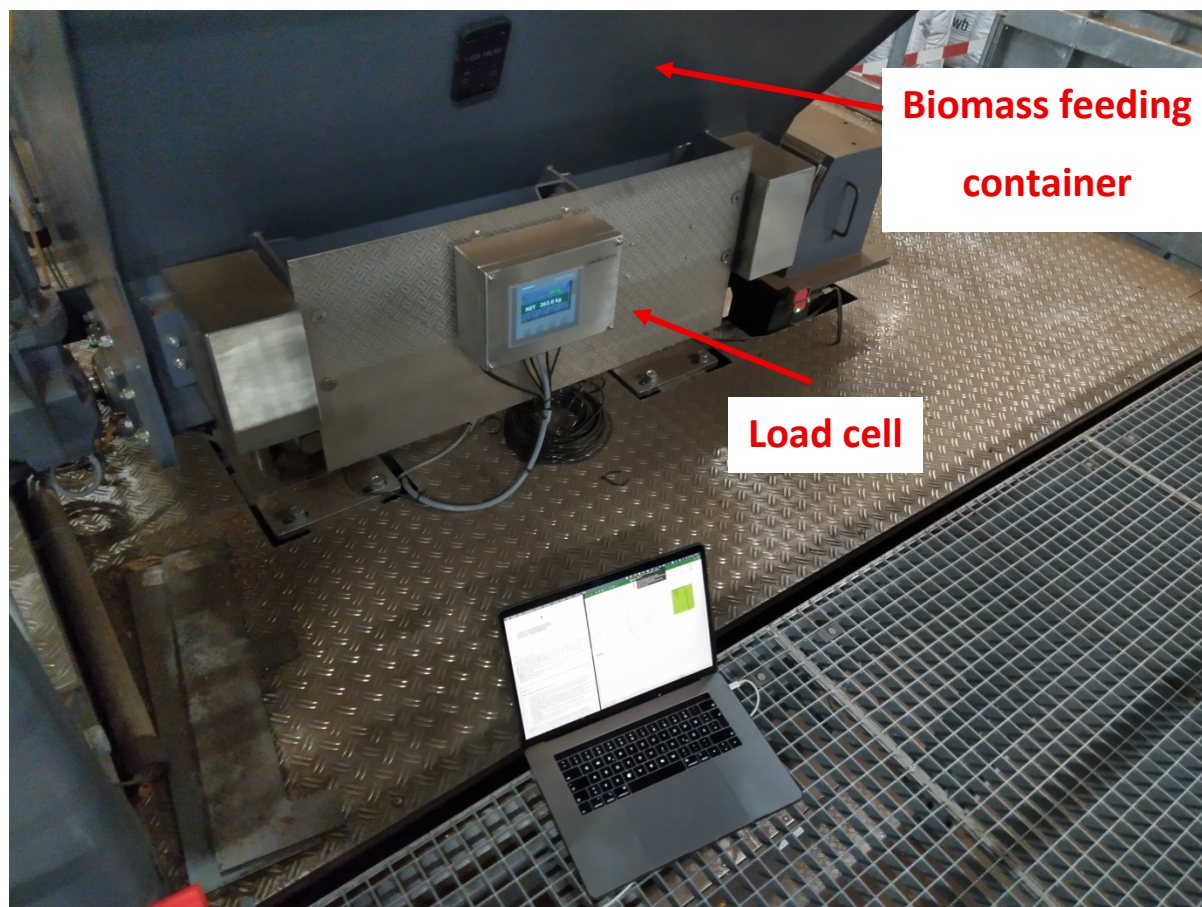


Figure S2: Load cell installed at the biomass feeding container. The load cell was recorded during the 15-minute time intervals during which the container was not filled but only emptied into the reactor. This way, a biomass mass flow into the reactor was obtained as an average value during the whole experiment.



Figure S3: Manual dosing of wood ash to the biomass feeding container installed on top of the pyrolysis reactors. The ash was added to the container during the short time interval (1 minute) during which the bunker was filled with wood, which happened every 15 minutes.

1.4. Ash, biomass and biochar analysis

Table S3: Ash, biomass and biochar analysis performed by Eurofins Umwelt Ost GmbH (Bobritzsch-Hilbersdorf, Germany) in accordance with the respective regulations.

Sample matrix	Parameter	References
Ash	pH	DIN ISO 10390 ¹
Ash	Ash content (550 °C)	DIN EN 15169 ²
Ash	Main Elements	DIN EN ISO 17294-2 ³
Ash	Trace Elements	DIN EN ISO 17294-2 DIN EN ISO 12846 ⁴
Ash, Biomass	Total Carbon	DIN EN ISO 16948 ⁵
Biomass	Ash content (550 °C)	DIN EN ISO 18122 ⁶
Biomass	Main and trace elements	DIN EN ISO 11885 ³ DIN EN ISO 17294-2 ³ 05.11.25 11:24:00
Biomass	Cellulose, Hemicellulose Lignin content	VDLUFA Method 6.5.3, volume III , 2012 ⁷
Biochar	Ash content (550 °C)	European Biochar Certificate ⁸
Biochar	Carbon, Hydrogen, Nitrogen, Sulfur content	European Biochar Certificate ⁸
Biochar	Polycyclic Aromatic Hydrocarbons (16 EPA PAH)	European Biochar Certificate ⁸
Biochar, Ash	Hexavalent chromium	DIN EN 16318 ⁹

1.5. Quantification of biochar mass yields

For the measurement of feedstock mass flow ($f_{feedstock}$, equation (1)), PYREKA was operated at room temperature to determine the mass of feedstock being transported through the reactor in a given time t ($M_{feedstock,t}$). Mass yield (y_M) of biochar was calculated as follows in equation (2):

$$f_{feedstock} = \frac{M_{feedstock,t}}{t} \quad (1)$$

$$y_M = \frac{M_{biochar,t}}{t} \cdot \frac{1}{f_{feedstock}} \cdot 100\% \quad (2)$$

where $M_{biochar,t}$ is the amount of biochar produced over the time period t . An average value for $f_{feedstock}$ was obtained by four replicate measurements recorded with $t \geq 10$ min. Mass of biochars during pyrolysis was determined without replicates with a one-time sampling interval of three residence times (RT), i.e., $t = 30$ min. Further, $f_{feedstock}$ was corrected for its dry matter content, which was determined in duplicates at 105 °C. The mass of biochar was measured instantly after production, which allowed assuming a dry matter content of 100%.

1.6. Quantification of dry and ash-free yield (y_{daf}) and carbon yield (y_C)

For each biochar sample, y_{daf} and y_C was calculated according to equation (3) and (4):

$$y_{daf} = y_M \cdot \frac{(1 - a_{BC})}{(1 - a_f)} \quad (3)$$

$$y_C = y_M \cdot \frac{c_{C,BC}}{x_{a,f} \cdot c_{C,a} + \sum_{n=0}^i x_{BM,i} \cdot c_{C,BM}} \quad (4)$$

where y_M is the dry biochar yield according to equation (2), a_{BC} and a_f are the ash contents of biochar and feedstock, respectively, $c_{C,BC}$, $c_{C,BM}$ and $c_{C,a}$ represent the total C content in the biochar, biomass and ash additive, respectively, $x_{a,f}$ and $x_{BM,i}$ represent the mass fraction of ash additive and each individual biomass in the pelleted feedstock. For the ash additive, $c_{C,a}$ was assumed to equal the loss on ignition of the sample at 850 °C. For the Zeglingen sample, the C content was separately quantified by elemental analysis.

1.7. Quantification of nitrogen yield increase

For ash addition in industrial pyrolysis, the change in nitrogen yield (y_N) was calculated based on nitrogen content (x_N) and mass yield (y_M) of pure (p) and ash-amended (a) biochar:

$$\Delta y_N = \frac{x_{N,a} \cdot y_{M,a}}{x_{N,p} \cdot y_{M,p}} \cdot 100\% - 100\% \quad (5)$$

1.8. Quantification of deviation of biochar yield on pilot-plant scale according to error propagation law

1.8.1. Biochar mass yield y_M

$$\Delta y_M = \sqrt{\left(\frac{\delta y_M}{\delta M_{biochar,t}} \cdot \Delta M_{biochar,t}\right)^2 + \left(\frac{\delta y_M}{\delta f_{feedstock}} \cdot \Delta f_{feedstock}\right)^2 + \left(\frac{\delta y_M}{\delta t} \cdot \Delta t\right)^2} \quad (6)$$

With $\Delta M_{biochar,t} = \Delta t = 0$ (not measured in replicates):

$$\begin{aligned} \Delta y_M &= \sqrt{\left(\frac{\delta y_M}{\delta f_{feedstock}} \cdot \Delta f_{feedstock}\right)^2} \\ &= \sqrt{\left(-\frac{M_{biochar,t}}{t} \cdot \frac{1}{f_{feedstock}^2} \cdot \Delta f_{feedstock} \cdot 100\%\right)^2} \end{aligned} \quad (7)$$

With $\Delta f_{feedstock}$ being the standard error of the feedstock mass flow.

1.8.2. Dry and ash-free biochar yield y_{daf}

$$\Delta y_{daf} = \sqrt{\left(\frac{\delta y_{daf}}{\delta y_M} \cdot \Delta y_M\right)^2 + \left(\frac{\delta y_{daf}}{\delta a_{BC}} \cdot \Delta a_{BC}\right)^2 + \left(\frac{\delta y_M}{\delta a_f} \cdot \Delta a_f\right)^2} \quad (8)$$

With $\Delta a_{BC} = \Delta a_f = 0$ (no replicated ash content analysis) and Δy_M from equation 7:

$$\Delta y_{daf} = \sqrt{\left(\frac{\delta y_{daf}}{\delta y_M} \cdot \Delta y_M\right)^2} = \sqrt{\left(\frac{(1 - a_{BC})}{(1 - a_f)} \cdot \Delta y_M\right)^2} \quad (9)$$

1.8.3. Carbon yield y_C

With $c_{C,BC} = x_{a,f} = c_{C,a} = x_{BM,i} \cdot c_{C,BM} = 0$ (no replicated C analysis, no deviation in x_{BM} and $x_{a,f}$ quantified), the deviation of y_C is calculated as follows:

$$\Delta y_C = \sqrt{\left(\frac{\delta y_C}{\delta y_M} \cdot \Delta y_M\right)^2} = \sqrt{\left(\frac{c_{C,BC}}{x_{a,f} \cdot c_{C,a} + \sum_{n=0}^i x_{BM,i} \cdot c_{C,BM}} \cdot \Delta y_M\right)^2} \quad (10)$$

1.9. Quantification of increases in y_{daf} and y_C

The increase in y_{daf} and y_C was calculated based on yields of ash-amended biochar (index a) related to those of the pure, non-amended biochar (index p):

$$y_{daf,In.} = \frac{y_{daf,a}}{y_{daf,p}} \cdot 100\% - 100\% \quad (11)$$

$$y_{C,In.} = \frac{y_{C,a}}{y_{C,p}} \cdot 100\% - 100\% \quad (12)$$

1.9.1. Deviation of $y_{daf,In.}$

With $y_{daf,a}$ and $y_{daf,p}$ being the y_{daf} of biochar production from a similar biomass with (index a) or without (index p) an ash amendment and $\Delta y_{daf,a}$ as well as $\Delta y_{daf,p}$ being the deviations of y_{daf} according to equation 9:

$$\begin{aligned} \Delta y_{daf,In.} &= \sqrt{\left(\frac{\delta y_{daf,In.}}{\delta y_{daf,a}} \cdot \Delta y_{daf,a}\right)^2 + \left(\frac{\delta y_{daf,In.}}{\delta y_{daf,p}} \cdot \Delta y_{daf,p}\right)^2} \\ &= \sqrt{\left(\frac{1}{y_{daf,p}} \cdot 100\% \cdot \Delta y_{daf,a}\right)^2 + \left(-\frac{y_{daf,a}}{y_{daf,p}^2} \cdot 100\% \cdot \Delta y_{daf,p}\right)^2} \end{aligned} \quad (13)$$

1.9.2. Deviation of $y_{C,In}$.

With $y_{C,a}$ and $y_{C,p}$ being the y_C of biochar production from a similar biomass with (index a) or without (index p) an ash amendment and $\Delta y_{C,a}$ as well as $\Delta y_{C,p}$ being the deviations of y_C according to equation 10:

$$\begin{aligned}\Delta y_{C,In} &= \sqrt{\left(\frac{\delta y_{C,In}}{\delta y_{C,a}} \cdot \Delta y_{C,a}\right)^2 + \left(\frac{\delta y_{C,In}}{\delta y_{C,p}} \cdot \Delta y_{C,p}\right)^2} \\ &= \sqrt{\left(\frac{1}{y_{C,p}} \cdot 100\% \cdot \Delta y_{C,a}\right)^2 + \left(-\frac{y_{C,a}}{y_{C,p}^2} \cdot 100\% \cdot \Delta y_{C,p}\right)^2}\end{aligned}\quad (14)$$

2. Supporting Results and Discussion

2.1. Properties of ashes and suitability for direct soil application

All ash samples had an ash content close to 100%, except for the Zeglingen sample, which was an ash-rich gasifier coke and had an ash content of 70% (Table S4) and a 25% C content. Among AAEM, Ca exhibited the highest amounts in the ashes, followed by K, Mg, and Na (Table S4). The total AAEM content was lowest in the Zeglingen and Sissach samples (333-387 g kg⁻¹) and highest in the Brislach sample (505 g kg⁻¹, Table S4). Overall, the composition of the ashes was well within the range reported in the literature^{10,11}.

According to XRD analysis of the ashes, a large fraction of AAEM (42-57%, Figure S4b) was present in amorphous structures. In the crystalline phase, AAEM were predominantly present in form of carbonates, oxides, hydroxides, and silicates (Figure S4a and b). AAEM were present to a negligible extent as phosphates and sulphates (Figure S4b). The Zeglingen sample had a significantly higher fraction of AAEM bound as CaCO₃ compared to the other ashes. The Sissach sample had the highest share of AAEM bound as Ca₂SiO₄ (Figure S2b), a mineral that was found in all ashes except the Zeglingen sample. The Zeglingen sample was further the only ash with a relevant AAEM allocation in K₂Ca₂(CO₃)₃. The XRD measurements recovered 43-67% of total AAEM content quantified by wet chemistry analysis, which matches the finding that 42-57% (w/w) of the ash samples were of amorphous character and thus not covered by XRD. The ashes comply with the mineral fingerprint of wood ashes usually obtained in a temperature range of 700-800 °C¹².

For all ashes, water-solubility of K was highest compared to the other AAEM, both in absolute and relative amounts, contributing up to 100% to the soluble fraction of AAEM (Table S5). The Sissach and Gruyère samples shared the lowest solubility of total K (20-34%, respectively) and total AAEM, while it was highest for the Zeglingen sample (81%, Table S5), matching with the high content of K₂SO₄ and K₂Ca₂(CO₃)₃ in the Zeglingen sample. Water solubility of K was well related to the K content determined by XRD present in the crystalline phase in the samples (R²=0.78, Figure S3), indicating that K contained in XRD-recovered crystalline structures in ashes and gasifier cokes might exhibit higher solubility compared to K in amorphous structures.

Chapter 2: Wood ash additives in biochar production and related formation of polychlorinated contaminants

Copper, zinc, chromium, and nickel were the most relevant quantified potentially toxic elements (PTE) in the ashes (Table S4). Additionally, the Sissach sample had a high Pb content compared to the other ashes, since the latter were intendedly selected from burning chambers using wood from forests that were at significant distance from busy roads. Due to its overall low concentrations of PTE, the Gruyère ash was selected to be used for the scale-up to industrial pyrolysis, as PTEs accumulate in biochar. The second sample of the Gruyère ash (Gruyère_large), however, had higher Cu and Cr contents, highlighting the variability in composition of wood ashes over time, even within the same combustion plant using the same input biomass (Table S4). The Brislach and Möhlin samples were characterized by the highest Cr(VI) contents (Table S4).

The use of ash in agriculture is subject to legal framework requirements in the European Union (EU), where wood ash is categorized in the compound material category (CMC) 13 (Thermal Oxidation Materials or Derivates) under Product Function Category (PFC) 1 (Inorganic Macronutrient Fertiliser) in the EU Fertilizer Product Regulation¹⁵. There are also country-specific regulations for agricultural soil application of wood ash, e.g., in Germany (BGH¹⁶) and Austria (BMLFUW¹⁷). All guidelines set a limit of 2 mg Cr(VI) kg⁻¹ (Table S4), to which only Sissach and Zeglingen ashes were compliant. Still, due to high PTE content in Sissach, only the Zeglingen ash would have been allowed for soil application (Table S4). All ashes and the gasifier coke that were used in this study are currently disposed of by the producers (landfill with special requirements), highlighting the necessity to develop recycling procedures to avoid losing plant nutrients from natural material cycles.

Chapter 2: Wood ash additives in biochar production and related formation of polychlorinated contaminants

Table S4: Elemental composition of wood ashes used for the pyrolysis experiments and limit values according to selected regulations. The Zeglingen sample was an ash-rich gasifier coke, all other samples were bottom ashes from biomass burning chambers. Phosphorus (P), calcium (Ca), magnesium (Mg), sodium (Na), potassium (K), lead (Pb), cadmium (Cd), copper (Cu), nickel (Ni), mercury (Hg), zinc (Zn), total chromium (Cr), hexavalent Cr (Cr^{VI}), arsenic (As), thallium (Tl). n.d.: not defined. The last three rows indicate compliance with various regulations^g.

	Ash Samples						Regulations		
	Sissach	Brislach	Möhllin	Gruyère ^a	Gruyère_large ^a	Zeglingen	BGH ^b	BMLFUW A/B ^c	EU-FPR ^d
Ash [%]	98.5	99.5	99.3	96.6	100.0	70.4	n.d.	n.d.	n.d.
P [g kg⁻¹]	14.4	11.8	12.9	17	13.9	5.6	n.d.	n.d.	n.d.
Ca [g kg⁻¹]	287.0	388.0	305.0	369.0	349.0	236.0	n.d.	n.d.	n.d.
Mg [g kg⁻¹]	19.7	37.9	33.9	18.3	24.0	12.2	n.d.	n.d.	n.d.
Na [g kg⁻¹]	2.4	0.6	1.9	2.1	2.4	0.2	n.d.	n.d.	n.d.
K [g kg⁻¹]	77.9	78.5	103.0	43.1	66.9	84.9	n.d.	n.d.	n.d.
Sum of AAEM^f [g kg⁻¹]	387.0	505.0	443.8	432.5	442.3	333.3	n.d.	n.d.	n.d.
Pb [mg kg⁻¹]	183	3	8	5	7	5	150	100/200	120
Cd [mg kg⁻¹]	<0.2	1.3	0.2	0.6	<0.2	0.6	1.5	5/8	3
Cu [mg kg⁻¹]	166	89	225	104	230	88	900	200/250	600
Ni [mg kg⁻¹]	22	68	72	31	44	21	30	150/200	100
Hg [mg kg⁻¹]	<0.07	<0.07	<0.07	<0.07	<0.07	<0.07	1	n.d.	1
Zn [mg kg⁻¹]	96	107	82	157	49	592	5000	1200/1500	1500
Cr [mg kg⁻¹]	39	75	57	78	204	7	n.d.	150/250	400

Chapter 2: Wood ash additives in biochar production and related formation of polychlorinated contaminants

Cr(VI) [mg kg ⁻¹]	1.6	19.0	17.0	4.5	7.5	<0.1	2	2/2	2
As [mg kg ⁻¹]	3.9	1.5	1.3	2.9	2.1	<0.8	40	20/20	40
TI [mg kg ⁻¹]	<0.2	<0.2	<0.2	<0.2	<0.2	<0.2	n.d.	n.d.	2
BGH	- (-)	- (-)	- (-)	- (+)	- (-)	+ (+)			
BMLFUW	-/+ (-/+)	- (+)	-/+ (-/+)	- (+)	- (-/+)	+ (+)			
EU-FPR	- (-)	- (+)	- (+)	- (+)	- (+)	+ (+)			

^a: Gruyère was used for pyrolysis on pilot-plant scale and Gruyère_large was used for the experiments on industrial scale.

^b: Germany: Threshold values for wood ashes to be used as soil or compost amendment according to the German Federal Quality Association Wood Ash (BGH).¹⁶

^c: Austria: Threshold values for the use of biomass ash on agricultural and forestry land according to the Austrian Ministry for Agriculture and Forestry, Environment and Water Management (BMLFUW) based on hydrofluoric acid digestion. Ashes that meet the limit values in category A are allowed for soil application without providing a soil analysis of the application site. Ashes with contents between threshold A and B are only allowed after providing a soil analysis of the application site and consideration of nutrient uptakes by plants.¹⁷

^d: European Union: EU Fertilizer Product Regulation (EU 2019/1009, EU-FPR): combined limit values for component material category CMC 13 (“Thermal Oxidation Materials or Derivates”) and product function category PFC 1(C)(I): Inorganic Macronutrient Fertilizer. There are additional limit values for vanadium and chlorine which are not considered here as their analysis was beyond the scope of this study.¹⁵

^f: Sum of the alkali and alkaline earth metals (AAEM) Na, K, Mg, and Ca.

^g: The compliance with regulations is evaluated when including or excluding (in brackets) Cr(VI) contents. Compliance is indicated with a ‘+’ and non-compliance by ‘-’. For BMLFUW, compliance is evaluated against subcategories A or B, separated by ‘/’. If no ‘/’ is indicated, evaluation refers to both subcategories.

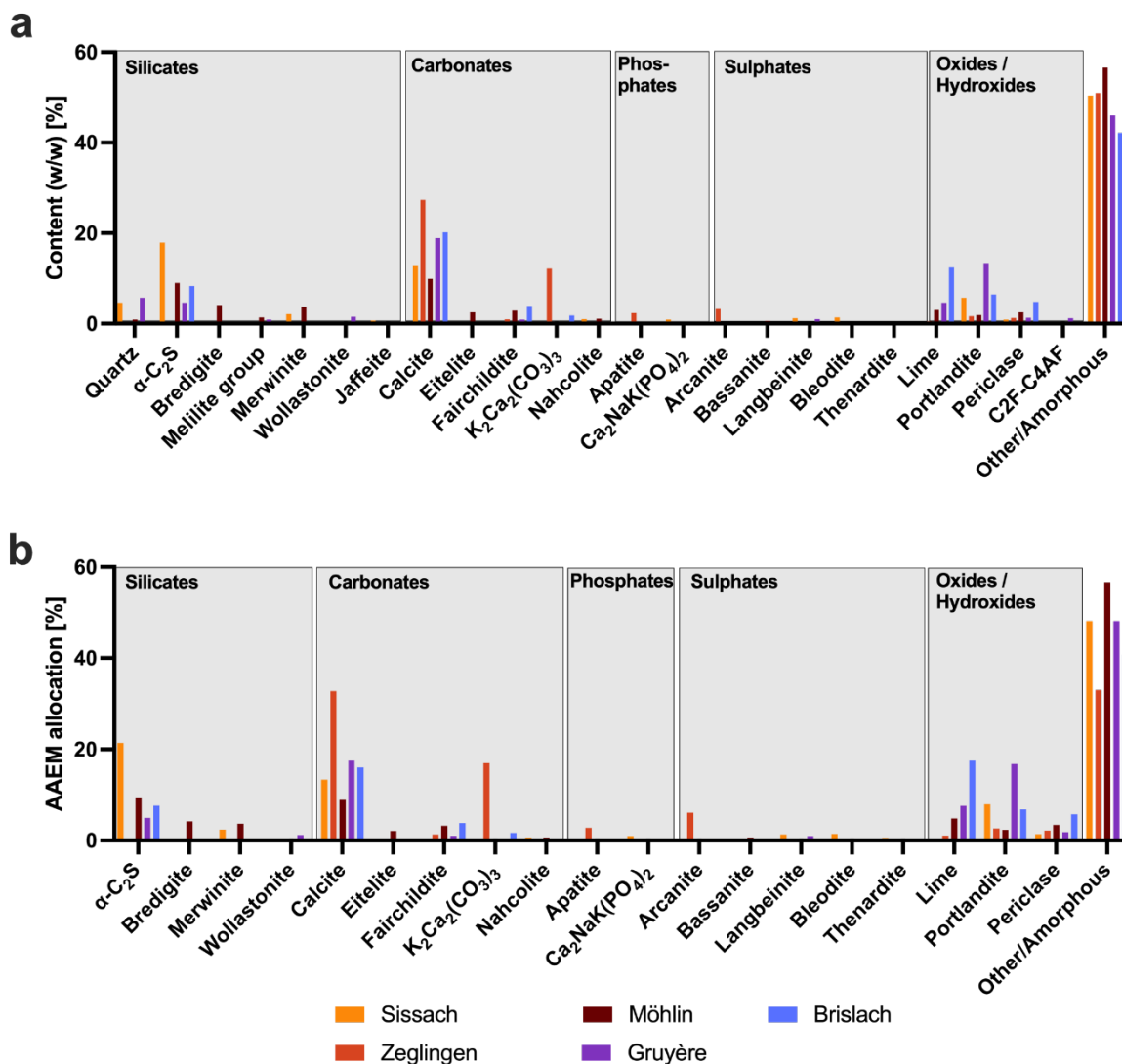


Figure S4: Quantitative X-ray diffraction (XRD) analysis of the five wood ash samples expressed as total content (w/w) of the mineral in the sample (a). Panel b presents the fraction of alkali and alkaline earth metals (AAEM) quantified by wet chemistry analysis in a specific ash, i.e., potassium, sodium, magnesium and calcium, which is allocated in a specific mineral quantified by XRD. X-ray diffraction analysis of the ashes was performed after drying the samples at 40 °C and dry-milling with an internal standard prior to measurement in the diffractometer (D8 Advance equipped with an XE-T detector; irradiation with Cu-K α -radiation, Bruker GmbH, Mannheim, Germany).

Chapter 2: Wood ash additives in biochar production and related formation of polychlorinated contaminants

Table S5: Water soluble amount and fractions of alkali and alkaline earth metals (AAEM) calcium (Ca), magnesium (Mg), potassium (K) and sodium (Na) and their total sum from the different ash samples. Values are based on elution of the ashes (1+10, m+V) for 1 hour. Errors indicate the standard deviation of three replicates, where available.

Sample	water solubility [g kg ⁻¹]					water solubility [%]				
	Ca	Mg	K	Na	∑AAEM	Ca	Mg	K	Na	∑AAEM
Sissach	4.9	9·10 ⁻⁴	15	0.3	21	1.7	<0.01	20	13	5.0
Zeglingen	0.02 ± 0.0	5·10 ⁻⁴	69 ± 2	0.1 ± 0.0	69 ± 2	<0.1	<0.01	81 ± 3	57 ± 1	20.7 ± 0.6
Möhlin	2.2 ± 0.0	2·10 ⁻⁴	44 ± 1	0.4 ± 0.0	47 ± 1	0.7 ± 0.0	<0.01	43 ± 1	22 ± 1	10.5 ± 0.2
Gruyère	4.7 ± 0.1	3·10 ⁻⁴	15 ± 1	0.3 ± 0.0	20 ± 1	1.3 ± 0.0	<0.01	34 ± 1	13 ± 1	4.6 ± 0.1
Brislach	1.8 ± 0.1	3·10 ⁻⁴	50 ± 1	0.2 ± 0.0	52 ± 1	0.5 ± 0.0	<0.01	64 ± 1	35 ± 1	10.3 ± 0.2

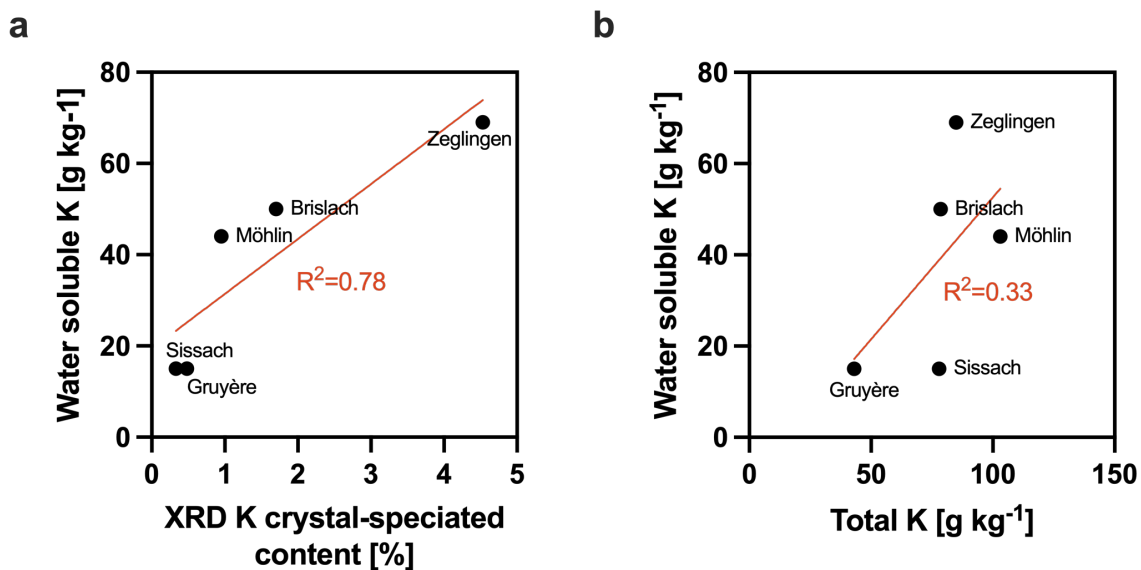


Figure S5: Water soluble content of potassium (K) in the wood ash samples (Sissach, Gruyère, Möhlin and Brislach) and the gasifier coke (Zeglingen) plotted over the K content in the ashes in crystalline structures according to X-ray diffraction analysis (panel a, in %, w/w) and plotted over the total K content in the samples determined by wet chemistry analysis (panel b). The R² values refer to linear regression through data points.

2.2. Biomass properties

Elemental and macromolecular composition varied considerably between biomasses (Table S6). The landscaping wood had the highest ash content (11%) followed by bark, grass, and straw while the lowest of 0.4-1.1% were present in forest and softwood (Table S6). Carbon content was in a narrow range (44-50%), despite larger differences in ash content. Calcium was the AAEM most present in biomasses, followed by K, Mg and Na (Table S6). The sum of AAEM contents was highest for the straw and bark (~200 mg kg⁻¹), followed by the grass and waste timber sample (~90 mg kg⁻¹) and was lowest for the landscaping wood, forest wood and softwood (4.5-39 mg kg⁻¹, Table S6). Thus, despite ash contents in a similar range for some of the biomasses, contents of individual AAEM and their sum had variation coefficients between 90 and 170%.

Lignin contents were highest for bark and the landscaping wood (42-45% (w/w)) and in a medium range for the other wood-based feedstocks (17-26% (w/w), Table S6). Straw and grass samples had the lowest lignin content (7%). Cellulose contents were highest for softwood, forest wood, and waste timber (55-61%). All other feedstocks had cellulose contents between 36 and 41%. Grass and straw had the highest hemicellulose contents (27-32%), followed by softwood, forest wood, and waste timber (16-22%), while bark as well as landscaping wood had only 3.1% of hemicellulose.

The softwood sample was delivered bark-free, while forest wood was delivered and processed with bark. The landscaping wood contained a high proportion of branches, explaining its relatively high lignin content. Further, this sample might have been partly microbial digested during storage, explaining its lower C and relatively higher ash contents, the latter might also have come from foliage residues.

Chapter 2: Wood ash additives in biochar production and related formation of polychlorinated contaminants

Table S6: Contents of Carbon, ash, lignin, cellulose, hemicellulose, potassium (K), calcium (Ca), magnesium (Mg), phosphorus (P), and sulfur (S) in the biomasses used for the pyrolysis experiments (dry basis).

Parameter	Softwood	Grass	Forest Wood	Straw	Waste Timber	Bark	Landscaping Wood ^a
Carbon [%]	50	47	50	44	49	49	48
Ash [%]	0.4	7.5	0.9	5.9	1.1	6.7	11
Lignin [%]	25	7	18	7	26	45	42
Cellulose [%]	55	36	61	40	55	39	41
Hemicellulose [%]	16	28	22	32	18	3	3
K [mg kg ⁻¹]	1	23	10	160	55	55	6
Ca [mg kg ⁻¹]	0.5	9	18	51	18	125	28
Mg [mg kg ⁻¹]	1	21	2	3	3	13	3
Na [mg kg ⁻¹]	2	37	1	2	5	4	2
Sum of AAEM^f [mg kg ⁻¹]	4.5	90	31	216	81	197	39
P [mg kg ⁻¹]	1	25	1	4	1	17	3
S [mg kg ⁻¹]	1	26	8	55	2	9	1
Pb [mg kg ⁻¹]	<2	<2	<2	<2	12	3	<2
Cd [mg kg ⁻¹]	<0.2	<0.2	<0.2	<0.2	0,2	<0.2	<0.2
Cu [mg kg ⁻¹]	<1	4	2	11	21	8	6
Ni [mg kg ⁻¹]	<1	4	1	2	1	8	4
Hg [mg kg ⁻¹]	<0.05	<0.05	<0.05	<0.05	<0.05	<0.05	<0.05

Chapter 2: Wood ash additives in biochar production and related formation of polychlorinated contaminants

Zn [mg kg ⁻¹]	4	22	6	9	165	37	25
Cr [mg kg ⁻¹]	<1	11	2	6	22	12	9
As [mg kg ⁻¹]	<0.8	<0.8	<0.8	<0.8	13.9	<0.8	<0.8

^a: Biomass used for pyrolysis at industrial scale

2.3. Further results on pyrolysis experiments

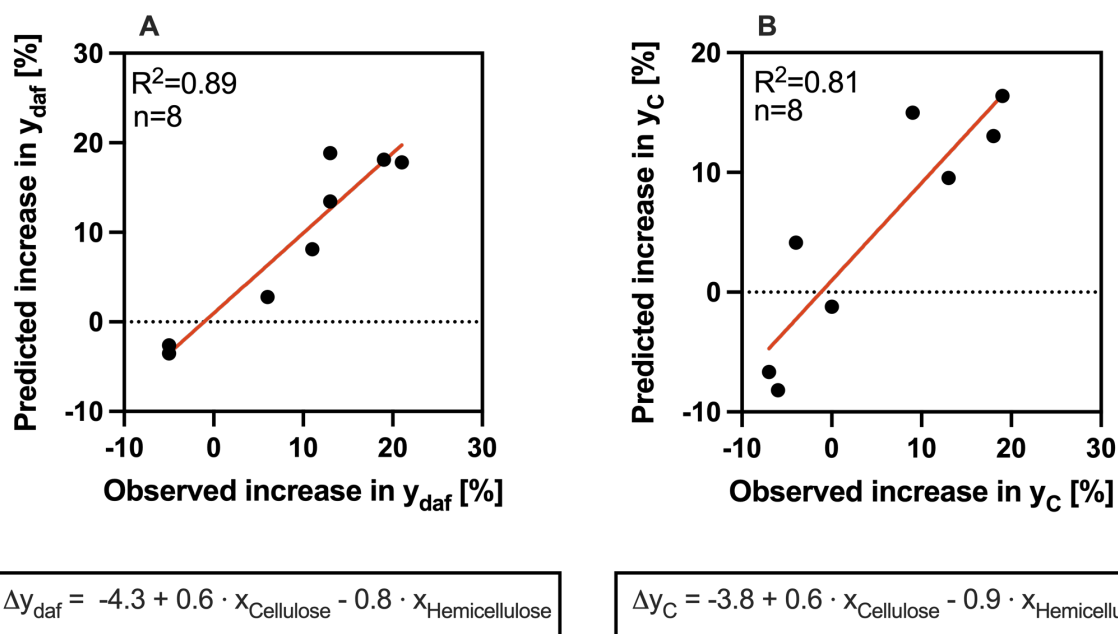


Figure S6: Predicted values of increase in dry and ash-free biochar yield (y_{daf} , a) or carbon yield (y_C , b) over observed increases in y_{daf} and y_C , respectively, in pyrolysis experiments using all biomasses, except waste timber, amended with 5% (w/w) of the Sissach ash performed at 500 °C with 10 minutes residence time. The predicted values were obtained from the presented multivariate models below the panels. The correlation coefficients correspond to the linear regression of predicted vs. observed values. $x_{Cellulose}$ and $x_{Hemicellulose}$ correspond to intrinsic contents of cellulose and hemicellulose in the biomasses, respectively. The other two input variables, i.e., intrinsic lignin and ash contents, had no significant impact on the model ($p>0.05$).

Chapter 2: Wood ash additives in biochar production and related formation of polychlorinated contaminants

Table S7: Pearson correlation of several total or water-soluble elemental contents in the ashes added at a rate of 5% (w/w) to the softwood with increases in dry and ash free biochar (y_{daf}) and carbon (y_C) yield. ns: not significant. Ash properties are presented in Tables S4 and S5 as well as Figures S2 and S3.

	increase in y_{daf} [%]	increase in y_C [%]	increase in y_N [%]
Ash content [wt%]	ns	ns	ns
AAEM [wt%]	ns	ns	ns
AAEM [mol%]	ns	ns	ns
Ca [wt%]	ns	ns	ns
K [wt%]	ns	ns	ns
Mg [wt%]	ns	ns	ns
Na [wt%]	ns	ns	ns
S [wt%]	ns	ns	ns
Pb [wt%]	ns	ns	ns
Cu [wt%]	ns	ns	ns
Fe [wt%]	ns	ns	ns
Ni [wt%]	ns	ns	ns
Zn [wt%]	ns	ns	ns
water-soluble Ca [wt%]	ns	ns	ns
water-soluble Mg [wt%]	ns	ns	ns
water soluble K [wt%]	ns	ns	ns
water soluble Na [wt%]	ns	ns	ns
water soluble AAEM [wt%]	ns	ns	ns
water soluble AAEM [mol%]	ns	ns	ns
AAEM as carbonates [wt%]	ns	ns	ns
AAEM as phosphates [wt%]	ns	ns	ns
AAEM as sulphates [wt%]	ns	ns	ns
AAEM as silicates [wt%]	ns	ns	ns

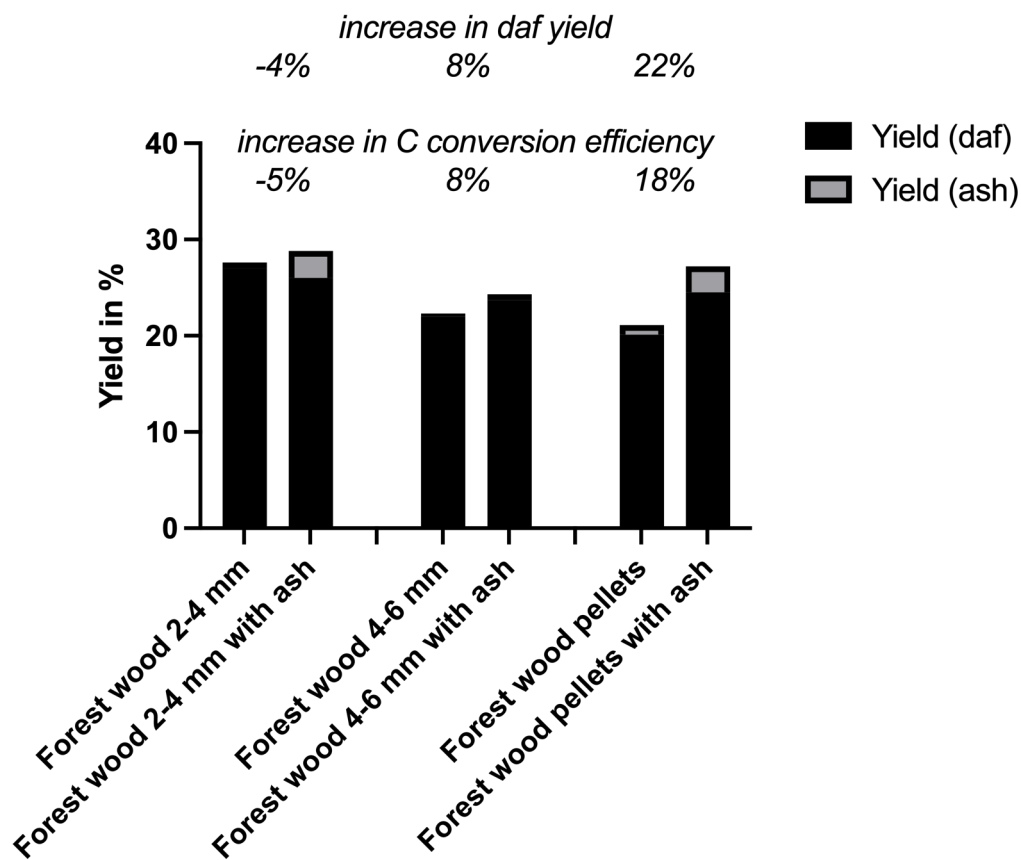


Figure S7: Yield of biochar production (total and dry and ash free (daf)) of the sieved forest wood (2-4 mm and 4-6 mm) in loose mixture with the amended ash in comparison to the pelleted forest wood amended without or with ash.

Chapter 2: Wood ash additives in biochar production and related formation of polychlorinated contaminants

Table S8: Potentially toxic elements biochars from the industrial pyrolysis experiment: arsenic (As), lead (Pb), cadmium (Cd), copper (Cu), nickel (Ni), quicksilver (Hg), zinc (Zn) and chromium (Cr). Limit values for AgroBio and Agro certification category in the European Biochar Certificate (EBC)⁸.

	Landscaping wood [mg kg ⁻¹]	Landscaping wood + ash [mg kg ⁻¹]	EBC AgroBio [mg kg ⁻¹]	EBC Agro [mg kg ⁻¹]
As	1.3	1.8	13	13
Pb	6.0	8.0	45	120
Cd	<0.2	<0.3	0.7	1.5
Cu	19.0	71.0	70	100
Ni	6.0	10.0	25	50
Hg	<0.07	<0.07	0.4	1.0
Zn	79.0	90.0	200	400
Cr	9.0	26.0	70	90

Chapter 2: Wood ash additives in biochar production and related formation of polychlorinated contaminants

Table S9: Contents of the 16 polycyclic aromatic hydrocarbons (PAH) prioritized by the Environmental Protection Agency (EPA) of the United States and the 8 PAH prioritized by the European Food Safety Authority (EFSA). Contents are given excluding the limit of detection (LOD) of the analysis method. Limit values in the European Biochar Certificate (EBC) are 6 mg kg⁻¹ for 16 EPA PAH, 1.0 mg kg⁻¹ for 8 EFSA PAH, and each 1 mg kg⁻¹ for Benzo[e]pyrene and Benzo[j]fluoranthene⁸, the latter two have not been quantified in the present study.

	mg kg ⁻¹	Landscaping wood	Landscaping wood + ash	
16 EPA PAH	Naphtalene	3.2 ± 0.2	3.1 ± 0.4	
	Acenaphthylene	<0.1	<0.1	
	Acenaphthene	0.1 ± 0.0	0.2 ± 0.0	
	Fluorene	0.7 ± 0.1	0.7 ± 0.1	
	Phenanthrene	1.0 ± 0.1	1.0 ± 0.0	
	Anthracene	0.3 ± 0.0	0.4 ± 0.0	
	Fluoranthene	0.3 ± 0.1	0.3 ± 0.0	
	Pyrene	0.4 ± 0.1	0.5 ± 0.0	
	8 EFSA PAH	Benzo[<i>a</i>]anthracene	0.1 ± 0.0	0.2 ± 0.0
		Chrysene	0.1 ± 0.0	0.1 ± 0.0
		Benzo[<i>b</i>]fluoranthene	<0.1	<0.1
		Benzo[<i>k</i>]fluoranthene	<0.1	<0.1
		Benzo[<i>a</i>]pyrene	<0.1	0.1 ± 0.0
		Indeno[1,2,3- <i>cd</i>]pyrene	<0.1	<0.1
		Dibenzo[<i>ah</i>]anthracene	<0.1	<0.1
		Benzo[<i>ghi</i>]perylene	<0.1	<0.1
16 EPA PAH excl. LOD	6.2 ± 0.3	6.8 ± 0.7		
8 EFSA PAH excl. LOD	0.2 ± 0.1	0.4 ± 0.1		

References

- (1) DIN EN ISO 10390:2022-08, Boden, Behandelte Bioabfälle Und Schlamm - Bestimmung Des pH-Werts (ISO_10390:2021); Deutsche Fassung EN_ISO_10390:2022. <https://doi.org/10.31030/3226922>.
- (2) DIN EN 15169:2007-05, Charakterisierung von Abfall - Bestimmung Des Glühverlustes in Abfall, Schlamm Und Sedimenten; Deutsche Fassung EN_15169:2007. <https://doi.org/10.31030/9771848>.
- (3) DIN EN ISO 17294-2:2024-03, Wasserbeschaffenheit - Anwendung Der Induktiv Gekoppelten Plasma-Massenspektrometrie (ICP-MS) - Teil 2: Bestimmung von Ausgewählten Elementen Einschließlich Uran-Isotope (ISO 17294-2:2023); Deutsche Fassung EN ISO 17294-2:2023, 2024. <https://doi.org/10.31030/3503779>.
- (4) DIN EN ISO 12846:2012-08, Wasserbeschaffenheit - Bestimmung von Quecksilber - Verfahren Mittels Atomabsorptionsspektrometrie (AAS) Mit Und Ohne Anreicherung (ISO_12846:2012); Deutsche Fassung EN_ISO_12846:2012. <https://doi.org/10.31030/1869854>.
- (5) DIN EN ISO 16948:2015-09, Biogene Festbrennstoffe - Bestimmung Des Gesamtgehaltes an Kohlenstoff, Wasserstoff Und Stickstoff (ISO 16948:2015); Deutsche Fassung EN ISO 16948:2015, 2015. <https://doi.org/10.31030/2244183>.
- (6) DIN e.V. DIN EN ISO 18122:2023-02, Biogene Festbrennstoffe - Bestimmung Des Aschegehaltes (ISO_18122:2022); Deutsche Fassung EN_ISO_18122:2022, 2023. <https://doi.org/10.31030/3379889>.
- (7) Verband Deutscher Landwirtschaftlicher Untersuchungs- und Forschungsanstalten. *VDLUFA Method 6.5.3*; VDLUFA-Verlag: Speyer, 2012; Vol. Volume III.
- (8) EBC 2012-2024. "European Biochar Certificate - Guidelines for a Sustainable Production of Biochar." Carbon Standards International (CSI), Frick, Switzerland. ([Http://European-Biochar.Org](http://European-Biochar.Org)). Version 10.4 from 20th Dec 2024, 2024.
- (9) DIN EN 16318:2016-07, Düngemittel Und Kalkdünger - Bestimmung von Chrom(VI) Mit Photometrie (Verfahren_A) Und Mit Ionenchromatographie Mit Spektrometrischer Detektion (Verfahren_B); Deutsche Fassung EN_16318:2013+A1:2016. <https://doi.org/10.31030/2415710>.
- (10) Bachmaier, H.; Kuptz, D.; Hartmann, H. Wood Ashes from Grate-Fired Heat and Power Plants: Evaluation of Nutrient and Heavy Metal Contents. *Sustainability* **2021**, *13* (10), 5482. <https://doi.org/10.3390/su13105482>.
- (11) Mayer, E.; Eichermüller, J.; Endriss, F.; Baumgarten, B.; Kirchhof, R.; Tejada, J.; Kappler, A.; Thorwarth, H. Utilization and Recycling of Wood Ashes from Industrial Heat and Power Plants Regarding Fertilizer Use. *Waste Management* **2022**, *141*, 92–103. <https://doi.org/10.1016/j.wasman.2022.01.027>.
- (12) Olanders, B.; Steenari, B.-M. Characterization of Ashes from Wood and Straw. *Biomass and Bioenergy* **1995**, *8* (2), 105–115. [https://doi.org/10.1016/0961-9534\(95\)00004-Q](https://doi.org/10.1016/0961-9534(95)00004-Q).
- (13) European Union. *REGULATION (EU) 2019/1009 OF THE EUROPEAN PARLIAMENT AND OF THE COUNCIL of 5 June 2019*; 2019. <https://eur-lex.europa.eu/legal-content/EN/TXT/?uri=CELEX%3A02019R1009-20241120> (accessed 2025-03-06).
- (14) BGH. *Bundesgütegemeinschaft Holzrasche: Verwertung von Holzraschen*. URL Accessed on 18.07.2021. https://www.kompost.de/fileadmin/docs/Archiv/Thema_Position/5.3.2_Thema_Verwertung_von_Holzraschen_2013-final.pdf (accessed 2021-02-08).

(15) Bundesministerium für Land- und Forstwirtschaft, Umwelt und Wasserwirtschaft; Fachbeirat für Bodenfruchtbarkeit und Bodenschutz. *Richtlinie Für Den Sachgerechten Einsatz von Pflanzenaschen Zur Verwertung Auf Land- Und Forstwirtschaftlich Genutzten Flächen.*; 2011. https://www.ages.at/download/sdl-eyJ0eXAiOiJKV1QiLCJhbGciOiJIUzI1NiJ9.eyJpYXQiOiJlMk0NTkyMDAsImV4cCI6NDA3MDkwODgwMCwidXNlciI6MCwiZ3JvdXBzIjpbMCwtMV0sImZpbGUiOiJmaWxlYWRTaW4vQUdFU18yMDIyLzVfVU1XRUXUL1JhZGlvYWt0aXZpdFh1MDBlNHQvUmFkaW9ha3Rpdml0XHUwMGU0dF9pb19kZXJfVW13ZWx0L1JpY2h0bGluaWVfZlx1MDBmY3Jfc2FjaGdlcmVjaHRlb19FaW5zYXR6X3Zvb19QZmxhbnplbmFzY2h1bi5wZGYiLCJwYWdlIjoxMjg0fQ.NWYqX15H8CdyRI0VdqxtlYP4-5YWKqSVHtl-RAxn9PE/Richtlinie_für_sachgerechten_Einsatz_von_Pflanzenaschen.pdf (accessed 2024-09-13).

Chapter 2b

Biochars from chlorine-rich feedstock are low in polychlorinated dioxins, furans and biphenyls

Jannis Grafmüller^{1,2,3}, Dilani Rathnayake^{1,4, 5}, Nikolas Hagemann^{1,4}, Thomas D. Bucheli⁴ and Hans-Peter Schmidt¹

¹Ithaka Institute, Arbaz (Switzerland) and Goldbach (Germany)

²Faculty of Process Engineering and Institute for Sustainable Energy Systems (INES), Offenburg University of Applied Sciences, Germany

³Plant Biogeochemistry, Tübingen University, Tübingen, Germany

⁴Environmental Analytics, Agroscope, Zurich, Switzerland

⁵Climate and Agriculture, Agroscope, Zurich, Switzerland

Published in:

Journal of Analytical and Applied Pyrolysis

First published: 16th September 2024

<https://doi.org/10.1016/j.jaap.2024.106764>

Material from:

J. Grafmüller, D. Rathnayake, N. Hagemann, T.D. Bucheli, H.-P. Schmidt, Biochars from chlorine-rich feedstock are low in polychlorinated dioxins, furans and biphenyls, Journal of Analytical and Applied Pyrolysis 183 (2024) 106764.

<https://doi.org/10.1016/j.jaap.2024.106764>.

The published article is re-printed in this thesis with permission from Elsevier B.V. The right to include the article in its published form in a thesis or dissertation is retained by the authors in accordance with Elsevier/ScienceDirect Journal Author Rights.

Chapter 2: Wood ash additives in biochar production and related formation of polychlorinated contaminants

Statement of personal and co-author contributions, plus non-listed contributors

Authors	Position of candidate in list of authors	Scientific ideas by the author [%]	Data generation by the author [%]	Analysis and interpretation by the author [%]	Paper writing done by the author [%]
Jannis Grafmüller	1	15	25	50	50
Dilani Rathnayake	2	10	25	10	10
Nikolas Hagemann	3	25	25	10	10
Thomas D. Bucheli	4	25	0	20	20
Hans-Peter Schmidt	5	25	0	10	10
Contribution by other parties not listed as authors (e.g., commercial analysis laboratories, student assistants)					
Eurofins Umwelt Ost GmbH, Bobritzsch Hilbersdorf, Germany		0	25	0	0
Publication status	published				
Explanations	The study was conceptualized by all co-authors and me. Vinayak Kamra assisted with feedstock pelleting, Henriette Tripke and Isabel Hilber supported me with drying of marine biomass. Jonas Geburzi and Sinnika Lennartz provided help with marine biomass identification. Biochar samples were produced by Dilani Rathnayake, Nikolas Hagemann and me. Biomass and biochar analysis was performed by Eurofins Umwelt Ost GmbH. Data analysis was performed by me and all authors assisted with their interpretation of the data. I wrote the first draft of the manuscript and all authors, with a particularly high contribution by Thomas D. Bucheli, improved its quality.				



Contents lists available at ScienceDirect

Journal of Analytical and Applied Pyrolysis

journal homepage: www.elsevier.com/locate/jaap



Biochars from chlorine-rich feedstock are low in polychlorinated dioxins, furans and biphenyls

Jannis Grafmüller^{a,b,c,d,e,*}, Dilani Rathnayake^{a,e,f}, Nikolas Hagemann^{a,b,e}, Thomas D. Bucheli^e, Hans-Peter Schmidt^{a,b}

^a Ithaka Institute, Arbaz, Switzerland

^b Ithaka Institute, Goldbach, Germany

^c Institute for Sustainable Energy Systems (INES), Offenburg University of Applied Sciences, Offenburg, Germany

^d Plant Biogeochemistry, University of Tübingen, Tübingen, Germany

^e Environmental Analytics, Agroscope, Zurich, Switzerland

^f Climate and Agriculture, Agroscope, Zurich, Switzerland

ARTICLE INFO

Keywords:

PCDD/F
PCB
Chlorine
Marine biomass
PVC
Slow pyrolysis

ABSTRACT

Chlorinated aromatic hydrocarbons like polychlorinated dibenzo-*p*-dioxins and -furans (PCDD/F) and polychlorinated biphenyls (PCB) are omnipresent in the environment due to historic production, use, and (unintended) release. Nowadays, their emission and maximum concentration in environmental compartments is strictly regulated. During biochar production, PCDD/F and PCB may be formed and retained on the solid pyrolysis product. Industrial biochars certified, e.g., under the European Biochar Certificate (EBC), exhibit concentrations that were always well below threshold values for soil application and even animal feed. However, this has not been sufficiently tested for chlorine (Cl) rich organic material such as marine biomass or polyvinyl chloride (PVC) contaminated feedstock. Here, we analyzed PCDD/F and PCB contamination in biochars produced at different temperatures from different biomasses with comparatively high Cl contents in the range from 0.2% to 3.8% (w/w, seagrass, two types of saltwater macroalgae, tobacco stalks, and PVC contaminated wood). All of the biochars produced showed PCDD/F and PCB contents well below the applicable threshold values given by the EBC ($< 20 \text{ ng TEQ kg}^{-1}$ for PCDD/F and $< 2 \times 10^5 \text{ ng kg}^{-1}$ for PCB). The EBC thresholds were undershot by a minimum of factor 1.5 for PCDD/F (mostly factor 20) and by a minimum of factor 90 for PCB. Between 1 and 27 ppb of feedstock Cl were transformed to Cl bound in PCDD/F and PCB in the biochars. No consistent correlation between biomass Cl contents and contents of PCDD/F and PCB were found but higher Cl contents in the feedstock led to a more diverse PCDD/F congener pattern in the biochars. Pyrolysis of PVC-amended wood resulted in consistently higher contamination of PCDD/F and PCB in the biochars compared to pyrolysis of the other biomasses, potentially due to differences in Cl speciation in the feedstocks i.e., Cl in PVC is already covalently bound to an organic carbon backbone. A high contamination in PCDD/F and PCB in biochar was intentionally triggered by separation of pyrogas and biochar in the reactor at $< 300 \text{ }^\circ\text{C}$ to promote condensation of contaminants on the solid product. Between 20% and 80% of feedstock Cl was released via the pyrogas, i.e., neutralization of HCl in burnt pyrogas might be necessary when pyrolyzing Cl-rich feedstock in industrial biochar production. Our results indicate that biochars produced from Cl-rich feedstocks with proper biochar production process control are conform with European certification guidelines for PCDD/F and PCB contamination. The results open the opportunity to exploit and valorize so far non-used marine or otherwise Cl enriched biomasses for the production of biochar and carbon sinks.

1. Introduction

Polychlorinated aromatic hydrocarbons such as polychlorinated

dibenzo-*p*-dioxins and -furans (PCDD/F) and (dioxin-like) polychlorinated biphenyls (PCB) are persistent, hydrophobic and toxic substances omnipresent in the environment, which has led to their entry

* Corresponding author at: Ithaka Institute, Goldbach, Germany.
E-mail address: grafmueller@ithaka-institut.org (J. Grafmüller).

<https://doi.org/10.1016/j.jaap.2024.106764>

Received 21 July 2024; Received in revised form 22 August 2024; Accepted 15 September 2024

Available online 16 September 2024

0165-2370/© 2024 The Authors. Published by Elsevier B.V. This is an open access article under the CC BY-NC-ND license (<http://creativecommons.org/licenses/by-nc-nd/4.0/>).

Chapter 2: Wood ash additives in biochar production and related formation of polychlorinated contaminants

J. Grafmüller et al.

Journal of Analytical and Applied Pyrolysis 183 (2024) 106764

into the food chain with subsequent bioaccumulation [1–3]. While PCB have intendedly been produced in high production volumes in the past to be used as additives in industrial products (e.g., insulators or plasticizers), PCDD/F are solely and unintendedly released as byproducts in chemical or thermal processes, such as waste incineration and can also be emitted in natural processes (e.g., volcanic activity) [4]. During combustion processes, these contaminants are likely to be formed, specifically during thermal treatment of chlorine (Cl) containing waste or fuels [4]. They may also form during the pyrolysis of Cl-rich biomass to produce biochar though pyrolysis differs fundamentally from combustion due to the absence of molecular oxygen [5].

Biochar is a carbon-rich material considered for carbon sequestration, as part of the carbon dioxide removal strategy referred to as Pyrogenic Carbon Capture and Storage (PyCCS) [6]. Application of biochar is most prominently practiced in agriculture as soil amendment [7,8] or feed additive [9], but it can also be used for other purposes such as additive in industrial products or building materials [10]. To limit the release of PCDD/F and PCB to the environment via biochar applications, the European Biochar Certificate (EBC) set a threshold value of 20 ng TEQ kg⁻¹ for the sum of PCDD/F (expressed as toxicological equivalents, TEQ, defined by the NATO Committee on the Challenges of Modern Society, I-TEQ NATO/CCMS [11]) and 0.2 mg kg⁻¹ for the sum of the six non-dioxin like (ndl) PCB congeners (28, 52, 101, 138, 153 and 180) plus the dioxin-like (dl) PCB congener 118, summarized as 7-PCB [12]. Those limits are based on Swiss and German soil protection regulations [13,14]. The limit values for biochars used in animal feed are

even lower [12].

The formation of PCDD/F and PCB during combustion is well understood [4,5,15], but has been less studied during pyrolysis. They can either form in homogeneous reactions in the gas-phase, or in heterogeneous reactions on the surface of solids (Fig. 1) [4]. While homogeneous reaction mechanisms are relevant in a temperature range of 500–800 °C, heterogeneous ones are limited to 200–400 °C [4]. At temperatures above 800 °C, formation rates of polychlorinated aromatic hydrocarbons decrease significantly and their destruction prevails [4]. The heterogeneous *de novo* formation of PCDD/F and PCB from elemental carbon and Cl is dependent on the presence of molecular oxygen, which is in contrast to their heterogeneous and homogeneous formation from precursors such as phenols, chlorobenzenes or chlorophenols alone (Fig. 1) [4].

Industrial biochar production by pyrolysis is usually carried out in the absence of molecular oxygen at pyrolysis temperatures above 500 °C. Heterogeneous formation of polychlorinated aromatic hydrocarbons via *de novo* reactions may, thus, not be relevant for biochar production [15]. However, it could play a certain role during initial (low) heating processes in the pyrolysis reactor [16,17]. Moreover, continuously operating pyrolysis plants are never completely airtight and the use of inert gas is not feasible in practice. Further, feedstock biomass itself contains oxygen [17]. Still, homogeneous formation of PCDD/F and PCB might be more relevant for biochar production since the temperature range for these reactions is 500–800 °C and they do not specifically require an oxidative atmosphere [4]. Here, a higher content of Cl in the feedstock

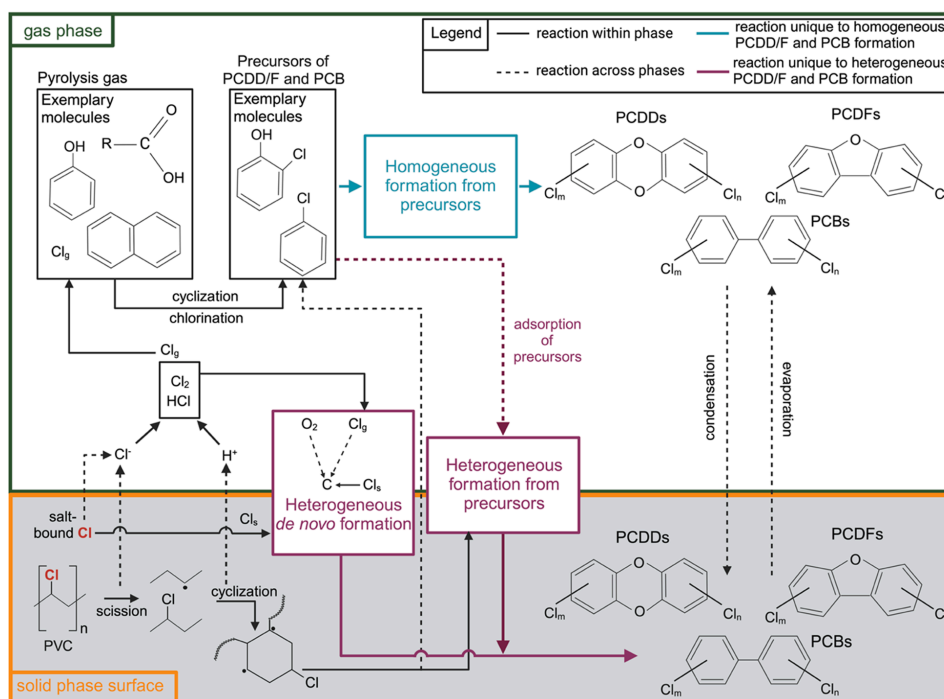


Fig. 1. Proposed scheme for the formation of polychlorinated dibenzo-*p*-dioxins (PCDDs), -furans (PCDFs) and polychlorinated biphenyls (PCBs) during pyrolysis of chlorine (Cl) rich biomass, based on literature available for the contaminant formation in combustion processes [4] and literature on pyrolysis of polyvinyl chloride (PVC) [18,19]. Heterogeneous reactions are relevant at temperatures between 200 °C and 400 °C, while homogeneous reactions dominate at temperatures between 500 °C and 800 °C [4]. For Cl, the indexes 's' and 'g' refer to 'solid', and 'gaseous', and 'm' and 'n' to the number of Cl atoms bound in a respective PCDD, PCDF and PCB congener. Red-colored Cl in the solid phase indicate an original Cl-speciation in the feedstock (e.g., salt-bound or PVC-bound Cl). Created with BioRender.com.

might lead to higher concentrations of Cl in the pyrogas, which could promote chlorination reactions of aromatic precursors (Fig. 1). They could potentially also be influenced by the Cl speciation in the feedstock. Finally, if PCDD/F and PCB would form in the gas phase of the pyrolysis system, there is a certain risk of them to condensate onto biochar particles (Fig. 1) in case local temperatures fall below the boiling points of the contaminants (185–537 °C [4,20]), as already observed with polycyclic aromatic hydrocarbons (PAH) [15,21]. A more detailed presentation of potential contamination paths of biochar with PCDD/F and PCB during pyrolysis is given in chapter 1 in the [Supplementary Information \(SI\)](#).

No matter which formation processes might actually occur, reported PCDD/F and PCB contents in biochar are usually well below the EBC thresholds [22–24]. Sobol et al. recently reviewed a set of 61 biochars for PCDD/F and found contents mostly below 1 ng TEQ kg⁻¹ and no biochar exceeded the EBC threshold value of 20 ng TEQ kg⁻¹ [24]. However, this study did not investigate in detail the influence of the Cl content and speciation in the feedstocks. Furthermore, pyrolysis was found to be a tool to remove PCDD/F and PCB from solids, when the pyrolysis feedstock was already contaminated [23]. Removal rates from the feedstocks were found to be above 96 % for all pyrolysis temperatures (500–800 °C) but in contrast, the condensed pyrooil from the pyrogas was highly contaminated with PCDD/F and PCB [23]. Most likely, the pyrolysis temperatures and residence times were sufficient for PCDD/F and PCB evaporation from the solid phase which contributed to the low contamination of the produced biochars, indicating a likely reason for the low contaminations found for biochars in general, especially at increasing pyrolysis temperatures [23,24]. Low levels of PCDD/F (0.005–1.2 ng TEQ kg⁻¹) were also found by Hale et al. in a variety of biochars produced from, e.g., paper mill waste, corn stover, pine wood, switch grass, and food waste in a temperature range between 300 and 900 °C [22].

Summarizing the existing literature on PCDD/F and PCB contents in biochars, there is a knowledge gap, particularly on how Cl-rich feedstock (> 1 %, w/w) affect biochar contamination. Some studies have shown that feedstocks with a higher Cl content tend to result in biochars with higher PCDD/F and/or PCB contents [22,25], whereas Sormo et al. found no such correlation [23]. However, the Cl contents of the feedstock materials of those studies were well below 1 %, which might be exceeded by e.g., marine biomasses used for biochar production.

To close this knowledge gap, pyrolysis experiments on Cl-rich biomasses are urgently needed. Such biomasses include marine biomasses like seagrass or macroalgae that pile up on shorelines, agricultural residues that accumulate Cl from contaminated soils during crop cultivation, and waste biomass streams that contain plastic contaminants, specifically PVC or polyvinylidene dichloride. Marine biomasses have recently been discussed as an undervalued biomass stream that could become important for carbon sequestration via PyCCS [26]. If biochars are produced from such biomasses with high Cl content, it is critical to guarantee that PCDD/F and PCB contents stay below the applicable threshold values.

In the present study, five different biomass samples with Cl contents between 0.2 % and 3.8 % (w/w) with different speciation, i.e., Cl salts or aliphatic-bound Cl in PVC, were pyrolyzed at different highest treatment temperatures (HTT) in a continuously operating pyrolyzer on pilot plant scale [27]. Most of the pyrolysis experiments were conducted at HTTs around 600 °C, where homogeneous formation of polychlorinated aromatic hydrocarbons is maximal [4]. We also performed experiments at the lower end of HTTs used for industrial biochar production (450 °C), where high biomass Cl contents are likely to result in increased PCDD/F and PCB formation via the heterogeneous formation pathways and are less likely to evaporate from the solids due to the low temperatures. Further, we investigate the risk of contaminant condensation on biochar, when the pyrogas is not separated sufficiently from the biochar at the reactor outlet. With the present study, we are aiming to get insights if biochars made from Cl-rich biomass are likely to be contaminated with

PCDD/F and PCB above applicable limit values or if they might be safely used for carbon sequestration in various applications.

2. Materials and methods

2.1. Biomass origin and preparation

Four different biomasses (Figures S1–S4) were sampled for the pyrolysis experiments either of marine or agricultural origin. For the marine biomasses, a mixture of seagrasses, dominated by *Zostera noltii* and *Z. marina* were sampled in December 2021 near Bages, France and referred to as Seagrass in the following. Further, two different mixtures of macroalgae originating from Cuba (species not identified) were sampled in May 2022 at Playa Santa Maria La Habana (Macroalgae_1) and Playa Miel (Macroalgae_2). Tobacco (*Nicotiana tabacum*) stalks were received from an agricultural farm near Ferrara, Italy in February 2023 and are referred to as Tobacco in the following. The Seagrass and Tobacco samples were oven-dried at 60 °C for 48 hours, the other feedstocks were received in already processable constitution (water content < 20 %, w/w). All feedstocks were milled to < 12 mm in a hammer mill. The marine biomasses were further processed in a pellet mill into pellets with a diameter of 6 mm. Before pelleting, the feedstocks were re-moistened to 20 % (w/w) water content with deionized water. The milled tobacco stalks were pyrolyzed without pelleting after sieving to 2–8 mm. Additionally, softwood (< 15 mm, Allspan Spanverarbeitung GmbH, Karlsruhe, Germany) was mixed with 10 % (w/w) milled PVC (PVC pipe, Gebr. Ostendorf Kunststoffwerk GmbH, Vechta, Germany), processed to pellets and labelled as PVC-Wood. Pelleting was performed without the use of any additional binder. All pellets were oven-dried at 60 °C for 16 hours to further increase mechanical stability.

2.2. Biochar production

The experimental pyrolysis was sequentially performed on a PYREKA research pyrolysis unit (Pyreg GmbH, Dörth, Germany), a continuously operated auger reactor which was described in detail by Hagemann et al. [27]. The reactor was purged with 2 L min⁻¹ N₂ and the pyrolysis gases passed the reactor (8 cm diameter) in the same direction as the solids (co-current). The temperature in the reactor is controlled by two separate heating circuits (first and second half of the reactor = first and second half of the total residence time) and was kept constant at the respective HTT during each experiment. The reactor was pre-heated to this temperature before biomass input started. Thermal conversion was performed in a range of HTT between 450 and 750 °C set for both heating circuits with a total residence time (RT) of 10 or 20 minutes of the biomass in the reactor. The HTT and RT used for each biochar production is indicated in the respective sample name (e.g., Seagrass 600–10 for the Seagrass sample pyrolyzed at 600 °C with 10 minutes RT). At the outlet of the reactor, where pyrogases are separated from the solids, a constant temperature of 400 °C was ensured. For a single biochar made from the PVC-Wood feedstock, only the first reactor heating circuit was operated at 600 °C, while the second heating circuit and the constantly operated heating system at the reactor outlet were switched off, to provoke condensation of volatiles onto the solids. Here, RT of the biomass in the heated zone was 10 minutes and the total residence time in the reactor was 20 minutes. Heating of the second reactor section by heat transfer was monitored and the temperature in the second reactor section never exceeded 300 °C. In the following, this experiment is referred to as *forced pyrogas condensation* and the sample was labelled PVC-Wood-Cond. 600–10.

To measure the mass flow of feedstock ($f_{\text{feedstock}}$), PYREKA was operated without heating the reactor to determine the mass of pellets or sieved particles being transported through the reactor in a given time t ($m_{\text{feedstock},t}$ Eq. 1).

Chapter 2: Wood ash additives in biochar production and related formation of polychlorinated contaminants

J. Grafmüller et al.

Journal of Analytical and Applied Pyrolysis 183 (2024) 106764

$$f_{\text{feedstock}} = \frac{m_{\text{feedstock},t}}{t} \quad (1)$$

The mass yield (y_m) of biochar was calculated as follows (Eq. 2):

$$y_m = \frac{m_{\text{biochar},t}}{t} \cdot \frac{1}{f_{\text{feedstock}}} \cdot 100\% \quad (2)$$

where $m_{\text{biochar},t}$ is the amount of biochar produced in a time t . An average value for $f_{\text{feedstock}}$ was obtained with four replicate measurements, which were recorded with $t \geq 10$ min. Before taking a sample for the analysis of the biochar, the biochar produced after a time equal to $4xRT$ was dismissed to ensure process stabilization and to minimize cross-contamination between different feedstocks. Further, the PVC-Wood-Cond. 600–10 sample was produced at the end of the pyrolysis experiments to avoid the contamination of other biochar samples. The analysis sample and the mass of biochars during pyrolysis was recorded without replicates with a one-time sampling interval equal to $3xRT$, i.e., $t = 30$ min for experiments conducted with 10 min RT. The mass flow of feedstock was corrected for its dry matter content, which was determined in duplicates at 105 °C. The mass of biochar was measured instantly after the production, which allowed assuming a dry matter content of 100 %.

2.3. Analysis of biochars and biomass

The biomasses were analyzed for (organic) carbon (C_{org} and C , respectively), ash and Cl contents, main and trace elements by a commercial lab (Eurofins Umwelt Ost GmbH, Bobritzsch-Hilbersdorf, Germany) according to relevant DIN EN ISO standards [28–33]. The different biochars produced were analyzed in the same lab using EBC-accredited methods for C, hydrogen (H), nitrogen (N), sulfur (S), Cl and ash content [12]. Electric conductivity (EC) was measured in the filtrates ($<0.45 \mu\text{m}$) of $n=2$ replicated suspensions made from 2 g of biochar and 20 mL of ultrapure water (water with $18.2 \text{ M}\Omega \times \text{cm}$ electrical resistance) after shaking for 1 hour according to the EBC [12] (WTW Cond 7110, Xylem Inc., Washington D.C, USA). Chloride (Cl⁻) contents in these filtrates were quantified by Eurofins using ion chromatography following DIN EN ISO 10304 [34]. Congeners of PCDD/F and PCB in the biochars were quantified by Eurofins according to the EBC-method with gas chromatography coupled to a high-resolution mass spectrometer (Trace GC Ultra and Trace 1310 coupled with DFS GC-HRMS, Thermo Fisher Scientific Inc., Waltham, USA), after Soxhlet extractions of the biochars in toluene for 24 hours. Quantified contaminants were the 17 PCDD/F congeners prioritized by NATO/CCMS [11], the six ndl PCB (congeners 28, 52, 101, 138, 153, and 180), referred to as ndl PCB in the following and the 12 dl PCB prioritized by the World Health Organization (WHO) [35], referred to as dl PCB in the following.

2.4. Data processing and visualization

Pyrolysis experiments and laboratory analyses of representative biochar samples were performed as individual replicates ($n=1$). The carbon conversion efficiency (CCE) of the pyrolysis process, i.e., the share of initial biomass carbon retained in the biochar, was calculated according to Eq. 3:

$$\text{CCE} = y_m \cdot \frac{C_{\text{C,biochar}}}{C_{\text{C,feedstock}}} \quad (3)$$

where $C_{\text{C,biochar}}$ and $C_{\text{C,feedstock}}$ are the gravimetric carbon contents of the biochar and the feedstock, respectively. Chlorine retention in the biochar in relation to total Cl contained in the feedstock was calculated according to Eq. 4:

$$\text{Cl retention} = y_m \cdot \frac{C_{\text{Cl,biochar}}}{C_{\text{Cl,feedstock}}} \quad (4)$$

where $C_{\text{Cl,biochar}}$ and $C_{\text{Cl,feedstock}}$ are the chlorine contents (w/w) in the biochar and the feedstock, respectively.

The water-extractable fraction of total Cl in the biochars was calculated according the Eq. 5:

$$\text{Extractable Cl} = \frac{C_{\text{Cl,extract}} \cdot V_{\text{extract}}}{C_{\text{Cl,biochar}} \cdot m_{\text{biochar}}} \cdot 100\% \quad (5)$$

where $C_{\text{Cl,extract}}$ is the quantified Cl content in the filtered biochar extract, V_{extract} is the total volume of added extractant (20 mL) and m_{biochar} is the weight of the extracted biochar sample (2 g).

Individual PCDD/F and PCB congeners are presented with their absolute gravimetric concentrations in the biochars, and sum parameters are given as TEQ, following both the NATO/CCMS [11] and the WHO guidelines [35]. For this purpose, gravimetric concentrations of individual congeners of PCDD/F or dl PCB were multiplied with their respective toxicological equivalent factor (TEF). Sum parameters were calculated both assuming a concentration of 0 ng TEQ kg^{-1} for individual congeners quantified below the limit of quantification (LOQ), i.e., excluding LOQ, or assuming the LOQ as content of the respective congener, thus including LOQ. Sum share of individual congeners of PCDD/F and PCB in % (w/w) were calculated as mean value across all biochars produced with at least one quantified congener above the LOQ. Congeners quantified below LOQ were set to zero for this calculation. The ratio of feedstock Cl (in parts per billion – ppb, $x_{\text{Cl,PCDD/F/PCB}}$) bound in PCDD/F and PCB in the biochar were calculated according to Eq. 6:

$$x_{\text{Cl,PCDD/F/PCB}} = \frac{\sum_{i=1}^n C_{\text{Cl,con},i} \cdot C_{\text{con},i,\text{biochar}}}{C_{\text{Cl,feedstock}}} \cdot y_m \cdot 10^9 \quad (6)$$

where $C_{\text{Cl,con},i}$ is the Cl content in PCDD/F or PCB congener i , and $C_{\text{con},i,\text{biochar}}$ is the content of PCDD/F or PCB congener i in the biochar. Data visualization was performed with Graphpad Prism (version 10.2.2, GraphPad Software LLC, Boston, USA).

3. Results and discussion

3.1. Biomass composition

The different feedstocks showed a wide range of C contents, being lowest for the Seagrass and Macroalgae samples (26–39 %) and highest for PVC-Wood (50 %, Table 1). With increasing C contents, lower ash contents were found in the feedstocks (Table 1). The highest ash contents were measured for Seagrass (57 %), and the lowest ash content for the PVC-Wood (1.8 %). Chlorine contents, potentially one of the main factors influencing the formation of PCDD/F and PCB during biochar production, ranged from 0.2 % to 3.8 % in the different feedstocks (Table 1). The sample Macroalgae_1 had a Cl content of 2.5 % while Macroalgae_2 showed a Cl content of only 0.2 %. The highest Cl contents were quantified for the PVC-Wood and the Seagrass sample (3.3 % and 3.8 %, respectively, Table 1). This indicates an impurity of the PVC used (filling materials in PVC pipe) or inaccuracy in preparation of the PVC-wood feedstock, as the theoretical Cl content in this feedstock would be 5.7 % assuming 57 % (w/w) Cl content in pure PVC. The low Cl content in Macroalgae_2 might be related to rain events that leached away Cl (as well as Na) from this marine biomass, once it was washed up on the coast (Table 1). The elevated Cl content in Tobacco (1.5 %) could be a result from excess KCl fertilization or a contamination of soil or stalks by sea breeze, since stalks were stored outside on the field for several months after harvest in the cultivation region approximately 25 km from the Adriatic Sea. Contents of the elements K, P, Mg and S were below 3 % in all feedstocks, while the Seagrass and both Macroalgae samples showed increased Ca (3.4–17 %) and Na contents (0.8–3.2 %, Table 1). The potentially toxic elements (PTE) arsenic and chromium were found in a higher range in Macroalgae_1 (21.3 and 53 mg kg^{-1} , respectively) and Macroalgae_2 (12.1 and 316 mg kg^{-1} , respectively, Table S1), which

4

Chapter 2: Wood ash additives in biochar production and related formation of polychlorinated contaminants

J. Grafmüller et al.

Journal of Analytical and Applied Pyrolysis 183 (2024) 106764

Table 1

Feedstock composition: carbon (C), ash, chlorine (Cl), potassium (K), phosphorus (P), sulfur (S), magnesium (Mg), calcium (Ca) and sodium (Na) contents in the different biomasses expressed in weight percent. Seagrass, two different samples of Macroalgae, tobacco stalks (Tobacco) and softwood pellets amended with 10 % milled polyvinyl chloride (PVC-Wood). Wood: softwood used for PVC-Wood feedstock; the pure softwood was not pyrolyzed alone.

Feedstock	C [%]	Ash [%]	Cl [%]	K [%]	P [%]	S [%]	Mg [%]	Ca [%]	Na [%]
Seagrass	26	57	3.8	0.8	0.1	0.4	0.8	17	2.6
Macroalgae_1	34	36	2.5	0.6	0.1	1.2	1.7	8.8	3.2
Macroalgae_2	39	19	0.2	0.1	<0.1	1.1	1.7	3.4	0.8
Tobacco	44	9.5	1.5	3.2	<0.1	0.1	0.1	0.6	<0.1
PVC-Wood	50	1.8	3.3	<0.1	<0.1	<0.1	<0.1	0.5	<0.1
Wood	50	0.2	n.d.	<0.1	<0.1	<0.1	<0.1	0.1	<0.1

might resulted from wastewater being discharged untreated as reported for other regions of Cuba [36]. Some algae have been reported to accumulate PTEs [37]. Copper, which is known to catalyze heterogeneous formation of PCDD/F and PCB [4], was present in low concentrations in Macroalgae_1 and Macroalgae_2, as well as in PVC-Wood (< 6 mg kg⁻¹, Table S1), and to a higher extent in Tobacco (11 mg kg⁻¹) and Seagrass (36 mg kg⁻¹).

3.2. Yield and main properties of biochars

Biochar yields (y_m) increased with the ash content of the respective biomass, which remains predominantly inert during pyrolysis (Table 2). The highest values for y_m were found for the Seagrass biochars (66 % and 68 %, respectively, Table 2), pyrolysis of both Macroalgae samples provided a biochar yield around 40 %, which is in line with literature on pyrolysis of macroalgae with comparable ash content [38]. Values for y_m of Tobacco ranged between 29 % and 36 %, and pyrolysis of PVC-wood provided biochar yields between 19 % and 35 %, depending on the HTT and RT of pyrolysis (Table 2). The CCE, i.e., the percentage of biomass-derived carbon that remains in the solid biochar product after pyrolysis, was highest for the Seagrass (57–60 %) and the Tobacco biochars (52 % at 600 °C), while the CCE at a comparative HTT of 600–650 °C ranged between 32 % and 41 % for the Macroalgae samples and was 34–46 % for the PVC-Wood biochars (Table 2). With that, most of CCEs observed in the HTT range from 450 to 650 °C are significantly higher compared to the pyrolysis of the pure softwood without PVC amendment pyrolyzed in the same reactor at 500 °C in an earlier study (CCE= 35 % [25]), potentially due to catalysis of biochar formation related to the high content of ash minerals in the feedstocks used in the present study [25]. The biochars' molar H/C_{org} ratios were all below the limit of 0.7 set by the EBC [12] and decreased with increasing pyrolysis temperatures, in line with the literature (Table 2) [39].

For the Seagrass, Macroalgae and Tobacco samples, Cl contents in the biochars increased with the Cl content in the feedstocks (Table 2). They were lowest for the biochar made from Macroalgae_2 (0.6 %, w/w) and ranged between 3.3 % and 5.2 % for the biochars produced from feedstock materials with higher Cl contents (Table 2). For the PVC-Wood, however, Cl contents in the biochars were only between 1.1 % and 2.6 % (w/w), despite the comparatively high Cl content in the feedstock. For pyrolysis experiments with Seagrass, Macroalgae and Tobacco, Cl retention in the biochars was around 80 %, i.e., most of the feedstock Cl remained in the solid product (Table 2). In contrast, for pyrolysis experiments with PVC-Wood, Cl retention in the biochars was only between 12 % and 21 %. The remaining Cl must have passed from the solid to the gas phase during pyrolysis. It was probably released via the gas phase and left the burning chamber, which is connected to the pyrolysis reactor and operated at > 650 °C, most likely as HCl [40,41]. Therefore, pyrolysis plants converting Cl-enriched biomasses should neutralize the exhaust from the pyrolysis gas combustion chamber, which is common practice in waste incineration, especially when dealing with PVC contaminated feedstocks. Our experiments indicate that Cl speciation affect the extent of Cl retention in the solids during pyrolysis. In the Seagrass, Macroalgae and Tobacco feedstocks, we

expect Cl to be predominantly present as readily dissolvable free ion undergoing electrostatic interaction, whereas in PVC, it is covalently bound to aliphatic, polymeric carbon. The latter might lead to a higher rate of Cl release to the gas phase, once the aliphatic structure is cracked by the pyrolysis process. The higher release of Cl from the PVC-contaminated feedstock also indicates a higher potential for homogeneous formation of PCDD/F and PCB due to potentially higher Cl concentrations in the gas phase. The biochar produced from Macroalgae_2 presented a Cl retention >100 % (Table 2), which indicates an inaccuracy in either biochar yield recordings, elemental analysis, or a problem with carryover of Cl in the reactor from previous pyrolysis experiments. The low Cl retentions for the PVC-Wood biochars in the present study are in contrast to an earlier study from Cao *et al.* who found up to 83 % Cl retention in the biochar for pyrolysis of an macroalgae mixed with 10 % (w/w) PVC before pyrolysis [38]. The authors attributed the high retention of Cl in the biochars to potential adsorption of, most likely, PVC-derived Cl from the gas phase by minerals or pyridinic nitrogen contained in the algal biochar [38]. As the softwood used in our study was low in minerals and nitrogen, this could be the reason why in the present study, pyrolysis of PVC-wood led to a low retention of Cl in the biochars. Conversely, Cao *et al.* found only 5 % Cl retention in the biochar produced from the pure macroalgae, which is in contrast to the high Cl retentions found in our study for the Seagrass and Macroalgae samples and indicates differences in Cl release between studies due to e.g., differences in the pyrolysis process used or biomass composition.

The electric conductivity (EC) in filtrates obtained from aqueous biochar suspensions, which represents a proxy for the salt content of biochar [12], was lowest for the PVC-Wood biochars and the biochar made from Macroalgae_2 (1.9–7.0 mS cm⁻¹, Table 2). Comparable higher EC values were quantified for the biochars made from Tobacco and Macroalgae_1 (24–35 mS cm⁻¹, Table 2) and EC generally increased with HTT both for the Tobacco and PVC-Wood biochars (Table 2). The EC values of the biochars measured in this study are in the range of literature values for biochars made from mineral-rich feedstock like wheat straw, digestate or greenhouse gardening residues (3–30 mS cm⁻¹) [42]. For the tested biochars made from both Macroalgae and Tobacco, all Cl that was contained in the biochars was water-extractable chloride (Cl⁻, 96–137 %, w/w, Table 2), i.e., it can be assumed that for feedstocks containing Cl predominantly in ionic form, all Cl is released as Cl⁻ to the soil pore water after application to soil. For the PVC-Wood biochars, the fraction of water extractable Cl⁻ increased with HTT and ranged between 46 % and 89 % (Table 2), indicating that not all Cl initially bound in PVC was transformed to Cl⁻ in these biochars or that Cl⁻ was immobilized to a higher extent in the wood-based biochar matrix.

An application of 2 t ha⁻¹ of a biochar produced from Cl-rich feedstock with a Cl content of 3–5 % (w/w) in water-extractable form, which is representative for the biochars produced in the present study, would transport 60–100 kg Cl ha⁻¹ to the field. This is below Cl amounts transported to the field via potassium-chloride (KCl) fertilizers (180 kg Cl ha⁻¹ year⁻¹ at 200 kg K fertilization ha⁻¹ year⁻¹), but potentially higher as compared to compost amendments [43] or manure amendments [44] (10–30 kg Cl ha⁻¹ year⁻¹ with 30 m³ compost and 20 m³ manure application ha⁻¹ year⁻¹). Agricultural application of biochars

5

Table 2
Pyrolysis yields and biochar properties: biochar yield (y_m), contents of total and organic carbon (C and C_{org} , respectively), hydrogen (H), nitrogen (N), sulfur (S), chlorine (Cl), ash and molar H/ C_{org} ratios of the biochars produced at different pyrolysis temperatures in °C and residence times in minutes, as indicated in the sample names. Carbon conversion efficiency of the pyrolysis process (CCE), Cl retention in the biochar in relation to total Cl in the feedstock, water-extractable ratio of Cl from the biochar and electric conductivity (EC) in the filtrate originating from an aqueous biochar suspension (1:10, m/V). Biochar feedstocks used were seagrass, two samples of macroalgae, tobacco stalks (Tobacco), softwood amended with 10 % (w/w) polyvinylchloride (PVC-Wood), and PVC-Wood pyrolyzed with forced condensation of pyrogas (PVC-Wood-Cond.). For extractable Cl, the deviations indicate the minimum and maximum quantified value of n=2 replicates. This deviation was <2 % in n=2 replicated extractions for EC values. n.d.: not determined.

Biochar	y_m [%]	C [%]	C_{org} [%]	H [%]	N [%]	S [%]	Cl [%]	ash [%]	H/ C_{org}	CCE [%]	Cl retention [%]	Extractable Cl [%]	EC [mS cm ⁻¹]
Seagrass 450-10	68	23	17	0.7	0.66	0.47	4.4	78	0.48	59	78	n.d.	n.d.
Seagrass 650-10	66	22	17	0.6	0.51	0.41	4.4	82	0.42	57	77	n.d.	n.d.
Macroalgae_1 650-10	42	26	23	0.6	0.31	1.6	5.2	80	0.32	33	87	103 ± 4	24
Macroalgae_2 650-10	42	38	35	0.8	0.54	1.9	6.6	64	0.27	41	127	96 ± 1	6.5
Tobacco 450-10	36	62	61	2.0	2.4	0.57	3.3	31	0.39	51	80	120 ^b	26 ^b
Tobacco 600-10	37	63	61	0.9	2.0	0.46	3.3	32	0.18	52	81	137 ± 5	28
Tobacco 750-10	29	58	56	0.2	2.5	0.56	4.3	39	0.04	38	82	129 ± 5	35
PVC-Wood 450-20	35	83	n.d.	3.3	0.35	n.d.	1.1	4.4	0.47 ^a	58	12	46 ± 1	1.9
PVC-Wood 600-20	25	87	n.d.	2.6	0.48	n.d.	2.5	6.9	0.36 ^a	46	19	83 ± 1	6.7
PVC-Wood 600-10	19	88	n.d.	2.7	0.54	n.d.	2.4	7.0	0.37 ^a	34	14	89 ± 1	7.0
PVC-Wood-Cond. 600-10	27	84	83	2.3	0.28	<0.03	2.6	7.5	0.33 ^a	45	21	n.d.	n.d.

^a H/C ratio was calculated based on total carbon in the biochar sample, since C_{org} was not determined.

^b Extraction was performed non-replicated due to shortage in sample.

produced from Cl-rich biomass should therefore be tested in field trials to investigate potential plant physiological effects of biochar's increased Cl content especially for Cl-sensitive plants [45], if Cl in the biochars is predominantly present as an ion. The EBC certification includes the measurement of the salt content in biochars, however, this method does not distinguish between Cl⁻ or other ions contributing to the total salt content. Therefore, it might be adequate to establish a measurement of extractable Cl⁻ from biochars in the EBC in the future.

The contents of PTE accumulated in the biochars according to the respective contents in the feedstocks (Table S2), as they are predominantly non-volatile at the pyrolysis temperatures applied in the experiments. With that, the contents of PTE generally increased at higher pyrolysis temperatures, in line with literature [39]. Beside the higher As contents for the biochars made from Macroalgae_1 and Macroalgae_2 and elevated Cr and Ni contents in the biochar produced from Macroalgae_2, all analytical parameters of the biochars produced were in line with the EBC Agro certification [12] (Table S2).

3.3. Contents of polychlorinated aromatic hydrocarbons in biochars

3.3.1. Contents PCDD/F in biochars

The sum of mass-based concentrations of PCDD/F ranged between <LOQ and 76 ng kg⁻¹ in the biochars produced under standard pyrolysis conditions, i.e., sufficient heating of solids throughout the whole length of the pyrolysis reactor (Table 3). The lowest mass-based concentrations were found for the biochars produced from Macroalgae_2 and Seagrass (0.7 – 1.6 ng kg⁻¹, Table 3), followed by the Tobacco biochars produced at 450 °C and 600 °C (6–27 ng kg⁻¹) while all PVC-Wood biochars and the biochar produced from Macroalgae_1 showed the highest concentrations (35–76 ng kg⁻¹). The biochar produced from the PVC-Wood with forced condensation of pyrogas showed the highest mass-based concentration of PCDD/F with 40700 ng kg⁻¹ (PVC-Wood-Cond. 600–10, Table 3).

The increase in pyrolysis temperature from 450 °C to 650 °C led to a decrease in PCDD/F by 41 ng kg⁻¹ (-54 %) for the PVC-Wood biochars (20 minutes residence time), while for the Tobacco and Seagrass biochars, the temperature rise from 450 °C to 600–650 °C increased PCDD/F by 21 ng kg⁻¹ (+340 %) and 0.3 ng kg⁻¹ (+23 %), respectively (Table 3). A further increase in pyrolysis temperature from 600 °C to 750 °C decreased the content below LOQ in the Tobacco biochar (Table 3). The increase in contamination for the Tobacco and Seagrass biochars between 450 and 600–650 °C cannot be confirmed by previous literature, as studies on comparable feedstocks are lacking, but the reduction in PCDD/F at higher HTT (>700 °C) is in line with recent studies that found decreasing contents of PCDD/F with increasing HTT [23,24].

The increase in RT from 10 minutes to 20 minutes for the PVC-Wood pyrolyzed at 600 °C decreased the content of PCDD/F in the biochar by 21 ng kg⁻¹ (-38 %, Table 3). This might indicate that heterogeneous formation took place during pyrolysis of this feedstock and with an increase in residence time, the chance was higher that the contaminants volatilized from the solid when the temperature of the produced biochar was high enough (Fig. 1), which might have been promoted by a longer residence time in the reactor. However, all these observations on the influence of pyrolysis temperature and residence time can only be reported as trends without statistical validation, since pyrolysis experiments were performed without repetitions and without the necessary resolution in variation of HTT and RT.

The greatest varieties of PCDD/F congeners were found for the biochars produced from Macroalgae_1 and PVC-Wood, i.e., 10–12 out of the 17 analyzed congeners were quantified above LOQ in these biochars (Fig. 2 and Table 3). In contrast, only 0–3 of the PCDD/F congeners were quantified above LOQ in the biochars produced from Seagrass, Macroalgae_2 and Tobacco (Fig. 2 and Table 3). With that, the biochar produced from Macroalgae_1 showed a more similar pattern as the PVC-Wood biochars and did not follow the pattern of the biochars made from the other marine biomasses, i.e., Macroalgae_2 and the Seagrass.

Chapter 2: Wood ash additives in biochar production and related formation of polychlorinated contaminants

J. Grafmüller et al.

Journal of Analytical and Applied Pyrolysis 183 (2024) 106764

Table 3
 Contents of polychlorinated dibenzo-p-dioxins and -furans (ng kg⁻¹) in the biochars produced from the different biomasses at the pyrolysis temperatures and residence times as indicated (in °C and minutes, respectively). Biochar feedstocks used were seagrass, two samples of macroalgae, tobacco stalks (Tobacco), softwood amended with 10 % (w/w) polyvinylchloride (PVC-Wood), and PVC-Wood pyrolyzed with forced condensation of pyrogas (PVC-Wood-Cond.). Contents exceeding the limit of quantification (LOQ) are indicated with bold letters. The sum of all congeners is given as mass-based concentration excluding LOQ, sum parameters presenting toxicological equivalence (TEQ) adjusted contents include the limit of quantification (LOQ) of each congener, following NATO/CCMS [11] and WHO [35] guidelines. The threshold set by the European Biochar Certificate is 20 ng TEQ kg⁻¹ for I-TEQ NATO/CCMS PCDD/F.

	Seagrass 450-10	Seagrass 650-10	Macroalgae_1 650-10	Macroalgae_2 650-10	Tobacco 450-10	Tobacco 600-10	Tobacco 750-10	PVC-Wood 450-20	PVC-Wood 600-20	PVC-Wood 600-10	PVC-Wood-Cond. 600-10
2,3,7,8-TetracDD	<0.18	<0.18	0.59	<0.18	<0.19	<0.19	<0.21	1.1	0.51	0.58	280
1,2,3,7,8-	<0.24	<0.24	0.83	<0.24	<0.25	<0.26	<0.28	1.1	0.73	1.0	440
PentaCDD	<0.48	<0.48	<0.48	<0.48	<0.51	<0.52	<0.56	<0.41	<0.45	<0.44	180
1,2,3,4,7,8-	<0.48	<0.48	<0.48	<0.48	<0.51	<0.52	<0.56	<0.41	<0.45	<0.44	180
HexaCDD	<0.48	<0.48	<0.48	<0.48	<0.51	<0.52	<0.56	<0.41	<0.45	<0.44	180
1,2,3,6,7,8-	<0.48	<0.48	<0.48	<0.48	<0.51	<0.52	<0.56	<0.41	<0.45	<0.44	160
1,2,3,7,8,9-	<0.48	<0.48	<0.48	<0.48	<0.51	<0.52	<0.56	<0.41	<0.45	<0.44	160
HexaCDF	<0.54	<0.54	2.2	<0.54	1.3	5.7	<0.63	<0.46	0.72	1.3	420
1,2,3,4,6,7,8-	<0.54	<0.54	<0.54	<0.54	1.3	5.7	<0.63	<0.46	0.72	1.3	420
HepaCDD	<2.2	<2.2	<2.2	<2.2	4.9	19.9	<2.6	<1.9	<2.1	<2.0	270
OctaCDD	<0.32	<0.32	8.0	<0.32	<0.34	<0.35	<0.37	22	5.4	7.1	4100
2,3,7,8-TetraCDF	<0.44	<0.44	6.0	<0.44	<0.46	<0.47	<0.51	19	5.2	7.8	5500
1,2,3,7,8-PentaCDF	<0.44	<0.44	9.4	<0.44	<0.46	<0.47	<0.51	14	5.2	7.5	5500
2,3,4,7,8-PentaCDF	<0.44	<0.44	6.1	<0.44	<0.42	<0.43	<0.47	6.1	4.5	7.5	5100
1,2,3,4,7,8-	<0.40	<0.40	6.3	<0.40	<0.42	<0.43	<0.47	6.0	4.1	6.6	4500
HexaCDF	<0.40	<0.40	<0.40	<0.40	<0.42	<0.43	<0.47	6.0	4.1	6.6	4500
1,2,3,6,7,8-	<0.40	<0.40	<0.40	<0.40	<0.42	<0.43	<0.47	<1.5	0.68	<0.84	<380
HexaCDF	<0.40	<0.40	<0.40	<0.40	<0.42	<0.43	<0.47	<1.5	0.68	<0.84	<380
1,2,3,7,8,9-	<0.40	<0.40	<0.40	<0.40	<0.42	<0.43	<0.47	<1.5	0.68	<0.84	<380
HexaCDF	0.43	0.41	5.2	<0.40	<0.42	<0.43	<0.47	2.5	1.8	3.4	2500
2,3,4,6,7,8-	0.85	1.2	9.0	<0.38	<0.42	<0.43	<0.47	2.5	1.8	3.4	2500
HexaCDF	<0.38	<0.38	1.6	<0.38	<0.55	0.90	<0.61	3.1	5.9	12	9400
1,2,3,4,6,7,8-	<0.38	<0.38	1.6	<0.38	<0.40	<0.41	<0.44	1.2	0.55	0.79	920
HepaCDF	<3.2	<3.2	<3.2	<3.2	<3.4	<3.5	<3.7	<2.7	<3.0	<2.9	1400
OctaCDF	1.3	1.6	55	0.7	6.1	27	<LOQ	76	35	56	40700
Σ PCDD/F (excl. LOQ)	0.92	0.90	7.3	0.89	0.98	1.1	1.1	11	4.8	6.9	4300
TEQ WHO-PCDD/F	0.90	0.88	8.9	0.87	0.96	1.0	1.1	14	5.6	8.0	5300
I-TEQ NATO/CCMS	0.90	0.88	8.9	0.87	0.96	1.0	1.1	14	5.6	8.0	5300

Chapter 2: Wood ash additives in biochar production and related formation of polychlorinated contaminants

J. Grafmüller et al.

Journal of Analytical and Applied Pyrolysis 183 (2024) 106764

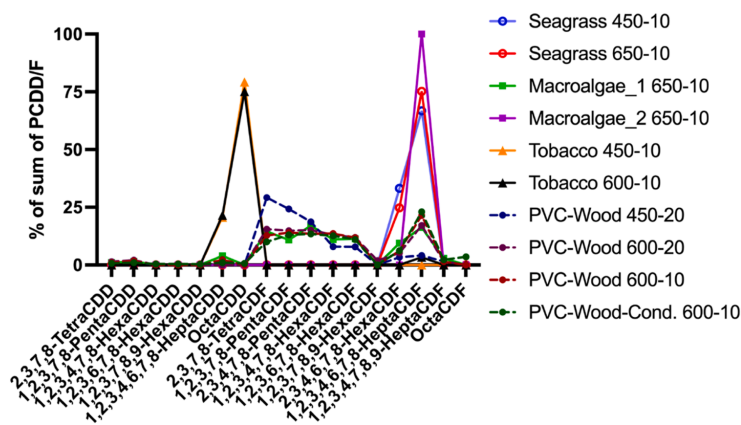


Fig. 2. Sum share of individual congeners of polychlorinated dibenzo-*p*-dioxins and -furans (PCDD/F) in % (w/w). Biochar feedstocks used were seagrass, two samples of macroalgae, tobacco stalks (Tobacco), softwood amended with 10 % (w/w) polyvinylchloride (PVC-Wood), and PVC-Wood pyrolyzed with forced condensation of pyrogas (PVC-Wood-Cond.). The pyrolysis temperature and residence time is indicated in each sample name, in °C and minutes, respectively. Only biochars with at least one quantified congener above the quantification limit were included in the analysis.

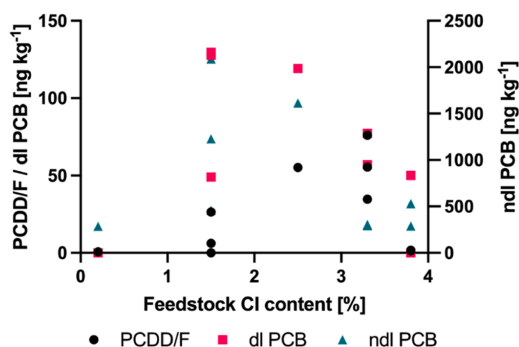


Fig. 3. Mass-based contents (excluding the limit of quantification) of polychlorinated dibenzo-*p*-dioxins and -furans (PCDD/F), dioxin-like polychlorinated biphenyls (dl PCB) and non-dioxin-like PCB (ndl PCB) in biochars plotted over the chlorine (Cl) content in the feedstock. The contents are reported as sum of the contents of all considered congeners in each group. The biochar produced from the PVC-amended softwood with forced pyrogas condensation was excluded from this analysis.

The review of the analysis protocols has shown that a mix-up of samples or cross-contamination could be ruled out. In general, PCDF were present to a higher extent compared to PCDD in the biochars, only the tobacco biochars showed a PCDD/PCDF ratio >1 (Table S4 and Fig. 2). This finding that the pyrolytic conditions favored PCDF formation instead of PCDD formation is in line with literature [46]. Except for the Tobacco biochars, 1,2,3,4,6,7,8-HeptaCDF consistently contributed to a high extent to the mass based PCDD/F content across all biochars (Fig. 2 and Table 3). Within each feedstock, variations in relative contributions by different congeners was relatively low, i.e., independent of the HTT or RT, PCDD/F congeners were present to a similar relative extent in biochars made from the same feedstock, even for the PVC-Wood biochar prepared with forced pyrogas condensation (Fig. 2). The most toxic congener among PCDD/F, which is 2,3,7,8-TCDD, also known as Seveso-Dioxin, only contributed below 1 % to the total sum share of

PCDD/F, if quantified above LOQ (Fig. 2 and Table 3). In previous studies, OctaCDD was the most dominant PCDD/F congener quantified in biochars [22,23], which was not the case for the biochars produced in the present study, except for the Tobacco biochars (Fig. 2).

There was a general trend for higher contents of PCDD/F with increasing Cl contents in the feedstock, however, it was not consistent for all feedstocks, as the Seagrass showed comparable low contents despite the highest Cl content in this feedstock (Fig. 3, Table 1 and Table 3). Still, the highest contamination was found for the biochars produced from the PVC-amended feedstock, which showed the second highest Cl content in the feedstock (3.3 %). The higher contents of PCDD/F for PVC-amended feedstock might further be related to speciation of Cl in the feedstock, for example, covalently bound Cl, as was the case for Cl in PVC, might be more readily available for formation of PCDD/F due to the formation of relevant chlorinated precursors [18,19] compared to Cl bound in ionic form (sea salt) in the biomasses, either via homogeneous or heterogeneous reactions. However, also biochars produced from marine biomass with high contents of Cl present as salts can have comparable higher PCDD/F contents as seen for the Macroalgae_1 650–10 sample (Table 3), which was not a result of feedstock contamination (no PCDD/F were found above LOQ in the Macroalgae_1 feedstock, data not shown and only measured for this feedstock). In general, between 0.01 and 0.5 ppb of feedstock Cl were transferred to PCDD/F in biochars produced under standard pyrolysis conditions where the sum of PCDD/F congeners exceeded the LOQ (Table S5). As Cl contents in the feedstocks increased, a higher number of different congeners was quantified above LOQ in the resulting biochars except for the Seagrass biochars (Figure S5).

The mass-based contents of PCDD/F in the set of biochars produced at 450 °C or between 600 °C and 750 °C did not significantly correlate with the contents of potential catalysts in the feedstocks such as copper [4], ash or other elements listed in Table S1 (Pearson linear correlation coefficient, correlation results not shown).

The high contamination of the PVC-Wood biochar produced under conditions with forced pyrogas condensation (+73800 % mass-based PCDD/F content, PVC-Wood-Cond. 600–10 compared to PVC-Wood 600–10, Table 3), confirmed that a high content of PCDD/F was present in the gas phase in the pyrolysis reactor when pyrolyzing feedstocks with elevated Cl content, either originating from homogeneous formation in the gas phase or from heterogeneous formation on the solids with

Chapter 2: Wood ash additives in biochar production and related formation of polychlorinated contaminants

J. Grafmüller et al.

Journal of Analytical and Applied Pyrolysis 183 (2024) 106764

Table 4

Content (ng kg⁻¹) of the non-dioxin-like polychlorinated biphenyls (ndl PCB) in the biochars produced from the different feedstocks (pyrolysis temperature and residence time in °C and minutes are indicated in the sample names, respectively). Biochar feedstocks used were seagrass, two samples of macroalgae, tobacco stalks (Tobacco), softwood amended with 10 % (w/w) polyvinylchloride (PVC-Wood), and PVC-Wood pyrolyzed with forced condensation of pyrogas (PVC-Wood-Cond.). Contents exceeding the limit of quantification (LOQ) are indicated with bold letters. The sum of all listed congeners is given as mass-based concentration excluding the LOQ and as mass-based concentration including the LOQ plus the mass-based concentration of the dioxin-like PCB118 ($\sum 7$ -PCB, value for PCB118 is given in Table 5). The threshold set by the European Biochar Certificate (EBC) [12] is 2×10^3 ng kg⁻¹ (including LOQ) for $\sum 7$ -PCB.

	Seagrass 450-10	Seagrass 650-10	Macroalgae_1 650-10	Macroalgae_2 650-10	Tobacco 450-10	Tobacco 600-10	Tobacco 750-10	PVC- Wood 450-20	PVC- Wood 600-20	PVC- Wood 600-10	PVC- Wood- Cond. 600-10
PCB 28	94	<80	450	140	350	180	660	<70	<77	<75	240
PCB 52	210	140	800	140	280	160	720	120	130	120	100
PCB 101	230	150	360	<98	250	110	470	170	180	180	220
PCB 138	<72	<72	<72	<72	120	<72	100	<72	<68	<66	470
PCB 153	<120	<120	<120	<120	160	<120	140	<99	<110	<110	220
PCB 180	<30	<30	<30	<30	66	<30	<30	<26	<28	<27	360
\sum ndl	534	290	1610	280	1326	450	2090	290	310	300	1610
PCB (excl. LOQ)											
$\sum 7$ -PCB (incl. LOQ)	796	620	1907	628	1405	706	2206	609	634	630	2410

Table 5

Content (ng kg⁻¹) of 12 dioxin-like polychlorinated biphenyls (dl PCB) in the biochars produced from the different feedstocks (pyrolysis temperature and residence time in °C and minutes are indicated in the sample names, respectively). Biochar feedstocks used were seagrass, two samples of macroalgae, tobacco stalks (Tobacco), softwood amended with 10 % (w/w) polyvinylchloride (PVC-Wood), and PVC-Wood pyrolyzed with forced condensation of pyrogas (PVC-Wood-Cond.). Contents exceeding the limit of quantification (LOQ) are indicated with bold letters. The sum of mass-based concentrations of all congeners are presented excluding the limit of quantification (LOQ) of each congener and the sum of dl PCB considered by the World Health Organization (WHO PCB) [35] expressed in toxicological equivalents (TEQ) are presented including the LOQ of each congener.

	Seagrass 450-10	Seagrass 650-10	Macroalgae_1 650-10	Macroalgae_2 650-10	Tobacco 450-10	Tobacco 600-10	Tobacco 750-10	PVC- Wood 450-20	PVC- Wood 600-20	PVC- Wood 600-10	PVC- Wood- Cond. 600-10
PCB 77	<3.6	<3.6	9.0	<3.6	11	5.0	13	8.2	4.5	7.1	1900
PCB 81	<0.8	<0.8	1.1	<0.8	<0.8	<0.8	<0.8	0.9	<0.8	<0.8	280
PCB 105	9.9	<7.8	25	<7.8	23	11	23	13	9.7	12	570
PCB 114	<0.9	<0.9	2.5	<0.9	1.7	<0.9	<0.9	1.1	<0.9	1.1	75
PCB 118	40	<28	75	<28	79	34	86	52	41	52	800
PCB 123	<0.8	<0.8	1.2	<0.8	<0.8	<0.8	<0.8	<0.7	<0.8	<0.7	87
PCB 126	<1.0	<1.0	3.4	<1.0	<1.0	<1.0	<1.0	2.1	1.8	2.5	1200
PCB 156	<4.4	<4.4	<4.4	<4.4	9.8	<4.4	6.0	<4.4	<4.1	<4.4	550
PCB 157	<0.9	<0.9	0.9	<0.9	1.3	<0.9	<0.9	<0.8	<0.8	<0.8	240
PCB 167	<2.2	<2.2	<2.2	<2.2	4.7	<2.2	<2.2	<2.2	<2.1	2.4	300
PCB 169	<2.4	<2.4	<2.4	<2.4	<2.4	<2.4	<2.4	<2.1	<2.3	<2.2	230
PCB 189	<0.8	<0.8	1.2	<0.8	1.2	<0.8	<0.8	<0.7	<0.8	<0.7	280
\sum dl PCB (excl. LOQ)	50	<LOQ	119	<LOQ	132	49	128	77	57	77	6512
TEQ WHO PCB (incl. LOQ)	0.2	0.2	0.4	0.2	0.2	0.2	0.2	0.3	0.3	0.3	125

subsequent evaporation (Fig. 1). Therefore, avoiding condensation of pyrogas on the solids through proper pyrolysis practice is the key prevention strategy to achieve biochars low in PCDD/F from Cl-rich feedstock. This, in turn, requires proper handling and treatment of the pyrooil and pyrogas, as also observed by Sørmo *et al.* [23], who found >96 % of PCDD/F in the separated pyrolysis oil when balancing across all three products of their pyrolysis (i.e., solid biochar, liquid oil, and pyrogas). We also found an increased contamination with PAH of the biochar produced with forced pyrogas condensation compared to the comparable biochar produced under standard conditions with sufficient heating throughout the whole reactor (23.6 vs. 3.1 mg kg⁻¹, 16 EPA PAH, Table S3). Therefore, to produce biochars low in PAH and PCDD/F, we recommend to design pyrolysis reactors in a way that ensures active

separation of the gas phase from the biochar at sufficiently high temperatures to reduce the risk of contaminant condensation onto biochar, as already proposed in literature for PAH [15,21].

The TEQ adjusted contents of PCDD/F ranged between LOQ and 14 ng TEQ kg⁻¹ (I-TEQ NATO/CCMS) when pyrolysis was performed under standard conditions, i.e., without forced pyrogas condensation (Table 3). With that, all biochars, independent of the Cl content of the feedstock, HTT, and RT were well below the limit value of 20 ng TEQ kg⁻¹ set by the EBC [12] (Table 3). The TEQ adjusted contents followed the same trend as absolute mass-based concentrations when comparing the different biochars with each other (Table 3). Only the Tobacco biochar produced at 600 °C had a mass-based content of PCDD/F congeners in the same order of magnitude as compared to the biochars made

Chapter 2: Wood ash additives in biochar production and related formation of polychlorinated contaminants

J. Grafmüller et al.

Journal of Analytical and Applied Pyrolysis 183 (2024) 106764

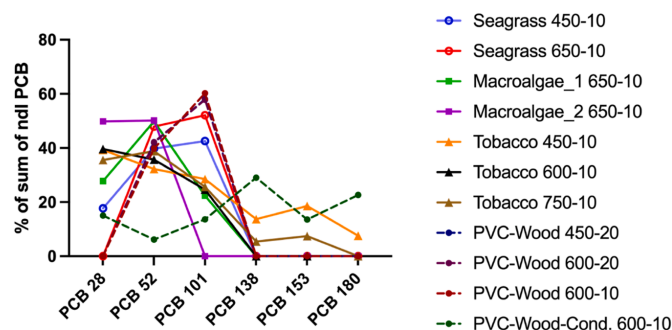


Fig. 4. Sum share of individual congeners of the non-dioxin-like polychlorinated biphenyls (ndl PCB) in % (w/w) calculated as mean value across biochars produced from an individual feedstock. Biochar feedstocks used were seagrass, two samples of macroalgae, tobacco stalks (Tobacco), softwood amended with 10 % (w/w) polyvinylchloride (PVC-Wood), and PVC-Wood pyrolyzed with forced condensation of pyrogas (PVC-Wood-Cond.). The pyrolysis temperature and residence time is indicated in each sample name, in °C and minutes, respectively. Only biochars with at least one quantified congener above the quantification limit were included in the analysis. The sample PVC-Wood 450–20 has a similar congener pattern as PVC-Wood 600–20 and PVC-Wood 600–10 and is therefore barely visible in the graph.

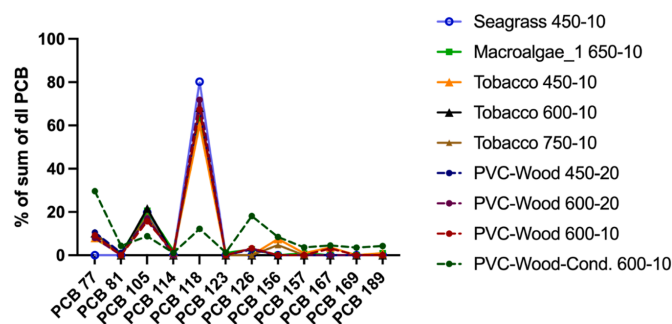


Fig. 5. Sum share of individual congeners of the dioxin-like polychlorinated biphenyls (dl PCB) in % (w/w) calculated as mean value across biochars produced from each individual feedstock. Biochar feedstocks used were seagrass, two samples of macroalgae, tobacco stalks (Tobacco), softwood amended with 10 % (w/w) polyvinylchloride (PVC-Wood), and PVC-Wood pyrolyzed with forced condensation of pyrogas (PVC-Wood-Cond.). The pyrolysis temperature and residence time is indicated in each sample name, in °C and minutes, respectively. Only biochars with at least one quantified congener above the quantification limit were included in the analysis.

from Macroalgae_1 and PVC-Wood, but the TEQ-adjusted content in this biochar was two orders of magnitude lower (Table 3), because PCDD/F were dominated by OctaCDD with a low TEF [47].

The biochar contamination with PCDD/F based on TEQ adjusted contents we investigated is comparable to previous studies [22–24]. Sørmo *et al.* found concentrations below $0.05 \text{ ng TEQ kg}^{-1}$ when feedstocks were pyrolyzed with initial concentrations of $>1\text{--}7 \text{ ng TEQ kg}^{-1}$ [23]. Hale *et al.* found dioxin concentrations in the range of $0.008\text{--}1.2 \text{ ng TEQ kg}^{-1}$ at various HTTs for biomasses with Cl contents below 1 % [22]. We found slightly higher concentrations of PCDD/F compared to these studies, potentially due to the higher Cl contents in our feedstocks, but contents in a similar range were also found by Sobol *et al.*, who did, however, not report Cl contents in the feedstocks used for pyrolysis [24].

3.3.2. Contents of PCB in biochars

The mass-based sum concentrations (excl. LOQ) of ndl PCB ranged between 280 and 2090 ng kg^{-1} (Table 4) and sum concentrations for dl PCB ranged between $<\text{LOQ}$ and 132 ng kg^{-1} for all regularly produced biochars (Table 5). With forced pyrogas condensation, the PVC-Wood biochar had a content of 1610 ng kg^{-1} for ndl PCB and 6512 ng kg^{-1} of dl PCB, i.e., an increase by 437 % and 8360 % was observed,

respectively, compared to the biochar produced under standard pyrolysis conditions (Table 4 and Table 5). The variation in PCB contents in biochars was not linked to the feedstock type but rather to the HTT used for pyrolysis. For the dl PCB, contents decreased with a HTT increase from 450 °C to $600\text{--}650 \text{ °C}$ for Seagrass, Tobacco and PVC-Wood (Table 5). For the ndl PCB, this was only the case for Seagrass and Tobacco, while contents in the PVC-Wood biochars remained unchanged upon the HTT increase (Table 4). A further increase in HTT from 600 °C to 750 °C drastically increased the contents of the ndl and dl PCB in the Tobacco biochar (Table 4 and Table 5).

Independent of the biochar feedstock, the ndl PCB congeners 28, 52 and 101 were present to the highest extent in the category of the 6 ndl PCB in the biochars, while PCB 138, 153 and 180 were only present to a low extent in the biochar produced from Tobacco at 450 °C and 750 °C (Fig. 4 and Table 4). The ndl PCB congeners found in the PVC-Wood biochar produced with forced pyrogas condensation were less dominated by PCB 52 and PCB 101. The remaining PCB congeners were more equally represented in this biochar, which distinguishes this sample from the PVC-Wood biochars produced under regular pyrolysis conditions (Fig. 4). In contrast to our study, Sørmo *et al.* found the congener 153 among the ndl PCB with highest concentrations in their biochars [23].

For the dl PCB, congener 118 made up the highest gravimetric percentage of all congeners quantified in the biochars, followed by PCB 105 and PCB 77 (Fig. 5). All other congeners only had low gravimetric contributions for the different feedstocks (Fig. 5). Again, PVC-Wood pyrolyzed with forced pyrogas condensation differed from the other PVC-Wood biochars: PCB 118 was present in a considerably lower amount in the PVC-Wood-Cond. biochar and PCB 77 as well as PCB 126 were present in a comparable higher relative extent in the PVC-Wood-Cond. biochar (Fig. 5). With that, both for ndl and dl PCB, the spectrum of congeners in the biochar was broadened with forced pyrogas condensation, which is in contrast to the PCDD/F pattern of this biochar, which did not differ from the other PVC-Wood biochars (Fig. 2). In general, the dominance of lighter ndl PCB in biochars produced under regular pyrolysis conditions in this study is different from ndl PCB patterns found globally in soils [1,48] where the heavier ndl PCB congeners 138, 153 and 180 are usually more dominant or compared to other biowaste streams like compost or digestate [23,49], where all ndl PCB congeners, except PCB28, are usually more equally represented.

The mass-based contents of the sum of ndl PCB were positively correlated with the sum of dl PCB ($R^2=0.62$, Figure S6), while there was no consistent linkage between ndl or dl PCB and the mass-based contents of PCDD/F in the biochars (Figure S7). Further, the mass-based contents of ndl and dl PCB were not consistently linked with the Cl contents in the different feedstocks, but contents of dl PCB were generally higher for feedstocks that contained $>1\%$ of Cl (Fig. 3). Between 0.9 and 27 ppb of feedstock Cl were transferred to ndl PCB and between 0.2 and 1.7 ppb were transferred to dl PCB in biochars produced under standard pyrolysis conditions where the sum of PCB congeners exceeded the LOQ (Table S5). The mass-based contents of ndl and dl PCB in the set of biochars produced at 450 °C or between 600 °C and 750 °C did not significantly correlate with the contents of potential catalysts in the feedstocks such as copper [4], ash or other elements listed in Table S1 (Pearson linear correlation coefficient, correlation results not shown).

The TEQ-adjusted contents of dl PCB ranged between $<LOQ$ and $0.4\text{ ng TEQ kg}^{-1}$ for all biochars produced under standard pyrolysis conditions and were increased by forced pyrogas condensation to $125\text{ ng TEQ kg}^{-1}$ (Sample PVC-Wood-Cond. 600–10, Table 5). The highest TEQ-adjusted concentrations were found for biochars produced from Macroalgae_1 and PVC-Wood. The mass-based contents of dl PCB quantified in the PVC-biochars were comparatively low but their TEQ adjusted PCB contents were amongst the highest (Table 5). This finding was mainly due to the presence of the non-ortho-substituted PCB 126 in the PVC-biochars, which has the highest TEF of all dl PCBs [35]. For two of the Tobacco biochars, it was the other way around, i.e., comparatively high gravimetric contents of the dl PCB were quantified but the TEQ-adjusted contents were rather low (Table 5). PCB congener 126 was also quantified in the biochar produced from Macroalgae_1, but not in all the other biochars.

The EBC sets a limit value of $2 \times 10^5\text{ ng kg}^{-1}$ for the sum of ndl PCB (including LOQ) plus the dl PCB118 (summarized as 7-PCB), while there is no limit value for the other dl PCB. This threshold was undershot in all biochars produced by a factor of 90–330, and with that, all biochars would be allowed for soil application independent of the feedstock type and pyrolysis conditions (Table 4). If once the PCDD/F limit value in the EBC is extended by the TEQ-adjusted contents of dl PCB, the threshold of 20 ng TEQ kg^{-1} for the sum PCDD/F and dl PCB would not be exceeded due to the additional contribution of the dl PCB for any biochar produced under standard pyrolysis conditions in this study (Table 3 and Table 5).

4. Conclusions

As contents of PCDD/F and PCB fell below the threshold of the EBC by a minimum of factor 1.5 for PCDD/F and by 90 for PCB, despite the high Cl contents in the investigated feedstocks, there is strong evidence that pyrolysis processes with well-suited process control, i.e., limited

oxygen input to the reactor, ensuring a sufficient separation of solids and gases at the biochar outlet, are not prone to produce biochars with PCDD/F and PCB contents of concern. Still, pyrooil and pyrogas need to be properly handled and treated to ensure work safety and avoid emissions of PCDD/F and PCB to the environment. Based on our results, currently, underused biomass such as macroalgae, seagrass, marine debris and PVC-contaminated biomass waste could be valorized and treated via slow pyrolysis and the produced biochar could be used for soil application, biochar-based materials and carbon sequestration. Our experiments showed, however, that Cl speciation in the biomass affects the extent of PCDD/F and PCB contamination of biochars. Therefore, care should be taken when biomasses are processed with elevated contaminations with PVC, where the Cl covalently-bound to a carbon backbone might be more readily available for PCDD/F and PCB formation compared to Cl present as salt in the biomass. Further, biochars obtained from gasifiers processing Cl enriched feedstocks should be investigated in detail for contaminations, since oxygen is a main component in the formation of PCDD/F and PCB via heterogeneous *de novo* formation. We suggest further research to improve the understanding of interactive PCDD/F and PCB formation reactions at different pyrolysis temperatures and residence times also with different Cl speciation in the feedstocks (salt-bound or covalently-bound Cl). Pyrolysis plants dealing with Cl-rich biomass should neutralize the exhaust gas to avoid corrosion and air pollution, since approximately 20 % of salt-bound and 80 % of polymer-bound Cl initially contained in the feedstocks is released via the pyrolysis gas, most likely as HCl when pyrogases are burnt.

Funding

JG was partly financed within the HyPErFarm project which has received funding from the European Union's Horizon 2020 research and innovation programme under grant agreement no. 101000828. Ithaka Institute was supported within the r4d call of the Swiss National Science Foundation (project Bio-C, grant-No.: IZ08Zo_177346). PVC-biochar production and analysis was part of the CoPyKu2 project funded by the Federal Office for the Environment, Switzerland (UTF 668.16.21).

CRedit authorship contribution statement

Jannis Grafmüller: Writing – original draft, Investigation, Formal analysis. **Dilani Rathnayake:** Writing – review & editing, Investigation. **Nikolas Hagemann:** Writing – review & editing, Investigation, Funding acquisition, Conceptualization. **Thomas D. Bucheli:** Writing – review & editing, Funding acquisition, Conceptualization. **Hans-Peter Schmidt:** Writing – review & editing, Funding acquisition, Conceptualization.

Declaration of Competing Interest

The authors declare the following financial interests/personal relationships which may be considered as potential competing interests: Hans-Peter Schmidt and Nikolas Hagemann report a relationship with Carbon Standards International AG that includes: board membership. If there are other authors, they declare that they have no known competing financial interests or personal relationships that could have appeared to influence the work reported in this paper.

Data availability

Data will be made available on request.

Acknowledgements

We acknowledge Samuel Gogniat for provision of macroalgae, Henriette Tripke and Isabel Hilber for help with seagrass drying. Vinayak Kamra is acknowledged for help with pelleting and pyrolysis

Chapter 2: Wood ash additives in biochar production and related formation of polychlorinated contaminants

J. Grafmüller et al.

Journal of Analytical and Applied Pyrolysis 183 (2024) 106764

work. We thank Severin Neukom for maintenance of the pyrolysis plant. Jonas Geburzi (LEIBNIZ CENTRE for Tropical Marine Research) and Sinnika Lennartz (University of Oldenburg) are acknowledged for assistance with marine biomass identification.

Appendix A. Supporting information

Supplementary data associated with this article can be found in the online version at [doi:10.1016/j.jaap.2024.106764](https://doi.org/10.1016/j.jaap.2024.106764).

References

- [1] P. Schmid, E. Gujer, M. Zennegg, T.D. Bucheli, A. Desaulles, Correlation of PCDD/F and PCB concentrations in soil samples from the Swiss soil monitoring network (NABO) to specific parameters of the observation sites, *Chemosphere* 58 (2005) 227–234, <https://doi.org/10.1016/j.chemosphere.2004.08.045>.
- [2] K. Srogi, Levels and congener distributions of PCDDs, PCDFs and dioxin-like PCBs in environmental and human samples: a review, *Environ. Chem. Lett.* 6 (2008) 1–28, <https://doi.org/10.1007/s10311-007-0105-2>.
- [3] J. Castro-Jiménez, S.J. Eisenreich, M. Ghiani, G. Mariani, H. Skejo, G. Umlauf, J. Wollgast, J.M. Zaldívar, N. Berrojalbiz, H.I. Reuter, J. Dachs, Atmospheric occurrence and deposition of polychlorinated dibenzo-*p*-dioxins and dibenzofurans (PCDD/Fs) in the open mediterranean sea, *Environ. Sci. Technol.* 44 (2010) 5456–5463, <https://doi.org/10.1021/es100718a>.
- [4] B.R. Stanmore, The formation of dioxins in combustion systems, *Combust. Flame* 136 (2004) 398–427, <https://doi.org/10.1016/j.combustflame.2003.11.004>.
- [5] W. Buss, C. Wurzer, J. Shepherd, T.D. Bucheli, *Organic contaminants in biochar. Biochar for Environmental Management: Science, Technology and Implementation*, third ed., Routledge, London, 2024 <https://doi.org/10.4324/9781003297673>.
- [6] H.-P. Schmidt, A. Anca-Couce, N. Hagemann, C. Werner, D. Gerten, W. Lucht, C. Kammann, Pyrogenic carbon capture and storage, *GCB Bioenergy* 11 (2019) 573–591, <https://doi.org/10.1111/gcbb.12553>.
- [7] H.-P. Schmidt, C. Kammann, N. Hagemann, J. Leifeld, T.D. Bucheli, M.A. Sánchez Monedero, M.L. Cayuela, Biochar in agriculture – a systematic review of 26 global meta-analyses, *GCB Bioenergy* 13 (2021) 1708–1730, <https://doi.org/10.1111/gcbb.12889>.
- [8] L. Ye, M. Camps-Arbestain, Q. Shen, J. Lehmann, B. Singh, M. Sabir, Biochar effects on crop yields with and without fertilizer: a meta-analysis of field studies using separate controls, *Soil Use Manag.* 36 (2020) 2–18, <https://doi.org/10.1111/sum.12546>.
- [9] H.-P. Schmidt, N. Hagemann, K. Draper, C. Kammann, The use of biochar in animal feeding, *PeerJ* 7 (2019) e7373, <https://doi.org/10.7717/peerj.7373>.
- [10] M. Legan, A.Z. Gotvajn, K. Zupan, Potential of biochar use in building materials, *J. Environ. Manag.* 309 (2022), <https://doi.org/10.1016/j.jenvman.2022.114704>.
- [11] F.W. Kutz, D.G. Barnes, D.P. Bottimore, H. Greim, E.W. Bretthauer, The international toxicity equivalency factor (I-TEF) method of risk assessment for complex mixtures of dioxins and related compounds, *Chemosphere* 20 (1990) 751–757, [https://doi.org/10.1016/0045-6535\(90\)90178-V](https://doi.org/10.1016/0045-6535(90)90178-V).
- [12] EBC (2012-2023), “European Biochar Certificate - Guidelines for a Sustainable Production of Biochar.” European Biochar Foundation (EBC), Arbaz, Switzerland. (<http://european-biochar.org/>). Version 10.3 from 5th April 2023, (2023).
- [13] Deutsches Bundesamt für Justiz, Bundes-Bodenschutz- und Altlastenverordnung vom 9. Juli 2021 (BGBl. I S. 2598, 2716), 2021.
- [14] Schweizerischer Bundesrat, Verordnung über Belastungen des Bodens (VBBo), 2016.
- [15] Bucheli, et al., Polycyclic aromatic hydrocarbons and polychlorinated aromatic compounds in biochar, in: J. Lehmann, S. Joseph (Eds.), *Biochar for Environmental Management*, second ed., Routledge, 2015, pp. 627–656, <https://doi.org/10.4324/9780203762264> (accessed December 31, 2020).
- [16] 2016, P. Quicker, K. Weber (Eds.), *Biokohle: Herstellung, Eigenschaften und Verwendung von Biomassekarbonisaten*, Springer Vieweg, Wiesbaden.
- [17] N. Hagemann, K. Spokas, H.-P. Schmidt, R. Kägi, M. Böhler, T. Bucheli, Activated carbon, biochar and charcoal: linkages and synergies across pyrogenic carbon’s ABCs, *Water* 10 (2018), <https://doi.org/10.3390/w10020182>.
- [18] J. Yang, Y. Wu, J. Zhu, H. Yang, Y. Li, L. Jin, H. Hu, Insight into the pyrolysis behavior of polyvinyl chloride using in situ pyrolysis time-of-flight mass spectrometry: Aromatization mechanism and Cl evolution, *Fuel* 331 (2023), <https://doi.org/10.1016/j.fuel.2022.125994>.
- [19] H. Meng, J. Liu, Y. Xia, B. Hu, H. Sun, J. Li, Q. Lu, Migration and transformation mechanism of Cl during polyvinyl chloride pyrolysis: the role of structural defects, *Polym. Degrad. Stab.* 224 (2024), <https://doi.org/10.1016/j.polymerdegradstab.2024.110750>.
- [20] W.Y. Shiu, D. Mackay, A critical review of aqueous solubilities, vapor pressures, Henry’s law constants, and octanol–water partition coefficients of the polychlorinated biphenyls, *J. Phys. Chem. Ref. Data* 15 (1986) 911–929, <https://doi.org/10.1063/1.555755>.
- [21] W. Buss, I. Hilber, M.C. Graham, O. Mašek, Composition of PAHs in Biochar and Implications for Biochar Production, *ACS Sustain. Chem. Eng.* 10 (2022) 6755–6765, <https://doi.org/10.1021/acssuschemeng.2c00952>.
- [22] S.E. Hale, J. Lehmann, D. Rutherford, A.R. Zimmerman, R.T. Bachmann, V. Shitumbanuma, A. O’Toole, K.L. Sundqvist, H.P.H. Arp, G. Cornelissen, Quantifying the total and bioavailable polycyclic aromatic hydrocarbons and dioxins in biochars, *Environ. Sci. Technol.* 46 (2012) 2830–2838, <https://doi.org/10.1021/es203984k>.
- [23] E. Sormo, K.M. Krahn, G.O. Flatabo, T. Hartnik, H.P.H. Arp, G. Cornelissen, Distribution of PAHs, PCBs, and PCDD/Fs in products from full-scale relevant pyrolysis of diverse contaminated organic waste, *J. Hazard. Mater.* 461 (2024), <https://doi.org/10.1016/j.jhazmat.2023.132546>.
- [24] L. Sobol, A. Dyjakon, K. Soukup, Dioxins and furans in biochars, hydrochars and torreficates produced by thermochemical conversion of biomass: a review, *Environ. Chem. Lett.* 21 (2023) 2225–2249, <https://doi.org/10.1007/s10311-023-01600-7>.
- [25] J. Grafmüller, A. Böhm, Y. Zhuang, S. Spahr, P. Müller, T.N. Otto, T.D. Bucheli, J. Leifeld, R. Giger, M. Tobler, H.-P. Schmidt, N. Dahmen, N. Hagemann, Wood Ash as an additive in biomass pyrolysis: effects on biochar yield, properties, and agricultural performance, *ACS Sustain. Chem. Eng.* 10 (2022) 2720–2729, <https://doi.org/10.1021/acssuschemeng.1c07694>.
- [26] J. Sun, O. Norouzi, O. Mašek, A state-of-the-art review on algae pyrolysis for bioenergy and biochar production, *Bioresour. Technol.* 346 (2022), <https://doi.org/10.1016/j.biortech.2021.126258>.
- [27] N. Hagemann, H.-P. Schmidt, R. Kägi, M. Böhler, G. Sigmund, A. Maccagnan, C. S. McArdell, T.D. Bucheli, Wood-based activated biochar to eliminate organic micropollutants from biologically treated wastewater, *Sci. Total Environ.* 730 (2020), <https://doi.org/10.1016/j.scitotenv.2020.138417>.
- [28] DIN EN ISO 18134-1:2015-12, Biogene Festbrennstoffe - Bestimmung des Wassergehaltes - Ofentrocknung - Teil 1: Gesamtgehalt an Wasser - Referenzverfahren (ISO 18134-1:2015); Deutsche Fassung EN ISO 18134-1:2015, (2015), <https://doi.org/10.31030/2311530>.
- [29] DIN EN ISO 18122:2016-03, Biogene Festbrennstoffe - Bestimmung des Aschegehaltes (ISO 18122:2015); Deutsche Fassung EN ISO 18122:2015, (2016), <https://doi.org/10.31030/2316155>.
- [30] DIN EN ISO 17294-2:2024-03, Wasserbeschaffenheit - Anwendung der induktiv gekoppelten Plasma-Massenspektrometrie (ICP-MS) - Teil 2: Bestimmung von ausgewählten Elementen einschließlich Uran-Isotope (ISO 17294-2:2023); Deutsche Fassung EN ISO 17294-2:2023, (2024), <https://doi.org/10.31030/3503779>.
- [31] DIN EN ISO 16994:2016-12, Biogene Festbrennstoffe - Bestimmung des Gesamtgehaltes an Schwefel und Chlor (ISO 16994:2016); Deutsche Fassung EN ISO 16994:2016, (2016), <https://doi.org/10.31030/2558210>.
- [32] DIN EN ISO 16948:2015-09, Biogene Festbrennstoffe - Bestimmung des Gesamtgehaltes an Kohlenstoff, Wasserstoff und Stickstoff (ISO 16948:2015); Deutsche Fassung EN ISO 16948:2015, (2015), <https://doi.org/10.31030/2244183>.
- [33] DIN EN ISO 11885:2009-09, Wasserbeschaffenheit - Bestimmung von ausgewählten Elementen durch induktiv gekoppelte Plasma-Atom-Emissionsspektrometrie (ICP-OES) (ISO 11885:2007); Deutsche Fassung EN ISO 11885:2009, (2009), <https://doi.org/10.31030/1530145>.
- [34] DIN EN ISO 10304-1:2009-07, Wasserbeschaffenheit - Bestimmung von gelösten Anionen mittels Flüssigkeits-Ionenchromatographie - Teil 1: Bestimmung von Bromid, Chlorid, Fluorid, Nitrat, Nitrit, Phosphat und Sulfat (ISO 10304-1:2007); Deutsche Fassung EN ISO 10304-1:2009, (2009), <https://doi.org/10.31030/1518948>.
- [35] M. Van Den Berg, L.S. Birnbaum, M. Denison, M. De Vito, W. Farland, M. Feeley, H. Fiedler, H. Hakansson, A. Hanberg, L. Haws, M. Rose, S. Safe, D. Schrenk, C. Tohyama, A. Tritscher, J. Tuomisto, M. Tysklind, N. Walker, R.E. Peterson, The 2005 World Health Organization reevaluation of human and mammalian toxic equivalency factors for dioxins and dioxin-like compounds, *Toxicol. Sci.* 93 (2006) 223–241, <https://doi.org/10.1093/toxsci/kf055>.
- [36] H. Gonzalez, L. Brüggemann, Heavy metals in sediments of Matanzas Bay, Cuba, *Chem. Ecol.* 4 (1989) 37–46, <https://doi.org/10.1080/02757548908035961>.
- [37] V. Van Ginneken, E. De Vries, Seaweeds as biomonitoring system for heavy metal (HM) accumulation and contamination of our oceans, *Am. J. Plant Sci.* 09 (2018) 1514–1530, <https://doi.org/10.4236/ajps.2018.97111>.
- [38] B. Cao, Y. Sun, J. Guo, S. Wang, J. Yuan, S. Esakimuthu, B. Bernard Uzojejinwa, C. Yuan, A.E.-F. Abomohra, L. Qian, L. Liu, B. Li, Z. He, Q. Wang, Synergistic effects of co-pyrolysis of macroalgae and polyvinyl chloride on bio-oil/bio-char properties and transferring regularity of chlorine, *Fuel* 246 (2019) 319–329, <https://doi.org/10.1016/j.fuel.2019.02.037>.
- [39] J.A. Ippolito, L. Cui, C. Kammann, N. Wrage-Mönnig, J.M. Estavillo, T. Fuertes-Mendizabal, M.L. Cayuela, G. Sigua, J. Novak, K. Spokas, N. Borchard, Feedstock choice, pyrolysis temperature and type influence biochar characteristics: a comprehensive meta-data analysis review, *Biochar* (2020), <https://doi.org/10.1007/s42773-020-00067-x>.
- [40] M.-Y. Wey, W.-Y. Ou, Z.-S. Liu, H.-H. Tseng, W.-Y. Yang, B.-C. Chiang, Pollutants in incineration flue gas, *J. Hazard. Mater.* 82 (2001) 247–262, [https://doi.org/10.1016/S0304-3894\(00\)00355-1](https://doi.org/10.1016/S0304-3894(00)00355-1).
- [41] H. Kuramochi, D. Nakajima, S. Goto, K. Sugita, W. Wu, K. Kawamoto, HCl emission during co-pyrolysis of demolition wood with a small amount of PVC film and the effect of wood constituents on HCl emission reduction, *Fuel* 87 (2008) 3155–3157, <https://doi.org/10.1016/j.fuel.2008.03.021>.
- [42] B. Singh, M. Mei Dolk, Q. Shen, M. Camps-Arbestain, *Biochar pH, electrical conductivity and liming potential*, in: *Biochar: A Guide to Analytical Methods*, CSIRO Publishing, Clayton, Victoria, 2017, pp. 10–23.
- [43] Bundesgütegemeinschaft Kompost, *Schwellenwerte und Grenzwerte*, (2023). (https://www.kompost.de/fileadmin/user_upload/Dateien/Guetesicherung/Do_kumente_Kompost/Dok_251-006-4_Schwellen_Grenzwerte.pdf) (accessed June 12, 2024).

Chapter 2: Wood ash additives in biochar production and related formation of polychlorinated contaminants

J. Grafmüller et al.

Journal of Analytical and Applied Pyrolysis 183 (2024) 106764

- [44] Landwirtschaftskammer Salzburg, Wirtschaftsdünger: Anfall, Lagerung, Verwertung, Umwelt, (2009). (https://www.infothek-biomasse.ch/images/205_2009_IK_Hofduenger_naehrstoffe_AUT.pdf) (accessed June 12, 2024).
- [45] C.-M. Geilfus, Review on the significance of chlorine for crop yield and quality, *Plant Sci.* 270 (2018) 114–122, <https://doi.org/10.1016/j.plantsci.2018.02.014>.
- [46] M. Altarawneh, B.Z. Dlugogorski, E.M. Kennedy, J.C. Mackie, Mechanisms for formation, chlorination, dechlorination and destruction of polychlorinated dibenzo-p-dioxins and dibenzofurans (PCDD/Fs), *Prog. Energy Combust. Sci.* 35 (2009) 245–274, <https://doi.org/10.1016/j.pecs.2008.12.001>.
- [47] P.R.S. Kodavanti, J. Valdez, J.-H. Yang, M. Curras-Collazo, B.G. Loganathan, Polychlorinated Biphenyls, Polybrominated Biphenyls, Polychlorinated Dibenzop-dioxins, and Polychlorinated Dibenzofurans. *Reproductive and Developmental Toxicology*, Elsevier, 2017, pp. 711–743, <https://doi.org/10.1016/B978-0-12-804239-7.00039-1>.
- [48] S.N. Meijer, W.A. Ockenden, A. Sweetman, K. Breivik, J.O. Grimalt, K.C. Jones, Global distribution and budget of PCBs and HCB in background surface soils: implications for sources and environmental processes, *Environ. Sci. Technol.* 37 (2003) 667–672, <https://doi.org/10.1021/es025809l>.
- [49] R.C. Brändli, T.D. Bucheli, T. Kupper, R. Furrer, W.A. Stahel, F.X. Stadelmann, J. Tarradellas, Organic pollutants in compost and digestate.: Part 1. Polychlorinated biphenyls, polycyclic aromatic hydrocarbons and molecular markers, *J. Environ. Monit.* 9 (2007) 456–464, <https://doi.org/10.1039/B617101J>.

**Supplementary Information to:
Biochars from chlorine-rich feedstock are low in polychlorinated dioxins, furans and biphenyls**

Jannis Grafmüller^{1,2,3}, Dilani Rathnayake^{1,4, 5}, Nikolas Hagemann^{1,4}, Thomas D. Bucheli⁴ and Hans-Peter Schmidt¹

¹Ithaka Institute, Arbaz (Switzerland) and Goldbach (Germany)

²Faculty of Process Engineering and Institute for Sustainable Energy Systems (INES), Offenburg University of Applied Sciences, Germany

³Plant Biogeochemistry, Tübingen University, Tübingen, Germany

⁴Environmental Analytics, Agroscope, Zurich, Switzerland

⁵Climate and Agriculture, Agroscope, Zurich, Switzerland

Supplementary information related to this chapter can be found under the following link on the publisher website: <https://doi.org/10.1016/j.jaap.2024.106764>
or directly under: <https://ars.els-cdn.com/content/image/1-s2.0-S0165237024004194-mmcl.pdf>

Chapter 3a

Root-zone amendments of biochar-based fertilizers: yield increases of white cabbage in temperate climate

Jannis Grafmüller^{1,2,3}, Hans-Peter Schmidt³, Daniel Kray¹ and Nikolas Hagemann^{2,3,4}

¹Institute of Sustainable Energy Systems and Institute of Process Engineering, Offenburg University of Applied Sciences, Offenburg Germany

²Ithaka Institute gGmbH, Goldbach, Germany; hagemann@ithaka-institut.org

³Ithaka Institute, Arbaz, Switzerland; schmidt@ithaka-institut.org

⁴Environmental Analytics, Agroscope Reckenholz, Zurich, Switzerland

Published in:

Horticulturae

First published: 5th April 2022

<https://doi.org/10.3390/horticulturae8040307>

Material from:

J. Grafmüller, H.-P. Schmidt, D. Kray, N. Hagemann, Root-Zone Amendments of Biochar-Based Fertilizers: Yield Increases of White Cabbage in Temperate Climate, Horticulturae 8 (2022) 307. <https://doi.org/10.3390/horticulturae8040307>.

The published article is re-printed in this thesis with permission from MDPI. The right to include the article in its published form in a thesis or dissertation is retained by the authors in accordance with MDPI Copyright and Licensing regulations.

Statement of personal and co-author contributions, plus non-listed contributors

Authors	Position of candidate in list of authors	Scientific ideas by the author [%]	Data generation by the author [%]	Analysis and interpretation by the author [%]	Paper writing done by the author [%]
Jannis Grafmüller	1	35	80	65	55
Hans-Peter Schmidt	2	20	0	10	15
Daniel Kray	3	20	0	10	15
Nikolas Hagemann	4	20	0	10	15
Contribution by other parties not listed as authors (e.g., commercial analysis laboratories, student assistants)					
Sara Cebulla		0	20	5	0
Bernhard Bauer		5	0	0	0
Publication status	published				
Explanations	The experiment was conceptualized by all co-authors and me. Alois Huber and Andreas Harlander from Krinner GmbH Agri-Photovoltaic division provided me with the soil for the plant growth study. Bernhard Bauer from Weihenstephan-Triesdorf University of Applied Sciences supported me with calculation of plant nutrient demand before the experiment. The experimental work was mainly conducted by me with support from Sara Cebulla during plant harvest and establishment of the Shovelomics method in our lab. Further, Barbara Anders from Offenburg University of Applied Sciences assisted during ascorbic acid quantification. The data analysis was performed by me and I wrote the first draft of the manuscript and all co-authors improved its quality.				



Article

Root-Zone Amendments of Biochar-Based Fertilizers: Yield Increases of White Cabbage in Temperate Climate

Jannis Grafmüller ^{1,2,3,4,*}, Hans-Peter Schmidt ⁴, Daniel Kray ^{1,2} and Nikolas Hagemann ^{3,4,5,*}

¹ Institute of Sustainable Energy Systems, Offenburg University of Applied Sciences, 77652 Offenburg, Germany; daniel.kray@hs-offenburg.de

² Institute of Process Engineering, Offenburg University of Applied Sciences, 77652 Offenburg, Germany

³ Ithaka Institute gGmbH, 63773 Goldbach, Germany

⁴ Ithaka Institute, 1974 Arbaz, Switzerland; schmidt@ithaka-institut.org

⁵ Environmental Analytics, Agroscope Reckenholz, 8046 Zurich, Switzerland

* Correspondence: jannis.grafmueller@hs-offenburg.de (J.G.); hagemann@ithaka-institut.org (N.H.)

Abstract: The use of biochar is an important tool to improve soil fertility, reduce the negative environmental impacts of agriculture, and build up terrestrial carbon sinks. However, crop yield increases by biochar amendment were not shown consistently for fertile soils under temperate climate. Recent studies show that biochar is more likely to increase crop yields when applied in combination with nutrients to prepare biochar-based fertilizers. Here, we focused on the root-zone amendment of biochar combined with mineral fertilizers in a greenhouse trial with white cabbage (*Brassica oleracea* convar. Capitata var. Alba) cultivated in a nutrient-rich silt loam soil originating from the temperate climate zone (Bavaria, Germany). Biochar was applied at a low dosage (1.3 t ha⁻¹). The biochar was placed either as a concentrated hotspot below the seedling or it was mixed into the soil in the root zone representing a mixture of biochar and soil in the planting basin. The nitrogen fertilizer (ammonium nitrate or urea) was either applied on the soil surface or loaded onto the biochar representing a nitrogen-enhanced biochar. On average, a 12% yield increase in dry cabbage heads was achieved with biochar plus fertilizer compared to the fertilized control without biochar. Most consistent positive yield responses were observed with a hotspot root-zone application of nitrogen-enhanced biochar, showing a maximum 21% dry cabbage-head yield increase. Belowground biomass and root-architecture suggested a decrease in the fine root content in these treatments compared to treatments without biochar and with soil-mixed biochar. We conclude that the hotspot amendment of a nitrogen-enhanced biochar in the root zone can optimize the growth of white cabbage by providing a nutrient depot in close proximity to the plant, enabling efficient nutrient supply. The amendment of low doses in the root zone of annual crops could become an economically interesting application option for biochar in the temperate climate zone.

Keywords: PyCCS; pyrogenic carbon capture and storage; nitrogen fertilizer; root architecture; Shovelomics



Citation: Grafmüller, J.; Schmidt, H.-P.; Kray, D.; Hagemann, N. Root-Zone Amendments of Biochar-Based Fertilizers: Yield Increases of White Cabbage in Temperate Climate. *Horticulturae* **2022**, *8*, 307. <https://doi.org/10.3390/horticulturae8040307>

Academic Editor: Xun Li

Received: 9 March 2022

Accepted: 1 April 2022

Published: 5 April 2022

Publisher's Note: MDPI stays neutral with regard to jurisdictional claims in published maps and institutional affiliations.



Copyright: © 2022 by the authors. Licensee MDPI, Basel, Switzerland. This article is an open access article distributed under the terms and conditions of the Creative Commons Attribution (CC BY) license (<https://creativecommons.org/licenses/by/4.0/>).

1. Introduction

Biochar is the solid product of biomass pyrolysis. Over the past two decades, it has attracted scientific attention as a beneficial soil amendment and as a carbon sink [1,2]. In soil, biochar can, e.g., improve water and nitrogen (N) use efficiencies, the root growth of plants, and reduce soil-borne N₂O emissions, thus contributing to both climate change adaptation and mitigation [2,3]. While environmental benefits are desirable and adaptation strategies are desperately needed in agriculture, mainstreaming biochar application will only succeed at a sufficient pace when farmers experience direct benefits, e.g., increases in crop yield. Global meta-analyses show that biochar amendment with or without fertilizer can increase crop yields compared to the fertilized control by 10% on average or by up to 25% when biochar is combined with mineral fertilizer compared to the fertilized control [4,5]. Biochar

can also provide crop yield increases when applied to the soil at low application rates in the range of 1 t ha^{-1} as a carrier for nutrients, which is termed as a biochar-based fertilizer [6,7]. However, crop yield increases after the amendment of biochar or biochar based-fertilizers have only been systematically achieved in soils under tropical or subtropical climate but rarely in soils in the continental and humid-temperate climate zone with a mean annual temperature lower than $10 \text{ }^\circ\text{C}$ [4]. Still, to the best of our knowledge, there is no evidence that biochar-based fertilization in general cannot increase crop yields under such climatic conditions. Thus, further research is needed to study the effect of different application modes of biochar-based fertilizers in soils under temperate climate.

Despite the large number of studies on different formulations of biochar-based (slow-release) fertilizers [7–11], there are no studies to our knowledge that have compared different types of biochar positionings in the field/pot; thus, this factor could not be investigated so far in any meta-analysis. Mostly, biochar or the biochar-based fertilizer was spread homogeneously onto the field and incorporated into the soil by (minimal) tillage. However, this approach results in low biochar concentrations in close proximity to the plant, when economically feasible amounts (e.g., $<2 \text{ t ha}^{-1}$) are amended to the soil. As a contrast, the root-zone amendment of biochar-based fertilizers was proposed as a beneficial strategy, since the biochar is placed where most of the plant roots are present, which allows a targeted and effective fertilization (Figure 1) [6,12]. Studies that applied biochar-based fertilizers in the root zone of annual crops prepared them by physical mixing of the biochar with nutrient-dense liquids or solids, achieving crop-yield increases independent of the crop that was cultivated in tropical and temperate/alpine climate zones [6,12–16]. Still, to date, no study has systematically investigated the combined effects of different types of biochar root-zone amendments and different mineral N compounds on the impact of biochar-based fertilization on plant productivity and root growth response, which is the focus of this study. Furthermore, we test whether biochar-based fertilization based on a priori mixing of biochar with N fertilizer (N-enhanced biochar) is superior to the soil amendment of pure biochar combined with a regular soil-surface N fertilization. We therefore conducted a greenhouse trial with white cabbage, applying two different types of root-zone amendments of low-dosed biochar (1.3 t ha^{-1}) with a combination of the above-mentioned experimental factors and two different N fertilizers to study the transferability of the results to different N fertilizer compounds. The aboveground biomass yields were analyzed and the root architecture of the plants was studied with the REST Shovelomics software to observe a potential effect of different root-zone amendments and N fertilization methods on root growth [17]. The Shovelomics approach allows one to characterize the architecture of rootstocks, which was previously successively applied in a study to evaluate differences in the root architecture of maize plants following a root-zone amendment of biochar in a tropical soil [18]. With this study, we aim to contribute to the understanding of new strategies in biochar-based fertilization, focusing on fertile soils in the temperate climate zone and their effects on crop yields and root development.

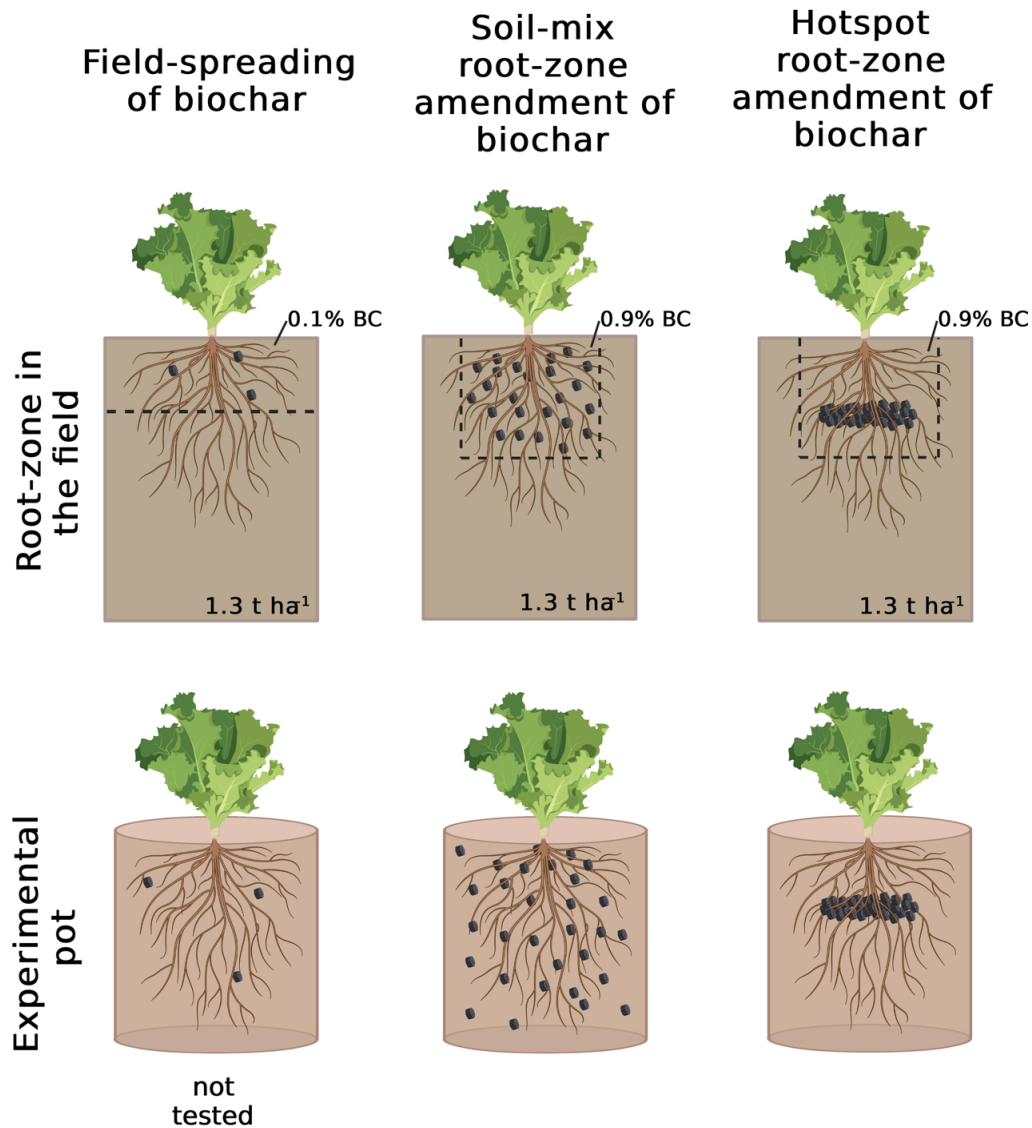


Figure 1. Illustrative comparison of the homogeneous field spreading of 1.3 tons of biochar (BC) per hectare (**left column**) with the two tested methods to prepare BC root-zone amendments in this study: soil-mix root-zone amendment (**middle column**) and hotspot root-zone amendment of BC (**right column**). For the homogeneous BC field spreading, the shown local BC weight concentration is based on an assumed soil bulk density of 1.3 t m^{-3} and an incorporation depth of biochar in the upper 10 cm. The local BC concentration in the soil-mix root-zone amendment of 0.9% was used in the greenhouse trial. The amount of BC applied per pot resulted from dividing the total amount of 1.3 t of BC applied per hectare by the number of plants growing per hectare (40,000). The graphic was created with BioRender.com (accessed on 4 March 2022).

2. Materials and Methods

2.1. Biochar Origin and Further Processing

Biochar was provided by Carbon Cycle GmbH & Co. KG (Rieden, Germany) and produced from untreated wood chips. The pyrolysis process was performed with a maximum temperature of 750 °C in an electrically heated vertical moving bed reactor (Carbon Technik Schuster GmbH, Dischingen, Germany). The biochar used was certified according to the European Biochar Certificate (Certification class AgroOrganic) [19], and a detailed analysis is provided in Table S1. After pyrolysis, biochar was milled with a hammer mill (Model HM420B with 11 kW and 12 mm sieve, Evertch GmbH, Rodgau, Germany) and stored in fabric bags until further processing.

2.2. Combining Biochar and N Fertilizer

All chemicals were of analytical grade (Carl Roth GmbH, Karlsruhe, Germany), and solutions were prepared with de-ionized (DI) water. To prepare N-enhanced biochar, 32 g of dry matter (DM) equivalent biochar (88% DM content) was mixed with 45 mL of ammonium nitrate or urea solution (54 g N L⁻¹) to achieve 80% of its water holding capacity (WHC = 1.8 mL g⁻¹) and an additional N content of 78 mg N (g char)⁻¹. The mixture was stored for 3 days at room temperature in a closed glass jar.

2.3. Greenhouse Trial

The pot trial was comprised of 11 treatments (Table 1) and was conducted for 70 days from 5th of July to 13th of September 2021 in a greenhouse with east–west orientation located in Offenburg, Germany. The treatment with ID11 had to be dismissed due to an error that occurred during fertilization (Table 1). A silt loam topsoil originating from Straßkirchen (Bavaria, Germany) was used, on which grass for hay harvest was grown and which received mineral fertilization in the years before. The soil contained high levels of available phosphorus (P), potassium (K), and magnesium (Mg), and a detailed soil analysis conducted by Eurofins Umwelt Ost GmbH (Jena, Germany) is provided in Tables S2–S4. White cabbage (variety Sunta F1, Bruno Nebelung GmbH, Everswinkel, Germany) was preplanted for 20 days in growing media. Five replicate pots were prepared for each treatment and arranged into a randomized complete block design. The pots were repositioned at random within each block on a weekly basis. The biochar and fertilizer dosages were calculated per pot, assuming a biochar application rate of 1.3 t ha⁻¹ (32 g biochar plant⁻¹) and a N fertilization rate of 100 kg N ha⁻¹ (2.5 g N plant⁻¹) with an assumed plant density of 40,000 plants ha⁻¹.

Table 1. Treatments prepared for the greenhouse trial with a three-factorial experimental setup: type of nitrogen (N) fertilizer, type of biochar (BC) root-zone amendment (none, hotspot, or soil-mix application), and the type of N fertilization method (N fertilization via N-enhanced biochar or soil-surface N fertilization). n.a.: not applicable.

Treatment ID	Nitrogen Fertilizer	Type of Biochar Root-Zone Amendment	Nitrogen Fertilization Method
1	none	none	n.a.
2	NH ₄ NO ₃	none	soil-surface fertilization
3	NH ₄ NO ₃	Hotspot	N-enhanced biochar
4	NH ₄ NO ₃	Hotspot	soil-surface fertilization
5	NH ₄ NO ₃	Soil-Mix	N-enhanced biochar
6	NH ₄ NO ₃	Soil-Mix	soil-surface fertilization
7	Urea	none	soil-surface fertilization
8	Urea	Hotspot	N-enhanced biochar
9	Urea	Hotspot	soil-surface fertilization
10	Urea	Soil-Mix	N-enhanced biochar
11 ^a	Urea	Soil-Mix	soil-surface fertilization

^a This treatment had to be dismissed due to organizational issues.

Pots with a volume of 4 L (21 cm height, 17 cm inner diameter at the top) were initially filled with 2590 g of DM equivalent soil (88% DM content at trial setup) and compacted by knocking on a table three times. For the treatments without biochar amendments, one seedling per pot was placed onto this amount of soil, which was properly enclosed by another 890 g of DM equivalent of soil. Two different root-zone amendments of biochar were conducted: a biochar–soil mix and the concentrated hotspot biochar root-zone amendment (Figure 1). In the pots for the soil-mix root-zone amendment of biochar, 3480 g of DM equivalent of soil was mixed with 32 g of DM equivalent of N-enhanced or pure biochar, and the above-described planting procedure was conducted in the same way. The soil-mix root-zone amendment represented a mixture of biochar and the soil in the planting basin in the field (Figure 1). In the treatments with hotspot biochar amendment, a cylinder with 8 cm diameter and 1 cm height was formed in the middle of the first portion of soil in which the biochar was subsequently placed (10 cm below soil surface). The biochar was then covered with a 1 cm soil layer of the remaining soil before the seedling was planted (Figure S1). Pots were stepwise (50 mL) watered to 65% of their WHC with well water, according to previous quantification of soil and biochar WHC. During the experiment, pots were watered daily with a fixed amount of water through a drip line (Figure S2). The daily water supply was adapted, if necessary, once a week after all pots were manually re-watered to 65% of maximum WHC. The soil in each pot was covered with 50 g of quartz sand to allow a homogeneous distribution of water from the drip line during the experiment (Figure S2).

Three days after planting, 100 mL of a nutrient solution was injected by means of a medical syringe in 2 cm soil depth at 8 different spots in the pot. Each plant received 2.5 g of N as ammonium nitrate or urea, 0.9 g of potassium as tri-potassium citrate, 1.0 g of sodium and 0.7 g sulfur as sodium sulfate, and 1.0 g of calcium as calcium acetate. The solution was prepared without additional N for the treatments with N-enhanced biochar. Phosphorus was not fertilized, since the soil already contained 35 mg of available P (100 g)^{−1} (Table S2).

2.4. Aboveground Biomass Harvest and Data Collection

After 69 days, dimensionless chlorophyll content was determined non-destructively with a handheld spectrophotometer (SPAD-502Plus, Konica Minolta, Marunouchi, Japan) on the three outer leaves of each plant. On the next day, total aboveground biomass was measured after cutting the stem at the lowest leaf base. The cabbage head was weighed after separating the outer protruding, nonmarketable leaves with a knife (Figure S3). The diameter of the cabbage head was measured by means of a caliper with 1 mm accuracy to calculate the head volume by assuming the geometry of an ellipsoid. Subsequently, the whole cabbage heads were manually rasped and homogenized manually to allow for better drying conditions and preparation of representative subsamples. An aliquot (40 g) was dried at 105 °C to a constant weight to calculate the dry matter content of aboveground biomass. A 20 g aliquot was immediately stored at −18 °C for the analysis of vitamin C content.

2.5. Belowground Biomass Analysis

Pots were overthrown into a cold-water bath and left for five minutes to enable an easier removal of soil particles from the roots. The soil was gently removed from the rootstocks by hand and shaking the rootstock inside the water bath to further pre-clean the roots. Each rootstock was separated into two halves by cutting the stem lengthwise with a knife. Each pre-cleaned half was washed under a stream of tap water for another 15 min, and all visible soil particles were removed. The rootstocks were stored in water to keep them moistened until photographs were taken from one half of the rootstock per plant within two days after washing.

Rootstocks were fixed in a sample holder in front of a black background in order to generate high-contrast images (Figure S4). The pictures were taken in a completely darkened room with two soft boxes to uniformly illuminate the samples from the left and right side, respectively. A Canon EOS 70D with an EF-S 18–55 mm objective (Canon AG,

Tokyo, Japan) was positioned on a tripod and used at a focal length of 35 mm, 0.8 s exposure time, and an f -number of $f/6.3$ in self-timer mode to avoid wiggling of the images. All camera settings, positions of lighting equipment, and distances of the samples relative to the camera and the black background were kept constant for all images. Unprocessed images were evaluated with the open-source software “Root Estimator for Shovelomics Traits” (REST), designed and presented in detail by Colombi and colleagues [17]. The root area, total projected structure lengths, and root fill factors were evaluated.

2.6. Vitamin-C Quantification

The content of vitamin C (L-(+)-ascorbic acid) in the cabbage-head biomass was estimated by iodometric titration [20]. In short, a subsample of the frozen cabbage head was extracted with DI water, and the extract was titrated with a potassium iodide and iodine solution by using a starch indicator solution. A detailed description of the procedure is provided in the Supporting Information (SI).

2.7. Data Analysis

The effects of all three factors (type of biochar root-zone amendment, N-fertilizer type, and N-fertilization method) were determined using three-way analysis of variance (ANOVA). When including the controls without biochar amendments, the interaction of the type of root-zone amendment and the N-fertilization method was not evaluable, since N fertilization via a N-enhanced biochar could not be performed without a biochar amendment. Therefore, ANOVA was also conducted for the biochar treatments alone to estimate the effect of this interaction. Means for different factor levels were compared at $p < 0.05$ using the Tukey HSD test or Student’s t -test (for comparison of only two means). Due to organizational issues, the treatment with soil-mixed biochar root-zone amendment and soil-surface urea fertilization had to be dismissed (treatment ID11, Table 1). Therefore, the pot trial represents a part-factorial experimental setup. To correct the unbalance in the experimental design, data are shown as least square means when data were averaged over a specific experimental factor. All statistical analysis was performed using JMP 10 (SAS Institute Inc., Cary, NC, USA).

3. Results and Discussion

3.1. Aboveground Biomass Yields

Fresh cabbage-head yields ranged within 200 and 270 g plant⁻¹ for the different treatments (Table 2). These rather low cabbage-head yields may be explained by the rather low N-fertilization rate (2.5 g N plant⁻¹) and the circumstance that the plants were grown in pots and not in the field with more space for root development. In general, the presence of a N fertilizer significantly increased aboveground biomass yields, which was reflected by the control without N fertilization, which yielded the lowest aboveground biomass and did not produce a cabbage head (Table 2). The increase in dry cabbage-head biomass averaged over all biochar amendments compared to the fertilized control without biochar was 12% ($p = 0.09$). The highest yield increase of dry cabbage-head biomass compared to the respective control was achieved with the NH₄NO₃ fertilizer with a hotspot pure-biochar amendment and additional soil-surface N fertilization (24% head yield increase) and for urea when the N-enhanced biochar was amended as a hotspot (14% head yield increase, Figure 2B). Still, for both N fertilizers, the amendment of a N-enhanced biochar as a hotspot in the root zone consistently provided high cabbage-head yield increases compared to the equally fertilized control without biochar (Figure 2). While the application of the N fertilizer loaded onto biochar provided head yield increases in all tested treatments, soil-surface fertilization with urea combined with a hotspot pure-biochar amendment had no effect on head yield increases compared to the urea fertilized no-biochar control (Figure 2).

Table 2. Aboveground biomass yields and parameters based on fresh matter (FM) and dry matter (DM) of cabbage plants for all treatments. The cabbage-head ratio presents the mass ratio of the cabbage head compared to the total aboveground biomass including the non-marketable part of the plant (based on DM). SPAD values present a proxy for the chlorophyll content in the plant tissue. Treatment identifiers refer to the explanations in Table 1. Errors are presented as standard errors of the mean ($n = 5$). Different letters within a column indicate a statistically significant difference between individual treatments (at $p < 0.05$, Tukey HSD post hoc test). n.a.: not applicable.

Treatment	Aboveground Biomass (FM)	Cabbage Heads (FM)	Aboveground Biomass (DM)	Cabbage-Head Ratio (DM)	Cabbage-Head Volume	SPAD	Vitamin C Content in Head Biomass	Dry Root Biomass
	g	g	g	wt%	cm ³		(mg(100 g) ⁻¹)	g
1: No N-Fert., no BC NH₄NO₃-Fertilizer	106.1 ± 6.9 b	n.a.	17.5 ± 1.5 b	n.a.	n.a.	48.0 ± 1.7 a	n.a.	1.4 ± 0.1 a
2: no BC-Control	430.9 ± 34.5 a	206.8 ± 32.5 a	29.4 ± 0.8 a	47.0 ± 4.0 b	2270.5 ± 313.1 a	53.6 ± 1.9 a	7.1 ± 0.2 a	1.4 ± 0.3 a
3: BC-Hotspot, N-enhanced BC	465.5 ± 5.4 a	271.7 ± 7.0 a	28.5 ± 0.9 a	58.4 ± 1.3 a	2874.1 ± 133.2 a	54.0 ± 1.7 a	7.4 ± 0.7 a	1.3 ± 0.1 a
4: BC-Hotspot, pure BC	470.9 ± 15.3 a	263.6 ± 8.1 a	30.8 ± 0.7 a	56.0 ± 0.9 ab	2803.5 ± 134.3 a	54.8 ± 1.7 a	8.5 ± 0.3 a	1.5 ± 0.1 a
5: BC-mixed, N-enhanced BC	436.9 ± 9.5 a	227.5 ± 7.0 a	29.2 ± 0.5 a	52.1 ± 1.1 ab	2420.3 ± 81.5 a	54.3 ± 1.7 a	7.0 ± 0.1 a	1.6 ± 0.2 a
6: BC-mixed, pure BC Urea-Fertilizer	465.1 ± 21.3 a	246.1 ± 12.6 a	30.9 ± 1.5 a	53.1 ± 2.3 ab	2464 ± 142.2 a	53.9 ± 1.7 a	8.1 ± 0.9 a	1.6 ± 0.2 a
7: no BC-Control	452.1 ± 10.5 a	236.8 ± 5.8 a	29.2 ± 0.6 a	52.4 ± 1.3 ab	2401.1 ± 106.5 a	54.5 ± 2.8 a	7.8 ± 0.4 a	1.4 ± 0.1 a
8: BC-Hotspot, N-enhanced BC	447.5 ± 4.6 a	258.9 ± 8.7 a	30.04 ± 0.9 a	57.8 ± 1.4 a	2691.8 ± 88.8 a	56.9 ± 2.8 a	8.0 ± 0.2 a	1.5 ± 0.1 a
9: BC-Hotspot, pure BC	433.7 ± 21.6 a	234.1 ± 21.5 a	27.9 ± 1.2 a	53.8 ± 3.5 ab	2557.3 ± 296.6 a	54.0 ± 1.2 a	7.7 ± 0.5 a	1.4 ± 0.1 a
10: BC-mixed, N-enhanced BC	439.5 ± 7.7 a	259.3 ± 7.9 a	27.9 ± 1.1 a	59.0 ± 1.1 a	2615.0 ± 195.3 a	56.7 ± 2.4 a	7.2 ± 0.2 a	1.5 ± 0.1 a
<i>p</i> -Value (ANOVA)	<0.0001	0.06	<0.0001	0.01	0.33	0.18	0.38	0.85

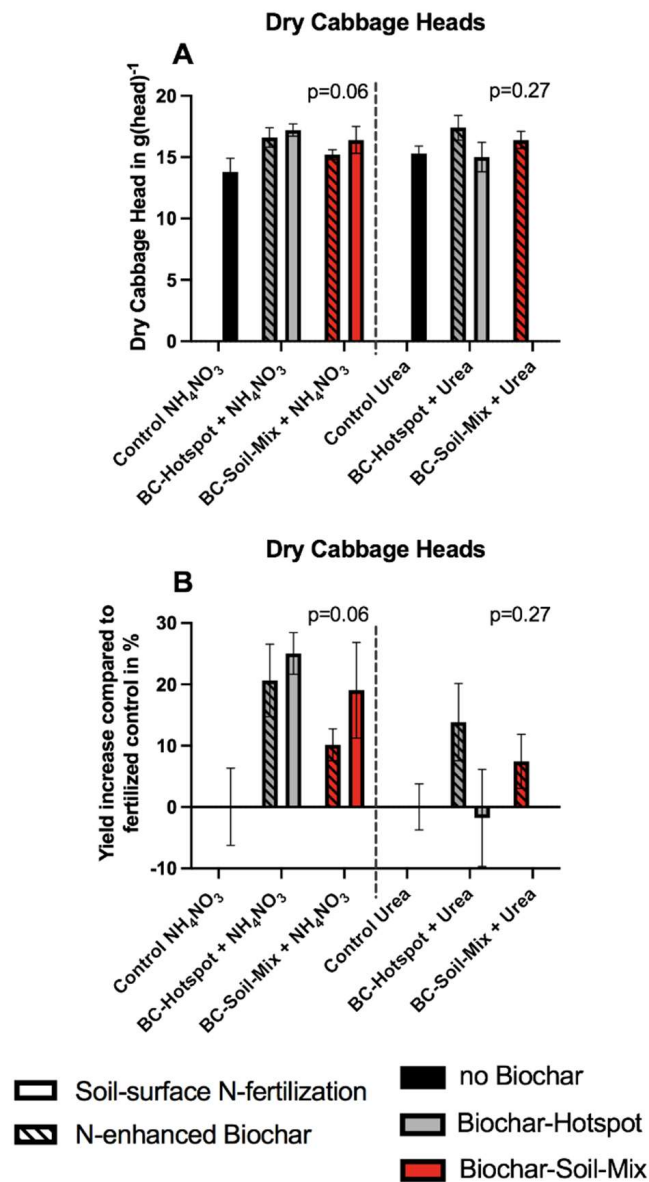


Figure 2. Dry cabbage-head weights (A) and yield increases of dry cabbage-head biomass (B) compared to the respective nitrogen (N) fertilized control (NH₄NO₃ or urea) for all biochar (BC) treatments, depending on the type of BC root-zone amendment (hotspot or soil-mix) and the N fertilization method (N-enhanced biochar or soil-surface N fertilization). Error bars indicate the standard error of the mean of replicated ($n = 5$) planting experiments. The p -values were derived from one-way ANOVA comparing all treatments fertilized with the same N compound.

Since the method of N fertilization (N-enhanced biochar vs. soil-surface N fertilization) did not change aboveground biomass parameters significantly (Table S5), it is appropriate to present data averaged over this experimental factor (Figure 3) [21]. Averaged over both approaches, the increases in dry cabbage-head biomass compared to the N fertilized no-biochar control were significantly intensified for the NH_4NO_3 -fertilized plants when biochar was amended as a hotspot in the root zone (22% yield increase with a hotspot and 14% with a soil-mix biochar amendment, Figure 3A). For the urea fertilizer, a biochar amendment in the root zone only showed a slight tendency (not significant, $p = 0.64$) to increase dry cabbage-head biomass compared to the no-biochar control (5% for hotspot and 7% for soil-mix root-zone biochar amendment, averaged over the N-fertilization method) (Figure 3A).

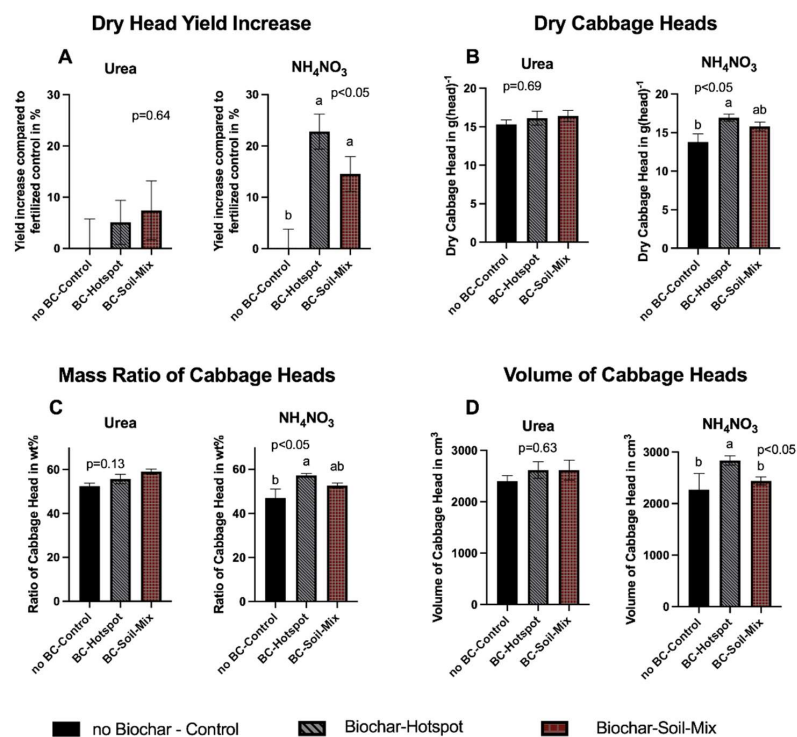


Figure 3. Aboveground biomass parameters averaged over the nitrogen (N) fertilization method and separated by the N-fertilizer type evaluated for fertilized plants without biochar amendment (no BC-Control) or biochar root-zone amendments (BC-Hotspot or BC-Soil-Mix) presented as least square means (processed with JMP10): (A) fresh cabbage-head biomass, (B) dry cabbage-head biomass, (C) mass ratio of cabbage heads (dry head biomass divided by total dry aboveground biomass), and (D) volume of cabbage heads. The error bars represent one standard error in each direction ($n = 10$ for no BC-control, $n = 20$ for BC-Hotspot and $n = 15$ for BC-Soil-Mix). Different letters above error bars indicate significant differences among the types of biochar root-zone amendments treated with the same N fertilizer ($p < 0.05$, Tukey HSD post hoc test).

This lower averaged increase in cabbage-head yield for the urea-fertilized biochar treatments can be explained by a better performance of the urea-fertilized control compared to the NH_4NO_3 -fertilized control (Table 2, Figure 3B); therefore, the type of N fertilizer

significantly influenced the extent of head yield increases provided by the different biochar root-zone amendments (Table S6, Figure 2).

Total aboveground biomass yields were not affected by biochar amendment (Tables 2 and S5). However, the mass ratio of cabbage heads related to the total biomass in presence of biochar increased significantly due to increases in the mass of cabbage heads ($p = 0.03$, Table S5 and Figure 3C). For the NH_4NO_3 -fertilized treatments, this ratio increased from 47% (no biochar) to 57% (hotspot biochar amendment), while for the urea fertilizer, the soil-mix biochar root-zone amendment maximized this ratio from 52% to 59% (Table 2 and Figure 3C). With that, the marketable part of the cabbage plant was increased in presence of biochar. Focusing on the biochar treatments, no significant difference was observed for this ratio for the type of root-zone amendment, the N fertilizer type, or the N-fertilization method (Table S6).

Within the biochar treatments, absolute cabbage-head yields were not significantly influenced neither by the type of root-zone amendment (hotspot vs. soil-mix root-zone application), the type of N fertilizer (ammonium nitrate vs. urea), nor the N-fertilization method (N-enhanced biochar vs. soil-surface N fertilization) (Table S6). Still, the interaction of the N-fertilization method and type of N fertilizer was almost significant ($p = 0.06$, Table S6), when plants were grown with biochar. This was reflected by the low cabbage-head yield in the treatment with hotspot biochar amendment with urea used as the soil-surface fertilizer, while in the complementary treatment fertilized with NH_4NO_3 , the overall highest dry head biomass was obtained (Table 2 and Figure 2). However, this contrast cannot be directly explained by the data we collected.

With higher cabbage-head yields in presence of the biochar amendments, the volume of cabbage heads was increased as well (Figure 3D); therefore, cabbage-head density was not altered by biochar amendment.

Vitamin C contents in frozen cabbage-head biomass (stored for two months at $-18\text{ }^\circ\text{C}$) were not altered by any factor applied in this study (Table 2). In general, vitamin C contents were within 7.0 and 8.5 mg $(100\text{ g})^{-1}$ for the different treatments and are in the lower range of reported vitamin C contents for white cabbage, which are typically within 5–30 mg $(100\text{ g})^{-1}$ but can reach up to 70 mg $(100\text{ g})^{-1}$ [22,23]. SPAD values of aboveground biomass, which represent a proxy for the chlorophyll content in plant tissues, were also not significantly different for the varying treatments (Table 2). Only in the control plants that did not receive any N fertilizer (no N-Fert., no BC) were the SPAD values slightly lower (Table 2). The influence of the different biochar root-zone amendments on the nutrient contents in plant tissues and the nutrient use efficiency should be conducted in future research.

In summary, the amendment of biochar in the root zone increased cabbage-head yields independent of the type of N fertilizer applied in this study but to a higher relative extent when fertilized with NH_4NO_3 . The hotspot amendment of a N-enhanced biochar in the root zone showed the most consistent positive impacts on cabbage-head yields for both N fertilizers (Figure 2). In this case, the biochar may act as a nutrient depot within close proximity to the root system, which may ease nutrient supply for the plant. This approach to obtain a biochar root-zone amendment in the field could be achieved by applying a biochar layer in the planting/seeding row. In contrast, the soil-mix root-zone amendment of biochar can be translated to field conditions as a mixture of biochar and soil in the planting basin of the cabbage plant and should not be confused with a homogeneous spreading of the biochar onto the whole field (Figure 1). For the homogeneous amendment of 1.3 t ha^{-1} of a biochar-based fertilizer onto the whole cabbage field, we would expect a less intense improvement in cabbage-head yield, since this would result in a biochar concentration of only 0.1–0.03% (w/w) when biochar is incorporated to a soil depth of 10–30 cm (assuming a soil-bulk density of 1.3 t m^{-3}), which is much lower than the biochar concentration that would result from the soil-mix root-zone amendment (0.9% w/w in our study, Figure 1).

The average yield increases in fresh cabbage-head biomass of 15% with biochar amendment and the maximum increase of 31% compared to the fertilized control are rather un-

usual when compared with meta-analyses that report no significant effect in crop yield increase when biochar is amended to soils in the humid-temperate climate zone [4]. Such a climate-dependent effect was not observed in a recently published meta-analysis when biochar was used as a fertilizer carrier at low biochar application rates (in the range of 1 t ha^{-1}), but still, biochar-based fertilizers only increased crop yields when applied to highly weathered or weakly developed soils and not when applied to already fertile soils, as was carried out in our study [7]. However, significant yield increases were reported before for various vegetable crops following the root-zone amendment of biochar that was enriched with a mineral NPK-fertilizer solution or cow urine as a nutrient source when added to fertile silt loam soils under temperate/alpine climate conditions in Nepal [6]. Thereby, the liquid nutrient enrichment of biochar with mineral NPK fertilizers provided lower crop yield increases (<50% increase compared to fertilized control) than biochar enriched with an organic nutrient source (i.e., cow urine with yield increases of up to 300%) [6]. The crop yield increases of up to 30% provided by the N-enriched biochar amended in the root zone in our study can therefore be seen in line with these results, and they indicate that a simple liquid nutrient enrichment of biochar positioned in the root zone is a promising strategy for biochar-based fertilization, as well as in fertile soils in the temperate climate zone. This may be due to a higher use efficiency of fertilized nutrients by the plants, which was also reported for conventional mineral fertilizer granules without biochar, when applied to the root zone of annual plants [24–26]. However, not only the nutrient-enriched biochar in our study promoted the growth of cabbage heads but the pure biochar along with soil-surface N fertilization as well, in most of the treatments. This is in contrast to a previous greenhouse pot study on quinoa where the addition of a pristine biochar (2% w/w) along with two different mineral N-fertilization levels to a nutrient poor sandy soil decreased aboveground biomass yields compared to the equivalently fertilized control without biochar [27]. However, Kammann and colleagues applied mineral fertilizer as a top-dress on average every nine days (nine doses within 82 days of cultivation), which could already be interpreted as a fertigation practice with probably nearly ideal nutrient supply. In contrast, we applied the soil-surface N fertilizer only once at the beginning of the cultivation; thus, the plants grown with biochar could take advantage of a nutrient depot when compared to the no-biochar controls.

Assuming the average fresh head yield increase of 20% provided by the N-enhanced biochar applied as a hotspot below the seedling in our study, a typical yield (fresh matter) of white cabbage heads in Germany of 90 t ha^{-1} would be increased to 108 t ha^{-1} . This would generate an approximate additional income of EUR 1200 ha^{-1} for the farmer, assuming a producer price of EUR 68.9 t^{-1} [28,29]. This additional income would cover the cost for the biochar at an application rate of 1.3 t ha^{-1} , and there would be a little but not significant added financial profit for the farmer within one season, assuming a commercial biochar price of EUR $500\text{--}1000 \text{ t}^{-1}$. Therefore, the biochar application rate and mode would have to be further optimized to create a higher economic incentive to apply this specific biochar-based fertilizer. However, it has to be considered that possible yield increases under field conditions may be different than in our greenhouse study, e.g., since we did not grow the cabbages to typical plant-specific head weights, which may be a result of the limited soil volume in our experimental pots ($<0.5 \text{ kg head}^{-1}$ in our study compared to commercial weights of approximately 1 kg head^{-1}).

3.2. Belowground Biomass Yields and Root Architecture

The different factors applied in the experiment had no impact on the absolute root biomass weights of white cabbage plants (Table 2) but significant impacts on the root architecture, including the root fill factor, area, and total projected structure length (Table S5, Figures 4 and S5). It should be noted that variations among the treatments compared to the head biomass cannot be resolved for the root biomass because of the low absolute root weights ($<2 \text{ g plant}^{-1}$, Table 2). The optical-based analysis of the root structure and total root area may be more sensitive and is an important additional tool to evaluate the root

growth under different biochar treatments. These root architecture-related parameters were evaluated with the REST Shovelomics software [17], which is based on processing high-contrast images from the washed rootstocks (Figure 5). The root-fill factor was most impacted by the type of root-zone amendment and the N-fertilization method ($p < 0.05$, Tables S5 and S6, Figure 4A). Lower fill factors were observed with the hotspot biochar amendment compared to both the fertilized no-biochar control and the soil-mix root-zone biochar amendment, especially for hotspot amendments of a N-enhanced biochar (Figures 4A and S5). The root fill factor in general is described as the number of root-derived pixels divided by the total number of pixels in the area of the photograph, in which 90% of root-derived pixels were registered. Therefore, the root fill factor is a measure for the root-hair density: low fill factors indicate a low root-hair density and with that fewer root hairs and more room between individual root hairs and vice versa. In a Shovelomics study on maize grown under field conditions, biochar mixed with soil in the planting basin resulted in a significant increase in root fill factor compared to the no-biochar control, which was not the case in our study for the comparable soil-mix biochar amendments (Figure 4A) [18]. However, biochar amendment in their (tropical) study (aeolian acidic sandy soil and sandy loam soil) also tended to increase both the above and belowground biomass compared to fertilized controls.

The area of the roots was not altered with the biochar amendments compared to the fertilized no-biochar control (Table S5, Figure S5), but within the biochar treatments, the interaction of the N-fertilization method and the type of biochar root-zone amendment significantly influenced root areas (Table S6, Figure 4B). For the hotspot biochar amendment, the application of a N-enhanced biochar led to lower root areas than for the soil-surface N fertilization (84 vs. 103 cm², Figure 4B). The exact opposite was registered for the soil-mix biochar amendments, where the N-enhanced biochar maximized the root area (Figure 4B). The same pattern as for the root areas was observed for the biochar treatments regarding the total projected structure lengths of the roots (Figure 4C). Furthermore, biochar-amended plants that received a fertilization with NH₄NO₃ had significantly higher root areas and total projected structure lengths than the plants fertilized with urea (Figure S6). As no difference in absolute root biomass production was registered among the different treatments (Table 2), a change in the root area is interpreted as a change in the total amount of root hairs and with that, the content of fine roots. Thereby, the results for the root area and projected structure lengths are consistent with the observed root fill factors, which all indicate that the content of fine roots was lower with hotspot N-enhanced biochar amendments compared to the mixed-soil amendment of the N-enhanced biochar.

The hotspot amendment of the N-enhanced biochar may act as a nutrient depot in close proximity to the plant, which in turn requires fewer fine roots for nutrient supply. In contrast, a soil-mix root-zone application of the N-enhanced biochar may require the development of more root hairs to reach the finely distributed N-carrying biochar particles in the pot. Furthermore, NH₄NO₃ is more mobile within the soil than urea and might spread more widely across the pot, which might explain the higher root area in the NH₄NO₃-fertilized treatments (Figure S6).

Data from a meta-analysis showed that root growth, especially for annual plants, is typically stimulated by large biochar amendments to soil (>10 t ha⁻¹), which was not the case for the low biochar amendments (1.3 t ha⁻¹) in our study [30]. However, our data show that biochar root-zone amendments and the N-fertilization method can influence the root architecture in a way that was not reported before. In summary, the reduced fine root development paired with higher aboveground biomass production in the treatments with N-enhanced biochar applied as a hotspot strongly indicated an improved plant nutrition of white cabbage plants. This should be studied under real field conditions to examine the potential positive or negative changes of crop nutrition and water supply of the plant through potential changes in its fine root biomass development when biochar is amended as a hotspot in the root zone.

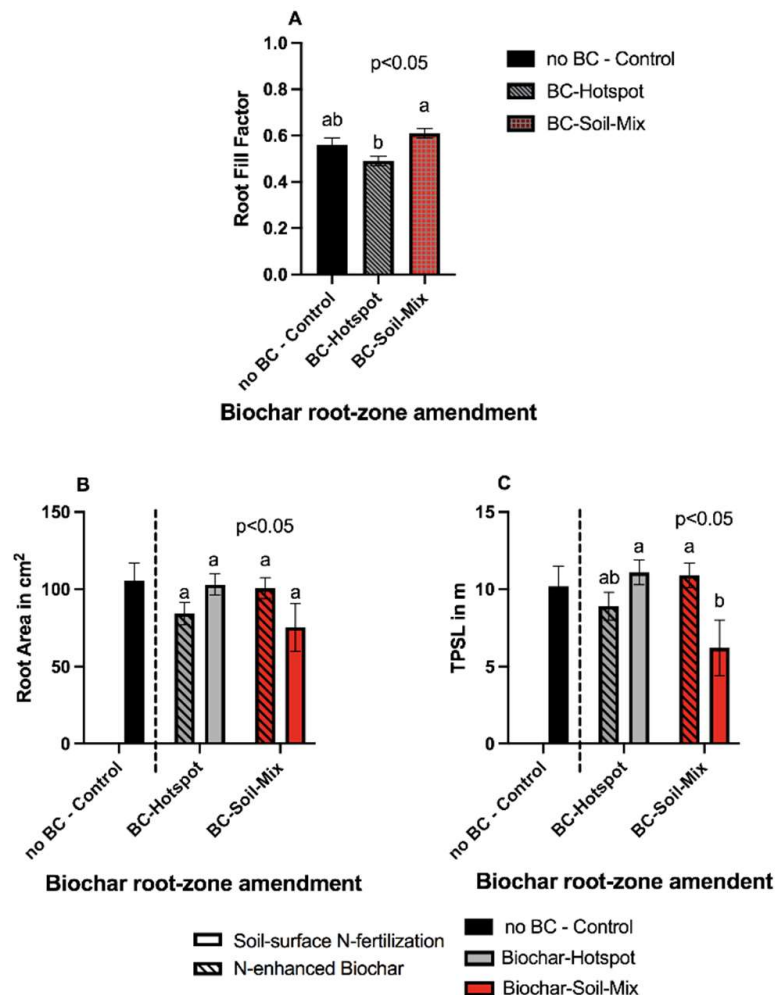


Figure 4. (A) Root fill factor depending on the biochar root-zone amendment (no-biochar (BC)-Control, BC hotspot in the root zone (BC-Hotspot), or BC mixed with soil (BC-Soil-Mix)) averaged over the type of nitrogen (N) fertilizer and the N-fertilization method. Data are provided as least square means (LSM), and the error bars represent one standard error in each direction calculated with the LSM method using JMP10 ($n = 10$ for no BC-Control, $n = 20$ for BC-Hotspot, and $n = 15$ for BC-Soil-Mix). (B,C) Root area and total projected structure lengths (TPSL) of the roots are averaged over the N-fertilizer type and separated by the N-fertilization method ($n = 10$). Parameters were determined from photographs of the rootstocks with the REST software (Colombi et al., 2015). Different letters above error bars indicate significant differences among the different variants (at $p < 0.05$, Tukey HSD post hoc test). The analysis of variance and the post hoc test in panel B and C only include the biochar treatments to examine the interactive effect of the type of root-zone amendment and the N-fertilization method. The no-BC-Control is only presented to ease interpretation of the results.

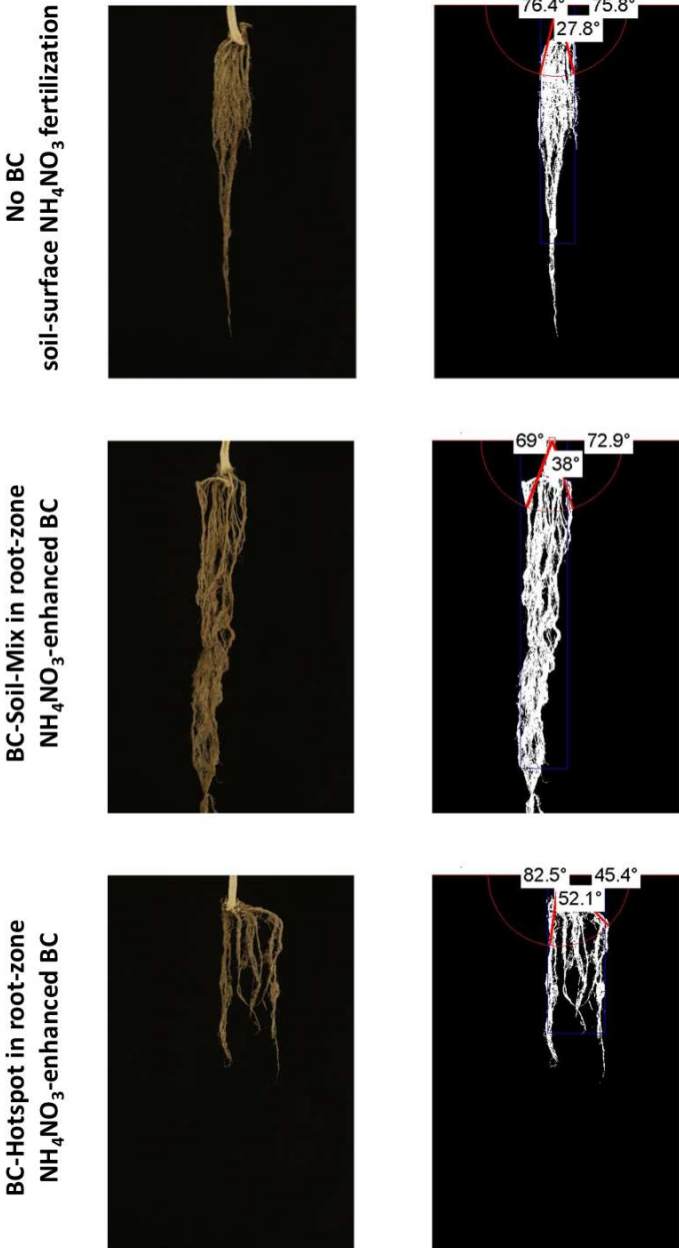


Figure 5. Photographs taken from the rootstock (left image) and the corresponding contrast image processed by the Shovelomics software REST [17] (right image) for selected plants fertilized with NH_4NO_3 and grown without biochar (BC) (top) and with root-zone-amended, NH_4NO_3 -enhanced biochar as soil mix (middle) or as hotspot (bottom).

4. Conclusions

Our results indicate that biochar-based fertilizers prepared by simple liquid nutrient enrichment positioned in the root zone of annual plants may also provide crop yield increases in fertile soils in the continental and humid-temperate climate zone. The use of the new method could provide an economic benefit for farmers, which was shown for white cabbage in our study. Field studies with low-dose root-zone amendments of biochar-based fertilizers are needed in temperate climates and should be conducted also with other cultivars to validate our results under field conditions and to find optimal biochar dosages and positions relative to the seedling. Technologies need to be further developed to perform such biochar root-zone amendments on a field scale. Future research is needed to understand the response of root growth and root architecture to the amendment of biochar-based fertilizers in the root zone of annual plants and its linkage with aboveground crop yields.

Supplementary Materials: The following are available online at <https://www.mdpi.com/article/10.3390/horticulturae8040307/s1>, Detailed description of vitamin C quantification; Figure S1: Photograph of the concentrated biochar amendment in the pot; Figure S2: Fixation of the drip line in the pot; Figure S3: Separation of the cabbage heads from residual, nonmarketable aboveground biomass; Figure S4: Photographic equipment for the Shovelomics analysis; Figure S5: Root biomass parameters for all fertilized treatments; Figure S6: Root area and total projected structure lengths of the rootstocks averaged over all plants that received a biochar amendment separated by the fertilizer type; Table S1: Biochar properties derived from batch analysis according to the EBC; Table S2: Basic soil properties and nutrient contents of the soil used in the greenhouse trial; Table S3: Cation exchange capacity of the soil used in the greenhouse trial; Table S4: Particle size distribution of the soil used in the greenhouse trial; Table S5: Analysis of variance for all treatments; Table S6: Analysis of variance for all biochar treatments.

Author Contributions: J.G.: conceptualization, investigation, formal analysis, and writing—original draft preparation; H.-P.S.: conceptualization, and writing—review and editing; D.K.: funding acquisition, conceptualization, and writing—review and editing; N.H.: conceptualization and writing—review and editing. All authors have read and agreed to the published version of the manuscript.

Funding: This research was conducted within the HyPErFarm project (<https://hyperfarm.eu/>) (accessed on 8 March 2022), which has received funding from the European Union's Horizon 2020 research and innovation programme under grant agreement no. 101000828. The Ithaka Institute was supported within the r4d call of the Swiss National Science Foundation (project Bio-C, grant-No.: IZ08Zo_177346).

Institutional Review Board Statement: Not applicable.

Informed Consent Statement: Not applicable.

Acknowledgments: We acknowledge Carbon Cycle GmbH & Co. KG for providing us with the biochar. We thank Sarah Cebulla for her support during the plant harvest and root analysis, and we are grateful for the help of Barbara Anders, Regina Brämer, Andrea Seigel, Almuth Henninger, Corinna Henninger, and Bernd Spangenberg in the labs at Offenburg University. We thank Sascha Rißmann and Sascha Himmelsbach for providing space for the root washing, Linda Künath-Ünver for the supply with the photographic equipment, and Christoph Pönisch with his help to set up the pot trial. We thank Alois Huber for excavating and providing the soil and the HyPErFarm Consortium in Germany, and especially Bernhard Bauer for valuable discussion.

Conflicts of Interest: The authors declare no conflict of interest. The funders had no role in the design of the study, in the collection, analyses, or interpretation of data, in the writing of the manuscript, or in the decision to publish the results.

References

1. Hagemann, N.; Spokas, K.; Schmidt, H.-P.; Kägi, R.; Böhler, M.; Bucheli, T. Activated Carbon, Biochar and Charcoal: Linkages and Synergies across Pyrogenic Carbon's ABCs. *Water* **2018**, *10*, 182. [CrossRef]
2. Schmidt, H.; Kammann, C.; Hagemann, N.; Leifeld, J.; Bucheli, T.D.; Sánchez Monedero, M.A.; Cayuela, M.L. Biochar in Agriculture—A Systematic Review of 26 Global Meta-analyses. *GCB Bioenergy* **2021**, *13*, 1708–1730. [CrossRef]
3. Kammann, C.; Ippolito, J.; Hagemann, N.; Borchard, N.; Cayuela, M.L.; Estavillo, J.M.; Fuertes-Mendizabal, T.; Jeffery, S.; Kern, J.; Novak, J.; et al. Biochar as a Tool to Reduce the Agricultural Greenhouse-Gas Burden—Knowns, Unknowns and Future Research Needs. *J. Environ. Eng. Landsc. Manag.* **2017**, *25*, 114–139. [CrossRef]
4. Ye, L.; Camps-Arbestain, M.; Shen, Q.; Lehmann, J.; Singh, B.; Sabir, M. Biochar Effects on Crop Yields with and without Fertilizer: A Meta-analysis of Field Studies Using Separate Controls. *Soil Use Manag.* **2020**, *36*, 2–18. [CrossRef]
5. Bai, S.H.; Omidvar, N.; Gallart, M.; Kämper, W.; Tahmasbian, L.; Farrar, M.B.; Singh, K.; Zhou, G.; Muqadass, B.; Xu, C.-Y.; et al. Combined Effects of Biochar and Fertilizer Applications on Yield: A Review and Meta-Analysis. *Sci. Total Environ.* **2022**, *808*, 152073. [CrossRef]
6. Schmidt, H.-P.; Pandit, B.H.; Cornelissen, G.; Kammann, C.I. Biochar-Based Fertilization with Liquid Nutrient Enrichment: 21 Field Trials Covering 13 Crop Species in Nepal: Biochar-Based Fertilization. *Land Degrad. Develop.* **2017**, *28*, 2324–2342. [CrossRef]
7. Melo, L.C.A.; Lehmann, J.; Carneiro, J.S.D.S.; Camps-Arbestain, M. Biochar-Based Fertilizer Effects on Crop Productivity: A Meta-Analysis. *Plant. Soil* **2022**, *472*, 45–58. [CrossRef]
8. Gwenzi, W.; Nyambishi, T.J.; Chaukura, N.; Mapope, N. Synthesis and Nutrient Release Patterns of a Biochar-Based N–P–K Slow-Release Fertilizer. *Int. J. Environ. Sci. Technol.* **2018**, *15*, 405–414. [CrossRef]
9. Liu, X.; Liao, J.; Song, H.; Yang, Y.; Guan, C.; Zhang, Z. A Biochar-Based Route for Environmentally Friendly Controlled Release of Nitrogen: Urea-Loaded Biochar and Bentonite Composite. *Sci. Rep.* **2019**, *9*, 9548. [CrossRef]
10. Shi, W.; Ju, Y.; Bian, R.; Li, L.; Joseph, S.; Mitchell, D.R.G.; Munroe, P.; Taherymoosavi, S.; Pan, G. Biochar Bound Urea Boosts Plant Growth and Reduces Nitrogen Leaching. *Sci. Total Environ.* **2020**, *701*, 134424. [CrossRef]
11. Shi, W.; Bian, R.; Li, L.; Lian, W.; Liu, X.; Zheng, J.; Cheng, K.; Zhang, X.; Drosos, M.; Joseph, S.; et al. Assessing the Impacts of Biochar-blended Urea on Nitrogen Use Efficiency and Soil Retention in Wheat Production. *GCB Bioenergy* **2022**, *14*, 65–83. [CrossRef]
12. Cornelissen, G.; Martinsen, V.; Shitumbanuma, V.; Alling, V.; Breedveld, G.; Rutherford, D.; Sparrevik, M.; Hale, S.; Obia, A.; Mulder, J. Biochar Effect on Maize Yield and Soil Characteristics in Five Conservation Farming Sites in Zambia. *Agronomy* **2013**, *3*, 256–274. [CrossRef]
13. Blackwell, P.; Krull, E.; Butler, G.; Herbert, A.; Solaiman, Z. Effect of Banded Biochar on Dryland Wheat Production and Fertiliser Use in South-Western Australia: An Agronomic and Economic Perspective. *Soil Res.* **2010**, *48*, 531. [CrossRef]
14. Schmidt, H.; Pandit, B.; Martinsen, V.; Cornelissen, G.; Conte, P.; Kammann, C. Fourfold Increase in Pumpkin Yield in Response to Low-Dosage Root Zone Application of Urine-Enhanced Biochar to a Fertile Tropical Soil. *Agriculture* **2015**, *5*, 723–741. [CrossRef]
15. Zhang, L. Participation of Urea-N Absorbed on Biochar Granules among Soil and Tobacco Plant (*Nicotiana tabacum*, L.) and Its Potential Environmental Impact. *Agric. Ecosyst. Environ.* **2021**, *313*, 107371. [CrossRef]
16. Altaf, F.; Gul, S.; Chandio, T.A.; Rehman, G.B.; Kakar, A.-R.; Khan, N.; Shaheen, U.; Shahwani, M.N.; Ajmal, M.; Manzoor, M. Influence of Biochar Based Organic Fertilizers on Growth and Concentration of Heavy Metals in Tomato and Lettuce in Chromite Mine Tailing Contaminated Soil. *Sarhad J. Agric.* **2021**, *37*, 315–324. [CrossRef]
17. Colombi, T.; Kirchgessner, N.; Le Marié, C.A.; York, L.M.; Lynch, J.P.; Hund, A. Next Generation Shovelomics: Set up a Tent and REST. *Plant. Soil* **2015**, *388*, 1–20. [CrossRef]
18. Abiven, S.; Hund, A.; Martinsen, V.; Cornelissen, G. Biochar Amendment Increases Maize Root Surface Areas and Branching: A Shovelomics Study in Zambia. *Plant. Soil* **2015**, *395*, 45–55. [CrossRef]
19. EBC (2012–2022) "European Biochar Certificate—Guidelines for a Sustainable Production of Biochar." European Biochar Foundation (EBC), Arbaz, Switzerland. Available online: <http://european-biochar.org> (accessed on 10 January 2022).
20. Spínola, V.; Mendes, B.; Câmara, J.S.; Castilho, P.C. Effect of Time and Temperature on Vitamin C Stability in Horticultural Extracts. UHPLC-PDA vs. Iodometric Titration as Analytical Methods. *LWT-Food Sci. Technol.* **2013**, *50*, 489–495. [CrossRef]
21. Piepho, H.P.; Edmondson, R.N. A Tutorial on the Statistical Analysis of Factorial Experiments with Qualitative and Quantitative Treatment Factor Levels. *J. Agro. Crop Sci.* **2018**, *204*, 429–455. [CrossRef]
22. Singh, J.; Upadhyay, A.K.; Bahadur, A.; Singh, B.; Singh, K.P.; Rai, M. Antioxidant Phytochemicals in Cabbage (*Brassica oleracea*, L. *Var. Capitata*). *Sci. Hortic.* **2006**, *108*, 233–237. [CrossRef]
23. Dominguez-Perles, R.; Mena, P.; García-Viguera, C.; Moreno, D.A. Brassica Foods as a Dietary Source of Vitamin C: A Review. *Crit. Rev. Food Sci. Nutr.* **2014**, *54*, 1076–1091. [CrossRef]
24. Mazid Miah, M.A.; Gaihre, Y.K.; Hunter, G.; Singh, U.; Hossain, S.A. Fertilizer Deep Placement Increases Rice Production: Evidence from Farmers' Fields in Southern Bangladesh. *Agron. J.* **2016**, *108*, 805–812. [CrossRef]
25. Liu, X.; Wang, H.; Zhou, J.; Chen, Z.; Lu, D.; Zhu, D.; Deng, P. Effect of Nitrogen Root Zone Fertilization on Rice Yield, Uptake and Utilization of Macronutrient in Lower Reaches of Yangtze River, China. *Paddy Water Environ.* **2017**, *15*, 625–638. [CrossRef]
26. Jiang, C.; Lu, D.; Zu, C.; Zhou, J.; Wang, H. Root-Zone Fertilization Improves Crop Yields and Minimizes Nitrogen Loss in Summer Maize in China. *Sci. Rep.* **2018**, *8*, 15139. [CrossRef]

27. Kammann, C.I.; Schmidt, H.-P.; Messerschmidt, N.; Linsel, S.; Steffens, D.; Müller, C.; Koyro, H.-W.; Conte, P.; Joseph, S. Plant Growth Improvement Mediated by Nitrate Capture in Co-Composted Biochar. *Sci. Rep.* **2015**, *5*, 11080. [[CrossRef](#)]
28. Bavarian State Agency for Agriculture Contribution Margins and Calculation Data—White Cabbage (Industrial Product). Available online: <https://www.stmelf.bayern.de/idb/weisskohl.html> (accessed on 9 February 2022).
29. German Federal Statistical Office Farms, Areas under Cultivation, Yields and Harvest Quantities of Vegetables. Available online: <https://www.destatis.de/DE/Themen/Branchen-Unternehmen/Landwirtschaft-Forstwirtschaft-Fischerei/Obst-Gemuese-Gartenbau/Tabellen/betriebe-anbau-erntemenge-gemuese.html#fussnote-A-123138> (accessed on 9 February 2022).
30. Xiang, Y.; Deng, Q.; Duan, H.; Guo, Y. Effects of Biochar Application on Root Traits: A Meta-Analysis. *GCB Bioenergy* **2017**, *9*, 1563–1572. [[CrossRef](#)]

Supplementary Information to:

Root-zone amendments of biochar-based fertilizers: yield increases of white cabbage in temperate climate

Jannis Grafmüller^{1,2,3}, Hans-Peter Schmidt³, Daniel Kray¹ and Nikolas Hagemann^{2,3,4}

¹Institute of Sustainable Energy Systems and Institute of Process Engineering, Offenburg University of Applied Sciences, Offenburg Germany

²Ithaka Institute gGmbH, Goldbach, Germany; hagemann@ithaka-institut.org

³Ithaka Institute, Arbaz, Switzerland; schmidt@ithaka-institut.org

⁴Environmental Analytics, Agroscope Reckenholz, Zurich, Switzerland

Supplementary information related to this chapter can be found under the following link on the publisher website: <https://doi.org/10.3390/horticulturae8040307>
or directly under: <https://www.mdpi.com/article/10.3390/horticulturae8040307/s1>

Chapter 3b

Preparation of biochar microparticles by milling: effect on biochar and soil water holding capacity, biochar porosity and growth of white cabbage

Jannis Grafmüller^{1,2,3}, Jens Möllmer⁴, Daniel Kray¹, Stephanie Spahr⁵, Hans-Peter Schmidt²,
Nikolas Hagemann^{2,6}

¹Institute for Sustainable Energy Systems (INES), Offenburg University of Applied Sciences, Germany

²Ithaka Institute, Arbaz (Switzerland) and Goldbach (Germany)

³Plant Biogeochemistry, Tübingen University, Tübingen, Germany

⁴Institut für Nichtklassische Chemie e.V. (INC), Leipzig, Germany

⁵Leibniz Institute of Freshwater Ecology and Inland Fisheries, Berlin, Germany

⁶Environmental Analytics, Agroscope Zurich, Switzerland

Working paper

Statement of personal and co-author contributions, plus non-listed contributors

Authors	Position of candidate in list of authors	Scientific ideas by the author [%]	Data generation by the author [%]	Analysis and interpretation by the author [%]	Paper writing done by the author [%]
Jannis Grafmüller	1	60	50	60	100
Jens Möllmer	2	0	20	20	0 ^a
Daniel Kray	3	10	0	5	0 ^a
Stephanie Spahr	4	0	20	5	0 ^a
Hans-Peter Schmidt	5	15	0	5	0 ^a
Nikolas Hagemann	6	15	0	5	0 ^a
Contribution by other parties not listed as authors (e.g., commercial analysis laboratories, student assistants)					
Mohammed Kusaybati		0	5	5	0
Lea Elena Anders		5	5	0	0
Publication status	unpublished				
Explanations	The study was conceptualized by Nikolas Hagemann, Hans-Peter Schmidt, Daniel Kray and me. The WHC measurements and plant growth experiment were mainly conducted by me with assistance from Mohammed Kusaybati and Lea Elena Anders. The gas adsorption experiments were performed and evaluated by Jens Möllmer. Steve Ullmann from INC e.V. Leipzig, Germany supported me with elemental analysis data of the biochars. Stephanie Spahr and a student assistant, who is not known by name, conducted the particle size distribution analysis. The data analysis and writing of the manuscript was performed by me.				

^a: Contribution set to 0 as c-author did not yet review the manuscript.

Abstract

Biochar has to be provided as microparticles (1-1000 μm) for production of biochar-based fertilizers (BBF) e.g., via granulation or for integration in fertigation. However, little is known how biochar microparticles obtained from different milling processes differ in properties such as water holding capacity (WHC), micro- and mesoporosity and their effect on plant growth. In this study, five different biochars produced both from wood or straw were either milled with an impact mill to coarser or with a ball mill to finer microparticles. After impact milling, biochar microparticles were obtained with an average diameter (d_{50}) between 22 and 104 μm while ball milling reduced d_{50} to the range of 6-18 μm . Impact milled biochars had a WHC between 140% and 240% (w/w), ball milling reduced WHC to 85-115%. As micro- and mesoporosity of biochars based on CO_2 and N_2 sorption did not differ between milling methods, the higher WHC of impact milled biochars is likely due to the storage of water in pore spaces between the coarser biochar microparticles, i.e., interporosity, not by changes in intraporosity of biochar particles. In a sandy soil, intermixed impact milled biochars significantly increased WHC by 5-17% compared to pure soil, while ball-milled biochars did not increase it, likely linked with the lower particle sizes of ball milled biochars creating less pore spaces between biochar and soil particles for water storage. Biochar might also be applied as concentrated layer in seeding or planting rows. Soil amended with three of the ball milled biochars with lowest d_{50} had higher WHC when biochar was applied as layer compared to homogeneous application to soil, which we associate with a potential water barrier built up by the fine ball milled biochar particles limiting water drainage from the above soil layer, thus reducing hydrological connectivity. In a silt loam, biochar amendments, independent of biochar type or milling technique, did not affect aboveground cabbage yields compared to non-amended soil. On average, biochar increased root biomass by 12% compared to non-amended soil. To conclude, if biochar must be provided in microparticles for BBF production, we recommend using the largest possible particle size to benefit from highest possible biochar-induced soil WHC increases.

1. Introduction

Application of biochar in agriculture as biochar-based fertilizer (BBF) aims to integrate biochar in fertilization strategies resulting in repeatedly application of low-dosed biochar amendments without the need for a separate biochar application step¹. This is to ease adoption of biochar application and thus biochar-based carbon sequestration in agriculture. Among various strategies to produce biochar-based fertilizers¹, the integration of biochar in granulated fertilizers and in fertigation strategies might be most scalable in practice, since both fertilization techniques are used widely^{2,3}. Granulated or pelleted compound fertilizers are applied during cultivation of both field and vegetable crops. Fertigation strategies, i.e. fertilizer solutions applied via drip irrigation systems, are widely applied in vegetable cultivation and on fruit orchards³. In addition, solubilized fertilizer can be applied as foliar fertilizers⁴, which has also been demonstrated with biochar suspensions⁵.

These fertilization strategies have in common that biochar would have to be supplied as fine powder to either enable granulation or pelleting and to avoid blockage of e.g., drippers or spraying nozzles of fertigation systems. For granulation processes, particles with a size of < 200 μm up to < 500 μm are recommended⁶, while insoluble components in fertilizer suspensions for fertigation have been applied with particle sizes of < 50 μm ⁷. Particles in this size range are termed as microparticles (1-100 μm or 1-1000 μm depending on definition)^{8,9}. Biochar producers usually use coarse wood chips or pelleted feedstocks for pyrolysis. The biochar product has thus irregular particle sizes which are usually in the range of 10-50 mm, which must be reduced to make biochar available for granulation, pelleting or fertigation. Such a comminution of biochar to obtain microparticles in the abovementioned relevant size range for BBF production can be achieved by milling of biochar.

Potential milling strategies include e.g. impact milling or ball milling. However, milling might not only reduce the average particle size of biochar but could also alter biochar properties relevant for soil application of biochar. By milling, the morphology of biochar particles is changed, and the porous structure of biochar might be destructed. This could reduce its potential to increase water holding capacity (WHC) of soil, which is a positive effect after biochar application especially observed in sandy soils^{10,11}. On the other hand, biochar milling to microparticles increases the external surface area of biochar, which can improve biochar interactions with plant roots leading to increased crop growth and nutrient uptake¹². Still, there are also contrasting results indicating that plant growth is reduced under soil amendment of finely ground particles (<63 μm and 63-500 μm)¹³.

This study aimed to investigate if two different biochar milling techniques, specifically impact milling and ball milling, can be used to provide biochar microparticles for BBF production and how the biochars after milling differ in biochar porosity, WHC (both of pure biochar and in a soil matrix) and in their effects on growth of white cabbage in biochar-amended soil, depending on the milling technique. Two different milling methods were chosen to obtain microparticles of biochars in different particle size ranges: the impact mill was equipped with a sieve of < 2 mm, which allows the preparation of a comparable coarser particle size fraction (< 500 μm based on pre-experiments), while ball milling allows micronization to lower particle size (< 100 μm based on pre-experiments). To cover a broader spectrum of biochars, we used three different wood-based biochars produced on industrial scale with different reactor techniques and varying pyrolysis temperatures (650-850 $^{\circ}\text{C}$). Further, two biochars were produced on pilot plant-scale at 500 $^{\circ}\text{C}$ both from pelleted wood or straw, to further integrate a different lignocellulosic biomass type and lower pyrolysis temperature in the experimental setup. The effect on WHC was quantified in a sandy soil to maximize the presumed biochar-induced improvements¹⁴ and thus differences between individual biochars and milling methods. The crop study was performed in a silty loam where reference data from an earlier greenhouse trial for one of the biochar sample was available¹⁵. We aim to give practical recommendations which biochar milling method should be used to provide biochar microparticles for BBF production.

2. Materials and methods

2.1. Biochar origin and production

Industrial wood-based biochars (IWBC) were obtained from three different pyrolysis reactor types, which were either manufactured by Syncraft Engineering GmbH, Schwaz, Austria (IWBC-01, provided by Energiewerk Ilg GmbH, Dornbirn, Austria), Carbon Technik Schuster GmbH (IWBC-02, produced by Carbon Cycle GmbH & Co. KG, Rieden, Germany) or Pyreg GmbH, Dörth, Germany (IWBC-03, produced by ASF Freiburg GmbH, Freiburg, Germany). The pyrolysis temperatures were 850 $^{\circ}\text{C}$ for IWBC-01, 750 $^{\circ}\text{C}$ for IWBC-02 and 650 $^{\circ}\text{C}$ for IWBC-03. In addition, two biochars were produced with a PYREKA pyrolysis reactor on pilot-plant scale (Pyreg GmbH, Dörth, Germany) at a temperature of 500 $^{\circ}\text{C}$ and 10 minutes residence time from wood-pellets (oecoplan wood pellets, AEK Pellet AG4502 Solothurn, Switzerland) or selfmade cereal straw pellets and labelled as PWBC and PSBC, respectively. Details on the PYREKA pyrolysis plant can be found elsewhere¹⁶.

2.2. Biochar milling and characterization

Biochars were milled in an impact mill through a sieve of 2 mm (PX-MFC 90D, Kinematica AG, Malters, Switzerland) or for 30 minutes in a planetary ball mill (TOB-XQYMD-2, TOB Xiamen CO LTD., Fujian Province, China). Bulk biochar obtained for IWBC-02 was milled to < 12 mm in an impact mill (HM420B, Evertec, Dieburg, Germany) prior to milling with the abovementioned techniques.

2.2.1. Elemental analysis and particle size distribution

Elemental analysis of biochars for carbon (C), hydrogen (H), nitrogen (N) and sulfur (S) was performed on a vario MACRO cube only for ball milled samples (Elementar Analysensysteme GmbH, Langenselbold, Germany). Ash contents of biochar samples were analyzed according to DIN EN ISO 18122¹⁷ at 550°C. Particle size distribution was recorded for all milled biochars with a Mastersizer device (Malvern Panalytical, Kassel, Germany). From these measurements, the volume-based particle size sum distribution Q_3 and the volume-based particle size density distribution q_3 was obtained according to DIN 66144¹⁸. The 10th, 50th and 90th percentile of the Q_3 distribution are referred to as d_{10} , d_{50} and d_{90} , respectively.

2.2.2. Water holding capacity of biochar and biochar-soil mixtures

The WHC of milled biochar samples was measured according to DIN EN ISO 14238 Annex A¹⁹, with a saturation of the biochar samples in the water bath for 14 hours and subsequent drainage on a dry sand bed for 2 hours²⁰. For that, 20 g of biochar (dry matter equivalent) were weighed in plastic cylinders equipped with a 0.5 mm stainless steel mesh and a water permeable membrane filter (0.45 µm nylon mesh) at the bottom. The WHC on mixtures of the milled biochar samples and a sandy-loamy soil (standard soil 2.3, LUFA, Speyer, Germany) were measured as described above in two different ways: homogeneous distribution of the biochar in the soil or biochar applied as concentrated layer. The cylinders contained 1.84 g biochar and 90 g soil (all dry matter equivalents), which resulted in a biochar concentration in the mixture of 2% (w/w). For the homogeneous application, biochar and soil were manually homogenized in a glass beaker for two minutes and transferred to the cylinders (Figure S 1a). For the layer application, half the soil mass was filled in the cylinder, followed by the whole biochar mass spread evenly on the soil; the second half of the soil mass was put on top (Figure S 1b). The WHC of the pure soil was also measured. All measurements were done in duplicates.

2.2.3. Gas adsorption on biochar samples

Carbon dioxide (CO₂) and nitrogen (N₂) adsorption isotherms were recorded for milled biochar samples on an Autosorb iQ (Quantachrome Instruments, Anton Paar GmbH, Ostfildern-Scharnhausen, Germany) at 273.15 K in a relative pressure range of $3 \cdot 10^{-5}$ - $3 \cdot 10^{-2}$ for CO₂ and at 77 K in a relative pressure range of $1 \cdot 10^{-3}$ – $9.9 \cdot 10^{-1}$ for N₂. Specific surface area (SSA), was calculated using either the Brunauer-Emmett-Teller²¹ (BET) or the density functional theory²² (DFT). Micropore volumes (pore width < 2nm) were calculated based on CO₂ adsorption and the sum of micro- and mesopores (< 50 nm) was calculated based on N₂ adsorption.

2.3. Greenhouse trial

The greenhouse experiment was conducted with white cabbage (*Brassica oleracea* convar. Capitata var. Alba, Sunta F1, Bruno Nebelung GmbH, Everswinkel, Germany) and was set up for 11 weeks from April to June 2022 in a greenhouse located in Offenburg, Germany (48°29'00.6"N 7°56'23.8"E). Seedlings were grown for four weeks before trial start (Figure S 2). A silt loam was used originating from Straßkirchen, Germany, which had a pH of 7.1, a soil organic matter content of 3.7%, a mineralized N content of 19 mg kg⁻¹ and plant-available contents of phosphorus, potassium and magnesium of 353 mg kg⁻¹, 272 mg kg⁻¹ and 298 mg kg⁻¹, respectively. A basic soil analysis performed by Eurofins Umwelt Ost GmbH (Bobritzsch-Hilbersdorf, Germany) is given in Table S 1-Table S 3.

The experimental factors were the biochar type (IWBC-01, IWBC-02, IWBC-03, PWBC and PSBC) and the milling method (impact mill < 2 mm; ball mill). Additionally, a control without any biochar was included. All biochar treatments were set up with five and the Control with ten replicate pots, which lead to a total of 60 pots that were arranged on the greenhouse table in a randomized complete block design with five blocks (Figure S 3, each two control pots within one block). The fifth block had to be excluded from the analysis due to shading problems recognized early in the experiment, i.e., only four or eight replicates per treatment or control, respectively, were harvested. The different biochar samples were applied as a concentrated layer which was 8 cm in diameter in 4 L pots at a rate of 0.8% (w/w, i.e., 32g pot⁻¹ dry equivalent) at 8 cm soil depth (Figure S 4). The soil weight was 3900 g pot⁻¹ (dry equivalent). The biochar layer was covered by a thin layer of soil before one seedling per pot was planted and the remaining soil was filled to the pots (Figure S 4). Plants were adjusted to 60% of the maximum WHC of each soil mixture (calculated based on WHC of pure soil and pure BC) once per week and irrigated daily through an automated drip line with well water. Pots were randomly rearranged within each block on a weekly basis. Two weeks after planting, the pots

were fertilized with 120 ml of an ammonium nitrate solution to fertilize all pots with 2.5 g N pot⁻¹. After 5 weeks, plants were fertilized with 1.1 g K pot⁻¹ via 80 mL of a potassium sulfate solution.

After 11 weeks, cabbage plants were harvested by cutting the stem beyond the lowest leaf base to determine total aboveground cabbage biomass. Subsequently, the outer protruding leaves were removed to determine the mass of the cabbage head alone. Root biomass was removed from the soil and washed under tap water to remove soil particles, stones and other artefacts. Dry matter of all biomass fractions was determined after drying to mass constancy at 80 °C.

2.4. Data analysis

Data analysis and visualization were performed with GraphPad Prism (version 10.4.1, GraphPad Software LLC, Boston MA, USA). Water holding capacities and plant yields were compared with a two-way analysis of variance (ANOVA) with the factors Biochar type (IWBC-01, -02, -03; PWBC and PSBC) and the biochar milling method (impact mill < 2 mm; ball mill). Block effects in the greenhouse were considered with the repeated-measures function in Prism. Cabbage yields in the Control group (no biochar) were compared with yields under biochar amendments (averaged over all amendments, independent on biochar type and particle size) with an unpaired t-test. Water holding capacities of biochar-amended soils were also compared to the non-amended soil in a one-way ANOVA followed by a Dunnett's test. Pearson correlation coefficients for correlation of WHC of pure biochars with SSA and pore volumes based on BET and DFT as well as with the average particle diameter d_{50} were obtained both for correlation within each milling method and across both different milling types. Pearson correlation coefficients were only reported for statistically significant correlations.

3. Results

3.1. Elemental analysis of biochars

Carbon content was with 67.1% lowest in PSBC while all wood-based biochars had C contents in the range of 84-94% (Table 1). In contrast, the ash content was with 24% highest for PSBC and all wood-based biochars had ash contents below 12% (Table 1). The H/C ratios decreased with the pyrolysis temperature: biochars PWBC and PSBC, which were produced at 500 °C, had ratios around 0.45 which decreased to 0.27-0.11 for industrially produced biochars at higher temperature (Table 1).

Table 1: Elemental composition of biochars: carbon (C), hydrogen (H), nitrogen (N), sulfur (S) and ash content (all w/w) and molar H/C ratio. IWBC: Wood-based biochar pyrolyzed on industrial scale at 850 °C (01), 750 °C (02) or 650 °C (03) and wood-based (PWBC) and straw-based (PSBC) biochar pyrolyzed on pilot-plant scale at 500 °C.

	C [%]	H [%]	N [%]	S [%]	H/C	Ash [%]
IWBC-01	86.2	0.8	0.4	<0.05	0.11	12.1
IWBC-02	94.0	1.9	0.4	<0.05	0.24	1.4
IWBC-03	87.5	2.0	0.4	<0.05	0.27	7.1
PWBC	84.8	3.4	0.2	0.05	0.48	1.4
PSBC	67.1	2.4	0.7	0.09	0.43	23.6

3.2. Particle size distribution of milled biochar samples

Biochar particle sizes were reduced to < 0.5 mm after milling with the impact mill and to < 0.1 mm after ball milling (Figure 1a and c, Table 2). In general, ball milled biochars had monomodal particle size density distributions (q_3), while particle size of impact milled biochars were bimodally distributed including peak overlapping (Figure 1b and d).

The 90th percentile of the particle diameter of impact milled biochars was mostly in the range of 73-104 μm , only PWBC had a d_{90} of 324 μm (Table 2). Impact milling resulted in d_{50} values between 22 μm and 104 μm (Table 2). Biochars microparticles obtained by ball milling had d_{90} values below 50 μm and d_{50} values in the range of 6-18 μm , thus significantly lower as compared to impact milled biochars.

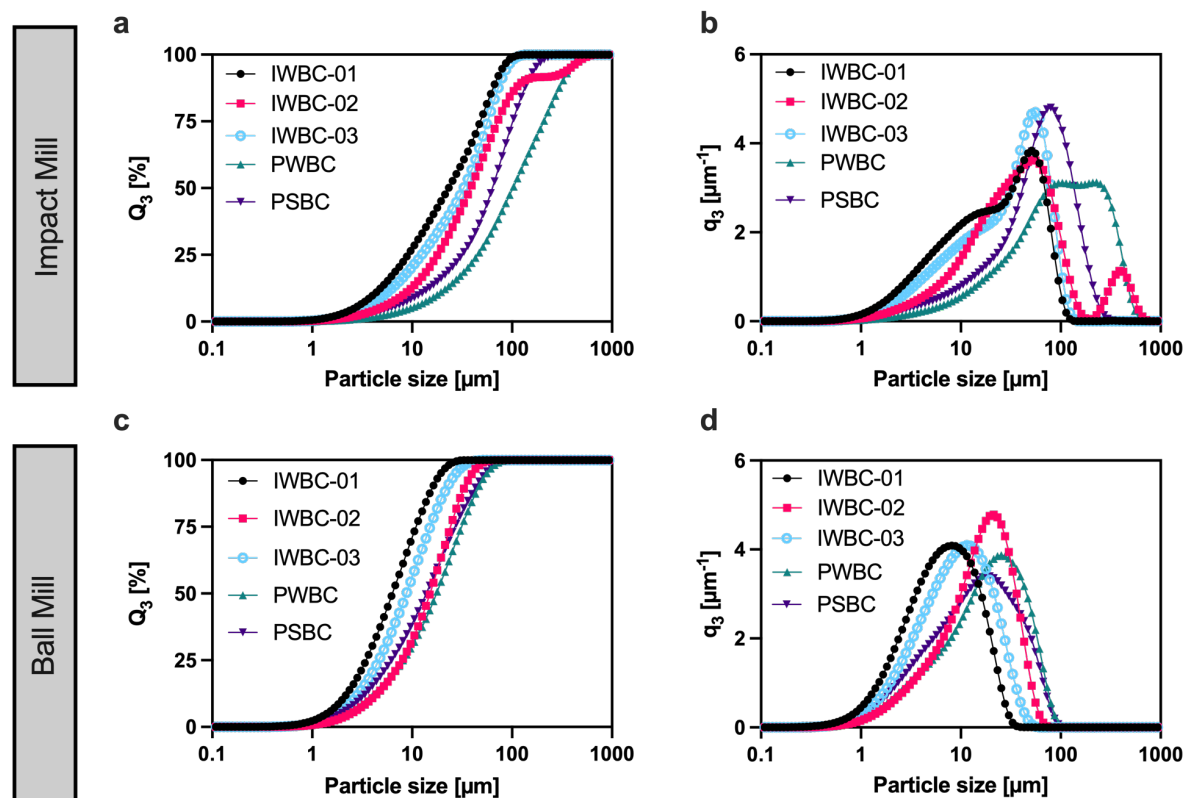


Figure 1: Volume weighed particle sum distribution (Q_3) of biochar samples milled with an impact mill (a) or with a ball mill (c). First derivate of Q_3 with respect to particle size (q_3), i.e., volume-weighted density distribution of particle size of biochar samples milled with an impact mill (b) or with a ball mill (d). IWBC: Wood-based biochar pyrolyzed on industrial scale at 850 °C (01), 750 °C (02) or 650 °C (03) and wood-based (PWBC) and straw-based (PSBC) biochar pyrolyzed on pilot-plant scale at 500 °C.

Table 2: Parameters of the Q_3 sum distribution of biochars milled with the impact or ball mill: 10th, 50th and 90th percentile of the particle size sum distribution Q_3 (d_{10} , d_{50} and d_{90} , respectively). IWBC: Wood-based biochar pyrolyzed on industrial scale at 850 °C (01), 750 °C (02) or 650 °C (03) and wood-based (PWBC) and straw-based (PSBC) biochar pyrolyzed on pilot-plant scale at 500 °C.

	Impact Mill			Ball Mill		
	d_{10} [μm]	d_{50} [μm]	d_{90} [μm]	d_{10} [μm]	d_{50} [μm]	d_{90} [μm]
IWBC-01	4	22	73	2	6	16
IWBC-02	8	39	135	4	15	33
IWBC-03	6	33	80	3	9	23
PWBC	18	104	324	4	18	47
PSBC	13	64	147	3	14	43

3.3. Biochar micro- and mesoporosity

Biochars produced on industrial scale in the temperature range of 650 °C to 850 °C had considerably higher micro- and mesopore SSA (<2 nm and 2-50 nm, respectively) based on N₂ sorption, which ranged between 72-354 m²g⁻¹ and 66-310 m²g⁻¹ (BET and DFT theory, respectively) compared to biochars produced on pilot plant scale at 500 °C, which had N₂-based SSA below 21 m²g⁻¹ (Table 3, impact milled to < 2 mm or ball milled). Specific surface areas of micropores (< 2 nm) based on CO₂ sorption were in a narrower range for all biochars which was 236-425 m²g⁻¹ calculated according to the BET theory and between 321-617 m²g⁻¹ based on DFT (Table 3). Thus, there was a large fraction of SSA in the micropore-range, especially for pore widths < 1 nm (Figure 2) that could not be detected by N₂ but with CO₂ sorption, especially for PWBC and PSBC. Cumulative pore volumes mirrored the trends observed for SSA, both based on N₂ and CO₂ sorption (Table 3). In general, the different milling processes, i.e., impact milling to < 2mm or ball milling, and thus, the different resulting particle size distribution of biochars did not affect micro- and mesoporosity based on CO₂ and N₂ sorption (Table 3). Only for biochars produced on pilot plant scale at 500°C, ball milling to lower particle size increased N₂-based SSA compared to impact milling, yet absolute porosity based on N₂ sorption remained comparable low (Table 3). Further, IWBC-02, which was also measured as coarser particle size fraction (impact milled to < 12 mm), had considerably lower N₂-based SSA compared to the two finer milling fractions (Table 3).

The pore size distribution of micropores (< 2 nm) was not affected by the milling method for any biochar and the pore widths contributing to the highest extent to the cumulative pore volume were 0.35 nm, 0.5 nm and 0.8 nm for all biochars (Figure 2a, c, e, g and i). The different milling techniques had a more pronounced effect on shifts in pore size distribution based on N₂ sorption (Figure 2b, d, f, h and j). For example, biochars PWBC and PSBC had pores present with a width of 1.8 nm when ball milled, which were not detectable when biochars were processed by impact milling (Figure 2 h and j). For IWBC-03, pores with a width of 1 nm were present to a considerably lower extent after ball milling compared to the impact milled sample, which was also observed for IWBC-02, but not for IWBC-01 (Figure 2 b, d and f). In general, mesopores > 2-50 μm only contributed to a low extent to cumulative pore volumes and were only detectable to a comparable high extent in IWBC-01 (Figure 2 b, d and f).

Table 3: Porosity characteristics of the biochar samples milled with an impact mill to < 2 mm or with a ball mill to < 0.1 mm: Specific surface area (SSA) based on CO₂ and N₂ adsorption isotherms according to the Brunauer-Emmett-Teller theory (BET) or the Density Functional Theory (DFT) and pore volumes of micro- and mesopores derived from N₂ adsorption and of micropores based on CO₂ adsorption according to the DFT theory. IWBC: Wood-based biochar pyrolyzed on industrial scale at 850 °C (01), 750 °C (02) or 650 °C (03) and wood-based (PWBC) and straw-based (PSBC) biochar pyrolyzed on pilot-plant scale at 500 °C. IWBC-02 was also characterized by N₂ sorption after impact milling to < 12 mm.

Biochar	Milling method	BET SSA (N ₂) [m ² g ⁻¹]	BET SSA (CO ₂) [m ² g ⁻¹]	DFT SSA (N ₂) [m ² g ⁻¹]	DFT SSA (CO ₂) [m ² g ⁻¹]	DFT Micro- & mesopore volume (N ₂) [cm ³ g ⁻¹]	DFT Micropore volume (CO ₂) [cm ³ g ⁻¹]
IWBC-01	Impact mill	187	360	203	479	0.175	0.138
	Ball mill	199	368	186	492	0.178	0.141
	Impact mill (< 12 mm)	14	n.d.	13	n.d.	0.015	n.d.
IWBC-02	Impact mill	72	393	66	575	0.035	0.157
	Ball mill	83	377	87	564	0.050	0.152
IWBC-03	Impact mill	354	425	310	617	0.185	0.167
	Ball mill	267	383	302	561	0.131	0.153
PWBC	Impact mill	1	304	2	421	0.004	0.120
	Ball mill	19	324	21	435	0.019	0.126
PSBC	Impact mill	0	236	3	326	0.012	0.092
	Ball mill	10	237	14	321	0.020	0.091

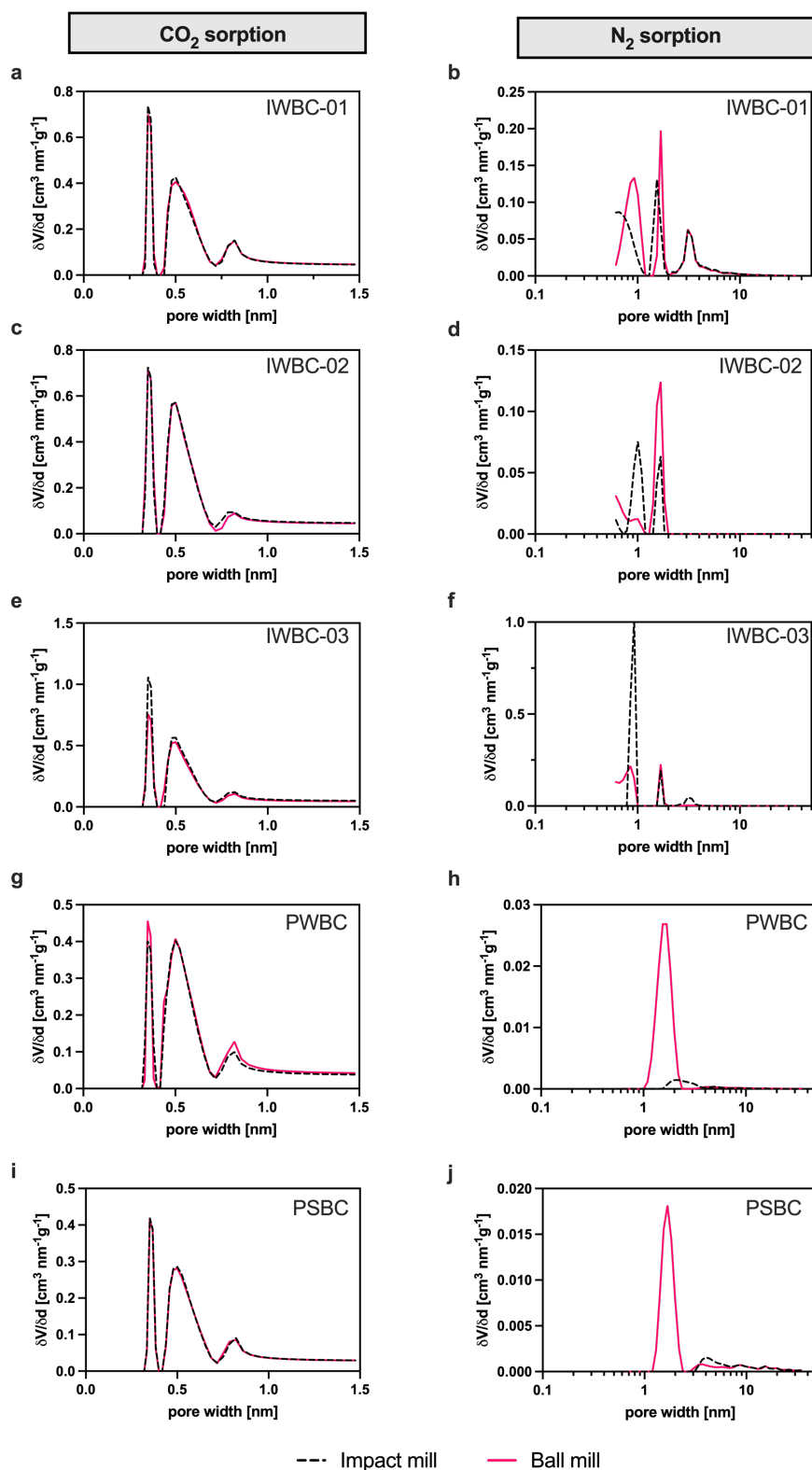


Figure 2: Pore size distribution weighed by pore volume derived from CO_2 sorption (panels a, c, e, g and i) and from N_2 sorption (panels b, d, f, h and j) for the different biochar types and milling methods impact milling or ball milling. Pore size distribution was calculated with the density functional theory. IWBC: Wood-based biochar pyrolyzed on industrial scale at $850\text{ }^\circ\text{C}$ (01), $750\text{ }^\circ\text{C}$ (02) or $650\text{ }^\circ\text{C}$ (03) and wood-based (PWBC) and straw-based (PSBC) biochar pyrolyzed on pilot-plant scale at $500\text{ }^\circ\text{C}$.

3.4. Water holding capacity of biochar and biochar-soil mixtures

Water holding capacities of pure biochars ranged between 140% and 240% (w/w) after impact milling and differed significantly from each other, despite IWBC-01 and PSBC, which had a WHC in a similar range (Figure 3). Biochar IWBC-03 had the highest WHC and PWBC the lowest after impact milling. After ball milling, WHCs were more unified across different biochar types and ranged between 85% and 115% (Figure 3). Only IWBC-01 had a WHC significantly higher compared to the other biochars, except compared to the PSBC (Figure 3). Thus, ball milling of biochars to finer particle size significantly reduced WHC compared to the biochars processed in the impact mill. The WHC of pure biochars was not linearly correlated (analysis not shown) with any parameter describing biochar porosity listed in Table 3 nor with the average particle diameter d_{50} listed in Table 2. This was both tested individually within each biochar milling method and expanded on all biochar samples, independent of the milling method. For IWBC-02, also a larger milling fraction after impact milling to < 12 mm was analyzed for WHC (Figure S 5). For this biochar, every decrease in particle size resulted in a further decrease in WHC (Figure S 5).

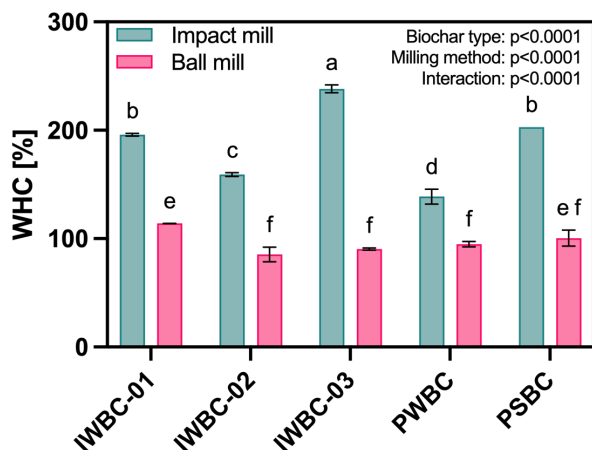


Figure 3: Water holding capacities of pure biochar samples milled with an impact mill or with a ball mill. IWBC: Wood-based biochar pyrolyzed on industrial scale at 850 °C (01), 750 °C (02) or 650 °C (03) and wood-based (PWBC) and straw-based (PSBC) biochar pyrolyzed on pilot-plant scale at 500 °C. The error bars indicate the minimums and maximums of $n=2$ measurements. Different letters above error bars indicate significant differences between all samples (two-way ANOVA, Tukey's post hoc test, $p < 0.05$).

Homogeneous mixtures of soil and impact milled biochars had WHCs between 31.6% and 35.2%, which was higher compared to the pure soil without any biochar amendment (30.1% WHC), and also significantly higher compared to most soil mixtures containing ball milled biochars, which had WHCs between 30.4% and 32.1% (Figure 4a). Both the biochar

type and the milling method significantly affected the WHC of the homogeneously biochar-amended soil ($p < 0.0001$, Table S 4). Only for PWBC, the direct comparison between the different milling methods was not statistically significant (Figure 4a). For impact milled biochars, soil homogeneously amended with IWBC-03 had the highest WHC (Figure 4a), in line with WHC of pure biochars (Figure 3). For ball milled biochars, PSBC maximized the WHC of the soil mixture (Figure 4a). On a relative basis, all impact milled biochars under homogeneous amendment significantly increased WHC by 5-17% ($p < 0.05$) while only PSBC in ball milled form significantly increased WHC by 6% compared to soil without a biochar amendment ($p < 0.05$, one-way ANOVA followed by Dunnett's test against the no BC control, analysis data not shown). For ball milled industrial biochars, WHC of homogeneously biochar-amended soils were similar to the WHC of the pure soil (Figure 4a).

Biochar application as layer increased WHC of the soil mixtures in the range of 5-11% for impact milled biochars and between 4-9 % for ball milled biochars compared to pure soil (Figure 4b). Compared to the control, increases were only significant for impact milled IWBC-03 and PSBC ($p < 0.05$, one-way ANOVA followed by Dunnett's test). Ball milled biochars increased WHC to a similar extent as impact milled biochars, only for IWBC-03, impact milling significantly increased WHC compared to ball milling (Figure 4b, Table S 4). Impact milled biochars had similar WHC under layer application as compared to homogeneous soil application. The mixtures containing ball milled IWBCs as concentrated layer application had higher WHC compared to their homogeneous application (Figure 4b). Thus, differences between ball milled and impact milled biochars were smaller in concentrated layer application compared to homogeneous application (Figure 4).

Estimation of WHCs of soil-biochar-mixtures by calculation from WHC of pure biochars and soil were close to actual measurements for all biochar types, both milling and application methods of the biochar (Figure 4 c and d). The deviation of measured from estimated WHCs ranged between -6.1% and 3.0% for homogeneous mixtures and between -3.3% and 3.4% for biochar applications as layer. The sum of squares of deviations from estimated to measured WHCs was 50% lower for data obtained for the application of biochar as layer in soil.

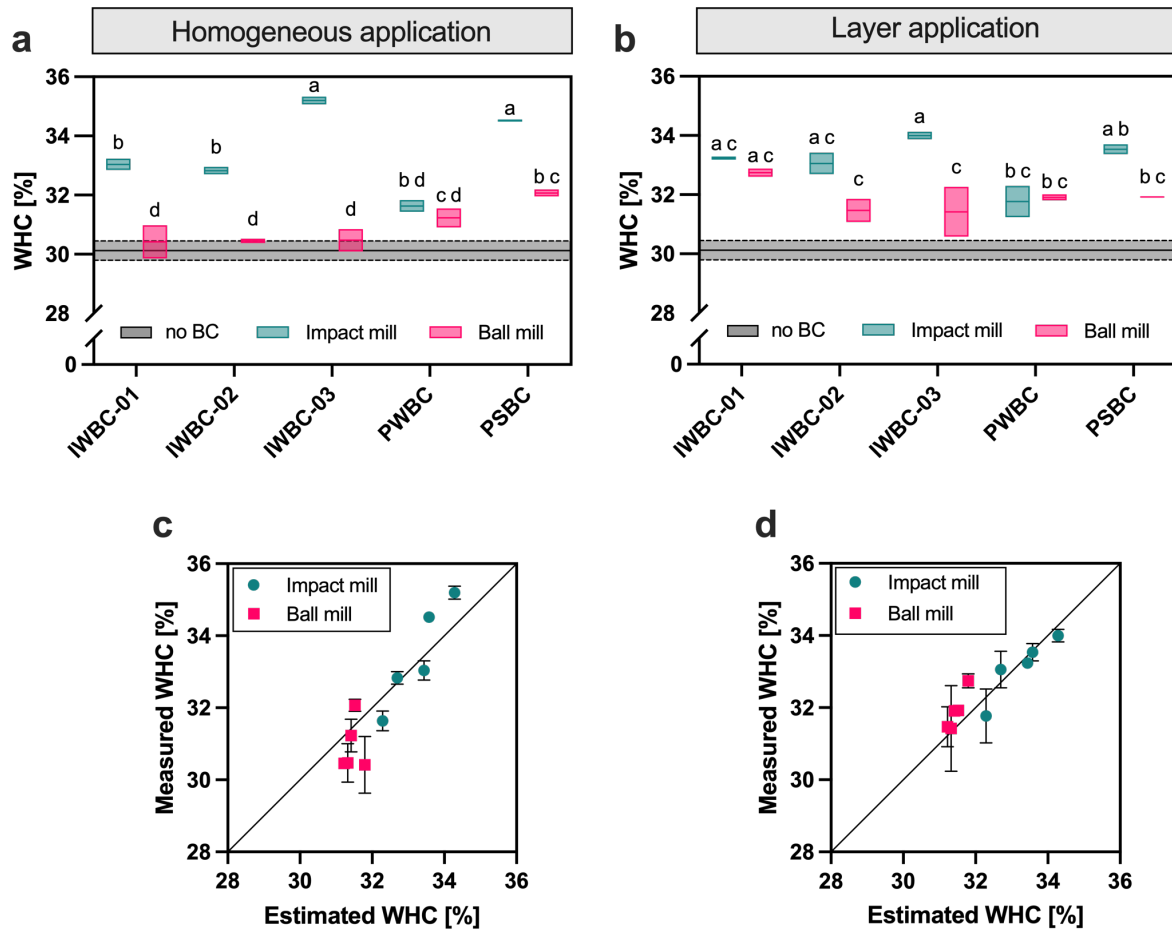


Figure 4: Water holding capacity (WHC) of soil-biochar mixtures (2%, w/w) where biochar was applied homogeneously (a) or as concentrated layer (b) derived from milling with an impact mill (<2 mm) or with a ball mill. Measured WHC plotted over estimated WHC based on individually measured WHCs of pure soil and biochar for the soil-biochar mixtures, where biochars were applied homogeneously to the soil (c) or as concentrated layer (d). IWBC: Wood-based biochar pyrolyzed on industrial scale at 850 °C (01), 750 °C (02) or 650 °C (03) and wood-based (PWBC) and straw-based (PSBC) biochar pyrolyzed on pilot-plant scale at 500 °C. The box range indicates the minimum and maximum of n=2 measurements with the average indicated as horizontal line. Different letters above error bars indicate significant differences between all samples (two-way ANOVA, Tukey's post hoc test, p<0.05).

3.5. Cabbage growth

Dry yields of aboveground biomass were around 40 g plant⁻¹ and cabbage head yields were around 25 g plant⁻¹ and they were similar for all biochar treatments compared to the Control (Figure 5a, b, c and d). The biochar type significantly affected cabbage head yields ($p = 0.037$), which was reflected by the lower yield for plants grown on soil amended with IWBC-03 compared to soil amended with PSBC (Figure 5c). The milling method had no significant impact on yield of any plant part of white cabbage (Figure 5a, c and e). Root biomass ranged between 2 g plant⁻¹ and 3.6 plant⁻¹ for all plants (Figure 5e) and was on average 12% higher with a biochar amendment compared to non-amended Control, i.e., pure soil without biochar ($p=0.014$, Figure 5f).

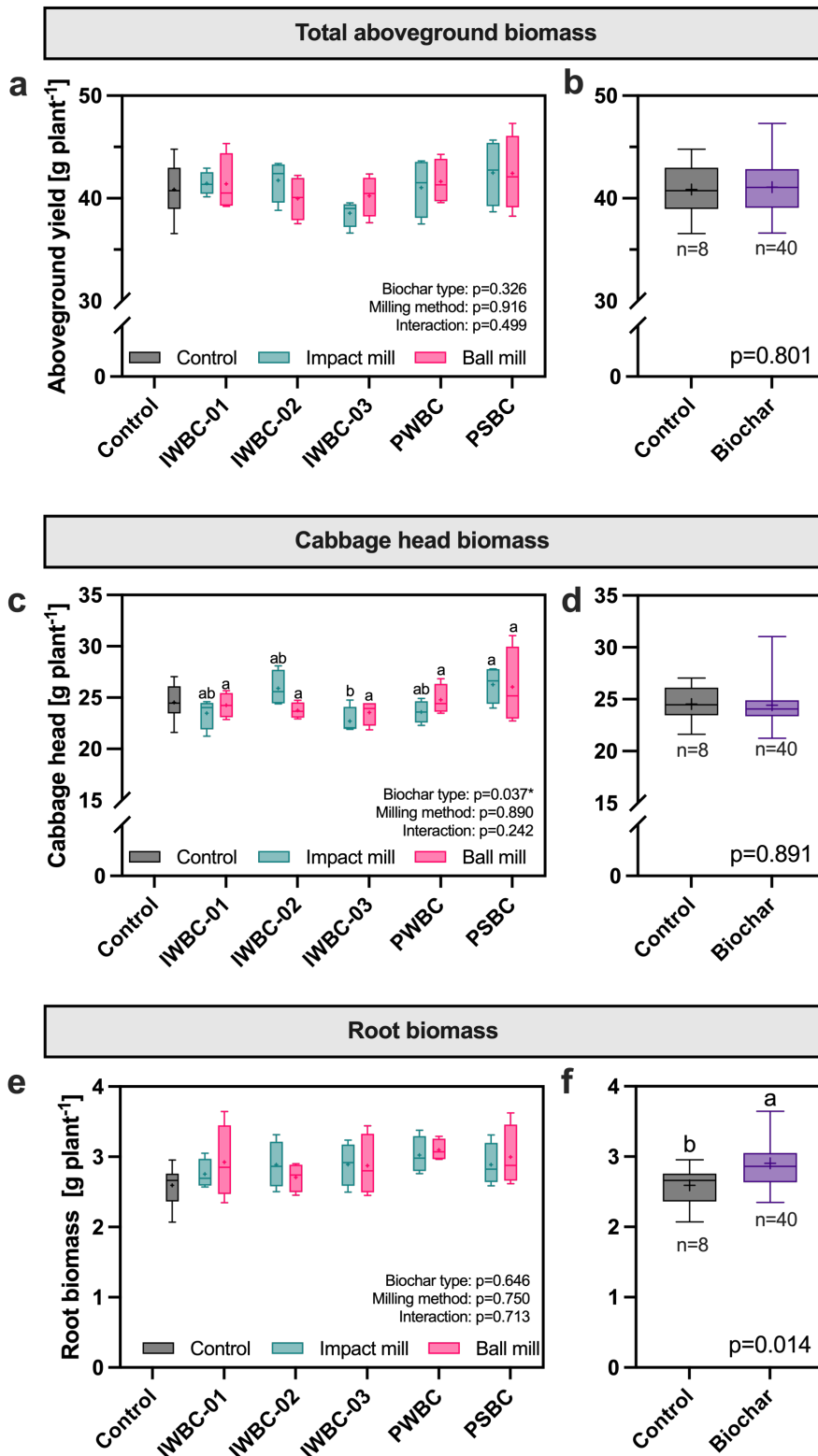


Figure 5: Dry biomass yields of white cabbage plants: total aboveground biomass (a and b), cabbage heads (c and d) and cabbage roots (e and f). The soil was amended with 0.8% of different biochars derived from milling with an impact mill or with a ball mill as concentrated layer or without any biochar (Control). IWBC: Wood-based biochar pyrolyzed on industrial scale at 850 °C (01), 750 °C (02) or 650 °C (03) and wood-based (PWBC) and straw-based (PSBC) biochar pyrolyzed on pilot-plant scale at 500 °C. For panel b, d and f, 'Biochar'

represents the average of all biochar treatments, independent of biochar type and milling method. Whiskers in boxplots represent the minimum to maximum value of the replicates, mean values are indicated with "+". Each individual biochar treatment had four replicates; the Control had eight replicates. In panels a, c and e, different letters indicate a significant difference between the treatments within milling method ('Impact mill' or 'Ball mill', two-way analysis of variance, Tukey's post hoc test, $p < 0.05$). In panel b, d and f, different letters above error bars indicate a significant difference between the Control and the average of all biochar treatments (unpaired t -test, $p < 0.05$).

4. Discussion

This study investigated the effect of two different milling techniques to produce biochar microparticles on biochar particle size distribution, biochar porosity as well as WHC of biochars and of biochar-soil mixtures. Further, the effect of the different biochars and milling methods on yield of white cabbage was studied, when biochar was applied as concentrated layer in the root-zone of cabbage seedlings.

Ball milling resulted in fine biochar powders with significantly lower particle size as compared to impact milling. Still, both milling methods provided biochar powders with particle sizes below 500 μm , which is considered as maximum particle diameter e.g., for biochar to be used in granulation processes for BBF production⁶. Despite applying the same milling method, different biochars had different particle size distributions after milling. Biochars produced on pilot plant scale were in general less finely milled as compared to biochars produced on industrial scale. There are two possible reasons for this observation. For pyrolysis on pilot-plant scale, pelleted biomass was used while non-pelleted wood was used for pyrolysis on industrial scale. As pelleting results in a more dense and harder feedstock material, the resulting biochar might be harder as well, lowering its grindability compared to biochars produced from non-pelleted feedstock. Further, the biochars produced on pilot plant scale were made at significantly lower pyrolysis temperature, i.e., at 500 °C compared to 650-850 °C which were used for industrial pyrolysis. Higher pyrolysis temperatures made biochars more porous, which might have also improved its grindability.

Despite the considerable differences in particle size distributions of biochars between the different milling methods, the micro- and mesoporosity of biochars was not changed based on CO₂ and N₂ sorption. Thus, the accessible biochar surface for these gases was not further increased through ball milling, in contrast to what was observed in some earlier studies^{23,24}, presumably because internal surface area of biochars was already well accessible before any milling or after impact milling. Coarser milled biochar (> 2 mm) was unfortunately only

analyzed for IWBC-02 in the present study, where N₂ accessible SSA was significantly increased by impact-milling to < 2 mm or ball-milling. It was withdrawn to include non-milled or coarser milled for all biochars to have more equal comparisons between individual biochar types, as biochars differed in bulk particle size due to variation in feedstock material and process conditions. For example, IWBC-01 is obtained from the pyrolysis process in already relatively fine powder <1 mm, while all other biochars had particle sizes in the range of 20 mm after pyrolysis.

The fact that WHC of pure biochars was significantly decreased through ball milling, despite similar micro- and mesoporosity, highlights that WHC of biochars is substantially affected by interporosity, i.e., the presence of pore space between individual biochar particles and not by intraporosity predicted from N₂ or CO₂ physisorption²⁵. Ball milling significantly reduced the particle size and thus the space between individual biochar particles, which lowers interpore space for water storage. It must be noted that biochar macroporosity (pore widths > 50 μm) was not quantified in the present study and thus, the influence of the different milling methods on macropores contributing to the intraporosity and WHC of the biochar samples cannot be concluded from our study. Ball milling will likely have destroyed macropores to a greater extent than impact milling, further limiting the WHC of pure biochars.

Impact milled biochars increased WHC of soil mixtures to a higher extent than ball milled biochars, mirroring the results obtained for WHC of pure biochars. Most likely, coarser, impact milled microparticles with its larger and more irregular particle size (multimodal q_3 distributions, Figure 2b) created additional interpore space in the soil matrix under homogeneous application. For ball milled samples, this was only observed for PSBC, which also had the broadest q_3 particle size distribution among ball milled biochars, i.e. particles were present in a larger range of particle sizes. These results are in line with increased WHC of pure sand amended with coarse (0.853-2 mm) and medium (0.251-0.853 mm) sized biochar particles at 2% (w/w) compared to amendment of fine biochar particles (< 0.251 mm)²⁵. As plant available water is positively correlated with WHC of biochar-amended soils²⁵, trends observed for WHC among biochar-amended soils in the present study might be transferable to plant-available water values.

The comparatively higher WHC of soil amended with layered compared to the homogeneous application of ball milled biochar with lowest and most narrowly distributed particle sizes (IWBC-01, IWBC-02 and IWBC-03) might be associated with a development of a water barrier by the layer of finely milled biochars, inhibiting water drainage from the topsoil by a potential reduction of hydrological connectivity in the soil column. However, this would need further

investigation, also with a higher number than only two experimental replications and with a separate measurement of water contents after drainage in the upper and lower soil layer.

More general, WHC of biochar-soil-mixtures could be well predicted from WHC of the pure soil and biochar, even better when biochar was applied as layer. This might be since the layer application, i.e., pure soil layers interrupted by a pure biochar layer, better reflects the WHC measurement situation of the pure soil and biochars. The good agreement of measured and estimated WHC is in line with reported linear increase in WHC with biochar amendments to sandy soil of up to 10% (w/w)²⁶. We tested both homogeneous and layer application in this study, as homogeneous spreading of biochar to soil is most common practice in biochar application¹, still, positive crop response was also achieved under concentrated, layered BBF applications in the root-zone of plants^{15,27-29}. Based on our results, if ball milling of biochar is technically necessary to achieve a specific particle size, it should rather be applied layered and not homogeneously distributed to soil to maximize WHC. Still, this should also be tested when biochar is amended as layered stripes, i.e., horizontal interruption of the biochar layer by soil, which would reflect a field scenario with biochar applied in planting or seeding stripes.

Aboveground biomass yields of white cabbage remained unaffected of any biochar amendment, independent of biochar type or milling method. Positive, but also negative, effects on plant growth with biochar microparticle amendments as observed for rice¹², cowpea or velvetleaf¹³ or general higher agronomic benefits of soil amendment with cereal residue-based biochar produced at low pyrolysis temperature³⁰, which would be represented by the biochar sample PSBC, could thus not be confirmed in our plant growth study. Potential negative effects on reduced WHC of soil amended with ball milled biochar might only have become relevant under drought simulation during the experiment, but not with the sufficient irrigation on a daily basis and the use of a silt loam soil, which has higher water retention capacity compared to sandy soils, and is thus less responsive to biochar amendments in terms of increases in WHC and plant-available water¹⁴. Therefore, a follow up experiment should be conducted with different soil types and two different irrigation regimes, e.g., irrigation at the level of the permanent wilting point³¹ and regular irrigation to 60% WHC, as was done in the present study. For such an experiment, a biochar like IWBC-03 should be used which had the highest difference in WHC of impact milled compared to ball milled particles.

The biochar IWBC-02 was applied as a concentrated layer in the root zone of white cabbage in an earlier greenhouse experiment to the same soil, where it increased cabbage head yields in combination with a NH_4NO_3 fertilization by 27% while yield was not changed in combination with urea fertilization compared to similarly fertilized controls without any biochar

amendment¹⁵. This could highlight the deviation in plant growth response on biochar amendments even between individual trials performed in the greenhouse as e.g., affected by climatic conditions or sun irradiance. More important, it has to be noted that IWBC-02 was amended as coarser particles (impact milled to < 12 mm) in the previous trial, which does not allow a direct comparison of the trial results. In the present trial, differences in cabbage growth might have occurred e.g., under drought conditions, were plants grown on soil amended with impact milled biochars would have benefited from the higher substrate WHC and higher water content at the permanent wilting point²⁵. The 12% increase in root growth averaged over all biochar applications is well in line with meta-analysis of biochar effects on root growth³². As there were no positive effects of biochar comminution via ball milling e.g., on biochar porosity, WHC or plant growth, the largest possible particle size should be chosen if biochar is needed in the form of microparticles, e.g., for granulation processes or for application of biochar via drip irrigation. This, in the light of the results of the present study, is to ensure highest possible elevation of soil WHC with a biochar amendment. Impact milled biochars, when using a milling sieve with 2 mm mesh size, had a particle sizes in the range of mostly 5-150 μm , which would be well suitable for drum granulation processes to produce granulated BBF⁶.

5. Conclusions

Micronization of biochar to particle sizes below 50 μm , e.g. by ball milling, would make biochar utilizable for BBF granulation or BBF-based fertigation, but comes at the expense of WHC of biochar and biochar-amended soil. Reductions of particle size to mostly <200 μm was also achieved by impact milling, which would be a well applicable particle size for granulation processes in BBF production, while providing higher WHC in soil. Whenever possible, it seems that the largest possible particle size of biochar should be applied to soil, at least in the size range between 1-1000 μm . Differences in hydrological properties of biochar-amended soil could also influence nutrient leaching. Therefore, biochar microparticles applied via BBF might also affect nutrient leaching compared to application of coarser milled biochar, which should be tested in future research.

References

1. Melo, L. C. A., Lehmann, J., Carneiro, J. S. da S. & Camps-Arbestain, M. Biochar-based fertilizer effects on crop productivity: a meta-analysis. *Plant Soil* (2022) doi:10.1007/s11104-021-05276-2.
2. Izydorczyk, G., Mikula, K., Skrzypczak, D., Witek-Krowiak, A. & Chojnacka, K. Granulation as the method of rational fertilizer application. in *Smart Agrochemicals for Sustainable Agriculture* 163–184 (Elsevier, 2022). doi:10.1016/B978-0-12-817036-6.00003-0.
3. Hagin, J. & Lowengart, A. Fertigation for minimizing environmental pollution by fertilizers.
4. Niu, J., Liu, C., Huang, M., Liu, K. & Yan, D. Effects of Foliar Fertilization: a Review of Current Status and Future Perspectives. *J Soil Sci Plant Nutr* **21**, 104–118 (2021).
5. Kumar, A. *et al.* Fertilizing behavior of extract of organomineral-activated biochar: low-dose foliar application for promoting lettuce growth. *Chem. Biol. Technol. Agric.* **8**, 21 (2021).
6. Bowden-Green, B. & Briens, L. An investigation of drum granulation of biochar powder. *Powder Technology* **6** (2016).
7. Äijälä, H. & Ahlnäs, T. A suspension fertilizer suitable for irrigation fertilization, and a process for its preparation. (1997).
8. Vert, M. *et al.* Terminology for biorelated polymers and applications (IUPAC Recommendations 2012). *Pure and Applied Chemistry* **84**, 377–410 (2012).
9. Verma, D. *et al.* Advancements on microparticles-based drug delivery systems for cancer therapy. in *Advanced Drug Delivery Systems in the Management of Cancer* 351–358 (Elsevier, 2021). doi:10.1016/B978-0-323-85503-7.00003-1.
10. Atkinson, C. J. How good is the evidence that soil-applied biochar improves water-holding capacity? *Soil Use and Management* **34**, 177–186 (2018).
11. Basso, A. S., Miguez, F. E., Laird, D. A., Horton, R. & Westgate, M. Assessing potential of biochar for increasing water-holding capacity of sandy soils. *GCB Bioenergy* **5**, 132–143 (2013).
12. Chew, J. *et al.* Biochar-based fertiliser enhances nutrient uptake and transport in rice seedlings. *Science of The Total Environment* 154174 (2022) doi:10.1016/j.scitotenv.2022.154174.
13. Tang, E., Liao, W. & Thomas, S. C. Optimizing Biochar Particle Size for Plant Growth and Mitigation of Soil Salinization. *Agronomy* **13**, 1394 (2023).
14. Rabbi, S. M. F., Minasny, B., Salami, S. T., McBratney, Alex. B. & Young, I. M. Greater, but not necessarily better: The influence of biochar on soil hydraulic properties. *European J Soil Science* **72**, 2033–2048 (2021).
15. Grafmüller, J., Schmidt, H.-P., Kray, D. & Hagemann, N. Root-Zone Amendments of Biochar-Based Fertilizers: Yield Increases of White Cabbage in Temperate Climate. *Horticulturae* **8**, 307 (2022).
16. Hagemann, N. *et al.* Wood-based activated biochar to eliminate organic micropollutants from biologically treated wastewater. *Science of The Total Environment* **730**, (2020).
17. DIN e.V. DIN EN ISO 18122:2023-02, Biogene Festbrennstoffe_ - Bestimmung des Aschegehaltes (ISO_18122:2022); Deutsche Fassung EN_ISO_18122:2022. (2023) doi:10.31030/3379889.
18. DIN e.V. DIN 66144:1974-03, Darstellung von Korn-(Teilchen-)größenverteilungen; Logarithmisches Normalverteilungsnetz. (1974) doi:10.31030/1301604.
19. DIN e.V. DIN EN ISO 14238:2014-03, Bodenbeschaffenheit - Biologische Verfahren-Bestimmung der Stickstoffmineralisierung und -nitrifizierung in Böden und der Einflüsse von Chemikalien auf diese Prozesse (ISO_14238:2012); Deutsche Fassung EN_ISO_14238:2013.

(2014) doi:10.31030/2081435.

20. EBC 2012-2024. 'European Biochar Certificate - Guidelines for a Sustainable Production of Biochar.' Carbon Standards International (CSI), Frick, Switzerland. (<http://european-biochar.org>). Version 10.4 from 20th Dec 2024. (2024).
21. Brunauer, S., Emmett, P. H. & Teller, E. Adsorption of Gases in Multimolecular Layers. *Journal of the American Chemical Society* **60**, 309–319 (1938).
22. Hohenberg, P. & Kohn, W. Inhomogeneous Electron Gas. *Phys. Rev.* **136**, B864–B871 (1964).
23. Lyu, H. *et al.* Effects of ball milling on the physicochemical and sorptive properties of biochar: Experimental observations and governing mechanisms. *Environmental Pollution* **233**, 54–63 (2018).
24. Peterson, S. C., Jackson, M. A., Kim, S. & Palmquist, D. E. Increasing biochar surface area: Optimization of ball milling parameters. *Powder Technology* **228**, 115–120 (2012).
25. Liu, Z., Dugan, B., Masiello, C. A. & Gonnermann, H. M. Biochar particle size, shape, and porosity act together to influence soil water properties. *PLoS ONE* **12**, e0179079 (2017).
26. Yu, O.-Y., Raichle, B. & Sink, S. Impact of biochar on the water holding capacity of loamy sand soil. *Int J Energy Environ Eng* **4**, 44 (2013).
27. Abiven, S., Hund, A., Martinsen, V. & Cornelissen, G. Biochar amendment increases maize root surface areas and branching: a shovelomics study in Zambia. *Plant Soil* **395**, 45–55 (2015).
28. Cornelissen, G. *et al.* Biochar Effect on Maize Yield and Soil Characteristics in Five Conservation Farming Sites in Zambia. *Agronomy* **3**, 256–274 (2013).
29. Schmidt, H. *et al.* Fourfold Increase in Pumpkin Yield in Response to Low-Dosage Root Zone Application of Urine-Enhanced Biochar to a Fertile Tropical Soil. *Agriculture* **5**, 723–741 (2015).
30. Ye, L. *et al.* Biochar effects on crop yields with and without fertilizer: A meta-analysis of field studies using separate controls. *Soil Use Manage* **36**, 2–18 (2020).
31. Haider, G. *et al.* Biochar but not humic acid product amendment affected maize yields via improving plant-soil moisture relations. *Plant Soil* **395**, 141–157 (2015).
32. Xiang, Y., Deng, Q., Duan, H. & Guo, Y. Effects of biochar application on root traits: a meta-analysis. *GCB Bioenergy* **9**, 1563–1572 (2017).

Supplementary Information to:

Preparation of biochar microparticles by milling: effect on biochar and soil water holding capacity, biochar porosity and growth of white cabbage

Jannis Grafmüller^{1,2,3}, Jens Möllmer⁴, Daniel Kray¹, Stephanie Spahr⁵, Hans-Peter Schmidt²,
Nikolas Hagemann^{2,6}

¹Institute for Sustainable Energy Systems (INES), Offenburg University of Applied Sciences, Germany

²Ithaka Institute, Arbaz (Switzerland) and Goldbach (Germany)

³Plant Biogeochemistry, Tübingen University, Tübingen, Germany

⁴Institut für Nichtklassische Chemie e.V. (INC), Leipzig, Germany

⁵Leibniz Institute of Freshwater Ecology and Inland Fisheries, Berlin, Germany

⁶Environmental Analytics, Agroscope Zurich, Switzerland

Chapter 3: Physical modification of biochar for use in biochar-based fertilizers

Table S 1: Basic soil properties and nutrient contents of the soil used in the Greenhouse Trial. Reproduced with permission from Grafmüller et al., 2022, *Horticulturae*, MDPI.

Parameter	Unit	Value	Method
Humus content	wt%	3.7	DIN ISO 10694: 1996-08
Total Organic Carbon	wt%	2.1	DIN ISO 10694: 1996-08
pH	1	7.1	VDLUFA Methodenbuch Band I, Kapitel 5.1.1, 7.Teillieferung, 2016
Electric Conductivity	μScm^{-1}	79	VDLUFA Methodenbuch Band I, Kapitel 10.1.1, 1991
Salt content	$\text{mg}(100\text{g})^{-1}$	42	VDLUFA Methodenbuch Band I, Kapitel 10.1.1, 1991
Kjeldahl-N	wt%	0.23	DIN 19684-4
NH ₄ -N	$\text{mg}(100\text{g})^{-1}$	<0.05	VDLUFA Methodenbuch Band I, 3. Teillieferung, Kapitel 6.1.4.1, 2002
NO ₃ -N	$\text{mg}(100\text{g})^{-1}$	1.9	VDLUFA Methodenbuch Band I, 3. Teillieferung, Kapitel 6.1.4.1, 2002
S _{min}	$\text{mg}(100\text{g})^{-1}$	0.51	VDLUFA Methodenbuch I, A 6.3.1 (2016), Extraktion mit 0,0125 M CaCl ₂
Potassium (K)	$\text{mg}(100\text{g})^{-1}$	27.2	Calcium lactate extract, VDLUFA Methodenbuch Band I, 6.Teillieferung, Kapitel 6.2.1.1, 2012
Phosphorus (P)	$\text{mg}(100\text{g})^{-1}$	35.3	Calcium lactate extract, VDLUFA Methodenbuch Band I, 6.Teillieferung, Kapitel 6.2.1.1, 2012
Magnesium (Mg)	$\text{mg}(100\text{g})^{-1}$	29.8	Calcium lactate extract, VDLUFA Methodenbuch Band I, 6.Teillieferung, Kapitel 6.2.1.1, 2012
Boron (B)	mgkg^{-1}	0.9	CAT extract, VDLUFA Methodenbuch Band I, 3. Teillieferung, Kapitel 6.4.1, 2002
Manganese (Mn)	mgkg^{-1}	160	CAT extract, VDLUFA Methodenbuch Band I, 3. Teillieferung, Kapitel 6.4.1, 2002
Copper (Cu)	mgkg^{-1}	4.2	CAT extract, VDLUFA Methodenbuch Band I, 3. Teillieferung, Kapitel 6.4.1, 2002
Zinc (Zn)	mgkg^{-1}	10	CAT extract, VDLUFA Methodenbuch Band I, 3. Teillieferung, Kapitel 6.4.1, 2002

Table S 2: Cation exchange Capacity of the Soil used in the Greenhouse Trial. Reproduced with permission from Grafmüller et al., 2022, *Horticulturae*, MDPI.

Parameter	Unit	Value	Method
Cation Exchange Capacity (eff. ^a)	cmol ⁺ kg ⁻¹	23.6	DIN EN ISO 11260:2011-09
Exchange Acidity	cmol ⁺ kg ⁻¹	<0.1	DIN EN ISO 11260:2011-09
Exchangable Mg (eff. ^a)	cmol ⁺ kg ⁻¹	4.1	DIN EN ISO 11260:2011-09
Exchangable Ca (eff. ^a)	cmol ⁺ kg ⁻¹	24.5	DIN EN ISO 11260:2011-09
Exchangable Na (eff. ^a)	cmol ⁺ kg ⁻¹	<0.1	DIN EN ISO 11260:2011-09
Exchangable K (eff. ^a)	cmol ⁺ kg ⁻¹	1.2	DIN EN ISO 11260:2011-09
Sum of exchangeable Cations (eff. ^a)	cmol ⁺ kg ⁻¹	29.8	DIN EN ISO 11260:2011-09
Cation Exchange Capacity (pot. ^b)	cmol ⁺ kg ⁻¹	22.2	DIN ISO 13536: 1997-04
Exchangable Mg (pot. ^b)	cmol ⁺ kg ⁻¹	2.4	DIN ISO 13536: 1997-04
Exchangable Ca (pot. ^b)	cmol ⁺ kg ⁻¹	17	DIN ISO 13536: 1997-04
Exchangable Na (pot. ^b)	cmol ⁺ kg ⁻¹	<0.1	DIN ISO 13536: 1997-04
Exchangable K (pot. ^b)	cmol ⁺ kg ⁻¹	0.9	DIN ISO 13536: 1997-04
Sum of exchangeable Cations (pot. ^b)	cmol ⁺ kg ⁻¹	20	DIN ISO 13536: 1997-04

^aeff.: effective

^bpot.: potential

Table S 3: Particle Size Distribution of the soil used in the Greenhouse Trial. Reproduced with permission from Grafmüller et al., 2022, Horticulturae, MDPI.

Parameter	Unit	Value	Method
Clay (<2µm)	wt%	28	DIN ISO 11277:2002:08
Coarse Sand (0.63 - 2mm)	wt%	2	DIN ISO 11277:2002:08
Medium Sand (0.2 - 0.63mm)	wt%	2	DIN ISO 11277:2002:08
Fine Sand (0.063 - 0.2mm)	wt%	5	DIN ISO 11277:2002:08
Coarse Silt (20-63 µm)	wt%	31	DIN ISO 11277:2002:08
Medium Silt (6.3 - 20 µm)	wt%	24	DIN ISO 11277:2002:08
Fine Silt	wt%	24	DIN ISO 11277:2002:08
Gravel (>2 mm)	wt%	<1	DIN ISO 11277:2002:08
Coarse Soil (>2mm)	wt%	<1	DIN ISO 11277:2002:08

Table S 4: Results of two-way analysis of variance (ANOVA) for water holding capacity of homogeneous mixtures of biochar and soil: sum of squares (SS), degree of freedom (DF), mean sum of squares (MS), F and p value.

Homogeneous biochar application to soil					
	SS	DF	MS	F (DFn, DFd)	p
Biochar type x Milling method	9.366	4	2.342	F (4, 10) = 17.05	0.0002
Biochar type	10.89	4	2.724	F (4, 10) = 19.83	<0.0001
Milling method	31.62	1	31.62	F (1, 10) = 230.2	<0.0001

Table S 5: Results of two-way analysis of variance (ANOVA) for water holding capacity of homogeneous mixtures of biochar and soil: sum of squares (SS), degree of freedom (DF), mean sum of squares (MS), F and p value.

Layered biochar application to soil					
	SS	DF	MS	F (DFn, DFd)	p
Biochar type x Milling method	4.512	4	1.128	F (4, 10) = 4.193	0.0300
Biochar type	3.323	4	0.8307	F (4, 10) = 3.088	0.0674
Milling method	7.511	1	7.511	F (1, 10) = 27.92	0.0004

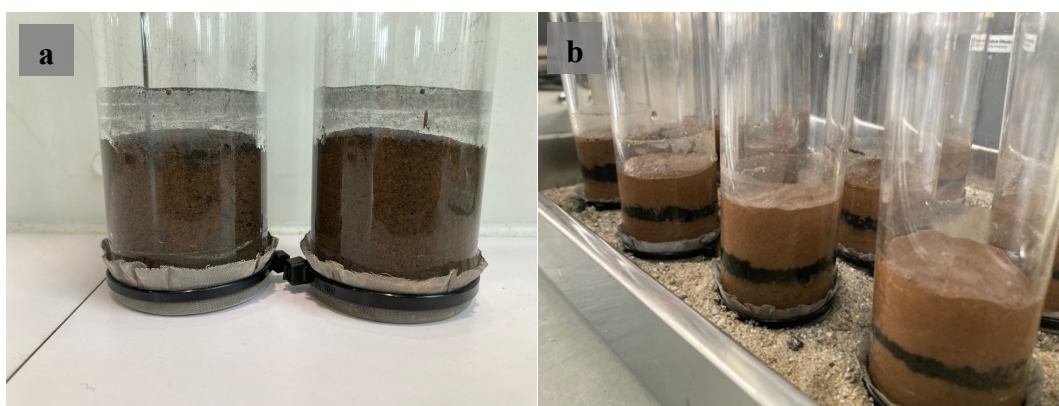


Figure S 1: Soil columns after water saturation and drainage with 2% (w/w) biochar amendment as homogeneous application (a) or layer application (b).



Figure S 2: White cabbage seedlings just before transplantation to experimental pots.



Figure S 3: White cabbage plants in the greenhouse 2.5 weeks after transplanting seedling into pots (a) and after 8 weeks, i.e., 3 weeks before final harvest (b).

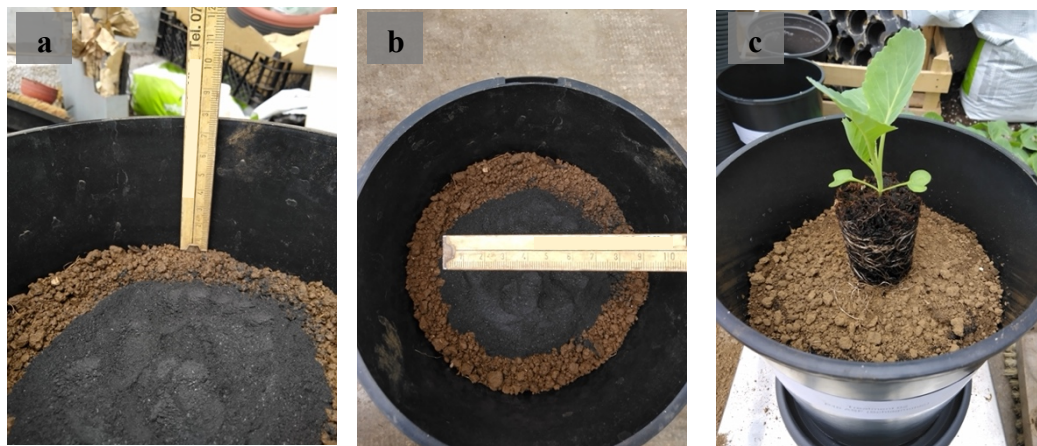


Figure S 4: Concentrated biochar layer in 8 cm soil depth (a) with a diameter of 8 cm (b) and transplanted seedling on top of the biochar which was covered by a thin (<1 cm) soil layer. The pot was then filled up with the remaining soil (not shown).

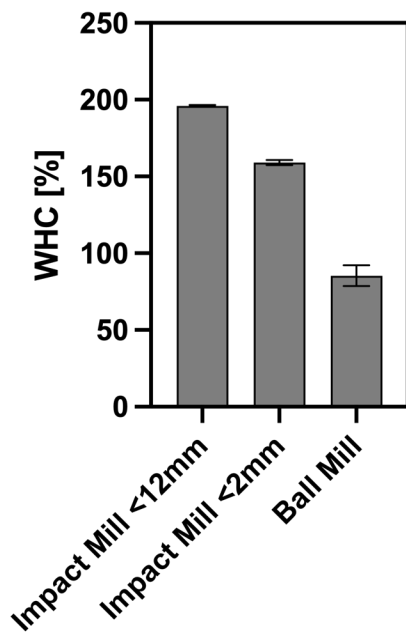


Figure S 5: Water holding capacity (WHC) of industrial wood biochar produced at 750 °C in a pyrolysis plant manufactured by Carbon Technik Schuster GmbH (biochar IWBC-02). Biochar was processed in an impact mill either to particles <12 mm, < 2 mm or in a ball-mill.

References

J. Grafmüller, H.-P. Schmidt, D. Kray, N. Hagemann, Root-Zone Amendments of Biochar-Based Fertilizers: Yield Increases of White Cabbage in Temperate Climate, *Horticulturae* 8 (2022) 307. <https://doi.org/10.3390/horticulturae8040307>.

Chapter 3c

Granulation compared to co-application of biochar plus mineral fertilizer and its impacts on crop growth and nutrient leaching.

Jannis Grafmüller^{1,2,3,4}, Jens Möllmer⁵, E. Marie Muehe^{3,6}, Claudia I. Kammann⁷, Daniel Kray¹, Hans-Peter Schmidt² and Nikolas Hagemann^{2,4}

¹Institute of Sustainable Energy Systems (INES), Offenburg University of Applied Sciences, Germany

²Ithaka Institute, Arbaz (Switzerland) and Goldbach (Germany)

³Plant Biogeochemistry, Department of Geosciences, University of Tübingen, Tübingen, Germany

⁴Environmental Analytics, Agroscope, Zurich, Switzerland

⁵Institut für Nichtklassische Chemie e.V. (INC), Leipzig, Germany

⁶Plant Biogeochemistry, Department of Applied Microbial Ecology, Helmholtz Centre for Environmental Research - UFZ, Leipzig, Germany

⁷Department of Applied Ecology, Hochschule Geisenheim University, Geisenheim, Germany

Published in:

Scientific Reports

First published: 17th July 2024

<https://doi.org/10.1038/s41598-024-66992-0>

Material from:

J. Grafmüller, J. Möllmer, E.M. Muehe, C.I. Kammann, D. Kray, H.-P. Schmidt, N. Hagemann, Granulation compared to co-application of biochar plus mineral fertilizer and its impacts on crop growth and nutrient leaching, *Sci Rep* 14 (2024) 16555.

<https://doi.org/10.1038/s41598-024-66992-0>.

The published article is re-printed in this thesis with permission from Springer Nature. The right to include the article in its published form in a thesis or dissertation is retained by the authors in accordance with Springer Nature Journal Author Rights.

Statement of personal and co-author contributions, plus non-listed contributors

Authors	Position of candidate in list of authors	Scientific ideas by the author [%]	Data generation by the author [%]	Analysis and interpretation by the author [%]	Paper writing done by the author [%]
Jannis Grafmüller	1	70	60	65	40
Jens Möllmer	2	0	10	10	5
E. Marie Muehe	3	0	0	5	10
Claudia I. Kammann	4	5	0	5	10
Daniel Kray	5	10	0	5	10
Hans-Peter Schmidt	6	5	0	5	10
Nikolas Hagemann	7	10	0	5	15
Contribution by other parties not listed as authors (e.g., commercial analysis laboratories, student assistants)					
Lea Elena Anders and Viola Bartsch		0	10	0	0
Regina Brämer and Barbara Anders		0	5	0	0
Martin Zuber		0	5	0	0
Eurofins Umwelt Ost GmbH, Bobritzsch Hilbersdorf, Germany		0	5	0	0
Schneider Planta Chemicals GmbH, Eppelborn, Germany		0	5	0	0
Publication status	published				
Explanations	<p>The study was conceptualized by Nikolas Hagemann, Daniel Kray, Hans-Peter Schmidt, Claudia Kammann and me. Ulrike Planta from Schneider-Planta Chemicals GmbH, Eppelborn, Germany produced granulated fertilizers in a commercial subcontract according to my specifications. Jens Möllmer performed the gas sorption experiments on biochar and granulated fertilizers. All other experimental work was performed by me, except the basic characterization of pristine biochar and soil, which was performed by Eurofins Umwelt Ost GmbH, Bobritzsch-Hilbersdorf, Germany. Regina Brämer and Barbara Anders at Offenburg University of Applied Sciences supported me during ICP measurements and Martin Zuber at Agroscope, Zurich, Switzerland supported me during N quantification in plant tissue. Thomas Margenfeld provided soil for the greenhouse experiment. Olivia Bartsch and Lea Elena Anders supported me during plant cultivation and harvest. The first draft of the manuscript was written by me and the quality was greatly improved by all co-authors.</p>				



OPEN Granulation compared to co-application of biochar plus mineral fertilizer and its impacts on crop growth and nutrient leaching

Jannis Grafmüller^{1,2,3,4,5✉}, Jens Möllmer⁶, E. Marie Muehe^{4,7}, Claudia I. Kammann⁸, Daniel Kray¹, Hans-Peter Schmidt^{2,3} & Nikolas Hagemann^{2,3,5}

Mechanized biochar field application remains challenging due to biochar's poor flowability and bulk density. Granulation of biochar with fertilizer provides a product ready for application with well-established machinery. However, it's unknown whether granulated biochar-based fertilizers (gBBF) are as effective as co-application of non-granulated biochar with fertilizer. Here, we compared a gBBF with a mineral compound fertilizer (control), and with a non-granulated biochar that was co-applied at a rate of 1.1 t ha⁻¹ with the fertilizer in a white cabbage greenhouse pot trial. Half the pots received heavy rain simulation treatments to investigate nutrient leaching. Crop yields were not significantly increased by biochar without leaching compared to the control. With leaching, cabbage yield increased with gBBF and biochar-co-application by 14% ($p > 0.05$) and 34% ($p < 0.05$), respectively. Nitrogen leaching was reduced by 26–35% with both biochar amendments. Biochar significantly reduced potassium, magnesium, and sulfur leaching. Most nitrogen associated with gBBF was released during the trial and the granulated biochar regained its microporosity. Enriching fertilizers with biochar by granulation or co-application can improve crop yields and decrease nutrient leaching. While the gBBF yielded less biomass compared to biochar co-application, improved mechanized field application after granulation could facilitate the implementation of biochar application in agriculture.

Keywords Biochar-based fertilizer, BBF, Pyrolysis, PyCCs, White cabbage

Biochar is being considered for application in agriculture to improve crop yields and make soils more resilient to global warming induced challenges while creating long-term carbon sinks. Biochar can be implemented in different agricultural practices, e.g., as a soil amendment^{1,2}, feed supplement³, compost additive⁴, or as a component of fertilizers to reduce N losses from soils⁵. The combination of biochar and fertilizer is known as biochar-based fertilizer (BBF)⁶. A recent meta-analysis found that BBFs increased crop productivity by 10% compared to fertilized controls without biochar amendment⁶. This might be due to improved retention of fertilizer by biochar in soil, which can lead to increased nutrient use efficiencies and higher crop yields compared to conventional fertilizers without biochar^{2,7–10}.

A BBF is produced through (1) sorption of nutrients by biochar from a liquid^{11–14}, (2) infusing nutrients into biochar by heating a mixture of biochar and fertilizer under controlled conditions¹⁵, (3) coating of solid, granulated fertilizers with biochar⁷, or (4) pelleting and granulation of biochar with solid nutrient-rich materials^{8,16}. Granulation of biochar and fertilizer results in a granulated BBF (gBBF) with a homogeneous particle size distribution and improved flowability, which eases mechanized application to soil. With that, current challenges

¹Institute of Sustainable Energy Systems (INES), Offenburg University of Applied Sciences, Offenburg, Germany. ²Ithaka Institute, Arbaz, Switzerland. ³Ithaka Institute, Goldbach, Germany. ⁴Plant Biogeochemistry, Department of Geosciences, University of Tübingen, Tübingen, Germany. ⁵Environmental Analytics, Agroscope, Zurich, Switzerland. ⁶Institut für Nichtklassische Chemie e.V. (INC), Leipzig, Germany. ⁷Plant Biogeochemistry, Department of Applied Microbial Ecology, Helmholtz Centre for Environmental Research - UFZ, Leipzig, Germany. ⁸Department of Applied Ecology, Hochschule Geisenheim University, Geisenheim, Germany. ✉email: jannis.grafmueller@hs-offenburg.de

Granulation of biochar and fertilizer results in a granulated BBF (gBBF) with a homogeneous particle size distribution and improved flowability, which eases mechanized application to soil. With that, current challenges during application of biochar with common agricultural machinery might be overcome, such as blockages of fertilizer spreaders due to the inhomogeneity in biochar particle size and its low bulk density.

However, to the best of our knowledge, no study so far investigated whether gBBF is as effective as the co-application of non-granulated (and non-milled) biochar and fertilizer to soil. Granulation processes require raw material particle sizes below 300–500 μm , i.e., biochar must be milled. Additionally, granulation reduces the number of particles per mass unit of biochar resulting in fewer particles being applied to a volume of soil. Thus, there is less direct exchange interface between biochar and soil as long as the granules retain their shape. Both effects could affect plant growth in comparison to the application of non-granulated biochar. In addition, granulation with fertilizer can reduce biochar's porosity¹⁷, which is an important parameter for the interaction of biochar with soil nutrients. However, it is unknown how porosity of gBBF evolves after soil application. Still, the leaching of nutrients from soils amended with a gBBF might be reduced compared to the co-application of biochar and fertilizer, as the interaction between nutrients and biochar could be enhanced to a higher extent in granulated gBBFs¹⁰.

In the present study, a gBBF was produced from milled biochar (< 1 mm) using 0.02% (w/w) of binding agent (carboxymethyl cellulose), which is considerably lower than in some earlier studies^{7–9,15–17} and allows to study the impact of the biochar's granulation on crop growth and nutrient leaching without secondary effects of such additives. In addition, biochar was loosely mixed into the soil along with the granulated NPK fertilizer (B + NPK), reflecting the most frequent pathway of biochar uses in agriculture (co-application). For this purpose, biochar was milled to < 12 mm for practical reasons, but not finely milled as for granulation (collard mill, < 1 mm). Both treatments were compared to an NPK-fertilizer control without biochar (NPK, Fig. S1). The aim was to assess how the granulation process impacts the effects of biochar on crop growth and nutrient leaching, i.e., if B + NPK would differ from gBBF. We hypothesized that gBBF would improve nutrient retention and crop growth more effectively than co-applied B + NPK, due to the close contact of biochar and nutrients in gBBF. We assumed that granulation may allow enhanced nutrient sorption onto biochar surfaces and into biochar pores. Furthermore, we studied the changes in porosity that the biochar incorporated in the gBBF underwent after soil application.

Materials and methods

Production of fertilizers

Biochar certified according to the European Biochar Certificate (EBC)¹⁸ was obtained from an industrial pyrolysis plant using untreated wood chips (Carbon Cycle GmbH & Co. KG, Rieden, Germany, <https://www.eurobiochar.org/cert/4py5-h7f2-xwj6-v6w8/en>) at a maximum pyrolysis temperature of 750 °C. Biochar was processed in a hammer mill to < 12 mm and further milled to < 1 mm in a collard mill (Type SJM00F, Gebr. G. Fischer AG, Schaffhausen, Switzerland). For the production of gBBF, biochar (13.3 kg, < 1 mm), 3.4 kg urea (N source, without urease and nitrification inhibitors), 1.2 kg mono-potassium phosphate (phosphorus (P) and potassium (K) source), and 2.5 kg Patentkali® (P, K, magnesium (Mg) and sulfur (S) source, all of technical purity grade, dry matter equivalents) were mixed in a granulator (Type SK G1, Gustav Eirich GmbH, Hardheim, Germany). Water (4 kg) followed by 0.6 kg of a 0.8% (w/w) solution of hydroxypropyl methyl cellulose (Arbocel® CE2910 HE 50 LV, J. Rettenmaier & Söhne GmbH + Co. KG, Rosenberg, Germany) were stepwise added to the biochar-nutrient mix via a sprayer nozzle, which resulted in a binding agent concentration of 0.02% (w/w) in the end product. The granulated fertilizer without the addition of biochar was produced under otherwise unchanged conditions but with less water addition, keeping the binder-to-nutrient ratio constant, and was labeled as NPK. After the particles had agglomerated to the desired granule size range, the product was sieved to 2–4 mm and dried at 90 °C for 90 min to reach sufficient mechanical stability. Both types of granulated fertilizers and the pure biochar (< 12 mm milling fraction) were packed in air-tight bags and stored under ambient conditions in the dark until further usage.

Basic characterization of granulated fertilizers and biochar

Biochar, gBBF, and NPK were analyzed for total carbon, nitrogen, hydrogen, and sulfur content (CHNS), macro and microelements, and ash content according to the EBC analytical guidelines¹⁸ by a commercial lab (Eurofins Umwelt Ost GmbH, Bobritzsch-Hilbersdorf, Germany). The pH of biochar, gBBF, and NPK was measured after shaking for 1 h in 0.01 M CaCl₂ (1:10, w/w). The porosity of pristine biochar (< 1 mm after collard milling), gBBF, and NPK was characterized by recording CO₂ and N₂ adsorption isotherms on an Autosorb iQ (Quantachrome Instruments, Anton Paar GmbH, Ostfildern-Scharnhausen, Germany), as described in section 1.1 of the SI. Specific surface area (SSA) was calculated using either the Brunauer–Emmett–Teller¹⁹ (BET) method or the density functional theory²⁰ (DFT). Scanning Electron Microscopy (SEM) and electron dispersive X-ray (EDX) mapping were performed for gBBF as described in section 1.2 of the SI.

N release from fertilizers

The release of N from NPK, gBBF, and B + NPK was determined by repeated extraction with CaCl₂ and incubation in distilled water. For the repeated extraction, samples were weighed into 100 mL Erlenmeyer flasks (equivalent of 0.4 g of N per flask), where 50 mL of a 0.0125 M CaCl₂ solution was added. The flasks were shaken at 125 rpm on a horizontal shaker for 1 h. After decanting and addition of fresh extractant to the sample, a second and third extraction step was performed (with shaking for a further 2 h and 45 h, respectively; for details see section 1.3 in the SI). Filtered extracts (< 0.45 μm) were quantified for total dissolved nitrogen (TN) by chemiluminescence as described below in the “Analysis of N species in fertilizer extracts, leachates, and soil extracts” section. Extracted TN was calculated after each extraction step as described in section 1.3 of the SI.

For the incubation study, fertilizers (equivalent to 0.4 g N) were incubated in 100 mL of de-ionized water in triplicates in Schott bottles at 20 °C without shaking as was suggested by Liu et al.¹⁵. After 1, 3, 6, 20, 24, 120, and 220 h, 5 mL liquid was sampled and filtered to <0.45 µm and de-ionized water (5 mL) was added to the bottle to maintain a constant solid-to-liquid ratio. Samples were measured for dissolved TN and release of N was calculated as detailed in the SI (section 1.3).

Greenhouse pot experiment

Origin and analysis of the soil used for the pot experiment

Sandy topsoil (0–20 cm) with a pH of 7.4 and organic matter content of 7.7% was excavated in March 2022 from an arable field in the Ortenau Region near river Rhein (48° 32′ 23.7″ N, 7° 48′ 50.6″ E, Kehl-Sundheim, Germany), sieved to < 10 mm and thoroughly homogenized before taking a representative subsample for the analysis²¹ at Eurofins Umwelt-Ost GmbH (Jena, Germany, Tables S2–S4). The soil was stored under dry conditions for 3 months in air-permeable plastic bags until further usage. The amount of soil used for the pot experiment was re-homogenized before the experiment.

Pot setup and management

Pots with a volume of 4 L (17 cm inner diameter at the top, 21 cm height) equipped with a 2 mm Nylon mesh at the bottom were filled with a homogeneous mixture of 4000 g dry matter equivalent of the soil and 3.5 g N in one of the three different fertilizer types: (1) NPK, (2) gBBF and (3) B + NPK (Table 1). This corresponds to 140 kg N ha⁻¹, assuming a plant density of 40,000 plants ha⁻¹. Detailed information on resulting nutrient dosage (P, K, Mg, S) per pot can be found in Table S5. The biochar application rates in the gBBF and B + NPK treatments were both 26.7 g dry weight pot⁻¹, corresponding to 1.1 t biochar ha⁻¹ assuming the above-mentioned plant density. Five replicate pots per treatment were either prepared for cultivation with or without leaching events, the latter including a non-fertilized control (CTRL-0) to test for leaching of native soil nutrients and mineralized N (Table 1). A control group without fertilizer/biochar application and without leaching events was not conducted as a pre-trial showed that no cabbage head development could be expected¹³. Five additional pots for NPK, gBBF, and B + NPK without leaching were set up for repeated sampling to measure soil N speciation and urease activity over time (cf. “Soil sampling and analysis” section). In total 50 pots were set-up. In the middle of each soil-filled pot, two seeds of white cabbage were sown on 5th of August 2022 and reduced to one plant per pot two weeks after sowing (cabbage variety Sunta F1, Bruno Nebelung GmbH, Everswinkel, Germany). Pots were arranged in a randomized block design on a greenhouse table. Soils were kept at 65% water holding capacity (WHC), further details on trial maintenance can be found in section 1.4 of the SI.

Leaching events

The simulation of extreme rain events was performed 35 and 63 days after sowing in treatments ID4–ID7 (cf. Table 1). Pots were irrigated with tap water to achieve 65% WHC and placed on a pipe socket with a sealed bottom (Fig. S5). For each pot, a total of 0.7 L of distilled water was added within 60 min in steps of 0.1 L every 8 min, which corresponds to an extreme precipitation event²² of 30 mm calculated based on the soil surface of the pot. 30 min after the simulated rain event, leachate samples were filtered to <0.45 µm and immediately stored on ice and analyzed for nitrate-N (NO₃⁻-N), ammonium-N (NH₄⁺-N) and total dissolved N (TN) as described in the “Analysis of N species in fertilizer extracts, leachates, and soil extracts” section. After storage at -20 °C, the samples were also analyzed for P, K, Mg and S by Inductively Coupled Plasma Optical Emission Spectroscopy (ICP-OES, icap 7000 series, Thermo Scientific, Waltham, USA).

Biomass harvest and analysis

Cabbage plants were harvested 116 days after sowing by cutting the stem below the lowest leaf base. The fresh weight of total aboveground biomass and the cabbage head alone was recorded after removing outer protruding leaves (Fig. S6). All the harvested biomass was rasped, mixed and an aliquot of 50 g was dried to mass constancy at 80 °C for further analysis and to determine dry matter content. Roots were excavated, washed and dried at 80 °C to determine dry weights. The dried aboveground biomass was ground to < 1 mm (Retsch ZM 200) and measured for total N contents (CN928, LECO Corporation, St. Joseph, USA). The content of other main nutrients (P, K, Mg, S, Ca) and trace elements (Mn, Cu, Zn) was measured using ICP-OES after microwave digestion of the

Treatment ID	Treatment	Leaching
1	NPK	None
2	gBBF	None
3	B + NPK	None
4	CTRL-0	30 L m ⁻² (twice)
5	NPK	30 L m ⁻² (twice)
6	gBBF	30 L m ⁻² (twice)
7	B + NPK	30 L m ⁻² (twice)

Table 1. Treatments prepared for the greenhouse trial. NPK: granulated, mineral nitrogen, phosphorus and potassium fertilizer. gBBF: granulated biochar-based NPK fertilizer. B + NPK: co-application biochar and granulated NPK fertilizer to the soil. CTRL-0: non-fertilized control.

biomass (Mars 5 Xpress, CEM GmbH, Kamp-Lintfort, Germany, cf. section 1.5 of the SI for details). Nutrient uptake in the aboveground cabbage biomass was calculated by multiplying the measured nutrient contents in cabbage tissues with the aboveground biomass yield.

Soil sampling and analysis

Soil samples were taken with a soil core sampler (10 mm diameter) in five redundantly prepared pots for the NPK, gBBF, and B + NPK treatments without leaching 35 and 70 days after sowing for the whole soil depth (21 cm, Table 1, Fig. S4). Samples were stored at $-20\text{ }^{\circ}\text{C}$ for analysis of extractable N species ($\text{NH}_4^+\text{-N}$, $\text{NO}_3^-\text{-N}$ and TN) and at $4\text{ }^{\circ}\text{C}$ for quantification of soil urease activity²³. After harvest, the soil separated from the rootstock was mixed manually, representatively sampled (50 mL), and stored at $-20\text{ }^{\circ}\text{C}$ for analysis of extractable N species and at $4\text{ }^{\circ}\text{C}$ for quantification of soil urease activity. For soluble N extraction, 5 g of soil (fresh weight) was extracted in 20 mL 0.0125 M CaCl_2 in closed 100 mL-Erlenmeyer flasks for 1 h on a rotary shaker at 125 rpm, based on DIN 19746²⁴. The suspension was filtered to $<0.45\text{ }\mu\text{m}$ and stored at $-20\text{ }^{\circ}\text{C}$ if not measured directly for $\text{NH}_4^+\text{-N}$, $\text{NO}_3^-\text{-N}$, and TN content as described in the “Analysis of N species in fertilizer extracts, leachates, and soil extracts” section and reported based on soil dry matter. Soil pH values were measured according to DIN EN 15,933 on 5 mL air-dried samples in 25 mL 0.01 M CaCl_2 (Titroline alpha Plus, SI Analytics GmbH, Mainz, Germany).

Extraction of residual nitrogen and SSA of soil-aged gBBF granules

Individual intact granules of gBBF (Fig. S7) found in the remaining soil of each pot after harvest and representative soil sampling were sampled and stored both for analysis at $4\text{ }^{\circ}\text{C}$ (for porosity measurements) and $-20\text{ }^{\circ}\text{C}$ (for residual N content). From each pot, a mass of 0.3–0.5 g (dry weight) of sampled granules was transferred to 100 mL Erlenmeyer flasks and dried to mass constancy at $55\text{ }^{\circ}\text{C}$. Samples were subsequently extracted with 20 mL of 2 M KCl for 2 h on a horizontal shaker with 150 rpm at room temperature. The suspension was filtered to $<0.45\text{ }\mu\text{m}$ and analyzed for TN as described in the “Analysis of N species in fertilizer extracts, leachates, and soil extracts” section. The SSA of soil-aged gBBF granules (dried at $40\text{ }^{\circ}\text{C}$, but otherwise untreated after extraction from soil) sampled from three individual pots per treatment were characterized by CO_2 adsorption as described in the “Basic characterization of granulated fertilizers and biochar” section.

Analysis of N species in fertilizer extracts, leachates, and soil extracts

$\text{NH}_4^+\text{-N}$ concentrations in the leachates, soil, and fertilizer extracts were quantified with a Berthelot reaction according to Rhine and colleagues²⁵ on 96 well microtiter plates with a microplate reader (Epoch2, Biotek Instruments, Winooski, USA). For $\text{NO}_3^-\text{-N}$ quantification, a microplate reader method adapted from Hagemann et al.²⁶ was applied using UV transparent 96 well microplates (UV-Star[®], Greiner Bio-One GmbH, Frickenhausen, Germany). Total dissolved N in the leachates and extracts were quantified by chemiluminescence on a TOC-VCN equipped with the TN measurement unit TNM-1 (Shimadzu Corporation, Kyoto, Japan). The difference between TN and the sum of $\text{NO}_3^-\text{-N}$ and $\text{NH}_4^+\text{-N}$ was defined as organic N (N_{org}). Analytical techniques are described in more detail in section 1.6 of the SI.

Data analysis

All statistical analyses were performed with Graphpad Prism (version 10.0.3, GraphPad Software LLC, Boston, USA). For biomass yields and nutrient uptakes, two-way analysis of variance (ANOVA) was performed using the factors fertilizer type (NPK/gBBF/B + NPK) and leaching (no leaching/including leaching) followed by Tukey’s post-hoc test at $\alpha = 0.05$. For nutrient leaching, one-way ANOVA was performed, followed by Tukey’s post-hoc test to identify significant differences between different treatments at $\alpha = 0.05$. Block effects were taken into account via the repeated measures function in Graphpad Prism.

Results

Fertilizer composition and morphology

The biochar used in the experiment had a molar H/C ratio of 0.2, a low ash content of 2% (w/w), and a low content of macronutrients like K or Mg (Table 2). Trace metal contents in the biochar were below limit values of the certification class AgroBio of the European Biochar Certificate¹⁸ (Table S7). The NPK fertilizer granule contained the desired amounts of N, P, and K (Table 2), and low concentrations of trace metals (Table S7). As the biochar was added at 65% (w/w) to the fertilizer to prepare the gBBF, the contents of the main elements and trace metals in gBBF were accordingly lower (Tables 2 and S7).

The biochar had a microporous character (pore width $\leq 1.5\text{ nm}$) and was low in mesopores (pore width $1.5\text{ nm} < \times < 50\text{ nm}$), which was indicated by (1) a steep increase in adsorbed volume of CO_2 at low relative pressures in the CO_2 adsorption isotherms and (2) only low adsorption amounts of N_2 leading to a BET and DFT SSA of $358\text{ m}^2\text{ g}^{-1}$ and $516\text{ m}^2\text{ g}^{-1}$, respectively, when based on CO_2 adsorption compared to only $20\text{ m}^2\text{ g}^{-1}$ of BET SSA when based on N_2 adsorption (Table 2, Figs. S8a and S9a). The CO_2 -based SSA of the gBBF was only $155\text{ m}^2\text{ g}^{-1}$ (BET) and $116\text{ m}^2\text{ g}^{-1}$ (DFT, Table 2). Three distinct pore sizes of approximately 0.35 nm, 0.5 nm and 0.8 nm were identified in the biochar, using the first derivative of the cumulative pore volume (calculated via DFT, Fig. S10). The pore size distribution of gBBF granules was of more multimodal character, with a decrease in the peak at 0.35 nm, a clear widening of the distribution at around 0.5 nm, and a higher contribution by pore widths at around 0.8 nm compared to the pure biochar (Fig. S10). The wider and multimodal pore size distribution at around 0.5 nm in gBBF reflected the more heterogeneous matrix compared to pure biochar, as the NPK fertilizer had a similar pore size distribution in that region (Fig. S10). The relative increase in pores with 0.8 nm

Sample	C (%)	H (%)	N (%)	S (%)	Ash (%)	pH	P ₂ O ₅ (gkg ⁻¹)	K ₂ O (gkg ⁻¹)	MgO (gkg ⁻¹)	BET SSA ^a (N ₂) (m ² g ⁻¹)	BET SSA ^a (CO ₂) (m ² g ⁻¹)	DFT SSA ^b (CO ₂) (m ² g ⁻¹)
Biochar	93.3	1.4	0.31	<0.03	2.0	9.1	0.6	2.5	1.1	21 ^d	358 ^d ± 43	516 ^d ± 52
NPK	10.2	3.7	23.0	6.3	46.3	5.2	85.2	159.0	31.5	7	42	n.a. ^e
gBBF	61.4	2.3	8.74	2.63	19.1	6.1	33.6	62.9	11.4	5	155 ± 26	116 ± 8

Table 2. Elemental analysis (carbon (C), hydrogen (H), nitrogen (N), and sulfur (S)), and contents of macronutrients (phosphorus as P₂O₅, potassium as K₂O, and magnesium as MgO) in biochar and fertilizers. Specific surface area (SSA) of the biochar, the pure NPK fertilizer (NPK) and the granulated biochar-based NPK fertilizer (gBBF). Errors indicate the range of minimum to maximum measured values of n = 2 measurements, where applicable. ^aBET SSA: Specific surface area calculated with the Brunauer–Emmet–Teller (BET) method based on either N₂ or CO₂ adsorption isotherms. ^bDFT SSA: Specific surface area calculated with the density functional theory (DFT) based on CO₂ adsorption isotherms. ^cn.a.: not applicable since the adsorption isotherm did not show a Type-I isotherm characteristic. ^dBiochar after milling with a collar mill.

width in gBBF was clearly linked with the added mineral fertilizer, which harbors a relatively high presence of pores in that dimension (Fig. S10).

Elemental mapping with EDX suggested that the nutrients in gBBF were homogeneously distributed onto the carbonaceous surfaces of the biochar, which was demonstrated by imaging the cross-section of individual granules after slicing with a scalpel (Figs. S12–S15). Furthermore, the EDX mappings indicated that some pores of the biochar in gBBF were filled with mineral nutrients from the added fertilizer (Fig. S14) and that individual biochar particles were compressed and embedded in each other (Fig. S11).

Nitrogen release from granulated fertilizers and fertilizer-biochar mixture

In repeated extractions with 0.01 M CaCl₂, NPK and B + NPK released virtually all N during the first extraction step of 1 h with 102% and 95%, respectively (Fig. 1a). For the gBBF, the first extraction step only liberated 76% of total N, followed by extraction of 11% each after 3 and 48 h (Fig. 1a). A slower release of N from the gBBF compared to NPK and B + NPK was also observed in the liquid incubation experiment without continuous shaking of the incubation medium (Fig. 1b). While NPK and B + NPK released 100% and 92% of N to the liquid during the first day of incubation, respectively, gBBF only released 34% within the same period of time (Fig. 1b). The release of N from gBBF to the incubation liquid was significantly lower during the whole incubation period compared to the other treatments. For gBBF, 90% of N-release was achieved after nine days of incubation ($p < 0.05$). It has to be noted that biochar in B + NPK was milled to < 12 mm, while gBBF was produced after additional milling of biochar to < 1 mm. However, nutrient release from mixtures of biochar and NPK was not affected by particle sizes within the range relevant to this study, as detailed in the SI (Fig. S16).

Biomass yield and nutrient uptake

Dry cabbage head yields ranged between 15 and 20 g plant⁻¹ in treatments without leaching events and between 12 and 16 g plant⁻¹ for the same treatments including leaching events (Fig. 2). Leaching decreased cabbage

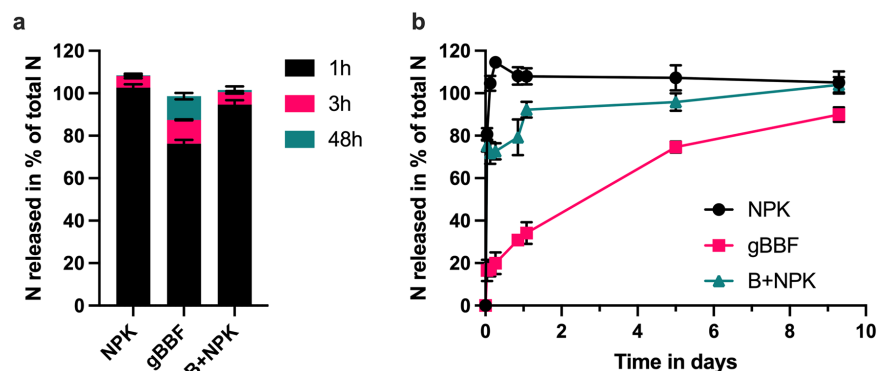


Figure 1. Nitrogen released from granulated NPK fertilizer (NPK) and granulated biochar-based fertilizer (gBBF) and the mixture of NPK with non-granulated biochar (B + NPK) in repeated extractions with 0.0125 M CaCl₂ during the indicated time intervals (a), and during incubation in distilled water for nine days (b). Data are presented as means ± standard deviation (n = 3). Released N is presented as a percentage of the total N contained in the different fertilizers.

Treatment	Fresh total aboveground biomass in g	Fresh cabbage heads in g	Dry total aboveground biomass in g	Dry root biomass in g
No leaching events				
NPK	376 ± 47 a	232 ± 61 a	24.8 ± 3.1 a	1.6 ± 0.2 a
gBBF	380 ± 10 a	250 ± 13 a	24.7 ± 1.0 a	1.3 ± 0.3 ab
B + NPK	418 ± 21 a	281 ± 14 a	28.8 ± 3.8 a	1.1 ± 0.1 b
Incl. leaching events				
NPK	340 ± 12 B	188 ± 33 B	21.9 ± 1.6 B	1.0 ± 0.1 A
gBBF	363 ± 34 AB	211 ± 42 AB	23.8 ± 1.7 AB	0.9 ± 0.1 A
B + NPK	395 ± 9 A	246 ± 17 A	26.1 ± 1.8 A	1.1 ± 0.1 A

Table 3. Aboveground biomass and root biomass of cabbage plants. NPK: granulated mineral nitrogen (N), phosphorus (P) and potassium (K) fertilizer. gBBF: granulated biochar-based NPK fertilizer. B + NPK: co-application of non-granulated biochar and NPK fertilizer to the soil. Data are presented as means ± standard deviation (n = 5). Different lowercase letters within a row indicate significant differences between the treatments cultivated without leaching events. Different uppercase letters indicate significant differences between the treatments including two leaching events (two-way analysis of variance, $p < 0.05$, followed by Tukey's post-hoc test).

Final biomass harvest	Total biomass		Cabbage heads		Roots	
	F	<i>p</i>	F	<i>p</i>	F	<i>p</i>
Leaching	3.61	0.099	4.89	0.063	10.91	0.013
Fertilizer type	5.58	0.017	6.56	0.010	3.181	0.073
Leaching × fertilizer type	0.11	0.898	0.06	0.941	9.017	0.003
Block	1.39	0.282	1.90	0.141	1.869	0.151

Table 4. Statistical results of two-way analyses of variance of dry matter aboveground and belowground biomass yields. Factors: 'Leaching' (no leaching /incl. leaching), 'Fertilizer type' (NPK/gBBF/B + NPK) and the interaction of both individual factors. Additionally, the block effect is presented 'Block'. Significant values are displayed in bold.

head yields compared to the equally fertilized plants grown in the absence of leaching (Fig. 2, Table 4, $p = 0.06$). Fertilizer type did not significantly affect dry cabbage head yields when plants were cultivated without leaching events (Fig. 2). Still, B + NPK tended to increase cabbage head yield compared to NPK (+27%, $p = 0.07$). For the plants grown with leaching events, the amendment of B + NPK significantly increased dry cabbage head yields by 34% relative to the NPK treatment ($p < 0.05$), while the increase under gBBF relative to NPK was not statistically significant ($p = 0.53$, Fig. 2).

Total aboveground biomass yields mirrored the yields of cabbage heads. The amendment of B + NPK tended to increase dry aboveground biomass without leaching events and significantly increased it by 19% compared to NPK in the presence of leaching ($p < 0.05$, Tables 3 and 4). Dry root biomass was significantly affected by the fertilizer type in absence of leaching events (Tables 3 and 4). The NPK treatment yielded the highest root biomass of 1.6 g plant⁻¹, while the B + NPK treatment had the lowest with 1.1 g plant⁻¹ ($p < 0.05$, Table 3). Root growth with gBBF was with 1.3 g plant⁻¹ in between these two different treatments (Table 3). Leaching events reduced root biomass to 0.9–1.0 g plant⁻¹ for the NPK and gBBF treatments, but remained unchanged with B + NPK (Tables 3 and 4).

Nitrogen uptake in the aboveground biomass was in the range of 1.0–1.2 g plant⁻¹ and it was not significantly affected by the leaching treatment nor the fertilizer type (Fig. 3a, Table S10). Nitrogen use efficiencies ranged between 30 and 35% for all plants, based on N uptakes into the aboveground biomass related to the applied N fertilizer (Fig. S20). Without leaching events, B + NPK significantly increased P, Mg, S, Mn and Cu uptakes compared to the gBBF treatment, and for Mn also compared to the NPK treatment ($p < 0.05$, Fig. 3). The lower uptakes of these nutrients with gBBF under no-leaching conditions were not only a result of lower aboveground biomass yields with gBBF compared to B + NPK (Table 3), but also due to lower contents for most of these nutrients in the aboveground cabbage tissues (Fig. S17). With the leaching treatment, B + NPK significantly increased the uptakes of Mg, S, Ca, and Mn compared to NPK and gBBF ($p < 0.05$, Fig. 3). Moreover, leaching significantly increased the plants' uptake of P, S and Cu compared to the plants grown without leaching, independent of the fertilization treatment (Table S10, Fig. 3).

Nutrient leaching from planted pots

When the first leaching event was performed, at 35 days after sowing, the cabbage plants had developed to the sixth unfold foliage (BBCH 16²⁷), and at the time of the second leaching event, at 63 days after sowing, cabbage head formation had started (BBCH 41²⁷). The biochar amendment significantly reduced total N losses in both individual leaching events in the range of 26–35%, compared to NPK, independent of the biochar application method (Fig. 4a,c). Cumulative TN losses were significantly reduced with gBBF and B + NPK compared to NPK

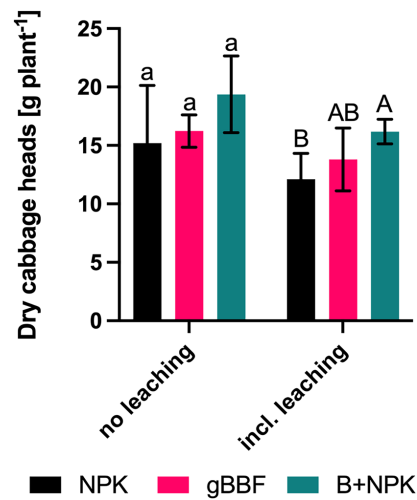


Figure 2. Yields of dry cabbage heads for the different fertilizer types for plants that were grown without leaching events (no leaching) or with two leaching events (incl. leaching, each 30 L m⁻²). NPK: granulated, mineral nitrogen, phosphorus and potassium fertilizer. gBBF: granulated biochar-based NPK fertilizer. B + NPK: co-application of non-granulated biochar and granulated NPK fertilizer to the soil. Data are presented as means \pm standard deviation (n = 5). Different letters above each error bar indicate a significant difference between treatments without or with leaching events (lowercase and uppercase letters, respectively, two-way analysis of variance and Tukey's post-hoc test at $p < 0.05$).

by 31% and 30%, respectively ($p < 0.05$, Tables 5 and 6). TN losses summed up to 15% of initially fertilized N for gBBF and B + NPK and to 21% for NPK. In the non-fertilized pots, all the native mineralized N from the soil was leached during the first leaching event; no N remained to be leached at the second leaching (Fig. 4). NH₄⁺-N loss was significantly reduced by 45% ($p < 0.05$) with gBBF and by 23% ($p = 0.10$) with B + NPK during the first leaching event compared to the NPK treatment (Fig. 4b). In the second leaching event, the NH₄⁺-N losses were significantly decreased by 58% and 63% with gBBF and B + NPK ($p < 0.05$), respectively, with lower absolute NH₄⁺-N losses for all treatments compared to the first leaching event (Fig. 4d). Cumulative NH₄⁺-N leaching was reduced by 49% with gBBF and by 35% with B + NPK compared to NPK ($p < 0.05$, Tables 5 and 6) and made up 13–17% of TN lost via leaching. Therefore, NH₄⁺-N retention was less critical than leaching of other N species, most importantly nitrate. NO₃⁻-N leaching was reduced with gBBF and B + NPK in both individual leaching events compared to NPK fertilized pots, but not statistically significant (Fig. 4b,d, Tables 5 and 6). Leaching of organic N (N_{org}) was reduced with gBBF and B + NPK compared to NPK during both individual leaching events (Fig. 4b,d) and statistically significant for the cumulative N_{org} loss for B + NPK compared to NPK (-59% , $p < 0.05$, Table 5). In general, the leaching of N_{org} was higher in the first leaching event as compared to the second.

Cumulatively leached amounts of K ranged between 13 and 15% of the fertilized K. Mg leaching summed up to 20–30% of fertilized Mg, and S leaching was between 18 and 23% of fertilized S in the different treatments. Cumulative K leaching was significantly reduced by 21% with B + NPK and by 18% with gBBF compared to the NPK treatment ($p < 0.05$ Fig. 5a, Table 7). Cumulative Mg leaching loss was significantly reduced with gBBF by 28% and by 27% with B + NPK compared to NPK ($p < 0.05$, Fig. 5b, Table 7). Further, gBBF significantly reduced Mg leaching by 36% compared to NPK during the first leaching event ($p < 0.05$), while B + NPK only reduced it by 25% ($p > 0.05$, Fig. 5b). Sulfur leaching was consistently reduced with gBBF during both leaching events compared to NPK, summing up to a cumulative reduction by 25% ($p < 0.05$, Fig. 5c). The B + NPK treatment reduced S leaching by 38% in the second leaching event compared to NPK ($p < 0.001$), but the cumulative S loss was not significantly reduced compared to NPK (Fig. 5c). Phosphorus leaching was not affected by the different treatments during both leaching events and ranged between 0.3 and 0.8 mg P pot⁻¹ (Table S8). Leachate volumes were not affected by biochar addition within the fertilized treatments (Table S8).

Soil N content, N balance, and soil pH

Extractable N fractions from the soil after 36 and 70 days, i.e., shortly after the nutrient leaching events, were, when cumulated over all N fractions, not significantly changed by the different amendments (Fig. S19). Still, extractable NH₄⁺-N contents were significantly lower for gBBF and B + NPK compared to NPK after 36 days and for B + NPK also after 70 days, but absolute NH₄⁺-N contents were in general lower compared to NO₃⁻-N and N_{org} (Fig. S19). Soil urease activity was not affected by the different fertilizer amendments based on samples

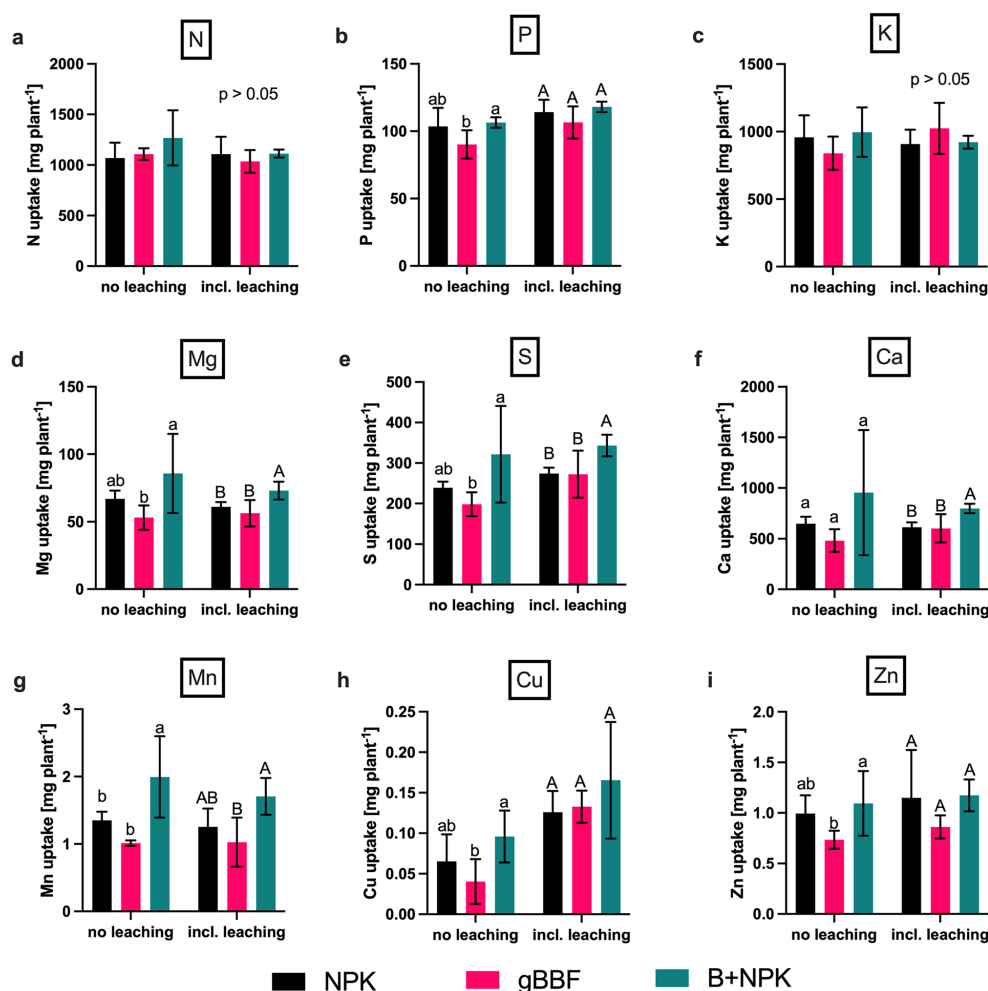


Figure 3. Nutrient uptake in aboveground cabbage biomass cultivated without (no leaching) or with two leaching events (incl. leaching, 30 L m⁻² each 35 and 63 days after sowing): nitrogen (N), potassium (K), phosphorus (P), magnesium (Mg), sulfur (S), calcium (Ca), manganese (Mn), copper (Cu) and zinc (Zn). NPK: granulated, mineral fertilizer. gBBF: granulated biochar-based NPK fertilizer. B + NPK: co-application of non-granulated biochar and granulated NPK fertilizer to the soil. Data are presented as means ± standard deviation (n = 5). Different letters above error bars indicate a statistically significant difference within the no leaching or the incl. leaching treatments (lowercase and uppercase letters, respectively, two-way analysis of variance and Tukey's post-hoc test, $p < 0.05$).

taken after 70 days and at the harvest on day 116 (Fig. S18). After harvest, a considerable amount of 0.01 M CaCl₂ extractable N remained in the soil in all treatments except in the leached non-fertilized control (Table S9). Treatments that included leaching events had between 25 and 55% lower residual extractable soil N contents compared to the treatments without leaching (Fig. 6 and Table S9). Virtually all N that remained in the soil was present as NO₃⁻-N and ranged between 290 to 390 mg kg⁻¹ for fertilized treatments without leaching events and from 180 to 200 mg kg⁻¹ for fertilized treatments with leaching events (Table S9). In the treatments without leaching, NPK fertilized control pots had significantly higher extractable NO₃⁻-N contents compared to gBBF and B + NPK ($p < 0.05$, Fig. 6 and Table S9). Non-accounted N ranged between 20 and 35% of total N in the pots (fertilizer + native extractable, mineral soil N, Fig. 6). The non-accounted N is assumed to be the sum of N in

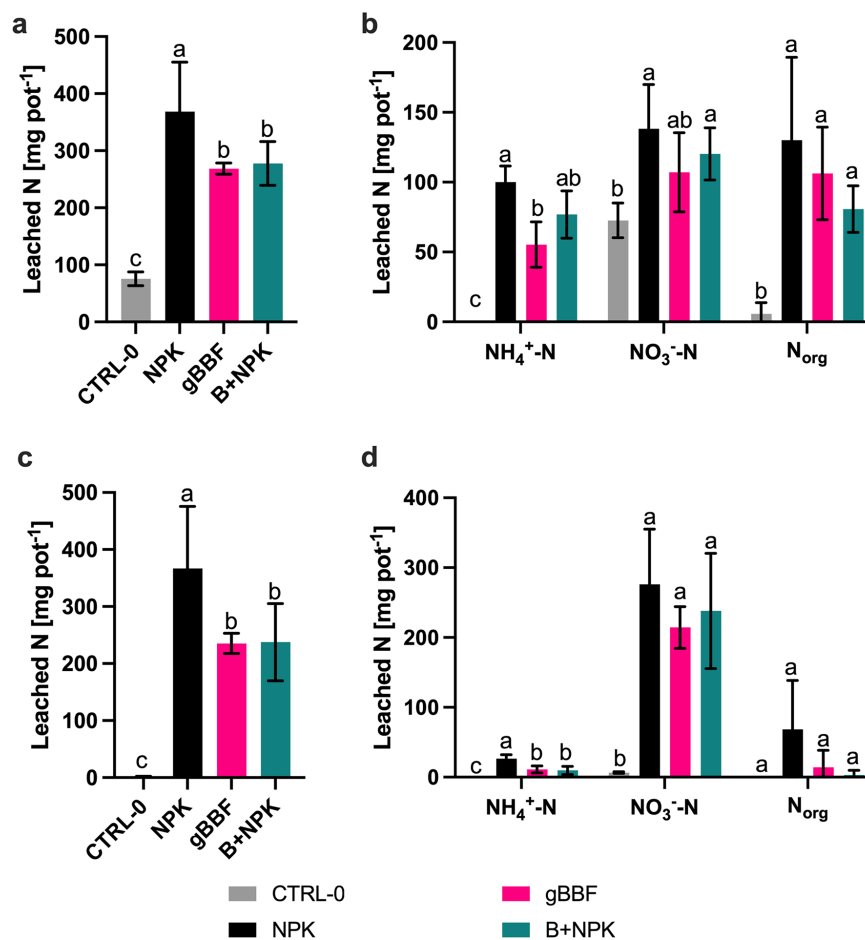


Figure 4. Total nitrogen (N) and individual N fractions leached from the pots during a leaching event after 35 days (a, b) and 63 days (c, d) with 30 L m⁻² each. Different N fractions are presented as ammonium-N, nitrate-N and organic N (NH₄⁺-N, NO₃⁻-N and N_{org}, respectively). Data are presented as means ± standard deviation (n = 5). CTRL-0: non-fertilized control. NPK: granulated mineral fertilizer. gBBF: granulated biochar-based NPK fertilizer. B + NPK: co-application of non-granulated biochar and granulated NPK fertilizer. Different letters above error bars indicate significant differences between the treatments within each N fraction (one-way analysis of variance, *p* < 0.05, Tukey's post-hoc test).

(1) below-ground biomass (roots were not analyzed for N content), (2) N emitted during the pot trial as NH₃, N₂O, or N₂, (3) soil N that was non-extractable with 0.01 M CaCl₂ and (4) N attached to leachate particles not quantified due to leachate filtration to < 0.45 μm before analysis.

The leaching events contributed to a significant pH change in the NPK treatment from 7.6 in the non-leached soils to 8.0 in the leached soils (*p* < 0.05, Table S9). For gBBF and B + NPK, soil pH did not increase significantly during the trial after leaching and ranged between 7.7 and 7.8 (Table S9).

Impact of soil incubation on N content and porosity of gBBF

Low residual amounts of N were quantified in gBBF granules sampled from the soil after harvest in the pots treated with or without the conduction of leaching events (1.3–1.4 mg g⁻¹; i.e., 1.5% of the initial N content, Fig. 7a). Thus, almost all N originally contained in the gBBF fertilizer (87 mg g⁻¹) was released to the soil during

Treatment	TN	NO ₃ ⁻ -N	NH ₄ ⁺ -N	N _{org}
CTRL-0	85 ± 12 c	79 ± 13 b	< LOQ	6 ± 8 c
NPK	736 ± 194 a	415 ± 98 a	127 ± 12 a	199 ± 121 a
gBBF	504 ± 22 b	322 ± 52 a	65 ± 18 b	123 ± 46 ab
B+NPK	516 ± 102 b	358 ± 89 a	86 ± 14 b	81 ± 18 b

Table 5. Cumulative leaching of nitrogen (N) fractions during leaching events (in mg N pot⁻¹): total dissolved N (TN), nitrate-N (NO₃⁻-N), ammonium-N (NH₄⁺-N) and organic N (N_{org}). Data are presented as means ± standard deviation (n = 5). Different letters show significant differences between the treatments within each N fraction (one-way analysis of variance, $p < 0.05$, Tukey's post-hoc test). LOQ: limit of quantification. CTRL-0: non-fertilized control. NPK: granulated mineral fertilizer. gBBF: granulated biochar-based NPK fertilizer. B+NPK: co-application of non-granulated biochar and granulated NPK fertilizer.

Cumulative Leaching	Total N		Ammonium		Nitrate		N _{org}	
	F	p	F	p	F	p	F	p
Fertilizer type	7.62	0.014	19.18	< 0.001	1.55	0.269	4.38	0.052
Block	2.36	0.140	0.63	0.655	0.86	0.526	2.40	0.136

Table 6. Statistical results of one-way analyses of variance of the cumulative nitrogen (N) leaching losses from two leaching events for total dissolved N and each individual N fraction for the factor 'fertilizer type' (NPK, gBBF, B+NPK, excluding the non-fertilized control (CTRL-0)). Additionally, the block effect is presented 'Block'. N_{org}: organic N. Significant values are displayed in bold.

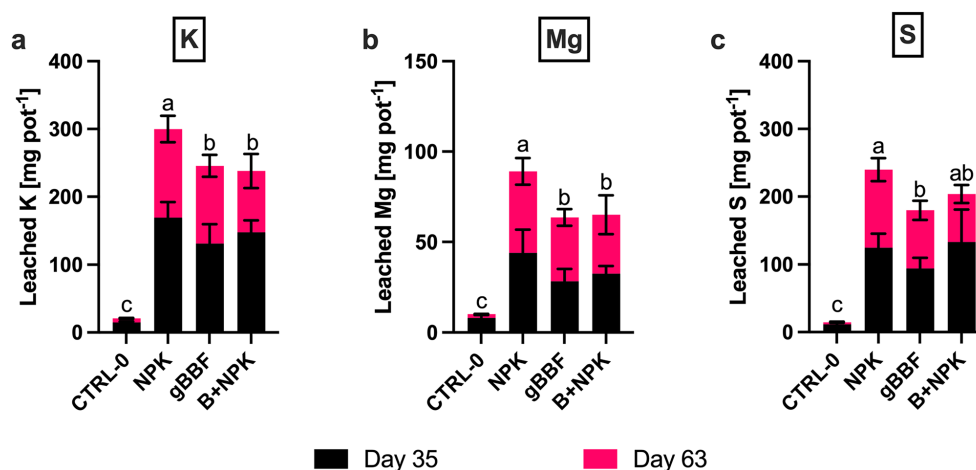


Figure 5. Amount of (a) potassium (K), (b) magnesium (Mg) and (c) sulfur (S) leached from cabbage pots as the result of two leaching events (each 30 L m⁻² precipitation) at 35 days and 63 days after sowing. CTRL-0: non-fertilized control. NPK: granulated mineral fertilizer. gBBF: granulated biochar-based NPK fertilizer. B+NPK: co-application of non-granulated biochar and granulated NPK fertilizer. Data are presented as means ± standard deviation (n = 5). Different letters above error bars indicate a significant difference in cumulative nutrient loss between the different treatments (one-way analysis of variance, $p < 0.05$, Tukey's post hoc test).

the greenhouse trial. Still, the extractable N content in gBBF granules were approximately six times higher compared to the CaCl₂-extractable N from the bulk soil in the respective treatments (0.2–0.3 mg g⁻¹, Table S9).

The gBBF granules sampled from the soil after harvest had a significantly higher SSA based on CO₂ adsorption compared to the original, non-incubated gBBF samples, independent of whether leaching events were applied or not ($p < 0.001$, Fig. 7b). The soil-aged gBBF granules had a SSA in the range of 300–360 m² g⁻¹ (BET method) and 400–480 m² g⁻¹ (DFT method) based on CO₂ adsorption. This is in the same range of SSA measured for the pristine non-granulated biochar (358 m² g⁻¹ (BET) and 516 m² g⁻¹ (DFT), Table 2). The adsorption isotherms

Cumulative Leaching	K		Mg		S	
	F	<i>p</i>	F	<i>p</i>	F	<i>p</i>
Fertilizer type	4.948	0.040	6.75	0.019	6.97	0.020
Block	0.6838	0.623	2.07	0.177	0.56	0.697

Table 7. Statistical results of one-way analyses of variance of the cumulative potassium (K), magnesium (Mg) and sulfur (S) leaching loss from two leaching events for the factor 'fertilizer type' (NPK, gBBF, B+NPK, excluding the non-fertilized control (CTRL-0)). Additionally, the block effect is presented 'Block'. Significant values are displayed in bold.

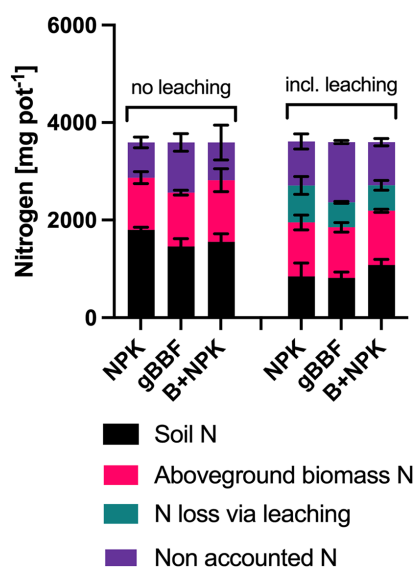


Figure 6. Nitrogen (N) balance for all fertilized treatments: residual total N in the soil after harvest, based on soil extractions with 0.01M CaCl₂, total N quantified in aboveground biomass, total N lost via leaching and non-quantified N. Non accounted N was calculated as difference between the total fertilizer addition to the soil (including native mineralized soil-N at the start of the experiment) and the sum of the other N pools. NPK: granulated mineral fertilizer. gBBF: granulated biochar-based NPK fertilizer. B+NPK: co-application of non-granulated biochar and granulated NPK fertilizer to the soil. Data are presented as means ± standard deviation (n = 5).

recorded for the soil-aged gBBF were well aligned to the isotherm recorded for the pristine, non-granulated biochar, which was also the case for the pore size distributions (Figs. S21 and S22).

Discussion

The plant growth study confirmed the potential of granulated BBFs to maintain crop productivity while improving soil nutrient retention compared to mineral fertilization alone. Still, the experiments indicated better plant growth in terms of aboveground biomass yield and nutrient uptake in the presence of non-granulated biochar co-applied with fertilizer. Three different mechanisms might be relevant for this observation. First, under optimized soil moisture (constant 65% WHC, no leaching event), the gBBF decreased the uptake of important macronutrients such as P, Mg, and S compared to the co-application of biochar with fertilizer, indicating immobilization of these nutrients in the gBBF potentially due to the closer contact of nutrients and biochar in the gBBF and subsequent higher nutrient adsorption on biochar surfaces. Secondly, in line with the literature¹⁷, combined granulation of biochar and fertilizer significantly decreased the porosity of the biochar contained in the gBBF, which could be due to compression of the individual biochar particles by granulation and biochar pore blockage by the fertilizer, as indicated by gas adsorption, SEM and EDX results. The reduction in biochar porosity might negatively impact the otherwise positive effects of pure biochar (co-applied with NPK) on soil properties and plant growth. However, our results also confirmed that the biochar in the gBBF regained its original

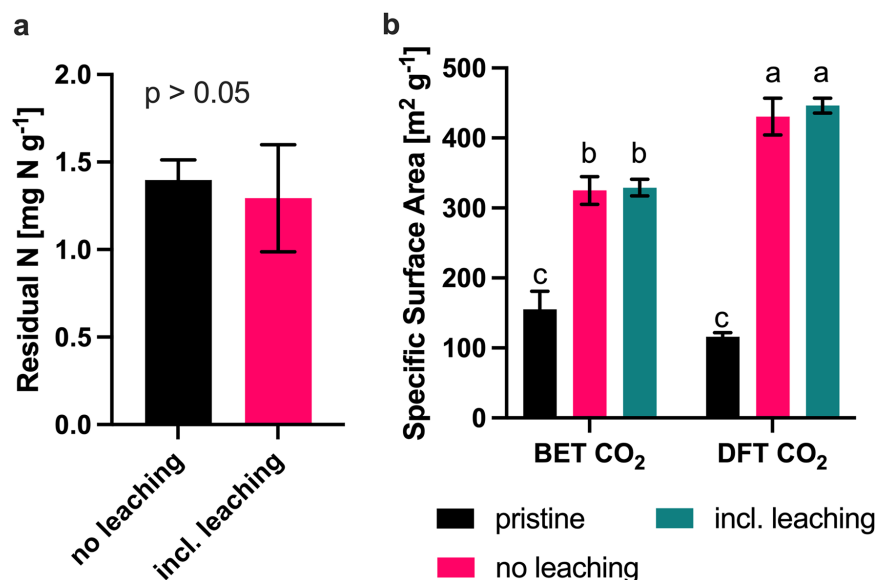


Figure 7. (a) Residual nitrogen (N) extracted with 2 M KCl solution for 2 h from granulated biochar-based fertilizer (gBBF) that was sampled from the soil after the harvest of white cabbage plants. (b) The specific surface area of pristine gBBF and soil-incubated gBBF was calculated based on CO₂ adsorption isotherms according to the Brunauer-Emmet-Teller (BET) model or Density Functional Theory (DFT). Samples were analyzed both from the pots without or including two leaching events. Data are presented as means \pm standard deviation ($n = 5$ in panel a and $n = 3$ in panel (b)). Different letters above error bars indicate a significant difference between the different treatments at $p < 0.05$ (one way analysis of variance, $p < 0.05$, Tukey's post hoc test).

microporosity during soil incubation, which we explain by the dissolution of nutrients in soil pore water. Thirdly, with the gBBF, individual biochar particles were less uniformly distributed in the soil compared to co-applied biochar, which might limit the potential of positive biochar impacts on plant-soil interactions.

Improved crop growth with leaching in the biochar treatments was not consistently linked to higher nutrient uptake, even though improved soil nutrient retention was observed with biochar amendments compared to pure mineral fertilization, most likely due to the high fertilization level used in the experiment. Under a more limited fertilization scheme, biochar-amended plants might have yielded higher cabbage yields compared to sole mineral fertilization since the reduced nutrient leaching with biochar would have had a more pronounced positive effect on crop growth. The still higher biomass production with biochar in the leaching treatments might be explained by the stabilization of soil pH close to a range more favorable for cabbage growth (i.e., a pH between 6.0 and 7.5²⁸) while soil pH rose to 8.0 with sole NPK fertilization. The soil pH measurements indicated that biochar retained more protons in the soil, i.e., derived from organic acids in root exudates or from the mineral fertilizer (which had a slightly acidic pH).

Our initial hypothesis, that combined granulation of biochar and fertilizer would improve biochar's nutrient retention effectivity in soil, was valid for NH₄⁺-N leaching during the first leaching event. However, total N losses were not impacted by biochar pretreatment during both leaching events. The hypothesis was further valid for Mg and S leaching during the first leaching event. However, cumulative reductions in nutrient leaching were reduced to the same extent for both biochar application methods compared to sole NPK fertilization. It is therefore suggested that although there is an initial improvement in the retention of some nutrients with the gBBF, this difference between gBBF and biochar-co-application with fertilizer will even out over time likely due to the progressing nutrient release from the gBBF largely restoring initial biochar properties, even despite the additional milling to < 1 mm. Nonetheless, biochar properties will change over time by aging in soil^{29,30}, but this requires considerably longer periods of time than in the present study.

In the present study, lower nutrient losses from soil amended with biochar were observed. This is likely due to the interaction of fertilizer components with the biochar surface since leachate volumes were not affected by the treatments. The fact that the biochar used here was more microporous than mesoporous indicates a relevant role of biochar micropores to improve soil nutrient retention. However, we did not quantify biochar macroporosity (e.g., by mercury intrusion), which might also contribute to interaction with dissolved nutrients.

Nitrogen was applied to the pots exclusively as urea, which, in a first step, is mineralized in soil to NH₄⁺-N by urease enzymes³¹. Urea-N was better retained in the gBBF during the extraction and incubation experiments

compared to the loose mixture of B + NPK, which is in line with literature^{15,16}, likely due to improved electrostatic interactions between the NH_2 groups in urea and negatively charged surface sites of the biochar. Urea molecules trapped in biochar pores in gBBF were potentially less available for ammonification until they were diffused out of the biochar pores to the soil, which was also partly indicated by less extractable $\text{NH}_4^+\text{-N}$ from the gBBF-amended soil samples taken 36 days after the beginning of the pot trial. Still, since the first leaching event in the greenhouse experiment was conducted after 35 days, most of the urea might have already been released and mineralized from the gBBF granule as indicated by the incubation experiments, where after 9 days, almost all N was released to the incubation liquid. If the leaching events had occurred at an earlier stage of the experiment, the reduction in N leaching provided by gBBF may have been more pronounced. Still, once urea was released from gBBF, it was mineralized closer to the biochar matrix compared to B + NPK, which may have eased $\text{NH}_4^+\text{-N}$ adsorption on biochar surfaces with the gBBF³² and can explain the lower leaching of $\text{NH}_4^+\text{-N}$ with gBBF compared to B + NPK in the first leaching event. Adsorption of $\text{NH}_4^+\text{-N}$ and urea-N on the biochar surface might be attributed to negatively charged carboxyl and phenolic groups^{32,33} on biochar, which can also explain the general lower leaching loss of K^+ and Mg^{2+} in the treatments with biochar amendments in line with the literature^{34,35}. Dissolved cations might also be retained in biochar pores by interaction with OH- π -bound water or water bound by Van-der-Waal force at the biochar surface³⁶. The improved retention of anions like nitrate (NO_3^-) and sulfur, most likely present as sulfates (SO_4^{2-}), may be attributed to positively charged biochar surface sites, such as O⁻-heteroatoms in aromatic rings that can form during pyrolysis above 700 °C, which applies to the biochar used in our study^{33,37}. Still, non-modified and non-aged biochars have only low nitrate adsorption and anion exchange capacities, which might be the reason why $\text{NO}_3^-\text{-N}$ leaching only tended to be reduced with biochar amendments in the present study compared to the control. Nitrate retention in biochar has been shown to rather evolve during soil aging of biochar surfaces and interaction with organic soil amendments or potentially organic acids derived from root exudates^{30,32,33,38–41}. The lower extractable soil $\text{NO}_3^-\text{-N}$ content in gBBF and B + NPK treatments compared to NPK in the absence of leaching after harvest might indicate that at the end of the experiment, some $\text{NO}_3^-\text{-N}$ was captured by biochar that was not extractable with 0.0125 M CaCl_2 .

We observed a reduction in cumulative N leaching by 32% with the gBBF compared to NPK. Three earlier studies found either no reduction in N leaching¹⁷, reductions by 44–61%⁹, or 6–9%⁴² with the application of gBBFs compared to fertilization without biochar. The observation that different studies on gBBFs found contrasting results on relative changes in N leaching losses may be explained by (1) an interaction of N leaching from gBBFs and soil type and (2) the gBBF characteristics (e.g., N speciation, biochar type, biochar to N ratio, and additive content). We prepared a gBBF using only trace amounts of a binding agent to be able to solely elucidate the impact of biochar itself in the gBBF on nutrient leaching. In earlier studies, additives like bentonite or paraffin wax were added to the gBBFs at significantly higher quantities, not just traces (e.g. ~50% w/w), which might have affected their agronomic impact e.g., on N leaching^{7–9,15–17}. Furthermore, all these studies only included a fertilizer-only control, but no control that included the additives, or biochar concomitant to the fertilizer. Therefore, the observed differences in N leaching between different studies might be linked to the additives used in the different BBFs.

The heavy precipitation events conducted during the present study of 30 mm within 1 h reflect events that will likely occur more often during crop cultivation periods in temperate climates in the future with progressing climate change^{43,44}. The reduction in nutrient leaching provided by the gBBF is promising as less environmental impact per unit of produced crop could be achieved. However, the additional incorporation of biochar into the granulated fertilizer at a rate of 65% (w/w) would increase fertilizer material costs by 930–1850 € per ton of mineral fertilizer, assuming a biochar cost of 500–1000 € t⁻¹; it would also require additional fuel for field application of the same amounts of nutrients, since more mass has to be transported to and on the field. Further, additional costs might occur during the production of the gBBF, e.g., due to biochar milling, which would have to be addressed in follow-up studies. At the same time, the CO₂ sequestration potential of 6.3 t CO₂ per ton of mineral fertilizer that is achieved by a gBBF as used here would translate to an income of 1000 € for the producer of the biochar-based fertilizer by CDR trading/carbon sink service revenues, assuming a biochar price index⁴⁵ of 180 \$ (t CO₂)⁻¹.

Conclusion

In the sandy soil used in the present study, biochar amendment had no statistically significant benefit on biomass yields under optimal growing conditions. With heavy rainfall (leaching) events, biochar increased yields significantly when co-applied with NPK fertilizer. Nutrient uptake of several macronutrients was significantly lower with gBBF compared to co-application of biochar and fertilizer in absence of leaching events, indicating immobilization in gBBF. In contrast to our hypothesis, granulation of biochar with mineral fertilizers did not significantly alter biochar effects on nutrient leaching compared to the co-application of non-granulated biochar with mineral fertilizer. Leaching events reduced yields across all treatments, however, biochar amendment counteracted the negative effect to some degree, especially with co-application of biochar, by improving plant nutrition with macronutrients. Since the granulated BBF provided similar crop yields compared to standard mineral fertilization, the combination of biochar and fertilizer via granulation can be recommended to enable biochar use with standard agricultural machinery. Further, biochar application provided an improved ratio of environmental effects (in particular reduced leaching) per unit of crop produced. Our study highlighted that granulated BBF can easily be produced without large amounts of various (binding) additives, as done in some earlier studies. A limitation of the current study is that the experiments included only one type of biochar, soil and crop and further, the results for crop growth and nutrient leaching might be different in the field due to the different environmental conditions as compared to the greenhouse. Future studies should investigate and optimize the effects of different biochar types and particle sizes, biochar-to-nutrient ratios, nutrient speciation,

and production techniques of granulated or pelleted BBFs on plant growth, nutrient retention, and soil-borne greenhouse gas emissions in different soils (since reductions in N₂O emissions are a common finding with biochar use⁵) both in greenhouse and field trials. Combined granulation of biochar and fertilizer is a way to ease adopting biochar application in agriculture to convey the positive environmental effects of biochar application to soils on a broader scale.

Data availability

The original data of this study is available on Zenodo with the following link: <https://doi.org/10.5281/zenodo.12098693>.

Received: 16 May 2024; Accepted: 8 July 2024

Published online: 17 July 2024

References

- Joseph, S. *et al.* How biochar works, and when it doesn't: A review of mechanisms controlling soil and plant responses to biochar. *GCB Bioenerg.* **13**, 1731–1764 (2021).
- Schmidt, H.-P. *et al.* Biochar in agriculture: A systematic review of 26 global meta-analyses. *GCB Bioenerg.* <https://doi.org/10.1111/gcb.12889> (2021).
- Schmidt, H.-P., Hagemann, N., Draper, K. & Kammann, C. The use of biochar in animal feeding. *PeerJ* **7**, e7373 (2019).
- Hagemann, N. *et al.* Effect of biochar amendment on compost organic matter composition following aerobic composting of manure. *Sci. Total Environ.* **613–614**, 20–29 (2018).
- Borchard, N. Biochar soil and land-use interactions that reduce nitrate leaching and N₂O emissions: A meta-analysis. *Sci. Total Environ.* **651**, 2354–2364 (2019).
- Melo, L. C. A., Lehmann, J., da Carneiro, J. S. S. & Camps-Arbestain, M. Biochar-based fertilizer effects on crop productivity: A meta-analysis. *Plant Soil* <https://doi.org/10.1007/s11104-021-05276-2> (2022).
- Jia, Y., Hu, Z., Ba, Y. & Qi, W. Application of biochar-coated urea controlled loss of fertilizer nitrogen and increased nitrogen use efficiency. *Chem. Biol. Technol. Agric.* **8**, 3 (2021).
- Shi, W. *et al.* Assessing the impacts of biochar-blended urea on nitrogen use efficiency and soil retention in wheat production. *GCB Bioenerg.* **14**, 65–83 (2022).
- Shi, W. *et al.* Biochar bound urea boosts plant growth and reduces nitrogen leaching. *Sci. Total Environ.* **701**, 134424 (2020).
- Rasse, D. P. *et al.* Enhancing plant N uptake with biochar-based fertilizers: Limitation of sorption and prospects. *Plant Soil* **475**, 213–236 (2022).
- Joseph, S. *et al.* Shifting paradigms: Development of high-efficiency biochar fertilizers based on nano-structures and soluble components. *Carbon Manag.* **4**, 323–343 (2013).
- Schmidt, H.-P., Pandit, B. H., Cornelissen, G. & Kammann, C. I. Biochar-based fertilization with liquid nutrient enrichment: 21 field trials covering 13 crop species in Nepal—biochar-based fertilization. *Land Degrad. Dev.* **28**, 2324–2342 (2017).
- Grafmüller, J., Schmidt, H.-P., Kray, D. & Hagemann, N. Root-zone amendments of biochar-based fertilizers: Yield increases of white cabbage in temperate climate. *Horticulturae* **8**, 307 (2022).
- Meyer Zu Drewer, J. *et al.* Impact of different methods of root-zone application of biochar-based fertilizers on young cocoa plants: Insights from a pot-trial. *Horticulturae* **8**, 328 (2022).
- Liu, X. *et al.* A biochar-based route for environmentally friendly controlled release of nitrogen: Urea-loaded biochar and bentonite composite. *Sci. Rep.* **9**, 9548 (2019).
- Bakshi, S., Banik, C., Laird, D. A., Smith, R. & Brown, R. C. Enhancing biochar as scaffolding for slow release of nitrogen fertilizer. *ACS Sustain. Chem. Eng.* <https://doi.org/10.1021/acssuschemeng.1c02267> (2021).
- Tahery, S. *et al.* A comparison between the characteristics of a biochar-NPK granule and a commercial NPK granule for application in the soil. *Sci. Total Environ.* **832**, 155021 (2022).
- EBC (2012–2023). 'European Biochar Certificate: Guidelines for a Sustainable Production of Biochar' European Biochar Foundation (EBC), Arbaz, Switzerland. (<http://european-biochar.org>). Version 10.3 from 5th April 2023. (2023).
- Brunauer, S., Emmett, P. H. & Teller, E. Adsorption of gases in multimolecular layers. *J. Am. Chem. Soc.* **60**, 309–319 (1938).
- Hohenberg, P. & Kohn, W. Inhomogeneous electron gas. *Phys. Rev.* **136**, B864–B871 (1964).
- Bucheli, T. D. *et al.* On the heterogeneity of biochar and consequences for its representative sampling. *J. Anal. Appl. Pyrolysis* **107**, 25–30 (2014).
- German Weather Service. Weather lexicon: Heavy rainfall. <https://www.dwd.de/DE/service/lexikon/begriffe/S/Starkregen.html>.
- Kandeler, E. & Gerber, H. Short-term assay of soil urease activity using colorimetric determination of ammonium. *Biol. Fertil. Soils* <https://doi.org/10.1007/BF00257924> (1988).
- DIN 19746:2005-06, Bodenbeschaffenheit - Bestimmung von mineralischem Stickstoff (Nitrat und Ammonium) in Bodenprofilen (Nmin-Laborverfahren). <https://doi.org/10.31030/9607286>.
- Rhine, E. D., Mulvaney, R. L., Pratt, E. J. & Sims, G. K. Improving the Berthelot reaction for determining ammonium in soil extracts and water. *Soil Sci. Soc. Am. J.* **62**, 473 (1998).
- Hagemann, N. *et al.* Does soil aging affect the N₂O mitigation potential of biochar? A combined microcosm and field study. *GCB Bioenerg.* **9**, 953–964 (2017).
- Meier, U. Entwicklungsstadien mono- und dikotyler Pflanzen: BBCH Monografie. (2018). <https://doi.org/10.5073/20180906-075119>.
- Cornell University. Growing guide: Cabbage. <http://www.gardening.cornell.edu/homegardening/scenes5fdd.html>.
- Joseph, S. *et al.* Microstructural and associated chemical changes during the composting of a high temperature biochar: Mechanisms for nitrate, phosphate and other nutrient retention and release. *Sci. Total Environ.* **618**, 1210–1223 (2018).
- Hagemann, N. *et al.* Organic coating on biochar explains its nutrient retention and stimulation of soil fertility. *Nat. Commun.* **8**, 1089 (2017).
- Hagemann, N., Harter, J. & Behrens, S. Elucidating the impacts of biochar applications on nitrogen cycling microbial communities. in *Biochar Application* 163–198 (Elsevier, 2016). <https://doi.org/10.1016/B978-0-12-803433-0.00007-2>.
- Gai, X. *et al.* Effects of feedstock and pyrolysis temperature on biochar adsorption of ammonium and nitrate. *PLoS ONE* **9**, e113888 (2014).
- Banik, C., Lawrinenko, M., Bakshi, S. & Laird, D. A. Impact of pyrolysis temperature and feedstock on surface charge and functional group chemistry of biochars. *J. Environ. Qual.* **47**, 452–461 (2018).
- Lehmann, J. *et al.* Nutrient availability and leaching in an archaeological anthrosol and a ferralsol of the central amazon basin: Fertilizer, manure and charcoal amendments. *Plant Soil* **249**, 343–357 (2003).
- Liao, W., Drake, J. & Thomas, S. C. Biochar granulation, particle size, and vegetation effects on leachate water quality from a green roof substrate. *J. Environ. Manage.* **318**, 115506 (2022).

Supplementary information to:

Granulation compared to co-application of biochar plus mineral fertilizer and its impacts on crop growth and nutrient leaching.

Jannis Grafmüller^{1,2,3,4}, Jens Möllmer⁵, E. Marie Muehe^{3,6}, Claudia I. Kammann⁷, Daniel Kray¹, Hans-Peter Schmidt² and Nikolas Hagemann^{2,4}

¹Institute of Sustainable Energy Systems (INES), Offenburg University of Applied Sciences, Germany

²Ithaka Institute, Arbaz (Switzerland) and Goldbach (Germany)

³Plant Biogeochemistry, Department of Geosciences, University of Tübingen, Tübingen, Germany

⁴Environmental Analytics, Agroscope, Zurich, Switzerland

⁵Institut für Nichtklassische Chemie e.V. (INC), Leipzig, Germany

⁶Plant Biogeochemistry, Department of Applied Microbial Ecology, Helmholtz Centre for Environmental Research - UFZ, Leipzig, Germany

⁷Department of Applied Ecology, Hochschule Geisenheim University, Geisenheim, Germany

Supplementary information related to this chapter can be found under the following link on the publisher website: <https://doi.org/10.1038/s41598-024-66992-0>

or directly under: https://static-content.springer.com/esm/art%3A10.1038%2Fs41598-024-66992-0/MediaObjects/41598_2024_66992_MOESM1_ESM.pdf

Chapter 3d

Contrasting effects of granulated biochar-based fertilizer on nitrogen leaching in sandy loam and silt loam

Jannis Grafmüller^{1,2,3}, Rebekka Goldbach⁴, Nikolas Hagemann^{2,5}, Daniel Kray¹

¹Institute for Sustainable Energy Systems (INES), Offenburg University of Applied Sciences, Offenburg, Germany

²Ithaka Institute, Arbaz (Switzerland) and Goldbach (Germany)

³Plant Biogeochemistry, Tübingen University, Tübingen, Germany

⁴Faculty of Mechanical and Process Engineering, Offenburg University of Applied Sciences, Offenburg, Germany

⁵Environmental Analytics, Agroscope Zurich, Zurich, Switzerland

Working paper

Statement of personal and co-author contributions, plus non-listed contributors

Authors	Position of candidate in list of authors	Scientific ideas by the author [%]	Data generation by the author [%]	Analysis and interpretation by the author [%]	Paper writing done by the author [%]
Jannis Grafmüller	1	70	20	60	100
Rebekka Goldbach	2	10	80	30	0 ^a
Nikolas Hagemann	3	10	0	5	0 ^a
Daniel Kray	4	10	0	5	0 ^a
Publication status	unpublished				
Explanations	The greenhouse experiment was conceptualized by Rebekka Goldbach and me. Rebekka Goldbach conducted the experimental work as part of her bachelor thesis under my supervision, with contributions from myself during trial setup, the conduction of the leaching events, plant harvest and laboratory analyses. Rebekka Goldbach and I analyzed the data and Daniel Kray and Nikolas Hagemann supported during data interpretation. The manuscript was written by me.				

^a: Contribution set to 0, as the co-author did not yet review the manuscript.

Abstract

The use of granulated biochar-based fertilizer (gBBF) can ease biochar application in agriculture while improving crop growth and reducing nitrogen (N) leaching. Still, it is unknown how effects on both crop yield and N leaching vary across soil types. In this study, a gBBF was applied to two different soils, a sandy or a silt loam, to quantify its effect on N leaching and ryegrass (*Lolium multiflorum*) growth. Soil amended with granulated compound fertilizer without biochar was used as reference (NPK). The gBBF amendment equaled a biochar application rate of 3 t biochar ha⁻¹. Nitrogen leaching was reduced by 33% with gBBF compared to NPK management in sandy loam, while ryegrass yields were similar for both amendments. In silt loam, however, gBBF application increased N leaching by 32% compared to NPK, potentially contributing to a 6% lower yield in ryegrass biomass after a total of four harvests. The differences in N leaching mirrored the differences of absolute leachate volumes, which might indicate that gBBF disturbed the soil structure of silt loam leading to increased macropore formation and thus resulted in higher leachate volumes compared to NPK amended soil. This study demonstrated that effects of gBBF amendment on N leaching vary with soil type. Potential faster disaggregation of gBBF in soil under field conditions, e.g., due to the presence of macrofauna, could reduce this effect, which should be assessed by future studies.

1. Introduction

The majority of agricultural crop production relies on application of synthetic nitrogen (N) fertilizer to soil, posing a risk of N leaching, mainly in the form of nitrate (NO_3^-), leading to groundwater contamination¹. Despite the implementation of so-called good agricultural practices, which include e.g., fertilization according to nutrient requirement of cultivars under consideration of soil nutrient content, and a general decline in the number of groundwater monitoring sites exceeding the NO_3^- limit of 50 mg l⁻¹, e.g. in Germany, many water bodies in agricultural regions still exceed this threshold².

The use of biochar-based fertilizers (BBF) might be a promising approach to address this challenge³. On a global average, biochar application can reduce NO_3^- leaching from soil by 13%¹, however, this has not yet been thoroughly investigated for application of biochar as granulated BBF (gBBF). Effects of gBBF amendment on crop growth but especially N leaching depending on soil texture are largely unexplored.

The soil texture regulates soil hydrological properties and nutrient dynamics⁴ and may also impact the effect of biochar application on e.g., water holding capacity (WHC), saturated hydraulic conductivity and with that also on nutrient leaching^{1,5}. While these effects are well documented for non-granulated biochar, research on granulated biochar remains scarce. Recent findings indicate that gBBF can reduce N leaching by up to 35% in sandy loam⁶, yet this effect may not be transferable to other soil types, as sandy soils are particularly responsive to biochar amendment¹.

Biochar applications to sandy soils generally stabilize or reduce saturated hydraulic conductivity, a measure for water transfer velocity through soil⁴, whereas in soils with higher clay and silt content, they tend to increase it⁵. As gBBF would be applied in a particle size range of 2-4 mm, to ensure compatibility with common agricultural machinery, especially in fine textured soil, i.e. soils with higher silt and clay content, the soil pore structure could be disrupted which might lead to different effects on N leaching as observed after application to sandy soil with an inherently coarser particle structure⁴.

In this study, a gBBF was applied to two contrasting soil types, a sandy or a silt loam. Effects on plant growth and N leaching in a simulated heavy precipitation event were quantified and compared to soil fertilization with a granulated compound fertilizer without biochar. The sandy loam was used to provide a reference to an earlier pot trial using the similar gBBF⁶ and ryegrass was used as experimental plant, as this opens up the possibility to quantify potential differences on crop yields caused by differences in N leaching via multiple harvests until full nutrient depletion in soil.

2. Materials and methods

2.1. Biochar and fertilizers

Granulated fertilizers were similar as used in a previous study⁶. In short, a granulated fertilizer without biochar addition was prepared from urea, mono-potassium-phosphate and patentkali to obtain a N, P and K content of 23.0%, 3.7% and 13.0% (w/w), respectively, and labelled as NPK. For the gBBF, biochar was added to the mixture at a rate of 65% (w/w) before granulation to obtain 8.7% N, 1.5% P and 52.2% K in the product. The biochar was prepared from forest wood at 750 °C in a pyrolysis plant manufactured by Carbon Technik Schuster GmbH (Dischingen, Germany) which was operated by Carbon Cycle GmbH & Co. KG (Rieden, Germany). Biochar and fertilizer characteristics are described in detail elsewhere⁶.

2.2. Soil origin and analysis

Two different soils were used in the present study and labelled according to their soil type. The *sandy loam* was sampled in March 2022 in the Ortenau region close to river Rhein in the upper 20 cm of soil depth and had an organic matter content of 7.7% and a pH of 7.4. The *silt loam* was obtained from Straßkirchen (Germany) in April 2021 and had a pH of 7.1 and an organic matter content of 3.7%. Basic soil characteristics were determined by Eurofins Umwelt Ost GmbH (Bobritsch-Hilberdorf, Germany) and are presented in Table S1-Table S3. Both soils were used in two earlier greenhouse trials^{6,7}. Soils were homogenized and sieved to < 10 mm before further usage.

2.3. Greenhouse trial

The pot trial was conducted between 17th November 2022 and 22nd May 2023 in a greenhouse located in Offenburg, Germany (48° 27' 29.6'' N, 7° 57' 6.9'' E). Over the whole experiment, averaging temperature was 19 ± 3 °C, relative humidity was 66 ± 13% and atmospheric CO₂ concentration was 486 ± 67 ppm. A weight of 4430 g of sandy loam or 3390 g of silt loam were homogenized with either 4.35 g NPK or 11.44 g gBBF (all dry matter equivalent), filled to 4 L planting pots (21 cm pot height with 17 cm inner diameter) and knocked on the floor for three times from a height of 20 cm for soil compaction. Pots were equipped with a 2 mm mesh size nylon layer at the bottom. Each treatment contained eight replicate pots. A total of 30 seeds of Italian ryegrass (*Lolium multiflorum*, variety Shakira) were sown and the soil was watered with 100 ml tap water. In the following three days, soil water content was adjusted to 60% WHC (Figure S1), which was maintained throughout the whole trial by watering three times a week with tap water. Pots were arranged in a randomized complete block design on a greenhouse

table with artificial lighting (Figure S2). Pots were re-arranged within each block on a weekly basis. Two weeks after sowing, germination rates were recorded (Figure S3), and plant number was reduced to 20 seedlings per pot. Aboveground biomass was harvested 2 cm above soil level on 11th January 2023, 06th February 2023, 15th March 2023 and 22nd May 2023. Harvested biomass was dried at 80 °C to mass constancy to determine dry weights. On 17th of January 2023, a heavy precipitation event equal to 30 l m⁻² was simulated in five replicate pots of each treatment by placing the pots on pipe sockets and adding a total of 0.7 l separated into watering steps of 175 ml every 15 minutes. After drainage had stopped after 45 minutes, the leachate volume was determined by weighing the pipe socket and a sample of 20 ml of the leachate was filtered into a 50 ml centrifuge tube and directly stored on wet ice in the greenhouse before storage at -18 °C in the lab. Soil from the three replicated pots in each treatment not receiving a leaching event was destructively sampled (50 ml after homogenization of root-freed soil) on 18th of January 2023 and stored at -18 °C for later extractable N quantification.

2.4. Soil extractions

A weight of 10 g of thawed soil samples taken from pots not receiving a leaching event were extracted in 40 ml of a 0.1 M CaCl₂ following DIN 19746⁸. Extracts were filtered to < 0.45 µm as described above and stored at -18 °C until further analysis.

2.5. Nitrogen analysis in soil extracts and leachates

Total N in soil extracts and leachates was quantified on a TOC-VCPN-TNM-1 (Shimadzu Corporation, Kyoto, Japan). Nitrate was quantified using an adapted method from Hagemann et al.⁹ in UV-transparent 96-well microplates (UV-Star, Greiner Bio-One GmbH, Frickenhausen, Germany). Ammonium was quantified according to Rhine et al.¹⁰ in 96 well microtiter plates. An Epoch 2 microplate reader was used (Biotek Instruments, Winooski, USA).

2.6. Data analysis

Data visualization and analysis was performed with Prism (version 10.4.1, GraphPad Software Inc., La Jolla (CA), USA). All data were analyzed with a two-way analysis of variance (ANOVA) including the factors *Soil* (sandy loam and silt loam) and *Fertilizer* (NPK and gBBF) followed by Tukey's post hoc test at alpha = 0.05. Only data of soil extractions was analyzed by a mixed effect model with similar factors as described above, as only two replicates of NPK amended to sandy loam could be analyzed in the lab compared to three replicates for all other

treatments. Block effects were considered with the repeated measures function. For aboveground ryegrass yields, N leaching and soil extractions, the analysis was performed separately for each harvest or N speciation.

3. Results

3.1. Aboveground ryegrass biomass

Total dry aboveground ryegrass yield after four individual harvests ranged between 26.5 g pot⁻¹ and 30.6 g pot⁻¹ and was generally higher for plants grown on sandy loam compared to silt loam (Figure 1 and Table S4). The type of fertilizer had no significant impact on total ryegrass yields, but there was a significant interaction of soil type and fertilizer ($p=0.0171$ and Table S4): yields for NPK and gBBF amendment were similar in sandy loam while gBBF treatment yielded 6% lower total biomass compared to NPK treatment in silt loam (Figure 1 and Table S4). The first harvest contributed to the lowest extent to total yields (3.9-4.9 g pot⁻¹), the third harvest yielded most biomass for all treatments (10.9-12.7 g pot⁻¹), while the second and fourth harvests yielded similar biomass (4.9-7.6 g pot⁻¹). Still, yield stagnation was indicated during the fourth harvest in relation to the length of growing period, which took a total of 68 days, compared to only 26 days and 37 days for the second and third growing period, respectively. Individual harvests in the sandy loam mirrored each other for NPK and gBBF amendments. In the silt loam, plants under gBBF management yielded lower biomass compared to NPK management with the first ($p=0.0121$, direct comparison) and fourth ($p=0.0368$) harvest, which was slightly compensated by plants fertilized with gBBF with the second harvest ($p=0.2585$, Table S4).

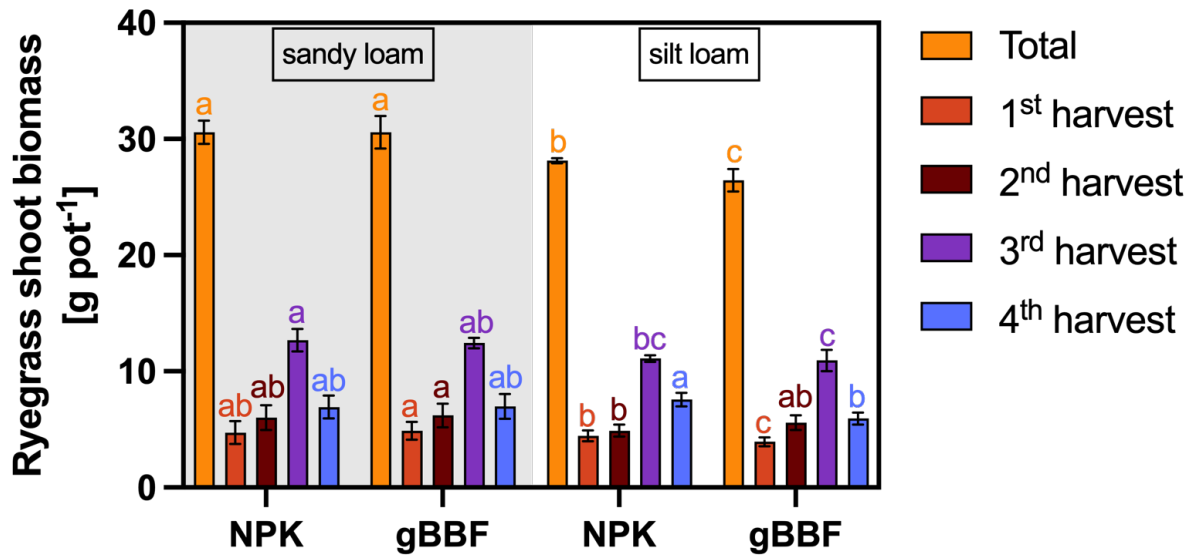


Figure 1: Dry aboveground yield of ryegrass during four individual harvests and their sum (Total). Two different soils, a sandy loam and a silt loam, were either amended with a granulated nitrogen, phosphorus and potassium fertilizer (NPK) or a granulated, biochar-based NPK fertilizer (gBBF). Different letters indicate significant differences between all treatments within a harvest category (two-way analysis of variance, Tukey's post-hoc test, $p < 0.05$). Error bars indicate the standard deviation of five replicates, except for the first harvest, where eight replicates are included.

3.2. Nitrogen leaching and extractability from soil

The volume of leachate obtained after the simulated heavy precipitation event 61 days after sowing was higher for pots filled with silt loam compared to sandy loam (Figure 1a). The amendment of gBBF reduced leachate volume obtained from sandy loam compared to NPK amendment (-21%), while the opposite was observed in silt loam (+12% with gBBF). In sandy soil, total N leaching was 33% lower under gBBF management compared to NPK management, while in silt loam, gBBF increased N leaching by 32% compared to NPK amendment. Nitrate made up an average of 93% of total N across all fertilizer soil combinations, ammonium was below the quantification limit in all leachates (Figure S4). The fraction of leached N compared to fertilized N (1000 mg pot⁻¹) ranged between 8% and 18% for all treatments. N concentrations in leachates mirrored the trends as observed for leachate volumes and absolute N leaching, but no statistically significant differences between the treatments were observed (Figure S5).

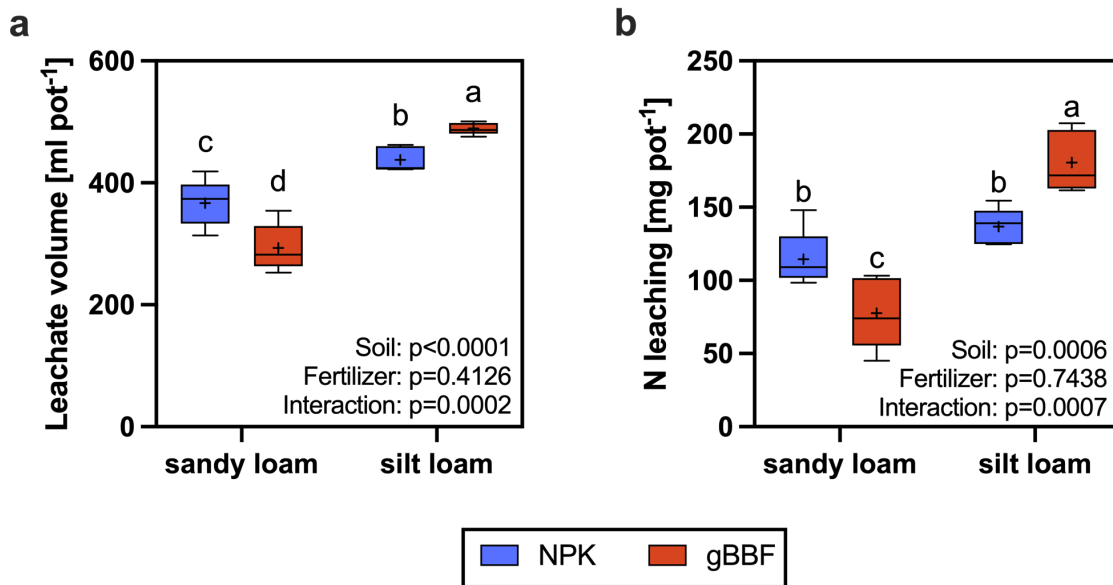


Figure 2: Leachate volume (a) and total amount of nitrogen (N) leached in the heavy precipitation event (30 l m^{-2}) 61 days after sowing. Two different soils, a sandy loam and a silt loam, were either amended with a granulated nitrogen, phosphorus and potassium fertilizer (NPK) or a granulated, biochar-based NPK fertilizer (gBBF). Whiskers in boxplots represent the minimum to maximum value of five replicates for each treatment, mean values are indicated with “+”, different letters indicate a significant difference between all treatments (two-way analysis of variance, Tukey’s post-hoc test, $p < 0.05$). Nitrate contributed close to 100% to total N (Figure S5).

Extractable N from non-leached soil, quantified in samples taken one day after the remaining pots were leached, was slightly higher in silt loam ($300\text{-}316 \text{ mg kg}^{-1}$) compared to sandy loam ($242\text{-}262 \text{ mg kg}^{-1}$, Figure 3 and Table S5). Yet, there was no significant difference in total extractable N between gBBF or NPK amendments in each soil type. Nitrate content was similar in all treatments and made up between 80% and 90% of total N across individual treatments, thus NH_4^+ and organic N only contributed to a comparable low extent. It is indicated that N uptake by plants was low with the first harvest as calculated N contents (fertilized N + native NO_3^- and NH_4^+) at the trial start were 315 mg kg^{-1} for silt loam and 250 mg kg^{-1} for sandy loam.

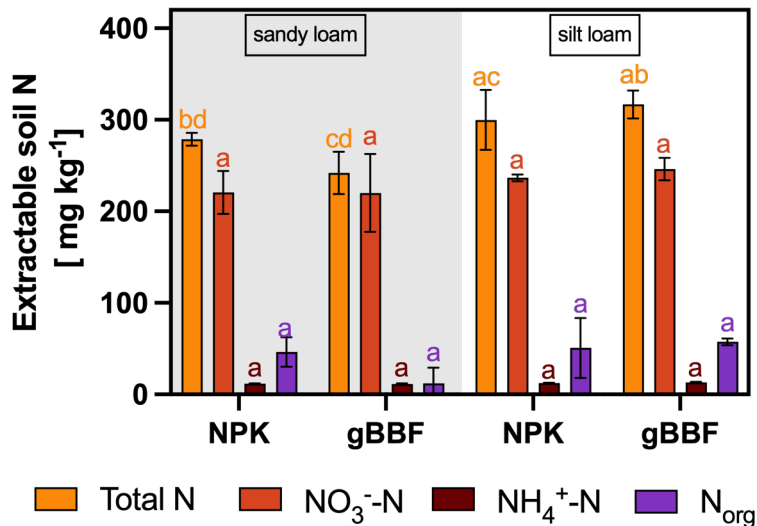


Figure 3: Soil nitrogen (N) fractions extracted with 0.01 M CaCl₂ from soil samples taken from pots that did not receive a leaching event. Soil samples were taken one day after all other pots underwent the leaching event. N fractions are divided into nitrate-N (NO₃⁻-N), ammonium-N (NH₄⁺-N), organic N and total N as the sum of the first three fractions. Two different soils, a sandy loam and a silt loam, were either amended with a granulated nitrogen, phosphorus and potassium fertilizer (NPK) or a granulated, biochar-based NPK fertilizer (gBBF). Different letters indicate significant differences between all treatments within a N fraction (two-way analysis of variance, Tukey's post-hoc test, $p < 0.05$). Error bars indicate the standard deviation of three replicates, except for NPK amendment in sandy soil, where only two replicates are presented.

4. Discussion

Contrasting effects on N leaching during a simulated heavy precipitation event were observed in the current experiment with gBBF amendment to either sandy or silt loam. The differences in N leaching between treatments cannot be explained by major differences in N uptake by ryegrass, since extractable soil N was similar in all treatments at the time the leaching event was conducted and ryegrass biomass yield was generally low after the first harvest, i.e. one week before the leaching event. Instead, differences in hydrological soil properties following gBBF amendment appear to have dominated N leaching, as indicated by the differences in leachate volumes. It is important to note that the difference in N leaching under gBBF management in either soil resulted from a combination of both leachate volume and N concentration, both parameters having consistent trends. However, only leachate volumes were significantly affected by gBBF amendment in the two soils.

Sandy loam, with its inherently coarser particle structure, naturally contains a higher fraction of macropores compared to silt loam⁴, the latter being characterized by a high proportion of

fine silt and clay and only minor sand content (<10% sand content, w/w, Table S3). The amendment of gBBF to sandy soil might have clogged existing macropores, potentially explaining the lower leachate volume compared to NPK amendment in this soil. In contrast, the coarse gBBF agglomerates might have introduced macropores by disturbing soil aggregate formation between fine silt and clay particles in the silt loam, leading to higher absolute leachate volumes under gBBF management. This finding is in line with previous studies that reported reduced or stabilized soil hydraulic conductivity following biochar amendment to sandy soil while the opposite was observed in soils with higher silt and clay content^{5,11}. Effects on hydraulic conductivity by gBBF amendment were not quantified in the current study and should be subject to a follow-up study.

The fact that NPK, applied in a similar particle size as gBBF, did not affect leachate volumes like gBBF in both soils is probably due to solubilization of NPK in the soil porewater and thus an absent sustained impact on soil structure. It is likely that NPK already fully solubilized at the time the leaching event was conducted as this was 61 days after sowing during which the soil moisture was kept at 60% WHC. In contrast, gBBF likely retained its granular shape in the soil over extended periods (>100 days as shown in a previous study⁶), affecting soil porosity and water movement still after nutrients were released. It must be noted that this might be different under real field conditions, where so called bioturbation⁴, i.e., mixing of soil structure through e.g. worm activity, might lead to disintegration of gBBF granules into individual particles with time. The results of the present study might therefore only reflect conditions shortly after gBBF amendment under real field conditions, where such bioturbation processes did not yet result in a potential granule disruption.

The increased leachate volume from gBBF-amended silt loam is not necessarily contradictory to the observed increase in WHC following gBBF amendment (Figure S1), as the measurement conditions differ fundamentally between these two parameters. During WHC measurement, soil was fully submerged in water for 18 hours, allowing time for gBBF-induced pores, even those with poorer accessibility, to fill with water, thereby enhancing water retention. During the heavy precipitation event, however, the rapid influx of water was preferentially channeled through additional macropores potentially created by the gBBF amendment, which might have dominated water transport under leaching conditions.

In sandy loam, N leaching was reduced by ~30% under gBBF treatment compared to NPK amendment, consistent with a previous study using the similar materials⁶, despite 3.5 times lower amendment rates to soil in the present study. The relative change in N leaching compared

to NPK therefore appears to be independent of the absolute biochar application rate resulting from gBBF amendment to soil, the biochar:N ratio in BBF could be more decisive.

As ryegrass yields were not increased in sandy loam under gBBF compared to NPK management, despite significantly lower N losses via leaching, N was likely not the limiting nutrient for plant growth in this soil or the difference in N leaching of only three percentage points, relative to total fertilized N, was too low to impact crop growth. In silt loam, higher N leaching under gBBF management might have contributed to the 6% lower ryegrass yield compared to NPK, yet this would have to be verified by N analysis in plant tissues. Differences in yield response might also be attributed to the leaching of other macro- and micronutrients, which were however not quantified in leachates or plant tissue in this study.

The relative low biochar application rate achieved with gBBF amendment of $\sim 3 \text{ t ha}^{-1}$ (0.2% biochar concentration in soil, w/w), may explain why potential biochar-induced improvements of crop yields¹² were absent in the present study in either of the soils. The yield decline observed for all treatments with the fourth harvest indicated that the plants used up the accessible nutrient pool in the soils and that an additional growing period would not have changed the overall findings of the present study.

5. Conclusion

This study demonstrated that effects of gBBF on N leaching strongly depend on soil type and point into the direction that effects on hydrological properties already observed for non-granulated biochar in earlier studies are similar for granulated biochar. As this experiment was conducted under controlled conditions in the greenhouse, field studies are needed to include factors such as soil biota, weather variability and long-term soil structure development to be able to conclude if the observed effects are transferable to field conditions. A more accelerated deagglomeration of gBBF in soil or the use of different granule sizes might avoid the negative effects on N leaching observed in silt loam, which should be considered for further optimization of gBBF.

References

1. Borchard, N. Biochar, soil and land-use interactions that reduce nitrate leaching and N₂O emissions: A meta-analysis. *Sci. Total Environ.* **11** (2019).
2. Bundesministerium für Ernährung und Landwirtschaft (BMEL) & Bundesministerium für Umwelt, nukleare Sicherheit und Verbraucherschutz (BMUV). Bericht der Bundesrepublik Deutschland gemäß Richtlinie 91/676/EWG zum Schutz der Gewässer vor Verunreinigung durch Nitrat aus landwirtschaftlichen Quellen: Nitratbericht 2024. (2024).
3. Melo, L. C. A., Lehmann, J., Carneiro, J. S. da S. & Camps-Arbestain, M. Biochar-based fertilizer effects on crop productivity: a meta-analysis. *Plant Soil* (2022) doi:10.1007/s11104-021-05276-2.
4. Amelung, W. *et al.* *Scheffer/Schachtschabel Lehrbuch der Bodenkunde*. (Springer Spektrum, Berlin, 2018).
5. Rabbi, S. M. F., Minasny, B., Salami, S. T., McBratney, Alex. B. & Young, I. M. Greater, but not necessarily better: The influence of biochar on soil hydraulic properties. *Eur. J. Soil Sci.* **72**, 2033–2048 (2021).
6. Grafmüller, J. *et al.* Granulation compared to co-application of biochar plus mineral fertilizer and its impacts on crop growth and nutrient leaching. *Sci. Rep.* **14**, 16555 (2024).
7. Grafmüller, J., Schmidt, H.-P., Kray, D. & Hagemann, N. Root-Zone Amendments of Biochar-Based Fertilizers: Yield Increases of White Cabbage in Temperate Climate. *Horticulturae* **8**, 307 (2022).
8. DIN e.V. DIN 19746:2005-06, Bodenbeschaffenheit - Bestimmung von mineralischem Stickstoff (Nitrat und Ammonium) in Bodenprofilen (Nmin-Laborverfahren). (2005) doi:10.31030/9607286.
9. Hagemann, N. *et al.* Does soil aging affect the N₂O mitigation potential of biochar? A combined microcosm and field study. *GCB Bioenergy* **9**, 953–964 (2017).
10. Rhine, E. D., Mulvaney, R. L., Pratt, E. J. & Sims, G. K. Improving the Berthelot Reaction for Determining Ammonium in Soil Extracts and Water. *Soil Sci. Soc. Am. J.* **62**, 473 (1998).
11. Ajayi, A. E. & Horn, R. Modification of chemical and hydrophysical properties of two texturally differentiated soils due to varying magnitudes of added biochar. *Soil Tillage Res.* **164**, 34–44 (2016).
12. Ye, L. *et al.* Biochar effects on crop yields with and without fertilizer: A meta-analysis of field studies using separate controls. *Soil Use Manag.* **36**, 2–18 (2020).

Supplementary Information to:

Contrasting effects of granulated biochar-based fertilizer on nitrogen leaching in sandy loam and silt loam

Jannis Grafmüller^{1,2,3}, Rebekka Goldbach⁴, Nikolas Hagemann^{2,5}, Daniel Kray²

¹Institute for Sustainable Energy Systems (INES), Offenburg University of Applied Sciences, Offenburg, Germany

²Ithaka Institute, Arbaz (Switzerland) and Goldbach (Germany)

³Plant Biogeochemistry, Tübingen University, Tübingen, Germany

⁴Faculty of Mechanical and Process Engineering, Offenburg University of Applied Sciences, Offenburg, Germany

⁵Environmental Analytics, Agroscope Zurich, Zurich, Switzerland

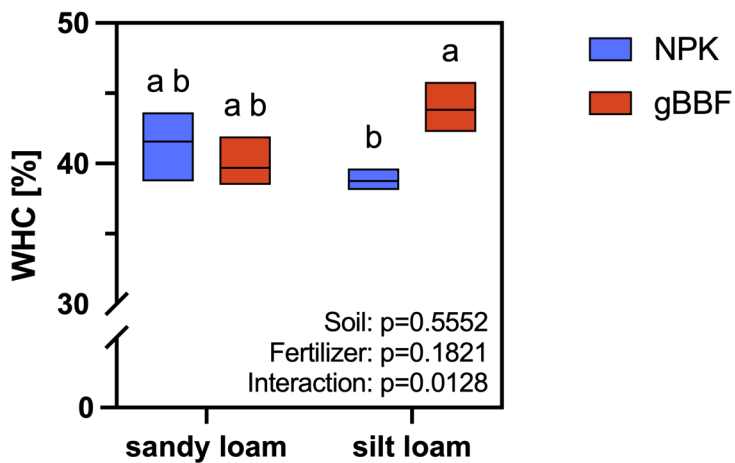


Figure S1: Water holding capacity (WHC) of two different soils, a sandy loam and a silt loam, either amended with a granulated nitrogen, phosphorus and potassium fertilizer (NPK) or a granulated, biochar-based NPK fertilizer (gBBF). Box plots indicate the range of minimum to maximum WHC of three replicates, the horizontal line in each box represents the average WHC. Different letters indicate a significant difference between all treatments (two-way analysis of variance, Tukey's post-hoc test, $p < 0.05$).

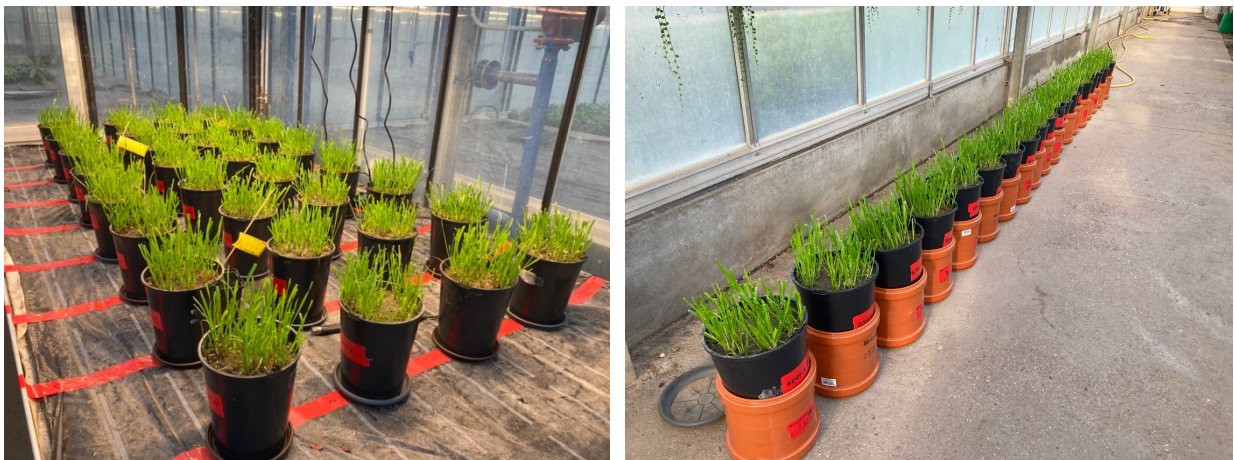


Figure S2: Pot arrangement in randomized complete block design on greenhouse table (left) and on the day of the leaching event where pots were placed on pipe sockets for leachate sampling (left).

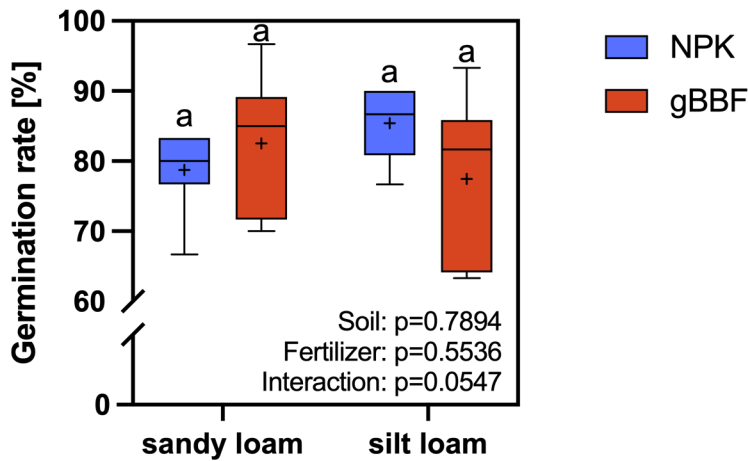


Figure S3: Germination rate as fraction (in %) of a total of 30 seeds initially applied per pot. Seedlings were counted 14 days after sowing. The two different soils, a sandy loam and a silt loam, were either amended with a granulated nitrogen, phosphorus and potassium fertilizer (NPK) or a granulated, biochar-based NPK fertilizer (gBBF). Whiskers in boxplots represent the minimum to maximum value of eight replicates for each treatment, mean values are indicated with “+”.

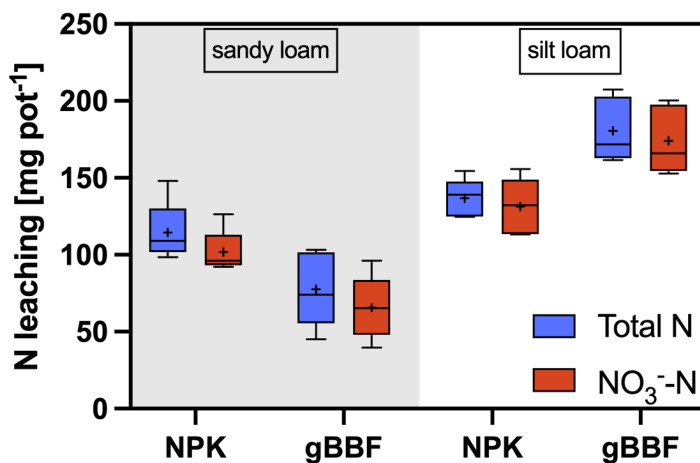


Figure S4: Amount of nitrogen N leached in a heavy precipitation event 61 days after sowing separated by total N and nitrate-N (NO₃-N). The two different soils, a sandy loam and a silt loam, were either amended with a granulated nitrogen, phosphorus and potassium fertilizer (NPK) or a granulated, biochar-based NPK fertilizer (gBBF). Whiskers in boxplots represent the minimum to maximum value of five replicates for each treatment, mean values are indicated with “+”.

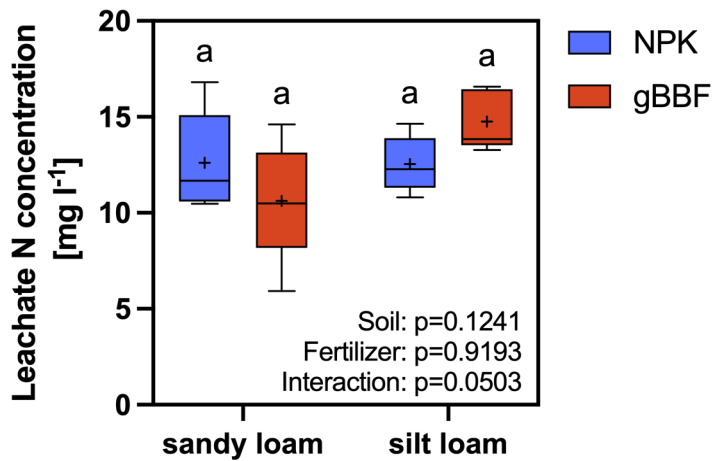


Figure S5: Nitrogen (N) concentration in leachates obtained from a heavy precipitation event 61 days after sowing. The two different soils, a sandy loam and a silt loam, were either amended with a granulated nitrogen, phosphorus and potassium fertilizer (NPK) or a granulated, biochar-based NPK fertilizer (gBBF). Whiskers in boxplots represent the minimum to maximum value of five replicates for each treatment, mean values are indicated with “+”.

Chapter 3: Physical modification of biochar for use in biochar-based fertilizers

Table S1: Main characteristics of the soil used in the greenhouse study. Concentrations are given based on dry matter, were applicable. SOM: Soil organic matter. TOC: Total organic carbon. EC: Electric conductivity. CAL: Calcium lactate extract. CaCl₂: Calcium chloride extract. Partly reproduced with permission from Grafmüller et al., 2022 and 2024, Horticulturae – MDPI and Scientific Reports – Springer Nature.

Parameter	Unit	Sandy loam	Silt loam	Method
SOM	wt%	7.7	3.7	DIN ISO 10694: 1996-08
TOC	wt%	4.5	2.1	DIN ISO 10694: 1996-08
pH	1	7.4	7.1	VDLUF A Method book volume I, Chapter 5.1.1, 7 th partial delivery, 2016
EC	μScm ⁻¹	110	79	VDLUF A Method book volume I, Chapter 10.1.1, 1991
Salt content	mg(100g) ⁻¹	58	42	VDLUF A Method book volume I, Chapter 10.1.1, 1991
Total Nitrogen	wt%	0.15	0.23	DIN ISO 13878:1998-11
NH ₄ -N	mg(100g) ⁻¹	<0.05	<0.05	VDLUF A Method book volume I, 3 rd partial delivery, Chapter 6.1.4.1, 2002
NO ₃ -N	mg(100g) ⁻¹	2.17	1.9	VDLUF A Method book volume I, 3 rd partial delivery, Chapter 6.1.4.1, 2002
S _{min}	mg(100g) ⁻¹	0.51	0.51	VDLUF A Method book volume I, A 6.3.1 (2016), Extraction with 0.0125 M CaCl ₂
Potassium (K)	mg(100g) ⁻¹	24.6	27.2	CAL, VDLUF A Method book volume I, 6 th partial delivery, Chapter 6.2.1.1, 2012
Phosphorus (P)	mg(100g) ⁻¹	13.0	35.3	CAL, VDLUF A Method book volume I, 6 th partial delivery, Chapter 6.2.1.1, 2012
Magnesium (Mg)	mg(100g) ⁻¹	8.8	29.8	CaCl ₂ , VDLUF A Method book volume I, Chapter 6.2.4.1, 1991; ISO 22036:2008
Boron (B)	mgkg ⁻¹	0.3	0.9	CAT, VDLUF A Method book volume I, 3 rd partial delivery, Chapter 6.1.4.1, 2002
Manganese (Mn)	mgkg ⁻¹	20	160	CAT, VDLUF A Method book volume I, 3 rd partial delivery, Chapter 6.1.4.1, 2002
Copper (Cu)	mgkg ⁻¹	4.6	4.2	CAT, VDLUF A Method book volume I, 3 rd partial delivery, Chapter 6.1.4.1, 2002
Zinc (Zn)	mgkg ⁻¹	9.5	10	CAT, VDLUF A Method book volume I, 3 rd partial delivery, Chapter 6.1.4.1, 2002

Table S2: Potential (pot.) and effective (eff.) cation exchange capacity of the soil used in the greenhouse study. Partly reproduced with permission from Grafmüller et al., 2022 and 2024, *Horticulturae* – MDPI and Scientific Reports – Springer Nature.

Parameter	Unit	Sandy Silt		Method
		loam	loam	
Cation exchange capacity (eff.)	cmol ⁺ kg ⁻¹	17.5	23.6	DIN EN ISO 11260:2011-09
Exchange acidity	cmol ⁺ kg ⁻¹	0.1	<0.1	DIN EN ISO 11260:2011-09
Exchangable Mg (eff.)	cmol ⁺ kg ⁻¹	0.5	4.1	DIN EN ISO 11260:2011-09
Exchangable Ca (eff.)	cmol ⁺ kg ⁻¹	13.2	24.5	DIN EN ISO 11260:2011-09
Exchangable Na (eff.)	cmol ⁺ kg ⁻¹	<0.1	<0.1	DIN EN ISO 11260:2011-09
Exchangable K (eff.)	cmol ⁺ kg ⁻¹	0.7	1.2	DIN EN ISO 11260:2011-09
Sum of exchangeable cations (eff.)	cmol ⁺ kg ⁻¹	14.4	29.8	DIN EN ISO 11260:2011-09
Cation exchange capacity (pot.)	cmol ⁺ kg ⁻¹	15.4	22.2	DIN ISO 13536: 1997-04
Exchangable Mg (pot.)	cmol ⁺ kg ⁻¹	0.5	2.4	DIN ISO 13536: 1997-04
Exchangable Ca (pot.)	cmol ⁺ kg ⁻¹	12.3	17	DIN ISO 13536: 1997-04
Exchangable Na (pot.)	cmol ⁺ kg ⁻¹	<0.1	<0.1	DIN ISO 13536: 1997-04
Exchangable K (pot.)	cmol ⁺ kg ⁻¹	0.7	0.9	DIN ISO 13536: 1997-04
Sum of exchangeable cations (pot.)	cmol ⁺ kg ⁻¹	13.5	20	DIN ISO 13536: 1997-04

Table S3: Particle size distribution and texture of the soil used for the greenhouse study. Partly reproduced with permission from Grafmüller et al., 2022 and 2024, *Horticulturae* – MDPI and Scientific Reports – Springer Nature.

Parameter	Unit	Sandy Silt		Method
		loam	loam	
Clay (<2µm)	wt%	11	28	DIN ISO 11277:2002:08
Coarse sand (0.63 - 2mm)	wt%	2	2	DIN ISO 11277:2002:08
Medium sand (0.2 - 0.63mm)	wt%	8	2	DIN ISO 11277:2002:08
Fine sand (0.063 - 0.2mm)	wt%	42	5	DIN ISO 11277:2002:08
Coarse silt (20-63 µm)	wt%	13	31	DIN ISO 11277:2002:08
Medium silt (6.3 - 20 µm)	wt%	14	24	DIN ISO 11277:2002:08
Fine silt	wt%	9	8	DIN ISO 11277:2002:08
Coarse soil (>2mm)	wt%	1	<1	DIN ISO 11277:2002:08

Table S4: Two-way analysis of variance of aboveground ryegrass yields (total, 1st to 4th harvest). Factors: Fertilizer (NPK and gBBF) and Soil (sandy loam and silt loam). SS: sum of squares. DF: Degrees of freedom. MS: mean square value. F value and p value.

Total ryegrass yield					
ANOVA table	SS	DF	MS	F (DFn, DFd)	P value
Fertilizer	3,596	1	3,596	F (1, 4) = 3,192	P=0,1485
Soil	53,86	1	53,86	F (1, 4) = 55,15	P=0,0018
Fertilizer x Soil	3,494	1	3,494	F (1, 4) = 15,46	P=0,0171
Ryegrass yield 1st harvest					
ANOVA table	SS	DF	MS	F (DFn, DFd)	P value
Fertilizer	0,2346	1	0,2346	F (1, 7) = 3,234	P=0,1152
Soil	3,038	1	3,038	F (1, 7) = 7,222	P=0,0312
Fertilizer x Soil	0,8911	1	0,8911	F (1, 7) = 17,38	P=0,0042
Ryegrass yield 2nd harvest					
ANOVA table	SS	DF	MS	F (DFn, DFd)	P value
Fertilizer	0,9331	1	0,9331	F (1, 4) = 43,49	P=0,0027
Soil	3,837	1	3,837	F (1, 4) = 15,65	P=0,0167
Fertilizer x Soil	0,3075	1	0,3075	F (1, 4) = 1,319	P=0,3147
Ryegrass yield 3rd harvest					
ANOVA table	SS	DF	MS	F (DFn, DFd)	P value
Fertilizer	0,194	1	0,194	F (1, 4) = 0,5914	P=0,4848
Soil	11,72	1	11,72	F (1, 4) = 11,54	P=0,0273
Fertilizer x Soil	0,008405	1	0,008405	F (1, 4) = 0,02988	P=0,8712
Ryegrass yield 4th harvest					
ANOVA table	SS	DF	MS	F (DFn, DFd)	P value
Fertilizer	3,113	1	3,113	F (1, 4) = 8,913	P=0,0405
Soil	0,2142	1	0,2142	F (1, 4) = 0,3640	P=0,5788
Fertilizer x Soil	3,638	1	3,638	F (1, 4) = 10,78	P=0,0304

Table S5: Two-way analysis of variance of extractable nitrogen (N) fractions from soil samples taken in pots without a leaching event on the day after the other pots underwent leaching. Factors: Fertilizer (NPK and gBBF) and Soil (sandy loam and silt loam). A fixed-effect analysis was performed due to different numbers in replicates per treatment. F value and p value.

Total N		
Fixed effects (type III)	P value	F (DFn, DFd)
Fertilizer	0,9463	F (1, 2) = 0,005785
Soil	0,0051	F (1, 2) = 194,9
Fertilizer x Soil	0,063	F (1, 1) = 101,3
Nitrate-N		
Fixed effects (type III)	P value	F (DFn, DFd)
Fertilizer	0,924	F (1, 2) = 0,01161
Soil	0,4314	F (1, 2) = 0,9556
Fertilizer x Soil	0,2869	F (1, 1) = 4,272
Ammonium-N		
Fixed effects (type III)	P value	F (DFn, DFd)
Fertilizer	0,5014	F (1, 2) = 0,6615
Soil	0,0936	F (1, 2) = 9,214
Fertilizer x Soil	0,2736	F (1, 1) = 4,760
Organic N		
Fixed effects (type III)	P value	F (DFn, DFd)
Fertilizer	0,8905	F (1, 2) = 0,02426
Soil	0,0773	F (1, 2) = 11,46
Fertilizer x Soil	0,2738	F (1, 1) = 4,754

References

J. Grafmüller, H.-P. Schmidt, D. Kray, N. Hagemann, Root-Zone Amendments of Biochar-Based Fertilizers: Yield Increases of White Cabbage in Temperate Climate, *Horticulturae* 8 (2022) 307. <https://doi.org/10.3390/horticulturae8040307>.

Grafmüller, J., Möllmer, J., Muehe, E.M., Kammann, C.I., Kray, D., Schmidt, H.-P., Hagemann, N., 2024. Granulation compared to co-application of biochar plus mineral fertilizer and its impacts on crop growth and nutrient leaching. *Sci Rep* 14, 16555. <https://doi.org/10.1038/s41598-024-66992-0>

Chapter 3e

Soil-borne N₂O emissions were not reduced with granulated biochar-based fertilizer at agricultural relevant biochar and nitrogen dosages

Jannis Grafmüller^{1,2,3}, E. Marie Muehe^{3,5}, Claudia I. Kammann⁶, Daniel Kray¹, Hans-Peter Schmidt², Nikolas Hagemann^{2,4}

¹Institute for Sustainable Energy Systems (INES), Offenburg University of Applied Sciences, Offenburg, Germany

²Ithaka Institute, Arbaz (Switzerland) and Goldbach (Germany)

³Plant Biogeochemistry, Tübingen University, Tübingen, Germany

⁴Environmental Analytics, Agroscope, Zurich, Switzerland

⁵Plant Biogeochemistry, Department of Applied Microbial Ecology, Helmholtz Centre for Environmental Research - UFZ, Leipzig, Germany

⁶Department of Applied Ecology, Hochschule Geisenheim University, Geisenheim, Germany

Working paper

Statement of personal and co-author contributions, plus non-listed contributors

Authors	Position of candidate in list of authors	Scientific ideas by the author [%]	Data generation by the author [%]	Analysis and interpretation by the author [%]	Paper writing done by the author [%]
Jannis Grafmüller	1	50	65	75	50
E. Marie Muehe	2	10	0	5	10
Claudia I. Kammann	3	10	0	5	10
Daniel Kray	4	10	0	5	10
Hans-Peter Schmidt	5	10	0	5	10
Nikolas Hagemann	6	10	0	5	10
Contribution by other parties not listed as authors (e.g., commercial analysis laboratories, student assistants)					
Lea Elena Anders		0	5	0	0
Regina Brämer and Barbara Anders		0	5	0	0
Alexandra Schuld		0	10	0	0
Paul-Georg Richter and Mara Breit		0	10	0	0
Martin Zuber		0	5	0	0
Publication status	unpublished				
Explanations	<p>The experiment was conceptualized by all co-authors and me. Christina Funk from Geisenheim University of Applied Sciences provided chambers for greenhouse gas enrichment and sampling equipment. The greenhouse trial and gas sampling was conducted by Lea Elena Anders and me. Elemental analyses of plant tissue and soil samples was performed by me, with support from Regina Brämer and Barbara Anders at Offenburg University of Applied Sciences and Martin Zuber at Agroscope Zurich, Switzerland. The gas samples were analyzed by Alexandra Schuld at Geisenheim University of Applied Sciences and Carolyn Görres supported with feedback on greenhouse gas flux calculations. E. Marie Muehe supported me with her advice and protocols on soil sampling for microbiological analyses, offering lab infrastructure for the analyses and with data interpretation. During conduction of microbiological analyses, I was greatly supported by Paul-Georg Richter and Mara Breit from UFZ Leipzig, Germany. The manuscript was written by me and was improved by all co-authors.</p>				

Abstract

Reduction of soil-borne nitrous oxide (N₂O) emissions is a well-researched benefit of biochar (BC) application to soil. However, little is known whether biochar-based fertilizers (BBF), resulting in low BC application rates, may also reduce soil-borne N₂O emissions. Here, we quantified N₂O emissions from soil amended with granulated BBF (gBBF) or with co-application of the same or tenfold amount of non-granulated biochar and conventional compound fertilizer (NPK) in a greenhouse trial. As reference, NPK was applied without a biochar amendment. The BC concentration in soil was 0.17% (w/w, 1.2 t ha⁻¹) with both gBBF and low-dosed non-granulated BC compared to 2% with high dosage of non-granulated BC (15 t ha⁻¹), reflecting a positive control for N₂O reductions. All treatments received nitrogen fertilization at 150 kg ha⁻¹. Spinach (*Spinacia oleracea*) yields were not affected by gBBF when compared to the pure NPK amendment but significantly increased by 10 and 14%, respectively, when compared to co-application of non-granulated biochar at both low and high dosage. It highlighted that plant growth was more stimulated by loosely mixed biochar particles than by gBBF, which was probably due to nutrient immobilization. Soil borne N₂O emissions were not reduced with low biochar dosage applied as gBBF or were even increased by 15% compared to pure NPK application with low dosage of non-granulated biochar. In contrast, the higher dosage of non-granulated biochar significantly reduced cumulative N₂O emissions compared to low-dose biochar treatments and to the pure NPK treatment. The latter could only be demonstrated on individual measurement days, but not on a cumulative basis. Still, at high biochar dosage, 22% less N₂O per amount of spinach biomass was emitted when compared to NPK. Further, this biochar treatment increased nitrogen use efficiency by 14% compared to NPK alone, indicating that N fertilization could be reduced with high biochar dosage while providing similar biomass production under a general lower risk for N₂O emissions. Functional marker gene abundance in soil after harvest compared to initial values indicated that N₂O was rather produced via nitrification-related paths than via conventional denitrification, which was expected at 25% water-filled pore space. Low biochar applications of 1 t ha⁻¹, as would be used in BBF strategies, are likely not sufficient to reduce soil-borne N₂O emissions when they are first applied, compared to conventional fertilization. From the perspective of N₂O emission reduction, gBBF is likely to be useful only after annual application over a longer period of time to allow biochar accumulation (>10 t ha⁻¹ after >10 years).

1. Introduction

Biochar application to soil reduces soil-borne nitrous oxide (N₂O) emissions¹, but this has only been consistently shown for high biochar dosages of >10-20 t ha⁻¹. Still, applying biochar at such dosage is not economically feasible for farmers due to high biochar prices (despite C-sink certification), low crop growth effects under temperate climates² and the absence of compensation payments for biochar ecosystem services³. Therefore, it is of interest to use biochar at the lowest possible application rates that result in agronomic and environmental benefits. A promising way to achieve this is the production of biochar-based fertilizers (BBF), i.e., biochar combined with nutrients in a single product instead of applying both individually and separated in time⁴. This could enhance the interaction of biochar and nutrients also at low biochar application rates of 0.5-2 t ha⁻¹, since the fertilizer is applied, solubilized and mineralized in or close to the biochar matrix in soil⁴⁻⁶. Moreover, BBF would be applied repeatedly, potentially annually, and result in an accumulation of biochar and its related positive effects. Ideally, such BBF are produced in a way that allows its application with common agricultural machinery, which would be achieved with granulated BBF (gBBF).

Nitrous oxide is a highly potent greenhouse gas, has a global warming potential of 265 on the basis of a 100 year time span and its atmospheric concentration has gradually increased since 1980⁷. Approximately 40% of annual N₂O emissions originate from anthropogenic sources, predominantly emerging from agricultural soils due to N fertilization^{8,9}. While only 1% of fertilized N is emitted as N₂O from agricultural soil¹⁰, N₂O emissions cause more than 50% of total CO₂-equivalents emitted during N fertilizer production and application¹¹. Soil-borne N₂O is produced during microbial metabolization of N, i.e., during nitrification and denitrification processes^{8,12}. Abiotic production of N₂O in soils is considered negligible on a global scale⁸.

Biochar's potential to reduce soil-borne N₂O emissions and the involved mechanisms were extensively researched in the past and summarized in an evaluation of 18 individual meta-analyses¹. According to this study, biochar soil application reduced N₂O emissions by 39% on average¹. Mechanisms that have been found to be relevant include:

1. Biochar stimulates *nosZ* gene abundance and activity associated with complete denitrification under low oxygen availability, i.e., the reduction of N₂O to N₂¹³⁻¹⁵, specifically in combination with
2. the entrapment of N₂O in water-filled pores of biochar¹⁴.
3. Biochar immobilizes nitrate and ammonium in its pores, leading to lower solubilized soil N concentrations and thus lower nitrification and denitrification rates¹⁶⁻¹⁸.

4. The liming effect of biochar could mitigate N₂O emissions under conditions with low oxygen availability by improving complete denitrification of NO₃⁻ to N₂¹⁶.
5. The sorption of labile carbon species at biochar surfaces could reduce substrate availability¹⁷.

Still, biochar can also increase N₂O emissions by promoting ammonia oxidation leading to higher N₂O production via nitrification-related paths, specifically *nitrifier-nitrification* and *nitrifier-denitrification*¹⁹.

Earlier studies on N₂O emissions used biochar application rates between 2-5% (w/w), equal to approximately 20-100 t ha⁻¹, which resulted in biochar to fertilized N ratios (BC:N_{Fert.}) between 150:1 and 500:1^{14,16,20,21}. Agricultural relevant compound fertilizers usually contain around 10% N (w/w). Lower N contents would limit the practicality, since the effort of fertilizer spreading would be too high due to the additional mass and volume. In synthetic fertilizers, N is mostly provided as urea, calcium ammonium nitrate, ammonium sulfate (salpeter) or ammonium nitrate-urea, which contain N at a rate of 21-46% (w/w)²². The maximum amount of biochar that could, thus, be added to a BBF with 10% N content would range between 60-80% (w/w), leading to ratios of BC:N_{Fert.} between 6:1 and 8:1. Additions of other macronutrients, such as phosphorus (P), potassium (K), magnesium (Mg), and sulfur (S), or an increase in N content, would further reduce the practically possible biochar content in the BBF and the BC:N_{Fert.} ratio. With standard fertilization rates of 100-200 kg N ha⁻¹, such a BBF with 10% N and 60-80% biochar would add 0.6-1.6 t ha⁻¹ biochar to a soil. Both the BC:N_{Fert.} ratio and biochar application rate would thus be 92-99% lower for BBF applications compared to the above-mentioned studies. So far, it is unknown if such low BC:N_{Fert.} and BC application rates can still provide reductions of N₂O emissions due to more efficient biochar use when N fertilizer is applied in a biochar matrix as BBF and not separate.

This study aims to elucidate whether reductions in N₂O emissions can be achieved with BBF applications using yearly agricultural relevant biochar dosages below 2 t ha⁻¹ and thus a low resulting BC:N_{Fert.} ratio. A gBBF was produced with a BC:N_{Fert.} ratio of 8:1, using urea as N source. We hypothesized that under low biochar application rates and BC:N_{Fert.} ratios, the gBBF would be more effective in reducing N₂O emissions than co-application of biochar with urea compared to urea alone, because the combined granulation of fertilizer and biochar could slow down N release to the soil pore water²³ and reduce the overall risk for N₂O production. To find out if the applied biochar in general reduces N₂O emissions compared to N fertilization alone

when applied at high, potentially sufficient dosage, it was also applied separately with the same N fertilizer but in tenfold dosage as with gBBF.

2. Materials and methods

2.1. Biochar and fertilizers

We used commercial biochar made from wood chips at a pyrolysis temperature of 750 °C in a pyrolysis plant designed by Carbon Technik Schuster GmbH (Neresheim, Germany), operated by Carbon Cycle GmbH & Co. KG (Rieden, Germany). The biochar was analyzed by Eurofins Umwelt Ost GmbH (Bobritsch-Hilbersdorf, Germany) according to the analytical guidelines of the European Biochar Certificate (EBC, 2012) and had a carbon content of 93%, N content of 0.3%, ash content of 2% (all w/w), molar H/C ratio of 0.18 and a pH of 9.1 (Table S1). The same biochar batch was used in greenhouse trials before^{23,24}. The biochar was processed by hammer-milling to <12 mm followed by collard-milling to <1mm (Type SJM00F, Gebr. G. Fischer AG, Schaffhausen, Switzerland). The gBBF and granulated, biochar-free compound fertilizer (NPK) were produced with urea as N source (excluding urease and nitrification inhibitors) and P, K, Mg and S source as described in literature²³. The products were sieved to 2-4 mm and contained 9% N, 1.5% P, 5% K, 0.7% Mg, 3% S and 65% biochar for gBBF and 23% N, 3.8% P, 13% K, 2% Mg and 6% S for NPK (Tables S1 and S2).

2.2. Greenhouse trial

The experiment was conducted from 10th of October 2022 until 24th of November 2022 in a greenhouse located in Offenburg, Germany (48° 27' 29.6'' N, 7° 57' 6.9'' E), with averaging temperature of 19.6 ± 4.5 °C, relative humidity of $69 \pm 14\%$, and atmospheric CO₂ concentration of 500 ± 80 ppm (10-minute measurement interval averaged over the whole experimental period). The soil used was a sandy loam taken from 0-20 cm soil depth of an agricultural field in the Ortenau region (48° 32' 23.7'' N, 7° 48' 50.6'' E, Kehl-Sundheim, Germany) in spring 2022. The soil was sieved to <16 mm and had an organic carbon content of 4.5% and a pH of 7.4. Soil analysis was performed by Eurofins Umwelt Ost GmbH and can be found in Tables S3-S5. The same soil was used in an earlier experiment²³. The fertilizer application was set to 0.2 g N pot⁻¹, corresponding to 150 kg N ha⁻¹ based on the soil surface of pots. Four different treatments were prepared (Table 1): soil amended homogeneously with NPK, gBBF, or a mixture of non-granulated biochar (<1 mm) and NPK either at low (0.17%, w/w) or high (2%) biochar concentration in the soil (NPK+BC_low and NPK+BC_high, respectively). With gBBF, biochar concentration in soil was 0.17%. Beside N, each pot

contained 0.03 g P, 0.12 g K, 0.16 g Mg and 0.05 g S amended via NPK or gBBF. A separate mixture of amendments, if applicable, and soil was homogenized and transferred to a rectangular shaped pot (11 x 11 x 12 cm³, length x width x height, Lambrecht-Verpackungen GmbH, Göttingen, Germany). For each treatment, five pots were prepared as replicates and positioned in a randomized complete block design surrounded by additional pots fertilized with NPK that were set up to eliminate edge effects but not included in the later data acquisition. This resulted in a total of 20 experimental pots and 18 surrounding pots. They were irrigated with 100 mL well water to initial ~30% water holding capacity (WHC), five holes with a depth of 1 cm were prepared on the horizontal bisecting line in each pot and two seeds of spinach (*Spinacia oleracea*, variety Corvair F1, Bruno Nebelung GmbH, Everswinkel, Germany) were sown into each hole (Figure S1). In the following two days, the water content in the pots was increased to 65% WHC (Figure S2a) with well water. Seven days after sowing, the number of seedlings was reduced to five plants per pot, equal to 5×10^6 plants ha⁻¹, and the germination rate was recorded (Figure S2b and Figure S3). The pots were manually watered three times a week to 65% WHC, equal to 25% WFPS²⁵ and randomly re-positioned within each block on a weekly basis. After 45 days, spinach plants were harvested by cutting the aboveground biomass 1 cm above soil level. Fresh and dry aboveground biomass weights were recorded, the latter after drying to mass constancy at 80 °C. Roots were washed under tap water to remove soil (Figure S4) and were dried at 80 °C to mass constancy to obtain dry weights.

Table 1 Biochar and fertilizer amounts mixed with 860 g pot⁻¹ of soil (dry matter equivalents) for each treatment. NPK: granulated, mineral nitrogen (N), phosphorus (P) and potassium (K) fertilizer. gBBF: granulated, biochar-based NPK fertilizer. gBBF contained 65% (w/w) milled biochar. NPK+BC: milled biochar co-applied with NPK fertilizer to the soil at low (0.17%) or high (2%) biochar concentration (w/w) in the soil mixture, as indicated. n.a.: not applicable.

ID	Treatment	Biochar concentration in soil [%]	Co-applied biochar [g pot ⁻¹]	NPK [g pot ⁻¹]	gBBF [g pot ⁻¹]
1	NPK	0	n.a.	0.9	n.a.
2	gBBF	0.17	n.a.	n.a.	2.3
3	NPK+BC_low	0.17	1.5	0.9	n.a.
4	NPK+BC_high	2.0	17.6	0.9	n.a.

2.3. Measurement of N₂O emissions

Gas sampling was performed with a static closed chamber method²⁶ by placing an air-tight plastic container around each pot with installed septum in the top cover for sampling (Figure S5). After closing the container, a steel cannula connected to a gas-tight syringe was inserted into the septum and the syringe was flushed three times with 15 ml gas from the container before a gas sample of 25 mL was taken. The sample was injected into a pre-vacuumed (< 10 mbar), hermetically sealed glass vial (Labco exetainer® 738W, 12 ml, Soda Glass, 738W). The procedure was repeated after 1 hour of gas enrichment in the container to obtain a second gas sample. A total of 1.7% of gas headspace volume was removed with both samples and the resulting low pressure in the container of ~10 mbar per sampling was not compensated. During gas enrichment in the container, the chambers were covered with a black plastic foil to inhibit photosynthesis. The N₂O concentration in the gas samples was quantified on a gas chromatograph (model 8610C, SRI Instruments Europe GmbH, Bad Honnef, Germany) equipped with an electron capture detector. Concentrations of CO₂ and CH₄ in the samples were also quantified via flame ionization detector (FID) and methane converter (in the case of CO₂). Gas sampling was performed on day 2, 4, 9, 16, 23, 30 and 37 after trial setup. Area-based N₂O gas flux (N_2O_{flux}) in µg N₂O-N m⁻² h⁻¹ were calculated with equation (1) in accordance to literature²⁶:

$$N_2O_{flux} = \frac{c_{t1} - c_{t0}}{t_1 - t_0} \cdot x_1 \cdot V_G \cdot \rho_G \cdot \frac{1}{A} \cdot x_2 \cdot x_3 = \frac{c_{t1} - c_{t0}}{t_1 - t_0} \cdot x_{conv.} \cdot (V_B - V_S - V_W) \cdot \frac{p \cdot M}{R \cdot T} \cdot \frac{1}{A} \cdot x_2 \cdot x_3 \quad (1)$$

where t_0 is the start and t_1 the end time (in hours) of N_2O enrichment in the chamber, c_{t0} and c_{t1} are the quantified N_2O concentrations (in parts per billion – ppb) in samples taken at t_0 and t_1 , respectively, x_1 is a conversion factor for transforming gas concentrations from ppb to m^3 (10^{-9}), V_G is the total gas volume surrounding the pot inside the chamber in m^3 , ρ_G is the density of N_2O in $kg\ m^{-3}$ at the temperature T (in K) and atmospheric pressure p (in Pa) during N_2O enrichment in the box, A is the top soil surface in the pot (in m^2), x_2 is for transforming kg in μg ($10^{-9}\ \mu g\ kg^{-1}$), x_3 is for transforming N_2O in N_2O -N mass equivalents ($=0.64$), V_B is the inside box volume, V_S is the soil particle volume in each pot (approximated by the total soil mass and particle densities of $2.65\ g\ cm^{-3}$ for sand, and $2.0\ g\ cm^{-3}$ both for silt and clay²⁷), V_W is the water volume at 65% WHC in each pot, M is the molecular weight of N_2O ($0.044\ kg\ mol^{-1}$) and R is the ideal gas constant ($8.314\ J\ mol^{-1}\ K^{-1}$).

Cumulative N_2O emissions ($N_2O_{cum.}$) were calculated assuming linear progression between individual values for the seven N_2O_{flux} measured over the time applying equation (2). Similar fluxes for day and nighttime were assumed. Yield-based cumulative emissions were obtained by division of $N_2O_{cum.}$ with dry aboveground spinach yields.

$$N_2O_{cum.} = \sum_{i=0}^7 (N_2O_{flux,i+1} - N_2O_{flux,i}) \cdot (t_{i+1} - t_i) \quad (2)$$

2.4. Spinach biomass analyses

Dried spinach shoot biomass was ground in a centrifugal mill to $<1\ mm$ (ZM 200, Retsch GmbH, Haan, Germany). Carbon and N contents were quantified with a CN928 (LECO Corporation, St. Joseph, USA) via combustion. Other main nutrients (P, K, Mg, S, Ca) as well as trace elements (Mn, Cu, Zn) were quantified following digestion of 120 mg dried sample in 3 mL 65% HNO_3 and 2 mL 30% H_2O_2 (analytical grade, Carl Roth, Germany) in a microwave at $180\ ^\circ C$ for 15 minutes (15 minutes ramp to $180\ ^\circ C$ in a Mars 5 Xpress, CEM GmbH, Kamp-Lintfort, Germany)²⁸. Quantification of elements in the digests was performed with ICP-OES in axial measurement configuration for all elements (icap 7000 series, Thermo Scientific, Waltham, USA). The digestion and ICP measurements were validated by digestion of a certified reference material (Table S6, ERM-CD281, European Commission DG JRC, Geel, Belgium). Nutrient uptakes with aboveground biomass were calculated by multiplication of nutrient contents and aboveground dry spinach yields. Nitrogen use efficiency (NUE) was calculated as a fraction of N uptake based on the sum of fertilized N plus initial native ammonium and nitrate N in the soil (NH_4^+ -N and NO_3^- -N, respectively, Table S3).

2.5. Soil geochemical analyses

After extracting the majority of roots from each pot during spinach harvest (manually, no water used yet), the remaining soil in each pot was homogenized manually for two minutes. A subsample of 7.5 g (stored at -20 °C) was extracted in 50 ml centrifuge tubes on a horizontal shaker at 150 rpm with 30 ml of a 1 M KCl in two sequential steps. After the first extraction step of 1 hour, samples were centrifuged at 10^4 g for 5 minutes (Megafuge 16, Thermo Fisher Scientific, Waltham, USA). A subsample of 15 ml of the supernatant was filtered for storage at -20 °C and the rest was decanted. The centrifuge tubes were weighed to correct for residual liquid and already eluted N before fresh 30 ml KCl solution was added for the second extraction step for 24 hours on the shaker. Ammonium according to Rhine et al.²⁹, NO₃⁻-N according to Hagemann et al.²⁰ and total N (TN, measured on a TOC-VCPN with TNM1, Shimadzu Corporation, Kyoto, Japan) was quantified in all filtered (<0.45 μm) extracts to calculate extractable N species based on soil dry matter. Dry matter of soil samples was quantified via drying to mass constancy at 105 °C. Organic N (N_{org}) in the extracts was calculated by subtraction of NH₄⁺-N and NO₃⁻-N from TN concentrations. For balancing N in different fractions (N uptake in aboveground biomass, N emitted as N₂O and extractable soil N left after harvest), soil N values were calculated by multiplication of TN concentrations in soil (in mg kg⁻¹) based on both extraction steps with dry matter of soil and biochar in each pot.

2.6. Soil DNA and RNA extraction and quantification

From the homogenized soil, a subsample of 0.5 g was weighted into cryo vials (Lysing Matrix E 2 mL, MP Biomedicals, Santa Ana - California, USA) and immediately stored on dry ice and subsequently at -80 °C. Non-amended soil was also stored in duplicates at -80 °C upon the start of the experiment to obtain initial gene abundance and activity. DNA and RNA was co-extracted from the soil³⁰ using a FastPrep-24 (MP Biomedicals, Santa Ana - California, USA) for the initial lysis step. The extracted DNA and RNA samples, diluted in a buffer made from Tris-HCl and EDTA (10 mM and 1 mM final concentration, respectively), were tested with Nanodrop for extraction quality and Qubit for DNA and RNA concentration (Table S8, NanoDrop One and Qubit Flex Fluorometer, both from Thermo Fisher Scientific, Waltham Massachusetts, USA). The extracts were aliquoted for upcoming analyses and stored at -80°C. For complementary DNA (cDNA) synthesis, DNA in the extracts was digested with the TURBO DNA-free KIT (Invitrogen, Thermo Fisher Scientific, Waltham Massachusetts, USA). Absence of DNA in these samples was verified by PCR and subsequent gel electrophoresis using the primers 515F and 806R³¹(Table S9). Reverse transcription of RNA to

cDNA was done with the SuperScript III reverse transcription kit (Invitrogen, Thermo Fisher Scientific, Waltham Massachusetts, USA). Synthesis of cDNA was confirmed by PCR and gel electrophoresis using the primers 515F and 806R. The cDNA samples were stored at -20 °C. Quantification of DNA and cDNA in the extracts was performed for the genes *amoA* (bacterial: AOB and archaeal: AOA), *nirK*, *nirS*, typical and atypical *nosZ*, *nifH* and bacterial *16S rRNA* (see Table S9 for primers). The quantitative PCRs (qPCR) were performed using a CFX96 attached to a C1000 Touch ® thermal cycler (Biorad-Laboratories, Hercules, California, USA). Individual qPCR mixtures and thermal profiles of qPCRs can be found in Table S10. Individual gene copy numbers per qPCR reaction volume were obtained from simultaneous analysis of a standard gene template (Table S9) serially diluted and previously measured for DNA content with Qubit, as described above. The CFX Maestro software (version 3.1.1517.0823, Biorad-Laboratories, Hercules, California, USA) was used for programming of qPCR thermal profiles and data analysis. Copy or transcript numbers per gene were reported based on soil dry matter. Abundance of 16S rRNA genes were divided by 5.5 gene copies cell⁻¹ to obtain cell numbers based on soil mass³².

2.7. Soil enzyme activities

Urease activity (UA) in the soil samples taken after harvest (stored at 4 °C) was measured using a non-buffered method one day after sampling³³. The NH₄-N concentration in the final extract was quantified according to literature²⁹. Nitrate reductase activity (NRA) was quantified after storing the soil samples six days at 4 °C following literature^{34,35}. Both methods were down-scaled to 1.25 g fresh soil weight and methodological details are given in the method section in the SI.

2.8. Statistical Analysis

Statistical analysis was performed with GraphPad Prism (version 10.3.1, GraphPad Software LLC, Boston, USA). Data were analyzed with a one-way analysis of variance (ANOVA) with the factor 'Treatment' (NPK, gBBF, NPK+BC_low, NPK+BC_high) followed by Tukey's post hoc test at alpha = 0.05. The repeated measures function implemented in GraphPad Prism was used to consider block effects. The mentioned p-values in the text, when comparing two different treatments, reflect adjusted p-values for the direct comparison obtained from one-way ANOVA. Data visualization was also performed in GraphPad Prism.

3. Results

3.1. Biomass yields and nutrient uptakes

Fresh and dry aboveground spinach yields were not significantly changed for gBBF compared to NPK (Figure 2a and b). Soil amended with NPK+BC_low and NPK+BC_high increased fresh yields compared to soil under NPK amendment by 13% and 26%, respectively, and dry yields by 10% and 14%, respectively (Figure 1a and b, Table S11). Spinach grown on gBBF-amended soil yielded 9% lower dry aboveground biomass relative to NPK+BC_high amendment ($p = 0.028$, Figure 1b). The root biomass was similar in all treatments (0.32-0.36 g plant⁻¹), but data scattering was highest when gBBF was amended to soil (Figure 1c). Similarly, root : shoot ratios varied most for plants grown on gBBF-amended soil (Figure 1d). Only the amendment of NPK+BC_high significantly reduced the root : shoot ratio compared to NPK-amended soil (-22%, $p=0.041$, Figure 1d).

Uptake of N, P, K, Mg and S, i.e., the nutrients that were contained in the fertilizers, in aboveground spinach biomass was not significantly changed under gBBF compared to NPK management (Figure 2). Uptake of N, P and S significantly increased when soils were amended with NPK+BC_low and NPK+BC_high compared to NPK, specifically 11-12% for N, 20-21% for P, and 17-24% for S (Figure 2, Table S12). This finding was primarily caused by the higher aboveground biomass yields under both NPK+BC amendments but can also partly be attributed to higher nutrient contents in spinach biomass (Figure S8). Further, NPK+BC_high increased K uptake by 63% compared to NPK ($p = 0.001$, Figure 2), also contributed by higher K contents in the aboveground biomass (Figure S8). Within the different biochar treatments, uptakes of P, K, and Mg were significantly lower from gBBF-managed soils as compared to both NPK+BC treatments ($p < 0.05$, Figure 2). Uptake of calcium and micronutrients is presented in Figure S9 but not further discussed here.

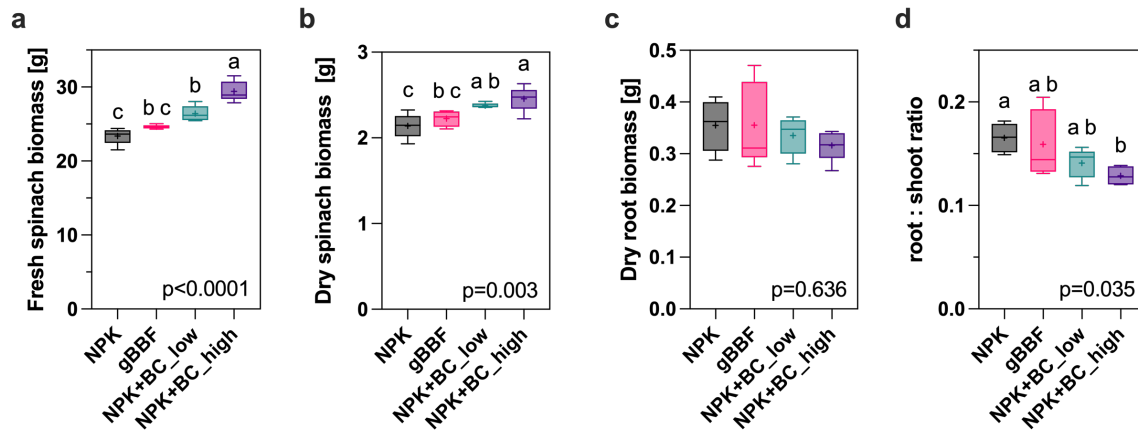


Figure 1 Fresh and dry aboveground biomass yields, dry root biomass and root : shoot ratio of spinach plants (panel a-d, respectively). NPK: granulated nitrogen (N), phosphorus (P) and potassium (K) fertilizer. gBBF: granulated, biochar-based NPK fertilizer. NPK+BC_low: milled biochar (< 1 mm) co-applied at 0.2% to the soil with NPK. NPK+BC_high: milled biochar (< 1 mm) co-applied at 2% to the soil with NPK. Whiskers in boxplots represent the minimum to maximum value of five replicates for each treatment, mean values are indicated with “+”, different letters indicate a significant difference between the treatments (one-way analysis of variance, Tukey’s post hoc test, $p < 0.05$).

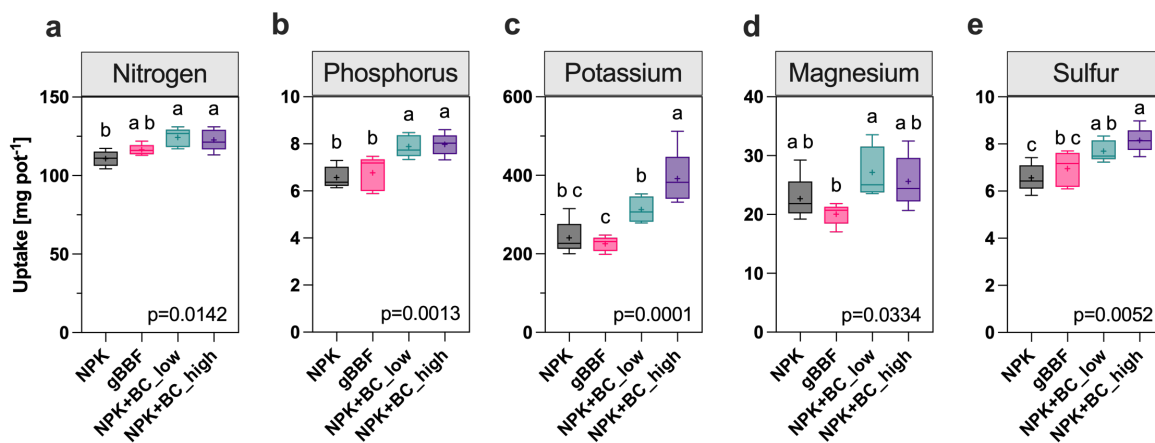


Figure 2 Uptake of nutrients in aboveground spinach biomass in panels a-e: nitrogen (N), phosphorus (P), potassium (K), magnesium (Mg) and sulfur (S). NPK: granulated nitrogen (N), phosphorus (P) and potassium (K) fertilizer. gBBF: granulated, biochar-based NPK fertilizer. NPK+BC_low: milled biochar (< 1 mm) co-applied at 0.2% to the soil with NPK. NPK+BC_high: milled biochar (< 1 mm) co-applied at 2% to the soil with NPK. Whiskers in boxplots represent the minimum to maximum value of five replicates for each treatment, mean values are indicated with “+”, different letters indicate a significant difference between the treatments (one-way analysis of variance, Tukey’s post hoc test, $p < 0.05$).

3.2. Soil-borne N₂O emissions

Emissions of N₂O ran with the same dynamics for all treatments, with highest emissions during the first 9 days of the experiment and ceased to around fivefold lower emission rates by day 16 (Figure 3a). Soil amended with gBBF emitted most N₂O during the first 9 days of up to 720 μg N₂O-N m⁻²h⁻¹ on day 4, without significant differences compared to NPK but with significantly higher emissions compared to NPK+BC_high (p=0.032, Figure 3a). Further, gBBF-amended soil consistently had the lowest emissions from day 16 onwards, which was significant compared to NPK+BC_low on day 23 (p=0.049). Like gBBF, NPK+BC_low had significantly higher emissions compared to NPK+BC_high on day 4 (p=0.043). The NPK+BC_high treatment had the lowest emissions until day 9, which was significant on day 2 compared to NPK (p=0.045) and compared to all other treatments on day 4 (p values of individual comparisons between 0.001 and 0.043, Figure 3a). With that, only NPK+BC_high reduced N₂O emissions significantly compared to NPK on individual days.

Cumulative N₂O emissions ranged between 157 and 196 mg N₂O-N m⁻² (Figure 3b). For soil amended with gBBF, no significant differences were observed compared to NPK- or NPK+BC_low-amended soils, but emissions were significantly higher relative to NPK+BC_high amendment (+16%, p=0.013). For NPK+BC_low-amended soil, cumulative emissions were significantly higher compared to soil amended with NPK (+16%, p=0.005) and NPK+BC_high (+22%, p<0.001). In soil with NPK+BC_high amendment, cumulative N₂O emissions were reduced by 7% compared to NPK, but not significantly (p=0.342). Spinach-yield normalized N₂O emissions were similar for soil amended with gBBF, NPK or NPK+BC_low but were significantly lower from NPK+BC_high-amended soils compared to the other treatments (-16 to -21%, p <0.0001, Figure 3c). Soil-borne emissions of CH₄ and CO₂ were similar in all treatments and are not discussed further at this point (Table S17, Figure S7).

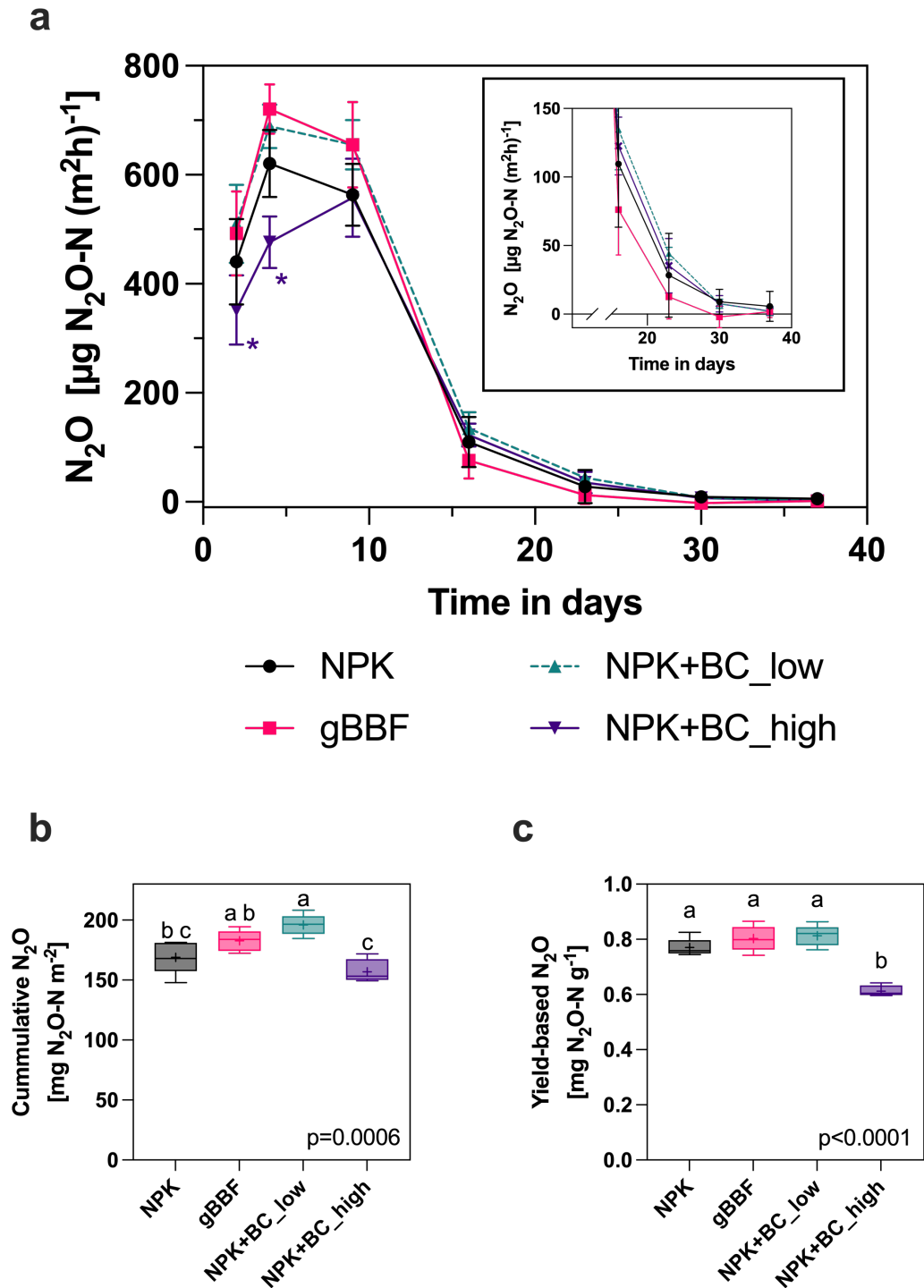


Figure 3 Nitrous oxide (N_2O) fluxes from the pots derived from seven individual measurements (a). Area-based cumulative N_2O emissions (b) and cumulative N_2O emissions based on dry aboveground spinach biomass (c). NPK: granulated nitrogen (N), phosphorus (P) and potassium (K) fertilizer. gBBF: granulated, biochar-based NPK fertilizer. NPK+BC_low: milled biochar (< 1 mm) co-applied at 0.2% to the soil with NPK. NPK+BC_high: milled biochar (< 1 mm) co-applied at 2% to the soil with NPK. Data are presented as means \pm standard deviation of five replicates in panel a.

Whiskers in boxplots (panel b and c) represent the minimum to maximum value of five replicates for each treatment, mean values are indicated with “+”, different letters indicate a significant difference between the treatments (one-way analysis of variance, Tukey’s post hoc test, $p < 0.05$) An asterisk in panel a below an error bar indicates a significant difference compared to the treatment ‘NPK’.

3.3. Nitrogen balance

Losses of N via soil-borne N₂O emissions only contributed to 0.7-0.9% of the sum of fertilized N and initial native mineral N in the soil (total of 220 mg N pot⁻¹, Figure 4a). The majority of N was equally distributed between uptake in spinach leaves and extractable N in soil after harvest (Figure 4a). Nitrogen use efficiency based on N uptake in aboveground spinach biomass was lowest under NPK and gBBF soil management with 50% and 53%, respectively. The NPK+BC amendments increased spinach’s NUE significantly to 57% compared to NPK ($p = 0.017$ for low and $p = 0.038$ for high BC dosage, Figure 4a). Total soil N after harvest, based on two sequential extraction steps of soil samples in 1 M KCl was similar for gBBF compared to NPK (Figure 4a and b). Soil amended with NPK+BC_high had the lowest remaining extractable total N, which was significant compared to gBBF management ($p = 0.007$) and almost significant compared to NPK management ($p = 0.053$, Figure 4). Further, soil amended with NPK+BC_high released a higher amount of N during the second extraction step compared to all other treatments (Figure S10). In soils with either treatment, N was predominantly present as NO₃⁻ after harvest (69-74%), followed by organic N (18-24%) and NH₄⁺ (4-8%, Figure 4b). Averaged N recovery (sum of on N in aboveground spinach biomass, remaining mineral soil N and emitted N₂O) ranged between 99% and 109% and was similar in all treatments (based on initial 220 mg N pot⁻¹, Figure S11).

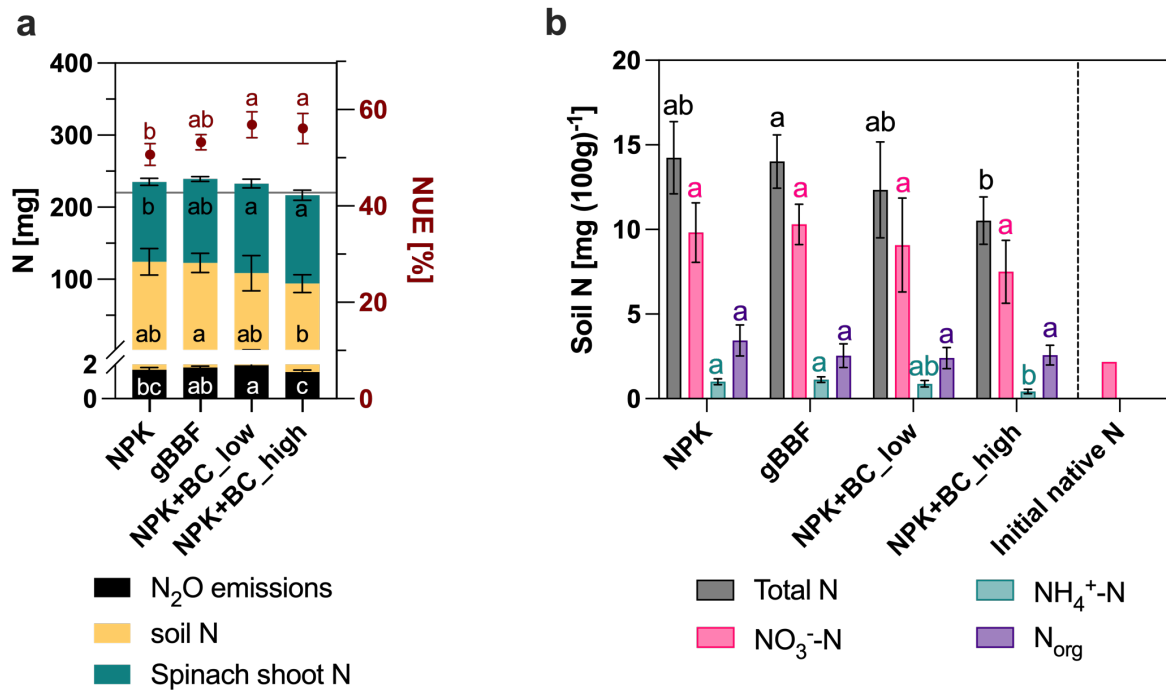


Figure 4 (a) Nitrogen (N) allocation (stacked bars) divided into losses via N₂O emissions, residual soil N after harvest (based on two subsequent elutions of soil samples in 1 M KCl and quantification of total N in eluates), N uptake in aboveground spinach biomass and non-recovered N. Nitrogen use efficiency (NUE, red symbols) for each treatment based on N uptake in aboveground biomass and fertilized N plus native soil N as a basis. The horizontal line in panel a at 220 mg N reflects the sum of fertilized N and mineral extractable native soil N at the beginning of the experiment. **(b)** N speciation in soil samples taken after harvest sequentially extracted in 1 M KCl for 1 hour followed by 24 hours in fresh extractant. N is fractionated in nitrate (NO₃⁻-N), ammonium (NH₄⁺-N) and organic N (N_{org}). NPK: granulated nitrogen (N), phosphorus (P) and potassium fertilizer. gBBF: granulated, biochar-based NPK fertilizer. NPK+BC_low: milled biochar (< 1 mm) co-applied at 0.2% to the soil with NPK. NPK+BC_high: milled biochar (< 1 mm) co-applied at 2% to the soil with NPK. Values for native extractable N in initial soil is also presented (only NO₃⁻ and NH₄⁺ analysis, unicate extraction), NH₄⁺ was below the quantification limit. Data are presented as means ± standard deviation of five replicates. Different letters within or above bars indicate significant differences between the treatments within each N allocation category or for NUE in panel a or within a N fraction in panel b (one-way analysis of variance, Tukey's post-hoc test, p < 0.05).

3.4. Prokaryotic abundance in soil after harvest

Total prokaryotic abundance in soil increased during the experiment from 1.1×10^{10} to $1.4\text{-}1.5 \times 10^{10}$ cells g^{-1} with no significant difference between the individual amendments (Table 2). Based on cDNA transcripts, total prokaryotic activity was significantly higher in NPK+BC_low compared to gBBF yet not compared to all other treatments (Table 2). In the nitrification path, abundance of *amo_AOB* genes associated with bacterial ammonia oxidation was significantly increased during the experiment compared to the initial baseline value for all amendments (Figure 6a). In the denitrification path, no difference in gene abundance between the treatments was observed for *nirS*, *nirK* and both typical and atypical *nosZ* genes, and only a tendency for increased abundance compared to initial values was observed (Figure 6b-d). The atypical variant of *nosZ* gene was 30% more abundant in the soil, independent of the amendment, compared to the typical one (Figure 6 c and d). The ratio of typical, atypical and total *nosZ* copies to *nirS+nirK* copies was similar for all treatments (Figure S12). Copy numbers of *amo_AOA* and *nifH* genes as well as urease and nitrate reductase activity are presented in the SI and not further discussed at this point (Figure S12 and Table S18, respectively). Despite relatively high RNA contents measured in the soil extracts (29-39 ng μl^{-1} , Table S8), the activities of all functional marker genes related to N cycling were below the quantification limit at the end of the trial, except for genes associated with archaeal ammonium oxidation (*amoA_AOA*, Figure S13).

Table 2 Cell number and transcript copy numbers per gram of dry soil for the prokaryotic 16S rRNA gene at the day of spinach harvest. NPK: granulated nitrogen (N), phosphorus (P) and potassium (K) fertilizer. gBBF: granulated, biochar-based NPK fertilizer. NPK+BC_low: milled biochar (< 1 mm) co-applied at 0.2% to the soil with NPK. NPK+BC_high: milled biochar (< 1 mm) co-applied at 2% to the soil with NPK. Initial: soil samples taken from native soil at the start of the experiment. Data are presented as means \pm standard deviation (n=5, except for gBBF and B-2%+NPK with n=4 and Initial with n=2). Different letters indicate a significant difference between the treatments (one-way analysis of variance, Tukey's post hoc test, $p < 0.05$). The 'Initial' group was excluded from the statistical test.

Treatment	16S rRNA gene DNA [10 ¹⁰ cells g ⁻¹]	16S rRNA transcript cDNA [10 ¹⁰ transcripts g ⁻¹]
NPK	1.5 \pm 0.4 a	1.8 \pm 1.7 ab
gBBF	1.4 \pm 0.2 a	0.6 \pm 0.3 b
NPK+BC_low	1.4 \pm 0.3 a	2.8 \pm 0.7 a
NPK+BC_high	1.4 \pm 0.3 a	0.7 \pm 0.4 b
Initial	1.1 \pm 0.1	0.4 \pm 0.1

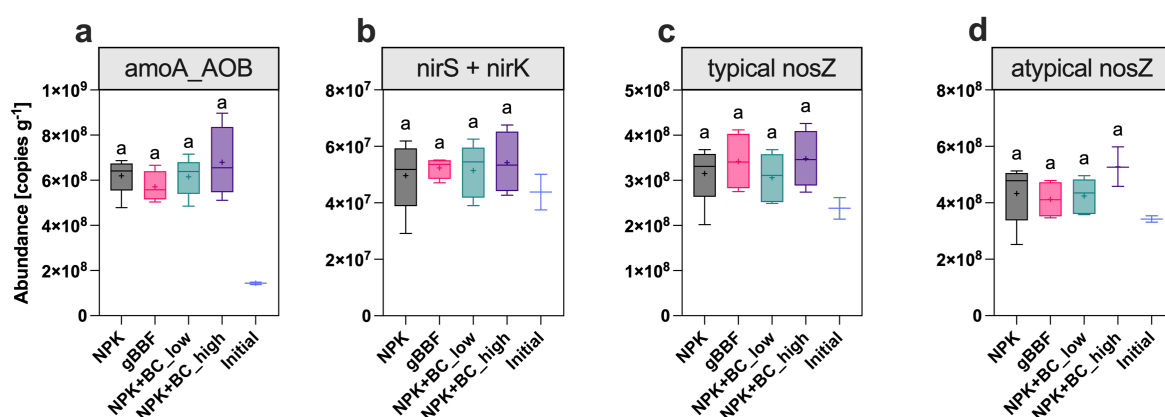


Figure 6 Copy numbers of genes involved in microbial nitrogen transformation per gram of dry soil: ammonium-oxidizing bacteria (*amoA_AOB*, panel a) sum of nitrite-reduction associated genes (*nirS+nirK*, panel b) and nitrous oxide reducing genes (typical and atypical *nosZ*, panel c and d, respectively). NPK: granulated nitrogen (N), phosphorus (P) and potassium (K) fertilizer. gBBF: granulated, biochar-based NPK fertilizer. NPK+BC_low: milled biochar (< 1 mm) co-applied at 0.2% to the soil with NPK. NPK+BC_high: milled biochar (< 1 mm) co-applied at 2% to the soil with NPK. Initial: soil samples taken from native soil at the start of the experiment. Box plots represent the minimum and maximum of replicated pots for the different treatments (n=5, except for gBBF and B-2%+NPK with n=4 and initial samples with n=2). Different letters above error bars indicate a significant difference between

treatments (at $p < 0.05$, Tukey's post-hoc test). The 'Initial' group was excluded from the statistical test.

4. Discussion

When biochar was applied with low application rate, only co-application but not granulation of biochar with NPK fertilizer resulted in significantly higher spinach yield compared to NPK alone. In gBBF amended soil, spinach plants had similar yields and nutrient uptakes compared to NPK alone. These results are in line with previous findings from a pot trial on growth of white cabbage fertilized with gBBF, NPK+BC or NPK²³ and indicate plant growth benefits from homogeneous distribution of individual biochar particles in the soil compared to the amendment of agglomerated biochar particles applied combined with fertilizer as gBBF. A potential mechanism for the lower growth in presence of gBBF compared to NPK+BC is supposed to be a higher immobilization of fertilizer nutrients in the matrix of granulated biochar, indicated by the lower uptakes of Mg, K, P and S with gBBF compared to co-application, as those nutrients were all present in gBBF and NPK. Lowest root : shoot ratios with co-applied biochar, especially at high dosage, further indicated better nutrient availability in these treatments compared to NPK. In addition, aboveground biomass yield was more increased with the high than low co-applied biochar dosage and this was more pronounced for fresh than dry biomass yields, indicating better water availability with higher biochar dosage.

We found that 0.7-0.9% of fertilized N was lost via N₂O emissions, which is in line with the general assumption of 1% of fertilized N emitted as N₂O in agriculture¹⁰. Area based N₂O losses in our study of 1.6-2.0 kg N₂O-N ha⁻¹ were in a similar range compared to those observed in a field trial including biochar amendment (1-2.7 kg N₂O-N ha⁻¹)²⁰.

Biochar-induced reductions in N₂O emissions were consistently reported for biochars with a H/C ratio below 0.3³⁶. Significant lower N₂O fluxes during day two and four in soil amended with NPK+BC_high compared to sole NPK amendment proved that the biochar applied in this study with a H/C ratio of 0.18 was in general capable of reducing emissions. Still, the absence of a significant reduction of cumulative area-based emissions with NPK+BC_high compared to NPK contrasts with some earlier studies using biochars with comparable H/C ratios amended at relatively high dosage of 2-5%^{16,20,21,25}. As the applied BC:N_{Fert.} ratios in these studies were with 150:1 – 500:1 essentially higher than the ones in our experiment, which were 8:1 for gBBF and NPK+BC_low as well as 90:1 with NPK+BC_high, it is likely that the biochar dosage in all biochar treatments, yet especially in gBBF and NPK+BC_low, was not sufficient to significantly reduce absolute N₂O emissions. Still, there are also observations were biochar

application of 20 t ha⁻¹, in the range of the NPK+BC_high amendment, did not reduce N₂O emissions³⁷. Compared to NPK, NPK+BC_low amendment even increased cumulative area-based N₂O emissions by 15%, which was partly offset by biochar granulation (no significantly higher N₂O emissions with gBBF compared to NPK) and is against a previous hypothesis that biochar more efficiently reduces N₂O emissions the more homogeneous it is distributed in soil¹⁷. In light of the abovementioned studies and lower initial N₂O fluxes with NPK+BC_high compared to all other treatments, our experiment indicates that applying biochar at a yearly economic application rate (<2 t ha⁻¹) combined with an agricultural relevant N fertilization (160 kg N ha⁻¹), either as gBBF or as co-applied biochar with fertilizer, does not instantly result in reductions in N₂O emissions on an area basis. Low yearly quantities of biochar that add up over several years may still lead to N₂O emission reduction, once a critical biochar concentration in soil is reached, as the potential of biochar to reduce N₂O emissions was generally maintained over several years, yet a reduction in the effect size was observed with time^{1,20}. Further, yield increases after several biochar applications become more likely, which would further reduce N₂O emissions per unit of crop produced, as was observed with the NPK+BC_high amendment. Our study suggests that BBF would need to be applied for 10 years to achieve an effective biochar concentration in the soil (2 t ha⁻¹ yr⁻¹ x 10 yr = 20 t ha⁻¹). Nitrogen use efficiencies, in addition, were increased with both co-application treatments of biochar compared to NPK-fertilized plants. This indicates that similar crop yields could be achieved with reduced N fertilization co-applied with biochar, which would further reduce the risk of absolute N₂O emissions in the first place.

The predominant mechanism for N₂O production in our study can be deduced from the type of N source applied as fertilizer and the applied water regime determining the availability of gaseous oxygen in soil pores. The applied urea was first solubilized in the soil pore water and mineralized by the urease enzyme to CO₂ and NH₃, the latter being present as NH₄⁺ at a soil pH of 7. During nitrification, NH₄⁺ is metabolized by ammonia oxidizers (*amoA*) to hydroxylamine (NH₂OH) and nitrification is completed by further oxidation to NO₂⁻ and, ultimately, to NO₃⁻²⁵. Nitrification is favored under oxic conditions, which was the case in our soil due to watering to a maximum of 65% WHC every 2-3 days, equaling ~25% WFPS. Here, N₂O can derive as a co-product during NH₂OH transformation by bacterial ammonium oxidizers via *nitrifier-nitrification* evident for oxidoreductases obtained from *Nitrosomonas spp.*³⁸ or from NO₂⁻ via *nitrifier-denitrification*¹², demonstrated for *Nitrosomonas and Nitrosospira spp.*³⁹. Chemodenitrification of NH₂OH or NO₂⁻ as an abiotic source of N₂O under oxic conditions is less relevant⁴⁰. As the urea fertilization initially must have increased the NH₄⁺ content in the

soil, ammonia oxidation was promoted, as indicated by the significant increased abundance of *amoA_AOB* genes at the end of the experiment compared to the initial abundance in soil (Figure 6). With a higher concentration of NH_4^+ as the educt, there is also a higher potential for N_2O to be formed during ammonia oxidation, which could explain why most N_2O emissions occurred at the beginning of the experiment until 10-15 days. It is plausible that most urea mineralization happened during this time, as no urease-inhibitor was contained in the fertilizers. Relevant contribution to N_2O emissions by conventional, stepwise denitrification of NO_3^- to N_2 , where N_2O is an obligatory intermediate product, is unlikely as it is predominant under anoxic conditions with WFPS $>70\%$ ²⁵, which does not apply to our irrigation regime. Under such conditions with WFPS $>70\%$, biochar can stimulate complete denitrification by increasing the ratio of *nosZ:nirK+nirS* genes¹⁵. Denitrification might have occurred in microsites in soil or biochar pores²⁵, as was indicated by a minimal increase in *nirK*, *nirS* and *nosZ* gene abundance in all treatments compared to initial values in soil and measurable nitrate-reductase activity (Table S18), but this increase in gene abundance was not as significant as observed for *amoA_AOB* and due to the rather oxic conditions, it is unlikely that denitrification was the predominant source path for N_2O emissions in our experiment. Further, if denitrification had played an important role, N_2O could have been produced in relevant amounts to a longer time than only 10-15 days, as the main N speciation at the end of the experiment in soil was NO_3^- and represented around 30% of initially fertilized N (Figure 4b).

The initial increase in higher production of N_2O but also CO_2 (Figure S7) might also partly be associated with the Birch-effect, which reflects an increased microbial activity instantly after dry soils are re-wetted⁴¹. However, this effect terminates on a time scale of a few hours to two days⁴² and might therefore have only contributed to a small extent to the recorded N_2O peak, which occurred after 10-15 days. To summarize, it is most likely that *nitrifier-nitrification* and *nitrifier-denitrification* by ammonium oxidizing bacteria were the most relevant paths of N_2O production in the present experiment.

Any decrease in urea release to the soil pore water or an immobilization of NH_4^+ after urea mineralization is likely to have resulted in decreased N_2O emissions in our setup. But urea release was presumably not retarded in soil amended with gBBF and NPK+BC_low compared to NPK amendment, as initial N_2O emissions in these biochar treatments were even higher. Our initial hypothesis that gBBF would lead to lower N_2O emissions due to a slower observed N release to an aqueous phase compared to NPK and NPK+BC_low²³ can thus not be confirmed. The increases of N_2O fluxes with the low amount of biochar might have been due to a promotion of ammonia oxidation and thus nitrification-related N_2O production by biochar, in line with a

previous study¹⁹. In the NPK+BC_high-amended soil, the higher biochar dosage likely improved urea and NH_4^+ immobilization, which could explain the shift of the peak maximum of N_2O emissions to a later time of the experiment (Figure 1). Higher N immobilization in NPK+BC_high-amended soil was at least measured at the end of the experiment, as a higher amount of N was only released in the second extraction step compared to the other treatments. To what extent the N_2O emission reduction by NPK+BC_high was the result of higher N immobilization, or due to a shift in microbial N transformation cannot be stated based on our results, since microbial abundance was only measured at the end of the experiment and not during the time at which N_2O emissions were highest. Harter and colleagues showed that biochar can promote entrapment of N_2O can be a path biochar-induced N_2O emission reduction, however their data was generated at 90% WFPS to promote denitrification¹⁴. We do not know how our individual amendments might have affected N_2O under such conditions. Further, the high soil organic carbon content of 4.5% might have promoted N_2O formation in general and meta-analyses indicate that biochar reduces N_2O emissions to a lower extent in soils with organic carbon contents above 2%^{1,43}, which could further have limited the relative reduction of N_2O emissions with biochar in our experiment.

The decline in N_2O emissions with an increase in biochar application rate is in line with literature^{1,43}. Further, it was already found before that low biochar concentrations in soil (< 0.5%) co-applied with N fertilizer can increase soil-borne N_2O emissions compared to N fertilization without biochar^{44,45}. In a soil column study, relative changes in N_2O emissions compared to the fertilized no-biochar control negatively correlated with the biochar-carbon-to-fertilized-N ratio in soil and N_2O emissions were only reduced at ratios higher than 60⁴⁵, which is in line with our results. Further, urea infusion into biochar applied at low dosage (0.06% and 0.14%, w/w, at BC: $\text{N}_{\text{Fert.}}$ ratios of 15 and 34, respectively) significantly reduced N_2O emissions compared to urea alone and also compared to biochar co-applied with urea⁴⁴. Thus, infusion of N fertilizer into biochar pores might be more effective to reduce N_2O emissions than combination by granulation, which should be compared in a follow up study. The maximal amount of N that could be attached to biochar via urea solubilization and infusion, based on 160% WHC of the biochar used in the present study and urea solubility of 1200 g l^{-1} , would amount to 30% N in the urea-loaded biochar, while further attachment of P and K sources, not via infusion but e.g., via simple mixing with solid biochar, would result in a maximal possible N content of 19% in the BBF. Thus, the 8% N content of gBBF used in this study could also be achieved by N infusion to biochar. A combination of both, N infusion into biochar pores and

biochar granulation at BC:N_{Fert.} ratios as wide as possible, might be a way to provide N₂O emission reduction and good applicability of BBF to soil with agricultural machinery.

5. Conclusion

Low, yearly economically viable biochar application rates of <2 t ha⁻¹ combined with agricultural relevant N fertilization at e.g., 150 kg N ha⁻¹ did not result in instant reduced soil-borne N₂O emission under a water regime where nitrification-related N₂O production was likely to be dominant. To achieve this effect, higher biochar application rates are necessary. Accumulation of low yearly biochar application rates is still likely to result in N₂O emissions once an effective biochar concentration in soil is reached, as meta-analyses indicate that biochar can reduce N₂O emissions over several years. The higher nitrogen use efficiencies obtained with low and high biochar dosage co-applied with NPK fertilizer and lower emissions per spinach biomass produced with the higher biochar dosage indicated that N fertilization could be reduced with co-applied biochar while maintaining crop yields and reducing absolute N₂O emissions. Studies on the development of BBF should include the biochar type and biochar ratio as well as N speciation and content in a BBF as experimental factors potentially influencing soil-borne N₂O emissions. Further, components that can slow-down the N release from a BBF could be integrated, such as gelling additives, which would reduce mineral N availability in soil and thus microbial N₂O production. Different water regimes should also be included to differentiate biochar effects on nitrification- or denitrification-based N₂O emissions.

References

1. Kaur, N., Kieffer, C., Ren, W. & Hui, D. How much is soil nitrous oxide emission reduced with biochar application? An evaluation of meta-analyses. *GCB Bioenergy* **15**, 24–37 (2023).
2. Ye, L. *et al.* Biochar effects on crop yields with and without fertilizer: A meta-analysis of field studies using separate controls. *Soil Use Manag.* **36**, 2–18 (2020).
3. Bach, M., Wilske, B. & Breuer, L. Current economic obstacles to biochar use in agriculture and climate change mitigation. *Carbon Manag.* **7**, 183–190 (2016).
4. Melo, L. C. A., Lehmann, J., Carneiro, J. S. da S. & Camps-Arbestain, M. Biochar-based fertilizer effects on crop productivity: a meta-analysis. *Plant Soil* (2022) doi:10.1007/s11104-021-05276-2.
5. Schmidt, H.-P., Pandit, B. H., Cornelissen, G. & Kammann, C. I. Biochar-Based Fertilization with Liquid Nutrient Enrichment: 21 Field Trials Covering 13 Crop Species in Nepal: Biochar-Based Fertilization. *Land Degrad. Dev.* **28**, 2324–2342 (2017).
6. Shi, W. *et al.* Biochar bound urea boosts plant growth and reduces nitrogen leaching. *Sci. Total Environ.* **701**, 134424 (2020).
7. *Climate Change 2013: The Physical Science Basis.* (Cambridge university press, New York, 2014).
8. Braker, G. & Conrad, R. Diversity, Structure, and Size of N₂O-Producing Microbial

Communities in Soils—What Matters for Their Functioning? in *Advances in Applied Microbiology* vol. 75 33–70 (Elsevier, 2011).

9. Reay, D. S. *et al.* Global agriculture and nitrous oxide emissions. *Nat. Clim. Change* **2**, 410–416 (2012).
10. Shcherbak, I., Millar, N. & Robertson, G. P. Global metaanalysis of the nonlinear response of soil nitrous oxide (N₂O) emissions to fertilizer nitrogen. *Proc. Natl. Acad. Sci.* **111**, 9199–9204 (2014).
11. Heinzlmaier, F. CO₂ Fussabdruck der Mineraldünger. *Landesarbeitskreis Düngung Bayern* https://www.landwirtschaft-bw.de/site/pbs-bw-new/get/documents/MLR.Energieberatung/Unterlagen/03_Wissensbasis/Archiv%20Fachartikel/Klimagase/CO2%20Fussabdruck%20der%20Minerald%20C3%BCnger_BLW_23_2013.pdf?attachment=true (2013).
12. Wrage, N., Velthof, G. L., van Beusichem, M. L. & Oenema, O. Role of nitrifier denitrification in the production of nitrous oxide. *Soil Biol.* (2001).
13. Harter, J., El-Hadidi, M., Huson, D. H., Kappler, A. & Behrens, S. Soil biochar amendment affects the diversity of nosZ transcripts: Implications for N₂O formation. *Sci. Rep.* **7**, 3338 (2017).
14. Harter, J. *et al.* Gas entrapment and microbial N₂O reduction reduce N₂O emissions from a biochar-amended sandy clay loam soil. *Sci. Rep.* **6**, 39574 (2016).
15. Harter, J. *et al.* Linking N₂O emissions from biochar-amended soil to the structure and function of the N-cycling microbial community. *ISME J.* **8**, 660–674 (2014).
16. Cayuela, M. L. *et al.* Biochar and denitrification in soils: when, how much and why does biochar reduce N₂O emissions? *Sci. Rep.* **3**, 1732 (2013).
17. Felber, R., Leifeld, J., Horák, J. & Nefel, A. Nitrous oxide emission reduction with greenwaste biochar: comparison of laboratory and field experiments. *Eur. J. Soil Sci.* **65**, 128–138 (2014).
18. Singh, B. P., Hatton, B. J., Singh, B., Cowie, A. L. & Kathuria, A. Influence of Biochars on Nitrous Oxide Emission and Nitrogen Leaching from Two Contrasting Soils. *J. Environ. Qual.* **39**, 1224–1235 (2010).
19. Sánchez-García, M., Roig, A., Sánchez-Monedero, M. A. & Cayuela, M. L. Biochar increases soil N₂O emissions produced by nitrification-mediated pathways. *Front. Environ. Sci.* **2**, (2014).
20. Hagemann, N. *et al.* Does soil aging affect the N₂O mitigation potential of biochar? A combined microcosm and field study. *GCB Bioenergy* **9**, 953–964 (2017).
21. Kammann, C., Ratering, S., Eckhard, C. & Müller, C. Biochar and Hydrochar Effects on Greenhouse Gas (Carbon Dioxide, Nitrous Oxide, and Methane) Fluxes from Soils. *J. Environ. Qual.* **41**, 1052–1066 (2012).
22. FAO. Inorganic fertilizers 2002-2022. (2024) doi:<https://doi.org/10.4060/cd1485en>.
23. Grafmüller, J. *et al.* Granulation compared to co-application of biochar plus mineral fertilizer and its impacts on crop growth and nutrient leaching. *Sci. Rep.* **14**, 16555 (2024).
24. Grafmüller, J., Schmidt, H.-P., Kray, D. & Hagemann, N. Root-Zone Amendments of Biochar-Based Fertilizers: Yield Increases of White Cabbage in Temperate Climate. *Horticulturae* **8**, 307 (2022).
25. Hagemann, N., Harter, J. & Behrens, S. Elucidating the Impacts of Biochar Applications on Nitrogen Cycling Microbial Communities. in *Biochar Application* 163–198 (Elsevier, 2016). doi:10.1016/B978-0-12-803433-0.00007-2.
26. *Measuring Emission of Agricultural Greenhouse Gases and Developing Mitigation Options Using Nuclear and Related Techniques: Applications of Nuclear Techniques for GHGs.* (Springer International Publishing, Cham, 2021). doi:10.1007/978-3-030-55396-8.
27. Schön, J. *Petrophysik: Physikalische Eigenschaften von Gesteinen Und Mineralen.* (De Gruyter, 1983). doi:10.1515/9783112707715.

28. Muehe, E. M., Wang, T., Kerl, C. F., Planer-Friedrich, B. & Fendorf, S. Rice production threatened by coupled stresses of climate and soil arsenic. *Nat. Commun.* **10**, 4985 (2019).
29. Rhine, E. D., Mulvaney, R. L., Pratt, E. J. & Sims, G. K. Improving the Berthelot Reaction for Determining Ammonium in Soil Extracts and Water. *Soil Sci. Soc. Am. J.* **62**, 473 (1998).
30. Drabesch, S. *et al.* Climate induced microbiome alterations increase cadmium bioavailability in agricultural soils with pH below 7. *Commun. Earth Environ.* **5**, 637 (2024).
31. Earth microbiome project. 16S Illumina Amplicon Protocol. <https://earthmicrobiome.org/protocols-and-standards/16s/> (2018).
32. Větrovský, T. & Baldrian, P. The Variability of the 16S rRNA Gene in Bacterial Genomes and Its Consequences for Bacterial Community Analyses. *PLoS ONE* **8**, e57923 (2013).
33. Kandeler, E. & Gerber, H. Short-term assay of soil urease activity using colorimetric determination of ammonium. *Biol. Fertil. Soils* **6**, (1988).
34. Abdelmagid, H. M. & Tabatabai, M. A. Nitrate reductase activity of soils. *Soil Biol. Biochem.* **19**, 421–427 (1987).
35. Kandeler, E. Nitrate Reductase Activity. in *Methods in Soil Biology* 176–179 (Springer Berlin Heidelberg, Berlin, Heidelberg, 1996). doi:10.1007/978-3-642-60966-4_11.
36. Cayuela, M. L., Jeffery, S. & Van Zwieten, L. The molar H:Corg ratio of biochar is a key factor in mitigating N₂O emissions from soil. *Agric. Ecosyst. Environ.* **202**, 135–138 (2015).
37. Hüppi, R., Felber, R., Neftel, A., Six, J. & Leifeld, J. Effect of biochar and liming on soil nitrous oxide emissions from a temperate maize cropping system. *SOIL* **1**, 707–717 (2015).
38. Hooper, A. B. & Terry, K. R. Hydroxylamine oxidoreductase of *Nitrosomonas*. *Biochim. Biophys. Acta BBA - Enzymol.* **571**, 12–20 (1979).
39. Shaw, L. J. *et al.* *Nitrosospira* spp. can produce nitrous oxide via a nitrifier denitrification pathway. *Environ. Microbiol.* **8**, 214–222 (2006).
40. Bremner, J. M. Sources of nitrous oxide in soils. *Nutr. Cycl. Agroecosystems* **49**, 7–16 (1997).
41. Jarvis, P. *et al.* Drying and wetting of Mediterranean soils stimulates decomposition and carbon dioxide emission: the ‘Birch effect’. *Tree Physiol.* **27**, 929–940 (2007).
42. Kostyanovsky, K. I., Huggins, D. R., Stockle, C. O., Morrow, J. G. & Madsen, I. J. Emissions of N₂O and CO₂ Following Short-Term Water and N Fertilization Events in Wheat-Based Cropping Systems. *Front. Ecol. Evol.* **7**, 63 (2019).
43. Borchard, N. Biochar, soil and land-use interactions that reduce nitrate leaching and N₂O emissions: A meta-analysis. *Sci. Total Environ.* **11** (2019).
44. Castejón-del Pino, R., Sánchez-Monedero, M. A., Sánchez-García, M. & Cayuela, M. L. Fertilization strategies to reduce yield-scaled N₂O emissions based on the use of biochar and biochar-based fertilizers. *Nutr. Cycl. Agroecosystems* (2023) doi:10.1007/s10705-023-10313-w.
45. Feng, Z. & Zhu, L. Impact of biochar on soil N₂O emissions under different biochar-carbon/fertilizer-nitrogen ratios at a constant moisture condition on a silt loam soil. *Sci. Total Environ.* **584–585**, 776–782 (2017).

Supplementary Information to:

Soil-borne N₂O emissions were not reduced with granulated biochar-based compound fertilizer at agricultural relevant biochar and nitrogen dosage

Jannis Grafmüller^{1,2,3}, E. Marie Muehe^{3,5}, Claudia I. Kammann⁶, Daniel Kray¹, Hans-Peter Schmidt², Nikolas Hagemann^{2,4}

¹Institute for Sustainable Energy Systems (INES), Offenburg University of Applied Sciences, Germany

²Ithaka Institute, Arbaz (Switzerland) and Goldbach (Germany)

³Plant Biogeochemistry, Tübingen University, Tübingen, Germany

⁴Environmental Analytics, Agroscope, Zurich, Switzerland

⁵Department of Environmental Microbiology, Helmholtz Centre for Environmental Research - UFZ, Leipzig, Germany

⁶Department of Applied Ecology, Hochschule Geisenheim University, Geisenheim, Germany

Supplementary Tables

Table S1 Elemental analysis (carbon (C), hydrogen (H), nitrogen (N), and sulfur (S)), and contents of macronutrients (phosphorus as P₂O₅, potassium as K₂O, and magnesium as MgO) in biochar and fertilizers. Specific surface area (SSA) of the biochar, the pure NPK fertilizer (NPK) and the granulated biochar-based NPK fertilizer (gBBF). The gBBF and NPK contained urea (excluding urease and nitrification inhibitors), mono-potassium phosphate, and Patentkali® as N, P, K, Mg and S source (all technical purity grade, K+S Aktiengesellschaft, Kassel, Germany). A content of 0.02% hydroxypropyl methyl cellulose was contained as binding agent in gBBF and NPK. Errors indicate the range of minimum to maximum measured values of n=2 measurements, where applicable. Reproduced with permission from (Grafmüller et al. 2024), *Scientific reports*, Springer Nature.

Sample	C [%]	H [%]	N [%]	S [%]	Ash [%]	pH	P ₂ O ₅ [gkg ⁻¹]	K ₂ O [gkg ⁻¹]	MgO [gkg ⁻¹]	BET SSA ^a (N ₂) [m ² g ⁻¹]	BET SSA ^a (CO ₂) [m ² g ⁻¹]	DFT SSA ^b (CO ₂) [m ² g ⁻¹]
Biochar	93.3	1.4	0.31	<0.03	2.0	9.1	0.6	2.5	1.1	21 ^d	358 ^d ± 43	516 ^d ± 52
NPK	10.2	3.7	23.0	6.3	46.3	5.2	85.2	159	31.5	7	42	n.a. ^c
gBBF	61.4	2.3	8.74	2.63	19.1	6.1	33.6	62.9	11.4	5	155 ± 26	116 ± 8

^aBET SSA: Specific surface area calculated with the Brunauer-Emmet-Teller (BET) method based on either N₂ or CO₂ adsorption isotherms.

^bDFT SSA: Specific surface area calculated with the density functional theory (DFT) based on CO₂ adsorption isotherms.

^cn.a.: not applicable since the adsorption isotherm did not show a Type-I isotherm characteristic.

^dBiochar after milling with a collard mill.

Table S2 Content of trace elements arsenic (As), lead (Pb), boron (B), cadmium (Cd), chromium (Cr), copper (Cu), manganese (Mn), nickel (Ni), mercury (Hg), silver (Ag) and zin (Zn) in the biochar and fertilizers. NPK: mineral nitrogen, phosphorus and potassium (NPK) fertilizer granule. gBBF: granulated biochar-based mineral NPK fertilizer. Reproduced with permission from (Grafmüller et al. 2024), *Scientific reports, Springer Nature*.

Sample	As	Pb	B	Cd	Cr	Cu	Mn	Ni	Hg	Ag	Zn
mg kg ⁻¹											
Biochar	<0.8	3	5	<0.2	13	2	208	9	<0.07	<5	43
NPK	<0.8	<2	2	<0.2	<1	2	10	<1	<0.07	<5	5
gBBF	<0.8	2	4	<0.2	7	2	140	6	<0.07	<5	30

Table S3 Main characteristics of the soil used in the greenhouse study. Reproduced with permission from (Grafmüller et al. 2024), Scientific reports, Springer Nature.

Parameter	Unit	Value	Method
Organic matter	wt% DM	7.7	DIN ISO 10694: 1996-08
Total Organic Carbon	wt% DM	4.5	DIN ISO 10694: 1996-08
pH	1	7.4	VDLUFA Methodenbuch Band I, Kapitel 5.1.1, 7.Teillieferung, 2016
Electric Conductivity	μScm^{-1}	110	VDLUFA Methodenbuch Band I, Kapitel 10.1.1, 1991
Salt content	$\text{mg}(100\text{g})^{-1}$ DM	58	VDLUFA Methodenbuch Band I, Kapitel 10.1.1, 1991
Total Nitrogen	wt% DM	0.15	DIN ISO 13878:1998-11
NH ₄ -N	$\text{mg}(100\text{g})^{-1}$ DM	<0,05	VDLUFA Methodenbuch Band I, 3. Teillieferung, Kapitel 6.1.4.1, 2002
NO ₃ -N	$\text{mg}(100\text{g})^{-1}$ DM	2.17	VDLUFA Methodenbuch Band I, 3. Teillieferung, Kapitel 6.1.4.1, 2002
S _{min}	$\text{mg}(100\text{g})^{-1}$ DM	0.51	VDLUFA Methodenbuch I, A 6.3.1 (2016), Extraktion mit 0,0125 M CaCl ₂ Calcium lactate extract, VDLUFA Methodenbuch Band I, 6.Teillieferung, Kapitel
Potassium (K)	$\text{mg}(100\text{g})^{-1}$ DM	24.6	6.2.1.1, 2012
Phosphorus (P)	$\text{mg}(100\text{g})^{-1}$ DM	13.0	Calcium lactate extract, VDLUFA Methodenbuch Band I, 6.Teillieferung, Kapitel 6.2.1.1, 2012
Magnesium (Mg)	$\text{mg}(100\text{g})^{-1}$ DM	8.8	Calcium chloride extract, VDLUFA Methodenbuch Band I, Kapitel 6.2.4.1, 1991; ISO 22036:2008
Boron (B)	mgkg^{-1} DM	0.3	CAT extract, VDLUFA Methodenbuch Band I, 3. Teillieferung, Kapitel 6.4.1, 2002
Manganese (Mn)	mgkg^{-1} DM	20	CAT extract, VDLUFA Methodenbuch Band I, 3. Teillieferung, Kapitel 6.4.1, 2002
Copper (Cu)	mgkg^{-1} DM	4.6	CAT extract, VDLUFA Methodenbuch Band I, 3. Teillieferung, Kapitel 6.4.1, 2002
Zinc (Zn)	mgkg^{-1} DM	9.5	CAT extract, VDLUFA Methodenbuch Band I, 3. Teillieferung, Kapitel 6.4.1, 2002

Table S4 Potential (pot.) and effective (eff.) cation exchange capacity of the soil used in the greenhouse study. Reproduced with permission from (Grafmüller et al. 2024), Scientific reports, Springer Nature.

Parameter	Unit	Value	Method
Cation exchange capacity (eff.)	cmol ⁺ kg ⁻¹	17.5	DIN EN ISO 11260:2011-09
Exchange acidity	cmol ⁺ kg ⁻¹	0.1	DIN EN ISO 11260:2011-09
Exchangable Mg (eff.)	cmol ⁺ kg ⁻¹	0.5	DIN EN ISO 11260:2011-09
Exchangable Ca (eff.)	cmol ⁺ kg ⁻¹	13.2	DIN EN ISO 11260:2011-09
Exchangable Na (eff.)	cmol ⁺ kg ⁻¹	<0.1	DIN EN ISO 11260:2011-09
Exchangable K (eff.)	cmol ⁺ kg ⁻¹	0.7	DIN EN ISO 11260:2011-09
Sum of exchangeable cations (eff.)	cmol ⁺ kg ⁻¹	14.4	DIN EN ISO 11260:2011-09
Cation exchange capacity (pot.)	cmol ⁺ kg ⁻¹	15.4	DIN ISO 13536: 1997-04
Exchangable Mg (pot.)	cmol ⁺ kg ⁻¹	0.5	DIN ISO 13536: 1997-04
Exchangable Ca (pot.)	cmol ⁺ kg ⁻¹	12.3	DIN ISO 13536: 1997-04
Exchangable Na (pot.)	cmol ⁺ kg ⁻¹	<0.1	DIN ISO 13536: 1997-04
Exchangable K (pot.)	cmol ⁺ kg ⁻¹	0.7	DIN ISO 13536: 1997-04
Sum of exchangeable cations (pot.)	cmol ⁺ kg ⁻¹	13.5	DIN ISO 13536: 1997-04

Table S5 Particle size distribution and texture of the soil used for the greenhouse study. Reproduced with permission from (Grafmüller et al. 2024), Scientific reports, Springer Nature.

Parameter	Unit	Value	Method
Clay (<2µm)	wt%	11	DIN ISO 11277:2002:08
Coarse sand (0.63 - 2mm)	wt%	2	DIN ISO 11277:2002:08
Medium sand (0.2 - 0.63mm)	wt%	8	DIN ISO 11277:2002:08
Fine sand (0.063 - 0.2mm)	wt%	42	DIN ISO 11277:2002:08
Coarse silt (20-63 µm)	wt%	13	DIN ISO 11277:2002:08
Medium silt (6.3 - 20 µm)	wt%	14	DIN ISO 11277:2002:08
Fine silt	wt%	9	DIN ISO 11277:2002:08
Coarse soil (>2mm)	wt%	1	DIN ISO 11277:2002:08

Chapter 3: Physical modification of biochar for use in biochar-based fertilizers

Table S6 Recovery of phosphorus (P), potassium (K), magnesium (Mg), sulfur (S), calcium (Ca), copper (Cu), manganese (Mn) and zinc (Zn) from a certified reference material after microwave digestion and quantification with inductively coupled plasma optical emission spectroscopy (ICP-OES). The reference material was a rye grass listed as ERM-CD281 as sample no. 1010 by the European Commission. Errors indicate \pm one standard deviation of replicated ($n=5$) digestions. Reproduced with permission from (Grafmüller et al. 2024), Scientific reports, Springer Nature.

Element	Quantified content in mg g ⁻¹	Content according to analysis certificate in mg g ⁻¹	Recovery in % (w/w)
P	2.9 \pm 0.1	2.8	106.9 \pm 2.3
K	28.3 \pm 0.5	34.0	83.1 \pm 1.3
Mg	1.7 \pm 0.02	1.6	106.3 \pm 1.6
S	3.1 \pm 0.1	3.4	90.4 \pm 1.7
Ca	7.3 \pm 0.1	6.3	116.4 \pm 2.1
Cu	0.010 \pm 0.001	0.0102	99.5 \pm 12.7
Mn	0.084 \pm 0.001	0.082	102.7 \pm 1.8
Zn	0.031 \pm 0.002	0.0305	102.1 \pm 7.9

Table S7 Content of trace elements arsenic (As), lead (Pb), boron (B), cadmium (Cd), chromium (Cr), copper (Cu), manganese (Mn), nickel (Ni), mercury (Hg), silver (Ag) and zinc (Zn) in the biochar and fertilizers. NPK: mineral nitrogen, phosphorus and potassium (NPK) fertilizer granule. gBBF: granulated biochar-based NPK fertilizer. Reproduced with permission from (Grafmüller et al. 2024), Scientific reports, Springer Nature.

Sample	As	Pb	B	Cd	Cr	Cu	Mn	Ni	Hg	Ag	Zn
mg kg ⁻¹											
Biochar	<0.8	3	5	<0.2	13	2	208	9	<0.07	<5	43
NPK	<0.8	<2	2	<0.2	<1	2	10	<1	<0.07	<5	5
gBBF	<0.8	2	4	<0.2	7	2	140	6	<0.07	<5	30

Table S8 Concentration of DNA and RNA in soil extracts. NPK: granulated nitrogen (N), phosphorus (P) and potassium (K) fertilizer. gBBF: granulated, biochar-based NPK fertilizer. B-0.2% +NPK: milled biochar (< 1 mm) co-applied at 0.2% to the soil with NPK. B-2% +NPK: milled biochar (< 1 mm) co-applied at 2% to the soil with NPK. Start: soil samples taken from native soil at the start of the experiment. Data are presented as means \pm standard deviation ($n=5$, except for gBBF and B-2%+NPK with $n=4$ and Start with $n=2$).

Treatment	DNA [ng μl^{-1}]	RNA [ng μl^{-1}]
NPK	80 \pm 17	34 \pm 7
gBBF	83 \pm 6	39 \pm 4
B-0.2% + NPK	71 \pm 12	33 \pm 9
B -2% + NPK	76 \pm 8	29 \pm 2
Initial	79 \pm 11	37 \pm 4

Table S9 Primer description used for quantitative Polymerase chain reaction (qPCR) and their sequences.

Target gene	Primer	Primer sequence	Origin of standard template
16s rRNA	515F 806R	GTGYCAGCMGCCGCGGTAA GGACTACNVGGGTWTCTAAT	Thiomonas
archael amoA	amo19F crenamoA	ATGGTCTGGCTWAGACG GCCATCCABCKRTANGTCCA	Fosmid clone 54d9
bacterial amoA	amoA1F amoA2R	GGGGTTTCTACTGGTGGT CCCCTCKGSAAAGCCTTCTC	Nitrosomonas eutropha
nirK	nirK876c nirK1040	ATYGGCGGVCA YGGCGA GCCTCGATCAGRTRRTGG	Ensifer meliloti strain1021
nirS	nirSCd3aF nirSR3cd	AACG YSAAGGARACSGG GASTTCGGRTGSGTCTTSAYGAA	Ralstonia eutropha
typical nosZ	nosZ2F nosZ2R	CGCRACGGCAASAAGGTSMSSTG CAKRTGCAKSGCRTGGCAGAA	Ensifer meliloti strain1021
atypical nosZ	nosZ-II-F nosZ-II-R	CTNGGNCCNYTKCAYAC GCNGARCARAANTCBGTRC	Gemmatimonas
nifH	nifH-F nifH-R	AAAGGYGGWATCGGYAARTCCACCAC TTGTTSGCSGCRTACATSGCCATCAT	Acidithiobacillus ferrooxidans

Table S10 Reactants and reactant volumes for quantitative Polymerase chain reaction (qPCR). Cyclers settings, efficiency and correlation coefficient (R^2) of qPCR. Each qPCR started with a heating phase to 95 °C for 3 minutes and ended with recording a melting curve between 65 °C and 95 °C. For target genes shown twice, the qPCR was done individually for DNA or cDNA templates.

Target gene	qPCR reactants	Reactant volumes [μl]	Cycler settings	Efficiency [%]	R ²
16s rRNA (DNA)	SYBR® Green ^a 515F (5 μM)	5.0 0.3	98 °C/10 s 60 °C/30 s	79.4	0.99
16s rRNA (cDNA)	806R (5 μM) PCR water template	0.3 3.4 1.0	40 cycles	76.8	0.99
archael amoA	SYBR® Green ^a amo19F (5 μM) crenamoA (5 μM) PCR water template	5.0 0.5 0.5 3.0 1.0	95 °C/45 s 55 °C/45 s 72 °C/45 s 40 cycles	80.3	0.99
bacterial amoA (DNA)	SYBR® Green ^a amo19F (5 μM)	5.0 0.75	95 °C/45 s 60 °C/45 s	78.3	0.99
bacterial amoA (cDNA)	crenamoA (5 μM) PCR water template	0.75 2.5 1.0	72 °C/45 s 40 cycles	75.3	0.99
nirK	SYBR® Green ^a nirK876c (5 μM) nirK1040 (5 μM) PCR water template	5.0 0.5 0.5 3.0 1.0	95 °C/10 s 58 °C/20 s 40 cycles	86.7	0.99
nirS	SYBR® Green ^a nirSCd3aF (5 μM) nirSR3cd (5 μM) PCR water template	5.0 0.5 0.5 3.0 1.0	95 °C/30 s 57 °C/45 s 40 cycles	81.8	0.99
typical nosZ	SYBR® Green ^a nosZ2F (5 μM) nosZ2R (5 μM) BSA PCR water template	5.0 0.5 0.5 0.5 2.5 1.0	95 °C/15 s 60 °C/25 s 40 cycles	64.2	0.99
atypical nosZ	SYBR® Green ^a nosZ-II-F (50 μM) nosZ-II-R (50 μM) PCR water template	5.0 0.5 0.5 3.0 1.0	95 °C/30 s 58 °C/30 s 72 °C/45 s 80 °C/30 s 40 cycles	64.5	0.99
nifH (DNA)	SYBR® Green ^a nifH-F (5 μM)	5.0 0.5	95 °C/30 s 55 °C/30 s	83.2	0.99
nifH (cDNA)	nifH-R (5 μM) PCR water template	0.5 3.0 1.0	72 °C/30 s 40 cycles	90.0	0.99

^aiTaq™ Universal SYBR® Green Supermix

Table S11 *F and p value of one-way analysis of variance for spinach biomass yields. The factor ‘Treatment’ includes the comparison of the treatments ‘NPK’, ‘gBBF’, ‘B-0.2+NPK’ and ‘B-2%+NPK’. The Block effect was considered with the repeated measures function in the GraphPad Prism software. Significant p values ($p < 0.05$) are indicated in bold.*

Factor	Fresh aboveground biomass		Dry aboveground biomass		Dry root biomass	
	F	<i>p</i>	F	<i>p</i>	F	<i>p</i>
Treatment	27.42	<0.0001	8.44	0.003	0.585	0.636
Block	0.396	0.808	1.2	0.361	0.819	0.537

Table S12 *F and p value of one-way analysis of variance for uptake of several nutrients in aboveground spinach biomass. The factor ‘Treatment’ includes the comparison of the treatments ‘NPK’, ‘gBBF’, ‘B-0.2+NPK’ and ‘B-2%+NPK’. The Block effect was considered with the repeated measures function in the GraphPad Prism software. Significant p values ($p < 0.05$) are indicated in bold.*

Factor	Nitrogen		Phosphorus		Potassium	
	F	<i>p</i>	F	<i>p</i>	F	<i>p</i>
Treatment	5.363	0.014	10.15	0.001	16.51	0.0001
Block	0.328	0.854	1.451	0.277	1.779	0.198
Factor	Magnesium		Sulfur		Calcium	
	F	<i>p</i>	F	<i>p</i>	F	<i>p</i>
Treatment	4.048	0.033	7.14	0.005	2.431	0.116
Block	1.592	0.239	0.825	0.534	0.891	0.499
Factor	Manganese		Copper		Zinc	
	F	<i>p</i>	F	<i>p</i>	F	<i>p</i>
Treatment	1.254	0.334	4.35	0.027	2.596	0.101
Block	1.540	0.253	1.895	0.176	0.919	0.484

Table S13 *F* and *p* value of one-way analysis of variance for soil-borne nitrous oxide fluxes on individual days. The factor ‘Treatment’ includes the comparison of the treatments ‘NPK’, ‘gBBF’, ‘B-0.2+NPK’ and ‘B-2%+NPK’. The Block effect was considered with the repeated measures function in the GraphPad Prism software. Significant *p* values ($p < 0.05$) are indicated in bold.

Day	Treatment		Block	
	F	<i>p</i>	F	<i>p</i>
2	4.3	0.044	1.0	0.469
4	21.0	0.003	0.4	0.827
9	3.5	0.044	1.6	0.232
16	3.1	0.090	0.3	0.591
23	2.2	0.176	0.3	0.866
30	2.6	0.126	0.2	0.943
37	0.4	0.600	0.9	0.501

Table S14 *F* and *p* value of one-way analysis of variance for soil-borne nitrous oxide (N_2O emissions). The factor ‘Treatment’ includes the comparison of the treatments ‘NPK’, ‘gBBF’, ‘B-0.2+NPK’ and ‘B-2%+NPK’. The Block effect was considered with the repeated measures function in the GraphPad Prism software. Significant *p* values ($p < 0.05$) are indicated in bold.

Factor	Cumulative emissions		Yield-based emissions	
	F	<i>p</i>	F	<i>p</i>
Treatment	15.18	0.0003	38.77	<0.0001
Block	0.139	0.710	0.0979	0.754

Table S15 *F* and *p* value of one-way analysis of variance for 16S rRNA gene abundance (both for DNA copy number and cDNA transcript number) in soil samples taken after harvest of spinach plants. The factor ‘Treatment’ includes the comparison of the treatments ‘NPK’, ‘gBBF’, ‘B-0.2+NPK’ and ‘B-2%+NPK’. The Block effect was taken into account with the repeated measures function in the GraphPad Prism software. Significant *p* values ($p < 0.05$) are indicated in bold.

Factor	16S rRNA (DNA)		16S rRNA (cDNA)	
	F	<i>p</i>	F	<i>p</i>
Treatment	0.209	0.888	4.264	0.393
Block	0	>0.999	9.3 x 10 ⁻⁶	0.998

Table S16 *F* and *p* value of one-way analysis of variance for nitrogen cycling gene abundance in soil samples taken after harvest of spinach plants. The factor ‘Treatment’ includes the comparison of the treatments ‘NPK’, ‘gBBF’, ‘B-0.2+NPK’ and ‘B-2%+NPK’. The Block effect was taken into account with the repeated measures function in the GraphPad Prism software. Significant *p* values ($p < 0.05$) are indicated in bold.

Factor	amoA AOA		amoA AOB		nirS+nirK	
	F	<i>p</i>	F	<i>p</i>	F	<i>p</i>
Treatment	1.195	0.361	0.992	0.436	0.174	0.912
Block	0.733	0.392	0.856	0.355	0.009	0.924
Factor	typical nosZ		atypical nosZ		nifH	
	F	<i>p</i>	F	<i>p</i>	F	<i>p</i>
Treatment	0.492	0.694	1.424	0.299	5.279	0.023
Block	0	>0.999	0	>0.999	0.577	0.448

Table S17 Cumulative soil-born emissions of nitrous oxide (N₂O), methane (CH₄) and carbon dioxide (CO₂) based on soil surface, dry aboveground spinach biomass, aboveground nitrogen (N) uptake of spinach or fertilized N, as indicated in column headers. Errors indicate one standard error (n=5), different letters within each column indicate significant differences between treatments (Tukey's post-hoc test at p<0.05). NPK: granulated nitrogen (N), phosphorus (P) and potassium fertilizer. gBBF: granulated, biochar-based NPK fertilizer. NPK+BC_low: milled biochar (< 1 mm) co-applied at 0.2% to the soil with NPK. NPK+BC_high: milled biochar (< 1 mm) co-applied at 2% to the soil with NPK.

Treatment	Cumulative N ₂ O emissions		Cumulative CH ₄ emissions		Cumulative CO ₂ emissions	
	[mg N ₂ O-N m ⁻²]	[mg (g biomass) ⁻¹]	[mg m ⁻²]	[μg (g biomass) ⁻¹]	[g m ⁻²]	[g (g biomass) ⁻¹]
NPK	169 ± 14 bc	0.77 ± 0.03 a	-1.3 ± 1.2 a	-6.1 ± 5.3 a	346 ± 8 a	1.57 ± 0.04 a
gBBF	183 ± 9 ab	0.80 ± 0.05 a	-2.3 ± 1.1 a	-10.2 ± 4.7 a	352 ± 7 a	1.54 ± 0.03 a
NPK+BC_low	196 ± 9 a	0.81 ± 0.04 a	-0.3 ± 1.1 a	-1.4 ± 4.5 a	359 ± 4 a	1.49 ± 0.02 a
NPK+BC_high	157 ± 10 c	0.61 ± 0.02 b	-0.1 ± 1.1 a	-0.3 ± 4.5 a	338 ± 11 a	1.35 ± 0.04 b

Table S18: Activity of urease (UA) in ammonium-nitrogen ($\text{NH}_4\text{-N}$) production and nitrate reductase (NRA) in nitrite-nitrogen ($\text{NO}_2\text{-N}$) production per gram of dry soil and day in soil samples taken on the day of spinach harvest. NPK: granulated nitrogen (N), phosphorus (P) and potassium (K) fertilizer. gBBF: granulated, biochar-based NPK fertilizer. NPK+BC_low: milled biochar (< 1 mm) co-applied at 0.2% to the soil with NPK. NPK+BC_high: milled biochar (< 1 mm) co-applied at 2% to the soil with NPK. Initial: soil samples taken from native soil at the start of the experiment. Data are presented as means \pm standard deviation ($n=5$, except for gBBF and B-2%+NPK with $n=4$). Different letters indicate a significant difference between the treatments (one-way analysis of variance, Tukey's post hoc test, $p < 0.05$).

Treatment	UA	NRA
	[$\mu\text{g NH}_4\text{-N g}^{-1}\text{d}^{-1}$]	[$\mu\text{g NO}_2\text{-N g}^{-1}\text{d}^{-1}$]
NPK	56 \pm 5 a	0.3 \pm 0.3 b
gBBF	55 \pm 6 a	0.8 \pm 0.3 a
NPK+BC_low	59 \pm 9 a	0.4 \pm 0.04 ab
NPK+BC_high	60 \pm 3 a	0.4 \pm 0.2 ab

Supplementary Figures



Figure S1 Sowing of ten seeds of spinach variety Corvair F1 into the pots filled with the sandy loam.

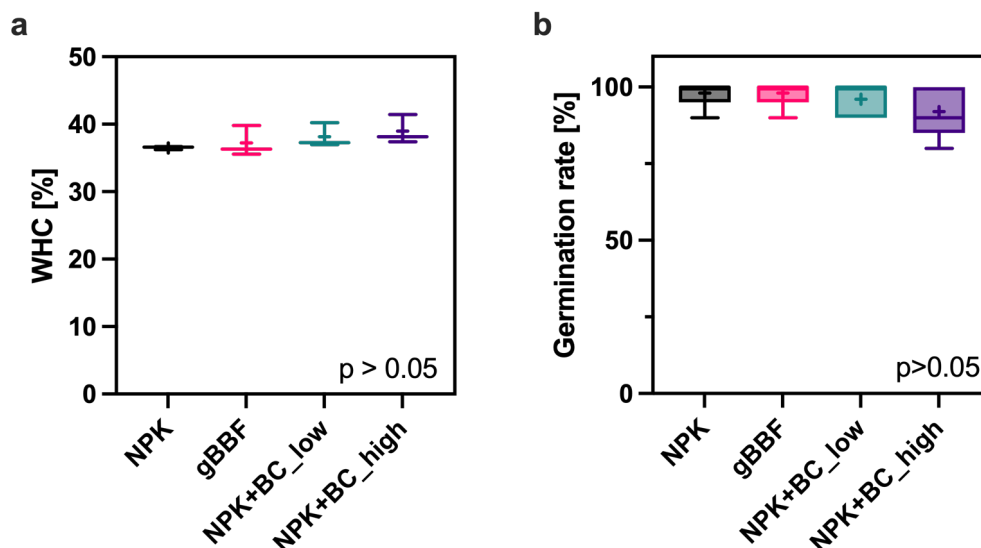


Figure S2 Water holding capacities (WHC) of the soil mixtures prepared for the pot trial (a) and germination rate in the pots prepared for the greenhouse trial 7 days after sowing spinach variety Corvair F1 (b). NPK: granulated nitrogen (N), phosphorus (P) and potassium fertilizer. gBBF: granulated, biochar-based NPK fertilizer. NPK+BC_low: milled biochar (< 1 mm) co-applied at 0.2% to the soil with NPK. NPK+BC_high: milled biochar (< 1 mm) co-applied at 2% to the soil with NPK. The water holding capacity was measured by saturation of the soil mixtures in a water bath for 16 hours followed by a drainage on a dry sand bed for 48 hours. The stored amount of water after drainage was related to the dry matter of the soil mixture to obtain the WHC. One-way analysis of variance indicated no significant differences between the treatments at $p < 0.05$.



Figure S3 (a) Pot after germination of the 10 seeds that were initially sown. (b) Pots after reducing the plant number to five seedlings per pot.



Figure S4 (a) Water basins for sequential root washing. (b) Pots from the greenhouse after harvesting the aboveground spinach biomass. (c) Separation of rootstocks from the soil. (d) Washed rootstocks after a last cleaning flush with distilled water.

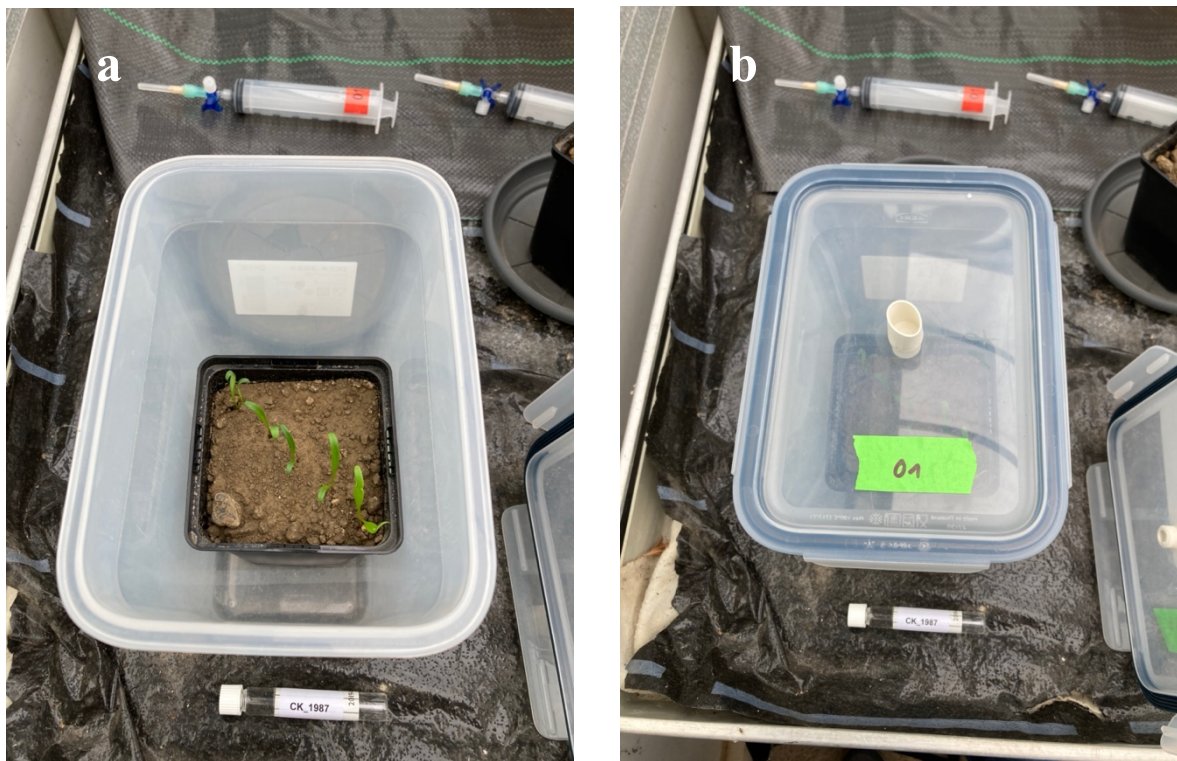


Figure S5 (a) Placement of the pots in the incubation container for determination of soil-borne greenhouse gas fluxes. (b) Pots in the incubation container with closed lid and septum in the lid for taking gas samples with a syringe.

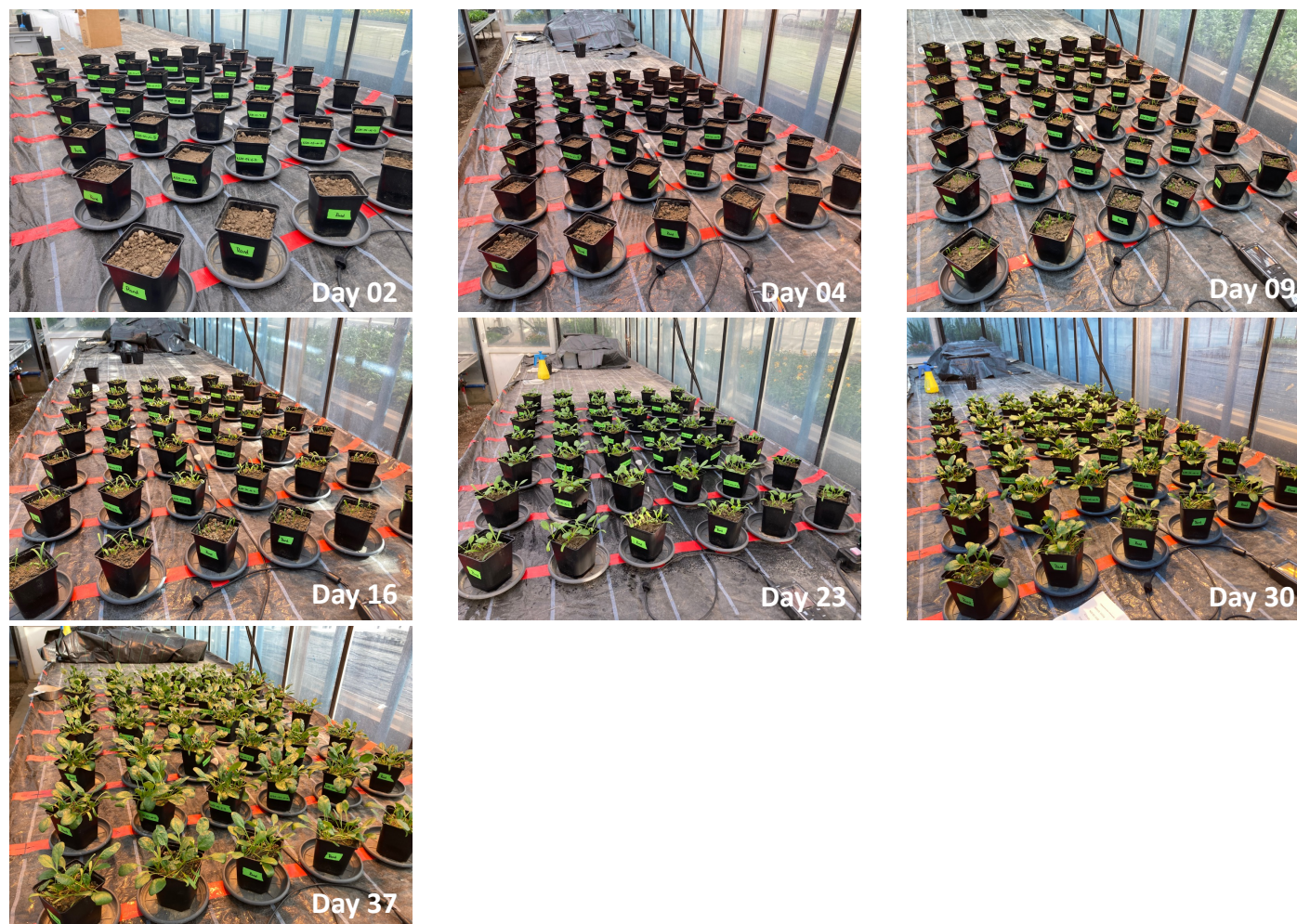


Figure S 6 Spinach plant development on the individual days of N₂O emission measurements.

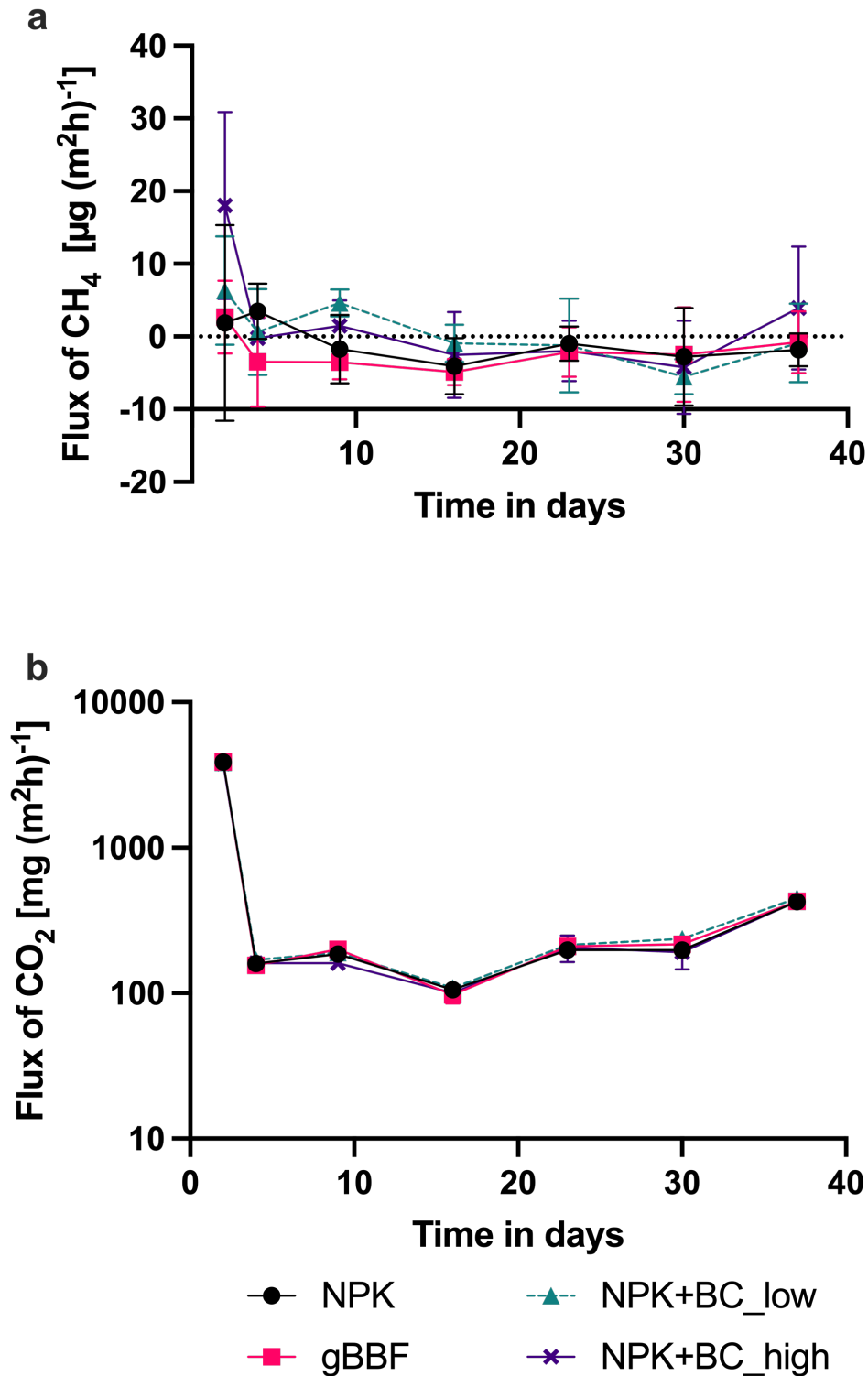


Figure S 7 Methane (CH₄, panel a) and Carbon Dioxide (CO₂, panel b) fluxes from the soil on seven individual measurement days. NPK: granulated nitrogen (N), phosphorus (P) and potassium (K) fertilizer. gBBF: granulated, biochar-based NPK fertilizer. NPK+BC_low: milled biochar (< 1 mm) co-applied at 0.2% to the soil with NPK. NPK+BC_high: milled biochar (< 1 mm) co-applied at 2% to the soil with NPK. Data are presented as means \pm standard deviation of five replicates.

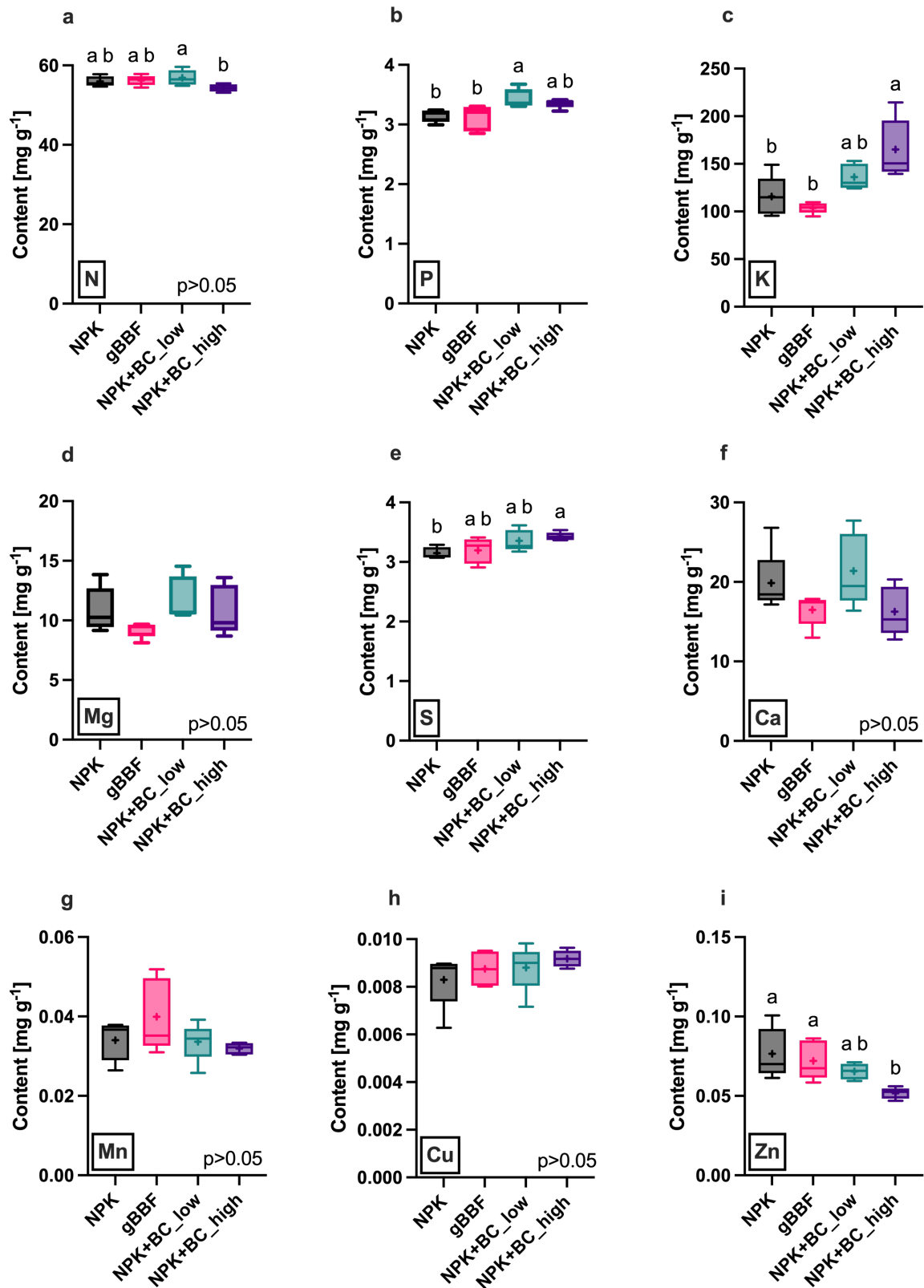


Figure S 8 Content of nutrients in aboveground spinach biomass based on dry matter in panels a to i: nitrogen (N), phosphorus (P), potassium (K), magnesium (Mg), sulfur (S), calcium (Ca), manganese (Mn), copper (Cu) and zinc (Zn). Whiskers in boxplots represent the minimum to maximum value of five replicates for each treatment, mean values are indicated with “+”,

different letters indicate a significant difference between the treatments (one-way analysis of variance, Tukey's post hoc test, $p < 0.05$). NPK: granulated nitrogen (N), phosphorus (P) and potassium (K) fertilizer. gBBF: granulated, biochar-based NPK fertilizer. NPK+BC_low: milled biochar (< 1 mm) co-applied at 0.2% to the soil with NPK. NPK+BC_high: milled biochar (< 1 mm) co-applied at 2% to the soil with NPK.

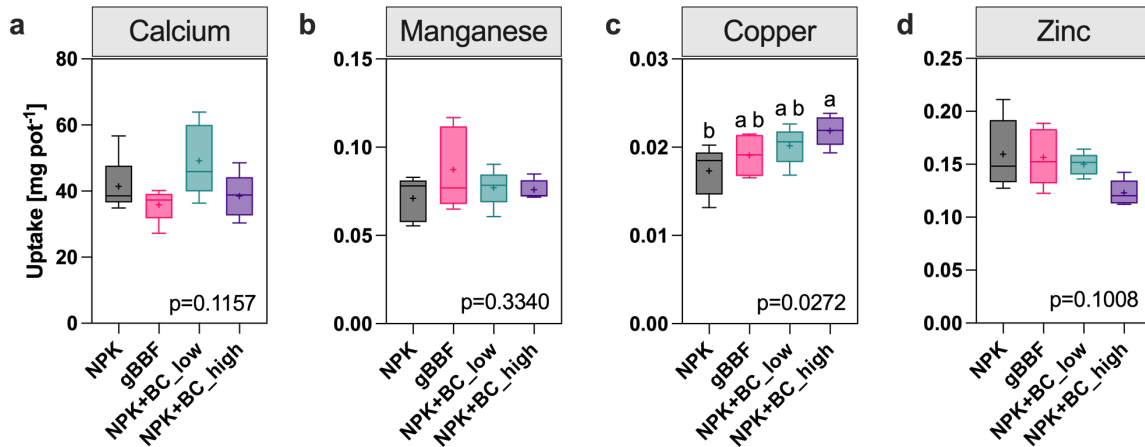


Figure S 9: Uptake of nutrients in aboveground spinach biomass for calcium, manganese, copper and zinc. NPK: granulated nitrogen (N), phosphorus (P) and potassium (K) fertilizer. gBBF: granulated, biochar-based NPK fertilizer. NPK+BC_low: milled biochar (< 1 mm) co-applied at 0.2% to the soil with NPK. NPK+BC_high: milled biochar (< 1 mm) co-applied at 2% to the soil with NPK. Whiskers in boxplots represent the minimum to maximum value of five replicates for each treatment, mean values are indicated with “+”, different letters indicate a significant difference between the treatments (one-way analysis of variance, Tukey's post hoc test, $p < 0.05$).

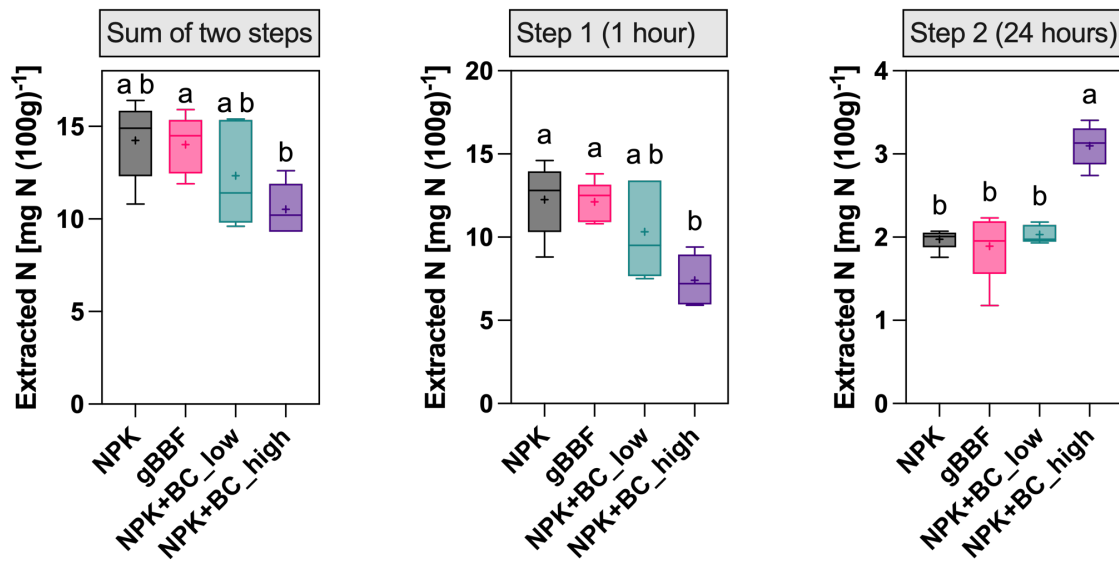


Figure S 10: Extractable total nitrogen (N) in 1 M KCl solution from soil samples at the end of the experiment in repetitive extraction steps: (a) sum of two extraction steps, (b) first extraction step for 1 hour and (c) second extraction step of 24 hours. gBBF: granulated, biochar-based NPK fertilizer. NPK+BC_low: milled biochar (< 1 mm) co-applied at 0.2% to the soil with NPK. NPK+BC_high: milled biochar (< 1 mm) co-applied at 2% to the soil with NPK. Whiskers in boxplots represent the minimum to maximum value of five replicates for each treatment, mean values are indicated with “+”, different letters indicate a significant difference between the treatments (one-way analysis of variance, Tukey’s post hoc test, $p < 0.05$).

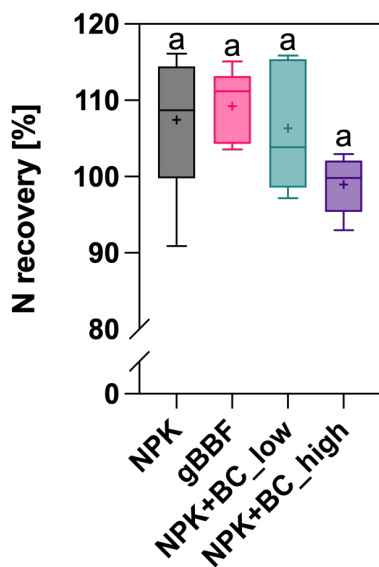


Figure S 11 Recovery of the sum of fertilized nitrogen (N) as urea and initial mineralized N in the soil at the experimental start (total of 220 mg N pot⁻¹) cummulated over N emitted as nitrous oxide, N quantified in aboveground spinach biomass and 1 M KCl-extractable N in soil after harvest. gBBF: granulated, biochar-based NPK fertilizer. NPK+BC_low: milled biochar (< 1 mm) co-applied at 0.2% to the soil with NPK. NPK+BC_high: milled biochar (< 1 mm) co-applied at 2% to the soil with NPK. Whiskers in boxplots represent the minimum to maximum value of five replicates for each treatment, mean values are indicated with “+”, different letters indicate a significant difference between the treatments (one-way analysis of variance, Tukey’s post hoc test, $p < 0.05$).

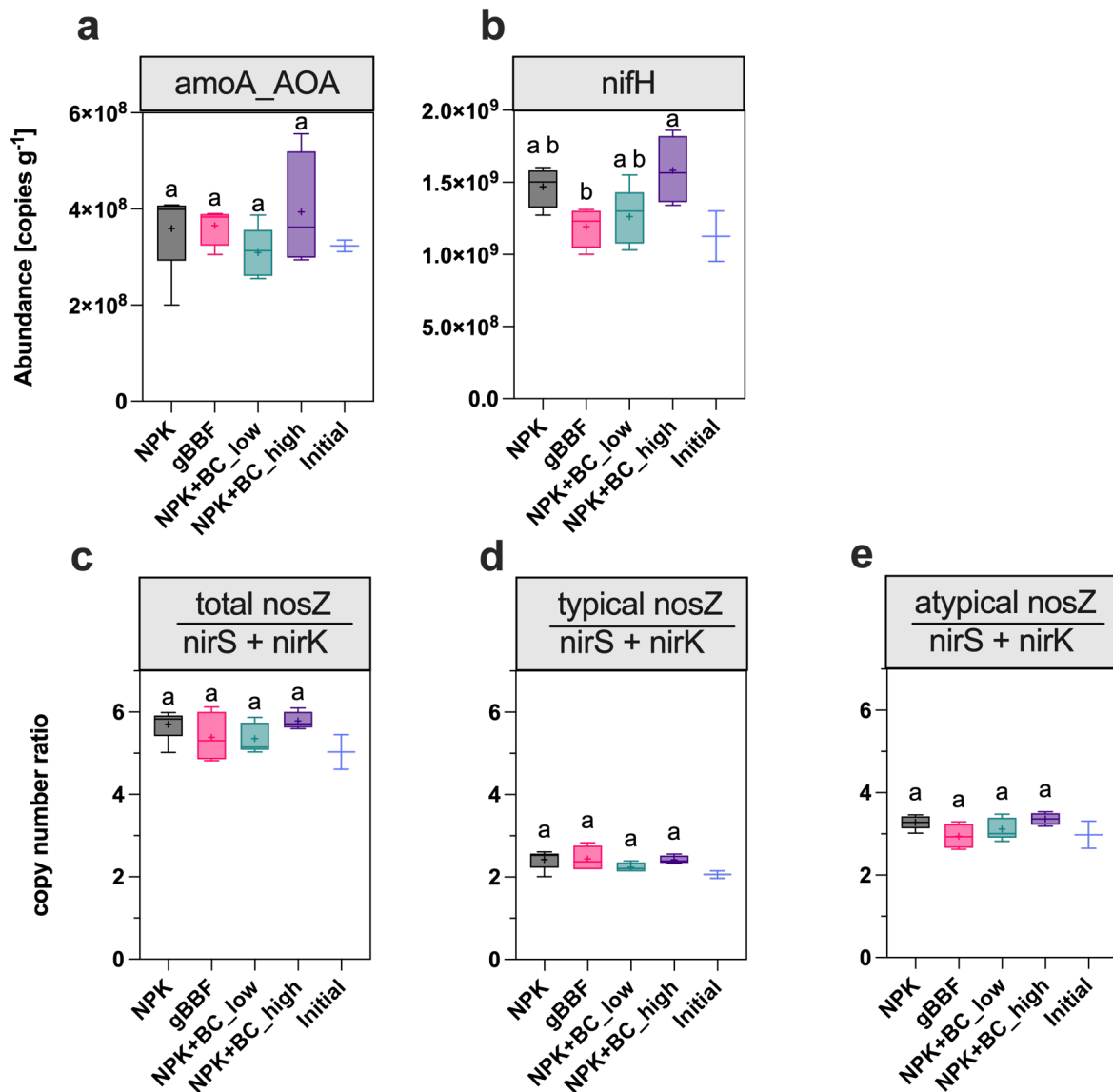


Figure S 12 Copy numbers per gram of dry soil for genes involved in microbial nitrogen transformation: archaeal ammonium oxidizers (*amoA* AOA, panel a) and gene associated with nitrogen fixation (*nifH*, panel b). Ratio of total, typical and atypical copy numbers of *nosZ* to *nirS*+*nirK* (panel c, d and e, respectively). NPK: granulated nitrogen (N), phosphorus (P) and potassium fertilizer. gBBF: granulated, biochar-based NPK fertilizer. NPK+BC_low: milled biochar (< 1 mm) co-applied at 0.2% to the soil with NPK. NPK+BC_high: milled biochar (< 1 mm) co-applied at 2% to the soil with NPK. Initial: soil samples taken from native soil at the start of the experiment. Box plots represent the minimum and maximum of replicated pots for the different treatments (n=5, except for gBBF and NPK+BC_high with n=4 and initial samples with n=2). Different letters above error bars indicate a significant difference between treatments (at p<0.05, Tukey's post-hoc test). The 'Initial' group was excluded from the statistical test.

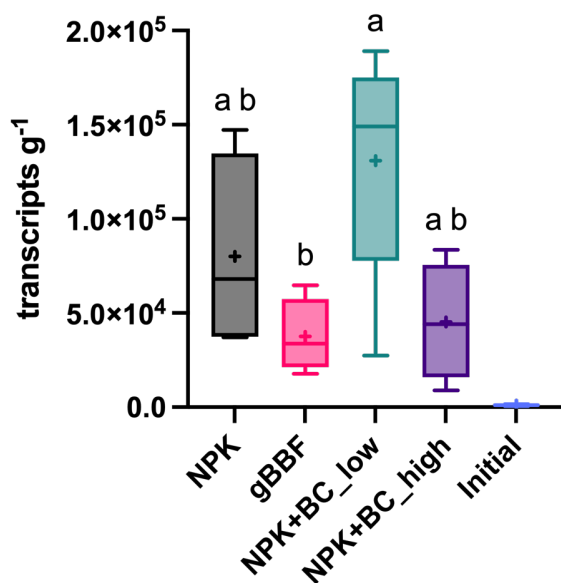


Figure S 13 Transcript numbers per gram of dry soil for gene associated with archaeal ammonium oxidation (*amoA AOA*). NPK: granulated nitrogen (N), phosphorus (P) and potassium (K) fertilizer. gBBF: granulated, biochar-based NPK fertilizer. NPK+BC_low: milled biochar (< 1 mm) co-applied at 0.2% to the soil with NPK. NPK+BC_high: milled biochar (< 1 mm) co-applied at 2% to the soil with NPK. Initial: soil samples taken from native soil at the start of the experiment. Box plots represent the minimum and maximum of replicated pots for the different treatments ($n=5$ for NPK+BC_low, $n=4$ for NPK, gBBF and NPK+BC_high and $n=2$ for Initial). Different letters above error bars indicate a significant difference between treatments (at $p<0.05$, Tukey's post-hoc test).

Supplementary methods

Urease activity (UA) in the soil samples taken after harvest (stored at 4 °C) was measured using a non-buffered method (Kandeler and Gerber 1988) one day after sampling. Fresh soil (1.25 g) was incubated with either 1.25 mL of an 80 mM urea solution or ultrapure water (blank) for two hours at 37 °C. After incubation, 12.5 mL of 1 M KCl solution was added and the samples were extracted for 30 minutes on a horizontal shaker. After filtration of the samples to < 0.45 µm, Blanks were used to correct for the native NH₄-N extracted from soil. Nitrate reductase activity (NRA) was quantified after storing the soil samples six days at 4 °C (Abdelmagid and Tabatabai 1987; Kandeler 1996). Fresh soil (1.25 g) was incubated with 0.45 mL of ultrapure water, 1.8 mL of a 2-4 Dinitrophenol (DNP) solution, and 0.25 mL of the substrate solution (25 mM KNO₃) or ultrapure water (blank) for 24 h at 25 °C. The necessary concentration of 2-4 DNP was determined to be 300 µg (g dry matter of soil)⁻¹, to inhibit nitrite reduction (Abdelmagid and Tabatabai 1987). After incubation, the samples were extracted with 2.5 mL of a 4 M KCl for 30 minutes at 150 rpm. Extracts were filtered to < 0.45 µm and nitrite concentration in the filtrates was measured colorimetric in a 96-well plate at 520 nm (Kandeler 1996). The NO₂ concentrations measured in the blanks were subtracted from the sample concentrations to correct for soil-native NO₂.

References

- Abdelmagid HM, Tabatabai MA (1987) Nitrate reductase activity of soils. *Soil Biol Biochem* 19:421–427. [https://doi.org/10.1016/0038-0717\(87\)90033-2](https://doi.org/10.1016/0038-0717(87)90033-2)
- Grafmüller J, Möllmer J, Muehe EM, et al (2024) Granulation compared to co-application of biochar plus mineral fertilizer and its impacts on crop growth and nutrient leaching. *Sci Rep* 14:16555. <https://doi.org/10.1038/s41598-024-66992-0>
- Kandeler E (1996) Nitrate Reductase Activity. In: *Methods in Soil Biology*. Springer Berlin Heidelberg, Berlin, Heidelberg, pp 176–179
- Kandeler E, Gerber H (1988) Short-term assay of soil urease activity using colorimetric determination of ammonium. *Biol Fertil Soils* 6:. <https://doi.org/10.1007/BF00257924>

Chapter 4a

Citric acid treated biochar reduced nitrate leaching but impaired macronutrient uptake in spinach, depending on biochar type

Jannis Grafmüller^{1,2,3}, Daniel Kray¹, Nikolas Hagemann^{2,4}

¹Institute for Sustainable Energy Systems (INES), Offenburg University of Applied Sciences, Offenburg, Germany

²Ithaka Institute, Arbaz (Switzerland) and Goldbach (Germany)

³Plant Biogeochemistry, Tübingen University, Tübingen, Germany

⁴Environmental Analytics, Agroscope Zurich, Zurich, Switzerland

Working paper

Statement of personal and co-author contributions, plus non-listed contributors

Authors	Position of candidate in list of authors	Scientific ideas by the author [%]	Data generation by the author [%]	Analysis and interpretation by the author [%]	Paper writing done by the author [%]
Jannis Grafmüller	1	70	85	80	100
Daniel Kray	2	15	0	10	0 ^a
Nikolas Hagemann	3	15	0	10	0 ^a
Contribution by other parties not listed as authors (e.g., commercial analysis laboratories, student assistants)					
Mohammed Kusaybati		0	5	0	0
Regina Brämer		0	5	0	0
Martin Zuber		0	5	0	0
Publication status	unpublished				
Explanations	The study was conceptualized by Nikolas Hagemann, Daniel Kray and me. The experimental work was mainly performed by me, with contributions from Mohammed Kusaybati during root harvest, Regina Brämer from Offenburg University of Applied Sciences during ICP measurements and Martin Zuber from Agroscope Zurich, Switzerland during N quantification in spinach biomass. The data analysis was performed by me, Daniel Kray and Nikolas Hagemann supported me with data interpretation. The manuscript was written by me.				

^a: Contribution set to 0, as co-author did not yet review the manuscript.

Abstract

The production of biochar-based fertilizers (BBF) that slowly release nutrients and thus reduce the risk of nutrient leaching from soil, most importantly nitrate (NO_3^-), requires biochar modification for improved nutrient retention. Here, NO_3^- -enriched BBF prepared from two biochars (BC1 and BC2) were acidified with citric acid to a pH of ~ 4.5 to quantify to what extent biochar acidification can reduce NO_3^- leaching during a heavy precipitation event in a greenhouse pot trial with spinach (*Spinacia oleracea*).

Compared to a fertilized soil without any biochar amendment (Control), both non-acidified BBF reduced NO_3^- leaching by 40-48% and both acidified BBF reduced it by 70%, indicating that biochar acidification might be a simple tool to improve NO_3^- retention in BBF amended soil. Independent of the acidification treatment, BBF amendment increased aboveground spinach yields by 16-20% compared to the Control under leaching, which reflected the lower NO_3^- loss during the precipitation event. When spinach cultivation was done without a leaching event, thus under drier conditions, acidification of BC2 reduced the uptake of phosphorus and sulfur likely due to decreased phosphate concentrations in soil porewater compared to non-acidified BC2, indicating immobilization of sulfate and phosphate by acidified BBF after NO_3^- was released from it. Biochar acidification via citric acid increased soil pH during the experiment, likely related to microbial decarboxylation of citrate. We suggest using inorganic acids, such as HNO_3 , for biochar acidification, which would directly add NO_3^- to the BBF and would further avoid the introduction of a negatively charged corresponding base that would interfere with NO_3^- sorption to biochar.

1. Introduction

Nitrate (NO_3^-) leaching from soil is estimated to account to up to 19-30% of fertilized nitrogen (N)^{1,2} and thus limits the efficiency of agricultural systems and causes groundwater pollution. Biochar amendment to soil reduces NO_3^- leaching by 13% on a global average, yet only consistently at relatively high application rates of $> 10\text{-}20 \text{ t ha}^{-1}$ and most effectively after 60-120 days following soil application³. As such biochar application rates with a single treatment are economically unfeasible for farmers, research is focusing on the development of biochar-based fertilizers (BBF), where biochar is enriched with nutrients, such as NO_3^- -bearing minerals, and applied in low application rates of $0.5\text{-}2 \text{ t ha}^{-1} \text{ year}^{-1}$ while biochar accumulates over time in soil⁴. Thus, modification techniques for biochar used in BBF that facilitate reductions in NO_3^- leaching directly after soil application and already at low, economical feasible biochar application rates are needed.

Probably the most important mechanisms that lead to biochar-induced reduction in NO_3^- leaching include electrostatic sorption of NO_3^- to the biochar surface⁵ and entrapment of NO_3^- in an organic coating developing after soil-application^{6,7}. To achieve direct benefits after biochar application to soil, the NO_3^- -sorption capacity of biochar should be increased, which would enable the production of slow-release BBF. Such a BBF should ideally release nutrients to the soil porewater in a way that nutrient requirements of plants are met, yet slow enough to reduce abrupt nutrient leaching during heavy precipitation events.

Modification techniques of biochar to improve sorption of NO_3^- to biochars include steam activation during pyrolysis to increase specific surface area of biochars⁸ or using metal additives, such as lanthanum oxide, magnesium oxide or potassium chloride during pyrolysis that increased sorption of anions on biochars⁹⁻¹¹. Improved sorption of NO_3^- to biochars has also been observed at acidic pH, as acids protonate the biochar surface, such as oxygen containing functional groups, which then represent a sorption site for anions¹²⁻¹⁴. In a direct, mole-equivalent comparison of different low-molecular weight organic acids that are also present in soil as root exudates, citric acid was found to be most effective in improving NO_3^- sorption to biochar¹⁴. Still, no study so far quantified the reduction potential of citric acid treated biochar for NO_3^- leaching in a soil environment and impacts of acidified BBF on plant growth. An acidification treatment in combination with nitrate-enrichment of biochar might produce a BBF with an optimized pH within biochar pores that improves NO_3^- sorption and thus the slow release of NO_3^- from the BBF to the soil porewater, as long as the pH in biochar pores did not yet equilibrate to higher soil pH.

Here, two industrially produced, wood-based biochars were used to produce NO_3^- - and citric acid-enriched BBF to study NO_3^- leaching and release to soil porewater in a pot trial with spinach. Biochars were acidified to a pH of 4.5-5.0, as this moderate pH range was identified to already improve sorption of NO_3^- significantly compared to sorption at native biochar pH for various wood-based biochars (Figure S 1). A soil with neutral pH was chosen for this experiment, as the sorption capacity of NO_3^- in non-acidified biochar might be more limited under such conditions compared to application to a more acidic soil. The aim of this study was to quantify to what extent the acidification treatment of BBF can reduce NO_3^- leaching from soil compared to non-acidified BBF and equally fertilized soil without any biochar amendment.

2. Materials and Methods

2.1. Biochar origin, characterization and modification

Two biochars produced from wood chips on industrial scale were used. Biochar BC1 was produced in an electrically heated pyrolysis plant at a highest treatment temperature (HTT) of 750 °C (plant manufactured by Carbon Technik Schuster GmbH, Neresheim, Germany operated by Carbon Cycle GmbH & Co. KG, Rieden, Germany). Biochar BC2 was produced with a HTT of 650 °C on a P500 (Pyreg GmbH, Dörth, Germany) operated by Abfallwirtschaftsgesellschaft Neckar-Odenwald-Kreis mbH, Buchen, Germany.

2.1.1. Characterization

Biochars were analyzed for carbon, hydrogen, nitrogen, sulfur (CHNS) and ash content, as well as contents of main and trace elements by a Eurofins Umwelt Ost GmbH (Bobritzsch-Hilbersdorf, Germany). Water holding capacity (WHC) of biochars was measured in line with the European Biochar Certificate¹⁵. The porosity of biochars was studied by N_2 and CO_2 physisorption as described in literature¹⁶.

2.1.2. BBF production

Biochars were milled to < 1mm in a centrifugal mill (ZM200, Retsch GmbH, Haan, Germany). Biochar-based fertilizers were produced by spiking biochars to a WHC of 80% with a solution of KNO_3 and, for acidified BBF, with addition of citric acid. Both biochars were spiked with 160 mg $\text{KNO}_3 \text{ g}^{-1}$ and, if applicable, with citric acid at 17.4 mg g^{-1} for BC1 or 85.4 mg g^{-1} for BC2 via a solution volume of ~1.4 ml g^{-1} for BC1 or ~1.5 ml g^{-1} for BC2. For the greenhouse trial, 18.15 g dry matter equivalent of biochars were weighed in 125 ml HDPE Nalgene bottles and spiked with the respective solution, closed with the cap, vortexed after 4 hours and left to

stand in the dark and at room temperature for three days. For pH measurements and N release experiments, biochar weights for BBF production as described above were downscaled to 2 g dry matter equivalent (in 50 ml centrifuge tubes) and 0.4 g dry matter equivalent (in 15 ml centrifuge tubes), respectively. The BBF were labelled as BC1-N or BC1-N+CA and BC2-N or BC2-N+CA. All BBF had a N content of 2.2% (w/w) and a pH measured according to the EBC of 8.9 and 4.7 for BC1-N and BC1-N+CA, respectively, and 9.1 and 4.5 for BC2-N and BC2-N+CA, respectively.

2.1.3. NO₃⁻ release from BBF

The NO₃⁻ release from BBF was studied in a 0.2 M phosphate buffer adjusted to pH 7 added at 10 ml to the BBF samples (cf. section 2.1.2) resulting in a solid:liquid ratio of 1:50 (w/w). The samples were shaken horizontally in 15 mL centrifuge tubes at 150 rpm. Aliquots of the suspension were sampled after 5, 15, 30 and 60 minutes, filtered (<0.45 µm) and stored at -18 °C for NO₃⁻ analysis.

2.2. Greenhouse trial

2.2.1. Trial setup

The pot trial was conducted between 2nd November 2023 and 5th January 2024 in a greenhouse located in Offenburg, Germany (48° 27' 29.6" N, 7° 57' 6.9" E) with averaging temperature of 18 ± 2 °C during daytime (8 am to 8 pm) and 14 ± 4 °C during night. Over the whole experiment, averaging temperature was 16 ± 3 °C, relative humidity was 65 ± 10% and atmospheric CO₂ concentration was 410 ± 40 ppm. In total, 10 treatments (Table 1) with each five replicates were set up using pots with a diameter and height of 12 cm. A sandy loam with pH 7.3 and a soil organic carbon content of 2.4% (w/w) was used and sieved to <3 mm. Basic soil properties can be found in Table S 1-Table S 3. A 1 mm nylon mesh was installed at the bottom of the pots. For pots without an amendment (ID 1 and 7, Table 1), 1.2 kg dry matter equivalent of soil were added and 40 ml of a KNO₃ solution (72.2 mg l⁻¹) were fertilized on top of the soil surface. After 24 hours, the pots were emptied into a container and the fertilized soil was homogenized manually for 1.5 minutes and put back into the pot. The pot content was compacted by knocking to ground for three times from a height of 15 cm. For pots with biochar amendments, the soil together with the respective BBF were directly homogenized as described above and transferred to the pot. Empty bottles containing the BBF were rinsed with 40 ml distilled water over the respective pots. The biochar concentration in soil was 1.5% (w/w) and 400 mg N were fertilized as KNO₃ in all pots. The WHC of soil mixtures (no amendment, 1.5%

BC1 and 1.5% BC2) was measured after saturation of three replicated pots in a water bath for 18 hours and subsequent drainage for 48 hours on a dry sand bed¹⁷ (Figure S 3). At 6 cm soil depth, a soil porewater sampling port was installed horizontally through the pot sidewall (Figure S 2, Rhizon MOM 5 cm, Article no. 19.21.22F, Rhizosphere Research Products bv, Wageningen, Netherlands). One day after pot setup, the water content in the pots was stepwise increased to 60% WHC with well water and positioned in a randomized complete block design. Eight seeds of spinach were sown into four holes arranged as a square on the soil surface (*Spinacia oleracea*, variety Corvair F1, Bruno Nebelung GmbH, Everswinkel, Germany, Figure S 4). Plant number was reduced to four plants per pot 11 days after sowing. Pots were irrigated during the whole trial to 60% WHC with well water three times the week.

Table 1: *Treatments prepared for the greenhouse pot trial. Two different biochars were applied at a rate of 1.5% (w/w): wood-based biochar produced in a pyrolysis plant from Carbon Technik Schuster GmbH (BC1) and a wood-based biochar produced in a P500 from Pyreg GmbH (BC2). Both biochars were enriched with KNO₃ to a nitrogen (N) content of 22 mg N g⁻¹ (BC1-N and BC2-N, respectively). Acidified and N enriched biochars are labeled as BC1-N+CA or BC2-N+CA. Leaching treatment to simulate heavy rainfall (~20 l m⁻²) was conducted 9 days after sowing.*

ID	Treatment	Biochar	Acidification	Leaching
1	Control	none	none	included
2	BC1-N	BC_1	none	included
3	BC1-N+CA	BC_1	included	included
4	BC2-N	BC_2	none	included
5	BC2-N+CA	BC_2	included	included
6	Control	none	none	none
7	BC1-N	BC_1	none	none
8	BC1-N+CA	BC_1	included	none
9	BC2-N	BC_2	none	none
10	BC2-N+CA	BC_2	included	none

2.2.2. Porewater sampling

Three hours before sampling, pots were adjusted to 60% WHC. Syringes with a volume of 10 ml were connected to the sampling ports. The plug was drawn up to 10 ml to apply negative pressure in the port and a wooden stick was installed to fix the plug of the syringe. Porewater was sampled (0.5-5 ml) for a duration of 1.5 hours and directly transferred to 2 ml reaction vessels and kept on wet ice in the greenhouse before permanent storage at -18 °C. Porewater samples were taken on day 2, 7, 17, 21, 32, 41, 47 and 61. On day 17, porewater was not sampled in pots that received a leaching treatment, as the water content in the soil was > 60% WHC, which would have biased the comparison of porewater concentrations from these samples with those sampled on other days.

2.2.3. Leaching event

Eight days after pot setup, a leaching event to simulate heavy precipitation was conducted for Treatments with ID 6-10 (Table 1). Pots, previously adjusted to 75% WHC, were placed on a plastic bucket and stepwise leached with a total of 200 ml DI water during 1 hour, equal to ~20 l m⁻² when related to the soil surface. After drainage had stopped, the leachate weight was recorded before filtration to < 0.45 µm. Leachates were kept on wet ice in the greenhouse before storage at -18 °C until further analysis.

2.2.4. Biomass harvest and analysis

Aboveground spinach biomass was harvested on day 43 and 63 by cutting spinach leaves 2 cm above soil level, leaving behind smaller leaves (< 5 cm) and the shoot axis on soil level to allow further growth in the following. Fresh weights were directly recorded to 10 mg accuracy and dry weights after drying to mass consistency at 80 °C to 1 mg accuracy. Aboveground spinach biomass was milled to < 1 mm (ZM200, Retsch GmbH) and analyzed without further preparation for N contents (CN928, LECO Corporation, St. Joseph, USA) and for contents of phosphorus (P), potassium (K), magnesium (Mg), sulfur (S), calcium (Ca), manganese (Mn), copper (Cu) and zinc (Zn) after digestion of 120 mg biomass with 3 ml of a 65% HNO₃ and 2 ml of a H₂O₂ in a microwave for 15 minutes at 180 °C (15 minute ramp to 180 °C, Mars 5 Xpress, CEM GmbH, Kamp-Lintfort, Germany) with subsequent analysis of the digests via Inductively Coupled Plasma Optical Emission Spectroscopy (ICP-OES, icap 7000 series, Thermo Scientific, Waltham, MA, USA). Root biomass was separated from the soil on day 64, washed in well water to remove soil particles and dried to mass consistency at 80 °C.

2.2.5. Analysis of soil pore water and leachates

Soil pore water was analyzed for nitrate (NO_3^-) in 96-well microtiter plates¹⁸ using a plate reader (Epoch2, Biotek Instruments, Winooski, USA). The calibration curve was derived from KNO_3 diluted to 0-2.5 mg N l⁻¹ in ultrapure water. Solubilized phosphate (PO_4^{3-}) was analyzed in 96-well microtiter plates following D'Angelo et al.¹⁹ using KH_2PO_4 as standard diluted in ultrapure water to 0-1 mg P l⁻¹. All chemicals were of analytical grade and either purchased from Carl Roth GmbH & Co. KG, Karlsruhe, Germany or Merck KGaA, Darmstadt, Germany. Leachates were analyzed for NO_3^- as described above and further analyzed for P, K, Mg, S and Ca via ICP-OES, as described above and pH was measured as well.

2.2.6. Soil geochemical analysis

Most soil was sampled from each pot during root excavation and manually homogenized for 1 minute. A subsample of 50 ml was taken and stored on wet ice and subsequently at -18 °C. Fresh soil samples (25 g) were weighed into 250 ml Nalgene bottles and extracted with 100 ml of a 0.0125 M CaCl_2 on a rotary shaker at 150 rpm for 1 hour following DIN 19746²⁰. The extract was filtered through ashless filter paper and the filter including decanted soil and biochar particles was put back in the extraction bottle. The extraction procedure was repeated twice as described above but with each fresh 1 M KCl added for extraction of 1 hour and subsequent 24 hours. All filtrates were further filtered to < 0.45 μm and stored at -18 °C. Nitrate in filtrates was quantified as described above using standards prepared with ultrapure water for diluted 0.0125 M CaCl_2 extracts or with 0.25 M KCl or 1 M KCl for KCl extracts measured either with four-fold or without any dilution, respectively. Ammonium (NH_4^+) was quantified in filtrates with a modified Berthelot reaction in 96-well microtiter plates²¹. Standards were prepared from $(\text{NH}_4)_2\text{SO}_4$ either in ultrapure water for 0.0125 M CaCl_2 extracts or 1 M KCl for KCl extracts, both measured without dilution. The bottles were weighed before each extraction step with 1 M KCl to correct for already extracted N by knowing tare weights of bottles and filter papers.

2.2.7. Statistical analysis

All data analysis and visualization were performed with GraphPad Prism (version 10.4.1, GraphPad Software LLC, Boston MA, USA). Nitrate release from BBF to phosphate buffer (cf. section 2.1.3) was modelled using the 'one phase association' model in Prism. Aboveground biomass yield for individual fractions (1st harvest, 2nd harvest and total harvest) was analyzed with one-way analysis of variance (ANOVA) separately for treatment groups with or without a leaching event. Cumulative nutrient uptakes were analyzed using two-way ANOVA with the

factors ‘Treatment’ and ‘Leaching’ and significant differences between individual treatments obtained from Tukey’s post-hoc test at $\alpha=0.05$ are only reported within the individual leaching groups (Treatment ID1-5 and ID6-10, Table 1). Nutrient leaching was analyzed by one-way ANOVA followed by Tukey’s post-hoc test. Average NO_3^- and PO_4^{3-} concentrations in soil pore water were obtained by integration of concentrations over time using the ‘Area under Curve’ tool in Prism (concentrations on individual days were connected using a linear model) and the net area was divided by the total number of days between first and last porewater sampling. Averaged porewater concentrations were analyzed with one-way ANOVA for each leaching group separately followed by Tukey’s post-hoc test. Block effects for all ANOVAs were considered with the repeated measured function implemented in GraphPad Prism.

3. Results

3.1. Biochar properties and NO_3^- release

Both biochars had relatively similar properties with low molar H/C ratios of 0.18-0.23, pH of 8.6-9.1 and low specific surface area (SSA) based on N_2 sorption compared to CO_2 sorption (Table 2).

For BC1-N, 93% of spiked NO_3^- was already released to the phosphate buffer after 5 minutes, while BC1-N+CA only released 83% during that time (Figure 1a). Nitrate release stabilized at 97% for BC1-N and 89% for BC1-N+CA (Figure 1a and Table S 4). The release from BC2 was in general lower as compared to BC1-N (Figure 1a). Release from BC2-N was 87% after 5 minutes and only 71% of NO_3^- were released from BC2-N+CA up to that time (Figure 1a). Nitrate release stabilized at 95% for BC2-N and at 77% for BC2-N+CA (Figure 1a and Table S 4). Averaged 4 mg N g^{-1} remained non-released in BC2-N+CA and 2 mg N g^{-1} in BC1-N+CA (Figure 1b). Non-acidified BC1-N and BC2-N only retained between 0.1 and 0.7 mg N g^{-1} after the extraction experiment (Figure 1b).

Table 2: Carbon (C), hydrogen (H), nitrogen (N) and sulfur (S) contents, molar H/C ratios, pH and specific surface area (SSA) derived from CO_2 and N_2 sorption of two different wood-based biochars (BC1 and BC2).

	C [%]	H [%]	N [%]	S [%]	H/C	pH	N_2 -SSA [$\text{m}^2 \text{ g}^{-1}$]	CO_2 -SSA [$\text{m}^2 \text{ g}^{-1}$]
BC1	93.3	1.4	0.3	<0.03	0.18	9.1	21	358
BC2	89.1	1.7	0.6	<0.03	0.23	8.6	9	388

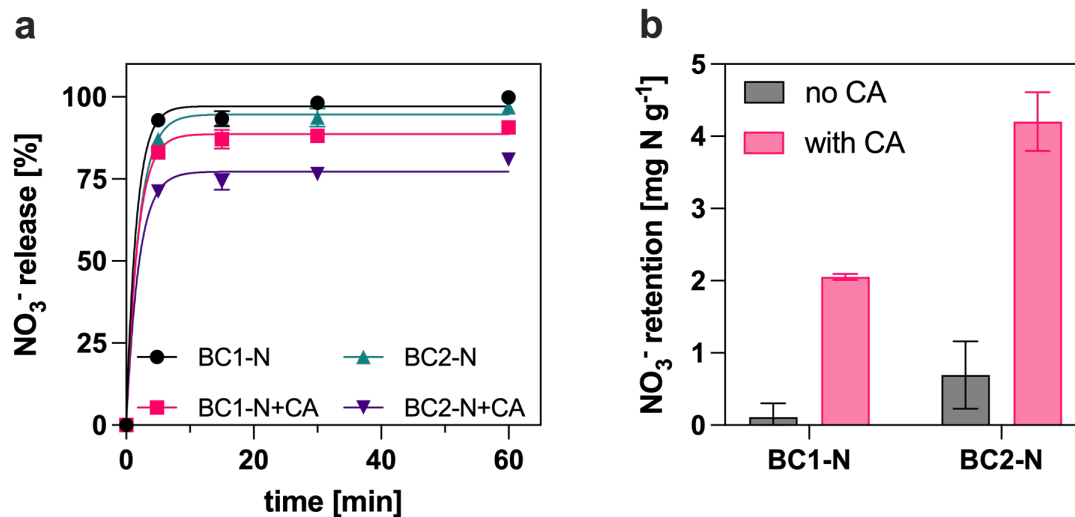


Figure 1: (a) Nitrate (NO_3^-) release from two NO_3^- enriched biochars (BC1-N and BC2-N) in percent of initial NO_3^- content during 1 hour. Nitrate enrichment was also combined with an acidification treatment using citric acid (BC1-N+CA and BC2-N+CA). (b) Retained NO_3^- in biochars that was not released during 1 hour of extraction. Release experiment was performed in a 0.2 M phosphate buffer adjusted to pH 7.0. Error bars indicate the standard deviation of three replicates. Model parameters from panel a can be found in Table S 4.

3.2. Spinach growth

In absence of leaching events, yield of aboveground spinach biomass was not significantly changed by any biochar amendment compared to the Control during both harvests and total harvests ranged between 7.8 and 8.1 g pot⁻¹ (Figure 2a). With the first harvest, soil amendment with BC2-N+CA significantly reduced spinach yield compared to soil amended with BC2-N ($p=0.018$, Figure 2a). Plants grown on BC2-N+CA amended soil yielded higher spinach biomass with the second compared to the first harvest, which was not observed for all other treatments (Figure 2a). The leaching treatment significantly decreased total aboveground spinach yields (Figure 2b and Table S 5). With the leaching treatment, total aboveground spinach yields were up to 20% higher for all plants grown on biochar-amended soil compared to the Control, but there were no significant differences between individual biochar treatments (Figure 2b). In leached soil amended with BC1-N+CA, spinach yields were significantly higher with the first harvest compared to the Control ($p=0.021$) and during the second harvest, soil under BC2-N+CA management increased yields significantly compared to both the Control ($p < 0.001$) and BC1-N+CA amended soil ($p = 0.008$, Figure 2b). Only plants grown on soil with BC2-N+CA yielded biomass in a similar range with the second harvest compared to the

first, while all other treatments generally had lower yields with the second harvest under leaching conditions (Figure 2b). Root biomass yields were not significantly changed with any soil amendment or by leaching (Figure S 5).

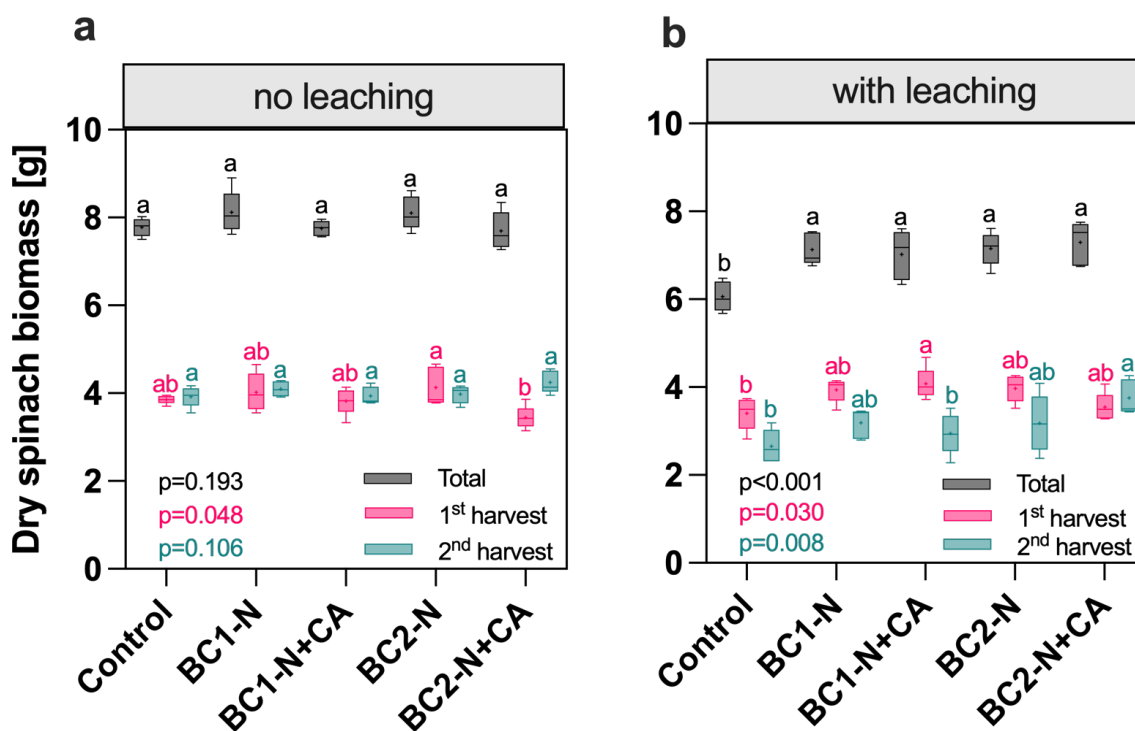


Figure 2: Aboveground dry spinach biomass harvested with two individual harvests (total yield and yield separated by each harvest). Plants were cultivated without (a) or with (b) a leaching event 9 days after sowing. The soil was either amended without (Control) or with two different biochars at 1.5% (w/w, BC1 and BC2). Biochars were enriched with 2.2% nitrogen (N) as KNO_3 (BC1-N and BC2-N). These N-enriched biochars were also applied after enrichment with citric acid (BC1-N+CA and BC2-N+CA). Whiskers in boxplots represent the minimum to maximum value of five replicates for each treatment, mean values are indicated with “+”, different letters indicate a significant difference between the treatments within each harvested fraction (one-way analysis of variance, Tukey’s post hoc test, $p < 0.05$).

In absence of leaching, total N uptake with aboveground biomass decreased significantly from 389 mg pot⁻¹ in the Control to 348 mg pot⁻¹ with BC2-N+CA amended soil ($p=0.002$), while all other BBF amendments did not significantly change N uptakes compared to the Control (Figure 3a). Further, plants grown on soil under BC2-N+CA management without leaching had 9% lower N uptake compared to BC2-N amendment ($p=0.001$, Figure 3a), which was related to lower uptakes with the first harvest (Figure S 11). Leaching decreased N uptakes in all treatments, especially for the Control to 255 mg pot⁻¹ (Figure 3a). All plants grown on biochar-amended soil had with 300-313 mg pot⁻¹ significantly higher N uptake compared to the Control

under leaching conditions (Figure 3a). Phosphorus uptakes were similar for all treatments either with or without leaching compared to the Control, only BC1-N+CA amended soil increased P uptake in plants compared to plants grown in the Control group with a leaching event (Figure 3b). Further, plants grown on BC2-N+CA amended soil had significantly lower P uptakes compared to BC2-N management in absence of leaching (-19%, $p=0.002$, Figure 3b). Similarly, S uptakes were not significantly changed compared to the Control with any biochar amendment in presence or absence of leaching, but soil management with BC2-N+CA significantly decreased S uptakes by up to 17% compared to all other biochar amendments to soil in absence of a leaching event (Figure 3c).

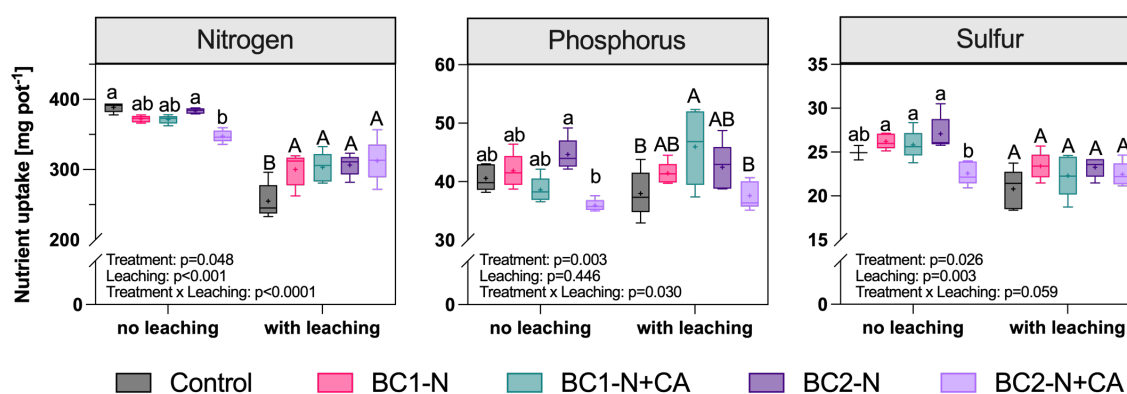


Figure 3: Uptake of nutrients in aboveground spinach biomass: nitrogen (a), phosphorus (b) and sulfur (c). The soil was either amended without (Control) or with two different biochars at 1.5% (w/w, BC1 and BC2). Biochars were enriched with 2.2% nitrogen (N) as KNO_3 (BC1-N and BC2-N). These N-enriched biochars were also applied after enrichment with citric acid (BC1-N+CA and BC2-N+CA). The soil in the Control treatment was spiked with similar amount of KNO_3 . Whiskers in boxplots represent the minimum to maximum value of five replicates for each treatment, mean values are indicated with “+”, different letters indicate a significant difference between the treatments within each leaching group (lowercase letters for ‘no leaching’, capital letters for ‘leaching’, two-way analysis of variance, Tukey’s post hoc test, $p < 0.05$).

3.3. Nutrient leaching and porewater analysis

Leaching of NO_3^- decreased with all biochar amendments to soil in the range of 40-70% compared to the Control, which was most pronounced for BC2-N+CA ($p = 0.004$) and BC1-N+CA ($p = 0.006$, Figure 4). There was no significant difference between non-acidified or acidified BC1 or BC2, respectively (Figure 4). Still, acidification decreased data scattering of NO_3^- leaching for both biochars and for BC1, NO_3^- leaching was only significantly reduced compared to the Control with the acidification treatment (Figure 4). All biochar treatments reduced K leaching significantly compared to the Control and BC2-N+CA amendment consistently reduced leaching of P, Mg, S and Ca compared to the control (Figure S 9).

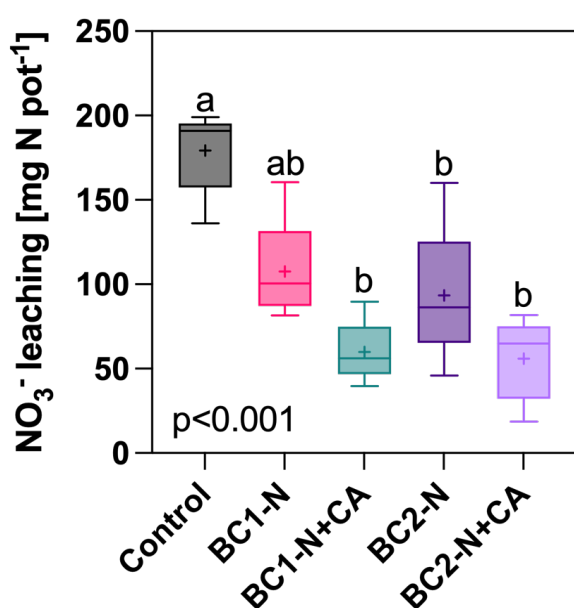


Figure 4: Nitrate (NO_3^-) leaching during simulated heavy precipitation (20 l m^{-2}) 9 days after experimental setup. The soil was either amended without (Control) or with two different biochars at 1.5% (w/w, BC1 and BC2). Biochars were enriched with 2.2% nitrogen (N) as KNO_3 (BC1-N and BC2-N). These N-enriched biochars were also applied after enrichment with citric acid (BC1-N+CA and BC2-N+CA). The soil in the Control treatment was spiked with similar amount of KNO_3 , equal to $400 \text{ mg N pot}^{-1}$. Whiskers in boxplots represent the minimum to maximum value of five replicates for each treatment, mean values are indicated with “+”, different letters indicate a significant difference between the treatments (one-way analysis of variance, Tukey’s post hoc test, $p < 0.05$).

Nitrate porewater concentrations were highest during the first 20 days in absence of a leaching event ($500\text{-}900 \text{ mg N l}^{-1}$) and gradually decreased from day 20 onwards towards 0 mg N l^{-1} , as aboveground biomass production increased (Figure 5a). Without a leaching treatment, averaged porewater NO_3^- concentration were significantly lower in both BC1 amended soils compared

to the Control during the whole trial and soil amended with either BC1 treatment had lower concentrations compared to treatments with BC2, but not significantly (Figure 5b). The decrease in NO_3^- concentrations in absence of leaching was significant for BC1-N on day 2, 7 and 17 and for BC1-N+CA on day 2 and 7 compared to the Control ($p < 0.05$), while treatments with either BC2 amendment did not differ significantly compared to the Control on individual measurement days (Figure 5a). The ratio of N uptake in aboveground biomass to average NO_3^- porewater concentrations was 90% higher in both BC1 amended soils compared to the Control and also 60% higher compared to both treatments that included a BC2 amendment, in absence of a leaching treatment (Figure 5c).

Following the leaching event, porewater NO_3^- concentrations increased in all biochar-amended soils while they remained at the same level in the Control compared to pre-leaching concentration (Figure 5b). In soil amended with BC1-N and BC1-N+CA, the decrease in NO_3^- concentrations, e.g., due to plant N uptake or re-sorption of released NO_3^- during the leaching event occurred earlier, i.e., between day 21 and 32, compared to BC2 amended soils (Figure 5b). Still, NO_3^- concentrations were not significantly different from each other for all treatments on individual days following the leaching event. Further, averaged NO_3^- concentrations during the whole experiment were not significantly different from each other during the whole experiment (Figure 5d).

Phosphate concentrations in porewater were significantly higher in pots amended with BC1-N compared to the Control on day 2 ($p = 0.009$), which was not the case for acidified BC1-N+CA (Figure 6a). Further, the amendment of BC2-N+CA significantly decreased PO_4^{3-} concentrations compared to the Control on the same day ($p < 0.0001$), also compared to soil amended with non-acidified BC2-N ($p < 0.0001$, Figure 6a). On day 7, soil under BC2-N+CA management had significantly lower PO_4^{3-} concentrations compared to BC1-N ($p = 0.001$) while in the following, no significant differences were observed between the different treatments without a leaching event and concentrations generally decreased after 20 days, as was observed for NO_3^- concentrations before (Figure 6a). Averaged PO_4^{3-} concentrations tended to be higher with BC1-N compared to the control and tended to be lowest with BC2-N+CA in absence of a leaching event (Figure S 12a). After the leaching event, porewater PO_4^{3-} concentrations were generally lowest in BC2-N+CA amended soil which was significant compared to the Control ($p = 0.040$) and compared to BC2-N ($p = 0.021$) on day 21. With leaching, averaged PO_4^{3-} concentrations during the whole experiment were not significantly changed with any BBF amendment compared to the control, only BC2-N+CA reduced them significantly compared to BC1-N (Figure S 12b).

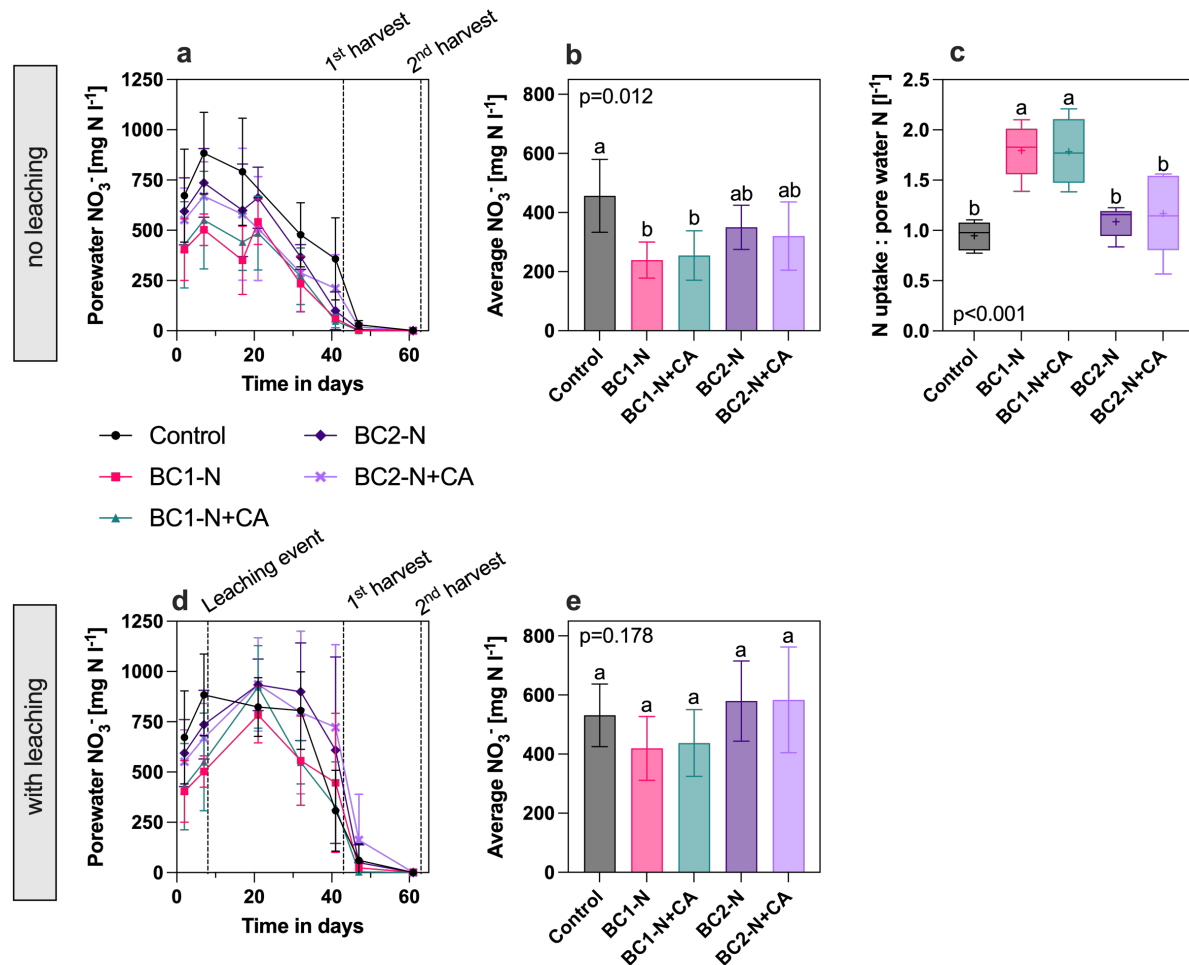


Figure 5: Nitrate (NO_3^-) concentration in porewater during spinach cultivation (over time and averaged for the whole experiment duration) without or with a leaching event after 9 days (panel a+b and d+e, respectively). Nitrogen (N) uptake with aboveground spinach biomass related to the averaged NO_3^- -N concentration in porewater during the whole cultivation period in absence of leaching (panel c). The soil was either amended without (Control) or with two different biochars at 1.5% (w/w, BC1 and BC2). Biochars were enriched with 2.2% N as KNO_3 (BC1-N and BC2-N). These N-enriched biochars were also applied after enrichment with citric acid (BC1-N+CA and BC2-N+CA). The soil in the Control treatment was spiked with similar amount of KNO_3 . Error bars in panel a and b indicate the standard deviation of ten replicates on day 2 and 7 and five replicates for the following days. Whiskers in boxplots (panels c and d) represent the minimum to maximum value of five replicates for each treatment, mean values are indicated with “+”, different letters indicate a significant difference between the treatments (one-way analysis of variance, Tukey’s post hoc test, $p < 0.05$).

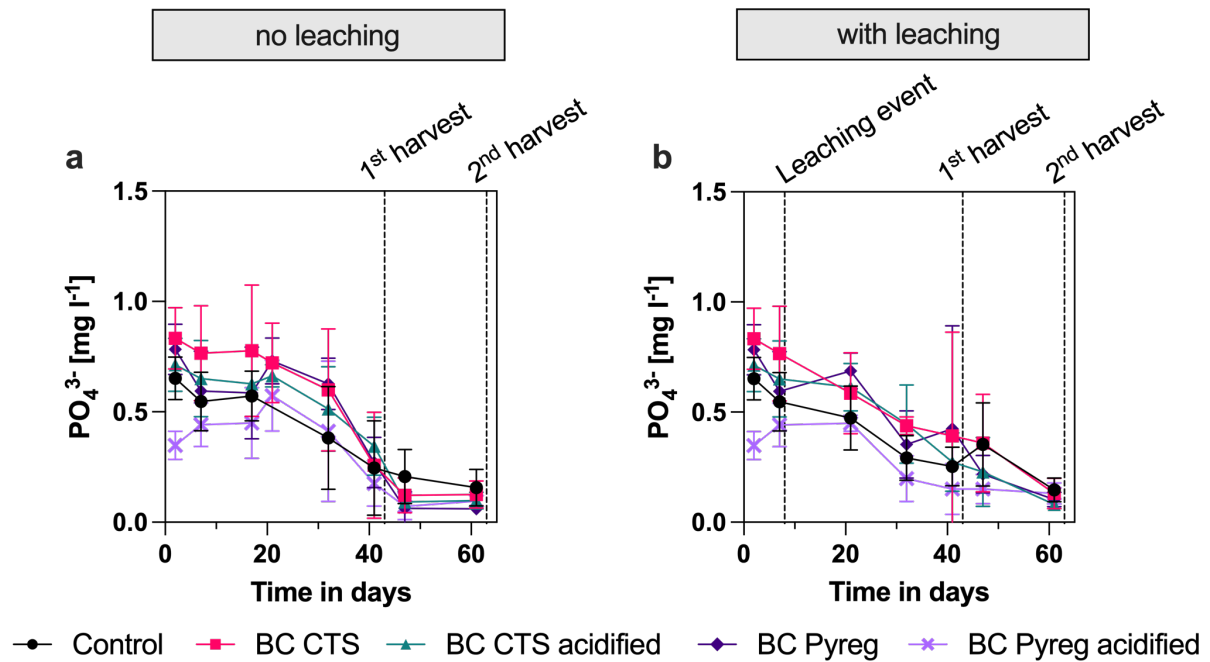


Figure 6: Phosphate solubilized in soil pore water in pots without a leaching event (a) and with one leaching event after 9 days (b). The soil was either amended without (Control) or with two different biochars at 1.5% (w/w, BC1 and BC2). Biochars were enriched with 2.2% nitrogen (N) as KNO_3 (BC1-N and BC2-N). These N-enriched biochars were also applied after enrichment with citric acid (BC1-N+CA and BC2-N+CA). The soil in the Control treatment was spiked with similar amount of KNO_3 . Error bars in panel a and b indicate the standard deviation of ten replicates on day 2 and 7 and five replicates for the following days.

3.4. Soil pH, extractable N in soil after harvest and N balance

The leaching event reduced soil pH values, independent of the soil amendment ($p=0.003$, Figure 7a). After harvest, soils amended with BC2-N+CA had pH values around 8.0-8.1, which was significantly higher compared to all other treatments including the Control, which had pH values in the range of 7.7-7.8 (Figure 7a). Soils amended with similar amounts of citric acid as added via BC1-N+CA and BC2-N+CA had slightly increased pH compared to the Control, which was more pronounced with the higher amount of added CA, which equaled the CA amendment via BC2-N+CA (Figure 7b). These increases in soil pH due to acidified BBF were mirrored by pH values in leachates obtained 9 days after experimental setup (Figure S 10). In absence of leaching, total, mineral extractable N, as sum of NH_4^+ and NO_3^- , ranged between 8 and $10.5 \text{ mg } (100\text{g})^{-1}$ and was significantly higher in BC2-N+CA amended soil compared to the Control ($p = 0.044$, Figure 8a). The BC1-N+CA amendment decreased total extractable N compared to the BC1-N treatment without acidification ($p = 0.013$, Figure 8a). Most N was extracted during 1 hour in 0.1 M $CaCl_2$ and the following extraction steps in 1 M KCl only

contributed further 10-20% of total extracted N (Figure 8a). Ammonium only contributed around 10% to total extractable N in all treatments without leaching.

The leaching treatment reduced total N concentrations to 0.3 mg (100g)⁻¹ in the Control treatment and to 1-1.3 mg (100g)⁻¹ in biochar-amended treatments (Figure 8b). Thus, extractable N contents were significantly higher in biochar-amended soil compared to the Control when leaching was included, especially for BC1-N+CA and both BC2-amended treatments (Figure 8b). In the Control, almost all N was already extracted during 1 hour with 0.01 M CaCl₂, while in all biochar-amended treatments, N release was delayed to later extraction steps in 1 M KCl (Figure 8b).

Recovery of N in soil and aboveground biomass ranged between 95% and 100% for all treatments when leaching was included (Figure 9a). With leaching, 89% of N were recovered for the Control while the recovery of N in soil, aboveground biomass and leachate decreased to 77% with acidified BBF (Figure 9b).

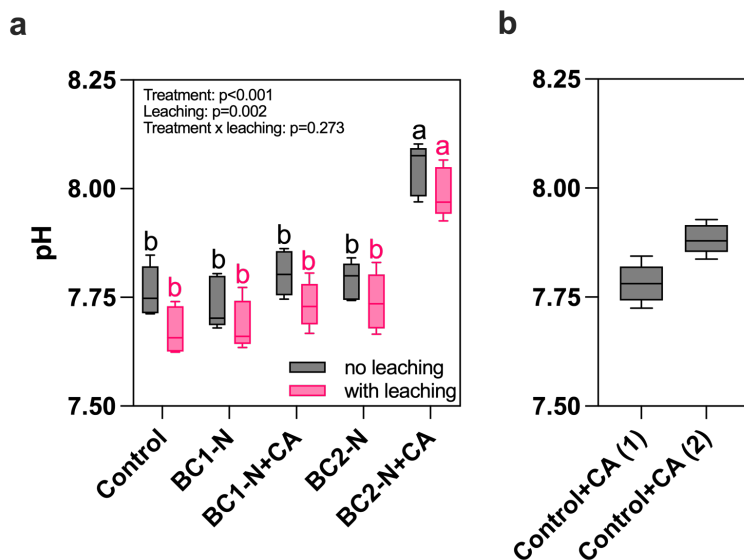


Figure 7: (a) Soil pH after harvest in pots with or without a leaching event and (b) in pots that received the similar amount of citric acid (CA) as with BC1-N+CA and BC2-N+CA amendments (Control+CA(1) equals CA amendment via BC1-N+CA and Control+CA(2) equals CA amendment via BC2-N+CA). The soil was either amended without (Control) or with two different biochars at 1.5% (w/w, BC1 and BC2). Biochars were enriched with 2.2% nitrogen (N) as KNO₃ (BC1-N and BC2-N). These N-enriched biochars were also applied after enrichment with CA (BC1-N+CA and BC2-N+CA). The soil in the Control treatment was spiked with similar amount of KNO₃. Whiskers in boxplots represent the minimum to maximum value of five replicates for each treatment, mean values are indicated with “+”, different letters indicate a significant difference between the treatments within leaching groups (two-way analysis of variance, Tukey’s post hoc test, $p < 0.05$).

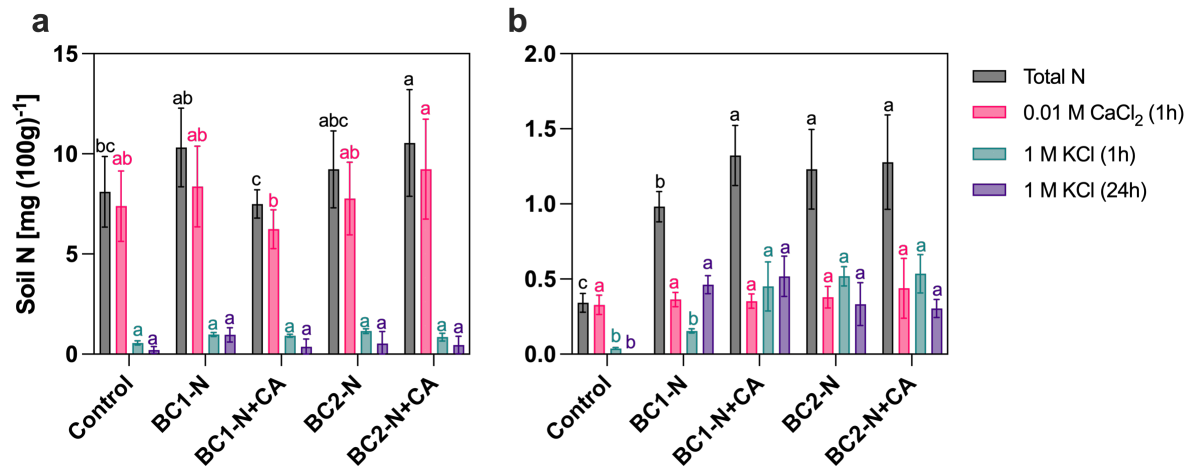


Figure 8: Extractable mineral nitrogen (N, sum of ammonium and nitrate) in soil samples taken during spinach harvest. Soil samples were sequentially extracted in either 0.01 M CaCl₂ for 1 hour or in 1 M KCl both for 1 hour or 24 hours. The soil was either amended without (Control) or with two different biochars at 1.5% (w/w, BC1 and BC2). Biochars were enriched with 2.2% nitrogen (N) as KNO₃ (BC1-N and BC2-N). These N-enriched biochars were also applied after enrichment with citric acid (BC1-N+CA and BC2-N+CA). The soil in the Control treatment was spiked with similar amount of KNO₃. Error bars indicate the standard deviation of five replicates. Different letters above error bars indicate significant differences within each N extraction step (two-way analysis of variance, Tukey's post-hoc test, $p < 0.05$). Please note the different axis scale in panel a and b.

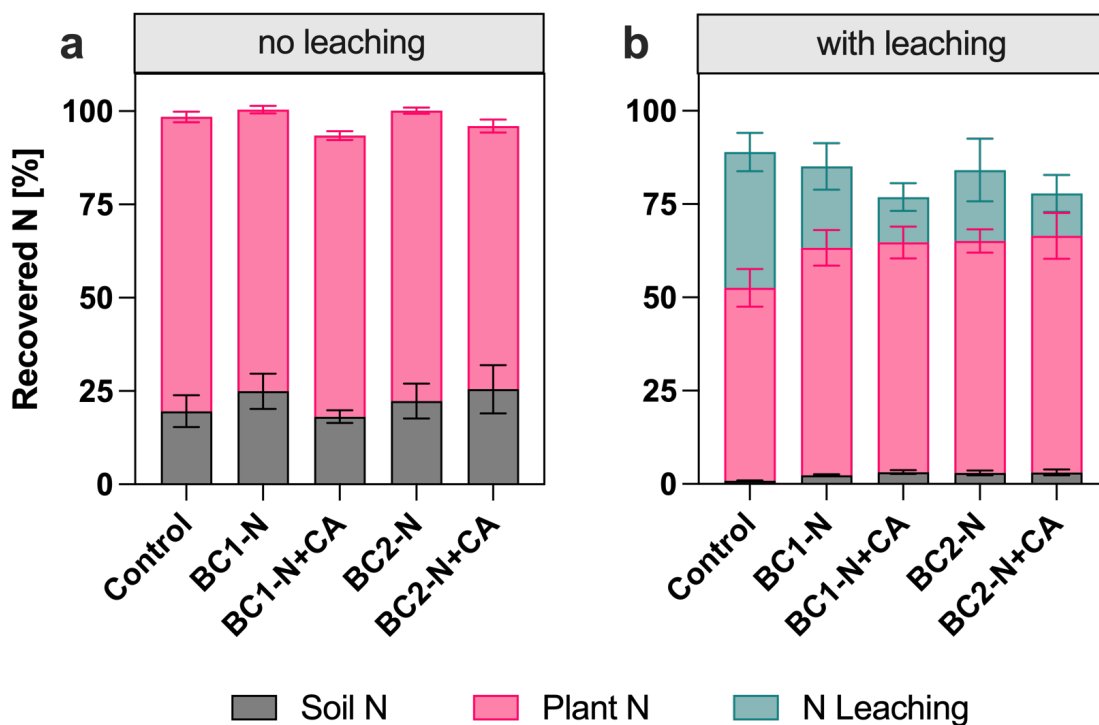


Figure 9: Recovered nitrogen (N) in soil after harvest (sum of ammonium and nitrate) in aboveground spinach biomass and in leachate as a fraction of the sum of total fertilized N and native mineral N in soil at the beginning of the experiment (total of 493 mg pot⁻¹) for cultivation without (a) or with a leaching event after 9 days (b). The soil was either amended without (Control) or with two different biochars at 1.5% (w/w, BC1 and BC2). Biochars were enriched with 2.2% N as KNO₃ (BC1-N and BC2-N). These N-enriched biochars were also applied after enrichment with citric acid (BC1-N+CA and BC2-N+CA). The soil in the Control treatment was spiked with similar amount of KNO₃. Error bars indicate the standard deviation of five replicates.

4. Discussion

This study investigated the potential of biochar acidification as a modification technique to reduce NO₃⁻ leaching from BBF amended soil. In simple release experiments in a phosphate buffer at pH 7, the acidification treatment decreased NO₃⁻ release from BBF, indicating that sorption of NO₃⁻ to acidified biochar was improved. In the greenhouse experiment, liquid nutrient enrichment of biochar alone without citric acid addition already decreased NO₃⁻ leaching during the heavy precipitation event by 40-48% compared to the Control, yet not significantly for BC1-N. With acidification, NO₃⁻ leaching was reduced significantly by 70% for both BBF compared to the Control, indicating that acidification can be a tool to improve NO₃⁻ retention in BBF-amended soil. The lower leaching loss with acidified BBF compared to non-acidified BBF were not predictable from NO₃⁻ concentrations in porewater, which were

similar for acidified or non-acidified BBF. Nitrate concentrations in porewater were rather influenced by the biochar type, as concentrations in soil amended with BBF prepared from BC1 were lower compared to those prepared from BC2 during the whole experiment in absence of leaching. The general differences in terms of NO_3^- release to the porewater between BC1 and BC2 are not explainable with biochar characteristics quantified in the present study, as both biochars had similar elemental composition and specific surface area (Table 2). In absence of leaching, the lower NO_3^- porewater concentrations in combination with similar spinach yield resulted in the highest ratio of N uptake related to NO_3^- porewater concentrations for spinach grown on soils amended with BBF produced from BC1, i.e., these treatments facilitated the highest N uptake in combination with the lowest overall risk for NO_3^- leaching. In combination with a leaching event, NO_3^- concentrations in porewater were generally higher, i.e., a higher mobilization of NO_3^- occurred likely due to the higher temporarily water content in soils.

Cumulative aboveground spinach yields were not affected by any amendment in absence of leaching but increased compared to the Control with all BBF amendments following the leaching event, reflecting the lower NO_3^- losses via leaching. The lower NO_3^- leaching losses from soil amended with acidified BBF were not translated to higher biomass yield or N uptakes compared to soil amended with non-acidified BBF. In absence of leaching, immobilization of N, P and S were indicated with acidified BBF produced from BC2, as indicated by lower cumulative nutrient uptakes in aboveground biomass, which was due to P and S deficiency as indicated by lower contents in spinach tissue. Phosphorus and S are mainly taken up by plants as phosphate and sulphate²². While non-acidified biochars, especially BC1-N, rather increased PO_4^{3-} concentrations in porewater, in line with literature²³, BC2-N+CA consistently decreased PO_4^{3-} concentrations compared to BC2-N (Figure 6a), which explains the lower P contents in spinach biomass and overall lower biomass growth on BC2-N+CA amended soil. The SO_4^{2-} porewater concentrations might have been affected in a similar way by BC2-N+CA amendment, but those were not quantified in the present study. The immobilization of PO_4^{3-} and the parallel release of NO_3^- in BC2-N+CA amended soil indicated that the effect of acidification on increasing sorption of anions to biochar remained after the initial release of NO_3^- , especially under drier conditions, i.e. in absence of a leaching event. This was not observed for BC1-N+CA, as BC1 generally provided a slower release of NO_3^- to the porewater, which might have limited potential sorption of other anions, such as PO_4^{3-} , from porewater.

While N recoveries in soil and harvested biomass for pots without a leaching treatment were close to 100%, recoveries were only 77-90% for treatments including leaching and they were at the lower end for pots that were amended with an acidified BBF. Denitrification-related

losses of N via N_2O or N_2 emissions might have been generally higher for pots with a leaching treatment, since the temporarily higher water content in soil likely caused anoxic conditions, which favored denitrification²⁴. However, losses via N_2O emissions may not explain the major difference between N recoveries observed between leaching and no leaching treatments, as they usually only make up 0.5-2% of total fertilized N²⁵. Yet, even lower N recoveries with acidified BBF and leaching treatment highlight the need for further research to find out, if the application of acidified BBF promotes the loss of N via denitrification. In a microcosm study, the acidification of biochar to pH 5.6, which represented the soil pH the biochar was applied to, increased N_2O emissions slightly compared to non-acidified, wood-based biochars²⁶. Further, the addition of citrate via acidified BBF as a low-molecular weight and thus labile source of carbon might have further promoted N_2O and N_2 emissions via denitrification²⁷. It is unlikely that the non-recovered N in pots that received leaching remained non-extractable in soil as the extractants were capable to recover approximately the tenfold amount of N from soils that were not subject to leaching (Figure 8). The general lower N recoveries in presence of leaching might also be related to analytical imprecision during NO_3^- quantification in leachates, as a dilution factor of 2000 had to be applied.

With BC1-N+CA and BC2-N+CA, 30 and 150 kg ha^{-1} of citric acid, respectively, would have been applied to soil at a biochar application rate of 2 t ha^{-1} in addition to 44 kg N ha^{-1} and 120 kg K ha^{-1} . For BC2, a significantly higher amount of citric acid was needed compared to BC1 to adjust its pH to ~ 4.5 , thus, BC2 had a higher alkalinity compared to BC1. Differences in biochar alkalinity despite ash contents and bulk pH values in a similar range can be confirmed by literature²⁸. As a side effect, the high amount of citric acid added with BC2-N+CA increased soil pH significantly compared to all other treatments. This increase in soil pH was most likely related to the microbial decarboxylation of citrate, which consumes H^+ ions²⁹. This was already observed for citrate additions to soil in the range of 0.25-1 mM (100g)⁻¹ which applies to citrate addition to soil via acidified BC2-N+CA (0.6 mM (100g)⁻¹)²⁹. This process occurs within 24 hours after soil application²⁹, which raises the probability that it was also the main mechanism of the pH increase in our experiment as the pH shift was already visible in leachates obtained after 9 days (Figure S 10). Such an increase in soil pH for an already rather alkaline soil, as used in this study, is not desired. Alternatively, inorganic acids could be used for biochar acidification. Here, HNO_3 would be the most obvious one for production of an acidified BBF, as acidification and NO_3^- enrichment of biochar could be achieved simultaneously while additional N might be added e.g., via KNO_3 . This would prevent the above discussed increase in soil pH and would also present a more cost-effective method for biochar acidification, as

HNO₃ is less expensive compared to citric acid and is a stronger acid, i.e. lower amounts would be needed to adjust pH of biochar. Further, via the usage of HNO₃ for acidification, the introduction of a negatively charged corresponding base (e.g., citrate) that competes with NO₃⁻ for sorption sites on the biochar surface could be avoided, which might further improve the NO₃⁻ retention in acidified BBF.

5. Conclusion

Citric acid treated BBF reduced NO₃⁻ leaching to the highest extent compared to fertilized soil without any biochar application. Thus, acidification might be a tool to increase the effectivity of biochar to improve NO₃⁻ retention in soil. However, in absence of a leaching event, i.e., under dryer conditions, acidification decreased the uptake of N, P and S in spinach plants for one of the biochars used. This highlights the need for further research on this modification technique. Further we propose to use HNO₃ for production of acidified and NO₃⁻ enriched BBF as a more cost-effective tool and with less environmental side effects of the acidified BBF, such as soil pH increase. The effect of biochar acidification on nitrate leaching should further be tested in different soil types varying in pH in combination with measurements on soil-borne N₂O emissions, as N recoveries in soil, plant tissue and leachate were lower for treatments that included an acidified BBF, indicating a potential higher loss of N from soil via denitrification.

References

1. Lin, B.-L., Sakoda, A., Shibasaki, R. & Suzuki, M. A Modelling Approach to Global Nitrate Leaching Caused by Anthropogenic Fertilisation. *Water Research* **35**, 1961–1968 (2001).
2. Wang, Y., Ying, H., Yin, Y., Zheng, H. & Cui, Z. Estimating soil nitrate leaching of nitrogen fertilizer from global meta-analysis. *Science of The Total Environment* **657**, 96–102 (2019).
3. Borchard, N. Biochar, soil and land-use interactions that reduce nitrate leaching and N₂O emissions: A meta-analysis. *Science of the Total Environment* **11** (2019).
4. Melo, L. C. A., Lehmann, J., Carneiro, J. S. da S. & Camps-Arbestain, M. Biochar-based fertilizer effects on crop productivity: a meta-analysis. *Plant Soil* (2022) doi:10.1007/s11104-021-05276-2.
5. Zhang, M. *et al.* Evaluating biochar and its modifications for the removal of ammonium, nitrate, and phosphate in water. *Water Research* **186**, 116303 (2020).
6. Hagemann, N. *et al.* Organic coating on biochar explains its nutrient retention and stimulation of soil fertility. *Nature Communications* **8**, 1089 (2017).
7. Haider, G. *et al.* Mineral nitrogen captured in field-aged biochar is plant-available. *Scientific Reports* **10**, 13816 (2020).
8. Borchard, N. *et al.* Physical activation of biochar and its meaning for soil fertility and nutrient leaching - a greenhouse experiment: Physical activation of biochar. *Soil Use and Management* **28**, 177–184 (2012).
9. Dieguez-Alonso, A. *et al.* Designing biochar properties through the blending of

- biomass feedstock with metals: Impact on oxyanions adsorption behavior. *Chemosphere* **214**, 743–753 (2019).
10. Wang, Z. *et al.* Biochar produced from oak sawdust by Lanthanum (La)-involved pyrolysis for adsorption of ammonium (NH₄⁺), nitrate (NO₃⁻), and phosphate (PO₄³⁻). *Chemosphere* **119**, 646–653 (2015).
 11. Zhang, M., Gao, B., Yao, Y., Xue, Y. & Inyang, M. Synthesis of porous MgO-biochar nanocomposites for removal of phosphate and nitrate from aqueous solutions. *Chemical Engineering Journal* **210**, 26–32 (2012).
 12. Chintala, R. *et al.* Nitrate sorption and desorption in biochars from fast pyrolysis. *Microporous and Mesoporous Materials* **179**, 250–257 (2013).
 13. Fidel, R. B., Laird, D. A. & Spokas, K. A. Sorption of ammonium and nitrate to biochars is electrostatic and pH-dependent. *Scientific Reports* **8**, 17627 (2018).
 14. Heaney, N., Ukpong, E. & Lin, C. Low-molecular-weight organic acids enable biochar to immobilize nitrate. *Chemosphere* **240**, 124872 (2020).
 15. EBC 2012-2024. ‘European Biochar Certificate - Guidelines for a Sustainable Production of Biochar.’ Carbon Standards International (CSI), Frick, Switzerland. (<http://european-biochar.org>). Version 10.4 from 20th Dec 2024. (2024).
 16. Grafmüller, J. *et al.* Granulation compared to co-application of biochar plus mineral fertilizer and its impacts on crop growth and nutrient leaching. *Sci Rep* **14**, 16555 (2024).
 17. Kammann, C. I. *et al.* Plant growth improvement mediated by nitrate capture in co-composted biochar. *Scientific Reports* **5**, 11080 (2015).
 18. Hood-Nowotny, R., Umana, N. H.-N., Inselbacher, E., Oswald- Lachouani, P. & Wanek, W. Alternative Methods for Measuring Inorganic, Organic, and Total Dissolved Nitrogen in Soil. *Soil Science Society of America Journal* **74**, 1018–1027 (2010).
 19. D’Angelo, E., Crutchfield, J. & Vandivere, M. Rapid, Sensitive, Microscale Determination of Phosphate in Water and Soil. *J of Env Quality* **30**, 2206–2209 (2001).
 20. DIN e.V. DIN 19746:2005-06, Bodenbeschaffenheit_ - Bestimmung von mineralischem Stickstoff (Nitrat und Ammonium) in Bodenprofilen (Nmin-Laborverfahren). (2005) doi:10.31030/9607286.
 21. Rhine, E. D., Mulvaney, R. L., Pratt, E. J. & Sims, G. K. Improving the Berthelot Reaction for Determining Ammonium in Soil Extracts and Water. *Soil Science Society of America Journal* **62**, 473 (1998).
 22. Amelung, W. *et al.* *Scheffer/Schachtschabel Lehrbuch der Bodenkunde*. (Springer Spektrum, Berlin, 2018).
 23. Gao, S., DeLuca, T. H. & Cleveland, C. C. Biochar additions alter phosphorus and nitrogen availability in agricultural ecosystems: A meta-analysis. *Science of The Total Environment* **654**, 463–472 (2019).
 24. Bateman, E. J. & Baggs, E. M. Contributions of nitrification and denitrification to N₂O emissions from soils at different water-filled pore space. *Biol Fertil Soils* **41**, 379–388 (2005).
 25. Shcherbak, I., Millar, N. & Robertson, G. P. Global metaanalysis of the nonlinear response of soil nitrous oxide (N₂O) emissions to fertilizer nitrogen. *Proc. Natl. Acad. Sci. U.S.A.* **111**, 9199–9204 (2014).
 26. Cayuela, M. L. *et al.* Biochar and denitrification in soils: when, how much and why does biochar reduce N₂O emissions? *Sci Rep* **3**, 1732 (2013).
 27. Senbayram, M. N₂O emission and the N₂O/(N₂O+N₂) product ratio of denitrification as controlled by available carbon substrates and nitrate concentrations. (2012).
 28. Fidel, R. B., Laird, D. A., Thompson, M. L. & Lawrinenko, M. Characterization and quantification of biochar alkalinity. *Chemosphere* **167**, 367–373 (2017).
 29. Yan, F., Schubert, S. & Mengel, K. Soil pH increase due to biological decarboxylation of organic anions. *Soil Biology and Biochemistry* **28**, 617–624 (1996).

Supplementary Information to:

**Citric acid treated biochar reduced nitrate leaching but impaired macronutrient uptake
in spinach, depending on biochar type**

Jannis Grafmüller^{1,2,3}, Daniel Kray¹, Nikolas Hagemann^{2,4}

¹Institute for Sustainable Energy Systems (INES), Offenburg University of Applied Sciences,
Offenburg, Germany

²Ithaka Institute, Arbaz (Switzerland) and Goldbach (Germany)

³Plant Biogeochemistry, Tübingen University, Tübingen, Germany

⁴Environmental Analytics, Agroscope Zurich, Zurich, Switzerland

Table S 1: Main characteristics of the soil used in the greenhouse study. Table structure reproduced with permission from Grafmüller et. al (2024), *Scientific Reports, Springer Nature*.

Parameter	Unit	Value	Method
Organic matter	wt% DM	4.2	DIN ISO 10694: 1996-08
Total Organic Carbon	wt% DM	2.4	DIN ISO 10694: 1996-08
pH	1	7.3	VDLUFA Methodenbuch Band I, Kapitel 5.1.1, 7.Teillieferung, 2016
Electric Conductivity	µS cm ⁻¹	142	VDLUFA Methodenbuch Band I, Kapitel 10.1.1, 1991
Salt content	mg(100g) ⁻¹ DM	75	VDLUFA Methodenbuch Band I, Kapitel 10.1.1, 1991
Total Nitrogen	wt% DM	0.25	DIN ISO 13878:1998-11
NH ₄ -N	mg(100g) ⁻¹ DM	0.11	VDLUFA Methodenbuch Band I, 3. Teillieferung, Kapitel 6.1.4.1, 2002
NO ₃ -N	mg(100g) ⁻¹ DM	7.68	VDLUFA Methodenbuch Band I, 3. Teillieferung, Kapitel 6.1.4.1, 2002
S _{min}	mg(100g) ⁻¹ DM	1.02	VDLUFA Methodenbuch I, A 6.3.1 (2016), Extraktion mit 0,0125 M CaCl ₂
Potassium (K)	mg(100g) ⁻¹ DM	27.2	Calcium lactate extract, VDLUFA Methodenbuch Band I, 6.Teillieferung, Kapitel 6.2.1.1, 2012
Phosphorus (P)	mg(100g) ⁻¹ DM	19.0	Calcium lactate extract, VDLUFA Methodenbuch Band I, 6.Teillieferung, Kapitel 6.2.1.1, 2012
Magnesium (Mg)	mg(100g) ⁻¹ DM	12.2	Calcium chloride extract, VDLUFA Methodenbuch Band I, Kapitel 6.2.4.1, 1991; ISO 22036:2008
Boron (B)	mgkg ⁻¹ DM	0.3	CAT extract, VDLUFA Methodenbuch Band I, 3. Teillieferung, Kapitel 6.4.1, 2002
Manganese (Mn)	mgkg ⁻¹ DM	12	CAT extract, VDLUFA Methodenbuch Band I, 3. Teillieferung, Kapitel 6.4.1, 2002
Copper (Cu)	mgkg ⁻¹ DM	3.9	CAT extract, VDLUFA Methodenbuch Band I, 3. Teillieferung, Kapitel 6.4.1, 2002
Zinc (Zn)	mgkg ⁻¹ DM	11	CAT extract, VDLUFA Methodenbuch Band I, 3. Teillieferung, Kapitel 6.4.1, 2002

Table S 2: Potential (pot.) and effective (eff.) cation exchange capacity of the soil used in the greenhouse study. Table structure reproduced with permission from Grafmüller et. al (2024), *Scientific Reports*, Springer Nature.

Parameter	Unit	Value	Method
Cation exchange capacity (eff.)	cmol ⁺ kg ⁻¹	18.0	DIN EN ISO 11260:2011-09
Exchange acidity	cmol ⁺ kg ⁻¹	<0.1	DIN EN ISO 11260:2011-09
Exchangable Mg (eff.)	cmol ⁺ kg ⁻¹	1.6	DIN EN ISO 11260:2011-09
Exchangable Ca (eff.)	cmol ⁺ kg ⁻¹	16.1	DIN EN ISO 11260:2011-09
Exchangable Na (eff.)	cmol ⁺ kg ⁻¹	<0.1	DIN EN ISO 11260:2011-09
Exchangable K (eff.)	cmol ⁺ kg ⁻¹	1.1	DIN EN ISO 11260:2011-09
Sum of exchangeable cations (eff.)	cmol ⁺ kg ⁻¹	18.8	DIN EN ISO 11260:2011-09
Cation exchange capacity (pot.)	cmol ⁺ kg ⁻¹	16.5	DIN ISO 13536: 1997-04
Exchangable Mg (pot.)	cmol ⁺ kg ⁻¹	1.7	DIN ISO 13536: 1997-04
Exchangable Ca (pot.)	cmol ⁺ kg ⁻¹	13.6	DIN ISO 13536: 1997-04
Exchangable Na (pot.)	cmol ⁺ kg ⁻¹	<0.1	DIN ISO 13536: 1997-04
Exchangable K (pot.)	cmol ⁺ kg ⁻¹	1.2	DIN ISO 13536: 1997-04
Sum of exchangeable cations (pot.)	cmol ⁺ kg ⁻¹	16.5	DIN ISO 13536: 1997-04

Table S 3: Particle size distribution and texture of the soil used for the greenhouse study. Table structure reproduced with permission from Grafmüller et. al (2024), *Scientific Reports*, Springer Nature.

Parameter	Unit	Value	Method
Clay (<2µm)	wt%	14	DIN ISO 11277:2002:08
Coarse sand (0.63 - 2mm)	wt%	3	DIN ISO 11277:2002:08
Medium sand (0.2 - 0.63mm)	wt%	9	DIN ISO 11277:2002:08
Fine sand (0.063 - 0.2mm)	wt%	29	DIN ISO 11277:2002:08
Coarse silt (20-63 µm)	wt%	18	DIN ISO 11277:2002:08
Medium silt (6.3 - 20 µm)	wt%	15	DIN ISO 11277:2002:08
Fine silt	wt%	12	DIN ISO 11277:2002:08

Table S 4: Model parameters of NO₃⁻ release from biochar-based fertilizers produced from two different biochars without or with citric acid (CA) treatment (BC1-N, BC2-N, BC1-N+CA and BC2-N+CA, respectively). To model the NO₃⁻ release (R) in weight percent, the equation $R = R_{max} \cdot (1 - e^{-k \cdot t})$ was used, where t is the time in minutes. The goodness of fit is reflected by R² values.

	R _{max}	k	R ²
BC1-N	97.2 ± 0.9	0.62 ± 0.08	0.99
BC1-N+CA	88.7 ± 0.7	0.55 ± 0.05	0.99
BC2-N	94.7 ± 0.7	0.51 ± 0.04	0.99
BC2-N+CA	77.2 ± 0.9	0.51 ± 0.06	0.99

Table S 5: Two-way analysis of variance of aboveground biomass yields (total, 1st and 2nd harvest). Factors: Treatment (Control, BC1-N, BC1-N+CA, BC2-N, BC2-N+CA) and Leaching (no Leaching, with Leaching). SS: sum of squares. DF: Degrees of freedom. MS: mean square value.

	Total aboveground biomass				
	SS	DF	MS	F (DFn, DFd)	P value
Treatment	3,415	4	0,8537	F (4, 16) = 6,970	P=0,0019
Leaching	11,52	1	11,52	F (1, 4) = 30,38	P=0,0053
Treatment x Leaching	2,346	4	0,5866	F (4, 16) = 6,298	P=0,0031

	Aboveground biomass (1 st harvest)				
	SS	DF	MS	F (DFn, DFd)	P value
Treatment	2,371	4	0,5927	F (4, 16) = 3,695	P=0,0258
Leaching	0,05534	1	0,05534	F (1, 4) = 3,117	P=0,1522
Treatment x Leaching	0,7102	4	0,1776	F (4, 16) = 2,120	P=0,1256

	Aboveground biomass (2 nd harvest)				
	SS	DF	MS	F (DFn, DFd)	P value
Treatment	2,847	4	0,7118	F (4, 16) = 6,163	P=0,0034
Leaching	9,979	1	9,979	F (1, 4) = 36,40	P=0,0038
Treatment x Leaching	0,7928	4	0,1982	F (4, 16) = 2,227	P=0,1120

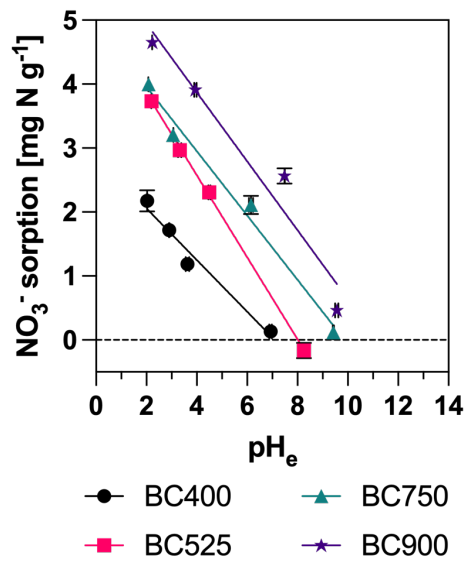


Figure S 1: (a) Sorption of nitrate (NO_3^-) at different equilibrium solution pH (pH_e) in presence of citric acid at an initial concentration of $20 \text{ mg NO}_3\text{-N L}^{-1}$ on the different biochars produced from beech wood at 400°C , 525°C , 750°C and 900°C (BC400, BC525, BC750 and BC900, respectively). Samples were equilibrated for seven days at 25°C and shaking at 200 rpm. Error bars indicate the standard deviation of three replicates. Sorption was modeled by linear regression over pH values.

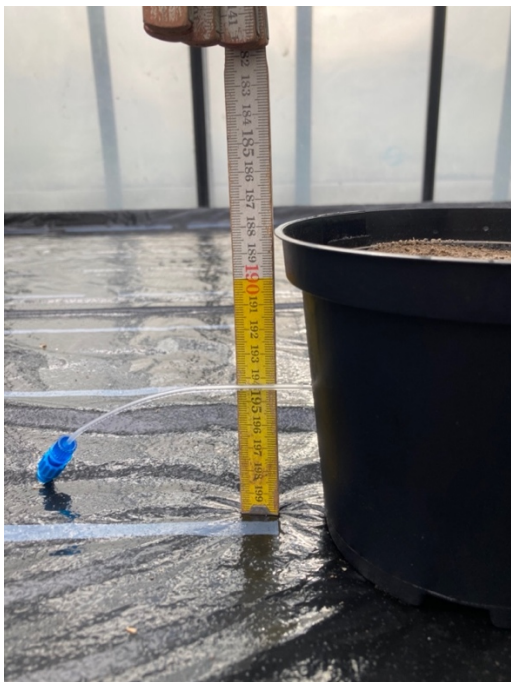


Figure S 2: Porewater sampling port installed in $\sim 5 \text{ cm}$ soil depth in horizontal position through the sidewall of pots (Rhizon MOM 5 cm, Article no. 19.21.22F, Rhizosphere Research Products by, Wageningen, Netherlands).

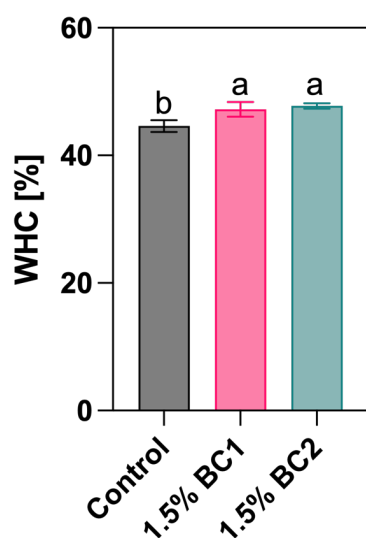


Figure S 3: Water holding capacity (WHC) of soil without any amendment (Control) or amended with two different biochars (BC1 and BC2) at 1.5% (w/w). Error bars indicate the standard deviation of three replicates. Different letters above error indicate significant differences (two-way analysis of variance, Tukey's post-hoc test, $p < 0.05$).



Figure S 4: Sowing of a total of eight seeds of spinach (*Spinacia oleracea*, variety Corvair F1, Bruno Nebelung GmbH, Everswinkel, Germany) in four holes with a depth of 1 cm.

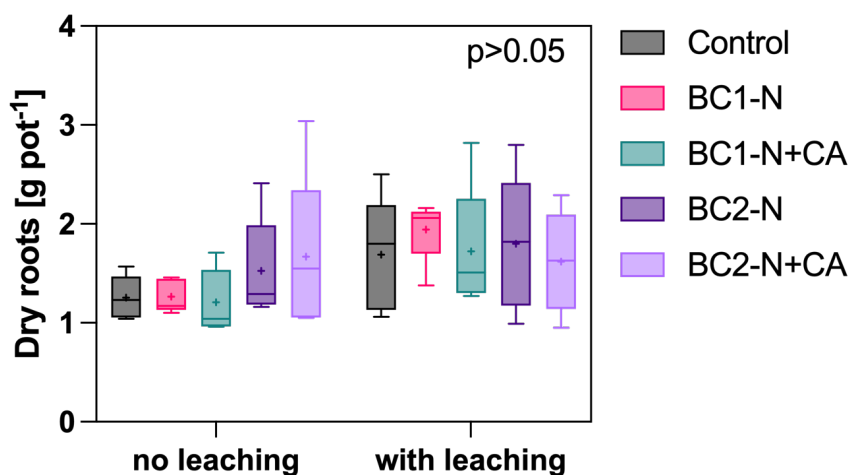


Figure S 5: Dry weight of spinach roots per pot at the end of the greenhouse experiment. The soil was either amended without (Control) or with two different biochars at 1.5% (w/w, BC1 and BC2). Biochars were enriched with 2.2% nitrogen (N) as KNO_3 (BC1-N and BC2-N). These N-enriched biochars were also applied after enrichment with citric acid (BC1-N+CA and BC2-N+CA). The soil in the Control treatment was spiked with similar amount of KNO_3 . Whiskers in boxplots represent the minimum to maximum value of five replicates for each treatment, mean values are indicated with “+”, different letters indicate a significant difference between the treatments within leaching groups (two-way analysis of variance, Tukey’s post hoc test, $p < 0.05$).

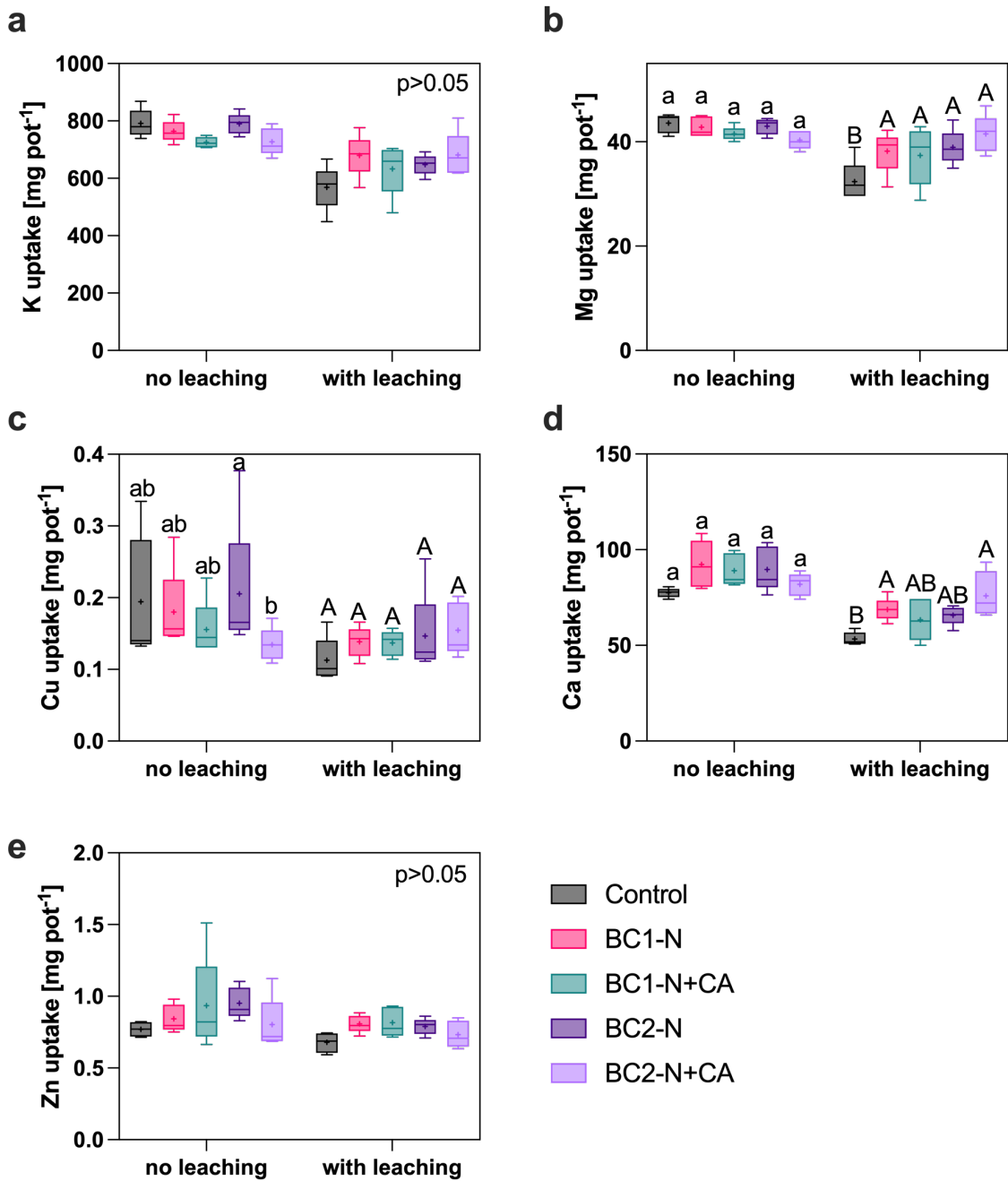


Figure S 6: Uptake of nutrients in aboveground spinach biomass cumulated over two harvests: potassium (K, panel a), magnesium (Mg, panel b), copper (Cu, panel c), calcium (Ca, panel d) and zinc (Zn, panel e). The soil was either amended without (Control) or with two different biochars at 1.5% (w/w, BC1 and BC2). Biochars were enriched with 2.2% nitrogen (N) as KNO_3 (BC1-N and BC2-N). These N-enriched biochars were also applied after enrichment with citric acid (BC1-N+CA and BC2-N+CA). The soil in the Control treatment was spiked with similar amount of KNO_3 . Whiskers in boxplots represent the minimum to maximum value of five replicates for each treatment, mean values are indicated with “+”, different letters indicate a significant difference within each leaching group (lowercase letters for ‘no leaching’, capital letters for ‘leaching’, two-way analysis of variance, Tukey’s post hoc test, $p < 0.05$).

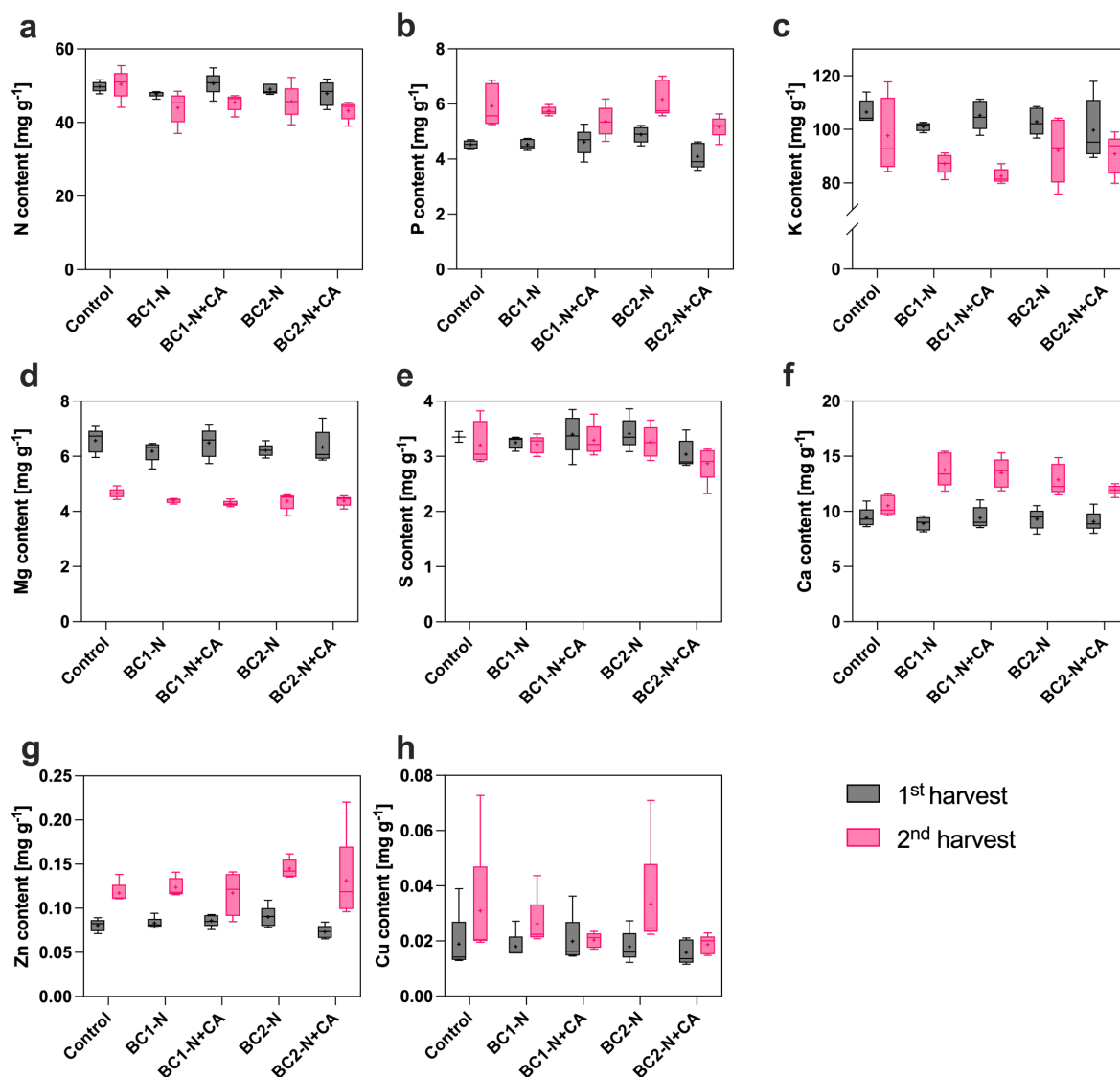


Figure S 7: Nutrient content in two harvests of spinach shoots cultivated without a leaching treatment: nitrogen (N, panel a), phosphorus (P, panel b), potassium (K, panel c), magnesium (Mg, panel d), sulfur (S, panel e), calcium (Ca, panel f) and zinc (Zn, panel e). The soil was either amended without (Control) or with two different biochars at 1.5% (w/w, BC1 and BC2). Biochars were enriched with 2.2% nitrogen (N) as KNO_3 (BC1-N and BC2-N). These N-enriched biochars were also applied after enrichment with citric acid (BC1-N+CA and BC2-N+CA). The soil in the Control treatment was spiked with similar amount of KNO_3 . Whiskers in boxplots represent the minimum to maximum value of five replicates for each treatment, mean values are indicated with “+”.

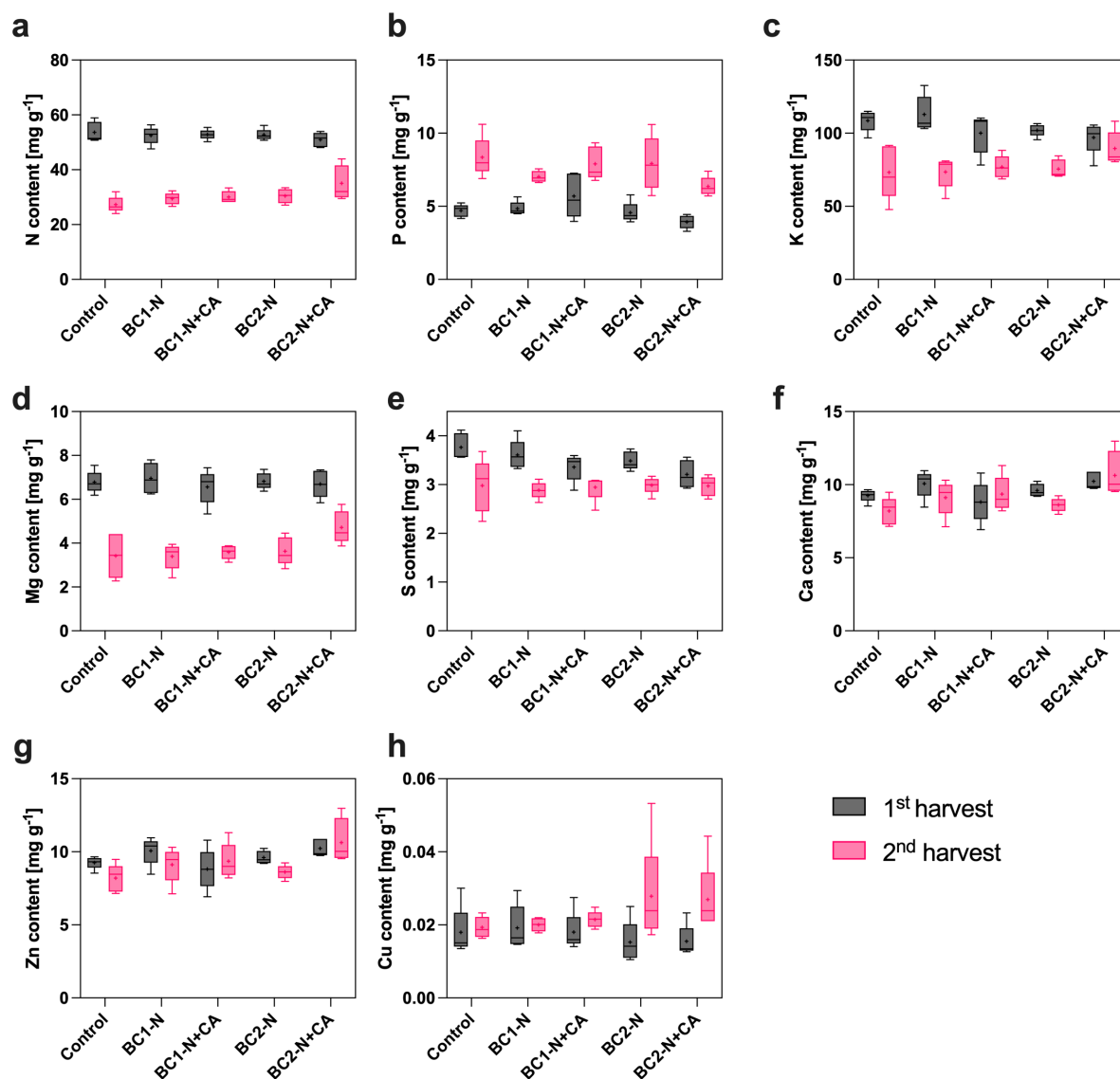


Figure S 8: Nutrient content in two harvests of spinach shoots cultivated with a leaching event after 9 days: nitrogen (N, panel a), phosphorus (P, panel b), potassium (K, panel c), magnesium (Mg, panel d), sulfur (S, panel e), calcium (Ca, panel f) and zinc (Zn, panel e). The soil was either amended without (Control) or with two different biochars at 1.5% (w/w, BC1 and BC2). Biochars were enriched with 2.2% nitrogen (N) as KNO₃ (BC1-N and BC2-N). These N-enriched biochars were also applied after enrichment with citric acid (BC1-N+CA and BC2-N+CA). The soil in the Control treatment was spiked with similar amount of KNO₃. Whiskers in boxplots represent the minimum to maximum value of five replicates for each treatment, mean values are indicated with “+”.

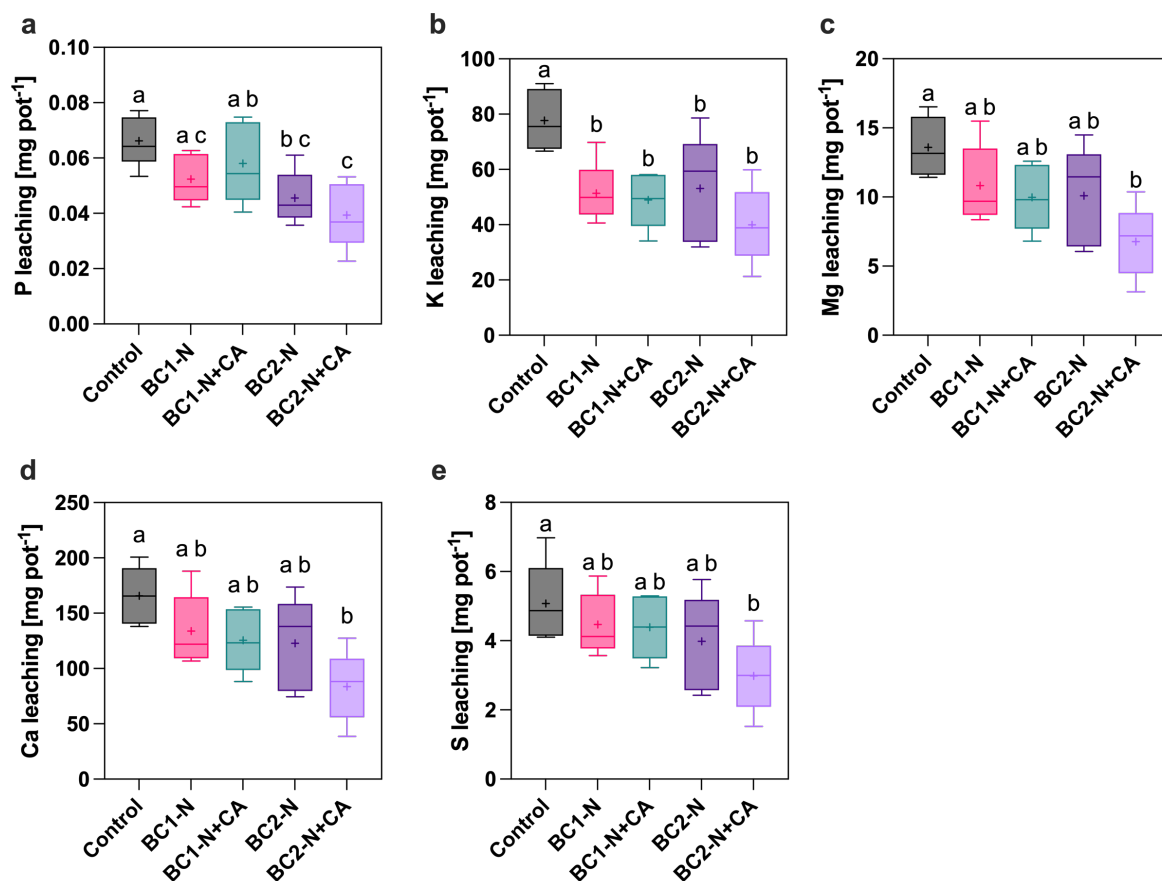


Figure S 9: Nutrient leaching during heavy rain simulation (20 L m⁻²) 10 days after sowing (in mg pot⁻¹): (a) nitrate-nitrogen (NO₃-N), (b) phosphorus (P), (c) potassium (K), (d) magnesium (Mg), (e) sulfur (S) and (f) calcium (Ca). The soil was either amended without (Control) or with two different biochars at 1.5% (w/w, BC1 and BC2). Biochars were enriched with 2.2% nitrogen (N) as KNO₃ (BC1-N and BC2-N). These N-enriched biochars were also applied after enrichment with citric acid (BC1-N+CA and BC2-N+CA). The soil in the Control treatment was spiked with similar amount of KNO₃. Whiskers in boxplots represent the minimum to maximum value of five replicates for each treatment, mean values are indicated with “+”, different letters indicate a significant difference between the treatments (one-way analysis of variance, Tukey’s post hoc test, p < 0.05).

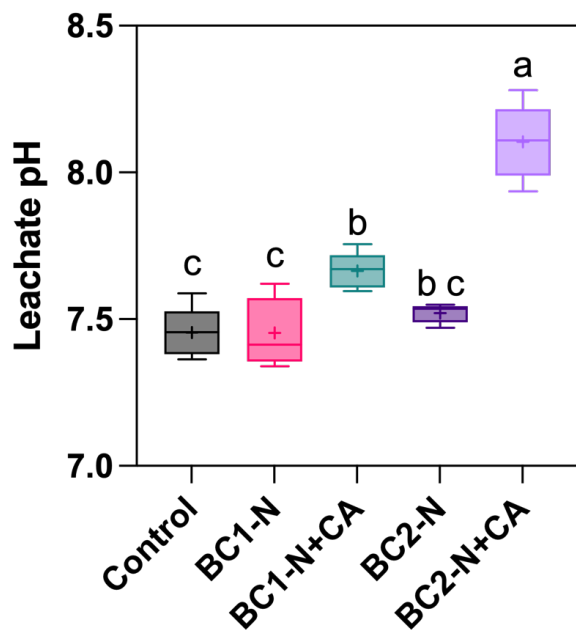


Figure S 10: pH of leachates from pots which received simulated heavy precipitation (30 l m^{-2}) 9 days after sowing. The soil was either amended without (Control) or with two different biochars at 1.5% (w/w, BC1 and BC2). Biochars were enriched with 2.2% nitrogen (N) as KNO_3 (BC1-N and BC2-N). These N-enriched biochars were also applied after enrichment with citric acid (BC1-N+CA and BC2-N+CA). The soil in the Control treatment was spiked with similar amount of KNO_3 . Whiskers in boxplots represent the minimum to maximum value of five replicates for each treatment, mean values are indicated with “+”, different letters indicate a significant difference between the treatments (one-way analysis of variance, Tukey’s post hoc test, $p < 0.05$).

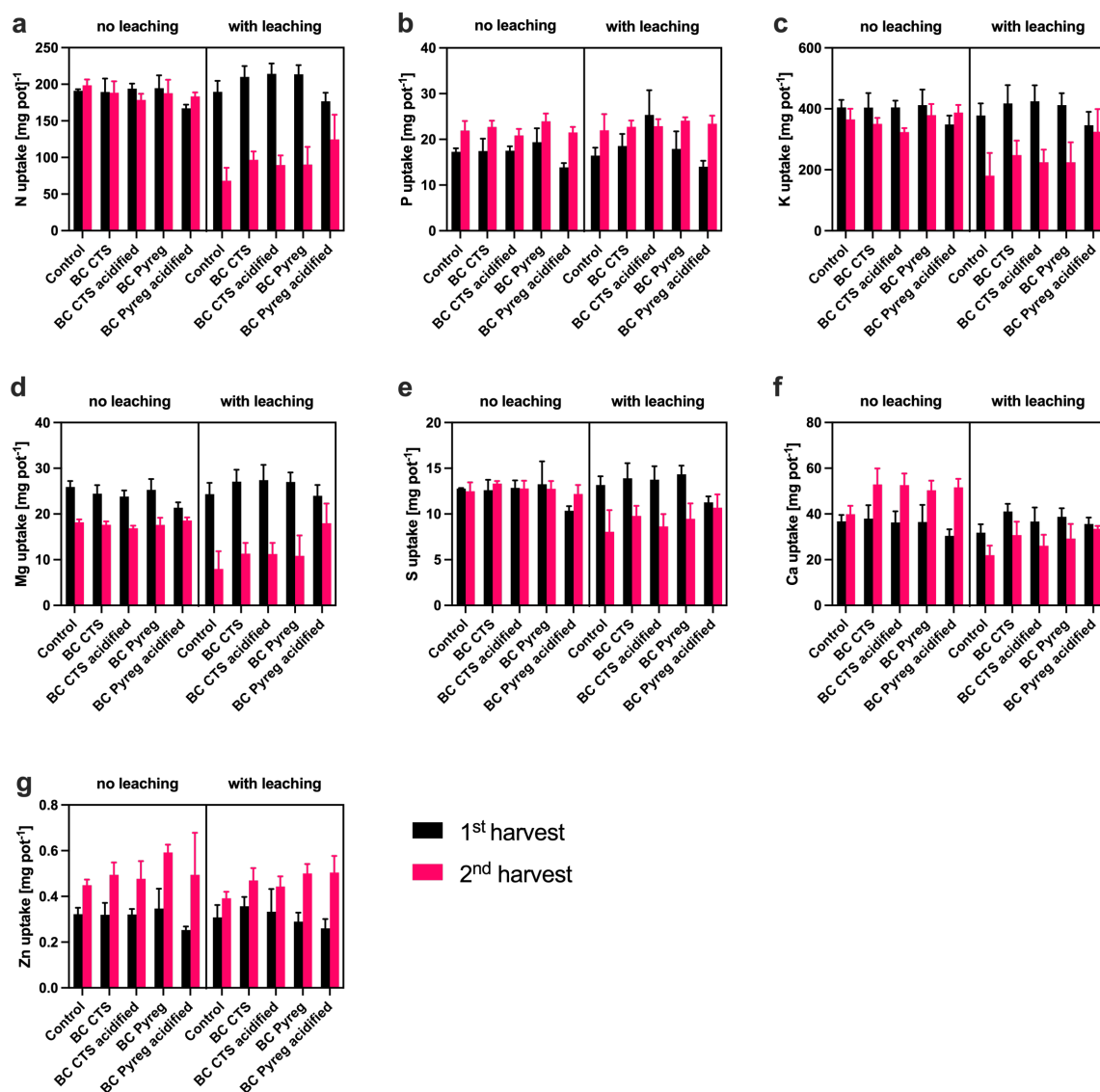


Figure S 11: Uptake of nutrients in aboveground spinach biomass during two subsequent harvests: nitrogen (N, panel a), phosphorus (P, panel b), potassium (K, panel c), magnesium (Mg, panel d), sulfur (S, panel e), calcium (Ca, panel f) and zinc (Zn, panel g). The soil was either amended without (Control) or with two different biochars at 1.5% (w/w, BC1 and BC2). Biochars were enriched with 2.2% N as KNO_3 (BC1-N and BC2-N). These N-enriched biochars were also applied after enrichment with citric acid (BC1-N+CA and BC2-N+CA). The soil in the Control treatment was spiked with similar amount of KNO_3 . Error bars indicate the standard deviation of five replicates.

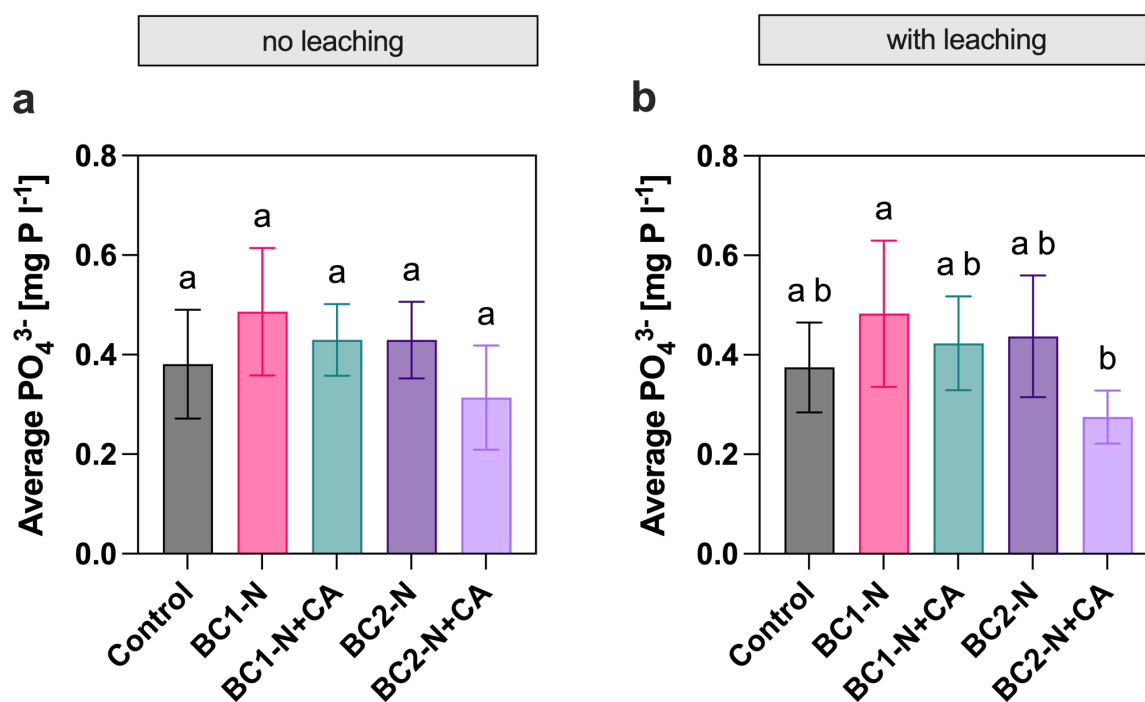


Figure S 12: Averaged phosphate (PO_4^{3-}) concentrations in soil porewater without (a) or with (b) the conduction of a leaching event after 9 days. The soil was either amended without (Control) or with two different biochars at 1.5% (w/w, BC1 and BC2). Biochars were enriched with 2.2% nitrogen (N) as KNO_3 (BC1-N and BC2-N). These N-enriched biochars were also applied after enrichment with citric acid (BC1-N+CA and BC2-N+CA). The soil in the Control treatment was spiked with similar amount of KNO_3 . Error bars indicate the standard deviation of $n=5$ replicates. Different letters above error bars indicate statistically significant differences in cumulative NO_3-N content between the treatments (one-way analysis of variance and Tukey's post-hoc test, $p<0.05$).

References

J. Grafmüller, J. Möllmer, E.M. Muehe, C.I. Kammann, D. Kray, H.-P. Schmidt, N. Hagemann, Granulation compared to co-application of biochar plus mineral fertilizer and its impacts on crop growth and nutrient leaching, *Sci Rep* 14 (2024) 16555. <https://doi.org/10.1038/s41598-024-66992-0>.

Chapter 4b

Biochar acidification increased sorption and reduced leaching of nitrate

Jannis Grafmüller^{1,2,3,4}, Hans-Peter Schmidt², Daniel Kray¹, Thomas D. Bucheli⁴, Haike Mäurer⁵, Jens Möllmer⁵, Heiko Peisert⁶, Nikolas Hagemann^{2,4}

¹Institute for Sustainable Energy Systems (INES), Offenburg University of Applied Sciences, Germany

²Ithaka Institute, Arbaz (Switzerland) and Goldbach (Germany)

³Plant Biogeochemistry, Department of Geosciences, University of Tübingen, Tübingen, Germany

⁴Environmental Analytics, Agroscope, Zurich, Switzerland

⁵Institut für Nichtklassische Chemie e.V. (INC), Leipzig, Germany

⁶Institute for Physical and Theoretical Chemistry, University of Tübingen, Tübingen, Germany

Published in:

Journal of Environmental Management

First published: 11th September 2025

<https://doi.org/10.1016/j.jenvman.2025.127224>

Material from:

Grafmüller, J., Schmidt, H.-P., Kray, D., Bucheli, T.D., Mäurer, H., Möllmer, J., Peisert, H., Hagemann, N., 2025. Biochar acidification increased sorption and reduced leaching of nitrate. *Journal of Environmental Management* 393, 127224.

<https://doi.org/10.1016/j.jenvman.2025.127224>

The published article is re-printed in this thesis with permission from Elsevier B.V. The right to include the article in its published form in a thesis or dissertation is retained by the authors in accordance with Elsevier/ScienceDirect Journal Author Rights.

Statement of personal and co-author contributions, plus non-listed contributors

Authors	Position of candidate in list of authors	Scientific ideas by the author [%]	Data generation by the author [%]	Analysis and interpretation by the author [%]	Paper writing done by the author [%]
Jannis Grafmüller	1	55	75	55	50
Hans-Peter Schmidt	2	10	0	5	5
Daniel Kray	3	0	5	5	5
Thomas D. Bucheli	4	20	0	10	15
Haike Mäurer	5	0	5	5	5
Jens Möllmer	6	5	5	5	5
Heiko Peisert	7	0	0	5	5
Nikolas Hagemann	8	10	0	10	10
Contribution by other parties not listed as authors (e.g., commercial analysis laboratories, student assistants)					
Syed Mustafa Hussein		0	10	0	0
Publication status	published				
Explanations	<p>The study was conceptualized by Thomas D. Bucheli, Nikolas Hagemann, Hans-Peter Schmidt and me. Biochars from pilot-plant scale were produced by Daniel Kray. The nitrate sorption and leaching experiments, FTIR measurements, Boehm titration for acidic groups, conductivity measurements and XPS analysis were conducted by me. Syed Mustafa Hussein and Heiko Peisert from Tübingen University supported me during XPS measurements and related data interpretation. Haike Mäurer performed Boehm titrations for basic functional groups and Jens Möllmer conducted gas adsorption experiments and evaluated the related data. All other data was evaluated by me, Hans-Peter Schmidt, Thomas D. Bucheli and Nikolas Hagemann supported me with their interpretation. The current version of the manuscript was written by me and Thomas D. Bucheli and Nikolas Hagemann greatly improved its quality, while all other authors provided input of a previous version of the manuscript with data included from pre-experiments.</p>				



Research article

Biochar acidification increased sorption and reduced leaching of nitrate

Jannis Grafmüller^{a,b,*}, Hans-Peter Schmidt^b, Daniel Kray^a, Thomas D. Bucheli^c,
Haike Mäurer^d, Jens Möllmer^d, Heiko Peisert^e, Nikolas Hagemann^{b,c}

^a Institute of Sustainable Energy Systems (INES), Offenburg University of Applied Sciences, Germany

^b Ithaka Institute, Arbaz, Switzerland and Goldbach, Germany

^c Environmental Analytics, Agroscope, Zurich, Switzerland

^d Institut für Nichtklassische Chemie e.V. (INC), Leipzig, Germany

^e Institute for Physical and Theoretical Chemistry, University of Tuebingen, Tuebingen, Germany



ARTICLE INFO

Keywords:

Pyrolysis
Protonation
Agriculture
Plant nutrients
biochar acidification
Nutrient leaching

ABSTRACT

Biochar can reduce nitrate (NO_3^-) leaching from soil, yet typically only at high, uneconomic application rates. Therefore, biochar should be produced and modified to achieve high sorption capacity. Increased NO_3^- sorption at acidic pH has been reported. However, the sorption mechanisms and potential of biochar acidification to reduce nitrate leaching remain unexplored. Here, NO_3^- sorption was quantified at soil-relevant pH of 5 and 7 on woody biochars produced at highest treatment temperatures (HTT) of 400–900 °C. Sorption capacities ranged between 700 and 6200 mg NO_3^- -N kg^{-1} at pH 5 and between 200 and 2500 mg NO_3^- -N kg^{-1} at pH 7. Thus, NO_3^- sorption to biochar might be higher in acidic compared to neutral soils and can be maximized by producing biochars at $\text{HTT} \geq 750$ °C. Correlation of sorption data with content of surface functional groups and proxies for biochar aromaticity suggest that NO_3^- is sorbed to protonated aromatic structures in biochars produced at >500 °C, while NO_3^- might sorb to protonated functional groups in biochar produced at 400 °C. Further, biochar acidification under NO_3^- enrichment was tested to reduce NO_3^- leaching. Both in aqueous suspension and in soil columns, full NO_3^- release from KNO_3 -enriched industrial biochar was prevented by biochar acidification, i.e., combined HNO_3 + KNO_3 enrichment. In soil with pH 5.7 or pH 7.4, only acidified biochar reduced NO_3^- leaching by up to 23% and 12%, respectively, compared to the soil-only control. Thus, acidification could be an interesting approach to produce biochar-based fertilizers with controlled NO_3^- release.

1. Introduction

Nitrogen (N) is often the primary limiting factor for crop production and thus a key component of fertilizers (Schubert, 2018). In mineral fertilizers, N can be added as nitrate (NO_3^-) or, if other N sources are used, soil microbes typically oxidize these to NO_3^- , which is subject to a high risk of leaching to groundwater due to the prevailing negatively charged surfaces of soils (Borchard et al., 2019). This limits the N use efficiency of agriculture.

Biochar is the solid product of biomass pyrolysis and is suggested for use as a soil amendment in agriculture (Lehmann and Joseph, 2015). Biochar reduces NO_3^- leaching by 13% on a global average (Borchard et al., 2019). Relevant reductions, however, are only obtained for biochar application rates of 10–40 t ha^{-1} (Borchard et al., 2019), which are economically challenging (Bach et al., 2016). Practical and economic applications are usually <2 t ha^{-1} and an effective amount of biochar in soil would only be achieved after several years of repeated input.

Biochar production and modification should therefore be optimized to generate a more effective sorbent for NO_3^- .

Mechanisms for biochar-induced reduction of NO_3^- leaching include the capture of NO_3^- in an organic coating developed through soil ageing or co-composting (Hagemann et al., 2017; Haider et al., 2020) and electrostatic sorption of NO_3^- (Fidel et al., 2018). As composting of biochar is a time-consuming process, more simple modification techniques are required to improve sorption, which is the focus of this study.

So far, NO_3^- sorption to biochar has been reported to be negligible with capacities $\ll 200$ mg NO_3^- -N kg^{-1} (Gai et al., 2014; Yang et al., 2017). However, the pH during batch experiments was barely controlled and, therefore, sorption was presumably measured at rather alkaline pH, given that biochar usually has a pH in the range of 8–10 (Ippolito et al., 2020). Indeed, biochars exhibit a significantly higher anion exchange capacity (AEC) at pH 5 compared to higher pH (Banik et al., 2018). Likewise, biochars had a limited NO_3^- sorption capacity at pH levels between 7 and 8 (<400 mg NO_3^- -N kg^{-1}), but sorption gradually

* Corresponding author. Institute of Sustainable Energy Systems (INES), Offenburg University of Applied Sciences, Germany.
E-mail address: jannis.grafmueller@hs-offenburg.de (J. Grafmüller).

<https://doi.org/10.1016/j.jenvman.2025.127224>

Received 16 June 2025; Received in revised form 2 September 2025; Accepted 5 September 2025

Available online 11 September 2025

0301-4797/© 2025 The Authors. Published by Elsevier Ltd. This is an open access article under the CC BY license (<http://creativecommons.org/licenses/by/4.0/>).

increased to 600 mg NO₃⁻-N kg⁻¹ at pH 6 and was maximized to 1400 mg NO₃⁻-N kg⁻¹ for a red oak biochar at pH 4.0 (Fidel et al., 2018). By adjusting the pH to 2.7 with citric acid, a rice husk biochar produced at a highest treatment temperature (HTT) of 700 °C could completely remove NO₃⁻ from aqueous solution, leading to sorption of 1400 mg NO₃⁻-N kg⁻¹, while no NO₃⁻ sorption occurred without addition of acid (pH 9) (Heaney et al., 2020). In line with that, biochar reduced NO₃⁻ leaching most effectively in soils with a pH < 5.5 (Borchard et al., 2019). Despite these consistent results of increased NO₃⁻ sorption at lower pH, no study has yet elucidated if acidification could be a method to optimize biochar's capacity to reduce NO₃⁻ leaching. The sorption mechanisms also remain uninvestigated. So far, biochar acidification has only been investigated in the context of phosphorus availability from biochar-based fertilizers (Kopp et al., 2023).

Different mechanisms might be relevant for improved sorption of anions at lower pH, including protonation of acidic functional groups on the biochar surface, protonation via uptake of protons by basic acting moieties, such as π-electrons on basal planes of graphitic structures, or the presence of O- and N-heterocycles that can impact pH-dependent AEC of biochars (Bartolomei et al., 2019; Boehm, 1994; Lawrinenko and Laird, 2015). These mechanisms add (net) positive surface charge to biochars when in contact with acids. Although pH dependent sorption increased for biochars produced at higher HTT (Fidel et al., 2018), it is unknown which of the abovementioned mechanisms dominate pH dependent sorption.

Due to their alkaline nature, biochar capacity to reduce NO₃⁻ leaching increases over time after soil application, likely as its pH decreases during the equilibration with the surrounding soil pH (Borchard et al., 2019). As the use of biochar-based fertilizers (BBF) has recently gained attention (Melo et al., 2022), simple pre-treatments that improve the NO₃⁻ sorption, like acidification, are of interest to ensure maximized leaching reduction right after soil application. Any acidified biochar will equilibrate to soil pH with time, determining its long-term pH-dependent sorption capacity. Still, acidification might prevent a rapid leaching of biochar-spiked NO₃⁻ immediately after soil application.

Here, NO₃⁻ sorption to wood-based biochars produced in an industrial-relevant pyrolysis process at HTT ranging from 400 to 900 °C was studied at soil-relevant pH (pH 5 and 7) along with in-depth biochar characterization, allowing to conclude about the relevance of oxygen containing functional groups and aromaticity of biochars for NO₃⁻ sorption. Nitric acid was used for pH control to add no further competitive anions to the experiments aiming to maximize NO₃⁻ sorption, contrasting to earlier studies (Chintala et al., 2013; Fidel et al., 2018; Heaney et al., 2020). The effect of biochar acidification on leaching of NO₃⁻ was studied in soil columns with two contrasting soils. This study aims to (1) improve our understanding of which biochar properties contribute and dominate pH dependent NO₃⁻ sorption and (2) answer the question whether acidification of biochar reduces NO₃⁻ leaching from BBF amended soil. We hypothesize that an increase in aromaticity can explain the increased pH dependent NO₃⁻ sorption previously reported for biochars produced at increased HTT and that biochar acidification reduces NO₃⁻ leaching from soil.

2. Materials and methods

2.1. Biochar materials

Biochar production was performed with a PYREKA research pyrolysis unit (Pyreg GmbH, Dörth, Germany) using milled and sieved beech wood particles (2 < x < 6 mm, Verora AG, Edlibach, Switzerland) with a residence time of 10 min at a HTT of 400 °C, 525 °C, 750 °C, and 900 °C. The pyrolysis reactor was electrically heated and is explained in more detail elsewhere (Hagemann et al., 2020). The biochars are referred to as BC400, BC525, BC750, and BC900. Wood was used as it is currently the most widely used feedstock for biochar production across Europe. Industrial wood biochar (BCi) was obtained from AWN GmbH (Buchen,

Germany), who used a Pyreg P500 pyrolysis reactor (Pyreg GmbH) at a HTT of ~650 °C and 20 min residence time (PYREG, 2025). The BCi had EBC-Feed certification according to the European biochar Certificate (EBC) under batch reference ba-de-54-1-2 (EBC 2012-2024, 2024). Biochars were milled to <200 μm with an impact mill (Kinematica AG, Lucerne, Switzerland) and stored in air-tight glass jars at ambient temperature in the dark for further usage. The biochars were characterized according to the methods described in chapter 1 in the Supplementary Information (SI). Where applicable, EBC methods were used (EBC 2012-2024, 2024).

2.2. Batch sorption experiments

Biochars were first conditioned over a total of 12 days to achieve the targeted pH values, i.e., pH 5.0 ± 0.1 or pH 7.0 ± 0.1, in a stock suspension (10 stock suspensions in total). To do so, ~0.4 g of dry biochar (actual weights were recorded to 0.1 mg accuracy) were weighed into 100 mL Schott bottles and 80 mL of ultrapure water was added. The bottles were placed on a magnet stirrer at room temperature. Over 9 days, the pH value of the suspensions was adjusted by adding diluted HNO₃, and the added volumes were recorded. From day 9 onwards, the pH of all stock suspensions was stable. On day 12, all suspensions were quantitatively transferred to a 100 mL graduated cylinder and filled up to the mark using either diluted HNO₃ with pH 5 or ultrapure water with pH 7.

For batch sorption experiments, 1.45 mL of the stock suspensions were aliquoted under constant stirring at 700 rpm into 2 mL polypropylene reaction vessels. A volume of 0.05 mL of five different KNO₃ solutions was pipetted to each reaction vessel to add additional 0, 10, 20, 50, 100, or 240 mg NO₃⁻-N L⁻¹ to the suspension besides already contained NO₃⁻ originating from HNO₃ in the stock suspension (Table S1). The resulting biochar concentration in each reaction vessel was 4 g L⁻¹. Establishment of equilibrium phase distribution was assured by initially following adsorption kinetics with 100 mg NO₃⁻-N L⁻¹ added to the suspensions in triplicates for either 1, 3, 6, 16, 24, or 48 h. For all other added NO₃⁻ concentrations, equilibration was done for only 48 h. The reaction vessels were equilibrated horizontally fixed on a rotary shaker at 220 rpm and 25 °C (KS 4000 ic control, IKA Werke GmbH&Co. KG, Staufen, Germany). Samples equilibrated for 48 h with either 20 or 100 mg NO₃⁻-N L⁻¹ were centrifuged after equilibration with 17,000×g at 25 °C (Fresco™ 17, Thermo Fisher Scientific, Waltham, USA), to obtain a biochar pellet for later NO₃⁻ desorption experiments (Fig. S1). The supernatants or suspensions, if not centrifuged, were filtered (<0.45 μm, Nylon, Chrompure, Membrane-Solutions LLC, Auburn (WA), USA) and filtrates were stored at -18 °C for later NO₃⁻ analysis.

2.3. Nitrate desorption from biochar

After centrifugation (cf. Section 2.2, Fig. S1), biochar pellets were resuspended in 1.5 mL of either diluted HNO₃ adjusted to pH 5 (for samples previously equilibrated at pH 5) or ultrapure water with pH 7 (for samples previously equilibrated at pH 7). Samples were equilibrated for 48 h and subsequently centrifuged and filtered as described above. A second desorption step was performed in the same way. Additional triplicate samples equilibrated in previous sorption experiments for 48 h with added 100 mg NO₃⁻-N L⁻¹ were used for desorption experiments as described above, but desorption was performed in 1 M KCl and only in a single step for 48 h. Before the first and second desorption steps, the reaction vessels including the biochar pellet were weighed to estimate the remaining non-decanted liquid volume to correct for already solubilized/desorbed NO₃⁻.

2.4. Experiments with BBF

2.4.1. BBF preparation

Two different BBF were prepared from BCI. The BCI was weighed into 50 mL centrifuge tubes and moistened with two different NO_3^- solutions to 80 % of its WHC (=230 %, w/w), which equaled 1.83 mL g^{-1} . For release experiments (cf. Section 2.4.2), 0.4 g, and for column leaching experiments (cf. Section 2.4.3), 0.09 g of dry matter equivalent of BCI was used. The first solution contained only KNO_3 at 138 g L^{-1} , the BBF enriched with this solution was termed BCI-N. The second solution contained a mixture of HNO_3 (27.4 mL concentrated $\text{HNO}_3 \text{ L}^{-1}$) and KNO_3 (95 g L^{-1}), in which 31 % of total NO_3^- originated from HNO_3 . The BBF prepared with this solution was labeled as BCI- HNO_3 . Each solution was pipetted onto the whole surface of the biochar, vortexed after 2 h, and left to stand for 3 days at room temperature. Both BBFs were enriched to a calculated NO_3^- content of 3.5 % N (w/w). After enrichment, BCI-N had a pH value of 9.0 and BCI- HNO_3 of 5.4.

2.4.2. Nitrate release from BBF

Nitrate release from BCI-N and BCI- HNO_3 was measured in triplicates in a 0.5 M phosphate buffer either adjusted to pH 5.7 or pH 7.4. The buffers were prepared from a stock solution of KH_2PO_4 and $\text{Na}_2\text{HPO}_4 \times 2\text{H}_2\text{O}$. A buffer volume of 20 mL was added to the centrifuge tube with the prepared BBF (cf. section 2.4.1), and samples were horizontally shaken at 150 rpm and room temperature. Four sequential desorption steps of each 48 h were performed. After each desorption step, samples were centrifuged at $10,000 \times g$ for 5 min (Megafuge 16, Thermo Fisher Scientific, Waltham, USA) and 15 mL of the supernatant were exchanged with fresh buffer while filtering a subsample of the supernatant through a syringe filter for storage at -18°C . For N release monitoring during the first desorption step, samples were centrifuged as described above after 1, 3, 8, and 24 h and 0.5 mL of the supernatant was sampled. Fresh 0.5 mL buffer were added to maintain a constant solid to liquid ratio. Total released N from the BBF into the buffer after each desorption step (R_{N_i}) in % (w/w) was calculated with equation (2) given in section 1.6 in the SI.

2.4.3. Nitrate leaching from BBF amended soil columns

Two different standard soils were used in the experiment, which are referred to as "soil-2.3" with pH 5.7 (silt sand) and "soil-2.4 N" with pH 7.4 (normal loam) according to the soil provider (LUFA, Speyer, Germany, for soil characteristics see Table S2). Columns were prepared by mixing 12 g dry matter of soil and biochar added via BCI-N or BCI- HNO_3 (0.75 % biochar concentration, w/w). A fertilized treatment without biochar was also included (Control), here a NO_3^- solution adding 3 mg N per column, as with BCI-N and BCI- HNO_3 , was applied. The spiked Control soil was left to stand for 3 days in 50 mL centrifuge tubes (similar as BCI-N and BCI- HNO_3 , cf. Section 2.4.1) before the soil was homogenized and packed into the columns. BCI-N and BCI- HNO_3 were homogeneously mixed with the soil and packed into columns. The columns were 10 mL polypropylene syringes and contained a 0.15 g glass wool layer at the bottom. Non-fertilized controls with or without BCI were also included. The water holding capacity (WHC) of each soil mixture was measured by submersion of the whole column in water for 24 h with a subsequent drainage of 2 h. The total H_2O remaining in the soil column after drainage was defined as 100 % WHC or one soil pore volume (SPV, corrected for contributions from syringe and glass wool). These soil columns for WHC measurement were prepared in addition and not used for later leaching experiments.

The columns were watered to 65 % WHC for three days and then to 95 % WHC on the fourth day after setup. On day 4, 7, 8, and 9, water was added on top of the columns, 2.3 mL for treatments with soil-2.3 and 2.98 mL for soil-2.4 N, both equal to 0.5 SPV (Fig. S2). Ultrapure water was used in all steps. Leachates were filtered and stored as described above. On day 12, 150 μL of a 144 g L^{-1} KNO_3 solution were pipetted on top of the column for re-fertilization with 3 mg NO_3^- -N. Further leaching

events were conducted on day 14, 15, 16, 17, and 18 as described above.

2.5. Nitrate quantification

NO_3^- concentrations in filtrates were measured in 96-well microplates and a microplate reader (Biotek Epoch 2, Agilent Technologies Inc., Santa Clara, USA) (Hood-Nowotny et al., 2010). A Thermomixer C (Eppendorf SE, Hamburg, Germany) was used for plate incubation for 1 h at 37°C and the calibration curve was recorded in a range of 0–2.5 mg NO_3^- -N L^{-1} with KNO_3 as standard. All reagents were of analytical grade and either purchased from Carl Roth GmbH & Co. KG (Karlsruhe, Germany) or Merck KGaA (Darmstadt, Germany).

2.6. Data analysis

Calculation of sorbed amounts of NO_3^- on biochars in batch sorption experiments (c_s in mg NO_3^- -N kg^{-1}) and their fitting to the Freundlich and Langmuir model are described in section 1.7 of the SI. The sorption capacities obtained from the Langmuir model ($c_{s,max}$) were normalized to different biochar properties according to section 1.8 in the SI to identify potential sorption mechanisms.

Data from release and column experiment was analyzed by an unpaired *t*-test at $\alpha < 0.05$ by either comparing BCI- HNO_3 with BCI-N (release experiment) or BCI- HNO_3 and BCI-N individually with the Control (column experiment), respectively, for each desorption or leaching step. Data normality and variance homogeneity were evaluated with a Shapiro-Wilk test and a Brown-Forsythe test, respectively. Data visualization and analysis was performed with GraphPad Prism (version 10.0.3, Graphpad Software LLC, Boston, USA).

3. Results

3.1. Chemical properties of biochars

The C and ash content, as well as pH of the biochars, increased with HTT (Table 1). By increasing HTT from 400°C to 525°C , SEC increased by four orders in magnitude and ultimately rose to $1.4 \cdot 10^3 \text{ mS cm}^{-1}$ and $1.3 \cdot 10^4 \text{ mS cm}^{-1}$ for a HTT of 750°C and 900°C , respectively, indicating higher aromaticity of biochars produced at higher HTT, in line with a reduction in hydrogen to organic carbon molar ratio (H/C_{org} , Table 1). Boehm titration indicated a decrease in the amount of acidic functional groups, i.e., total acidity of the biochars, with increasing HTT from 0.58 mmol g^{-1} (BC400) to 0.08–0.22 mmol g^{-1} (BC525-BC900, Table 1), but carboxylic groups were still detected for BC750 and BC900 (Fig. S3). In contrast, the amount of basic functional groups increased with HTT (Table 1). Spectroscopic analyses delivered evidence for decreased oxygen-containing functional group contents on the biochars produced at higher HTTs. The FTIR spectrums revealed a loss of H-bonded OH-groups ($3400\text{--}3200 \text{ cm}^{-1}$), a decrease in phenolic OH bending at 1390 cm^{-1} and a general loss of characteristic carboxylic group bands e. g., the C=O stretching band at 1690 cm^{-1} (from carboxylic acids or esters), the COO^- band at $\sim 1580 \text{ cm}^{-1}$ and carboxylic C-OH band at $\sim 1200 \text{ cm}^{-1}$ with increasing HTT (Fig. 1). The FTIR-band pattern of BCI was closely related to that of BC525 (Fig. 1). The XPS-derived surface O/C molar ratio decreased with an increase in HTT (Table 1 and Table S3) and the appearance of high binding energy satellite structures at around 291 eV may indicate an increase of aromaticity for BC750 and BC900 (Fig. S4). The SSA of biochars based on N_2 sorption increased drastically with HTT from 6 to $388 \text{ m}^2 \text{ g}^{-1}$ while SSA based on CO_2 sorption was generally higher (Table 1), indicating limited accessibility for N_2 at the applied measurement conditions (-195.8°C at 0.1 MPa), especially to the pore system in BC400. The SSA of pores with a diameter $> 0.67 \text{ nm}$, i. e., the range of pores most relevant for NO_3^- sorption due to the diameter of hydrated NO_3^- of 0.67 nm (Nightingale, 1959), were in a narrow range across biochars ($42\text{--}59 \text{ m}^2 \text{ g}^{-1}$), only BC525 had a SSA theoretically accessible for NO_3^- of only $28 \text{ m}^2 \text{ g}^{-1}$ (Table 1 and Fig. S7).

Table 1

Elemental analysis (carbon – C, organic carbon – C_{org}, hydrogen – H, nitrogen – N in % (w/w) and molar H/C_{org} ratio), ash content (w/w), pH, solid-state electric conductivity (SEC), surface molar O/C ratio (derived from X-ray photoelectron spectroscopy), total acidity and total basicity obtained from Boehm titration, as well as cumulative specific surface area (SSA) based on CO₂ and N₂ gas adsorption calculated with the Brunauer-Emmett-Teller model (CO₂- and N₂-SSA). The CO₂-SSA is also presented covering only pores with a width of >0.67 nm. The beech-wood biochars were produced at a highest treatment temperature of 400, 525, 750, and 900 °C (BC400, BC525, BC750 and BC900, respectively) and the industrial wood-based biochar at ~650 °C (BCi). n.d.: not determined. All analyzes were performed without repetitions, except the ash content and total acidity, which were performed as triplicate measurements.

	C [%]	C _{org} [%]	H [%]	N [%]	H/C _{org}	Ash [%]	pH	SEC [mS cm ⁻¹]	Surface O/C ratio [%]	Total acidity [mmol g ⁻¹]	Total basicity [mmol g ⁻¹]	CO ₂ -SSA [m ² g ⁻¹]	CO ₂ -SSA (>0.67 nm) [m ² g ⁻¹]	N ₂ -SSA [m ² g ⁻¹]
BC400	78.0	77.7	3.8	0.5	0.58	3.1 ± 0.1	6.9	9.6·10 ⁻⁷	0.16	0.58 ± 0.01	0.16	241	50	6
BC525	87.0	86.7	3.2	0.8	0.44	3.3 ± 0.2	9.1	9.3·10 ⁻³	0.12	0.08 ± 0.01	0.31	347	28	249
BC750	91.1	90.3	1.5	0.8	0.20	4.5 ± 0.1	9.4	1.4·10 ³	0.11	0.22 ± 0.01	0.79	410	42	372
BC900	91.4	90.8	1.5	0.9	0.20	4.9 ± 0.1	9.7	1.3·10 ⁴	0.09	0.22 ± 0.01	0.91	465	50	388
BCi	89.1	88.8	1.7	0.6	0.23	5.2	8.6	1.7·10 ⁷	n.d.	n.d.	n.d.	388	59	9

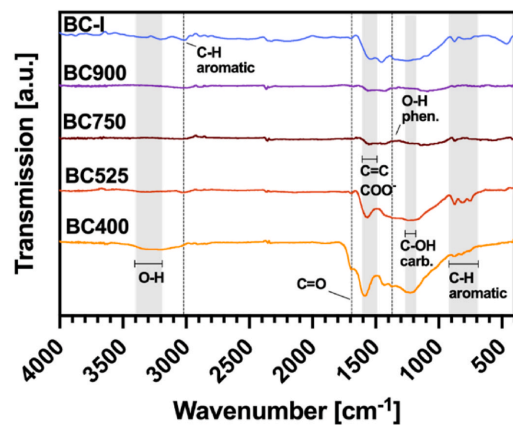


Fig. 1. (A) Baseline-corrected Fourier-Transform Infrared (FTIR) spectra of beech-wood biochars produced at pilot-plant scale at 400, 525, 750 and 900 °C (BC400, BC525, BC750 and BC900, respectively), and of industrial wood-based biochar (BCi, produced at ~650 °C). Band allocation was done according to literature (Singh et al., 2017). a.u.: arbitrary unit.

3.2. Nitrate sorption isotherms

Equilibrium water-biochar phase distribution of NO₃⁻ was stable after 48 h in preliminary tests for all biochars at both pH values (Fig. S8). Fig. 2 presents the calculated sorbed amount of NO₃⁻ on the different biochars over the c_w value and the fitted sorption models. The goodness of fit, i.e., R² values, were similar for the Langmuir and Freundlich sorption models (Table 2). Sorption was higher at pH 5 compared to pH 7 for all biochars (Fig. 2). At pH 5, NO₃⁻ Langmuir sorption capacities c_{s,max}, derived from adsorption data only, ranged between 650 mg NO₃⁻-N kg⁻¹ (BC400) and 6190 mg NO₃⁻-N kg⁻¹ (BC750), while at pH 7, c_{s,max} varied between only 180 mg NO₃⁻-N kg⁻¹ (BC400) and 2480 mg NO₃⁻-N kg⁻¹ (BC900, Fig. 2 and Table 2). For BC750 and BC900, c_{s,max} was in a similar range at pH 5 and it generally decreased in the following order: BC750 > BC900 > BCi > BC525 > BC400 at pH 5 and BC900 > BC750 > BCi > BC525 > BC400 at pH 7. The Freundlich exponent (1/n) was <1 for all biochars at all pH values, indicating favorable sorption (Table 2). Freundlich sorption coefficients K_F ranged between 450 and 2740 l kg⁻¹ at pH 5 and between 150 and 2030 l kg⁻¹ at pH 7 and decreased in the following order: BC900 > BCi > BC750 > BC525 > BC400 at pH 5 and BC900 > BC750 > BCi > BC525 > BC400 at pH 7.

There was a good positive linear correlation of c_{s,max} with the CO₂-based SSA (R² = 0.83–0.98, Fig. 3a), but no correlation was observed with CO₂-based SSA actually available for NO₃⁻ sorption (Fig. 3b), i.e.,

SSA contributed by pore widths >0.67 nm, which corresponds to the hydrated diameter of NO₃⁻ (Nightingale, 1959). High positive correlation was also observed with the decadic logarithm of SEC and the total basicity of the biochars (Fig. 3a-c and d). The c_{s,max} was negatively correlated with the molar H/C_{org} ratio and molar surface O/C ratio of biochars, but for the latter with lower goodness of fit, especially for sorption data obtained at pH 5 (Fig. 3e and f). There was no clear trend observable between c_{s,max} and total acidity quantified by Boehm titration (Fig. S11).

Normalization of c_{s,max} to available CO₂-based SSA (pore widths >0.67 nm) illustrated that monolayer sorption dominated at pH 7 while at pH 5, multilayer sorption was indicated for BC750 and BC900 (Fig. S9a). Normalization of c_{s,max} to total basicity reduced variation between different biochars to 23 % at pH 5 and 36 % at pH 7 (Fig. S9c), which is considerably lower compared to variation of non-normalized values for c_{s,max} (59 % at pH 5 and 54 % at pH 7).

Desorption experiments indicated hysteresis for BC525, BCi and BC900 at pH 5 and for BC525, BCi and BC750 at pH 7 (data points filled in white, outlined in color, Fig. 2).

3.3. Release of NO₃⁻ from BCi-N and BCi-HNO₃

Release of NO₃⁻ from two different BBF (BCi-N and BCi-HNO₃) was studied in a 0.5 M phosphate buffer, adjusted to pH 5.7 or 7.4, similar to the pH values of the soils used in the column leaching experiment (cf. Section 3.4). In the first desorption step, BCi-N and BCi-HNO₃ released respective 85 % and 81 % of NO₃⁻ at pH 5.7 (p = 0.25, Table S4), while respective 92 % and 83 % (p = 0.06, Table S4) were desorbed at pH 7.4 (Fig. 4a and c). All samples released an additional 3–4 % NO₃⁻ during the second desorption step, regardless of buffer pH. After four desorption steps, cumulative release from BCi-N and BCi-HNO₃ stabilized at respective 88 % and 85 % for pH 5.7 (p = 0.33) and at 96 % and 90 % at pH 7.4 (p = 0.10). After the fourth desorption step, respective 3.9 and 4.8 g NO₃⁻-N kg⁻¹ remained sorbed in BCi-N and BCi-HNO₃ at pH 5.7 (p > 0.05, Table S4), while 2.2 and 3.5 g NO₃⁻-N kg⁻¹ (p > 0.05), respectively, remained sorbed at pH 7.4. Initially, 35 g NO₃⁻-N kg⁻¹ were added to the biochar. Most NO₃⁻ was already desorbed after 1 h from all BBF during the first desorption step (Fig. 4 b and d, Table S5).

3.4. Nitrate leaching from soil amended with BCi-N and BCi-HNO₃

Amending BCi-HNO₃ to soil-2.3 with pH 5.7 significantly reduced cumulative NO₃⁻ leaching in the first four leaching events by 23 %, 13 %, 9 % and 8 %, respectively, compared to the Control (p < 0.05), which was not observed with BCi-N (Fig. 5a and c). Amendment of BCi-N resulted in a higher deviation between the three replicates (coefficient of variation - CV = 9 %) than observed both for the Control (CV = 2 %) and soil amended with BCi-HNO₃ (CV = 4 %). In soil-2.4 N with pH 7.4, BCi-HNO₃ significantly reduced cumulative NO₃⁻ leaching by 12 % compared to the Control after 0.5 SPV (p < 0.05) and by 16 % when correcting for native NO₃⁻ leached from the soil, but there was no

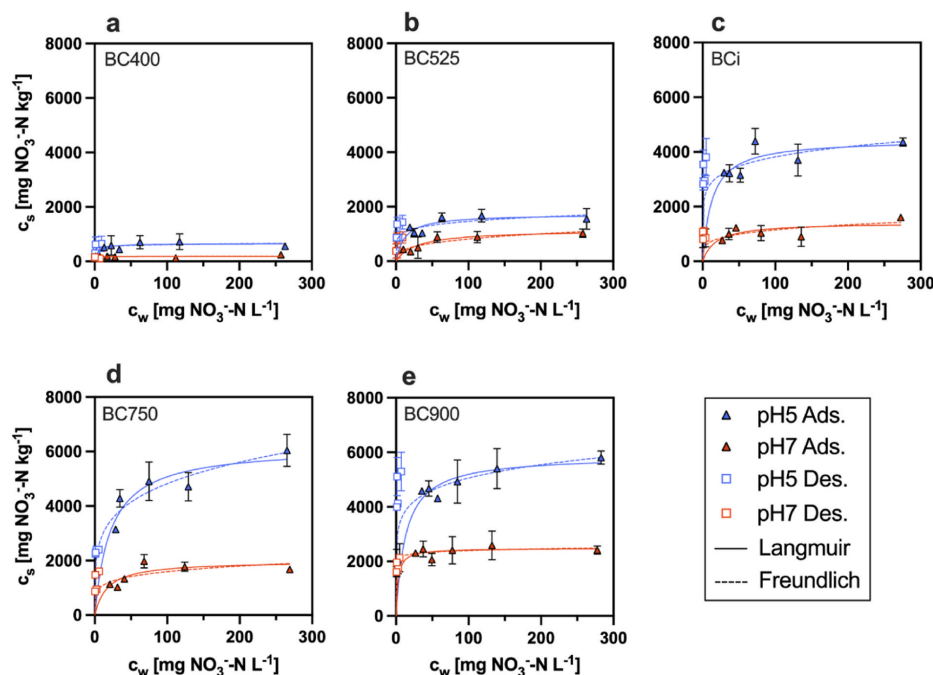


Fig. 2. Nitrate sorption isotherms of four wood-based biochars produced at pilot plant scale at 400, 525, 750, and 900 °C (BC400, BC525, BC750, and BC900 in panels a, b, d, and e, respectively) and at industrial scale (BCi, ~650 °C, panel c). Sorption was studied at pH 5.0 and 7.0 by equilibration in triplicates at 25 °C for 48 h. Filled data points represent the adsorption (Ads.) and white, color-bordered data points represent the desorption branch (Des.). c_s : calculated nitrate-nitrogen ($\text{NO}_3\text{-N}$) concentration in the solid phase (= sorbed on biochar). c_w : $\text{NO}_3\text{-N}$ concentration in liquid phase. Error bars indicate the standard deviation. Solid and dashed lines represent the fitted Langmuir and Freundlich sorption models, respectively. Fitting parameters are presented in Table 2.

Table 2

Fitting parameters and correlation coefficients of the Langmuir and Freundlich models (cf. equations (4) and (5) in section 1.7 in the Supplementary Information) for nitrate-nitrogen ($\text{NO}_3\text{-N}$) sorption onto biochars produced at pilot-plant scale at 400, 525, 750, and 900 °C (BC400, BC525, BC750, and BC900, respectively) and at industrial scale (BCi, produced at ~650 °C). Sorption experiments were conducted at pH 5.0 and 7.0 with equilibration at 25 °C for 48 h.

Biochar	Langmuir			Freundlich		
	$c_{s,max}$ [$\text{mg NO}_3\text{-N kg}^{-1}$]	K_L [L kg^{-1}]	R^2	1/n	K_F [L kg^{-1}]	R^2
pH 5.0						
BC400	650	0.240	0.87	0.067	450	0.86
BC525	1720	0.082	0.92	0.151	730	0.90
BC750	6190	0.046	0.96	0.219	1760	0.96
BC900	5880	0.076	0.98	0.133	2740	0.99
BCi	4450	0.078	0.95	0.135	2050	0.94
pH 7.0						
BC400	180	2.140	0.78	0.047	150	0.79
BC525	1140	0.034	0.93	0.305	200	0.91
BC750	1980	0.057	0.90	0.173	720	0.85
BC900	2480	0.385	0.97	0.036	2030	0.97
BCi	1420	0.054	0.82	0.216	430	0.85

significant difference compared to the Control in cumulative NO_3^- loss after 1.0, 1.5, and 2.0 SPV leached through the columns (Fig. 5b and d). With fertilization, almost all initial NO_3^- applied to the columns (3 mg $\text{NO}_3\text{-N}$) either by direct soil fertilization or via BCi-N and BCi- HNO_3 was released after leaching both soils with 2 SPV. For non-fertilized soil,

0.2–0.3 mg $\text{NO}_3\text{-N}$ were leached from soil-2.3 and 1.3 mg $\text{NO}_3\text{-N}$ were released from soil-2.4 N after 2 SPV, independent of a biochar amendment (Fig. 5a and b).

After re-fertilizing the columns by applying a fertilizer solution on top of the soil surface, BCi- HNO_3 significantly reduced cumulative leaching compared to the control by 15 % at 2.5 SPV, by 22 % at 3.0 SPV and by almost significant 10 % after 3.5 SPV ($p = 0.0534$) in soil-2.3 (Fig. 5a and c). BCi-N only reduced cumulative leaching significantly after 3.0 SPV by 10 % compared to the control (Fig. 5a and c). In soil-2.4 N, both BCi-N and BCi- HNO_3 significantly reduced cumulative leaching after 3 SPV by 7 % and BCi- HNO_3 further reduced it by 7 % after 3.5 SPV (Fig. 5b and d). In the following, no significant differences in cumulative N leaching were observed.

4. Discussion

4.1. NO_3^- sorption and desorption at soil-relevant pH

For all biochars, the decrease from pH 7 to pH 5 increased NO_3^- sorption capacities by a factor of 1.5–3.6 (average = 2.8). The increase in sorption capacity with a reduction in pH can be explained by biochar surface protonation under acidic conditions, which increases the net positive surface charge (Lawrinenko and Laird, 2015). As normalization of $c_{s,max}$ related to SSA accessible for hydrated NO_3^- ions, i.e., to pores with a width of >0.67 nm (Nightingale, 1959), did not level out differences between individual biochars, it can be concluded that higher sorption with higher HTT was less related to an increase in SSA, but

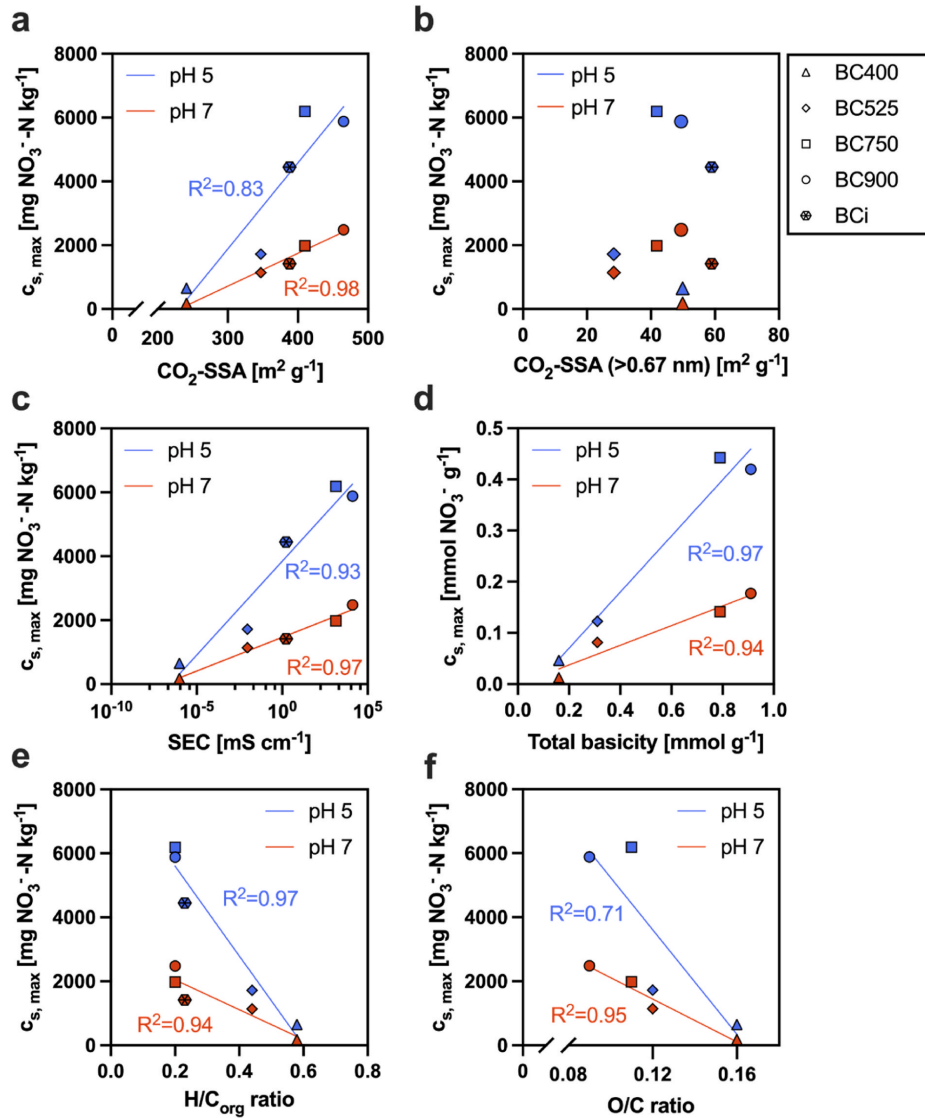


Fig. 3. Fitting parameter for nitrate-nitrogen sorption capacity obtained from Langmuir isotherm ($c_{s,max}$ in $\text{mg NO}_3\text{-N kg}^{-1}$ or in $\text{mmol NO}_3\text{-N g}^{-1}$ in panel d) of biochars plotted over biochar properties: specific surface area (SSA) derived from CO_2 sorption (total SSA and SSA contributed by pores >0.67 nm, panels a and b, respectively), solid state electric conductivity (SEC, logarithmic x-axis, panel c), total basicity (panel d), hydrogen/organic carbon molar ratio (H/C_{org}), and molar surface oxygen/carbon (O/C) ratio on the biochar surface derived from X-ray photoelectron spectroscopy (panel f). Correlation coefficients, where applicable, are related to linear regressions of the data each for $c_{s,max}$ recorded at pH 5 or pH 7.

rather to other biochar properties.

Oxygen-containing, deprotonated acidic functional groups on the biochar surface can take up protons, representing a partially positively charged sorption site for NO_3^- (Fidel et al., 2018). Boehm titration indicated that the overall acidity of biochars decreased with HTT, in line with the consensus that O-containing functional groups on biochar surfaces are degraded with increasing HTT (Banik et al., 2018).

However, a higher content of carboxylic groups was found for biochars produced at an HTT of 750 °C and 900 °C, which is not in line with literature (Gezahegn et al., 2019). This finding might be related to methodological biases in Boehm titration, which involves several pre-treatment steps that include acid-washing of biochar samples (Fidel et al., 2013). Residual acid might have been falsely detected as carboxylic groups for these biochars. Despite this, total acidity obtained

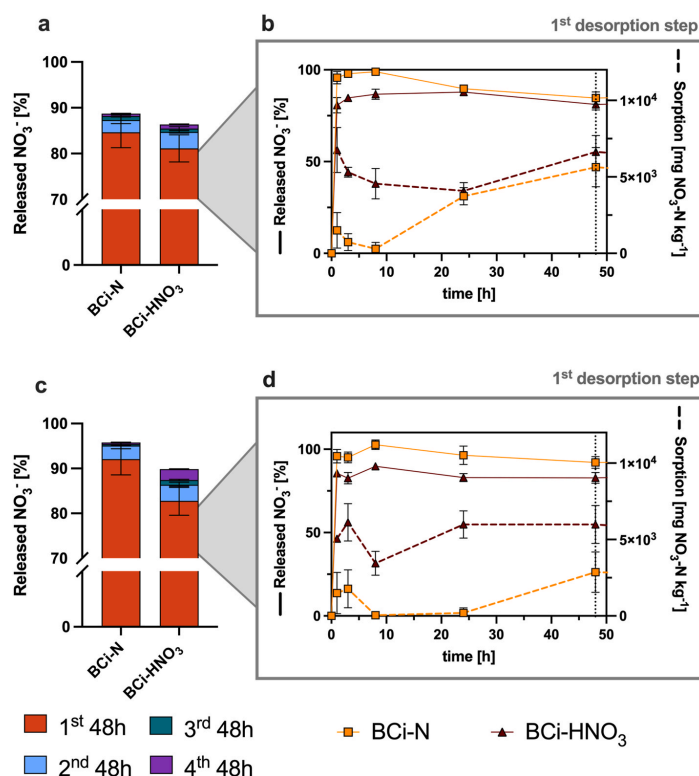


Fig. 4. Released nitrate (NO_3^-) from biochar produced at industrial scale, either enriched with HNO_3 and KNO_3 (BCi-H NO_3) or with only KNO_3 (BCi-N) to a N content of 3.5 % (w/w). Release experiments were performed either in a 0.5 M phosphate buffer adjusted to pH 5.7 (a, b) or to pH 7.4 (c, d) at 1:50 solid to liquid ratio and with shaking at 150 rpm. Panels a and c show the cumulative NO_3^- release during four desorption steps of each 48 h in fresh buffer (note the change in the y-axis scale at > 70 %). Panels b and d present the NO_3^- release (left axis, solid line) and the calculated mass of NO_3^- remaining sorbed onto biochar (right axis, expressed as NO_3^- -nitrogen, NO_3^- -N, dashed line) as a function of time during the first desorption step of 48 h. Error bars indicate the standard deviation of $n = 3$ replicates.

from Boehm titration as well as XPS and FTIR measurements coherently indicate a loss of the total O-containing functional group content with an increase in HTT. Therefore, the increased sorption of NO_3^- with decreasing pH and increasing HTT may have been less related to protonation of O-containing functional groups. Yet, it may be that NO_3^- sorption to BC400 was due to this mechanism, as molar-based sorption capacities ranged between 0.01 and 0.05 $\text{mmol NO}_3^- \text{g}^{-1}$, which is well below the quantified acidity of BC400 (0.5 mmol g^{-1} due to protonated phenols and lactols at pH 7 and 0.58 mmol g^{-1} by further contribution of protonated carboxylic groups at pH 5). However, for biochars with higher HTT, the observed sorption capacities of up to 0.4 $\text{mmol NO}_3^- \text{g}^{-1}$ cannot be attributed solely to the phenolic group content (0.05 mmol g^{-1} , Fig. S3) and potentially falsely detected carboxyl group content (0.15 mmol g^{-1}), which would anyway have only been present in the relevant protonated form during sorption experiments at pH 5, given their pK_a value of 6.4 (Fidel et al., 2013).

Protons may also be adsorbed on biochars by basic acting groups. Pyrone-like structures have basic character (Boehm, 2001), but since O/C ratios steadily decreased with higher HTT, it is unlikely that these contributed to the increased basicity at higher HTT. Sorption of protons can also occur on delocalized π -systems on the basal planes of graphitic structures (Boehm, 2001). With a higher HTT, graphitization of biochar is increased (Chia et al., 2015), which could explain their higher

basicity, leading to a higher degree of protonation and thus, higher NO_3^- sorption at lower pH. Further, SEC of biochars increases with aromaticity and graphitization of biochar (Issi, 2001; Mochizuki et al., 2003) while molar $\text{H}/\text{C}_{\text{org}}$ is reduced. The high goodness of fit for the correlation of NO_3^- sorption capacities with total basicity, SEC and $\text{H}/\text{C}_{\text{org}}$ ratios (Fig. 3) indicates that sorption of NO_3^- on protonated, aromatic structures was likely the main sorption mechanism, especially for biochars produced at $\text{HTT} > 500^\circ\text{C}$. This was also indicated by the lowest variation between different biochars upon normalization of $c_{s,\text{max}}$ to total basicity (Fig. S9), and is corroborated by lower molar $c_{s,\text{max}}$ values compared to the quantified basicity of all biochars (Fig. 3d). Still, it has to be mentioned that there is no validated method available for Boehm titration for biochar basicity as compared to quantification of acidity. Thus, the total basicity measurements might not only cover the uptake of H^+ by graphitic structures but also a neutralization of ash fractions. Still, while variation in ash content of the different biochars was only 19 %, total basicity varied by 58 % and was thus not dominated by the ash content.

The increase in NO_3^- sorption of biochars under acidic conditions and with HTT aligns with literature on pH-dependent NO_3^- sorption (Chintala et al., 2013; Fidel et al., 2018) and anion exchange capacities of biochars (Lawrinenko and Laird, 2015). The latter reported NO_3^- sorption capacities in a similar range as the present study: 1700–2000

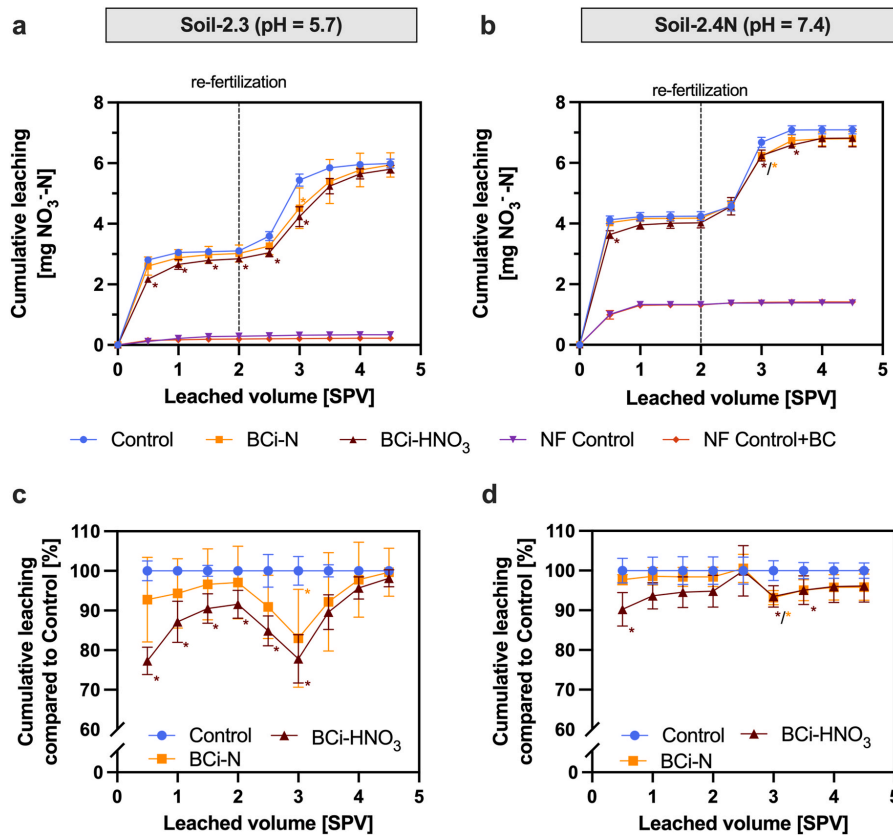


Fig. 5. Leaching of nitrate-nitrogen (NO_3^- -N) from soil columns without biochar (Control) or with biochar (0.75 %, w/w), either enriched with HNO_3 and KNO_3 (BCi- HNO_3 , bulk pH = 5.4) or with only KNO_3 (BCi-N, bulk pH = 9) plotted over cumulative leachate volume expressed as soil pore volume (SPV). Initial fertilization was 3 mg NO_3^- -N via direct soil fertilization or via enriched biochars. Re-fertilization occurred after four leaching events (=2 SPV) with 3 mg NO_3^- -N via KNO_3 solution added to the soil surface. Non-fertilized controls with or without pristine biochar were included (NF Control + BC and NF Control). Soil-2.3 had a pH of 5.7 (a, c) and soil-2.4 N had a pH of 7.4 (b, d). Panels (c) and (d) present relative cumulative leaching compared to the respective fertilized Control for each soil. Error bars indicate the standard deviation of triplicates for fertilized treatments and duplicates for non-fertilized treatments. Asterisks beside corresponding data points indicate significant differences compared to the Control (unpaired *t*-test, $p < 0.05$).

mg NO_3^- -N kg^{-1} for corn stover and red oak biochars at pH 3.7 (Fidel et al., 2018) as well as 700–6000 mg NO_3^- -N kg^{-1} at pH 5.0 and 560–4000 mg NO_3^- -N kg^{-1} at pH 7.0 for corn stover, pine wood, and switchgrass biochars (Chintala et al., 2013). This underscores that the type of acid and biochar production methods in the different studies were less influential for NO_3^- sorption capacities as compared to pH values during sorption experiments and HTT. In the light of the present study, the absent NO_3^- sorption capacities discovered by Gai et al. were likely due to a lack of pH control and resulting alkaline conditions (Gai et al., 2014).

As HNO_3 was used for pH control in our experiments, low equilibrium concentrations below 10–30 mg NO_3^- -N l^{-1} could not be covered in the sorption experiments. Therefore, sorption in this range cannot be described with sufficient certainty by our models. Still, this does not significantly affect the extent of the Langmuir sorption capacity $c_{s,\text{max}}$ derived from our model, which is the focus of our sorption experiment. The full release during desorption in 1 M KCl with average NO_3^- recovery rates of 80–115 % indicated a closed mass balance in the sorption-

desorption experimental series (Fig. S10).

4.2. NO_3^- release from BCI-N and BCI- HNO_3 in phosphate buffer

Biochar-based fertilizers were produced by enriching biochar with 35 g NO_3^- -N kg^{-1} , i.e., a significantly higher amount of N compared to the maximum sorption capacity of BCI (4.5 g NO_3^- -N kg^{-1} , Table 2). The acidification of biochar significantly reduced NO_3^- release during the initial hours of the first desorption step at both pH values (pH 5.7 and pH 7.4, Table S5), but differences between non-acidified and acidified BBF were generally small. Desorption of 80–90 % of applied N from all BBF in general occurred fast, i.e., within the first hour of desorption.

BCi-N demonstrated re-sorption of previously released NO_3^- during the first desorption step, with this effect being more pronounced at pH 5.7 than at pH 7.4. The initial pH of BCI-N was 9.0, and during the release experiment, BCI-N equilibrated to the pH of the buffers, which in turn increased its NO_3^- sorption capacity. This explains the alignment in residual sorbed and released NO_3^- of BCI- HNO_3 and BCI-N after 24 h

during the first two desorption steps at pH 5.7, when equilibration seemed complete. At pH 7.4, the differences in NO_3^- release between BCi-N and BCi- HNO_3 persisted for a longer period, i.e., until the third desorption step was finished. At higher environmental pH levels, biochar acidification could therefore improve NO_3^- sorption to biochar over a longer period than at lower pH.

The results generally imply that acidifying biochar can reduce the NO_3^- release from NO_3^- -enriched biochar, particularly in the short term after soil application. During this phase, the sorption capacity of pristine biochar may still be limited due to its alkalinity and delayed equilibration to soil pH. In contrast, acidified biochar exhibits a higher initial affinity for NO_3^- immediately upon application. In the long term, however, both acidified and non-acidified biochar will equilibrate to the surrounding soil pH, eliminating the effects of the acidification treatment, as observed in the release experiments, and both biochars would undergo ageing in soil contributing to NO_3^- capture in biochar (Hagemann et al., 2017; Haider et al., 2020).

The release dynamic of NO_3^- from biochar pores is not only regulated by NO_3^- sorption to the biochar surface, but also by mobility of water molecules inside biochar pores that hydrate NO_3^- ions (Conte and Schmidt, 2017). Both processes overlapped in the extraction experiment and can therefore not be differentiated. The effect of biochar acidification on water mobility within biochar pores could e.g., be separately studied by Fast-Field Cycling Nuclear Magnetic Resonance Relaxometry (Conte and Schmidt, 2017).

In general, the non-released NO_3^- after the release experiment for BCi-N was $4.5 \text{ g NO}_3^- \text{ N kg}^{-1}$ at pH 5.7 (13 % of initial N enrichment) and $1.4 \text{ g NO}_3^- \text{ N kg}^{-1}$ at pH 7.4 (4 % of initial N enrichment), which aligns with $c_{s,max}$ values calculated for BCi based on the batch sorption experiments (Table 2).

4.3. NO_3^- leaching in soil column experiment

In the first leaching event, NO_3^- leaching was significantly reduced only with BCi- HNO_3 but not with BCi-N compared to the respective Control in both soils, which is in good agreement with the release experiments in phosphate buffer. The effect of acidification in BCi- HNO_3 on reduction of NO_3^- leaching was only significantly maintained compared to the Control in soil-2.3 and not in the more alkaline soil-2.4 N during subsequent leaching events (until 2 SPV cumulative leaching), indicating that BCi- HNO_3 was faster equilibrated to environmental pH in the alkaline soil, which resulted in lower sorption of NO_3^- in BCi- HNO_3 . In soil-2.3, BCi- HNO_3 reduced NO_3^- leaching compared to the Control more significant as BCi-N after re-fertilization, indicating that biochar acidification still improved NO_3^- sorption to biochar even 12 days after application to soil. In soil-2.4 N, this effect did not occur, i.e., the initially higher NO_3^- sorption capacity of BCi- HNO_3 was lost. This synchronization effect of BCi-N and BCi- HNO_3 in terms of the NO_3^- leaching is the result of biochar equilibration to soil pH, which increases the NO_3^- sorption capacity for BCi-N (initial bulk pH of 9) and decreases sorption capacity of BCi- HNO_3 (initial bulk pH = 5.4). Equilibration of BCi-N to environmental pH might take longer in the soil with lower pH than at higher pH, leading to a longer maintained difference to BCi- HNO_3 in soil-2.3 N. At the same time, BCi- HNO_3 was already nearly at the same pH as soil-2.3 (= pH 5.7) and therefore maintained its initial NO_3^- sorption ability, while in soil-2.4 N, BCi- HNO_3 lost sorption capacity due to equilibration to higher pH, explaining the faster synchronization with BCi-N.

The soils not only differed in pH but also in texture, which might have affected the general potential of the biochar application on NO_3^- leaching reduction (Borchard et al., 2019), but likely not the differences observed between BCi-N and BCi- HNO_3 compared to the Control. Furthermore, the timing of the first leaching event after BBF application to soil (four days in the present study) and soil moisture content might be crucial for the extent of NO_3^- leaching reduction through the acidification treatment, as it affects pH equilibration to soil conditions. The

timing of the first leaching event was, however, not an experimental factor in the present study. Further, the soil moisture was adjusted to 65 % WHC on the initial three days after column setup. After the first leaching event, the soil was water saturated for the whole experiment, since a leaching event was conducted each day, and thus, soil moisture is not likely to have been a limiting factor for pH equilibration.

The leaching experiments were only performed with BCi due to a sample shortage of the biochars produced at pilot-plant scale. Higher reductions in NO_3^- leaching compared to the Control might have been achieved with BC750 and BC900 in both soils, as NO_3^- sorption to these biochars was higher in batch sorption experiments compared to BCi. The industrial biochar used here was produced at a moderate 650 °C, while there are also several industrial biochar production plants in operation that can use HTT of up to 900 °C. Ultimately, it must be mentioned that the small-scaled column leaching experiments can only reflect effects on NO_3^- leaching induced by physico-chemical soil-biochar interactions related to e.g., soil texture and pH, however, processes such as preferential flow, soil surface runoff or bioturbation are not covered.

4.4. Biochar modification to improve NO_3^- sorption

This study focused on modifying biochar with acid to improve its NO_3^- sorption capacity and potential to reduce NO_3^- leaching. Other modification techniques of biochar in this context include steam activation to increase available SSA of biochar (Borchard et al., 2012) or metal-enrichment of biomass prior to pyrolysis with e.g., lanthanum, potassium, or magnesium oxides to increase the number of anion sorption sites in biochar (Dieguez-Alonso et al., 2019; Wang et al., 2015; Zhang et al., 2012). Compared to acidification, the effects obtained from these methods might last longer after biochar soil application, as the effects of acidification may fade more quickly due to equilibration with environmental pH. However, steam activation will considerably decrease biochar yield by 30–70 % (Hagemann et al., 2020). Metal-enrichment, in contrast, may increase biochar yield (Grafmüller et al., 2022; Mašek et al., 2019), but to the best of our knowledge, optimizing both carbon yield and nitrate sorption capacity simultaneously has not been studied yet. Still, adding N as HNO_3 to biochar could be a cost-effective strategy to enhance its initial NO_3^- sorption capacity, as the cost of N added via HNO_3 or KNO_3 is comparable (approximately 7 € (kg N)^{-1} , (Chemishop24, 2025; Duengerexperte, 2025) and it can be implemented without modification of the pyrolysis process. Biochar acidification represents a tool to improve the short-term interaction of biochar with NO_3^- spiked into its pores during BBF production, independent of any pre-pyrolysis treatment of the biochar feedstock. To increase the effect of biochar acidification on increases in NO_3^- sorption capacity, physical activation could be considered based on the present study but also a maximization of aromaticity by choosing a high HTT during pyrolysis or increasing graphitization by using pyrolysis additives, such as isopropanol (Fornari et al., 2025).

4.5. Implications for practical biochar application in agriculture

The results of this study highlight the advantage of using biochar produced at a HTT >750 °C to increase NO_3^- sorption and thus improve the retention of NO_3^- in biochar amended soils. Based on release experiments in aqueous suspension and in soil columns, biochar acidification has the potential to improve the slow-release of NO_3^- from biochar-based fertilizers. This, however, needs to be studied in follow up experiments under field conditions to evaluate the practical relevance of the proposed treatment, also taking into account the risk of soil acidification under the proposed treatment. Such experiments would include effects such as preferential flow, surface runoff, or bioturbation, which can influence NO_3^- leaching. Our results can support scientists and practitioners by developing new formulations of biochar-based fertilizers for such field experiments.

5. Conclusions

The findings of this study suggest, in line with our hypothesis, that the dominant mechanism of pH-dependent NO_3^- sorption to biochar is related to sorption to protonated aromatic structures, especially for biochar produced at $\text{HTT} > 500^\circ\text{C}$. Nitrate sorption to biochar and thus, biochar's potential to reduce NO_3^- leaching increases as soil pH decreases and can be maximized by conducting pyrolysis at $\geq 750^\circ\text{C}$. With biochar repeatedly applied over several years and ultimately accumulating to $5\text{--}10\text{ t ha}^{-1}$, which is considered the optimistic economic break-even point reached after 10 years (Bach et al., 2016), $30\text{--}60\text{ kg N ha}^{-1}$ can maximally be sorbed and prevented from rapid leaching in slightly acidic soils and $10\text{--}25\text{ kg N ha}^{-1}$ in pH-neutral soils, which is of agricultural relevance. Acidification of biochar with HNO_3 can be a cost-neutral option for production of biochar-based fertilizers to reduce NO_3^- leaching instantly after biochar application to soil. Still, a long-term effect of the acidification treatment on NO_3^- leaching is unlikely due to biochar's equilibration to environmental pH. Thus, the relevance of this biochar treatment needs to be evaluated under field conditions. The focus of the present study was to investigate and enhance the sorption of NO_3^- to pristine biochar as it is the prevailing N species present in soils. To produce a BBF, however, also other mineral or organic N sources, which potentially have higher sorption affinity to pristine biochars compared to NO_3^- , like urea, should be considered to provide N-enriched biochars with optimal slow-release fertilization properties.

CRedit authorship contribution statement

Jannis Grafmüller: Writing – original draft, Investigation, Conceptualization. **Hans-Peter Schmidt:** Writing – review & editing, Supervision. **Daniel Kray:** Writing – review & editing, Supervision, Funding acquisition. **Thomas D. Bucheli:** Writing – review & editing, Conceptualization. **Haike Mäurer:** Writing – review & editing, Investigation. **Jens Möllmer:** Writing – review & editing, Investigation. **Heiko Peisert:** Writing – review & editing, Resources, Formal analysis. **Nikolas Hagemann:** Writing – review & editing, Supervision, Conceptualization.

Declaration of competing interest

The authors declare the following financial interests/personal relationships which may be considered as potential competing interests: Hans-Peter Schmidt and Nikolas Hagemann reports a relationship with Carbon Standards International AG that includes: board membership. If there are other authors, they declare that they have no known competing financial interests or personal relationships that could have appeared to influence the work reported in this paper.

Acknowledgments

This research was conducted within the HyPERFarm project (<https://hyperfarm.eu/>), which has received funding from the European Union's Horizon 2020 research and innovation programme under grant agreement no. 101000828. Syed Mustafa Hussain and colleagues at University of Tuebingen are acknowledged for the assistance during XPS measurements. Christian Gramlich from AWN GmbH is acknowledged for the provision of BCI, the industrially produced biochar. Rivka Fidel is acknowledged for valuable feedback on the methodology of the Boehm titration for acidic groups. We thank all the staff of the analytical chemistry lab at Offenburg University for assistance and provision of lab space and equipment, especially Andrea Seigel, Regina Brämer and Barbara Anders.

Appendix A. Supplementary data

Supplementary data to this article can be found online at <https://doi.org/10.1016/j.jenvman.2025.127224>.

Data availability

Data will be made available on request.

References

- Bach, M., Wilske, B., Breuer, L., 2016. Current economic obstacles to biochar use in agriculture and climate change mitigation. *Carbon Manag.* 7, 183–190. <https://doi.org/10.1080/17583004.2016.1213608>.
- Banik, C., Lawrinenko, M., Bakshi, S., Laird, D.A., 2018. Impact of pyrolysis temperature and feedstock on surface Charge and Functional Group chemistry of biochars. *J. Environ. Qual.* 47, 452–461. <https://doi.org/10.2134/jeq2017.11.0432>.
- Bartolomei, M., Hernández, M.L., Campos-Martínez, J., Hernández-Lamóneda, R., 2019. Graphene multi-protonation: a cooperative mechanism for proton permeation. *Carbon* 144, 724–730. <https://doi.org/10.1016/j.carbon.2018.12.086>.
- Boehm, H.P., 2001. Carbon surface chemistry. In: *Graphite and Precursors*, vol. 1. Gordon and Breach Science Publishers, pp. 141–178.
- Boehm, H.P., 1994. Some aspects of the surface chemistry of carbon blacks and other carbons. *Carbon* 32, 759–769. [https://doi.org/10.1016/0008-6223\(94\)90031-0](https://doi.org/10.1016/0008-6223(94)90031-0).
- Borchard, N., Schirrmann, M., Cayuela, M.L., Kammann, C., Wrage-Mönnig, N., Estavillo, J.M., Fuertes-Mendizábal, T., Sigua, G., Spokas, K., Ippolito, J.A., Novak, J., 2019. Biochar, soil and land-use interactions that reduce nitrate leaching and N₂O emissions: a meta-analysis. *Sci. Total Environ.* 651, 2354–2364. <https://doi.org/10.1016/j.scitotenv.2018.10.060>.
- Borchard, N., Wolf, A., Laabs, V., Aeckersberg, R., Scherer, H.W., Moeller, A., Amelung, W., 2012. Physical activation of biochar and its meaning for soil fertility and nutrient leaching - a greenhouse experiment: physical activation of biochar. *Soil Use Manag.* 28, 177–184. <https://doi.org/10.1111/j.1475-2743.2012.00407.x>.
- Chemieshop24, 2025. Salpetersäure 53% techn, 1200 kg Container [WWW Document]. Salpetersäure 53% techn. (1200kg Container). URL: <https://www.chemieshop24.de/salpetersaure-53-techn.-1200kg-container/1000409201002>. (Accessed 7 July 2025).
- Chia, 2015. Characteristics of biochar: physical and structural properties. In: Lehmann, J., Joseph, S. (Eds.), *Biochar for Environmental Management: Science, Technology and Implementation*. Routledge, Taylor & Francis Group, London/New York. <https://doi.org/10.4324/9780203762264-12>.
- Chintala, R., Mollinedo, J., Schumacher, T.E., Papiernik, S.K., Malo, D.D., Clay, D.E., Kumar, S., Gulbrandson, D.W., 2013. Nitrate sorption and desorption in biochars from fast pyrolysis. *Microporous Mesoporous Mater.* 179, 250–257. <https://doi.org/10.1016/j.micromeso.2013.05.023>.
- Conte, P., Schmidt, H.-P., 2017. Soil-Water interactions unveiled by fast field cycling NMR relaxometry. In: Harris, R.K., Wasylishen, R.L. (Eds.), *Emagres*. John Wiley & Sons, Ltd, Chichester, UK, pp. 453–464. <https://doi.org/10.1002/9780470034590.emrstm1535>.
- Dieguez-Alonso, A., Anca-Couce, A., Friskák, V., Moreno-Jiménez, E., Bacher, M., Bucheli, T.D., Cimó, G., Conte, P., Hagemann, N., Haller, A., Hilber, I., Husson, O., Kammann, C.I., Kienzl, N., Leifeld, J., Rosenau, T., Soja, G., Schmidt, H.-P., 2019. Designing biochar properties through the blending of biomass feedstock with metals: impact on oxyanions adsorption behavior. *Chemosphere* 214, 743–753. <https://doi.org/10.1016/j.chemosphere.2018.09.091>.
- Duengerexperte, de, 2025. Kaliumnitrat Multi-K RECI 13,5 - 0 - 46,5 [WWW Document]. Kaliumnitrat Multi-K RECI 13,5 - 0 - 46,5. URL: <https://www.duengerexperte.de/de/Kaliumnitrat.html>. (Accessed 7 July 2025).
- EBC 2012-2024, 2024. European Biochar Certificate - guidelines for a sustainable production of biochar. Carbon Standards International (CSI), Frick, Switzerland. 10 (4). <http://european-biochar.org>. from 20th Dec 2024.
- Fidel, R.B., Laird, D.A., Spokas, K.A., 2018. Sorption of ammonium and nitrate to biochars is electrostatic and pH-dependent. *Sci. Rep.* 8, 17627. <https://doi.org/10.1038/s41598-018-35534-w>.
- Fidel, R.B., Laird, D.A., Thompson, M.L., 2013. Evaluation of modified boehm titration methods for use with biochars. *J. Environ. Qual.* 42, 1771–1778. <https://doi.org/10.2134/jeq2013.07.0285>.
- Fornari, M.R., Hryniewicz, B.M., Matos, T.T.S., Schultz, J., Vidotti, M., Mangrich, A.S., 2025. Graphene-like biochars from pyrolysis of sugarcane bagasse and exhausted black acacia bark for the production of supercapacitors. *Biomass Bioenergy* 193, 107567. <https://doi.org/10.1016/j.biombioe.2024.107567>.
- Gai, X., Wang, H., Liu, J., Zhai, L., Liu, S., Ren, T., Liu, H., 2014. Effects of feedstock and pyrolysis temperature on biochar adsorption of ammonium and nitrate. *PLoS One* 9, e113888. <https://doi.org/10.1371/journal.pone.0113888>.
- Gezahegn, S., Sain, M., Thomas, S., 2019. Variation in feedstock wood chemistry strongly influences biochar liming potential. *Soil Syst.* 3, 26. <https://doi.org/10.3390/soilsystems3020026>.
- Grafmüller, J., Böhm, A., Zhuang, Y., Spahr, S., Müller, P., Otto, T.N., Bucheli, T.D., Leifeld, J., Giger, R., Tobler, M., Schmidt, H.-P., Dahmen, N., Hagemann, N., 2022. Wood ash as an additive in biomass pyrolysis: effects on biochar yield, properties, and agricultural performance. *ACS Sustain. Chem. Eng.* 10, 2720–2729. <https://doi.org/10.1021/acssuschemeng.1c07694>.

- Hagemann, N., Joseph, S., Schmidt, H.-P., Kammann, C.I., Harter, J., Borch, T., Young, R. B., Varga, K., Taherymoosavi, S., Elliott, K.W., McKenna, A., Albu, M., Mayrhofer, C., Obst, M., Conte, P., Dieguez-Alonso, A., Orsetti, S., Subdiaga, E., Behrens, S., Kappler, A., 2017. Organic coating on biochar explains its nutrient retention and stimulation of soil fertility. *Nat. Commun.* 8, 1089. <https://doi.org/10.1038/s41467-017-01123-0>.
- Hagemann, N., Schmidt, H.-P., Kägi, R., Böhler, M., Sigmund, G., Maccagnan, A., McArdell, C.S., Bücheli, T.D., 2020. Wood-based activated biochar to eliminate organic micropollutants from biologically treated wastewater. *Sci. Total Environ.* 730. <https://doi.org/10.1016/j.scitotenv.2020.138417>.
- Haider, G., Joseph, S., Steffens, D., Müller, C., Taherymoosavi, S., Mitchell, D., Kammann, C.I., 2020. Mineral nitrogen captured in field-aged biochar is plant-available. *Sci. Rep.* 10. <https://doi.org/10.1038/s41598-020-70586-x>, 13816.
- Heaney, N., Ukpong, E., Lin, C., 2020. Low-molecular-weight organic acids enable biochar to immobilize nitrate. *Chemosphere* 240, 124872. <https://doi.org/10.1016/j.chemosphere.2019.124872>.
- Hood-Nowotny, R., Umana, N.H.-N., Inselbacher, E., Oswald-Lachouani, P., Wanek, W., 2010. Alternative methods for measuring inorganic, organic, and total dissolved nitrogen in soil. *Soil Sci. Soc. Am. J.* 74, 1018–1027. <https://doi.org/10.2136/sssaj2009.0389>.
- Ippolito, J.A., Cui, L., Kammann, C., Wrage-Mönnig, N., Estavillo, J.M., Fuertes-Mendizabal, T., Cayuela, M.L., Sigua, G., Novak, J., Spokas, K., Borchard, N., 2020. Feedstock choice, pyrolysis temperature and type influence biochar characteristics: a comprehensive meta-data analysis review. *Biochar*. <https://doi.org/10.1007/s42773-020-00067-x>.
- Issi, J.-P., 2001. Electronic conduction. In: *Graphite and Precursors*, vol. 1. Gordon and Breach Science Publishers, pp. 45–70.
- Kopp, C., Sica, P., Lu, C., Tobler, D., Stoumann Jensen, L., Müller-Stöver, D., 2023. Increasing phosphorus plant availability from P-rich ashes and biochars by acidification with sulfuric acid. *J. Environ. Chem. Eng.* 11, 111489. <https://doi.org/10.1016/j.jece.2023.111489>.
- Lawrinenko, M., Laird, D.A., 2015. Anion exchange capacity of biochar. *Green Chem.* 17, 4628–4636. <https://doi.org/10.1039/C5GC00828J>.
- Lehmann, J., Joseph, S. (Eds.), 2015. *Biochar for Environmental Management: Science, Technology and Implementation*, second ed. Routledge, Taylor & Francis Group, London ; New York.
- Masek, O., Buss, W., Brownsort, P., Rovere, M., Tagliaferrro, A., Zhao, L., Cao, X., Xu, G., 2019. Potassium doping increases biochar carbon sequestration potential by 45%, facilitating decoupling of carbon sequestration from soil improvement. *Sci. Rep.* 9, 5514. <https://doi.org/10.1038/s41598-019-41953-0>.
- Melo, L.C.A., Lehmann, J., Carneiro, J.S. da S., Camps-Arbestain, M., 2022. Biochar-based fertilizer effects on crop productivity: a meta-analysis. *Plant Soil*. <https://doi.org/10.1007/s11104-021-05276-2>.
- Mochizuki, K., Soutric, F., Tadokoro, K., Antal, M.J., Tóth, M., Zelei, B., Várhegyi, G., 2003. Electrical and physical properties of carbonized charcoals. *Ind. Eng. Chem. Res.* 42, 5140–5151. <https://doi.org/10.1021/ie030358e>.
- Nightingale, E.R., 1959. Phenomenological theory of ion solvation. Effective radii of hydrated ions. *J. Phys. Chem.* 63, 1381–1387. <https://doi.org/10.1021/j150579a011>.
- PYREG, 2025. P1500 biomasse [WWW Document]. URL <https://www.pyreg.de/p1-500-biomasse/>.
- Schubert, S., 2018. *Pflanzenernährung*, 3. In: Auflage, vollständig überarb (Ed.), UTB Agrarwissenschaften. Verlag Eugen Ulmer, Stuttgart.
- Singh, B., Camps-Arbestain, M., Lehmann, J., 2017. *CSIRO (Australia). Biochar: a Guide to Analytical Methods*. CSIRO Publishing, Clayton, Victoria.
- Wang, Z., Guo, H., Shen, F., Yang, G., Zhang, Y., Zeng, Y., Wang, L., Xiao, H., Deng, S., 2015. Biochar produced from oak sawdust by Lanthanum (La)-involved pyrolysis for adsorption of ammonium (NH₄⁺), nitrate (NO₃⁻), and phosphate (PO₄³⁻). *Chemosphere* 119, 646–653. <https://doi.org/10.1016/j.chemosphere.2014.07.084>.
- Yang, J., Li, H., Zhang, D., Wu, M., Pan, B., 2017. Limited role of biochars in nitrogen fixation through nitrate adsorption. *Sci. Total Environ.* 592, 758–765. <https://doi.org/10.1016/j.scitotenv.2016.10.182>.
- Zhang, M., Gao, B., Yao, Y., Xue, Y., Inyang, M., 2012. Synthesis of porous MgO-biochar nanocomposites for removal of phosphate and nitrate from aqueous solutions. *Chem. Eng. J.* 210, 26–32. <https://doi.org/10.1016/j.cej.2012.08.052>.

Supplementary Information to:

Biochar acidification increased sorption and reduced leaching of nitrate

Jannis Grafmüller^{1,2,3,4}, Hans-Peter Schmidt², Daniel Kray¹, Thomas D. Bucheli⁴, Haike Mäurer⁵, Jens Möllmer⁵, Heiko Peisert⁶, Nikolas Hagemann^{2,4}

¹Institute for Sustainable Energy Systems (INES), Offenburg University of Applied Sciences, Germany

²Ithaka Institute, Arbaz (Switzerland) and Goldbach (Germany)

³Plant Biogeochemistry, Department of Geosciences, University of Tübingen, Tübingen, Germany

⁴Environmental Analytics, Agroscope, Zurich, Switzerland

⁵Institut für Nichtklassische Chemie e.V. (INC), Leipzig, Germany

⁶Institute for Physical and Theoretical Chemistry, University of Tübingen, Tübingen, Germany

Supplementary information related to this chapter can be found under the following link on the publisher website: <https://doi.org/10.1016/j.jenvman.2025.127224>
or directly under: <https://ars.els-cdn.com/content/image/1-s2.0-S0301479725032001-mmcl.pdf>

Chapter 5

Discussion and Conclusion

The main goal of the present thesis was to further understand the role of different pre- and post-pyrolysis treatments in BBF production on the pyrolysis process itself and the agricultural performance of BBF. In this context, wood ash as an additive in biochar production and the related presence of polychlorinated aromatic hydrocarbons (PCB+PCDD/F) in biochar produced from chlorine-containing feedstock was researched. Further, BBF produced via liquid nutrient enrichment, combined with or without acidification, but also granulation were studied for their impacts on crop growth, nutrient leaching and soil-borne N₂O emissions.

Relevance of the present thesis for the biochar industry and certification guidelines

Increased carbon and biochar yield obtained on industrial-scaled pyrolysis by mixing wood ash with biomass can increase revenues for biochar producers from carbon sink certification and improve both nutrient recycling and efficiency in biomass utilization of PyCCS. Thus, biochar cost could be further reduced for end consumers, potentially increasing the use of biochar in agriculture. While the EBC has paved the way for pyrolysis plant operators to use biomass ash as an additive¹, the forthcoming inclusion of biochar in EU Regulation 2019/1009² could hinder its adoption in the pyrolysis industry, at least in Europe, necessitating further legal review. Based on recent research^{3,4} and the results of the present thesis, using wood ash as an additive for pyrolysis of woody feedstock does not pose any known negative effects, provided that the resulting biochar complies with the EBC, which aligns with European soil protection and fertilizer regulations.

Furthermore, the results of this thesis have disproved concerns that including chlorine-containing additives, e.g. wood ash^{5,6}, or chlorine-rich biomass in pyrolysis could increase biochar contamination with PCB+PCDD/F. This finding broadens the range of viable biomass sources for biochar production, including marine biomass or biomass streams contaminated with plastic⁷ that can be added without concern in this respect to the positive list for biomasses in the EBC. However, PCB+PCDD/F contamination can still occur if pyrolysis process control is inadequate, underscoring the need for continued monitoring within the EBC framework.

From a toxicological perspective, the integrity of the EBC could be further strengthened by incorporating dioxin-like (dl) PCB into the current limit of 20 ng TEQ kg⁻¹ for PCDD/F, as these compounds have similar toxicological effect. This approach has already been implemented, for example, by the German Federal Compost Quality Association⁸.

Relevance of the present thesis for agricultural use of biochar-based fertilizers

In Figure D1, effects of BBF application on crop yield and N leaching, in comparison to the respective fertilized control, are summarized across all experiments conducted in this thesis. Results are categorized based on the BBF application method: gBBF, biochar co-applied with fertilizer or liquid-enriched biochar with fertilizer. For crop yields, effects were analyzed independent of the soil and plant type (Figure D1a). On average, BBF applications changed yields by $+5 \pm 9\%$ in the absence of leaching and by $+14 \pm 12\%$ under leaching conditions (Figure D1a). Thus, BBF application to soil may be more likely to increase crop yields under conditions limiting plant growth, e.g., reduced nutrient availability resulting from nutrient losses via leaching. Still, yield responses varied to a high extent across the experiments, i.e., from -9% to $+33\%$ compared to the fertilized control, highlighting the potential uncertainty farmers face when applying BBF to soil.

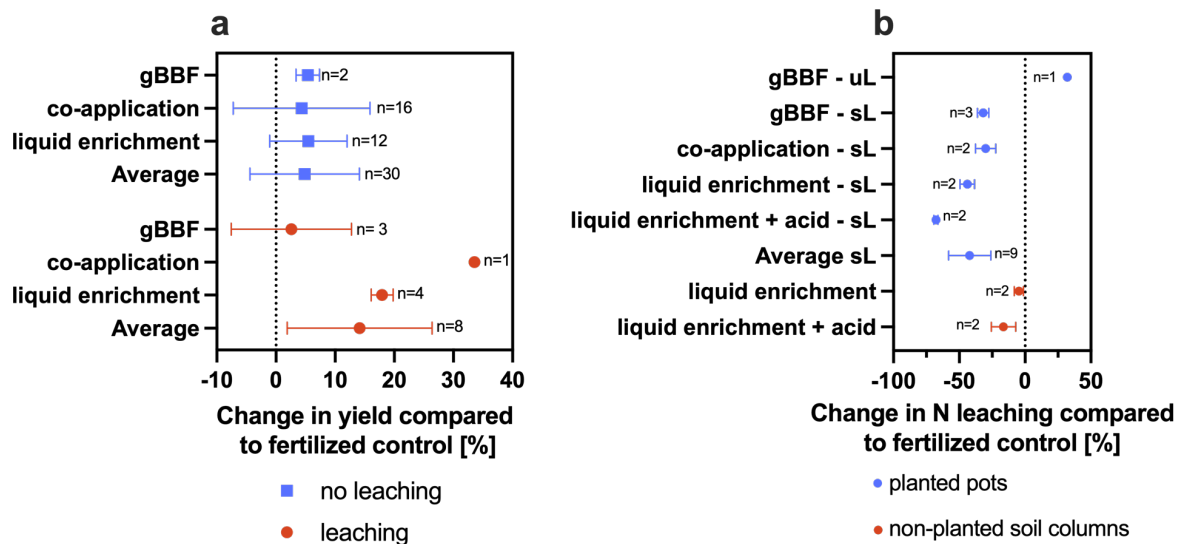


Figure D1: (a) Change in crop yield and (b) change in nitrogen (N) leaching with a biochar-based fertilizer (BBF) in an individual leaching event relative to fertilized control without BBF. Amendments were separated into three groups: granulated BBF (gBBF), biochar co-applied with fertilizer to soil or BBF prepared by liquid enrichment of biochar with fertilizer and with/without acid. Average changes are also presented, independent of BBF type. In panel a, comparisons were separated into leaching groups (leaching / no leaching). In panel b, data was further separated by study types: leaching of planted pots or non-planted soil columns. For planted pots, data was separated by soil type (silt loam (uL) or sandy loam (sL)), which was not done for soil column studies. For soil column studies, only the first leaching event was considered for better comparison with the other studies. Data is presented as mean \pm standard deviation, number of replicates are indicated beside data points.

Due to the variability in crop yield responses observed after BBF application, providing clear recommendations on optimal BBF application strategy remains challenging. However, the following key conclusions can be drawn from the individual studies conducted in this thesis:

1. A consistently achieved benefit from BBF amendment, independent of the biochar formulation technology used, was reduced N leaching from sandy soil, which was -42% on average in pot trials (Figure D1b). Thus, also low biochar application rates to soil (< 2-5 t ha⁻¹) with BBF can significantly improve N retention in such soil type. The opposite was observed for gBBF amendment to a soil with higher silt and clay content (+32%, Figure D1b), underscoring the need to include different soil types in studies on BBF evaluation.
2. Granulated biochar is less effective in promoting crop growth compared to non-granulated biochar. This was observed in two independent trials in a sandy loam (chapter 3c and e), potentially linked to a more homogeneous distribution of biochar in soil when applied non-granulated, allowing for a higher degree of interaction with e.g., soil porewater and plant roots, and avoiding nutrient immobilization due to concentrated biochar application with fertilizer in the case of gBBF.
3. Biochar effects on nutrient leaching are not affected by granulation compared to application of non-granulated biochar to sandy loam soil.
4. Preparing microparticles of biochar (size range 1-1000 µm) should be limited to the coarsest particle size possible necessary for further processing (e.g. granulation) to benefit from highest possible biochar-induced increase in soil WHC.
5. Quantification of SSA of micro- and mesopores is not a reliable proxy to estimate WHC of biochar.
6. To better forecast differences between BBF in nutrient leaching from soil based on release experiments in aqueous suspension, the pH in such experiments should be adjusted to soil conditions, as this can significantly impact e.g., NO₃⁻ sorption to biochar.
7. Biochar applied via BBF with initial biochar application rates <2 t ha⁻¹ is not sufficient to result in immediate reductions in soil-borne N₂O emissions. Emission reductions might be achieved after repeated BBF application over time, once a critical biochar concentration in soil is reached.
8. Application of BBF concentrated in the root zone of plants may decrease root growth due to improved nutrient availability, resulting in higher aboveground biomass yield.

9. Electrostatic sorption⁹ of NO_3^- to biochar at soil-relevant pH is likely to be dominated by sorption to protonated, condensed aromatic structures and not by sorption to protonated acidic functional groups.
10. Acidification of biochar combined with NO_3^- enrichment results in reduced NO_3^- leaching from soil and the effect is more likely to sustain in soil with a pH below 6.
11. Acidifying biochar with citric acid can lead to an unintended increase in soil pH, likely due to microbial decarboxylation of citrate, a reaction that consumes protons in soil¹⁰. The use of HNO_3 should be preferred, as it directly adds NO_3^- to the biochar, with the further advantage that no competitive anions for sorption sites on biochar are introduced to the BBF.

To summarize the attempts to further improve nutrient, but specifically nitrogen leaching from BBF amended soil, only acidification of biochar but not granulation led to an improvement compared to liquid nutrient enrichment of biochar or co-application of biochar and fertilizer, which served as the respective controls and already provided relative high reductions compared to non-amended soil (Figure D1b). The higher differences in NO_3^- leaching reduction relative to non-amended soil achieved with acidified BBF amendment in the greenhouse study (chapter 4a) compared to the soil column study (chapter 4b, Figure D1b) may be related to the higher N content in the BBF and the lower absolute biochar concentration in soil in the column leaching study in chapter 4b (2.2% N vs. 3.5% N and 1.5% vs. 0.75% biochar concentration in soil). These different approaches were chosen as the greenhouse study should provide a general prove of concept of the acidification treatment with a higher biochar concentration and a simultaneously lower N content in the BBF, while the soil column study should include a more practical biochar concentration with 0.75%, equal to $\sim 5\text{-}8 \text{ t ha}^{-1}$. Differences in conduction of the leaching experiment, i.e., applying distilled water to simulate 20 l m^{-2} precipitation in the greenhouse or leaching in steps of half pore volumes in the column study might further explain deviations, while differences in soil texture appear less influential, as both the greenhouse trial and the column study included a sandy textured soil.

All these findings may guide future research in further developing and optimizing production and application of BBF. The limitations of the present thesis and future research needs are discussed below. The experiments in the present study have shown that there is room for further optimization of BBF. Biochar-based fertilizers, at least those tested in this thesis, can so far be considered as a reliable tool for C sequestration when applied to soil but less reliable in its effect on crop yields. Thus, the economic efficiency of biochar application to soil remains uncertain

for farmers. Currently, biochar prices range from 800 to 1500 € t⁻¹ dry matter¹¹. With an annual BBF application equal to a biochar rate of 2 t ha⁻¹, an additional annual revenue of 1600 to 3000 € ha⁻¹ would need to be achieved to compensate biochar costs. This cannot be considered economic, as even a 5-10% yield increase only generates an additional 100-200 € ha⁻¹ on average for common arable crops grown across Europe¹¹. Further modifications to biochar, such as granulation, would only increase costs, making BBF applications even less economic, although application with common agricultural machinery would be eased. As a result, the widespread adoption of biochar in agriculture is unlikely under current conditions. A significant reduction in biochar procurement costs would be necessary, which could be achieved through higher compensation rates in the voluntary carbon market¹² for biochar producers, substantially exceeding the current 150 € (tCO_{2e})⁻¹, using additives that provide co-benefits in biomass pyrolysis, as outlined in chapter 2a, and lower cost for pyrolysis equipment.

Limitations and further research need

For experiments on wood ash as an additive in biochar production, the studied pyrolysis temperature of 500-550 °C was at the lower end of the typical industrial range of 500-900 °C. It is known from the addition of pure AAEM salts that their increasing effect on biochar yield remains constant within a 350-750 °C temperature range¹³. However, this should be validated for AAEM-containing additives such as wood ash. To provide a more mechanistic understanding, pure AAEM salts of different speciation should be used as additives in further pyrolysis experiments, which could also enable to forecast their effects on biochar yield in natural, more complex mixtures, such as wood ash. The co-benefits of such additives on increasing C yield of biochar production, enriching biochar with nutrients and potentially lowering NO_x emission¹⁴ from pyrolysis plants should be subject of further research. Another interesting recent observation is the use of an isopropanol-enriched atmosphere in pyrolysis reactor, promoting graphitization of biochar¹⁵ and with that, leading to a potential higher persistence when applied to soil. Given all these promising effects, the broader topic of pyrolysis additives should be further explored.

A key limitation of the pyrolysis experiments on pilot-plant scale in Chapter 2 was the lack of replication. Although biochar samples were collected across three residence times, making them representative of n=3 residence times, at least one specific experiment should have been performed in triplicates to account for intraday or day-to-day variability of the pyrolysis setup.

Despite for the soil column experiment in chapter 4b and in the greenhouse trial in chapter 3d, effects of BBF on plant growth, nutrient leaching and N₂O emissions were assessed using only

one specific soil and biochar type. Consequently, the results obtained in the other trials cannot be generalized across other biochar-soil combinations, due to high variation in physicochemical properties across different biochars and soils. For example, as observed in chapter 3d, N leaching from gBBF amended soil was soil-texture dependent. There might have been differences in the direct comparison of the gBBF with co-application of non-granulated biochar and fertilizer in the silt loam, which were not observable when only using sandy loam in chapter 3c. Similarly, the N₂O emission trial used a soil with relatively high organic matter content, which may be less responsive to biochar in terms of N₂O emission reductions^{16,17}. To obtain more generalizable results, future studies should include a broader range of soil and biochar types.

A further limitation concerns chapter 3a, which focused on the concentrated root-zone application of liquid-enriched biochar in white cabbage. The experiment directly compared BBF application methods with each other, however, we could not elucidate whether decreased root fill factors were solely biochar-related or rather an artifact of concentrated fertilizer application with the liquid enriched BBF applied below the cabbage plants. In this respect, the concentrated application of fertilizer without biochar below the seedling or the use of fertilizer-enriched inert minerals, such as zeolite, could have been applied to better isolate biochar induced effects. Furthermore, the interaction of biochar and the two different N sources were solely assessed based on effects on crop yield at the end of the experiment. A deeper mechanistic understanding of N availability and transformation could have been achieved through porewater or soil sampling throughout the experiment.

In chapter 3e, a non-fertilized control should have been included to differentiate between N₂O emissions induced by fertilization and emissions induced solely by soil re-wetting. Further, gas sampling should ideally have been performed via a minimum of four samples taken per pot and gas enrichment period, to calculate gas fluxes based on multi-point linear regression and not only by a two-point approach.

In this thesis, four different approaches were tested to reduce nutrient leaching compared to conventional fertilization without biochar amendment: co-application of biochar and fertilizer, liquid fertilizer enrichment of biochar, liquid fertilizer enrichment combined with acidification, and combined granulation of biochar and fertilizer. However, it would have been advantageous to also include previously developed BBF, for example metal or zeolite-modified BBF^{18,19}, as a reference to be able to better assess the effectiveness of the applied BBF in the present thesis.

For investigating specific mechanisms affecting e.g., N₂O emissions, nutrient leaching or nutrient availability in BBF amended soil, greenhouse trials remain a valuable tool to gain insights under controlled conditions. Yet, greenhouse trials may be less reliable to forecast the effect of soil-applied BBF on crop yields under field conditions. This is because they lack key environmental factors present in field conditions, such as macrofauna activity and greater variability in temperature, soil moisture (due to irregular precipitation) and light irradiation, all of which significantly influence crop growth and highlight the ongoing need of testing BBF in field trials.

References

1. EBC 2012-2024. 'European Biochar Certificate - Guidelines for a Sustainable Production of Biochar.' Carbon Standards International (CSI), Frick, Switzerland. (<http://european-biochar.org>). Version 10.4 from 20th Dec 2024. (2024).
2. European Union. *REGULATION (EU) 2019/1009 OF THE EUROPEAN PARLIAMENT AND OF THE COUNCIL of 5 June 2019*. (2019).
3. Buss, W., Jansson, S. & Mašek, O. Unexplored potential of novel biochar-ash composites for use as organo-mineral fertilizers. *J. Clean. Prod.* **208**, 960–967 (2019).
4. Grafmüller, J. *et al.* Wood Ash as an Additive in Biomass Pyrolysis: Effects on Biochar Yield, Properties, and Agricultural Performance. *ACS Sustain. Chem. Eng.* **10**, 2720–2729 (2022).
5. Vassilev, S. V., Baxter, D., Andersen, L. K. & Vassileva, C. G. An overview of the chemical composition of biomass. *Fuel* **89**, 913–933 (2010).
6. Davidsson, K. O. *et al.* Potassium, Chlorine, and Sulfur in Ash, Particles, Deposits, and Corrosion during Wood Combustion in a Circulating Fluidized-Bed Boiler. *Energy Fuels* **21**, 71–81 (2007).
7. Hilber, I. *et al.* Biochar Production From Plastic-Contaminated Biomass. *GCB Bioenergy* **16**, e70005 (2024).
8. Bundesgütegemeinschaft Kompost. Schwellenwerte und Grenzwerte. https://www.kompost.de/fileadmin/user_upload/Dateien/Guetesicherung/Dokumente_Kompost/Dok._251-006-4_Schwellen_Grenzwerte.pdf (2023).
9. Fidel, R. B., Laird, D. A. & Spokas, K. A. Sorption of ammonium and nitrate to biochars is electrostatic and pH-dependent. *Sci. Rep.* **8**, 17627 (2018).
10. Yan, F., Schubert, S. & Mengel, K. Soil pH increase due to biological decarboxylation of organic anions. *Soil Biol. Biochem.* **28**, 617–624 (1996).
11. Grafmüller, J., Hagemann, N. & Kray, D. Deliverable 4.2: Report on the comparison of pyrolysis with other CDR technologies available. *HyPERFarm EU Project* <https://hyperfarm.eu/wp-content/uploads/2025/03/D4.2.pdf> (2024).
12. CDR.FYI. CDR.FYI. <https://www.cdr.fyi>. accessed 25th March 2024. (2024).
13. Mašek, O. *et al.* Potassium doping increases biochar carbon sequestration potential by 45%, facilitating decoupling of carbon sequestration from soil improvement. *Sci. Rep.* **9**, 5514 (2019).
14. Guo, S. *et al.* Effects of calcium oxide on nitrogen oxide precursor formation during sludge protein pyrolysis. *Energy* **189**, 116217 (2019).
15. Fornari, M. R. *et al.* Graphene-like biochars from pyrolysis of sugarcane bagasse and exhausted black acacia bark for the production of supercapacitors. *Biomass Bioenergy* **193**, 107567 (2025).

16. Kaur, N., Kieffer, C., Ren, W. & Hui, D. How much is soil nitrous oxide emission reduced with biochar application? An evaluation of meta-analyses. *GCB Bioenergy* **15**, 24–37 (2023).
17. Borchard, N. Biochar, soil and land-use interactions that reduce nitrate leaching and N₂O emissions: A meta-analysis. *Sci. Total Environ.* 11 (2019).
18. Liu, X. *et al.* A Biochar-Based Route for Environmentally Friendly Controlled Release of Nitrogen: Urea-Loaded Biochar and Bentonite Composite. *Sci. Rep.* **9**, 9548 (2019).
19. Dieguez-Alonso, A. *et al.* Designing biochar properties through the blending of biomass feedstock with metals: Impact on oxyanions adsorption behavior. *Chemosphere* **214**, 743–753 (2019).